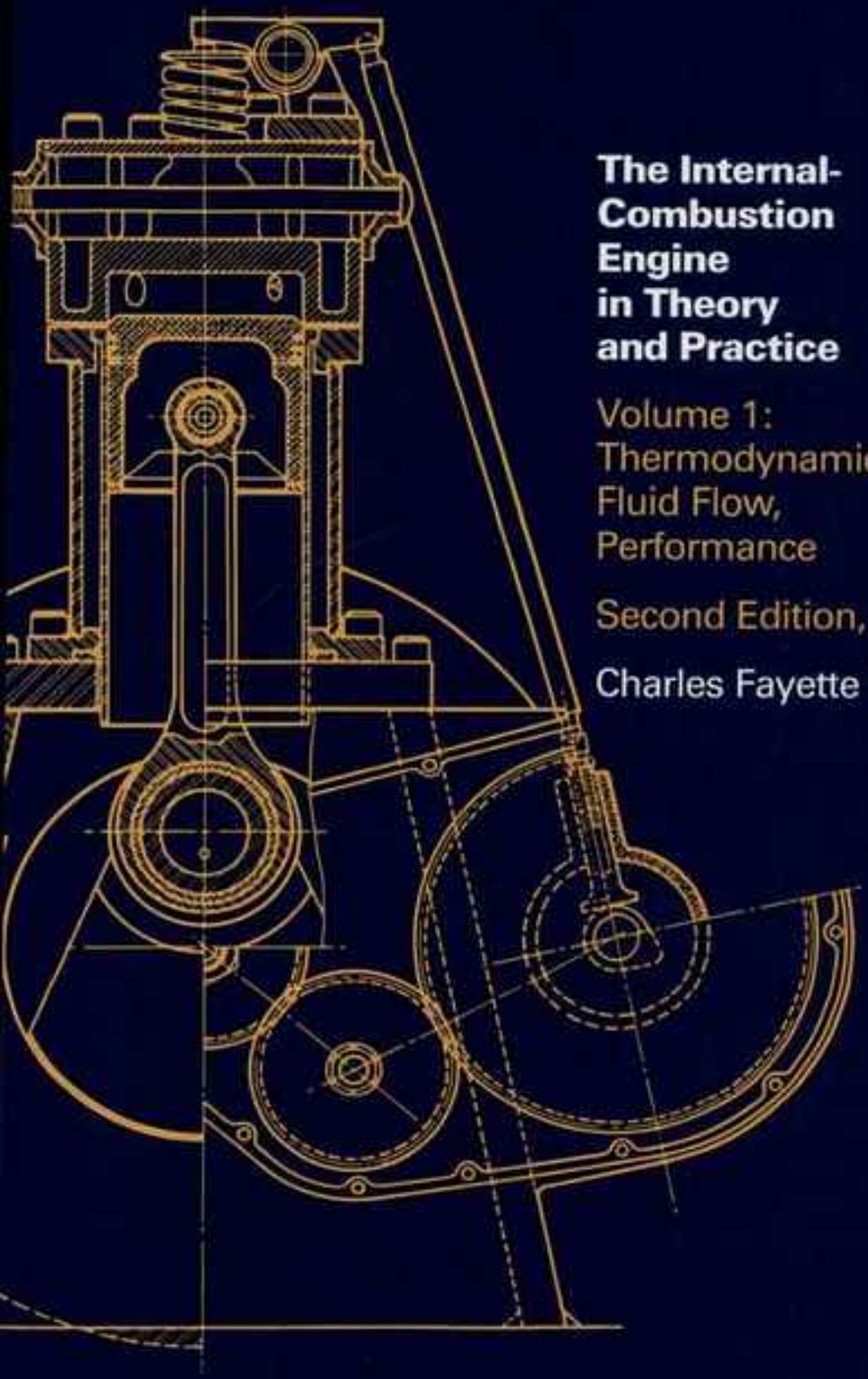

The Internal-Combustion Engine in Theory and Practice

Volume 1: Thermodynamics, Fluid Flow, Performance

Second Edition, Revised

Charles Fayette Taylor

The Internal-Combustion Engine in Theory and Practice

www.TechnicalBooksPDF.com

Volume I Thermodynamics, Fluid Flow, Performance

CHAPTER 1 Introduction, Symbols, Units, Definitions
2 Air Cycles
3 Thermodynamics of Actual Working Fluids
4 Fuel-Air Cycles
5 The Actual Cycle
6 Air Capacity of Four-Stroke Engines
7 Two-Stroke Engines
8 Heat Losses
9 Friction, Lubrication, and Wear
10 Compressors, Exhaust Turbines, Heat Exchangers
11 Influence of Cylinder Size on Engine Performance
12 The Performance of Unsupercharged Engines
13 Supercharged Engines and Their Performance

Volume II Combustion, Fuels, Materials, Design

CHAPTER 1 Combustion in Spark-Ignition Engines I: Normal Combustion
2 Combustion in Spark-Ignition Engines II: Detonation and Preignition
3 Combustion in Diesel Engines
4 Fuels for Internal-Combustion Engines
5 Mixture Requirements
6 Carburetor Design and Emissions Control
7 Fuel Injection
8 Engine Balance and Vibration
9 Engine Materials
10 Engine Design I: Preliminary Analysis, Cylinder Number, Size, and Arrangement
11 Engine Design II: Detail Design Procedure, Power-Section Design
12 Engine Design III: Valves and Valve Gear and Auxiliary Systems
13 Future of the Internal-Combustion Engine. Comparison with Other Prime Movers
14 Engine Research and Testing Equipment—Measurements—Safety

www.TechnicalBooksPDF.com

The Internal-Combustion Engine in Theory and Practice

Volume I: Thermodynamics, Fluid Flow, Performance

Second Edition, Revised

by Charles Fayette Taylor
Professor of Automotive Engineering, Emeritus
Massachusetts Institute of Technology

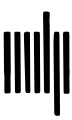

THE M.I.T. PRESS
Massachusetts Institute of Technology
Cambridge, Massachusetts, and London, England

www.TechnicalBooksPDF.com

Copyright © 1960 and 1966 and new material © 1985 by The Massachusetts Institute of Technology

All rights reserved. No part of this book may be reproduced in any form by any electronic or mechanical means (including photocopying, recording, or information storage and retrieval) without permission in writing from the publisher.

Printed and bound in the United States of America.

First MIT Press paperback edition, 1977
Second edition, revised, 1985

Library of Congress Cataloging in Publication Data

Taylor, Charles Fayette, 1894–
The internal-combustion engine in theory and practice.

Bibliography: v. 1, p.
Includes index.
Contents: v. 1. Thermodynamics, fluid flow,
performance.
1. Internal-combustion engines. I. Title.
TJ785.T382 1985 621.43 84-28885
ISBN 978-0-262-20051-6 (hc. : alk. paper)—978-0-262-70026-9 (pb. : alk. paper)

20 19 18 17 16 15 14

www.TechnicalBooksPDF.com

Preface

When the author undertook the task of teaching in the field of internal-combustion engines at the Massachusetts Institute of Technology, it was evident that commercial development had been largely empirical and that a rational quantitative basis for design, and for the analysis of performance, was almost entirely lacking. In an attempt to fill this gap, the Sloan Laboratories for Aircraft and Automotive Engines were established in 1929 at the Massachusetts Institute of Technology, largely through the generosity of Mr. Alfred P. Sloan, Jr., and the untiring enthusiasm of the late Samuel S. Stratton, then President of MIT.

The intervening years have been spent in research into the behavior of internal-combustion engines and how to control it. A large amount of the laboratory work has been done by students as part of their requirements for graduation. Other parts have been done by the teaching staff and the professional laboratory staff with funds provided by government or by industry.

The results of this work, translated, it is hoped, into convenient form for practical use in engine design and research, is the subject of these two volumes.

Grateful acknowledgment is made to all those who in various capacities —students, teaching staff, technical staff, and staff engineers—have contributed by their laboratory work, their writings, and their criticism.

www.TechnicalBooksPDF.com

Special acknowledgment and thanks are due to Professor E. S. Taylor, Director of the Gas Turbine Laboratory at MIT and long a colleague in the work of the Sloan Automotive Laboratories, and to Professors A. R. Rogowski and T. Y. Toong of the Sloan Laboratories teaching staff.

The author will be grateful to readers who notify him of errors that diligent proofreading may have left undiscovered.

C. FAYETTE TAYLOR

Cambridge, Massachusetts
November 1976

Preface to Second Edition, Revised

Since the publication of this volume in 1966 there have been no developments that require changes in the basic principles and relationships discussed in this volume. Neither have there been any important competitors to the conventional reciprocating internal-combustion engine for land and sea transportation and for most other purposes except aircraft, nuclear-powered vessels, and large electric generating stations. The total installed power of reciprocating internal-combustion engines still exceeds that of all other power sources combined by at least one order of magnitude (see p. 5).

On the other hand, there have been two important changes in emphasis, one toward improved fuel economy and the other toward reduced air pollution by engine exhaust gases.

The petroleum crisis of the 1970s caused the increased emphasis on fuel economy, especially in the case of road vehicles and large marine Diesel engines. In the case of passenger cars, the greatest gains have been made by reducing the size, weight, and air resistance of the vehicles themselves and by reducing engine size accordingly. This change, plus wider-range transmissions and reduced ratio of maximum engine power to car weight allow road operation to take place nearer to the engine's area of best fuel economy.

Increases in fuel economy of spark-ignition engines have been accomplished chiefly through improved systems of control of fuel-air ratio, fuel distribution, and spark timing. In the case of Diesel engines, supercharging to higher mean effective pressures, and in many cases reduction in rated piston speed, have achieved notable improvements in efficiency.

In the other major change in emphasis since the 1960s, public demand

www.TechnicalBooksPDF.com

for reduced air pollution has brought stringent government limitations on the amount of undesirable emissions from road-vehicle engines and other power plants. In the United States, the problem of reducing air pollution has resulted in more research, development, and technical literature than any other event in the history of the internal-combustion engine. The methods used for reducing pollution are outlined in Volume 2, together with references to the existing literature. See also the references on pages 555 and 556 of this volume.

The developments described above have been greatly assisted by the recent availability of powerful computers. These are now generally used in engine research, design, and testing. They make possible mathematical "modeling" of many aspects of engine behavior, including fluid flow, combustion, and stress distribution. Engine test equipment and procedures are now usually "computerized." An extremely important application of computers, now expanding rapidly, is the use of relatively small electronic computer systems applied to individual engine installations for purposes of control and the location of malfunctions. The use of such systems in road vehicles is becoming general in the United States, and it has assisted greatly in the control of exhaust emissions, as explained in Volume 2.

The developments mentioned here are covered in more detail at appropriate points in these two volumes.

C. Fayette Taylor

January 1984

www.TechnicalBooksPDF.com

DEDICATED TO THE MEMORY OF THE LATE

SIR HARRY R. RICARDO, L.L.D., F.R.S.,

WORLD-RENOWNED PIONEER IN

ENGINE RESEARCH AND ANALYSIS,

VALUED FRIEND AND ADVISER.

www.TechnicalBooksPDF.com

Contents

Volume I

Thermodynamics, Fluid Flow, Performance

Chapter	**1**	INTRODUCTION, SYMBOLS, UNITS, DEFINITIONS	**1**
	2	AIR CYCLES	**22**
	3	THERMODYNAMICS OF ACTUAL WORKING FLUIDS	**40**
	4	FUEL-AIR CYCLES	**67**
	5	THE ACTUAL CYCLE	**107**
	6	AIR CAPACITY OF FOUR-STROKE ENGINES	**147**
	7	TWO-STROKE ENGINES	**211**
	8	HEAT LOSSES	**266**
	9	FRICTION, LUBRICATION, AND WEAR	**312**

www.TechnicalBooksPDF.com

10 Compressors, Exhaust Turbines, Heat Exchangers 362

11 Influence of Cylinder Size on Engine Performance 401

12 The Performance of Unsupercharged Engines 418

13 Supercharged Engines and Their Performance 456

Appendix 1 Symbols and Their Dimensions 495

2 Properties of a Perfect Gas 500

3 Flow of Fluids 503

4 Analysis of Light-Spring Indicator Diagrams 510

5 Heat Transfer by Forced Convection between a Tube and a Fluid 514

6 Flow through Two Orifices in Series 516

7 Stresses Due to Motion and Gravity in Similar Engines 518

8 Basic Engine-Performance Equations 520

Bibliography 523

Charts

C-1, C-2, C-3, C-4 are folded in pocket attached to rear cover.

Index 557

www.TechnicalBooksPDF.com

one — Introduction, Symbols, Units, Definitions

Heat engines can be classified as the *external-combustion* type in which the working fluid is entirely separated from the fuel-air mixture, heat from the products of combustion being transferred through the walls of a containing vessel or *boiler*, and the *internal-combustion* type in which the working fluid consists of the products of combustion of the fuel-air mixture itself.

Table 1-1 shows a classification of the important types of heat engine. At the present time the reciprocating internal-combustion engine and the steam turbine are by far the most widely used types, with the gas turbine in wide use only for propulsion of high-speed aircraft.

A fundamental advantage of the reciprocating internal-combustion engine over power plants of other types is the absence of heat exchangers in the working fluid stream, such as the boiler and condenser of a steam plant.* The absence of these parts not only leads to mechanical simplification but also eliminates the loss inherent in the process of transfer of heat through an exchanger of finite area.

The reciprocating internal-combustion engine possesses another important fundamental advantage over the steam plant or the gas turbine, namely, that all of its parts can work at temperatures well below the maximum cyclic temperature. This feature allows very high maximum

* Gas turbines are also used without heat exchangers but require them for maximum efficiency.

www.TechnicalBooksPDF.com

Table 1-1

Classification of Heat Engines

Class	Common Name	Reciprocating or Rotary	Size of Units *	Principal Use	Status (1960)
External combustion	steam engine	reciprocating	S–M	locomotives	obsolescent
	steam turbine	rotary	M–L	electric power, large marine	active
	hot-air engine	reciprocating	S	none	obsolete
	closed-cycle gas turbine	rotary	M–L	electric power, marine	experimental
Internal combustion	gasoline engine	reciprocating	S–M	road vehicles, small marine, small industrial, aircraft	active
	Diesel engine	reciprocating	S–M	road vehicles, industrial, locomotives, marine, electric power	active
	gas engine	reciprocating	S–M	industrial, electric power	active
	gas turbine	rotary	M–L	electric power, aircraft	active
	jet engine	rotary	M–L	aircraft	active

* Size refers to customary usage. There are exceptions. L = large, over 10,000 hp, M = medium, 1000–10,000 hp, S = small, under 1000 hp.

cyclic temperatures to be used and makes high cyclic efficiencies possible.

Under present design limitations these fundamental differences give the following advantages to the reciprocating internal-combustion engine, as compared with the steam-turbine power plant, when the possibilities of the two types in question have been equally well realized:

1. Higher maximum efficiency.
2. Lower ratio of power-plant weight and bulk to maximum output (except, possibly, in the case of units of more than about 10,000 hp).
3. Greater mechanical simplicity.
4. The cooling system of an internal-combustion engine handles a much smaller quantity of heat than the condenser of a steam power plant of equal output and is normally operated at higher surface temperatures. The resulting smaller size of the heat exchanger is a great advantage in vehicles of transportation and in other applications in which cooling must be accomplished by atmospheric air.

These advantages are particularly conspicuous in relatively small units.

www.TechnicalBooksPDF.com

On the other hand, practical advantages of the steam-turbine power plant over the reciprocating internal-combustion engine are

1. The steam power plant can use a wider variety of fuels, including solid fuels.
2. More complete freedom from vibration.
3. The steam turbine is practical in units of very large power (up to 200,000 hp or more) on a single shaft.

The advantages of the reciprocating internal-combustion engine are of especial importance in the field of land transportation, where small weight and bulk of the engine and fuel are always essential factors. In our present civilization the number of units and the total rated power of internal-combustion engines in use is far greater than that of all other prime movers combined. (See Tables 1-2 and 1-3.) Considering the great changes in mode of life which the motor vehicle has brought about in all industrialized countries, it may safely be said that the importance of the reciprocating internal-combustion engine in world economy is second to that of no other development of the machine age.

Although the internal-combustion *turbine* is not yet fully established as a competitor in the field of power generation, except for aircraft, the relative mechanical simplicity of this machine makes it very attractive. The absence of reciprocating parts gives freedom from vibration comparable to that of the steam turbine. This type of power plant can be made to reject a smaller proportion of the heat of combustion to its cooling system than even the reciprocating internal-combustion engine —a feature that is particularly attractive in land and air transportation.

Cooling the blades of a turbine introduces considerable mechanical difficulty and some loss in efficiency. For these reasons most present and projected designs utilize only very limited cooling of the turbine blades, with the result that the turbine inlet temperature is strictly limited. Limitation of turbine inlet temperature imposes serious limitations on efficiency and on the output which may be obtained from a given size unit. Except in aviation, where it is already widely used, it is not yet clear where the internal-combustion turbine may fit into the field of power development. Its future success as a prime mover will depend upon cost, size, weight, efficiency, reliability, life, and fuel cost of actual machines as compared with competing types. Although this type of machine must be regarded as a potential competitor of the reciprocating internal-combustion engine and of the steam power plant, it is unlikely that it will ever completely displace either one.

www.TechnicalBooksPDF.com

Table 1-2

Estimated Installed Rated Power, United States, 1983

	Millions of hp.
(1) Road vehicles	20,000
(2) Off-road vehicles	250
(3) Diesel-electric power	60
(4) Small engines, lawnmowers, etc.	50
(5) Small water craft	250
(6) Small aircraft	36
(7) R.R. locomotives	7
Total I.C.E.	20,693
(9) Steam, hydroelectric, nuclear	700
(10) Jet aircraft (nonmilitary)	25
Total non I.C.E.	725
Ratio I.C.E. to other sources	28.7
(U.S. military and naval forces are not included)	

Method of Estimate

Item	No. Units and Estimated Unit Power	Source
(1)	160 million vehicles at 125 hp	WA
(2)	2.3 million farms at 100 hp, plus other off-road 10%	WA
(3)	8% of item 9	est.
(4)	25 million units at 2 hp	est.
(5)	5 million at 50 hp	est.
(6)	200,000 airplanes at 200 hp	SA
(7)	30,000 locomotives at 1200 hp	WA
(8)	853 vessels at 8000 hp	WA
(9)	from 1984 data	WA
(10)	2500 aircraft at 10,000 hp	SA

WA: *World Almanac*, 1984. SA: Statistical Abstracts, U.S. Dept. of Commerce, 1983. Average unit power is estimated.

Power plants which combine the reciprocating internal-combustion engine with a turbine operating on the exhaust gases offer attractive possibilities in applications in which high output per unit size and weight are of extreme importance. The combination of a reciprocating engine with an exhaust-gas turbine driving a supercharger is in wide use. (See Chapter 13.)

www.TechnicalBooksPDF.com

Table 1-3
Power Production in the United States, 1982

(1)	Electric power	
	Installed capacity (including Diesel)	760×10^6 hp
	1982 output	3×10^{12} hp-hr
	Use factor	0.45
(2)	Automobiles	
	No. passenger cars	144×10^6
	1982 output	864×10^9 hp-hr
	Use factor	0.007

Method of Estimate

(1) $$\text{Use factor} = \frac{3\times10^{12}}{760\times10^6\times365\times24} = 0.45.$$

(2) 160 million vehicles less 10% for trucks = 144 million. From *World Almanac*, average automobile goes 9000 miles per year. Estimate 30 mph = 300 hrs at 20 hp = 6000 hp-hr per car. At average rating of 100 hp per car,

$$\text{Use factor} = \frac{6000}{100\times365\times12} = 0.007.$$

Road vehicles used about half of U.S. petroleum consumption, or about 100 billion gallons, in 1982 (WA).

SYMBOLS

The algebraic symbols, subscripts, etc. used in this book are listed in Appendix 1. As far as possible, these conform with common U.S. practice. Definitions of symbols are also given in the text to the point at which they should be entirely familiar to the reader.

FUNDAMENTAL UNITS

The choice of the so-called *fundamental* units is largely a matter of convenience. In most fields of pure science these are three in number, namely, length (L), time (t) and either force (F) or mass (M). Through Newton's law, Joule's law, etc., all other quantities can be defined in terms of three units.

Since this book must, of necessity, use the results from many fields of scientific endeavor in which different systems of fundamental units oc-

www.TechnicalBooksPDF.com

cur,* it has been found convenient, if not almost necessary, to employ a larger number of fundamental dimensions, namely length (L), time (t), force (F), mass (M), temperature (θ), and quantity of heat (Q). How these are used and related appears in the next section.

Units of Measure

Throughout this book an attempt has been made to keep all equations in such form that any set of consistent units of measure may be employed. For this purpose Newton's law is written

$$F = Ma/g_0 \tag{1-1}$$

where F is force, M is mass, a is accelerations, and g_0 is a proportionality constant whose value depends upon the system of units used. The dimensions of g_0 are determined from Newton's law to be

$$\frac{\text{mass} \times \text{acceleration}}{\text{force}} = \frac{\text{mass} \times \text{length}}{\text{force} \times \text{time}^2} = MLt^{-2}F^{-1}$$

Under these conditions g_0 must appear in any equation relating force and mass in order that the equation shall be dimensionally homogeneous. (The word *mass* has been used whenever a quantity of material is specified, regardless of the units used to measure the quantity.) If the *technical* system of units is employed, that is, the system in which force and mass are measured in the same units, g_0 becomes equal in magnitude to the standard acceleration of gravity. Thus in the foot, pound-mass, pound-force, second system generally used by engineers $g_0 = 32.17$ lbm † ft per lbf † sec^2. In the foot, slug, pound-force, second system, or in the usual cgs system, g_0 is numerically equal to unity. g_0 must not be confused with the acceleration of gravity, g, which depends on location and is measured in units of length over time squared. In the technical system g has a value close to 32.17 ft per sec^2 at any point on the earth's surface.

In problems involving heat and work the dimensional constant J is defined as

$$w \mathrel{\widehat{=}} JQ \tag{1-2}$$

* For example, in American thermodynamic tables the unit of mass is the pound, whereas in many tables of density, viscosity, etc, the unit of mass is the slug.

† From this point on pound mass is written lbm and pound force, lbf.

www.TechnicalBooksPDF.com

in which the circle indicates a cyclic process, that is, a process which returns the system to its original state.

w is work done *by* a system minus the work done *on* the system, and Q is the heat added to the system, minus the heat released by the system.

The dimensions of J are

$$\frac{\text{units of work}}{\text{units of heat}} = \frac{\text{force} \times \text{length}}{\text{units of heat}} = FLQ^{-1}$$

and J must appear in any equation relating heat and work in order to preserve dimensional homogeneity.* In foot, pound-force, Btu units J is 778 ft lbf per Btu.

Another dimensional constant, R, results from the law of perfect gases:

$pV = (M/m)RT$
p = pressure
V = volume
M = mass of gas
m = molecular weight of gas
T = absolute temperature

Molecular weight may be considered dimensionless, since it has the same value in any system of units.†

R thus has the dimensions

$$\frac{\text{pressure} \times \text{volume}}{\text{temperature} \times \text{mass}} = \frac{\text{force} \times \text{length}}{\text{temperature} \times \text{mass}} = FL\theta^{-1}M^{-1}$$

In the foot, pound-force, pound-mass, degree Rankine (°F + 460) system R = 1545 ft lbf/°R for m lbm of material.

GENERAL DEFINITIONS

In dealing with any technical subject accurate definition of technical terms is essential. Whenever technical terms are used about whose

* For a more complete discussion of this question see refs 1.3 and 1.4.

† The official definition of molecular weight is 32 times the ratio of the mass of a molecule of the gas in question to the mass of a molecule of O_2.

www.TechnicalBooksPDF.com

definitions there may be some doubt, your author has endeavored to state the definition to be used. At this point, therefore, it will be well to define certain basic terms which appear frequently in the subsequent discussion.

Basic Types of Reciprocating Engine *

Spark-Ignition Engine. An engine in which ignition is ordinarily caused by an electric spark.

Compression-Ignition Engine. An engine in which ignition ordinarily takes place without the assistance of an electric spark or of a surface heated by an external source of energy.

Diesel Engine. The usual commercial form of the compression-ignition engine.

Carbureted Engine. An engine in which the fuel is introduced to the air before the inlet valve has closed.†

Carburetor Engine. A carbureted engine in which the fuel is introduced to the air by means of a carburetor. (Most spark-ignition engines are also carburetor engines.)

Injection Engine. An engine in which the fuel is injected into the cylinder after the inlet valve has closed. (All Diesel engines and a few spark-ignition engines are this type.)

Gas Turbines

In this book the words *gas turbine* are taken to mean the internal-combustion type of turbine, that is, one in which the products of combustion pass through the turbine nozzles and blades. External-combustion (closed cycle) gas turbines are not included.

DEFINITIONS RELATING TO ENGINE PERFORMANCE

Efficiency

In the study of thermodynamics the efficiency of a cyclic process (that is, a process which operates on a given aggregation of materials in

* It is assumed that the reader is familiar with the usual nomenclature of engine parts and the usual mechanical arrangements of reciprocating internal-combustion engines. If this is not the case, a brief study of one of the many descriptive books on the subject should be undertaken before proceeding further.

† Engines with fuel injected in the inlet ports are thus carbureted engines.

www.TechnicalBooksPDF.com

such a way as to return it to its original state) is defined as

$$\eta \equiv w/JQ' \tag{1-3}$$

where η = efficiency
w = useful work done by the process
J = Joule's law coefficient
Q' = heat which flows *into* the system during the process

Internal-combustion engines operate by burning fuel in, rather than by adding heat to, the working medium, which is never returned to its original state. In this case, therefore, the thermodynamic definition of efficiency does not apply. However, it is convenient to use a definition of efficiency based on a characteristic quantity of heat relating to the fuel. The method of determining this value, which is called the *heat of combustion* of the fuel, is somewhat arbitrary (see Chapter 3), but it is generally accepted in work with heat engines. If the heat of combustion per unit mass of fuel is denoted as Q_c, the efficiency, η, of any heat engine may be defined by the following expression:

$$\eta = P/J\dot{M}_f Q_c \tag{1-4}$$

where P = power
$\dot{M}_f$ = mass of fuel supplied per unit time
Q_c = heat of combustion of a unit mass of fuel

If the power, P, is the *brake power*, that is, the power measured at the output shaft, eq 1-4 defines the *brake thermal efficiency*. On the other hand, if the power is computed from the work done on the pistons, or on the blades in the case of a turbine, it is called *indicated power*, and eq 1-4 then defines the *indicated thermal efficiency*.

The ratio of brake power to indicated power is called *mechanical efficiency*, from which it follows that *brake* thermal efficiency is equal to the product of the indicated thermal and mechanical efficiencies.

Equation 1-4 is basic to the study of all types of heat engine. Several rearrangements of this equation are also important. One of these expresses power output:

$$P = J\dot{M}_a F Q_c \eta \tag{1-5}$$

in which $\dot{M}_a$ is the mass of air supplied per unit time and F is the mass ratio of fuel to air. Again, the power and efficiency terms may be *indicated*, or the equation may refer to *brake* power, in which case η is the brake thermal efficiency.

Another important arrangement of eq 1-4 is

$$\text{sfc} = \frac{\dot{M}_f}{P} = \frac{1}{JQ_c\eta} \tag{1-6}$$

www.TechnicalBooksPDF.com

in which $\dot{M}_f$ is the mass of fuel supplied per unit time and sfc is the *specific fuel consumption*, that is, the fuel consumed per unit of work. If P is indicated power and η is indicated thermal efficiency, sfc is the *indicated specific fuel consumption* and is usually written isfc. On the other hand, if P is brake power and η is the brake thermal efficiency, sfc is the *brake specific fuel consumption* and is usually written bsfc.

A third important arrangement of eq 1-4 is

$$\text{sac} = \frac{\dot{M}_a}{P} = \frac{1}{JFQ_c\eta} = \frac{\text{sfc}}{F} \tag{1-7}$$

in which sac is the *specific air consumption*, or mass of air consumed per unit of work. Again, we may use isac to designate *indicated specific air consumption* and bsac to indicate *brake specific air consumption.*

In eqs 1-4–1-7 power is expressed in (force × length/time) units. It is, of course, more usual to express power in units of horsepower, hp. For this purpose we note that hp $= P/K_p$, in which K_p is the value of 1 hp expressed in (force × length/time) units.

By using these definitions, eqs 1-4 and 1-5 may be written

$$\eta = \frac{\text{hp} \times K_p/J}{\dot{M}_f Q_c} \tag{1-8}$$

and

$$\text{hp} = \frac{J}{K_p} \dot{M}_a F Q_c \eta \tag{1-9}$$

Values for K_p and K_p/J are given in Table 1-4.

Table 1-4

United States and British Standard Horsepower

Force Unit	Length Unit	Time Unit	K_p	Units of K_p	$\frac{K_p}{J}$
pound	foot	sec	550	ft lbf/sec	0.707 Btu/sec
pound	foot	min	33,000	ft lbf/min	42.4 Btu/min
kilogram	meter	sec	76.04 *	kgf m/sec	0.178 kg cal/sec
dyne	centimeter	sec	76.04×10^9	dyne cm/sec	178 cal/sec

* A "metric" horsepower is 75 kgf m/sec = 0.986 × US horsepower.

www.TechnicalBooksPDF.com

For convenience, expressions 1-4 and 1-5 are given in the United States horsepower, pound, second, Btu system of units:

$$\eta = \frac{\text{hp} \times 0.707}{\dot{M}_f Q_c} \tag{1-10}$$

$$\text{hp} = 1.414 \dot{M}_a F Q_c \eta \tag{1-11}$$

Specific fuel consumption and specific air consumption are customarily given on an hourly basis; therefore,

$$\text{sfc} = \frac{0.707 \times 3600}{Q_c \eta} = \frac{2545}{Q_c \eta} \text{ lbm/hp-hr} \tag{1-12}$$

and, correspondingly,

$$\begin{aligned} \text{sac} &= 2545/FQ_c\eta \text{ lbm/hp-hr} \\ &= \text{sfc}/F \end{aligned} \tag{1-13}$$

CAPACITY AND EFFICIENCY

A most important measure of the suitability of a prime mover for a given duty is that of its *capacity*, or maximum power output, at the speed or speeds at which it will be used. An engine is of no use unless its capacity is sufficient for the task on hand. On the other hand, for a given maximum output it is desirable to use the smallest size of engine consistent with the requirements of rotational speed, durability, reliability, etc, imposed by any particular application. The size of any internal-combustion engine of a given type is greatly influenced by the maximum value of $\dot{M}_a$, the greatest mass of air per unit time that it must handle. Equation 1-5 shows that to attain minimum $\dot{M}_a$ at a given power output and with a given fuel conditions should be such that the product $F\eta$ has the maximum practicable value. In this way bulk, weight, and first cost of the engine for a given duty are held to a minimum. The conditions under which a maximum value of $F\eta$ prevails are not usually those that give maximum efficiency; hence to attain the highest practicable value of $F\eta$ specific fuel consumption may have to be high. However, fuel consumption at maximum output is usually unimportant because most engines run at maximum output only a small fraction of the time. In case an engine is required to run at its maximum output for long periods it may be necessary to increase its size so that it can operate at maximum efficiency rather than at the maximum value of $F\eta$.

www.TechnicalBooksPDF.com

Expression 1-6 shows that, with a given fuel, specific fuel consumption is inversely proportional to efficiency. From this relation it follows that wherever it is important to minimize the amount of fuel consumed engines should be adjusted to obtain the highest practicable efficiency at those loads and speeds used for long periods of time. For example, in self-propelled vehicles a high efficiency under *cruising*, or average road, conditions is essential for minimizing fuel loads and fuel costs.

Indirect Advantages of High Efficiency. In many cases an increase in indicated efficiency results in a lowering of exhaust-gas temperatures. (See Chapter 4.) Ricardo (refs 1.12, 1.13) was one of the first to point out that an improvement in indicated efficiency often results in an improvement in the reliability and durability of a reciprocating engine because many of the troubles and much of the deterioration to which such engines are subject are the result of high exhaust temperatures.

It is evident that capacity and efficiency are supremely important in any fundamental study of the internal-combustion engine and that they are closely related to each other and to other essential qualities. Much of the material in subsequent chapters, therefore, is considered with especial emphasis on its relation to these two essential quantities.

THE GENERAL ENERGY EQUATION

In the science of thermodynamics * the following relation applies to any *system*, or aggregation of matter, which goes through a *cyclic process*, that is, a process which returns the system to its original state.

$$Q \circleq \frac{w_t}{J} \tag{1-14}$$

In this equation Q is the heat † received by the system, minus the heat given up by the system, and w_t is the total work done *by* the system, minus the work done *on* the system during the process. By these definitions, Q is positive when more heat flows into the system than leaves the system and w_t is positive when more work is done by the system than is done on the system. (The circle indicates a cyclic process.)

* The material covered in this section can be found in several standard textbooks. However, it is so fundamental to the remainder of this book that it is considered desirable to include a brief presentation here.

† For definitions of heat, work, process, property, etc, in the thermodynamic sense, as well as for a discussion of the philosophic implications of eq 1-14, see refs 1.3, 1.4.

www.TechnicalBooksPDF.com

When a process is not cyclic, that is, when the system is left in a condition after the process which differs from its condition before the process, we can write

$$U_2 - U_1 = Q - (w_t/J) \tag{1-15}$$

U_1 is called the *internal energy* of the system at the beginning of the process, and U_2 is the internal energy at the end of the process.

Each of the terms in eq 1-15 may be divided by the mass of the system. Thus this equation is equally valid if we call U the internal energy per unit mass, Q the heat transferred per unit mass, and w_t the work per unit mass. From this point on these symbols apply to a unit mass of material, unless otherwise noted.

Equation 1-15 is often called the *general energy equation*, and it may be regarded as a definition of internal energy, since a change in this property is most conveniently measured by measuring Q and w_t/J. Because the absolute value of internal energy is difficult to define, its value above any arbitrary reference point can be determined by measuring $Q - (w_t/J)$ for processes starting from the reference point.

In practice, the difference in internal energy between any two states is manifested by a difference in temperature, pressure, chemical aggregation, electric charge, magnetic properties, phase (solid, liquid, or gas), kinetic energy, or mechanical potential energy. Potential energy may be due to elevation in a gravitational field, a change in elastic state, in the case of solids, or a change in surface tension, in the case of liquids.

In work with internal-combustion engines we are usually dealing with fluids under circumstances in which changes in electric charge, magnetic properties, and surface tension are negligible. We can usually make separate measurements of changes in mechanical potential energy. Kinetic energy may be measured separately, or, in the case of gases, as we shall see, its measurement may be automatically included because of the normal behavior of thermometers.

Let E be the internal energy per unit mass measured from a given reference state with the system at rest, and let it be assumed that changes in electrical, magnetic, and surface-tension energy are negligible and that there is no change in mechanical potential energy. Under these circumstances changes in E are attributable to changes in pressure, temperature, phase, and chemical aggregation only. For a unit mass of such a system expression 1-15 can be written

$$[E_2 + (u_2^2/2g_0J)] - [E_1 + (u_1^2/2g_0J)] = Q - (w_t/J) \tag{1-16}$$

www.TechnicalBooksPDF.com

in which u_1 is the velocity of the system at the beginning and u_2, the velocity at the end of the process. By reference to the definition of g_0 (see page 6), it is evident that $u^2/2g_0$ is the kinetic energy per unit mass.

Equation 1-16 is the common form of the general energy equation used in problems involving fluids, provided no significant changes in energy due to gravitational, electrical, magnetic, or surface-tension phenomena are involved. It is basic to the thermodynamic analysis of engine cycles discussed in the chapters which follow.

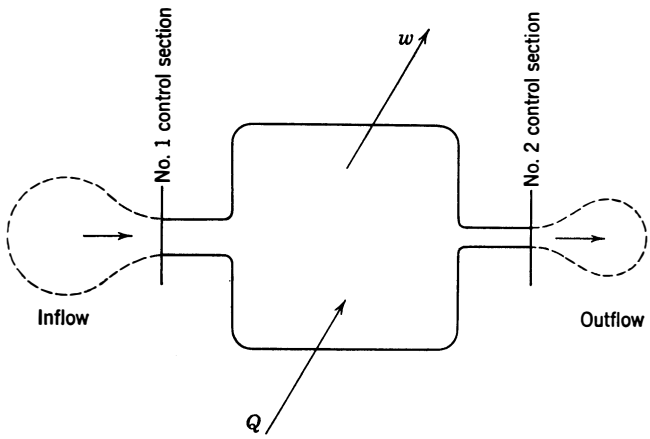

Fig 1-1. Steady-flow system (dashed lines indicate flexible boundaries).

Steady-Flow Process. An important application of the general energy equation to internal-combustion engines involves the type of process in which fluid flows into a set of stationary boundaries at the same mass rate at which it leaves them (Fig 1-1). If the velocities of inflow and outflow are constant with respect to time, such a process is called a *steady-flow process.* Let it be assumed that the velocities and internal energies are constant across the entrance and exit control cross sections, which are denoted by the subscripts 1 and 2, respectively. Let us consider a system whose boundaries include a flexible boundary around the unit mass of material about to flow through No. 1 control section. (See Fig 1-1.) As the entering unit mass flows in, a unit mass of material, surrounded by a flexible boundary, flows out of control section No. 2. Heat is supplied and released across the boundaries, and work crosses the boundaries through a shaft, both at a steady rate. Let the external (constant) pressures at the entrance and exit of the system be p_1 and p_2, respectively. For the process described, the work, w_t,

www.TechnicalBooksPDF.com

done by the system on its surroundings may be expressed as

$$w_t = w + p_2v_2 - p_1v_1 \tag{1-17}$$

in which v is volume per unit mass (specific volume). The quantity $(p_2v_2 - p_1v_1)$ is the work involved in forcing a unit mass of fluid out of and into the system, and w is the *shaft work* per unit mass. Since enthalpy per unit mass, H, is defined as $E + (pv/J)$, eq 1-15 can be written

$$[H_2 + u_2^2/2g_0J] - [H_1 + u_1^2/2g_0J] = Q - (w/J) \tag{1-18}$$

which is the basic equation for steady-flow systems conforming to the stated assumptions.

Stagnation Enthalpy. If we define stagnation enthalpy as

$$H_0 = H + u^2/2g_0J \tag{1-19}$$

the application of this definition to eq 1-18 gives

$$H_{02} - H_{01} = Q - (w/J) \tag{1-20}$$

Consider the case of flow through a heat-insulated passage. Because of the insulation the flow is adiabatic ($Q = 0$) and, since there are no moving parts except the gases, no shaft work is done; that is, $w = 0$. For this system we may write

$$H_{02} - H_{01} = 0 \qquad \text{(when } Q \text{ and } w = 0) \tag{1-21}$$

This expression shows that the stagnation enthalpy is the same at any cross section of a flow passage where the flow is uniform and when no heat or work crosses the boundaries of the passage. If the passage in which flow is taking place is so large at section 2 that u_2 is negligible, $H_{02} = H_2 = H_{01}$. From these relations it is seen that the stagnation enthalpy in any stream of gas in steady uniform motion is the enthalpy which would result from bringing the stream to rest adiabatically and without shaft work. Expression 1-21 also indicates that in the absence of heat transfer and shaft work the stagnation enthalpy of a gas stream in steady flow is constant. In arriving at this conclusion no assumption as to reversibility of the slowing-down process was necessary. *It is therefore evident that with no heat transfer and no shaft work stagnation enthalpy will be constant regardless of friction between the gas and the passage walls.*

www.TechnicalBooksPDF.com

APPLICATION OF STEADY-FLOW EQUATIONS TO ENGINES

Let the system consist of an internal-combustion engine with uniform steady flow at section 1, where the fuel-air mixture enters, and at section 2, where the exhaust gases escape. In this case H_{02} is the stagnation enthalpy per unit mass of exhaust gas and H_{01} is the stagnation enthalpy per unit mass of fuel-air mixture. Q is the heat per unit mass of working fluid escaping from the engine cooling system and from direct radiation and conduction from all parts between sections 1 and 2. Q will be a *negative* number, since a positive value for Q has been taken as heat flowing *into* the system. w is the shaft work done by the engine per unit mass of fuel-air mixture and is a positive quantity unless the engine is being driven by an outside source of power, as in friction tests (see Chapter 9).

By measuring three of the four quantities in eq 1-20, the other can be computed. For example, if H_{01}, H_{02}, and w are measured, the total heat loss is obtained. By measuring H_{01}, Q, and w, the enthalpy of the exhaust gases can be obtained.

One difficulty in applying eq 1-20 to reciprocating engines is the fact that the velocity at the inlet and the velocity and temperature at the exhaust may be far from steady and uniform. In engines with many cylinders connected to one inlet manifold and one exhaust manifold the fluctuations at the inlet and exhaust openings may not be serious enough to prevent reasonably accurate velocity, temperature, and pressure measurements. When serious fluctuations in velocity do exist, as in single-cylinder engines, the difficulty can be overcome by installing *surge tanks*, that is, tanks of large volume compared to the cylinder volume, as shown in Fig 1-2. With this arrangement, if the tanks are sufficiently large (at least 50 $\times$ cylinder volume), the conditions at sections 1 and 2 will be steady enough for reliable measurement.

With the arrangement shown in Fig 1-2, the inlet pressure and temperature, p_i and T_i, are measured in the inlet tank where velocities are negligibly small. Exhaust pressure is measured in the exhaust tank. However, temperature measured in the exhaust tank will not ordinarily be a reliable measure of the mean engine exhaust temperature for these reasons:

1. There is usually considerable heat loss from the tank because of the large difference in temperature between exhaust gases and atmosphere.
2. The gases may not be thoroughly mixed at the point where the thermometer is located.

www.TechnicalBooksPDF.com

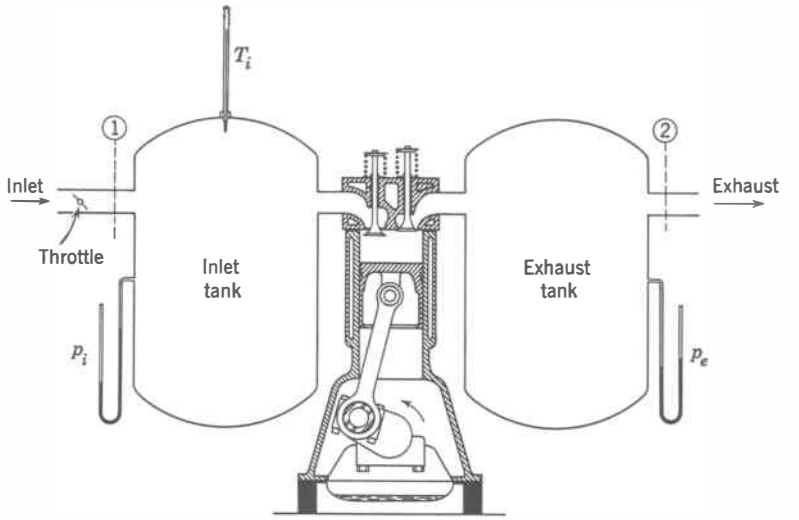

Fig 1-2. Single-cylinder engine equipped with large surge tanks and short inlet and exhaust pipes.

Methods of measuring exhaust temperature are discussed in ref 1.5. One method consists of measuring stagnation temperature at section 2, where flow is steady and the gases presumably are well mixed. In this case the exhaust tank must be provided with means, such as a water-jacket system, for measuring heat loss between exhaust port and section 2. If the heat given up by the exhaust tank is measured, the mean enthalpy of the gases leaving the exhaust port can be computed from eq 1-20, which can be written

$$H_{02} - H_{0e} = Q_e \tag{1-22}$$

In this equation H_{02} is determined from measurements of pressure in the exhaust tank and stagnation temperature at section 2. Q_e is the heat lost per unit mass from the exhaust tank. H_{0e}, then, is the mean stagnation enthalpy of the gases leaving the exhaust port. If the relation between enthalpy and temperature for these gases is known, the corresponding mean temperature may be determined.

FLOW OF FLUIDS THROUGH FIXED PASSAGES

Ideal flow of fluids through fixed passages, such as orifice meters and venturis, is usually based on these assumptions:

1. Q and w are zero (eq 1-20).
2. Fluid pressure, temperature, and velocity are uniform across the sections where measurements are made.

www.TechnicalBooksPDF.com

3. Changes in fluid pressures and temperatures are reversible and adiabatic.
4. Gases are perfect gases.
5. Liquids have constant density.

The use of these assumptions results in the equations for ideal velocity and ideal mass flow given in Appendix 2. These equations are referred to frequently in the chapters which follow.

The actual flow of fluids in real situations is generally handled by the use of a flow coefficient C, such that

$$\dot{M} = C\dot{M}_i \tag{1-23}$$

where $\dot{M}_i$ is the ideal mass flow computed from the appropriate equation in Appendix 2. It is found that under many practical circumstances C remains nearly constant for a given shape of flow passage. Thus, if the value of C is known for a given shape of flow passage, the actual flow can be predicted from eq 1-23. Further discussion of this method of approach to flow problems is given in subsequent chapters.

FURTHER READING

Section 1.0 of the bibliography lists references covering the history of the internal-combustion engine.

Section 1.1 refers to general books on internal-combustion engine theory and practice.

Reference 1.2 covers, briefly, engine balance and vibration. This subject is covered more fully in Vol 2 of this series.

ILLUSTRATIVE EXAMPLES

The following examples show how the material in this chapter can be used in computations involving power machinery.

Example 1-1. The following measurements have been made on the engine shown in Fig 1-2: $H_{01} = 1300$ Btu/lbm, $H_{02} = 500$ Btu/lbm. The heat given up to the exhaust-tank jackets is 14,000 Btu/hr. The flow of fuel-air mixture through section 1 is 280 lbm/hr. The engine delivers 40 hp.

Required: Heat lost by the engine and the ratio of heat lost to w/J.

Solution: From eq 1-18,

$$280(500 - 1300) = (-\dot{Q} - 14{,}000) - 40 \times 2545$$

$$\dot{Q} = 108{,}000 \text{ Btu/hr}$$

$$J\dot{Q}/w = 108{,}000/40 \times 2545 = 1.06$$

Example 1-2. Let Fig 1-2 represent an air compressor rather than an engine. The following measurements are made (pressures are in psia, temperatures in

www.TechnicalBooksPDF.com

°R): $p_i = 14.6$, $T_i = 520$, $p_e = 100$, $\dot{Q} = -3000$ Btu/hr (lost from compressor), $\dot{M} = 1000$ lbm air/hr. No heat is lost from the discharge tank. Power required is 45 hp.

Required: The mean temperature in the discharge tank, T_e.

Solution: Assuming air to be a perfect gas with specific heat at constant pressure, 0.24 Btu/lbm/°R (from eq 1-22),

$$H_e - H_i = 0.24(T_e - 520) \text{ Btu/lbm}$$

$$\dot{Q} = -3000/1000 = -3 \text{ Btu/lbm}$$

$$\frac{w}{J} = \frac{45 \times 33{,}000 \times 60}{778 \times 1000} = -114 \text{ Btu/lbm}$$

From eq 1-18,

$$0.24(T_e - 520) = (-3) - (-114) = 111$$

$$T_e = 982°\text{R}$$

In the following examples assume liquid petroleum fuel of 19,000 Btu/lbm whose chemically correct (stoichiometric) ratio, F_c, = 0.067 lbm/lbm air.

Example 1-3. Compute the air flow, fuel flow, specific fuel consumption, and specific air consumption for the following power plants:

(*a*) 200,000 hp marine steam-turbine plant, oil burning, $\eta = 0.20$, $F = 0.8F_c$.
(*b*) A 4360 in^3, 4-cycle airplane engine at 2500 bhp, 2000 rpm, $\eta = 0.30$, $F = F_c$.
(*c*) An automobile engine, 8 cylinders, $3\frac{3}{4}$-in bore $\times$ $3\frac{1}{2}$-in stroke, 212 hp at 3600 rpm, $\eta = 0.25$, $F = 1.2F_c$.
(*d*) Automobile gas turbine, 200 hp, $\eta = 0.18$, $F = 0.25F_c$.

Solution:

(*a*) From eq 1-4, $\dot{M}_f = \dfrac{2 \times 10^5 \times 42.4}{(19{,}000)\ (0.20)} = 2230$ lb/min

From eq 1-5, $\dot{M}_a = \dfrac{2230}{(0.8)\ (0.067)} = 41{,}600$ lb/min

From eq 1-6, sfc $= \dfrac{2230 \times 60}{200{,}000} = 0.669$ lb/hp-hr

From eq 1-7, sac $= \dfrac{41{,}600 \times 60}{200{,}000} = 12.48$ lb/hp-hr

(*b*) $\dot{M}_f = \dfrac{2500 \times 42.4}{19{,}000 \times 0.30} = 18.6$ lb/min

$\dot{M}_a = \dfrac{18.6}{1 \times 0.067} = 282$ lb/min

sfc $= \dfrac{18.6 \times 60}{2500} = 0.447$ lb/hp-hr

sac $= \dfrac{282 \times 60}{2500} = 6.77$ lb/hp-hr

www.TechnicalBooksPDF.com

(*c*) $\dot{M}_f = \dfrac{212 \times 42.4}{19{,}000 \times 0.25} = 1.89$ lbm/min

$$\dot{M}_a = \frac{1.89}{1.2 \times 0.067} = 23.5 \text{ lbm/min}$$

$$\text{sfc} = \frac{1.89 \times 60}{212} = 0.535 \text{ lbm/hp-hr}$$

$$\text{sac} = \frac{23.5 \times 60}{212} = 6.65 \text{ lbm/hp-hr}$$

(*d*) $\dot{M}_f = \dfrac{200 \times 42.4}{19{,}000 \times 0.18} = 2.48$ lbm/min

$$\dot{M}_a = \frac{2.48}{0.25 \times 0.067} = 148 \text{ lbm/min}$$

$$\text{sfc} = \frac{2.48 \times 60}{200} = 0.744 \text{ lbm/hp-hr}$$

$$\text{sac} = \frac{148 \times 60}{200} = 44.4 \text{ lbm/hp-hr}$$

Example 1-4. Estimate maximum output of a two-stroke model airplane engine, 1 cylinder, $\frac{3}{4}$-in bore $\times$ $\frac{3}{4}$-in stroke, 10,000 rpm, $\eta = 0.10$. Air is supplied by the crankcase acting as a supply pump. The crankcase operates with a volumetric efficiency of 0.6. One quarter of the fuel-air mixture supplied escapes through the exhaust ports during scavenging. The fuel-air ratio is $1.2F_c$. Assume atmospheric density 0.0765 lbm/ft^3.

Solution:

$$\dot{M}_a = \frac{\pi(0.75)^2}{4 \times 144} \times \frac{0.75}{12} \times 10{,}000 \times 0.0765 \times 0.6 \times 0.75 = 0.064 \text{ lbm/min}$$

$$\dot{M}_f = 0.064 \times 1.2 \times 0.067 = 0.00515 \text{ lbm/min (from eq 1-5)}$$

$$P = \frac{0.00515 \times 19{,}000 \times 0.10}{42.4} = 0.231 \text{ hp}$$

Example 1-5. Plot curve of air flow required vs efficiency for developing 100 hp with fuel having a lower heating value of 19,000 Btu/lb and fuel-air ratios of 0.6, 0.8, 1.0, and 1.2 of the stoichiometric ratio, F_c, which is 0.067. Let $F_R = F/F_c$.

Solution: Use eq 1-9 as follows:

$$100 = \frac{778}{33{,}000} M_a(0.067)F_R(19{,}000)\eta$$

$$\dot{M}_a = 3.33/F_R\eta \text{ lbm/min}$$

www.TechnicalBooksPDF.com

Plot $\dot{M}_a$ vs η for given values of F_R:

Air Flow for 100 hp, lbm/min

	F_R			
η	0.6	0.8	1.0	1.2
0.20	27.7	20.8	16.6	13.9
0.30	18.5	13.9	11.1	9.25
0.40	13.9	10.4	8.33	6.95
0.50	11.1	8.33	6.65	5.56

www.TechnicalBooksPDF.com

Air Cycles — two

IDEAL CYCLES

The actual thermodynamic and chemical processes in internal-combustion engines are too complex for complete theoretical analysis. Under these circumstances it is useful to imagine a process which resembles the real process in question but is simple enough to lend itself to easy quantitative treatment. In heat engines the process through which a given mass of fluid passes is generally called a *cycle*. For present purposes, therefore, the imaginary process is called an *ideal cycle*, and an engine which might use such a cycle, an *ideal engine*. The Carnot cycle and the Carnot engine, both familiar in thermodynamics, are good examples of this procedure.

Suppose that the efficiency of an ideal engine is η_0 and the indicated efficiency of the corresponding real engine is η. From eq 1-5, we can write

$$P = (J\dot{M}_a F Q_c \eta_0)\eta/\eta_0 \tag{2-1}$$

as an expression for the power of a real engine. The quantity in parentheses is the power of the corresponding ideal engine. It is evident that the power and efficiency of the real engine can be predicted if we can predict the air flow, the fuel flow, the value of η_0, and the ratio η/η_0. Even though the ratio η/η_0 may be far from unity, if it remains nearly constant over the useful range the practical value of the idealized cycle is at once apparent.

www.TechnicalBooksPDF.com

THE AIR CYCLE

In selecting an idealized process one is always faced with the fact that the simpler the assumptions, the easier the analysis, but the farther the result from reality. In internal-combustion engines an idealized process called the *air cycle* has been widely used. This cycle has the advantage of being based on a few simple assumptions and of lending itself to rapid and easy mathematical handling without recourse to thermodynamic charts or tables. On the other hand, there is always danger of losing sight of its limitations and of trying to employ it beyond its real usefulness.

The degree to which the air cycle is of value in predicting trends of real cycles will appear as this chapter develops.

Definitions

An *air cycle* is a cyclic process in which the medium is a perfect gas having under all circumstances the specific heat and molecular weight of air at room temperature. Therefore, for all such cycles molecular weight is 29, C_p is 0.24 Btu/lbm °F, and C_v is 0.1715 Btu/lbm °F.

A *cyclic process* is one in which the medium is returned to the temperature, pressure, and state which obtained at the beginning of the process.

A *perfect gas* (see Appendix 2) is a gas which has a constant specific heat and which follows the equation of state

$$pV = \frac{M}{m} RT \tag{2-2}$$

where p = unit pressure
V = volume of gas
M = mass of gas
m = molecular weight of gas
R = universal gas constant
T = absolute temperature

Any consistent set of units may be used; for example, if pressure is in pounds per square foot, volume is in cubic feet, mass is in pounds, molecular weight is dimensionless, temperature is in degrees Rankine (°R), that is, degrees Fahrenheit + 460, then R in this system is 1545 ft lbf/°F, for m lbm of gas. R/m for air using these units has the numerical value 53.3.

www.TechnicalBooksPDF.com

The internal energy of a unit mass of perfect gas measured above a base temperature, that is, the temperature at which internal energy is taken as zero, may be written

$$E = C_v(T - T_b) \tag{2-3}$$

and the enthalpy per unit mass,

$$\begin{aligned} H &= E + pV/J \\ &= E + RT/mJ \end{aligned} \tag{2-4}$$

where T = actual temperature
T_b = base temperature
p = pressure
V = volume

From these equations it is evident that internal energy and enthalpy depend on temperature only.

Other useful relations for perfect gases are given in Appendix 2.

Equivalent Air Cycles

A particular air cycle is usually taken to represent an approximation of some real cycle which the user has in mind. Generally speaking, the air cycle representing a given real cycle is called the *equivalent air cycle*. The equivalent cycle has, in general, the following characteristics in common with the real cycle which it approximates:

1. A similar sequence of processes.
2. The same ratio of maximum to minimum volume for reciprocating engines or of maximum to minimum pressure for gas turbines.
3. The same pressure and temperature at a chosen reference point.
4. An appropriate value of heat added per unit mass of air.

Constant-Volume Air Cycle. For reciprocating engines using spark ignition the equivalent air cycle is usually taken as the *constant-volume* air cycle whose pressure-volume diagram is shown in Fig 2-1. At the start of the cycle the cylinder contains a mass, M, of air at the pressure and volume indicated by point 1. The piston is then moved inward by an external force, and the gas is compressed reversibly and adiabatically to point 2. Next, heat is added at constant volume to increase the pressure to 3. Reversible adiabatic expansion takes place to the original volume at point 4, and the medium is then cooled at constant volume to its original pressure.

www.TechnicalBooksPDF.com

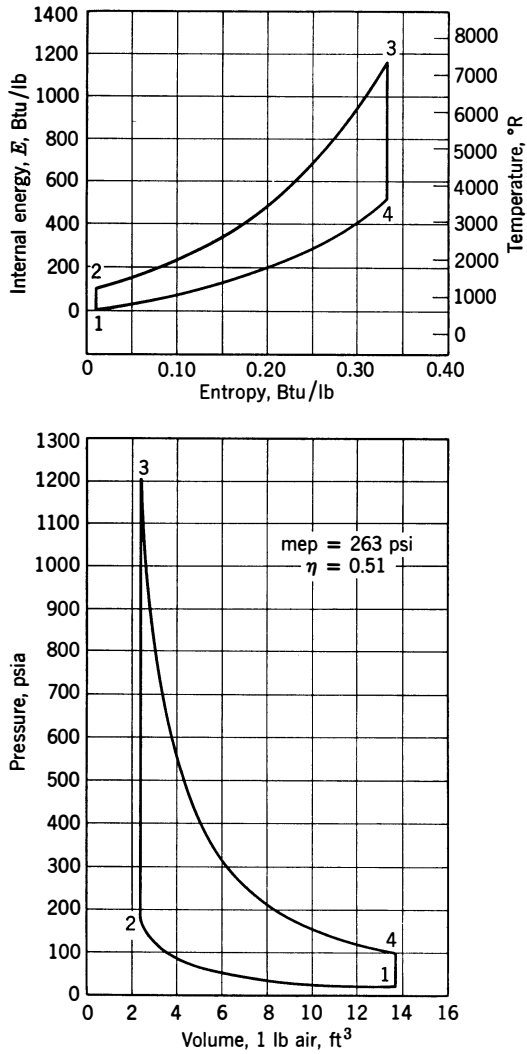

Fig 2-1. Constant-volume air cycle: $r = 6$; $p_1 = 14.7$ psia; $T_1 = 540°\text{R}$; $Q' = 1280$ $(r - 1)/r$ Btu/lbm; $Q'/C_vT_1 = 13.8(r - 1)/r$; E = zero at 520°R.

Figure 2-1 also shows the same cycle plotted on coordinates of internal energy vs entropy. The only difference between the two plots is the choice of ordinate and abscissa scales. On the p-V plot lines of constant entropy and constant internal energy are curved, and the same is true of constant pressure and constant volume lines on the E-S plot. Which

www.TechnicalBooksPDF.com

plot is used is a matter of convenience, but for work with reciprocating engines the p-V plot is usually the more convenient.

Since the process just described is cyclic, eq 1-2 applies, and we may write, for the process 1–2–3–4–1,

$$Q = (w/J) \tag{2-5}$$

In this cycle it is assumed that velocities are zero, and for any part of the process, therefore, eq 1-16 can be written

$$\Delta E = Q - w/J \tag{2-6}$$

where ΔE is the internal energy at the end of the process, minus the internal energy at the beginning of the process, and Q is the algebraic sum of the quantities of heat which cross the boundary of the system during the process. Heat which flows into the system is taken as positive, whereas heat flowing out is considered a negative quantity. w is the algebraic sum of the work done *by* the system on the outside surroundings and the work done *on* the system during the process. Work done *on* the system is considered a negative quantity. If we take as the *system* a unit mass of air, the cycle just described can be tabulated as shown in Table 2-1.

Table 2-1

Process (See Fig 2-1)	For Unit Mass of Air			
	Q	w/J	ΔE	ΔS
1–2	0	$-(E_2 - E_1)$	$E_2 - E_1$	0
2–3	$E_3 - E_2$	0	$E_3 - E_2$	$S_3 - S_2$
3–4	0	$-(E_4 - E_3)$	$E_4 - E_3$	0
4–1	$E_1 - E_4$	0	$E_1 - E_4$	$S_1 - S_4$
Complete cycle (by summation)	$E_1-E_2+E_3-E_4$	$E_1-E_2+E_3-E_4$	0	0

Since $\Delta E = MC_v\,\Delta T$, where ΔT is the final temperature minus the initial temperature, it follows that the work of the cycle can be expressed as

$$w/M = JC_v(T_1 - T_2 + T_3 - T_4) \tag{2-7}$$

For air cycles the efficiency η is defined as the ratio of the work of the cycle to the heat flowing *into* the system during the process which cor-

www.TechnicalBooksPDF.com

responds to combustion in the actual cycle. In this case process 2–3 corresponds to combustion and

$$Q_{2-3} = E_3 - E_2 = MC_v(T_3 - T_2)$$

$$\eta = JMC_v(T_1 - T_2 + T_3 - T_4)/JMC_v(T_3 - T_2)$$

Since $T_1/T_2 = T_4/T_3$,

$$\eta = \frac{T_2 - T_1}{T_2} = \frac{T_3 - T_4}{T_3} \tag{2-8}$$

The foregoing expression shows that the efficiency of this cycle is equal to the efficiency of a Carnot cycle operating between T_2 and T_1 or between T_3 and T_4.

The *compression ratio* r is defined by the relation

$$r = V_1/V_2 \tag{2-9}$$

From Appendix 2, for a reversible adiabatic process in a perfect gas, pV^k is constant, and it follows from eq 2-8 that

$$\eta = 1 - \left(\frac{1}{r}\right)^{k-1} \tag{2-10}$$

Since k is constant, this expression shows that the efficiency of this cycle is a function of compression ratio only (and is therefore independent of the amount of heat added, of the initial pressure, and of the initial volume or temperature).

Mean Effective Pressure. Although the efficiency of the cycle depends only on r, the pressures, temperatures, and the work of the cycle depend on the values assumed for p_1, T_1, and Q_{2-3} as well as on the compression ratio. A quantity of especial interest in connection with reciprocating engines is the work done on the piston divided by the *displacement* volume $V_1 - V_2$. This quantity has the dimensions of pressure and is equal to that constant pressure which, if exerted on the piston for the whole outward stroke, would yield work equal to the work of the cycle. It is called the *mean effective pressure*, abbreviated mep.

From the foregoing definitions

$$\text{mep} = \frac{w}{V_1 - V_2} = \frac{JQ_{2-3}\eta}{V_1 - V_2} \tag{2-11}$$

www.TechnicalBooksPDF.com

From eqs 2-2 and 2-9 eq 2-11 becomes

$$\text{mep} = \left(\frac{JQ_{2-3} \dfrac{p_1 m}{MRT_1}}{1 - \dfrac{1}{r}} \right) \eta \tag{2-12}$$

From this point on, Q_{2-3}/M, the heat added between points 2 and 3 *per unit mass* of gas, is designated by the symbol Q'.

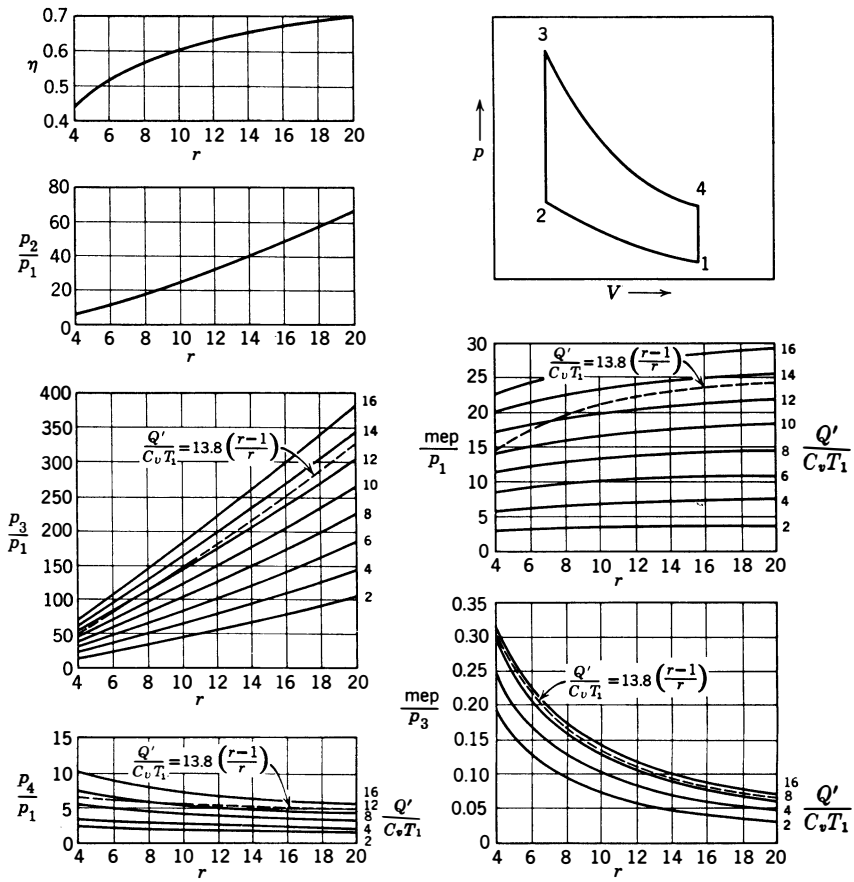

Fig 2-2. Characteristics of constant-volume air cycles: $r = V_1/V_2$; p = absolute pressure; T = absolute temperature; C_v = specific heat at constant volume; Q' = heat added between points 2 and 3; mep = mean effective pressure.

www.TechnicalBooksPDF.com

Dimensionless Representation of the Air Cycle

By substituting eqs 2-2 and 2-10 in eq 2-11 and rearranging,

$$\frac{\text{mep}}{p_1} = \frac{Q'}{T_1 C_v}\left[1 - \left(\frac{1}{r}\right)^{k-1}\right] \Big/ (k-1)\left(1 - \frac{1}{r}\right) \qquad (2\text{-}13)$$

which shows that for constant-volume cycles using a perfect gas the dimensionless ratio mep/p_1 is dependent only on the values chosen for Q', T_1, C_v, k, and r. With the values of k and C_v fixed, it is easy to show by a similar method that not only mep/p_1 but also all the ratios of corresponding pressures and temperatures, such as p_2/p_1, p_3/p_1, T_2/T_1, are determined when values are assigned to the two dimensionless quantities Q'/T_1C_v and r. We have already seen that one of these quantities, r, determines the dimensionless ratio called efficiency. Thus, by using the ratios mep/p_1 and Q'/T_1C_v in place of the separate variables from which they are formed, it is possible to plot the characteristics of a wide range of constant-volume air cycles in a relatively small space, as illustrated by Fig 2-2.

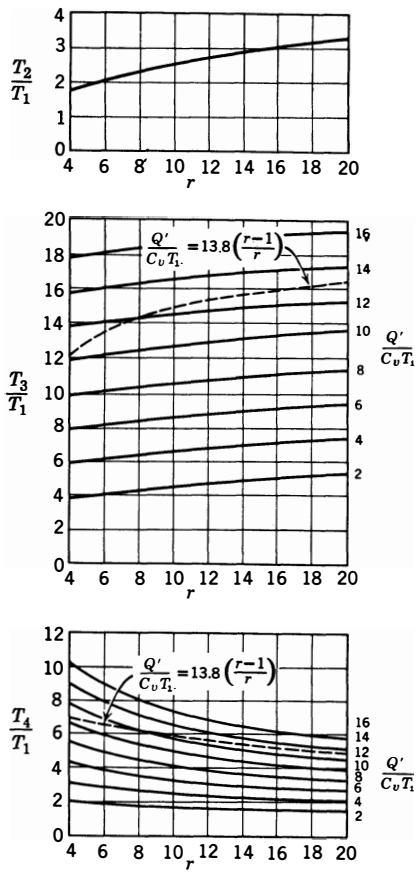

Fig 2-2. (*Continued*)

Examples of the use of the curves of Fig 2-2 are given in Illustrative Examples at the end of this chapter.

Choice of Q'. To be useful as a basis of prediction of the behavior of real cycles, the quantity Q' must be chosen to correspond as closely as possible with the real cycle in question.

A useful method of evaluating Q' is to take it as equal to the heat of

www.TechnicalBooksPDF.com

combustion (see Chapter 3) of the fuel in the corresponding real cycle, the *charge* being defined as the total mass of material in the cylinder when combustion takes place. Thus we may take

$$Q' = FQ_c \frac{M_a}{M_c} \tag{2-14}$$

where F is the ratio of fuel supplied to air supplied for the real engine, Q_c is the heat of combustion of the fuel per unit mass, and M_a and M_c are, respectively, the mass of fresh air supplied to the cylinder for one cycle and the total mass in the cylinder at the time of combustion.

At the chemically correct (stoichiometric) fuel-air ratio with a petroleum fuel the value of FQ_c is nearly 1280 Btu/lb air. It is often assumed that in an ideal four-stroke engine the fresh air taken in is enough to fill the piston displacement ($V_1 - V_2$) at temperature T_1, and the residual gases, that is, the gases left from the previous cycle, fill the clearance space (V_2) and have the same density. In this case $M_a/M_c = (r-1)/r$. Therefore the special value $Q' = 1280(r-1)/r$ Btu/lb air is plotted in Fig 2-2. More realistic values for the ratio M_a/M_c are discussed in subsequent chapters. (See especially Chapters 4 and 5.)

Limited-Pressure Cycle. An important characteristic of real cycles is the ratio of mep to the maximum pressure, since mep measures the useful pressure on the piston and the maximum pressure represents the pressure which chiefly affects the strength required of the engine structure. In the constant-volume cycle Fig 2-2 shows that the ratio (mep/p_3) falls rapidly as compression ratio increases, which means that for a given mep the maximum pressure rises rapidly as compression ratio goes up. For example, for 100 mep and $Q'/C_vT_1 = 12$ the maximum pressure at $r = 5$ is $100/0.25 = 400$, whereas at $r = 10$ it is $100/0.135 = 742$ psia. Real cycles follow this same trend, and it becomes a practical necessity to limit the maximum pressure when high compression ratios are used, as in Diesel engines.

Originally, Diesel engines were intended to operate on a *constant-pressure* cycle, that is, on a cycle in which all heat was added at the pressure p_2. However, this method of operation is difficult to achieve and gives low efficiencies. An air cycle constructed to correspond to the cycle used in modern Diesel engines is called a *limited-pressure* cycle, or sometimes a *mixed cycle*, since heat is added both at constant volume and at constant pressure.

The limited-pressure cycle is similar to the constant-volume cycle, except that the addition of heat at constant volume is carried only far

www.TechnicalBooksPDF.com

enough to reach a certain predetermined pressure limit. If more heat is then added, it is added at constant pressure. Figure 2-3 shows such a cycle.

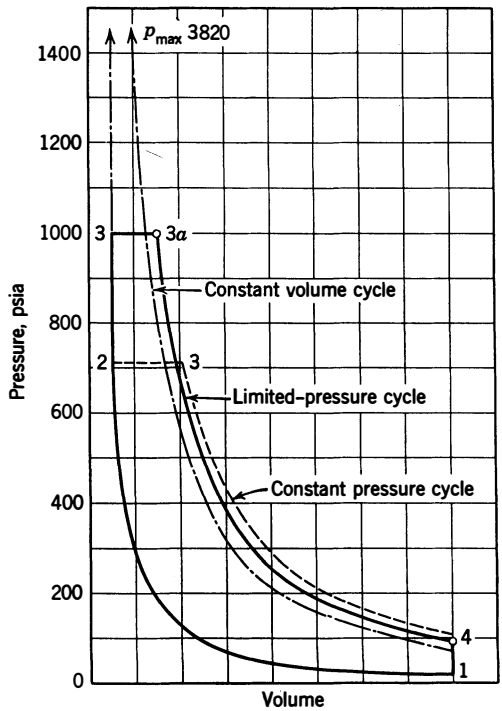

Fig 2-3. Limited pressure air cycles compared with a constant-volume cycle:

p_{max} for limited-pressure cycle $= 68p_1 = 1000$ psia

$r = 16$

$p_1 = 14.7$ psia

$T_1 = 540°\text{R}$

$$Q' = 1280\left(\frac{r-1}{r}\right) \text{ Btu/lb air}$$

Cycle	p_{max}, psia	mep, psi	$\frac{\text{mep}}{p_3}$	η
Constant volume	3820	338	0.0885	0.675
Limited pressure	1000	295	0.295	0.58
Constant pressure	715	265	0.371	0.53

www.TechnicalBooksPDF.com

Based on eqs 1-2, 1-16, and 1-18, the following tabulation may be constructed for this cycle:

Table 2-2

Process (See Fig 2-3)	For Unit Mass of Air		
	Q	w/J	ΔE
1–2	0	$-(E_2 - E_1)$	$E_2 - E_1$
2–3	$E_3 - E_2$	0	$E_3 - E_2$
3–3a	$H_{3a} - H_3$	$\frac{p_3}{J}(V_{3a} - V_3)$	$E_{3a} - E_3$
3a–4	0	$-(E_4 - E_{3a})$	$E_4 - E_{3a}$
4–1	$E_1 - E_4$	0	$E_1 - E_4$
Complete cycle	$E_3 - E_2$ $+H_{3a} - H_3$ $+E_1 - E_4$	$E_3 - E_2$ $+H_{3a} - H_3$ $+E_1 - E_4$	0

The symbol H denotes the enthalpy per unit mass, $E + pV/J$. For a perfect gas at constant pressure, $\Delta H = C_p \Delta T$. The process 2–3–3a corresponds to the combustion process. From these considerations, and from Table 2-2, the following relations may be derived for the limited-pressure cycle:

$$Q' = \frac{Q_{2-3a}}{M} = C_v(T_3 - T_2) + C_p(T_{3a} - T_3)$$

$$\frac{w}{M} = J[Q' - C_v(T_4 - T_1)]$$

$$\eta = \frac{w}{JQ_{2-3a}} = 1 - \frac{T_4 - T_1}{(T_3 - T_2) + k(T_{3a} - T_3)}$$

From the perfect-gas relations given in Appendix 2 the above relation can be written

$$\eta = 1 - \left(\frac{1}{r}\right)^{k-1}\left[\frac{\alpha\beta^k - 1}{(\alpha - 1) + k\alpha(\beta - 1)}\right] \tag{2-15}$$

where $\alpha = p_3/p_2$
$\beta = V_{3a}/V_3$

The constant-volume and the constant-pressure cycles can be considered as special cases of the mixed cycle in which $\beta = 1$ and $\alpha = 1$, respectively. Combustion in an actual engine is never wholly at constant volume nor wholly at constant pressure, some engines tending toward one extreme and some toward the other.

www.TechnicalBooksPDF.com

Figure 2-3 shows a constant-volume and a constant-pressure cycle, compared with a limited-pressure cycle. In a series of air cycles with varying pressure limit, at a given compression ratio and the same Q', the constant-volume cycle has the highest efficiency and the constant-pressure cycle the lowest efficiency. This fact may be observed from expression 2-15. For the constant-volume cycle, the expression in brackets is equal to unity. For any other case, it is greater than one.

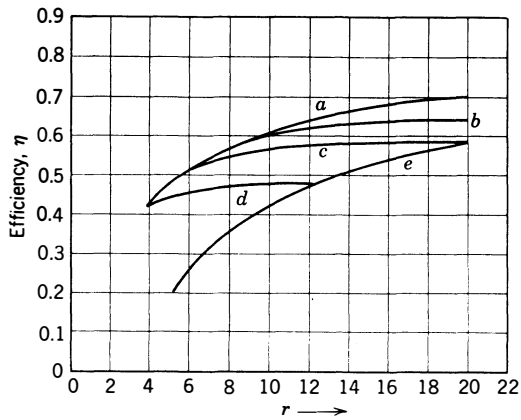

Fig 2-4. Efficiency of constant-volume, limited-pressure, and constant-pressure air cycles: a = constant-volume cycles; b = limited-pressure cycles; $p_3/p_1 = 100$; c = limited-pressure cycles; $p_3/p_1 = 68$; d = limited-pressure cycles; $p_3/p_1 = 34$; e = constant-pressure cycles. For all cycles $Q' = 1280\ (r - 1)/r$ Btu/lbm air.

Figure 2-4 gives a comparison of the efficiencies of the constant-volume, limited-pressure, and constant-pressure cycles at various compression ratios for the same value of $Q'(r - 1)/r$, for the same pressure and temperature at point 1, and for three values of p_3/p_1 for the limited-pressure cycle. It is interesting to note that efficiency is little affected by compression ratio above $r = 8$ for the limited-pressure cycle.

The ratio mep/p_3 for limited-pressure cycles with various pressure limits is given in Fig 2-5. It is evident that a considerable increase in this ratio, as compared to that of the constant-volume cycle, is achieved by the limited-pressure cycle at high compression ratios.

Gas-Turbine Air Cycle. Many cycles have been proposed for the gas turbine but nearly all are variations or combinations of what may be called the *elementary gas-turbine air cycle* shown in Fig 2-6. Air is compressed reversibly and adiabatically from 1 to 2; heat is added at constant pressure from 2 to 3; expansion from 3 to 4, the original pres-

www.TechnicalBooksPDF.com

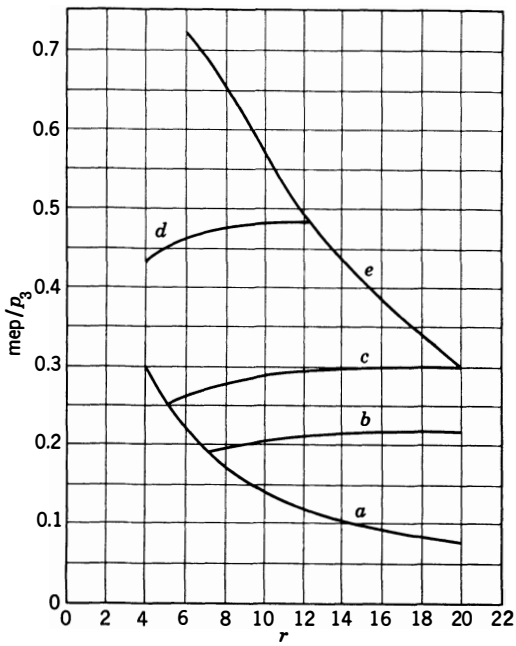

Fig 2-5. Ratio of mep to maximum pressure for the cycles of Fig 2-4: a = constant volume cycles; b = limited-pressure cycles; $p_3/p_1 = 100$; c = limited-pressure cycles; $p_3/p_1 = 68$; d = limited-pressure cycles; $p_3/p_1 = 34$; e = constant-pressure cycles.

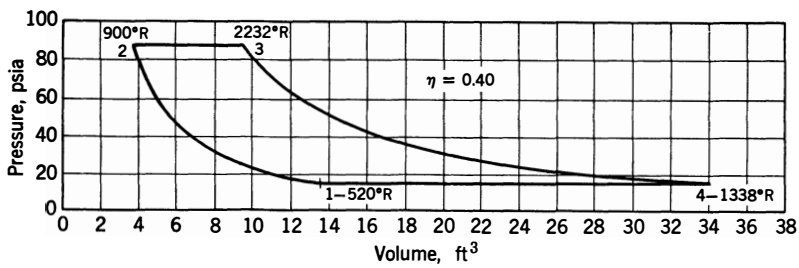

Fig 2-6. Gas-turbine air cycle for 1 lbm of air: $r_p = 6$; $p_1 = 14.7$ psia; $Q' = Q_{2-3} = 320$ Btu/lb air; $\eta = 0.40$; $w = 99{,}600$ ft lbf/lb air; $w/V_1 = 51$ psi; $T_1 = 520°R$; $T_2 = 900°R$; $T_3 = 2232°R$; $T_4 = 1338°R$.

sure, is reversible and adiabatic; and heat is rejected at constant pressure from 4 to 1. By a procedure similar to that given for the constant-volume cycle, it can be shown that eq 2-10 holds for this cycle also, provided r is defined as V_1/V_2. However, in the case of gas turbines it is

www.TechnicalBooksPDF.com

convenient to speak of the *pressure ratio*, p_2/p_1, rather than the compression ratio, V_1/V_2. It can easily be shown that for the gas-turbine cycle shown in Fig 2-6

$$\eta = 1 - \left(\frac{1}{r_p}\right)^{(k-1)/k} \tag{2-16}$$

where r_p is equal to p_2/p_1.

Gas turbines are generally run with maximum fuel-air ratios about $\frac{1}{4}$ of the chemically correct ratio. Hence the cycle illustrated in Fig 2-6 has been computed with $Q' = \frac{1280}{4} = 320$ Btu/lb air. There is nothing in a turbine corresponding to the clearance space in a cylinder. Consequently, M_a/M_c in eq 2-14 is taken as unity.

The gas turbine is a steady-flow machine, and its size is governed chiefly by the volume of air, at inlet conditions, which it is required to handle in a unit time. For a given power output the volume per unit time will be proportional to work per unit time divided by the product (mass of air per unit time by specific volume of inlet air). For the cycle of Fig 2-6, this ratio is w/V_1. This quantity has the dimensions of pressure, and it is that pressure which, multiplied by the inlet-air volume per unit time, would give the power delivered by the gas-turbine unit. Its significance is parallel to that of mean effective pressure in the case of reciprocating engines.

In the gas turbine a simple air cycle, such as the one described, shows the upper limit of possible efficiency. However, it does not predict trends in real gas-turbine efficiencies very well, even when compressor, turbine, and combustion-chamber efficiencies are assumed to be constant. On the other hand, trends in real gas-turbine performance can be predicted by a modified air-cycle analysis. (See ref 2.4.)

Comparison of Efficiencies of Air Cycles and Real Cycles

Figure 2-7 compares indicated efficiencies of a carbureted spark-ignition engine with the efficiencies of corresponding air cycles. This figure is typical for spark-ignition engines and shows that for this type of engine the air cycle gives a reasonably good prediction of the trends of efficiency vs compression ratio. On the other hand, the air cycle provides no indication of the observed effects of varying the fuel-air ratio in real cycles.

In Diesel engines compression ratios are held in the range 14–20, where the limited-pressure air cycle shows little change in efficiency (see Fig 2-4). Figure 2-8 compares Diesel-engine efficiencies with those of equivalent air cycles over the useful range of fuel-air ratios at $r = 16$.

www.TechnicalBooksPDF.com

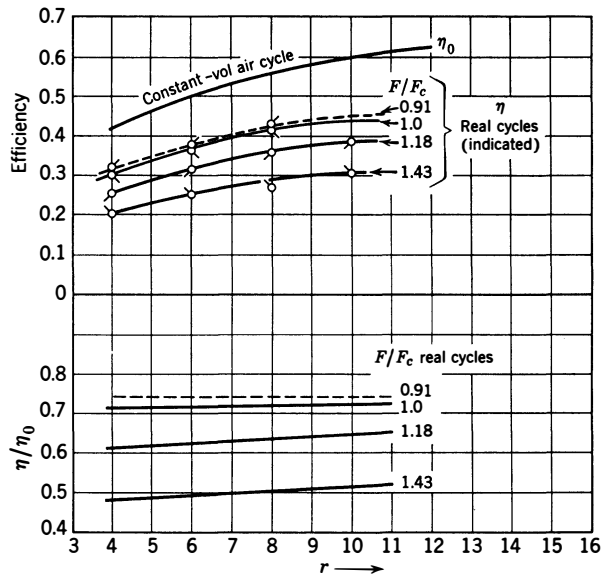

Fig 2-7. Comparison of efficiencies of real cycles and constant-volume air cycles: F/F_c = fuel-air ratio divided by stoichiometric fuel-air ratio of real cycles; η = efficiency of real cycle; η_0 = efficiency of air cycle. Real-cycle data, from tests made with CFR 3¼ x 4½ in single-cylinder engine in Sloan Automotive Laboratories. Fuel, butane; rpm, 1200; indicated work from indicator diagrams. (Van Duen and Bartas, ref 2.1)

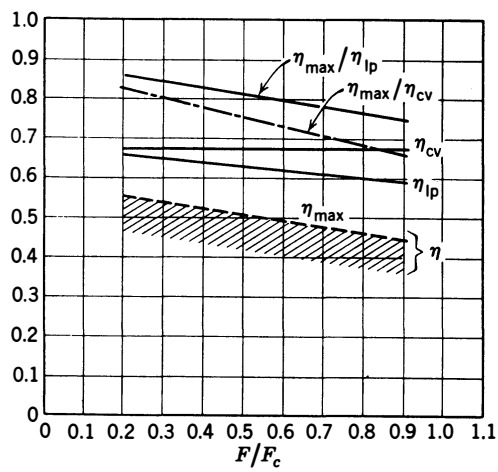

Fig 2-8. Comparison of Diesel-engine efficiencies with air-cycle efficiencies: η_{cv} = efficiency of constant-volume air cycle; $r = 16$; η_{lp} = efficiency of limited-pressure air cycle; $r = 16$; $p_3/p_1 = 68$; $Q' = 1280\ (F/F_c)\ [(r-1)/r]$; $T_1 = 600°R$; η = indicated efficiency of Diesel engines from Fig 5-27.

www.TechnicalBooksPDF.com

Figure 2-8 shows that the best efficiency of Diesel engines varies from 75 to 85% of the limited-pressure air-cycle efficiency, the ratio increasing as fuel-air ratio decreases. Here, again, a theoretical cycle which would more closely approximate the real cycle would be desirable.

ILLUSTRATIVE EXAMPLES

Example 2-1. Using Fig 2-2, find the efficiency, imep, pressures, and temperatures of a constant-volume air cycle with initial pressure 20 psia, initial temperature 600°R, compression ratio 10 and $Q' = 1280$ Btu/lb air.

Solution:

$$Q'/C_vT_1 = \frac{1280}{0.1715 \times 600} = 12.43$$

From Fig 2-2,

$$\eta = 0.603, \qquad \frac{\text{mep}}{p_1} = 21, \qquad \text{mep} = 21 \times 20 = 420$$

$$p_2 = 25 \times 20 = 500, \qquad p_3 = 150 \times 20 = 3000$$

$$p_4 = 6.5 \times 20 = 700, \qquad T_2 = 2.55 \times 600 = 1530$$

$$T_3 = 15 \times 600 = 9000, \qquad T_4 = 6 \times 600 = 3600$$

Pressures are in pounds per square inch and temperatures in degrees Rankine. More accurate values for the above quantities may be computed from the perfect-gas laws and the relations listed in Table 2-1.

Example 2-2. The sketch shows a thermodynamic process from initial state 1 to final state 2.

Assume $V_2 = 4V_1$, a perfect gas. Write an expression for p_2 and T_2 as a function of

$$p_1,\ V_1,\ Q,\ w,\ C_v,\ J,\ R, \text{ and } m$$

where Q = heat added per unit mass between 1 and 2
w = work done per unit mass between 1 and 2

Solution: For a unit mass,

$$E_2 - E_1 = Q - \frac{w}{J}$$

$$C_vT_2 - C_vT_1 = Q - \frac{w}{J}$$

$$T_1 = \frac{p_1V_1m}{R}$$

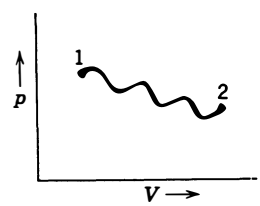

$$C_vT_2 - C_v\frac{p_1V_1m}{R} = Q - \frac{w}{J}$$

$$T_2 = \frac{Q - (w/J)}{C_v} + \frac{p_1V_1m}{R}$$

$$p_2 = \frac{RT_2}{mV_2} = \frac{RT_2}{4mV_1} = \frac{R}{4mV_1}\left[\frac{Q - (w/J)}{C_v}\right] + \frac{p_i}{4}$$

www.TechnicalBooksPDF.com

Example 2-3. The Lenoir air cycle consists of the following processes:
1–2 heating at constant volume
2–3 isentropic expansion
3–1 cooling at constant pressure
Required: Derive an expression for the efficiency of such a cycle in terms of k, T_1, T_2, and T_3, assuming a perfect gas with constant specific heat.
Solution:

$$\frac{\text{Work}}{J} = Q_{2\text{-}1} - Q_{3\text{-}1} = M[C_v(T_2 - T_1) - C_p(T_3 - T_1)]$$

$$\text{Heat supplied} = Q_{2\text{-}1} = MC_v(T_2 - T_1)$$

$$\eta = \frac{M[C_v(T_2 - T_1) - C_p(T_3 - T_1)]}{MC_v(T_2 - T_1)}$$

$$= 1 - k\left(\frac{T_3 - T_1}{T_2 - T_1}\right)$$

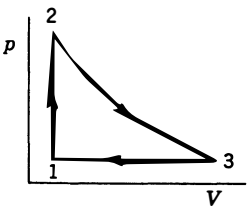

Example 2-4. Plot a curve of imep and efficiency for constant-volume air cycles in which p_1 varies from 1 to 6 atm, $r = 8$. $Q' = 1000$ Btu/lbm, $T_1 = 600°\text{R}$.
Solution: Figure 2-2 shows that efficiency is constant at $\eta = 0.57$, and at $Q'C_vT_1 = 1000/0.171 \times 600 = 9.75$, $\text{mep}/p_1 = 16$.

p_1	$\frac{\text{mep}}{p_1}$	mep, psi
14.7	16	235
14.7 × 2	16	470
14.7 × 3	16	705
14.7 × 4	16	930
14.7 × 5	16	1175
14.7 × 6	16	1410

Example 2-5. Compute the imep and efficiency of a limited-pressure air cycle for the following conditions:

$$p_1 = 14.7, \qquad T_1 = 600°\text{R}, \qquad p_{\max} = 1000 \text{ psia}$$

$$r = 16, \qquad Q' = 1000 \text{ Btu/lbm}$$

Solution: From Appendix 2, eq A-5,

$$p_2 = 14.7 \times (16)^{1.4} = 715 \text{ psia}, \quad \text{and} \quad \alpha = p_3/p_2 = 1.4$$

From eq A-6,

$$T_2 = 600(16)^{0.4} = 1820°\text{R}, \qquad T_3/T_2 = p_3/p_2,$$

$$T_3 = 1820 \times 1000/715 = 2540$$

www.TechnicalBooksPDF.com

From relations leading to eq 2-15,

$$Q' = 1000 = 0.171(2540 - 1820) + 0.24(T_{3a} - 2540)$$

$$T_{3a} = 6180°\text{R}, \qquad V_{3a}/V_3 = \tfrac{6180}{2540} = 2.43 = \beta$$

From eq 2-15,

$$\eta = 1 - \left(\frac{1}{16}\right)^{0.4}\left[\frac{1.4 \times 2.43^{1.4} - 1}{(0.4) + 1.4 \times 1.4(1.43)}\right] = 0.60$$

$$w/J = 1000 \times 0.60 = 600 \text{ Btu}$$

$$V_1 = \frac{MRT}{mp} = \frac{1544 \times 600}{29 \times 14.7 \times 144} = 15 \text{ ft}^3$$

and, from eq 2-11,

$$\text{mep} = \frac{778}{144} \times \frac{600}{15(1 - \frac{1}{16})} = 230 \text{ psi}$$

www.TechnicalBooksPDF.com

Thermodynamics of Actual Working Fluids —— three

Before studying internal-combustion engine cycles with their actual working fluids, it is necessary to consider the thermodynamic properties of these fluids. Since the process of combustion changes the properties of all working fluids to an appreciable extent, it is necessary to consider separately the thermodynamic properties before and after combustion.

THE WORKING FLUID BEFORE COMBUSTION

At the start of compression atmospheric air constitutes the major portion of the working fluid in all internal-combustion engines. In gas turbines atmospheric air alone is the medium throughout the compression process. In reciprocating engines, at the beginning of the inlet stroke, the cylinder always contains a certain fraction of *residual gas*, that is, gas left over from the previous cycle. If the fuel is supplied by a carburetor or its equivalent, the air also contains fuel which may be in gaseous or liquid form or partly in each of these phases. In Diesel and in some spark-ignition engines the fuel, either gaseous or liquid, is introduced during the compression process. Many different fuels and many different ratios of fuel to air may be used in each engine type. From these considerations it is evident that complete presentation of the

www.TechnicalBooksPDF.com

thermodynamic characteristics of all the media used in internal-combustion engines would be a formidable task.

Fortunately, the problem can be reduced to manageable proportions by confining our consideration to air and the more usual types of fuel and by using certain assumptions which simplify the procedure without introducing serious numerical errors.

COMPOSITION OF THE ATMOSPHERE

Dry atmospheric air consists of 23% oxygen and 76% nitrogen by weight, plus small amounts of CO_2 and "rare" gases, principal among

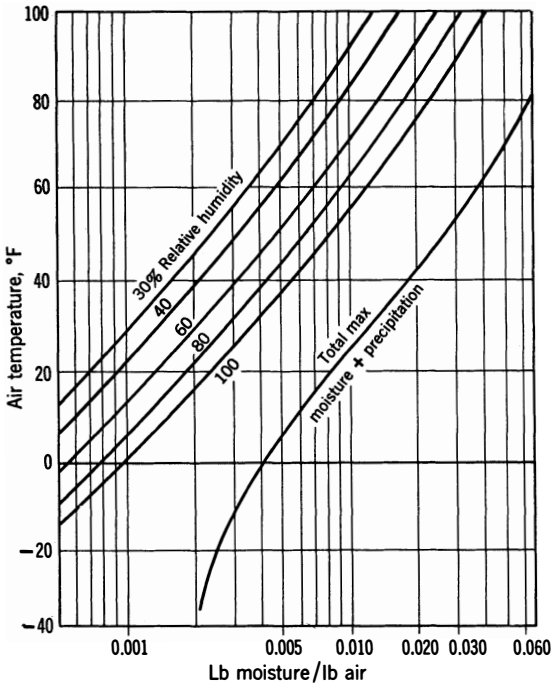

Fig 3-1. Moisture content of air. (Welsh, ref 12.189)

which is argon. By volume, these percentages are 21% O_2, 78% N_2 and, 1% other gases. For thermodynamic purposes the other gases are taken to be the equivalent of an equal amount of nitrogen. The molecular weight of dry air is 28.85, or 29 within the limits of accuracy of most computations.

www.TechnicalBooksPDF.com

In addition to the above ingredients, atmospheric air contains water vapor in percentages varying with temperature and the degree of *saturation*. The latter varies with time and place from near zero to near 100%. In addition to evaporated water, air may contain a considerable amount of water suspended in the form of droplets. Figure 3-1 shows limits of moisture and droplet content, and Fig 3-2 shows the influence of water vapor on thermodynamic properties.

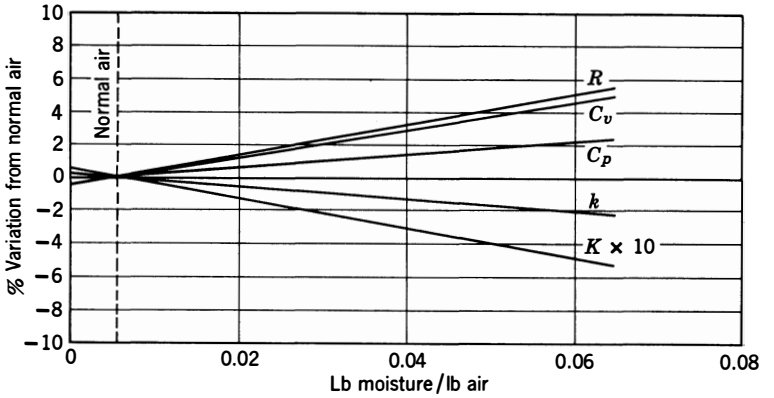

Fig 3-2. Effect of humidity on properties of air: R = universal R/m in eq 2-2; C_v = specific heat at constant volume; C_p = specific heat at constant pressure; k = ratio of specific heats; K = thermal conductivity.

THERMODYNAMIC PROPERTIES OF DRY AIR

The thermodynamic properties of air are presented in very complete and accurate form in the literature. (See refs 3.2—.)

Chart C-1 (folded inside back cover) gives thermodynamic properties of dry air up to 2500°R. (As is explained later, the auxiliary scales on either side of this chart can be used to obtain the thermodynamic characteristics of mixtures of gaseous octene and air, of their products of combustion, and of air containing water vapor.)

The mass base of C-1 is 1 lb mole of gas.*

The thermodynamic base assigns zero internal energy to dry air at 560°R (100°F).

* A *mole* is a mass proportional to molecular weight. If the pound is taken as the unit of mass, a mole of hydrogen is 2 lb, a mole of oxygen 32 lb, etc. Moles have the same volume at a given temperature and pressure. The *pound mole* is 408 cu ft at 100°F, 14.7 psia. 1 mole of air is 28.85 lbm, but 29 is used in the text and examples as being within the limits of accuracy required.

www.TechnicalBooksPDF.com

The symbols used in C-1 are defined as follows:

p = pressure, psia
T = temperature, °R
$V°$ = volume of 1 lb mole, ft^3 (see footnote *)
C_v = specific heat at constant volume, Btu/lbm °R
m = molecular weight
$E° = m\int_{560}^{T} C_v\, dT$ = internal energy above 560°R, Btu/lb mole
$H° = E° + pV°/J$ = enthalpy, Btu/lb mole
$S°$ = entropy, Btu/lb mole/°R

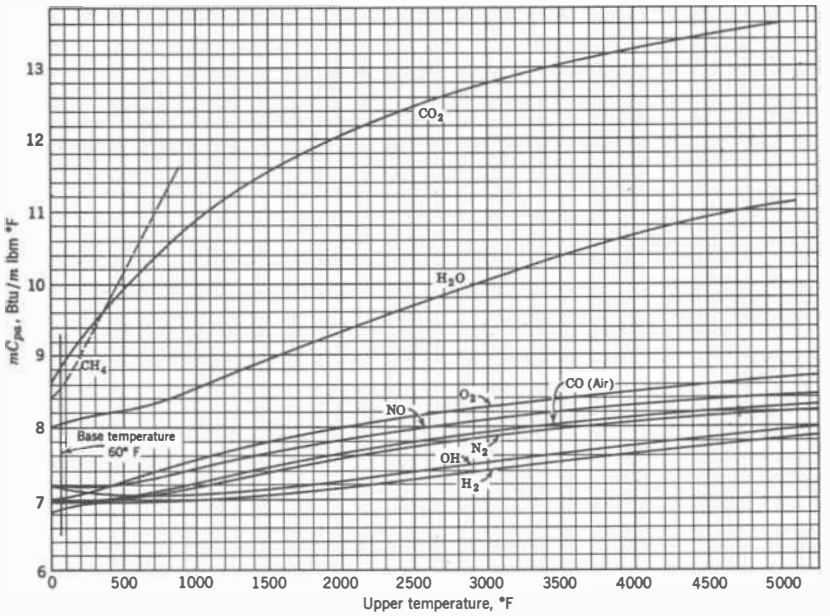

Fig 3-3. Heat capacity, mC_{pa} of gases above 60°F: m = molecular weight; C_{pa} = average specific heat at constant pressure; Btu/lbm °R between 520°R and abscissa temperature. (Hershey, Eberhardt, and Hottel, ref 3.43)

For dry air E° and H° are read along the lines where F_R, the relative fuel-air ratio, and f, the residual-gas fraction, are both zero.

The use of the base of zero internal energy at 560°R gives enthalpy zero at 397°R for pure dry air. Methods used in computing C-1 are fully explained in ref 3.20.

* Quantities based on 1 lb mole carry the superscript °.

www.TechnicalBooksPDF.com

The values of energy, enthalpy, and entropy are computed for zero pressure, but the assumption that they hold good over the range encountered in work with internal-combustion engines involves no serious error.†

Illustrative Examples at the end of this chapter show the method of using C-1 to find the thermodynamic properties of dry air.

Figure 3-3 provides data on the specific heat of dry air and the other gases of interest as a function of temperature. These data, corrected to the latest values wherever necessary, were used to construct the thermodynamic charts presented in this chapter. Chart C-1 may also be used for moist air, as will appear in subsequent discussion.

THERMODYNAMIC PROPERTIES OF FUELS

The commonest fuels for internal-combustion engines are of petroleum origin and consist of mixtures of many different hydrocarbons. The exact composition of such fuels is variable and not accurately known in most cases. However, for most purposes, the thermodynamic characteristics of a petroleum fuel can be satisfactorily represented by those of a single hydrocarbon having approximately the same molecular weight and the same hydrogen-carbon ratio. Thus, for thermodynamic calculations, C_8H_{16} (octene) may be taken as representing gasoline. In practice, fuels are used both in their gaseous and liquid states, so that their properties in each of these states must be considered.

Sensible Properties of Fuels. When fuels are used in association with air the possibility of releasing energy by chemical reaction is always present. The energy of such reactions is usually thought of as belonging to the fuel, and the thermodynamic properties of fuels are usually taken to include the possible contributions of such reactions.

However, in dealing with the processes of mixing fuel with air and of compressing fuel-air mixtures it has been found convenient to exclude questions of chemical reaction by basing the thermodynamic properties on the composition of the fuel before reaction. The base used here for this purpose assigns zero internal energy to fuel in gaseous form in its unburned state at 560°R. Properties computed on this basis are called *sensible* properties in order to distinguish them from properties computed from a base which takes chemical reaction into account. Sensible properties are designated by the subscript s, except for the properties on a mole basis given by C-1, all of which are sensible.

† Corrections for pressure are given in ref 3.20.

www.TechnicalBooksPDF.com

Using the base defined, the sensible enthalpy and internal energy of a unit mass of fuel are given by the following relations:

For gaseous fuels,

$$E_{sf} = \int_{560}^{T} C_v dT \tag{3-1}$$

$$H_{sf} = E_{sf} + pV/J \tag{3-2}$$

For liquid fuels,

$$(E_{sf})_l = E_{sf} + E_l \tag{3-3}$$

$$(H_{sf})_l = H_{sf} + H_l \tag{3-4}$$

In the foregoing equations

C_v = specific heat of the gaseous fuel at constant volume
E_{sf} = sensible internal energy per unit mass of gaseous fuel
H_{sf} = sensible enthalpy per unit mass of gaseous fuel
E_l = internal energy of a unit mass of liquid fuel minus its internal energy in the gaseous state
H_l = enthalpy of a unit mass of liquid fuel

Figure 3-4 gives values of H_{sf} for liquid and gaseous octene at various temperatures. Table 3-1 lists values for other fuels.

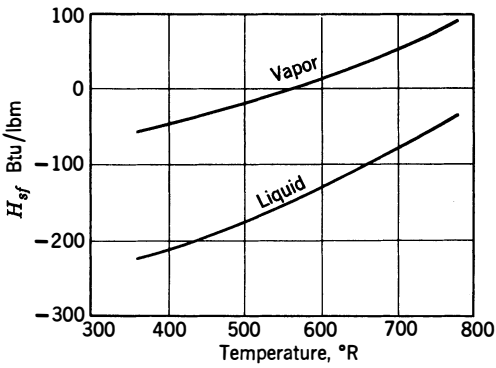

Fig 3-4. Sensible enthalpy of octene above 100°F. (Hottel et al., ref 3.20)

www.TechnicalBooksPDF.com

Table

Properties of Fuels used in

A. LIQUID FUELS—Pure Compounds

Name	Chemical Formula	Liquid Fuel						Fuel Vapor	
		m_f	Specific Gravity (60°F)	H_{lg} at 77°F	C_p 60–80°F	Q_c' (high)	Q_c (low)	C_p at 60°F	k
Normal Pentane	C_5H_{12}	72	0.631	−157	0.557	21,070	19,500	0.397	1.07
Normal Hexane	C_6H_{14}	86	0.664	−157	0.536	20,770	19,240	0.398	1.06
Normal Heptane	C_7H_{16}	100	0.688	−157	0.525	20,670	19,160	0.399	1.05
Normal Octane	C_8H_{18}	114	0.707	−156	0.526	20,590	19,100	0.400	1.05
Iso-Octane	C_8H_{18}	114	0.702	−141	0.515	20,570	19,080	0.400	1.05
Normal Decane	$C_{10}H_{22}$	142	0.734	−155	0.523	20,450	19,000	0.400	1.04
Normal Dodecane	$C_{12}H_{26}$	170	0.753	−154	0.521	20,420	18,980	0.400	1.03
Octene	C_8H_{16}	112	—	−145	0.525	—	19,035	0.400+	1.05+
Benzene	C_6H_6	78	0.884	−186	0.411	17,990	17,270	0.277	1.08
Methyl Alcohol	CH_3OH	32	0.796	−474		9,760	8,580	0.41	1.11+
Ethyl Alcohol	C_2H_5OH	46	0.794	−361		12,780	11,550	0.46	1.13

B. LIQUID FUELS—Typical Mixtures

Gasoline	C_8H_{17}	113	0.702	−150	0.50	20,460	19,020	0.4 approx	1.05 approx
Gasoline	—	126+	0.739	−142	0.48	20,260	18,900		
Kerosene	—	154+	0.825	−125	0.46	19,750	18,510		
Light Diesel Oil	$C_{12}H_{26}$	170	0.876	−115	0.45	19,240	18,250		
Med. Diesel Oil	$C_{13}H_{28}$	184	0.920	−105	0.43	19,110	18,000		
Heavy Diesel Oil	$C_{14}H_{30}$	198	0.960	−100	0.42	18,830	17,790		

C. SOLID FUELS

C to CO_2	C	12	—	—	—	14,520	14,520	—	—
C to CO	C	12	—	—	—	4,340	4,340	—	—

D. GASEOUS FUELS—Pure Compounds

Name	Chemical Formula	Fuel Alone					
		m_f	$\frac{\rho}{\rho_a}$	$\frac{C_p}{\Delta}$	Q_c' (high)	Q_c (low)	k
Hydrogen	H_2	2	0.069	3.41	61,045	51,608	1.41
Methane	CH_4	16	0.552	0.526	23,861	21,480	1.31
Ethane	C_2H_6	30	1.03	0.409	22,304	20,400	1.20
Propane	C_3H_8	44	1.52	0.388	21,646	19,916	1.13
Butane	C_4H_{10}	58	2.00	0.397	21,293	19,643	1.11
Acetylene	C_2H_2	26	0.897	0.383	20,880	20,770	1.26
Carbon Monoxide	CO	28	0.996	0.25	4,345	4,345	1.404
Air	—	29	1.00	0.24	—	—	1.40

E. GASEOUS FUELS—Typical Mixtures

Name	Fuel Alone											
	Composition by Volume										m_f	$\frac{\rho_f}{\rho_a}$
	CO_2	CO	C_2H_6	C_2H_4	H_2	CH_4	N_2	O_2	C_3H_8	C_6H_6		
Blast Furnace Gas	11.5	27.5	—	—	1.0	—	60.0	—	—	—	29.6	1.02
Blue Water Gas	5.4	37.0	—	—	47.3	1.3	8.3	0.7	—	—	16.4	0.57
Carb. Water Gas	3.0	34.0	—	6.1	40.5	10.2	2.9	0.5	—	2.8	18.3	0.63
Coal Gas	3.0	10.9	—	1.5	54.5	24.2	4.4	0.2	—	1.3	12.1	0.42
Coke-Oven Gas	2.2	6.3	—	3.5	46.5	32.1	8.1	0.8	—	0.5	13.7	0.44
Natural Gas	—	—	15.8	—	—	83.4	0.8	—	—	—	18.3	0.61
Producer Gas	4.5	27.0	—	—	14.0	3.0	50.9	0.6	—	—	24.7	0.86

Sources

(a) Maxwell, 3.33
(b) Taylor and Taylor, 1.10
\+ Estimated
x Estimated on basis of zero volume for carbon
(c) Handbook of Physics and Chemistry, p 1732
(d) Marks Handbook, McGraw-Hill 5 ed. p 364
(e) Marks Handbook. McGraw-Hill 5 ed. p 820
(f) Int Critical Tables, McGraw Hill 1929
(g) Hottel et al., 3.20

Symbols

m_f molecular weight fuel
H_{LG} enthalpy of liquid above vapor at 60°F, Btu/lbm
C_p specific heat at constant pressure, Btu/lbm°R
Q_c' higher heat of combustion, Btu/lbm
Q_c lower heat of combustion, Btu/lbm
k ratio of specific heats
m_m molecular weight of stoichiometric mixture
F_c stoichiometric fuel-air ratio

www.TechnicalBooksPDF.com

Internal-Combustion Engine

Chemically Correct Mixture Vapor and Air									
m_m	F_c	r_m	C_p (60°F)	k	$\frac{a}{\sqrt{T}}$	F_cQ_c	$\frac{1}{1+F_c\left(\frac{m_a}{m_f}\right)}$	Q_v	Source of Data
30.1	0.0657	1.05	0.25	1.360	47.3	1280	0.975	95.4	(a)
30.1	0.0658	1.05	0.25	1.357	47.3	1265	0.976	94.5	(a)
30.2	0.0660	1.06	0.25	1.355	47.2	1265	0.980	94.7	(a)
30.3	0.0665	1.06	0.25	1.355	47.2	1270	0.983	95.5	(a)
30.3	0.0665	1.06	0.25	1.355	47.2	1268	0.983	95.4	(a)
30.4	0.0668	1.06	0.25	1.353	47.1	1270	0.984	95.6	(a)
30.5	0.0672	1.06	0.25	1.350	47.0	1275	0.985	96.0	(a)
30.5	0.0678	1.05	0.25	1.355	47.2	1290	0.983	97.5	(f)
30.4	0.0755	1.01	0.248	1.350	47.5	1285	0.974	95.7	(a)
29.4	0.155	1.06	0.245	1.380	47.7	1410	0.876	94.5	(b)
30.2	0.111	1.06	0.262	1.340	46.9	1320	0.936	94.7	(b)
30.3	0.0670	1.06	0.25 approx	1.35 approx	47 approx	1275	0.984	95.6	(b)
30.3	0.0668	1.06				1265	0.987	94.8	(b)
30.4	0.0667	1.06				1240	0.988	91.0	+
30.5	0.0666	1.06				1220	0.989	88.5	(b)
30.6	0.0664	1.06				1215	0.989	88.3	+
30.7	0.0670	1.06				1210	0.990	90.5	+
29.0	0.0868	1.00[x]	0.24	1.40	49	1260	1.0	96.3	x
29.0	0.1736	0.825[x]	0.24	1.40	49	750	1.0	57.3	x

Chemically Correct Mixture										
m_m	F_c (vol)	F_c (mass)	r_m	C_p (60°F)	k (60°F)	$\frac{a}{\sqrt{T}}$	F_cQ_c	$\frac{1}{1+F\left(\frac{m_a}{m_f}\right)}$	Q_v	Source
21	0.418	0.0292	0.85	0.243	1.64	62.3	1510	0.704	81.2	(a)
27.7	0.105	0.0581	1.00	0.256	1.39	49.9	1248	0.904	86.4	(a)
29.0	0.0598	0.0623	1.03	0.249	1.38	48.6	1270	0.943	91.5	(a)
29.6	0.0419	0.0638	1.04	0.250	1.38	48.5	1270	0.961	93.5	(a)
29.8	0.0323	0.0647	1.05	0.250	1.38	48.4	1270	0.967	94.0	(a)
28.8	0.0837	0.075	0.96	0.250	1.38	48.7	1555	0.923	110.0	(c), (d)
28.7	0.418	0.404	0.85	0.241	1.43	49.3	1755	0.705	94.7	(c), (d)
28.85	—	—	—	0.240	1.40	49.0	—	1.0	—	—

Fuel Alone				Chemically Correct Mixture									Source
Q_c (Volume)		Q_c (Mass)		m_m	C_p	$\frac{a}{\sqrt{T}}$	F_c Vol	F_c Mass	r_m	F_cQ_c	$\frac{1}{1+F\left(\frac{m_a}{m_f}\right)}$	Q_v	
high	low	high	low										
92	91	1,170	1,160	29.4	0.245+	48.4	1.47	1.50	0.915	1740	0.405	53.9	(e)
289	262	6,550	5,980	25.0	—	52.6	0.476	0.266	0.864	1580	0.681	83.0	(e)
550	532	11,350	10,980	27.1	—	51.6	0.218	0.137	0.942	1505	0.821	94.4	(e)
532	477	16,500	14,800	26.9	—	51.6	0.220	0.092	0.940	1390	0.818	85.6	(e)
574	514	17,000	15,200	27.3	—	50.3	0.200	0.058	0.957	882	0.890	59.9	(e)
1129	1021	24,100	21,800	27.3	—	49.6	0.095	0.058	1.00	1265	0.916	88.2	(e)
163	153	2,470	2,320	27.0	—	—	0.813	0.700	0.913	1620	0.549	68.2	(e)

r_m ratio molecular weight before combustion to molecular weight after complete combustion of stoichiometric mixture
a velocity of sound in gas, ft/sec
T temperature, °R
m_a molecular weight of air = 28.95
Q_v heat of combustion of fuel vapor in one cubic foot of stoichiometric mixture at 14.7 psia, 60°F

www.TechnicalBooksPDF.com

THERMODYNAMIC PROPERTIES OF FUEL-AIR MIXTURES BEFORE COMBUSTION

The thermodynamic properties of fuel-air mixtures depend on the following characteristics:

1. Composition of the fuel
2. Fuel-air ratio
3. Water-vapor content
4. Residual-gas content

In general, separate charts would be required for each combination of these quantities. However, by introducing suitable approximations, it is possible to make a single chart cover a considerable range of values.

In dealing with such mixtures the following definitions are used:

F = mass ratio of fuel to *dry* air
F_c = stoichiometric or chemically correct fuel-air ratio
F_R = F/F_c, or the fraction of the chemically correct ratio, here called the *relative* fuel-air ratio
f = *residual-gas fraction*, defined as the ratio mass of residuals to the mass of dry air plus fuel plus residual gas
h = mass ratio water vapor to dry air.

From these relations

$$F = F_R F_c \tag{3-5}$$

and, since,

$$M = M_a + M_f + M_r + M_v \tag{3-6}$$

the following can be derived:

$$\frac{M_a}{M} = \frac{1 - f}{1 + F + h(1 - f)} \tag{3-7}$$

$$\frac{M_f}{M} = \frac{F(1 - f)}{1 + F + h(1 - f)} \tag{3-8}$$

$$\frac{M_r}{M} = \frac{f(1 + F)}{1 + F + h(1 - f)} \tag{3-9}$$

$$\frac{M_v}{M} = \frac{h(1 - f)}{1 + F + h(1 - f)} \tag{3-10}$$

www.TechnicalBooksPDF.com

where M is total mass of gaseous mixture, and subscripts a, f, r, and v refer to air, fuel, residual gas, and water vapor, respectively.

Since the total number of moles, N, is equal to the sum of the moles of each constituent,

$$N = N_a + N_f + N_r + N_v \tag{3-11}$$

it follows that

$$N = \frac{M_a}{29} + \frac{M_f}{m_f} + \frac{M_r}{m_r} + \frac{M_v}{18} \tag{3-12}$$

The molecular weight of the mixture is the total mass divided by the number of moles. Dividing eq 3-6 by eq 3-12 and substituting the masses shown by eqs 3-7–3-10 gives

$$m = \frac{M}{N} = \frac{1 + F + h(1 - f)}{(1/29 + F/m_f + h/18)(1 - f) + f(1 + F)/m_r} \tag{3-13}$$

where N is the number of moles and m is the molecular weight in each case. Since, in C-1, $N = 1$, the molecular weight and the mass of the mixture in that figure are given by eq 3-13. The molecular weight of octene is 112, and the molecular weight of dry octene-air mixtures both burned and unburned is given in Fig 3-5.

Since the internal energy of a mixture is equal to the sum of the internal energies of its constituents, we can write

$$E_s = \frac{(E_{sa} + FE_{sf} + hE_v)(1 - f) + fE_{sr}(1 + F)}{1 + F + h(1 - f)} \tag{3-14}$$

in which E_S refers to sensible internal energy per unit mass of mixture. The sensible enthalpy will have a corresponding relation to the enthalpy of a unit mass of each constituent. The energy and enthalpy of one mole of gas is obtained by multiplying eq 3-14 by the molecular weight, eq 3-13.

USE OF CHART 1 FOR FUEL-AIR MIXTURES

The scales of internal energy and enthalpy on the right-hand side of C-1 are m times the values computed by means of eq 3-14 and its corresponding form for enthalpy. The values given are *sensible* values because the base of zero energy is at 560°R for air, fuel, and residual gas in their original chemical compositions.

The mass base, as with air alone, is 1 lb mole of mixture.

www.TechnicalBooksPDF.com

Volumes for 1 mole depend only on temperature and pressure, and therefore the volume lines hold for all values of F_R and f.

Sensible Characteristics of Residual Gas. These characteristics are defined from a base of zero internal energy at 560°R in the gaseous

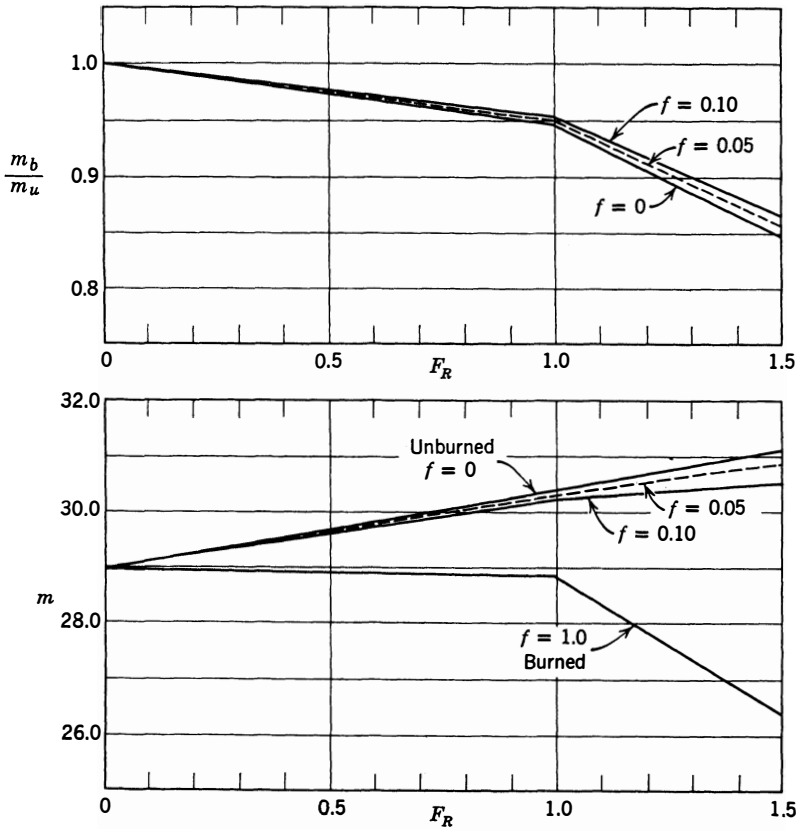

Fig 3-5. Molecular weight of octene-air mixtures and their products of combustion at 560°R: m = molecular weight; subscript b is burned; u is unburned. (Hottel et al., ref 3.20)

state and in their existing chemical composition. The curves on C-1 marked $f = 1$ are for burned mixtures of air and fuel, and therefore correspond to the residual gas in an engine. It is assumed that there is no change in chemical composition over the range of temperature of C-1.

Molecular weight of residual gas from octene-air mixtures is given by the curves for $f = 1.0$ in Fig 3-5.

www.TechnicalBooksPDF.com

Residual-gas content—curves for the values $f = 0$, $f = 0.05$, and $f = 1.0$ (burned mixture) are included in the auxiliary scales of C-1.

In reciprocating engines f usually lies between 0 and 0.10. Within this range interpolation or extrapolation by means of the curves $f = 0$ and $f = 0.05$ gives results within the accuracy of reading the plots.

Fuel-Air Ratio

F_R, the fuel-air ratio used in the charts is defined as follows:

$$F_R = F/F_c \tag{3-15}$$

where F_c is the "chemically correct," or stoichiometric fuel-air ratio (see Table 3-1). The charts are prepared for dry air, but a correction may be made for water-vapor as explained below. For octene, the base fuel for the thermodynamic charts reproduced here,

$F_c = 0.0678$ lbm/lbm air
$F_c° = 0.0175$ mole/mole air
m (molecular weight) $= 112$
$F = 0.0678F_R$
$F° = 0.0175F_R$

Constant-Entropy Lines. To perform a constant-entropy operation for a fuel-air mixture from a given point on the chart, *move parallel to the appropriate sloping entropy line* on the left of the chart. For pure dry air, $F_R = f = 0$, and the entropy lines are vertical. (See Illustrative Examples for an illustration of this operation.)

Water Vapor. Edson and Taylor (ref. 14.1) have shown that variations in residual-gas or water-vapor content have little effect on the efficiency of fuel-air cycles, and therefore for thermodynamic purposes water vapor can be treated as an equal mass of residual gas. Calling f' the residual fraction including water vapor:

$$f' = \frac{M_r + M_v}{M_a + M_f + M_r + M_v} \tag{3-16}$$

and therefore:

$$f' = \frac{f(1 + F) + h(1 - f)}{1 + F + h(1 - f)} \tag{3-17}$$

With water vapor, the charts should be used with the above value of f'. However, the molecular weight should be computed from eq 3-13 and eqs 3-7–3-14 should be used with the true values of f and h.

www.TechnicalBooksPDF.com

MIXING FUEL AND AIR

In many problems relating to internal-combustion engines the process of mixing fuel and air must be handled in thermodynamic terms. For mixing at constant volume without work or heat transfer,

$$E^*_{sm} = E_a^\circ/m + FE_{sf} \tag{3-18}$$

and at constant pressure

$$H^*_{sm} = H_a^\circ/m + FH_{sf} \tag{3-19}$$

Subscript m refers to the mixture, a to air, and f to fuel. The molal values may be read from C-1. E_{sf} and H_{sf} are computed as indicated by eqs 3-1–3-4, and m by eq 3-13. The asterisk indicates that the mass after mixing is $(1 + F)$ lbm.†

THERMODYNAMICS OF COMBUSTION

In spite of a great deal of research, knowledge concerning the chemical processes which take place during combustion is very limited. This is attributable to the fact that these processes normally take place with great rapidity and at very high temperatures.

In dealing with the process of combustion thermodynamically the end states only are considered. To establish the end state from a given initial state, we use the laws of conservation of energy and mass, plus the assumption of complete equilibrium after combustion. Thus mass stays constant, and we can write for the energy balance (eq 1-16), for a unit mass,

$$\left(E + \frac{u^2}{2g_0J}\right)_b - \left(E + \frac{u^2}{2g_0J}\right)_u = Q - w/J \tag{3-20}$$

in which the subscripts b and u refer to the burned and unburned states, respectively.

Equation 3-20 requires that the values of internal energy include their components resulting from chemical combination. As we have seen, these components are not included in the *sensible* properties, since the internal energy is taken as zero for the gases in their original chemical composition.

For present purposes the internal energy attributable to chemical reaction is included by assigning zero internal energy to the *products of complete combustion* at the base temperature.

† See "Thermodynamic Base," p. 59.

www.TechnicalBooksPDF.com

When the combustible material consists of hydrogen and carbon with air, complete combustion is taken to mean reduction of all material in the fuel-air mixture to CO_2, *gaseous* H_2O, O_2, and N_2 at the base temperature.

The relation between internal energy and enthalpy referred to the above base and the sensible properties of the unburned mixture can be expressed as follows for a unit mass of mixture:

$$E = E_{sm} + \Delta E \tag{3-21}$$

$$H = E_{sm} + \Delta E + \frac{PV}{J} = H_{sm} + \Delta E \tag{3-22}$$

where ΔE is the difference in energy attributable to the change of base. For an unburned mixture of air, fuel, and residual gas, since the air is already composed of O_2 and N_2, the value of ΔE depends entirely on the amount and composition of the fuel and of the residual gas. For a unit mass of mixture containing residual-gas fraction f, and with fuel-air ratio F, we can write

$$\Delta E = [(1 - f)FE_c + f(1 + F)q]/(1 + F) \tag{3-23}$$ *

where E_c may be called the *energy of combustion* of a unit mass of fuel and q, the energy of combustion of a unit mass of residual gas.

The numerical values of E_c and q can be computed from heat-of-combustion experiments, which are now described.

Heat of Combustion

This quantity is derived from calorimeter experiments. U.S. standards for measuring *heat of combustion* have been established by the American Society for Testing Materials. (See ref 3.34.)

Briefly, the heat of combustion of a fuel is measured by burning a known mass with an excess of oxygen in a constant-volume vessel called a *bomb calorimeter*. Fuels which are liquid at room temperature are introduced into the apparatus as liquids, and gaseous materials are introduced in gaseous form. The amount of oxygen is much in excess of the stoichiometric requirement in order that all carbon shall burn to CO_2, all hydrogen, to H_2O, all sulphur, to SO_2, etc.

Starting with the calorimeter and its contents at a known temperature, the mixture is ignited, after which the bomb and its contents are cooled to the initial temperature, which is usually low enough so that most of

* The product fFq in this equation is negligibly small and is omitted in subsequent computations.

www.TechnicalBooksPDF.com

the water in the products condenses to the liquid state. The heat released by this process, Q_e, is carefully measured. Since the process occurs at constant volume, Q_e is equal to the internal energy of the fuel-oxygen mixture above a base of zero energy of CO_2, H_2O, and O_2 at the temperature of the experiment.

The *heat of combustion* is the enthalpy of the process, that is:

$$Q_{ch} = \frac{1}{M_f}\left[Q_e + \frac{V}{J}(p_2 - p_1)\right] \tag{3-24}$$

where Q_e is the heat released during the experiment, M_f is the mass of fuel used, V is the container volume, and p_2 and p_1 are pressures in the bomb after and before combustion.

Q_{ch} is known as the *higher heat of combustion* of the fuel.

Another quantity, known as the *lower heat of combustion* of the fuel, is computed as follows:

$$Q_c = Q_{ch} + M_v H_v / M_f \tag{3-25}$$

where M_v is the mass of water vapor in the combustion products and H_v is the enthalpy of a unit mass of liquid water at the experimental temperature, referred to a base of water vapor. Since H_v is a negative number, Q_c is smaller than Q_{ch}.

Customarily, Q_c is used as the basis for computing the thermal efficiency of engines. All thermal efficiency values in this volume are computed on this basis.

Energy of Combustion

From previous discussion of this quantity, it can be defined as the internal energy of the unburned gaseous fuel at 560°R, referred to a base of zero energy for gaseous CO_2, H_2O, O_2, and N_2 at 560°R. This quantity could be measured by measuring the heat released at constant volume, starting with unburned gaseous fuel and O_2 at the base temperature and ending with gaseous CO_2, H_2O, and O_2 at the same temperature. Such an experiment is difficult to make, since many fuels, and also water, are normally liquid at 560°R. However, E_c can be computed from the bomb-calorimeter experiment previously described by using the following relation:

$$E_c = \frac{1}{M_f}(Q_e + M_v E_v) - E_{lg} \tag{3-26}$$

www.TechnicalBooksPDF.com

In the above expression

M_f = mass of fuel used
M_v = mass of water in products
E_v = internal energy of a unit mass of liquid water above a base of water vapor at the experimental temperature
E_{lg} = the internal energy of a unit mass of liquid fuel above a base of gaseous fuel at the experimental temperature. If the fuel was gaseous when put in the bomb, this quantity is taken as zero

Both E_v and E_{lg} are negative numbers, since the internal energy of the gas is greater than that of the liquid.

Equation 3-26 assumes that the bomb experiment was carried out at the base temperature for E_c. Small differences between the base and the experimental temperature can be ignored without appreciable error.

Energy of Combustion of Residual Gases. With fuel-air mixtures in which $F_R > 1.0$, the residual gases may contain appreciable amounts of such constituents as CO and H_2. By definition, such components have appreciable internal energy, referred to a base of CO_2 and H_2O. The energy of combustion of residual gas, q, is determined from the heats of combustion of such components as are not CO_2, gaseous H_2O, O_2, and N_2.

The following values apply to octene at a base temperature of 560°R:

For octene

$$Q_c = 19{,}035 \text{ Btu/lbm}$$

$$E_c = 19{,}180 \text{ Btu/lbm}$$

$$H_l = -145 \text{ Btu/lbm}$$

$$F_c = 0.0678$$

$$F = F_R \times 0.0678$$

For residual gases from octene-air mixtures where F_R is equal to or less than 1.0, $q = 0$. When F_R is greater than 1.0:

$$q = 1680\ (F_R - 1) \text{ Btu/lbm}$$

Similar data for other fuels are given in Table 3-1,† and the Illustrative Examples show how the foregoing relations may be used in practical problems.

† Q_c in Table 3–1 can be used for E_c with negligible error.

www.TechnicalBooksPDF.com

Chemical Equilibrium

Except in gas turbines and Diesel engines at very light loads, the temperatures during combustion and expansion in internal-combustion engines are so high that chemical composition is affected to an extent which cannot be ignored. Hence thermodynamic data must take into account this fact if they are to serve as accurate guides in this field.

For thermodynamic purposes it may be assumed that the products of combustion of the common fuels are made up of various combinations of oxygen, hydrogen, carbon, and nitrogen. The way in which these elements are combined after combustion and the proportion of the various compounds in the mixture depend not only on the proportions present in the original mixture but also on the temperature, the pressure, and the extent to which *chemical equilibrium* has been approached.

When two substances react chemically with each other the reaction does not necessarily proceed to the point at which one of the substances is completely consumed. Before this happens, an equilibrium condition may be reached in which not only products of the reaction are present but also appreciable amounts of the original reacting substances and, in many cases, intermediate compounds. The proportions at equilibrium of the products of a given reaction and the original or intermediate substances depend on the original proportions and on the temperature and pressure after the reaction has taken place. In general, exothermal reactions, that is, reactions which increase the temperature, such as the combustion process, are less complete at high temperatures than at low temperatures. In fuel-air mixtures at equilibrium after combustion appreciable amounts of the following substances may be present:

$$CO_2,\ H_2O,\ N_2,\ O_2,\ CO,\ H_2,\ OH,\ H,\ O,\ NO\ *$$

For a detailed discussion of the principles of chemical equilibrium and methods for its quantitative treatment the reader is referred to standard works in physical chemistry. Briefly, the quantitative treatment of chemical equilibrium rests upon a relationship of the partial pressures. For example, for the reaction

$$wA + xB \rightleftharpoons yC + zD$$

$$\frac{p_C^y \cdot p_D^z}{p_A^w \cdot p_B^x} = K \tag{3-27}$$

* In practice, complete equilibrium is never attained, and small amounts of additional substances, such as free carbon and various organic compounds, are often present in the exhaust gases. (See ref 4.81.) This discussion, however, includes all the substances for which it is necessary to account in thermodynamic problems dealing with engine cycles.

www.TechnicalBooksPDF.com

where w, x, y, and z are the respective numbers of moles of the substances involved, p is the partial pressure of the substance denoted by the subscript, and K is the *equilibrium coefficient*, which is a function of the temperature.

This general equation can be applied to the products of combustion of a fuel-air mixture containing compounds which tend to react with each other with a change in temperature. Examples of such reactions are

$$2CO + O_2 \rightleftharpoons 2CO_2$$

for which the equilibrium coefficient at a given temperature is

$$K_1 = \frac{(p_{CO_2})^2}{(p_{CO})^2(p_{O_2})} \tag{3-28}$$

and

$$CO_2 + H_2 \rightleftharpoons H_2O + CO$$

for which

$$K_2 = \frac{(p_{H_2O})(p_{CO})}{(p_{CO_2})(p_{H_2})} \tag{3-29}$$

These equilibrium coefficients, together with those for other possible reactions between the products of combustion, have been determined for various temperatures (ref 3.20) and may be used to determine the partial pressure ratios, hence the relative amounts of the various constituents at any given temperature. Figure 3-6 shows the equilibrium composition of the products of combustion of octane (C_8H_{18}) and air for three different fuel-air ratios over the range from 3000–5500°R.

Change in Number of Molecules. Since the composition of the working fluid changes almost continually throughout the cycle, it is not surprising to find that the number of molecules changes also. The greatest change in this respect is likely to occur during the process of combustion. For instance, taking the theoretically complete reaction of octene and air,

$$C_8H_{16} + 12O_2 + 45.2N_2 \rightarrow 8CO_2 + 8H_2O + 45.2N_2 \tag{3-30}$$

the number of molecules before combustion is proportional to $1 + 12 + 45.2 = 58.2$ and after combustion to $8 + 8 + 45.2 = 61.2$, or an increase of 5%. This increase, of course, means a similar increase in specific volume at a given temperature and pressure. In the actual case, however, the reaction does not proceed to completion, and the change may be still greater. Let us assume, for example, that two atoms of carbon burn only to CO and that one molecule of hydrogen remains un-

www.TechnicalBooksPDF.com

Fig 3-6. Equilibrium composition of products of combustion of mixtures of octane (C_8H_{18}) and air. (Hershey, Eberhardt, and Hottel, ref 3.43)

www.TechnicalBooksPDF.com

combined. The composition of the products of reaction now is

$$6CO_2 + 2CO + 7H_2O + H_2 + 1\tfrac{1}{2}O_2 + 45.2N_2 = 62.7 \text{ molecules}$$

an increase of 9% over the mixture before combustion.

It is evident that the change in number of molecules is dependent on the composition of the fuel, the fuel-air ratio, and on the completeness of the reaction. The number of molecules is greatest at high temperature where the chemical equilibrium involves considerable amounts of OH, NO, O_2, H_2, and CO. As the temperature falls, the number of molecules decreases, but even if combustion were complete most liquid fuels would give a larger total number of molecules after combustion than was contained in the original mixture of fuel and air. Figure 3-5 shows the ratio of molecular weight after combustion and cooling to 1600°R, or less, to molecular weight before combustion of C_8H_{16} at various values of F_R.

Specific Heat. As in the case of the mixture before combustion, the specific heat of each of the various constituents increases with temperature. Figure 3-3 includes data on specific heats of combustion products.

CHARTS FOR PRODUCTS OF COMBUSTION

The charts for products of combustion, C-2, C-3, and C-4, (to be found in pocket on back cover) have been constructed by means of the relations discussed in the foregoing section. These charts are for octene-air mixtures with $F_R = 0.8$, 1.0, and 1.2, respectively. Similar charts for $F_R = 0.9$, 1.1, and 1.5 are available in ref 3.20. This reference also gives further details on computation methods.

The mass basis for each of these diagrams is $(1 + F)$ lb of material. Quantities on this mass basis are designated by an asterisk.

Chemical equilibrium is assumed at all points in each chart.

Thermodynamic Base. These charts assign zero internal energy to gaseous CO_2, H_2O, O_2, and N_2 at 560°R at zero pressure.

Internal energy, E^*, is equal to the heat which would be released at constant volume by cooling $(1 + F)$ lbm of gas to 560°R and changing its composition to gaseous CO_2, O_2, H_2O, and N_2 at 560°R.

Enthalpy, H^*, is equal to $E^* + pV^*/J$, where V^* is the volume of $(1 + F)$ lbm of gas at the pressure p and the given temperature.

The entropy given in these charts is computed for $(1 + F)$ lbm of gas, assigning zero entropy to CO_2, gaseous H_2O, O_2, and N_2 at 560°R, 14.7 psia.

www.TechnicalBooksPDF.com

TRANSFER FROM C-1 TO CHARTS FOR PRODUCTS OF COMBUSTION

In dealing with processes involving combustion in which the temperature goes above 2500°R it is necessary to transfer the problem from C-1 to one of the charts for burned products.

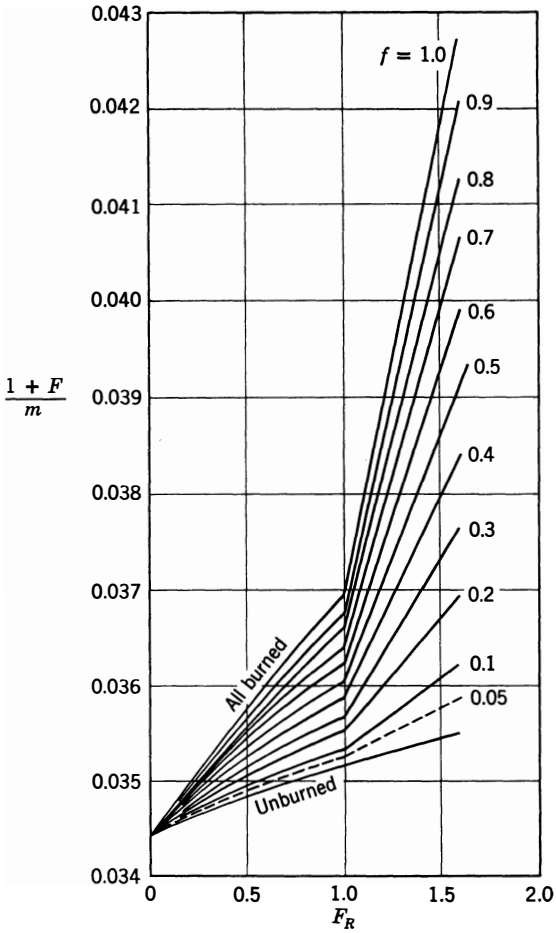

Fig 3-7. Values of $(1 + F)/m$ for octene-air mixtures. (Hottel et al., ref 3.20)

To effect this transfer, we use eq 3-20 for the combustion process. Values of E must include energy attributable to chemical reaction.

In terms of C-1, and the charts for products of combustion, for $(1 + F)$ lb of material eq 3-20 can be written

www.TechnicalBooksPDF.com

$$E^* - \left[\frac{(1+F)}{m} E^\circ + (1-f)FE_c + (1+F)fq\right] = Q^* - w^*/J \quad (3\text{-}31)$$

where E° is the value taken from C-1 for 1 lb mole of mixture at the same fuel-air ratio and at the same residual gas fraction.

The asterisks indicate that values are for $(1 + F)$ lb.

If the combustion process takes place at constant volume without heat loss, Q^* and w^* are zero. If the combustion process takes place at constant pressure without heat loss, Q^* is zero, $w = p(V_b^* - V_u^*)$, and we can write

$$H^* - \left[\frac{(1+F)}{m} H^\circ + (1-f)FE_c + (1+F)fq\right] = 0 \quad (3\text{-}32)$$

Values of $(1 + F)/m$ for octene-air-residual-gas mixtures are given in Fig 3-7. For other mixtures m can be computed from expression 3-13.

Residual Gas. In the charts for the products of combustion the characteristics are independent of the fraction of residual gas before combustion, since the residual gas has, by definition, exactly the same properties as the combustion products.

Water Vapor. When water vapor is present use f^1 [from equation (3–17)] instead of f in (3–32).

APPROXIMATE TREATMENT OF FUEL-AIR MIXTURES

The charts described here can be extended to cover other common hydrocarbon fuels and other fuel-air ratios without serious sacrifice in accuracy, provided the departure from the basic assumptions used in constructing the charts is not too great.

Fresh Mixture Chart C-1. To use this chart for fuels other than octene:

1. Since, for $F_R = 1$ on the chart, the molal ratio fuel-to-air is 0.0175,
   (*a*) calculate the molal fuel-air ratio of the new fuel, F_m;
   (*b*) read values on C-1 for $F_R = F_m/0.0175$.
2. Use f values for the new mixture without correction.

www.TechnicalBooksPDF.com

Transfer to Products Charts. Equations 3-31 and 3-32 should be used with values of m, E_c, and q computed for the fuel in question. (See Table 3-1.)

Products Charts. The products chart for the nearest value of F_R should be used. This rule should also be followed in the case of octene at values of F_R not included in the charts. (Reference 3.20 gives charts for several other F_R values with octene.)

By means of the above assumptions, the charts can be used for fuel-air ratios about $0.6 > F_R > 1.4$ and for petroleum-base fuels in the gasoline and Diesel-oil range without serious error. Example 3-7 illustrates the use of the charts for a fuel other than octene.

ILLUSTRATIVE EXAMPLES

Example 3-1. Dry Air.* Find pressure, temperature, volume, internal energy, enthalpy, and work done after compressing 1 lbm dry air from $T = 600$, $p = 14.7$ to $p = 500$ reversibly and without heat transfer.

(a) From C-1, at $T = 600$, $p = 14.7$, $F_R = 0$, $f = 0$, we read

$$E^\circ = 203, \qquad H^\circ = 1400, \qquad V^\circ = 440$$

From eq 3-13, $m = 29$; and, for 1 lbm,

$$E = 7, \qquad H = 48.3, \qquad V = 15.2$$

(b) Following a line of constant entropy (vertical) from initial point to $p = 500$, we read

$$T = 1580, \qquad V^\circ = 34.2, \qquad E^\circ = 5400, \qquad H^\circ = 8560$$

Dividing by 29,

$$V = 1.18, \qquad E = 186, \qquad H = 296$$

(c) For a reversible adiabatic process $E_2 - E_1 = w/J$,

$$w = -778(186-7) = -139{,}000 \text{ ft lbf}$$

Example 3-2. Air with Water Vapor. Same as example 3-1, except that air contains 0.04 lbm water vapor/lbm dry air.

(a) From eqs 3-7, 3-10, and 3-13,

$$M_a/M_m = 1/(1 + 0.04) = 0.962 \text{ lbm}$$

$$M_v/M_m = 0.04/1.04 = 0.038 \text{ lbm}$$

$$m = 1.04/(\tfrac{1}{29} + 0.04/18) = 28.4$$

* In these examples all temperatures are in degrees Rankine, pressures in psia, volumes in cubic feet, and energies and enthalpies in Btu. Mass base is 1 lbm except * indicates $(1 + F)$ lbm and ° indicates 1 lb mole.

www.TechnicalBooksPDF.com

(*b*) From eq 3-17, $f' = 0.04/1.04 = 0.0385$. Reading C-1 at $F_R = 0$, $T = 600$, $p = 14.7$ gives

$$V° = 440, \qquad E° = 200, \qquad H° = 1400$$

Dividing by 28.4,

$$V = 15.5, \qquad E = 7, \qquad H = 49.4$$

(*c*) From the above point, following a line parallel to the constant entropy line for $F_R = 0, f = 0.0385$,

$$V° = 34, \qquad T = 1575, \qquad E° = 5360, \qquad H° = 8540$$

Dividing by 28.4,

$$V = 1.2, \qquad E = 188, \qquad H = 300$$

(*d*) $w = -778(188 - 7) = -141{,}000$ lbf ft.

Example 3-3. Mixing Fuel and Air. Same as example 3-1, except that enough liquid octene is mixed with the air, both originally at 600°R, to give the chemically correct fuel-air mixture.

(*a*) From Fig 3-4, enthalpy of liquid octene at 600°R $= -127$ Btu/lbm,

$$F = 1 \times 0.0678 = 0.0678, \qquad f = 0$$

(*b*) From eqs 3-7, 3-8, and 3-13,

$$M_a/M = 1/1.0678 = 0.94$$

$$M_f/M = 0.0678/1.0678 = 0.06$$

$$m = \frac{1 + 0.0678}{\frac{1}{29} + 0.0678/112} = 30.4$$

(*c*) From C-1 at $T = 600$, $p = 14.7$, $F = 0$, $H° = 1400$, $V° = 440$, $H = 1400/29 = 48.2$. For the mixing process (eq 3-19),

$$H = 48.2 + 0.0678(-127) = 39.6$$

$$H° = 39.6(30.4)/(1 - 0.0678) = 1125$$

(*d*) From C-1 at $H° = 1125$, $p = 14.7$, $F_R = 1.0, f = 0$, read

$$T = 560°\text{R}, \qquad V° = 410, \qquad E° = 0$$

(*e*) Following constant entropy line parallel to line for $F_R = 1.0$ at the left of C-1, at $p = 500$, $F_R = 1.0$, read,

$$T = 1345, \qquad V° = 29.0 \qquad H° = 7470, \qquad E° = 4800$$

Dividing by 30.4,

$$V = 0.955, \qquad H = 246, \qquad E = 158$$

(*f*) $w = -778(158 - 0) = -123{,}000$ ft lbf

www.TechnicalBooksPDF.com

Example 3-4. Air with Water Vapor, Fuel, and Residuals. Same as example 3-1, except that at $T = 600$, $p = 14.7$, air contains gaseous octene at $F_R = 1.0$, residual gas at $f = 0.05$, and water vapor at $h = 0.04$.

(*a*) From Fig 3-5, $m_r = 28.8$ and from Table 3-1, $F_c = 0.0678$, and from eq 3-13,

$$m = \frac{1.0678 + 0.04(0.95)}{(\frac{1}{29} + 0.0678/(112) + 0.04/18)(0.95) + 0.05(1.0678)/28.8}$$

$$= 29.6$$

(*b*) From eq 3-17,

$$f' = \frac{0.05(1.0678) + 0.04(0.95)}{1.0678 + 0.04(0.95)} = 0.083$$

(*c*) On C-1 at $p = 14.7$, $T = 600$, $f = 0.083$, read

$$V_1° = 445, \qquad E_1° = 220, \qquad H_1° = 1430$$

(*d*) Following a line of constant entropy on C-1 (parallel to line $F_R = 1$, $f = 0.083$ at the left) to $p = 500$ gives $V_2° = 31$, $T_2 = 1430$, $E_2° = 5350$, $H_2° = 8180$

(*e*) Dividing by $m = 29.6$ gives

$$V_1 = 15.0 \qquad E_1 = 7.4 \qquad H_1 = 48.3$$

$$V_2 = 1.047 \qquad E_2 = 181 \qquad H_2 = 276$$

(*f*) From eq 1-16,

$$w = -J(E_2 - E_1) = -778(181 - 7.4) = -13.4(10)^4 \text{ lbf ft}$$

Example 3-5. The fuel-air mixture of example 3-3 ($F_R = 1.0$) is burned to equilibrium after compression to 500 psia. Burning takes place at constant pressure without heat loss or gain. Find properties at end of combustion.

(*a*) From Fig 3-7, $(1 + F)/m = 0.0351$.

(*b*) From eq 3-32,

$$H^* = 0.0351 \times 7580 + 0.0678 \times 19{,}180 = 1566$$

(*c*) On C-3 at $H^* = 1566$, $p = 500$, read

$$T = 4720, \qquad V^* = 3.8, \qquad E^* = 1220$$

Example 3-6. Assume that after compression the mixture ($F_R = 1.0$) of example 3-4 is burned at *constant volume* without heat loss or gain. Find the properties after burning.

(*a*) At the end of compression, example 3–4, the mixture is at 500 psia, $E° = 5350$; $(1 + F)/m = 1.0678/29.6 = 0.0395$.

www.TechnicalBooksPDF.com

(*b*) In this constant-volume process both Q^* and w^* in equation 3–31 are zero and:

$$E^* = 0.0395(5350) + (1 - 0.083)(0.0678)19{,}180 + 0 = 1401$$
$$V^* = 0.0395 \times 31 = 1.22$$

(*c*) Reading from C-3 at this point,

$$p = 1720, \qquad T = 5190, \qquad H^* = 1785$$

Example 3-7. Use of Fuel Other than Octene. A mixture of air and gaseous benzene (C_6H_6) at $F_R = 1$ is compressed from $T = 600$, $p = 14.7$ to $p = 500$, reversibly and without heat transfer. It is then burned at constant pressure without heat transfer. Find the thermodynamic properties at the end of this process.

(*a*) From Table 3-1, F_c for benzene is 0.076, $E_c = 17{,}500$. For $F_R = 1$, the molecular fuel-air ratio is

$$0.076 \times \tfrac{29}{78} = 0.0283$$

To use C-1 at the same *molecular* fuel-air ratio, we must read this figure at $F_R = 0.0283/0.0175 = 1.6$.

(*b*) The molecular weight of the benzene-air mixture, from eq 3-13, is

$$m = \frac{1.076}{1/29 + 0.076/78} = 30.3$$

(*c*) On C-1 at $T = 600$, $p = 14.7$, $F_R = 1.6$, read

$$V^\circ = 440, \qquad E^\circ = 230, \qquad H^\circ = 1440$$

Dividing by 30.3, $V = 14.5$, $E = 7.6$, $H = 47.5$. Following parallel to the $F_R = 1.6$ line to $p = 500$ gives

$$V^\circ = 29, \qquad T = 1360, \qquad E^\circ = 5330, \qquad H^\circ = 8050$$

Dividing by 30.3,

$$V = 0.96, \qquad E = 176, \qquad H = 266$$

(*d*) $w = -778(176 - 7.6) = -132{,}000$ lbf ft.

(*e*) For the combustion process at constant pressure, use eq 3-32:

$$H^* = \frac{1.076}{30.3} \times 8050 + 0.076 \times 17{,}500 = 1616$$

On C-3 ($F_R = 1.0$) at $H^* = 1616$ and $p = 500$, read

$$V^* = 3.85, \qquad T = 4800, \qquad E^* = 1256$$

www.TechnicalBooksPDF.com

(Note that these are substantially the same results obtained in example 3-5 for a similar process using octene.)

Table 3-2 compares the results of the examples in this section.

Table 3-2

Comparison of Examples in Section 3 of Illustrative Examples

A. Compression to 500 psia

Example	Material	F_R	f	h	T	V	H	E	$\frac{w}{1000}$
3-1	Dry air	0	0	0	1580	1.18	296	186	139
3-2	Air and water vapor	0	0	0.04	1575	1.2	300	188	141
3-3	Air and liquid fuel	1.0	0	0	1356	0.97	249	160	122
3-4	Air and fuel vapor, residuals, water vapor	1.0	0.05	0.04	1430	1.08	284	186	139
3-7	Air and C_6H_6	1.0	0	0	1360	0.96	266	176	132

B. Constant-Pressure Burning

Example	Material	F_R	f	h	T	V^*	H^*	E^*
3-5	Air and octene	1.0	0	0	4720	3.8	1566	1220
3-7	Air and benzene	1.0	0	0	4800	3.85	1616	1256

C. Constant Volume Burning

Example	Material	F_R	f	h	T	P	H^*	E^*
3-6	Air, fuel, water-vapor, residuals	1.0	0.05	0.04	5190	1720	1785	1401

Initial conditions, $T = 600°R$, $p = 14.7$ psia.
Isentropic compression.
In example 3-3 liquid fuel and air were at 600°R before mixing.

www.TechnicalBooksPDF.com

four Fuel-Air Cycles

A fuel-air cycle is here defined as an idealized thermodynamic process resembling that occurring in some particular type of engine and using as its working medium real gases closely resembling those used in the corresponding engine. In order to construct such cycles, thermodynamic data, such as those presented in Chapter 3, are necessary.

Since fuel-air cycles involve combustion, an irreversible process, the medium can never be returned to its original state, and therefore the process is not cyclic in the thermodynamic sense. For this type of process, and for the real process in engines, the term *cycle* is used as referring to one complete component of a repetitive process.

In dealing with the air cycle (Chapter 2) the term efficiency was used in the true thermodynamic sense, that is, as the ratio of work produced to heat supplied. In the case of the fuel-air cycle no heat is supplied during the process. Instead, a mixture of fuel and air is supplied and burned at the proper time. As stated in Chapter 3, the process of combustion involves a chemical transformation which, in the case of the usual type of fuel-air mixture, raises its temperature and pressure at a given volume or increases its temperature and volume at a given pressure. (When neither the volume nor pressure is held constant during combustion the result can be analyzed in terms of a summation of infinitesimal constant-volume or constant-pressure processes. (See ref 1.4.)

The work done in a fuel-air cycle can be measured, and the definition of efficiency may be handled in the same way as for an engine, that is, by assigning a thermal value to the fuel consumed. Since the objective of

www.TechnicalBooksPDF.com

a study of fuel-air cycles is to develop a basis of evaluating real cycles, the same efficiency base is used, namely, the *heat of combustion* of the fuel, Q_c, defined in Chapter 3. By using this base, eq 1-4 may be applied to fuel-air cycles as well as to engines. Heats of combustion of common fuels appear in Table 3-1.

DEFINITIONS

In fuel-air cycles, as well as in real cycles, the medium may consist of a mixture of several fluids. The definitions used in this book are as follows:

Reciprocating Engines

Fresh Air. The new air supplied to the cylinder for each cycle.

Fresh Fuel. The new fuel supplied for each cycle.

Fresh Mixture. The fresh air plus the fresh fuel supplied for each cycle in a carbureted engine or the fresh air in the case of Diesel and other injection engines.

Fuel-Air Ratio, F. The mass ratio of fresh fuel to fresh air, F.

Relative Fuel-Air Ratio, F_R. The fuel-air ratio divided by the stoichiometric ratio.

Residual-Gas Ratio, f. The mass ratio of gases left in the cylinder from the previous cycle, after all valves are closed, to the mass of the charge.

Charge. The total contents of the cylinder at any specified point in the cycle.

For gas turbines the medium before combustion is called the *fresh air* and the medium after combustion, the *burned gases*, or the *products of combustion*.

Assumptions

Assumptions commonly used for all fuel-air cycles are as follows:

1. There is no chemical change in either fuel or air before combustion.
2. Subsequent to combustion, the charge is always in chemical equilibrium.
3. All processes are adiabatic, that is, no heat flows to or from the containing walls.
4. In the case of reciprocating engines velocities are negligibly small.

These assumptions are used throughout this chapter.

www.TechnicalBooksPDF.com

Fuel-air cycles are usually assumed to begin at the start of the compression process. The ratios F and f are usually chosen to represent conditions prevailing in a real cycle or in a cycle having an idealized inlet and exhaust process. Such processes are discussed later in this chapter. The pressure and temperature at the beginning of compression are chosen in a similar way.

THE CONSTANT-VOLUME FUEL-AIR CYCLE USING CARBURETED MIXTURE

This cycle is taken as representing the ideal process for carbureted spark-ignition engines. It consists of these processes. (See Fig 4-1.)

Process 1–2. Compression of the charge reversibly and without heat transfer from volume 1 to volume 2, the compression ratio being V_1/V_2. For mixtures of gasoline, air, and residuals Chart C-1 may be used to evaluate such a process. (See examples 3-1, 3-2, 3-3.)

Process 2–3. The combustion process is taken as a transformation at constant volume, V_2, from the unburned charge to products of combustion at equilibrium. Only the end state, point 3, can be identified from charts of equilibrium conditions such as those given in Chapter 3.

In terms of those charts, for $(1 + F)$ lbm of gas,

$$E_3^* = \left(\frac{1 + F}{m}\right) E_2^\circ + (1 - f)FE_c + fq \tag{4-1}$$

The symbols are defined and evaluated in Chapter 3.

Process 3–4. Reversible adiabatic expansion from point 3, at volume V_2, to point 4, at volume V_1. Pressures and volumes are read along the constant-entropy line.

Work. Using eq 1-16 and taking Q and u as zero for $(1 + F)$ lbm, we can write

$$w^* = J\left\{(E_3^* - E_4^*) - \left(\frac{1 + F}{m}\right)(E_2^\circ - E_1^\circ)\right\} \tag{4-2}$$

Mean Effective Pressure. This quantity is defined as the work divided by the change in volume, that is,

$$\text{mep} = w^*/(V_1^* - V_2^*) \tag{4-3}$$

This quantity has the dimensions of pressure and is equal to the mean difference in pressure between the expansion and compression lines of the cycle.

www.TechnicalBooksPDF.com

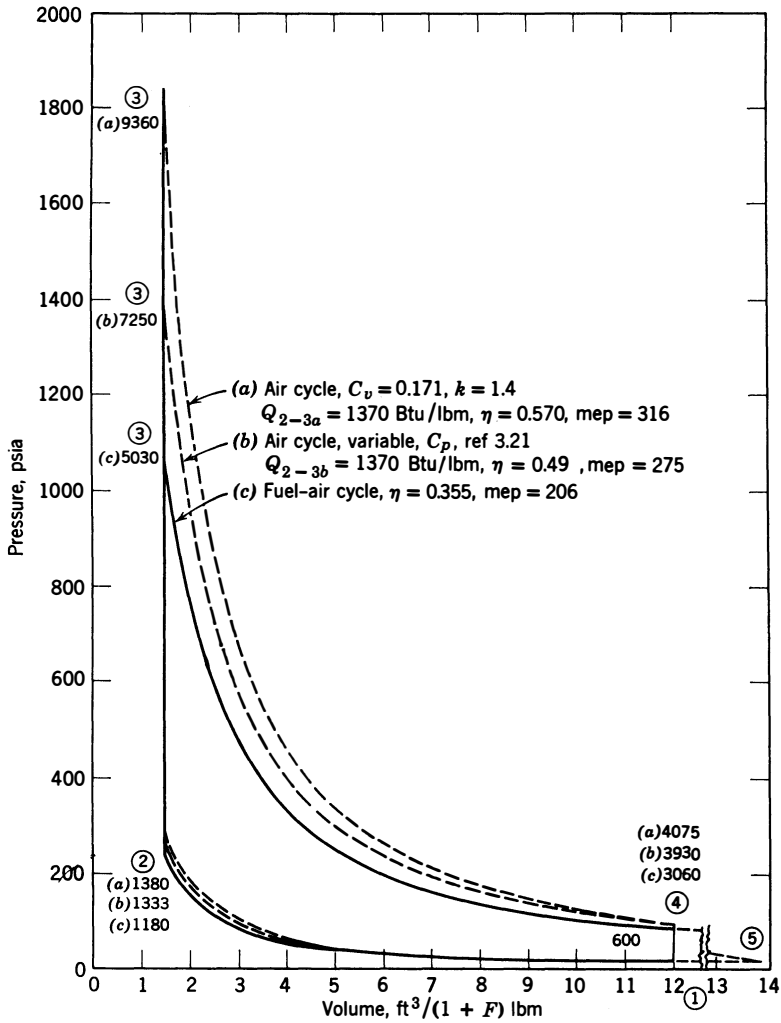

Fig 4-1. Constant-volume fuel-air cycle compared with air cycle: $r = 8$; $F_R = 1.2$; $p_1 = 14.7$; $T_1 = 600$; $f = 0.05$. Fuel is octene, C_8H_{16}. Numbers at each station are temperatures in °R: (*a*) air cycle; (*b*) air cycle, variable sp heat; (*c*) fuel-air cycle (example 4-1).

www.TechnicalBooksPDF.com

Efficiency. Using heat of combustion Q_c as a base, from eqs 3-7 and 3-8,

$$\eta = w^*/JM_a{}^*FQ_c = w^*/JFQ_c\left[\frac{(1+F)\,(1-f)}{1+F+h\,(1-f)}\right] \qquad (4\text{-}4)$$

Examples which show in detail how constant-volume cycles may be worked out from the thermodynamic charts of Chapter 3 are given at the end of this chapter.

Characteristics of Constant-Volume Fuel-Air Cycles

Figure 4-5 (p. 82) shows the characteristics of constant-volume cycles using octene (C_8H_{16}) fuel over the useful range of compression ratios, fuel-air ratios, and inlet conditions. Pressures are given in dimensionless form using p_1 as a base. Temperatures are given as ratios to the initial temperature, T_1.

The following general relations are apparent from Fig 4-5:

1. Efficiency is little affected by variables other than compression ratio and fuel-air ratio (*a*) through (*f*).*

2. When fuel-air ratio is the variable, efficiency decreases as fuel-air ratio increases (*b*). This relation is easily explained by noting that up to F_R = 1.0–1.1 increasing fuel-air ratio gives increasing temperatures after combustion (*p*) and thus increases specific heats and dissociation.

Above F_R = 1.0–1.1, expansion temperatures decrease with increasing fuel-air ratio (*p*), but in this region as fuel-air ratio increases the excess fuel burns to carbon monoxide, and the net result is decreasing efficiency with increasing F_R (*b*).

3. Mean effective pressure (*b'*). From eqs 4-3 and 4-4,

$$\frac{\text{mep}}{p_1} = JFQ_c\eta\left[\frac{(1+F)\,(1-f)}{1+F+h\,(1-\text{f})}\right] \div p_1V_1^*\left(1-\frac{1}{r}\right) \qquad (4\text{-}5)$$

With all initial conditions constant except F_R, the principal variable in eq 4-5 will be the product $F\eta$, which reaches a maximum with F_R near 1.10. This is evidently the point at which the favorable effect on efficiency of decreasing molecular weight (Fig 3-5) is offset by the unfavorable effect of burning more of the fuel to carbon monoxide.

* Letters in parenthesis refer to the various parts of Fig 4-5.

www.TechnicalBooksPDF.com

LIMITED-PRESSURE FUEL-AIR CYCLE

As explained in Chapter 2, cycles with an arbitrary limit on peak pressure are of interest chiefly in connection with Diesel engines, in which the injection characteristics and injection timing are often arranged to limit maximum pressure to an arbitrary value. The fuel-air cycle corresponding to this practice is taken as follows (Fig 4-2):

Process 1–2. Compression of air and residual gases (without fuel) from $V_1°$ to $V_2°$. (See Fig 4-2.)

Fuel Injection. It is assumed that liquid fuel is injected at point 2. For this process, taking heat-transfer as zero, after the fuel is injected,

$$E_2^* = \frac{E_2^\circ}{29} + (1 - f)F(E_c + H_l) + fq^\dagger \tag{4-6}$$

Definitions of the symbols can be found in Chapter 3. Values of E_{lg}, the internal energy of evaporation, are given in Table 3-1 for several fuels.

The last term is the work of injection, where V_f is the volume of liquid fuel injected. This quantity is so small that it may be taken as zero without appreciable error.

Process 2–3–3*A*. Combustion is assumed to take place at constant volume up to the pressure limit, p_3, and then at constant pressure. By applying eq 1-16 to this process for $(1 + F)$ lbm, $Q = 0$, velocities small,

$$E_{3A}^* = E_2^* - p_3(V_{3A}^* - V_2^*)/J \tag{4-7}$$

which can be written

$$H_{3A}^* = E_2^* + p_3V_2^*/J \tag{4-8}$$

The above equation is solved for H_{3A}^*, and conditions at point $3A$ can then be read at p_3, H_{3A}^* on a chart for the combustion products.

†$H_l + E_l + \left(\frac{pV}{J}\right)_l$ and thus the work of injecting the fuel is included.

www.TechnicalBooksPDF.com

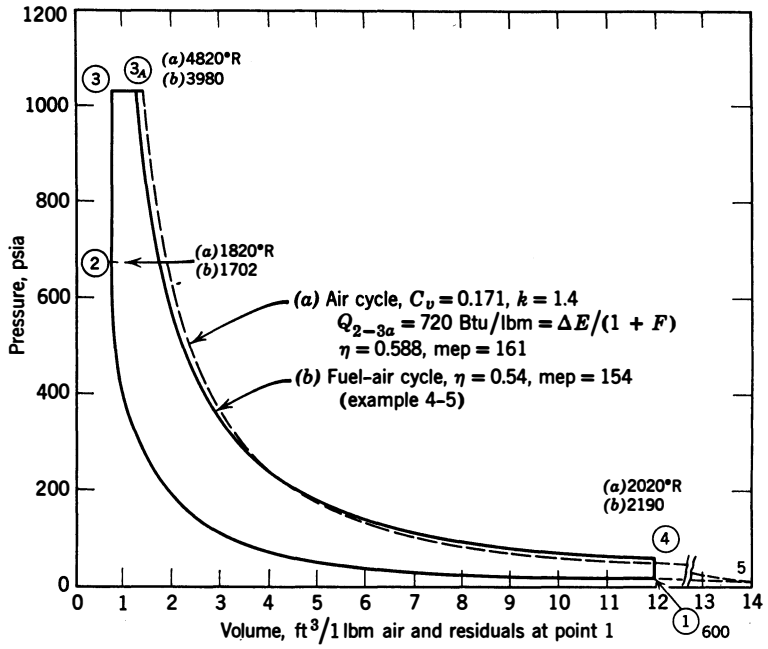

Fig 4-2. Limited-pressure fuel-air cycle compared with air cycle: $r = 16$; $F_R = 0.6$; $p_1 = 14.7$; $T_1 = 600$; $f = 0.03$; $p_3 = 70 \times p_1 = 1030$ psia. Numbers at each station are temperatures in °R.

Process 3*A*–4. Isentropic expansion from point $3A$ to V_1. Values of pressure and volume are read along the appropriate isentropic line.

Work. From eq 1-16 for the process 1–4,

$$w^* = J\left[\left(H_{3A}^* - \frac{p_3 V_3}{J} - E_4^*\right) - \frac{1}{m}(E_2^\circ - E_1^\circ)\right] \quad (4\text{-}8a)$$

mep and efficiency are calculated from eqs 4-3 and 4-4.

Examples at the end of this chapter show in detail how such cycles are worked out from the figures and charts in Chapter 3.

Characteristics of Limited-Pressure Fuel-Air Cycles

Figure 4-6 (p. 88) shows general characteristics of such cycles over the range of fuel-air ratios, compression ratios, and pressure limits of interest in connection with Diesel engines. These cycles were also computed with the idealized four-stroke inlet process to be described later.

www.TechnicalBooksPDF.com

Of general interest are the following relations:

1. The improvement in efficiency as the ratio p_3/p_1 increases. The higher this ratio, the larger the fraction of fuel burned at volume V_2. With no restriction on p_3, the cycle becomes a constant-volume cycle. Fuel burned at V_2 goes through a greater expansion ratio than fuel burned at larger volumes and therefore gives more work per unit mass.

2. The small variation of mep and efficiency with compression ratio, especially at $p_3/p_1 = 50$. This relation is explained by the fact that as compression ratio increases a larger fraction of the fuel is burned at constant pressure.

3. The small values of f at high compression ratios. This relation holds because of the small ratio of clearance volume V_2 to V_1.

4. The steady increase of efficiency with decreasing F_R. In this case not only the decrease in temperatures after combustion but also the reduced fraction of combustion at constant pressure account for this trend.

GAS-TURBINE FUEL-AIR CYCLES

In gas turbines combustion temperatures must be limited in order to avoid excessive nozzle and turbine-blade temperatures. In practice, combustion temperatures are limited by limiting the fuel-air ratio to values much less than the chemically correct value.

In practice the fuel-air ratios used are such that combustion temperatures do not reach the range at which the assumption that the products contain only CO_2, H_2O, O_2, and N_2 involves serious error. Thus charts such as C-1 and tables such as those of ref 3.21 can be used, even though they do not account for the effects of temperature on chemical equilibrium.*

The gas-turbine fuel-air cycle is taken as follows (Fig 4-3):

Process 1–2. Isentropic compression of *air only* from initial conditions to the given *pressure* p_2.

Locate point 1 on C-1 and follow an isentropic line for air ($F_R = 0$) to the given pressure p_2.

Process 2–3. Mixing and combustion. It is assumed that liquid C_8H_{16} is introduced and burned at constant pressure to equilibrium between points 2 and 3.

*It will be noted that C-1 is limited to 2500°F maximum temperature, at which point the author states that the effects of "dissociation" are negligibly small.

www.TechnicalBooksPDF.com

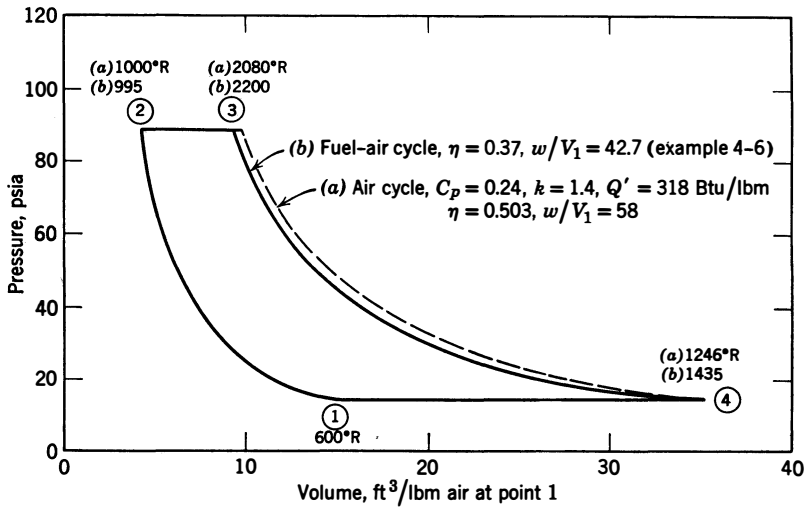

Fig 4-3. Gas-turbine fuel-air cycle compared with air cycle: $p_2/p_1 = 6$; $F_R = 0.25$; $p_1 = 14.7$; $T_1 = 600$. Numbers at each station are temperatures in °R.

For this process it is convenient to assume 1 lbm air and F lbm fuel by dividing the mole properties by the appropriate molecular weight. Then

$$(1 + F)\frac{H_3^\circ}{m_3} = \frac{H_2^\circ}{29} + F(E_{lg} + E_c) \tag{4-9}$$

m_3, the molecular weight at point 3, is found on Fig 3-5, and eq 4-9 is solved for H_3°.

Process 3–4. Locate H_3° on C-1 and follow an isentropic line (corresponding to the given value of F) to point 4 at the original pressure. Read properties at point 4 from C-1.

Work and efficiency are determined, in terms of the quantities given in C-1, as follows:

$$\frac{w^*}{J} = \frac{1 + F}{m_3}(H_3^\circ - H_4^\circ) - \frac{1}{29}(H_2^\circ - H_1^\circ) \tag{4-10}$$

$$\eta = \frac{w^*}{JFQ_c} \tag{4-11}$$

In gas turbines the ratio w/V_1, the work per unit volume of inlet air,

www.TechnicalBooksPDF.com

is more significant than mean effective pressure as an indicator of turbine effectiveness.

Values of efficiency and w/V_1 vs F_R and pressure ratio are given in refs 4.90–4.902.

IDEAL INLET AND EXHAUST PROCESSES

The fuel-air cycle can be extended to include idealized inlet and exhaust processes for any particular type of engine. Of particular interest is the idealized process for four-stroke engines.

Four-Stroke Ideal Process. In four-stroke carburetor engines the imep, hence the torque, is usually controlled by regulating the pressure in the inlet manifold. When this pressure is less than the pressure of the surrounding atmosphere the engine is said to be *throttled;* when it is substantially equal to the atmospheric pressure the engine is said to be operating *normally,* or at full *throttle.* When the inlet pressure is higher than that of the atmosphere the engine is said to be *supercharged.* These terms are used in connection with ideal cycles as well as actual engines.

As we have seen (Chapter 1), the pressures in the inlet and exhaust systems of real engines fluctuate with time. However, in the case of ideal inlet and exhaust processes these pressures are assumed to be steady. Such steady pressures are approached in the case of multi-cylinder engines or single-cylinder engines having inlet and exhaust *surge tanks* such as those illustrated in Fig 1-2.

Other assumptions used for idealized inlet and exhaust processes are as follows:

1. All processes are adiabatic
2. Valve events occur at top and bottom center
3. There is no change in cylinder volume while the pressure difference across an open valve falls to zero

Figure 4-4 shows typical diagrams of four-stroke idealized processes. The following description applies to any one of them, with appropriate intepretation.

At point 4 the exhaust valve opens to allow the exhaust gases to escape, and the pressure in the cylinder falls to the pressure p_e in the exhaust system. For the gases remaining in the cylinder this process is represented by the line 4–5. The volume of the remaining gases, however, is equal to V_1. The piston then returns on the exhaust stroke, forcing out additional exhaust gas at the constant pressure p_e. At top center

www.TechnicalBooksPDF.com

(point 6) the exhaust valve closes and the inlet valve opens. If p_e is not equal to p_i, there is flow of fresh mixture into the cylinder, or of residual gas into the inlet pipe, until the pressure in the cylinder is equal to the pressure in the inlet system (point 7). The piston then proceeds on the suction stroke until point 1 is reached, thus completing the cycle.

With our assumption of no heat transfer, the residual gas fraction of cycles of this character is fixed because the state of the residual gas remaining in the cylinder at the end of the exhaust stroke, point 6, is the same as its state at point 5 at the end of isentropic expansion of the gases in the cylinder to exhaust pressure. Since the volume of the residual gas remaining at the end of the exhaust stroke is equal to V_2, M_r for M lbm of charge can be found from the relation

$$M_r = M(V_2/V_5)$$

or

$$f = \frac{M_r}{M} = \frac{V_2}{V_5} \quad (4\text{-}12)$$

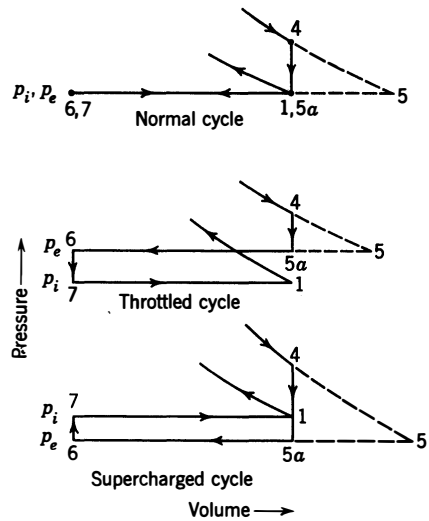

Fig 4-4. Ideal four-stroke inlet and exhaust processes: p_i = pressure in inlet system; p_e = pressure in exhaust system. (See Chapter 1 and Fig 1-2 for definition and measurement of p_i and p_e.)

In the normal idealized cycle there is no change in pressure of the residual gases when the exhaust valve closes and the inlet valve opens at point 6,7. In the throttled cycle, when the exhaust valve closes and the inlet valve opens, some of the residual gas flows back into the inlet system as the pressure in the cylinder falls to p_i. However, this gas is assumed to remain in the inlet pipe and to be returned to the cylinder during the first part of the inlet stroke. In the supercharged cycle the same valve events lead to a flow of fresh mixture into the cylinder, compressing the residual gas to p_i. Since the mass of residual gas is fixed at point 6 in each case, expression 4-12 holds for all three processes shown in Fig 4-4.

To find the characteristics of the charge at point 1 with the ideal inlet process, eq 1-16 can be used. For this purpose, let us take as the system the residual gases in the cylinder when the exhaust valve closes at the end of the exhaust process, point 6, and the fresh gases which

www.TechnicalBooksPDF.com

are about to enter the cylinder at p_i, V_i. The inlet process will be taken as that described by the paths 6–7–1 in Fig 4-4. Since velocities and heat transfer are assumed to be zero, we may write

$$(M_i + M_r)E_{s1} = M_iE_{si} + M_rE_{s6} - \frac{1}{J}\{-p_iV_i + p_1(V_1 - V_7)\} \tag{4-13}$$

Since $p_i = p_1$, $p_6 = p_e$, $V_6 = V_7 = V_2$, and $E_{s6} = E_{s5}$, we write

$$(M_i + M_r)H_{s1} = M_iH_{si} + M_rH_{s5} + \frac{V_2}{J}(p_i - p_e) \tag{4-14}$$

where M_i is the mass of fresh gas and M_r the mass of residual gas.

In order to use C-1 to solve eq 4-14, the unit-mass properties are multiplied by the appropriate molecular weights to give the properties of 1 mole. Since $f = M_r/(M_i + M_r)$, the resultant relation can be written

$$H_1^\circ = \frac{m_1}{m_i}(1 - f)H_i^\circ + \frac{m_1}{m_r}fH_5^\circ + V_2^\circ(p_i - p_e)\frac{144}{778} \tag{4-15}$$

in units of Btu, psia, and cubic feet.

When constructing cycles with idealized inlet processes the value of f may not be known in advance. In such cases it is necessary to take a trial value of f at point 1 and work out the cycle on this basis. If the trial value of f is not equal to V_2/V_5, a new value must be taken and the cycle recomputed; this process is repeated until the value of f determined by eq 4-12 agrees with the assumed value. Figure 4-5 gives values of f for idealized cycles of this kind so that within the range covered by this figure f can be evaluated closely from given values of r, F_R, p_e/p_i, and T_i. For example, suppose $r=8$, $F_R=1.2$, $T_i=800°$R, and $p_e/p_i=2.0$. From Fig 4-5 (ee), at $F_R=1.175$, $r=6$, $T_i=600$, $p_e/p_i=2$, $f=0.085$. Correcting for $r=8$ from (hh), $f=0.085\times0.03/0.04=0.064$. Correcting for $T_i=800$ from (ff), $f=0.064\times0.054/0.043=0.08$, which should be close to the proper value found by constructing the whole cycle. Example 4-1*a* shows how a fuel-air cycle with idealized inlet process is constructed.

Volumetric Efficiency. A very useful parameter in work with four-stroke reciprocating engines is the *volumetric efficiency*, defined as follows:

$$e_v = \frac{M_i}{(V_1 - V_2)\rho_i} \tag{4-16}$$

where M_i is the mass of fresh mixture supplied and ρ_i is the density of

www.TechnicalBooksPDF.com

the mixture at the pressure p_i and the temperature T_i. It is evident that the quantity $(V_1 - V_2)\rho_i$ is the mass of fresh mixture which would just fill the *piston displacement* at the density in the inlet system. For real engines this parameter is fully discussed in Chapter 6.

For fuel-air cycles the mass inducted is $(1 - f)$ times the mass base of the charts, so that for use with C-1 we can write

$$e_v = \frac{(1 - f)V_i^\circ}{V_1^\circ - V_2^\circ} \times \frac{m_1}{m_i} \tag{4-17}$$

where V_i° is the volume of 1 lb mole of fresh mixture at the pressure and temperature in the inlet manifold. Values of e_v are plotted in Fig 6-5, p. 157. It is evident that for the ideal four-stroke inlet process e_v is approximately equal to unity unless the exhaust and inlet pressures are not equal.

Pumping Work. Since, in the ideal process, both inlet and exhaust strokes take place at constant pressure, the work done on the piston during the inlet stroke is

$$w_i = p_i(V_1 - V_2) \tag{4-18}$$

and the work done on the piston during the exhaust stroke is

$$w_e = p_e(V_2 - V_1) \tag{4-19}$$

w_i and w_e are called the work of the inlet and exhaust strokes, respectively. The algebraic sum of these two, called the *pumping work*, w_p, may be expressed as follows:

$$w_p = (p_i - p_e)(V_1 - V_2) \tag{4-20}$$

When the inlet pressure is higher than the exhaust pressure pumping work is positive; that is, net work is done *by* the gases.

Pumping mep. Since mep is work divided by piston displacement, the mean effective pressures corresponding to the above equations are

$$\text{mep}_i = p_i \tag{4-21}$$

$$\text{mep}_e = p_e \tag{4-22}$$

$$\text{mep}_p = p_i - p_e \tag{4-23}$$

Net mep. We recall that mep has been defined on the basis of the compression and expansion strokes only; if we wish to take account of

www.TechnicalBooksPDF.com

the pumping mep, it is convenient to define the net mep as

$$\text{mep}_n = \text{mep} + \text{mep}_p$$

or, for the ideal process,

$$\text{mep}_n = \text{mep} + (p_i - p_e) \tag{4-24}$$

Efficiency based on net mep is called *net efficiency* and is evidently

$$\eta_n = \eta_i \frac{\text{mep}_n}{\text{mep}}$$

$$= \eta_i \left(1 + \frac{p_i - p_e}{\text{mep}}\right) \tag{4-25}$$

IDEAL TWO-STROKE INLET AND EXHAUST PROCESSES

Chapter 7 discusses two-stroke engines in considerable detail. In this type of engine (see Fig 7-1), near the bottom-center position of the piston, both inlet and exhaust ports are opened. The inlet pressure is higher than the exhaust pressure, so that when the ports open there is a flow of fresh mixture into the cylinder which causes exhaust gases to flow out. This process is called *scavenging*. The quantity of fresh mixture remaining in the cylinder at the end of the scavenging process depends on many factors which are fully discussed in Chapter 7.

For two-stroke engines the ideal process is based on the following assumptions:

1. The flow of fresh mixture into the cylinder, and of exhaust gas out of the cylinder, takes place at bottom dead center (volume V_1 of Fig 4-1) at the constant pressure p_1.
2. The process is adiabatic; that is, there is no exchange of heat between gases and engine parts.

The residual-gas content in the two-stroke engine is determined entirely by the scavenging process and is *not* related to the volume ratio V_2/V_5, as in the case of four-stroke engines. Thus the value of f may be taken as an independent given quantity in problems dealing with two-stroke engines. Since two-stroke engines may have much larger frac-

www.TechnicalBooksPDF.com

tions of residual gas than four-stroke engines, it is of interest to compute a cycle corresponding to example 4-1 but with a much larger value of f. Example 4-2 illustrates such a computation.

CHARACTERISTICS OF FUEL-AIR CYCLES

Figure 4-5 gives characteristics of constant-volume fuel-air cycles over a wide range of values of r, F_R, p_1, T_1, f, and h.

The data are presented in dimensionless form as far as is practicable. By means of these data, it is possible to construct cycles of this type very quickly. Numbered points are obtained directly from Fig 4-5. Only the lines connecting the numbered points need to be taken from the thermodynamic charts.

Figure 4-6 gives data similar to those of Fig 4-5 for the limited-pressure fuel-air cycle except that the ideal four-stroke inlet process was used for this figure. These data are limited to $T_i = 520°\text{R}$ and $p_e/p_i = 1.0$.

In Figs 4-5 and 4-6 the mep and efficiency values are based on the work of compression and expansion only. Net mep and net efficiency may easily be computed from eqs 4-24 and 4-25.

In addition to the general characteristics of these cycles, already discussed, the following trends are worthy of notice:

1. Initial pressure, p_1, has a very small effect on efficiency except near $F_R = 1.0$ with $p_1 < 1$ atmosphere.
2. Efficiency decreases with increasing values of T_1, because of increasing temperatures throughout the cycle.
3. Residual gas up to $f = 0.15$ and water vapor up to $h = 0.06$ have negligible effects on efficiency.

With both the efficiency and the conditions at point 1 known, from eqs 3-7, 4-3, and 4-4,

$$\frac{\text{mep}}{p_1} = \frac{Jm_1}{RT_1}(FQ_c\eta)\left(\frac{1-f}{1+F+h(1-f)}\right) \qquad (4\text{-}25a)$$

When T_1 is in degrees Rankine and Q_c in Btu per lbm, $J/R = 0.503$.

www.TechnicalBooksPDF.com

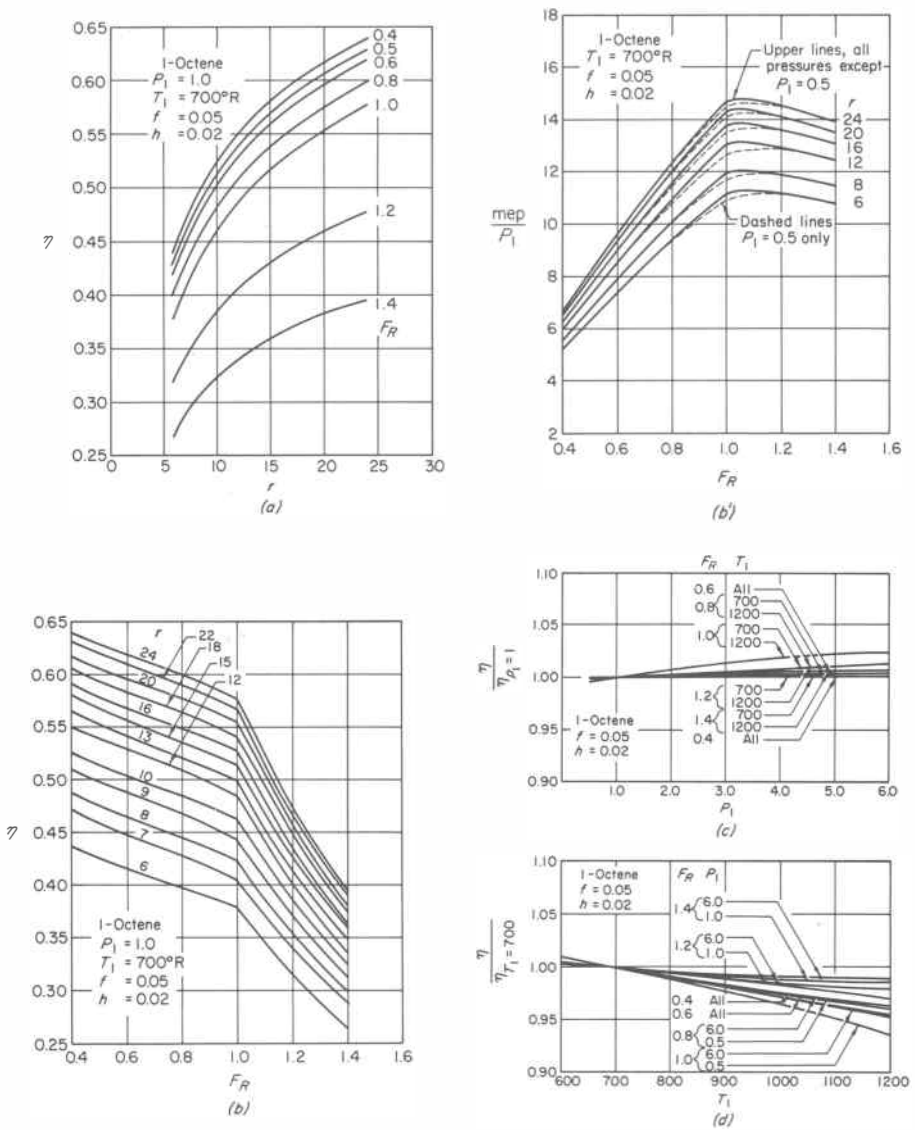

Fig 4-5. Characteristics of constant-volume fuel-air cycles with 1-octene fuel. (Edson and Taylor, ref 14.1)

www.TechnicalBooksPDF.com

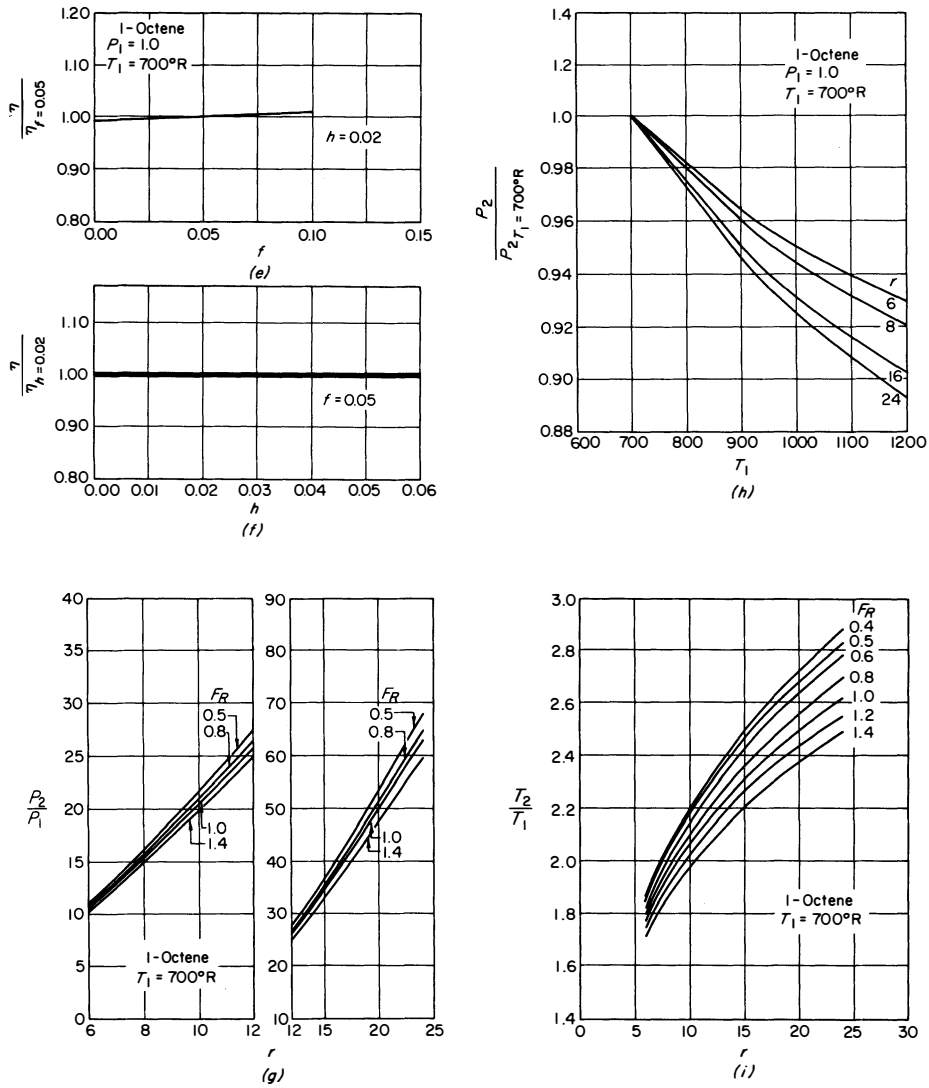

Fig 4-5. (*Continued*).

www.TechnicalBooksPDF.com

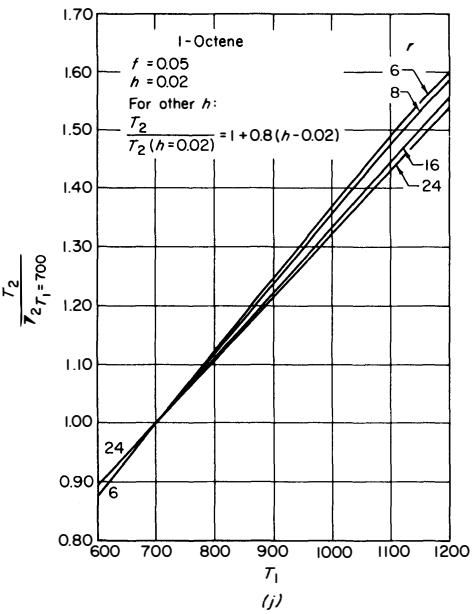

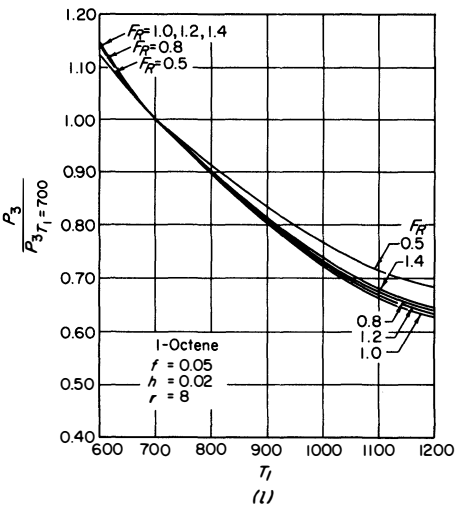

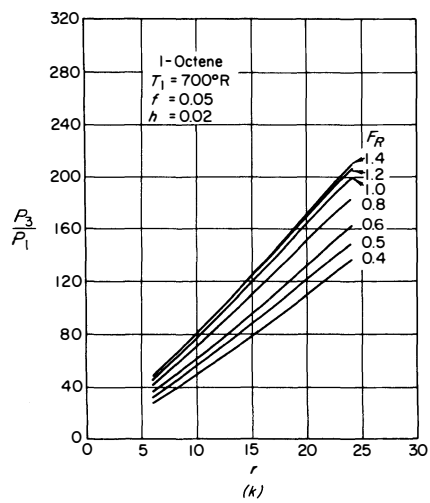

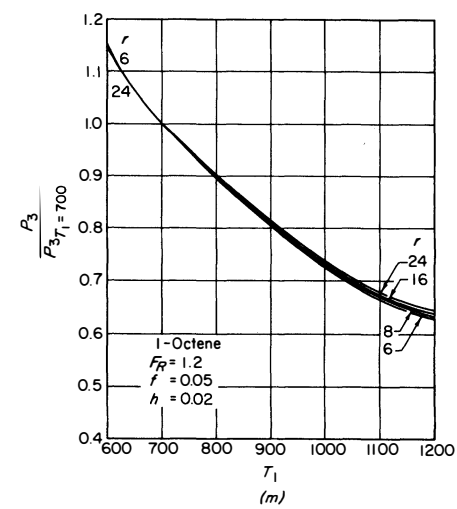

Fig 4-5. (*Continued*).

www.TechnicalBooksPDF.com

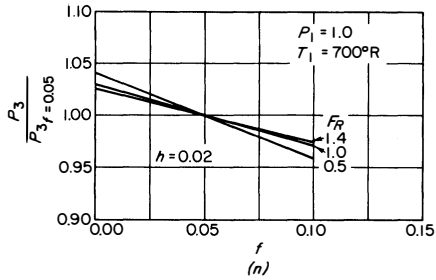

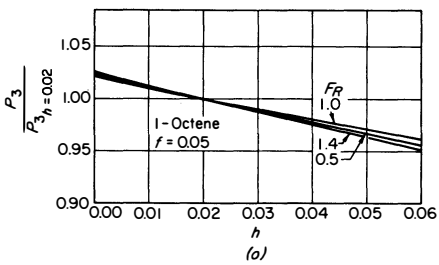

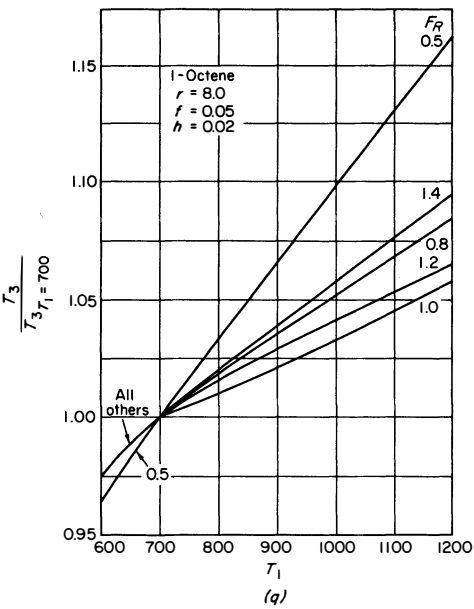

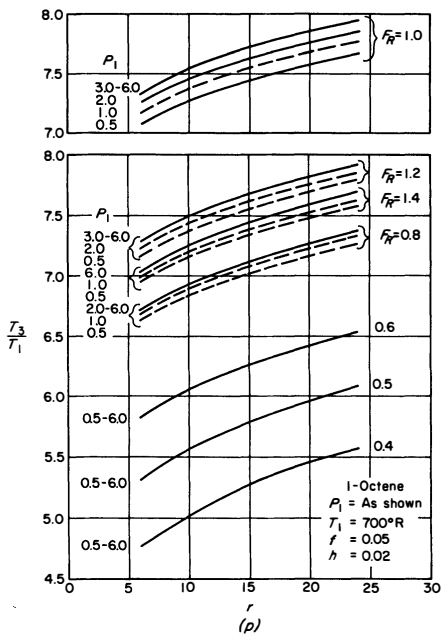

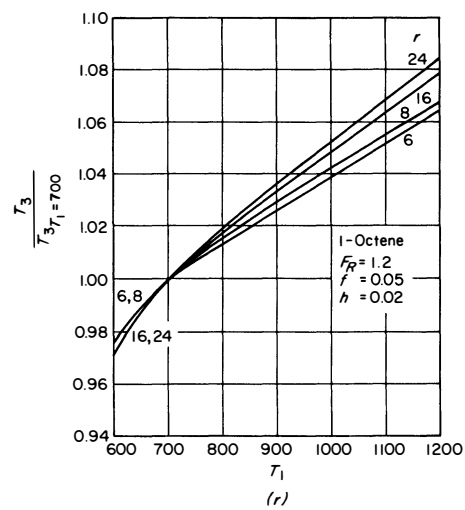

Fig 4-5. (*Continued*).

www.TechnicalBooksPDF.com

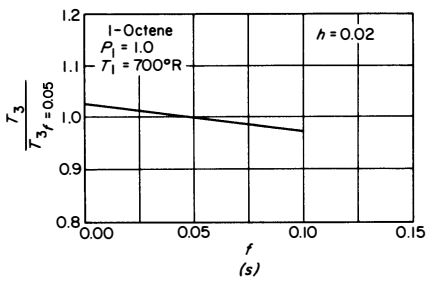

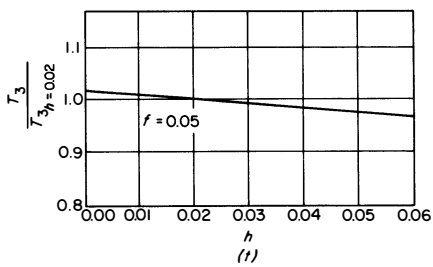

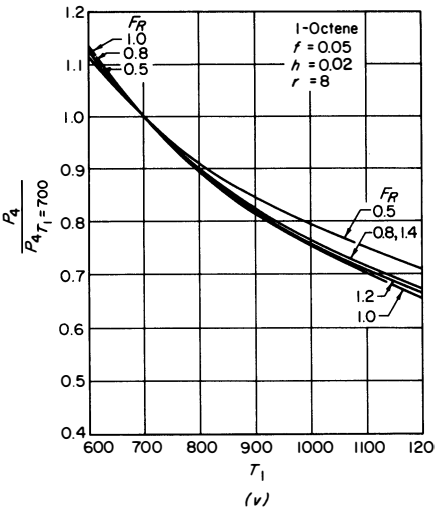

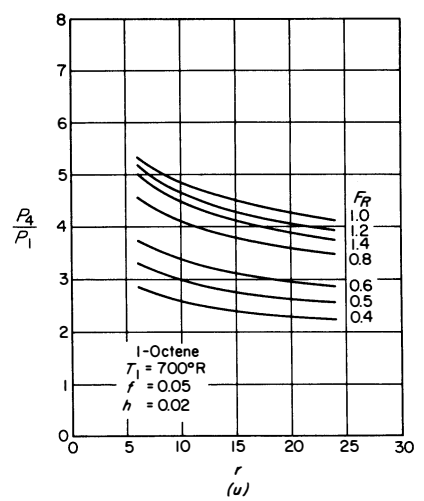

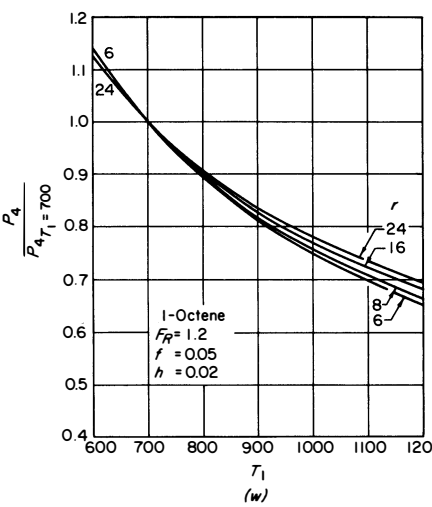

Fig 4-5. (*Continued*).

www.TechnicalBooksPDF.com

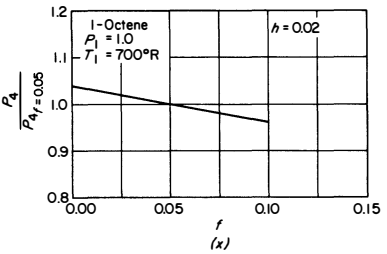

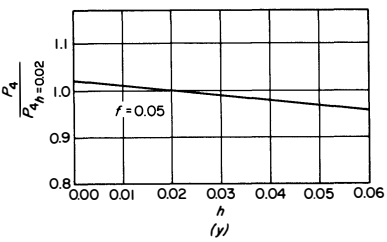

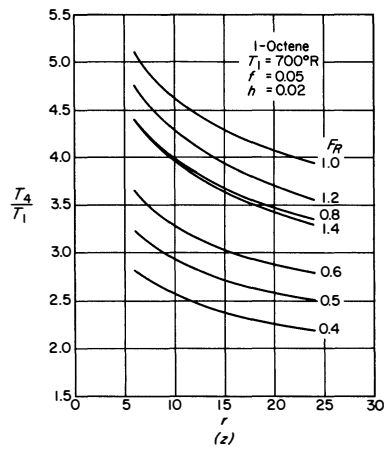

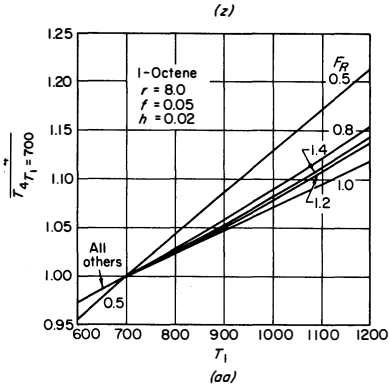

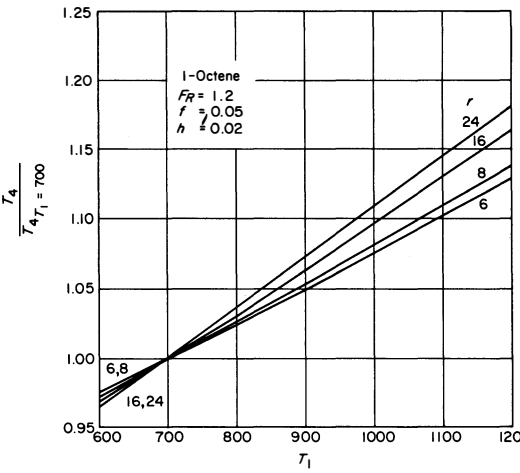

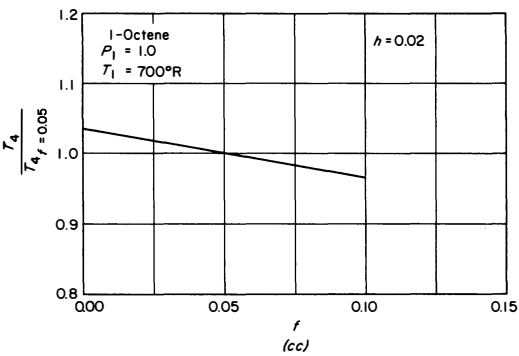

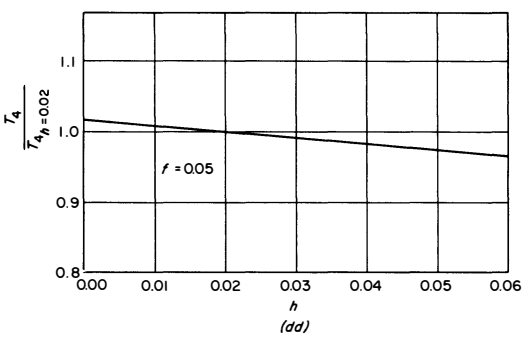

Fig 4-5 (*Continued*).

www.TechnicalBooksPDF.com

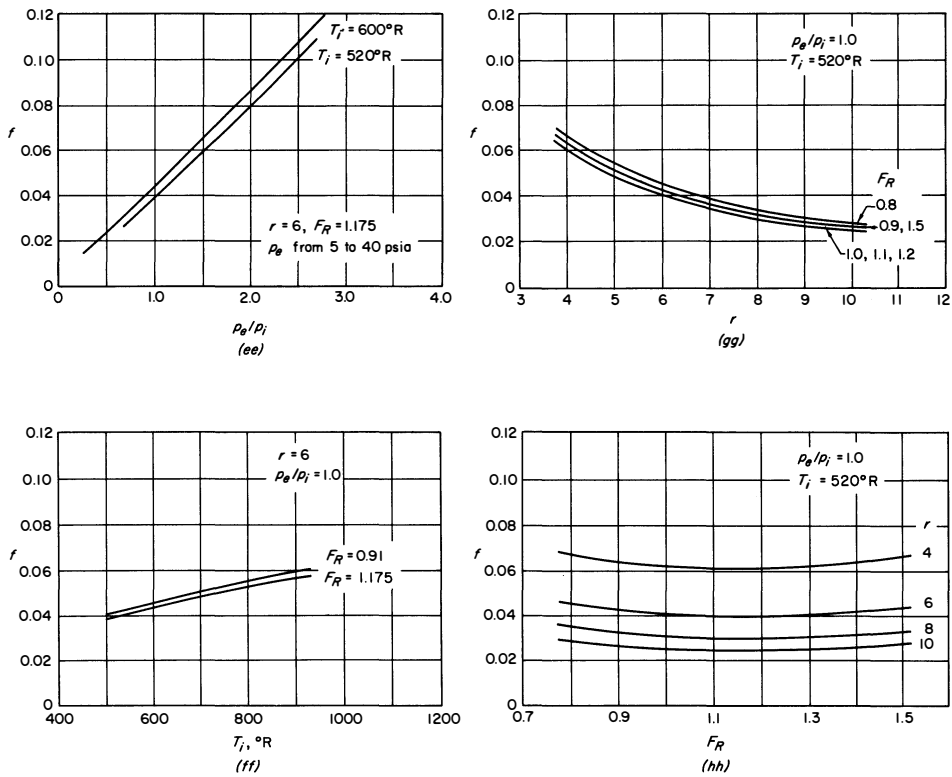

Curves for f with ideal four-stroke inlet process (from ref 1.10).

Fig 4-5 (*Continued*).

EQUIVALENT FUEL-AIR CYCLES

A fuel-air cycle having the same charge composition and density as an actual cycle is called the *equivalent* fuel-air cycle. Such cycles are of special interest, since they minimize differences resulting from the fact that the inlet and exhaust processes of a real engine are not the same as those proposed for the ideal inlet and exhaust processes.

In order to construct a fuel-air cycle on this basis, there must be available an indicator diagram for the actual cycle, such as Fig 4-7, as well as a

www.TechnicalBooksPDF.com

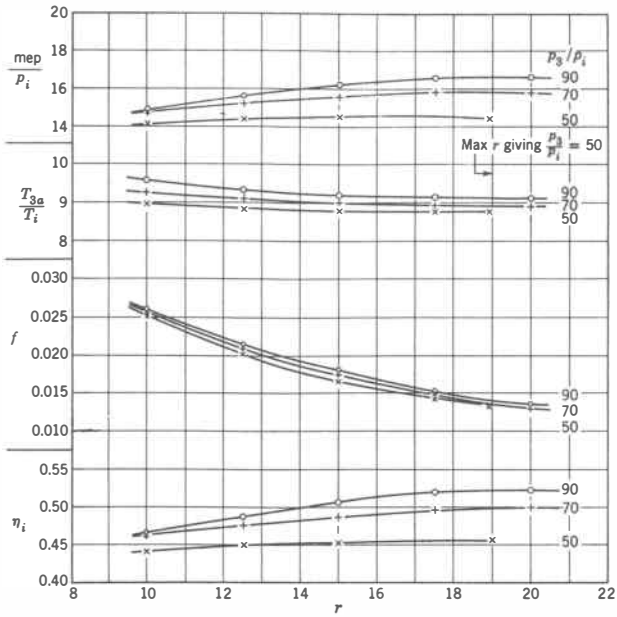

Part 1 $F_R = 0.91$

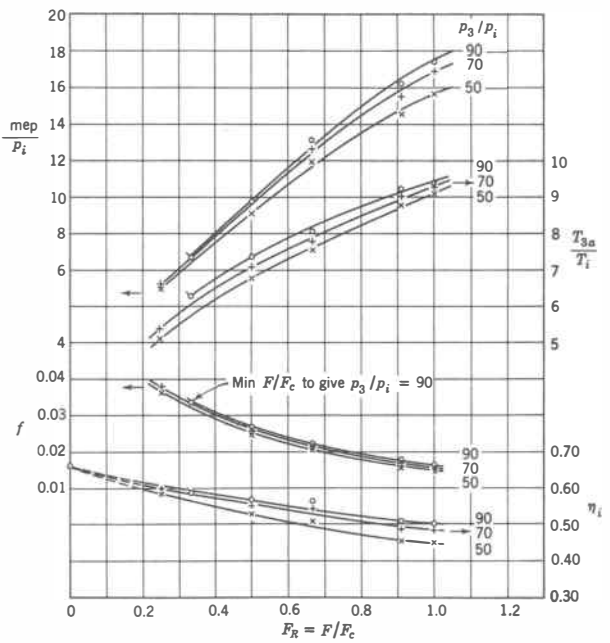

Part 2 $r = 15$

Fig 4-6. Limited-pressure fuel-air cycle characteristics: $T_i = 520°\text{R}$; $p_i = p_e = 14.7$ psia. (Computed from data in ref 3.43)

www.TechnicalBooksPDF.com

measurement of the mass of fresh air retained in the cylinder, per cycle, while the indicator diagram is being taken.

The composition and density in the equivalent fuel-air cycle is taken as the same as that in the corresponding actual cycle. Thus, at corresponding points in the two cycles, V/M, F, and f will be the same, where M is the mass of the charge.

At a given point between inlet closing and ignition, such as x in Fig 4-7, it is assumed that pressure and temperature will be the same in both

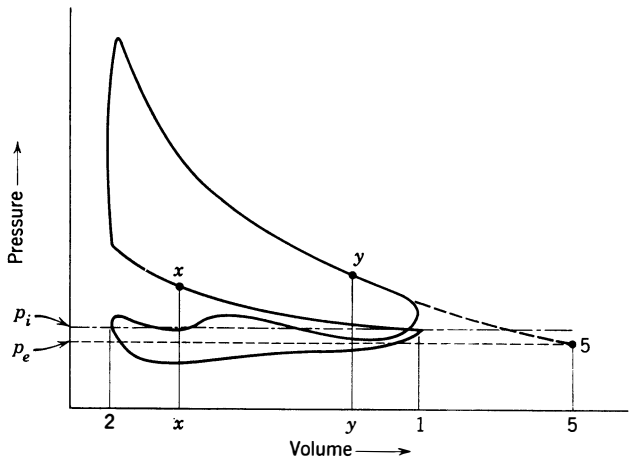

Fig 4-7. Method of correlating a fuel-air cycle with an actual cycle in order to establish equivalence.

cycles. If a temperature measurement is available, as by means of the sound-velocity apparatus described in ref 4.91, and the fuel-air ratio is known, the point corresponding to x on the appropriate thermodynamic chart can be located directly. If the temperature is not known, the chart volume at point x may be found from the following expression:

$$\frac{V_x}{V_{cx}} = \frac{M}{M_c} = \frac{M_a'(1 + F_x)}{(1 - f)M_c} \tag{4-26}$$

where, for the actual cycle,

V_x = cylinder volume above piston at point x
M = mass of charge after valves close
M_a' = the mass of fresh air retained per cycle
F_x = the fuel-air ratio at point x

www.TechnicalBooksPDF.com

For the thermodynamic chart V_{cx} is the chart volume at the point corresponding to x of the real cycle.

M_c is the mass base of the thermodynamic chart. In C-1 this is the molecular weight of the charge in pounds. For C-2, C-3, and C-4 it is $(1 + F)$ lbm, where F is the *chart* fuel-air ratio. (If a chart is not available for fuel-air ratio F_x, use the chart on which F is nearest F_x.)

Determination of M_a'. In four-stroke engines in which $p_e \geqq p_i$, or in which the *valve overlap* (see Chapter 6) is small, all the fresh air supplied is retained in the cylinder and M_a' is equal to M_a, the air *supplied* to the cylinder for one suction stroke. M_a is easily measured by means of an orifice meter.

In two-stroke engines, or four-stroke engines with considerable valve overlap and $p_e < p_i$, there is often an appreciable flow of fresh air out of the exhaust valves (or ports) while both valves are open. In such cases $M_a' < M_a$. Chapters 6 and 7 discuss the problem of measuring or estimating M_a' under such circumstances.

Determination of F_x. In carbureted engines, that is, in engines supplied with fuel through the inlet valve, $F_x = M_f/M_a'$, where M_f is the mass of fuel supplied per cycle. For four-stroke engines with small valve overlap, $F_x = F$, where F is the mass ratio of fuel and air supplied to the engine.

For engines in which the fuel is injected after the point x, F_x is zero, and the thermodynamic chart used must be for air and residual gases only. Diesel engines are an example of this type.

Determination of f for Real Cycles. The residual fraction must be determined for the real cycle not only for use in eq 4-26 but also for computing the internal energy of combustion. One possible method is to sample the gases during compression and to analyze them for CO_2. If the mass fraction* of CO_2 is determined at point x, f is equal to this fraction divided by the mass fraction of CO_2 in the residual gases before mixing. The latter fraction is a function of fuel-air ratio and is given in Fig 4-8.

Another method of determining f is available if the temperature of the gases at point x is known. Thus we can write

$$p_x V_x = \frac{M_a'(1 + F_x)}{(1 - f)m} RT_x \tag{4-27}$$

* *Note:* In analyzing gases by the Orsat apparatus, or its equivalent, percentages by volume with the water vapor condensed are usually found. These must be converted to a mass basis, including the water vapor in the gases.

www.TechnicalBooksPDF.com

Values of m, the molecular weight of fuel-air mixtures with various values of f, are given in Fig 3-5.

A method has been developed (see refs 4.91–4.92) by means of which a reasonably accurate temperature measurement in the cylinder gases can be made. Figure 4-9 shows values of f computed from eq 4-27 by using such measurements. The curves show that the residual fraction

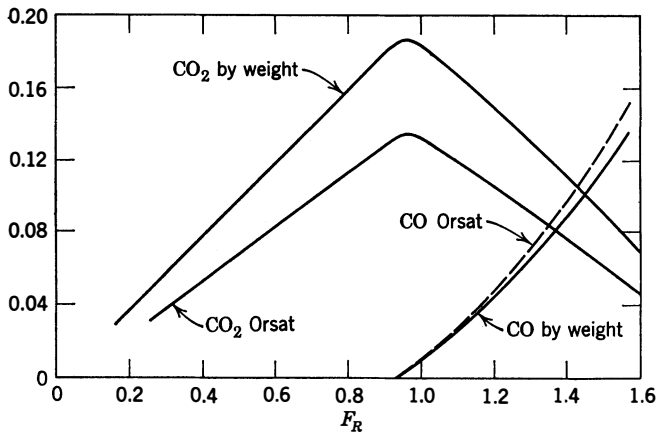

Fig 4-8. Carbon dioxide and monoxide content of combustion products for gasoline and Diesel engines. (D'Alleva and Lovell, ref 4.81, and Houtsma et al., ref 4.82)

in a real engine tends to be much larger than that for the ideal induction process. The reasons for this relation include

1. Heat losses during the expansion and exhaust strokes which result in lower residual-gas temperature than in the ideal process.
2. Resistance to flow through the exhaust valve which may cause residual pressure to be higher and the charge pressure to be lower than in the ideal process.

It is thus evident that residual-gas density will be greater in the actual than in the ideal process. Furthermore, pressure loss and heating as the fresh mixture passes through the inlet valve will reduce the density of the fresh mixture below that for the ideal process.

In general, two-stroke engines will have larger fractions of residual gas than four-stroke engines under similar circumstances. Chapters 6 and 7 discuss these questions in more complete detail.

www.TechnicalBooksPDF.com

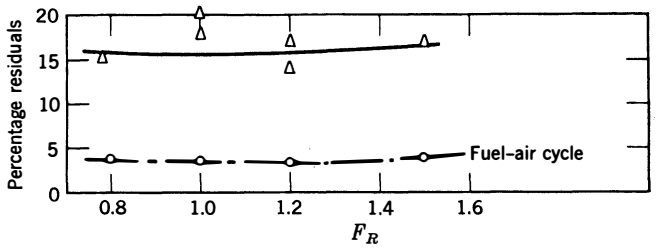

Effect of fuel–air ratio on residual percentage

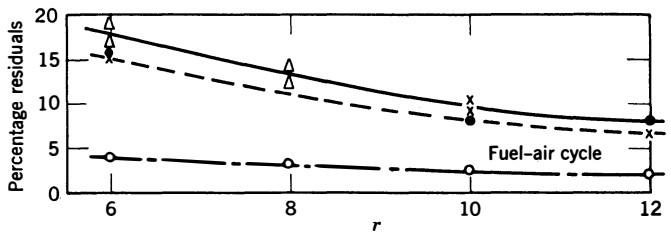

Effect of compression ratio on residual percentage

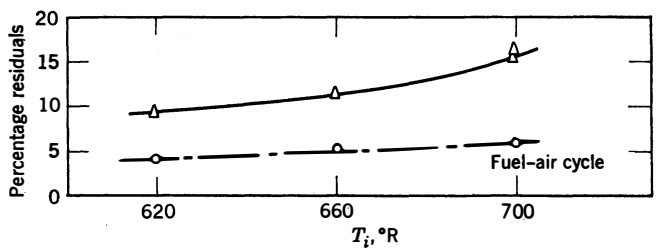

Effect of inlet temperature on residual percentage

o Ideal cycle, ref 5.17
• x Δ Based on sound-velocity-method measurements, ref 5.15

Fig 4-9. Comparison of residual-gas fraction for fuel-air cycles with the ideal four-stroke inlet process with measured values.

AIR CYCLES AND FUEL-AIR CYCLES COMPARED

In addition to the constant-volume fuel-air cycle already described, Fig 4-1 shows two other constant-volume cycles having the same compression ratio and initial conditions:

$$p_1 = 14.7, \qquad T_1 = 600, \qquad r = 8$$

www.TechnicalBooksPDF.com

Cycle a is an air cycle with $C_p = 0.24$, $k = 1.4$.

Cycle b is an air cycle with the actual specific heat of air which varies with temperature, as indicated in Fig 3-3.

Cycle c is the constant-volume fuel-air cycle with octene fuel, $F_R = 1.2$, $f = 0.05$, $r = 8$ already described and computed in example 4-1.

In order to make the cycles comparable, the addition of heat between points 2 and 3 of the air cycles is made equal to the energy of combustion of the fuel in the fuel-air cycle; that is,

$$Q' = (1 - f)FE_c/(1 + F) = 1370 \text{ Btu/lbm} \qquad (4\text{-}28)$$

in which Q' is the heat added per lbm air between points 2 and 3 of cycles a and b, and E_c is the internal energy of combustion of octene, 19,180 Btu/lbm.

The differences between cycles a and b are due entirely to the differences in specific heat.

Since the specific heat characteristics of the fuel-air cycle are nearly the same as those of cycle b, the differences between cycles b and c are caused chiefly by the changes in chemical composition which occur in the fuel-air cycle after point 2 is reached.

We have seen that the value of E_c is based on complete reaction of the fuel to CO_2 and H_2O. However, in the fuel-air cycle chemical equilibrium at point 3 is reached before combustion to CO_2 and H_2O is complete. (Figure 3-6 shows chemical compositions in the range of point 3 of Fig 4-1.) Thus in cycle c not all of the chemical energy of the fuel has been released at point 3 and temperature T_3 is lower than in cycle b.

Change in Number of Molecules. The reaction which occurs between points 2 and 3 of the fuel-air cycle usually involves a change in the number of molecules and, therefore, a change in molecular weight.

Referring to eq 4-5, because the same pressure and temperature are chosen at point 1, M/V is substantially * the same for corresponding points in all three cycles. Although T_3 is lower in cycle c than in cycle b, due to incomplete chemical reaction, the pressures at point 3 in the two cycles are not proportional to the temperatures because of the change in molecular weight in cycle c. For the particular fuel and fuel-air ratio used in this cycle there is an increase in the number of molecules (a decrease in m) during combustion which causes the pressure p_3 to be higher than it would be for a constant molecular weight.

* At point 1 in all three cycles $M/V = pm/RT$. The molecular weight for the air cycles is 29 and for the fuel-air cycle, 30.5.

www.TechnicalBooksPDF.com

Table 3-1 (p. 46) shows the change in molecular weight due to combustion for a number of fuels. For the usual petroleum fuels a decrease in molecular weight due to combustion is typical.

Expansion. For the expansion line of the air cycle pV^k is constant. In the modified air cycle k increases as the temperature falls, and curve b approaches that of the air cycle at point 4.

In the fuel-air cycles, in addition to an increasing k, chemical reaction becomes more complete as expansion proceeds and the various con-

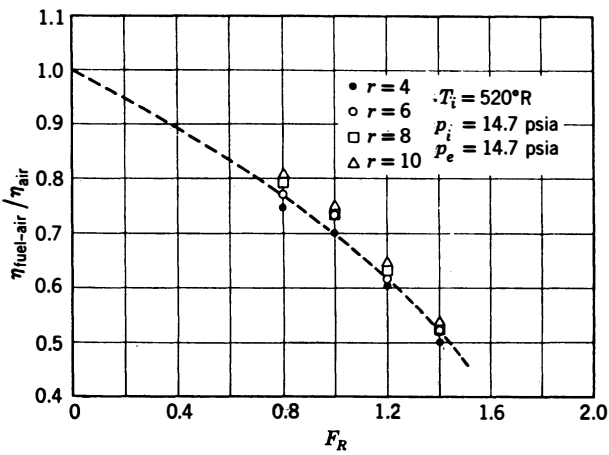

Fig 4-10. Ratio of fuel-air-cycle to air-cycle efficiencies.

stituents in the charge react toward CO_2, H_2O, and N_2. At point 4 in the fuel-air cycle these reactions are virtually complete.

It is interesting to note that the pressure of all three cycles is nearly the same at point 4.

Figure 4-1 can be taken as representative in a qualitative sense, but the magnitude of the differences between fuel-air cycles and the corresponding air cycles will depend on the following conditions:

1. Character of the cycle
2. Fuel-air ratio
3. Compression ratio
4. Chemical composition of the fuel

In order to evaluate them in any particular case, the fuel-air cycle must be constructed from data on the thermodynamic properties of the fuel-air mixture in question.

Figure 4-10 shows the ratio of fuel-air cycle to air cycle efficiency as a function of compression ratio and fuel-air ratio. The ratio of fuel-air

www.TechnicalBooksPDF.com

cycle efficiency to air cycle efficiency increases slightly with increasing compression ratio because most of the chemical reactions involved tend to be more complete as the pressure increases. The fuel-air cycle efficiency approaches air cycle efficiency as the amount of fuel becomes extremely small compared with the amount of air. With a very low fuel-air ratio, the medium would consist, substantially, of air throughout the cycle; and, since the temperature range would be small, the air would behave very nearly as a perfect gas with constant specific heat. The air cycle efficiency thus constitutes a limit which the efficiency of the fuel-air cycle approaches as the fuel-air ratio decreases.

The foregoing comparison is based on the constant-volume cycle, but similar considerations apply to other types of cycle. When combustion at constant pressure is involved, as in limited-pressure and gas-turbine cycles, the volume at the end of combustion will be less in the fuel-air cycle, as compared to the air cycle, for the same reasons that the pressure is less with constant-volume combustion. Figures 4-2 and 4-3 illustrate this difference.

Effect of Fuel Composition. Except for small differences due to the heat of dissociation of the fuel molecule, mixtures of air with hydrocarbon fuels having the same atomic ratio between hydrogen and carbon will have the same thermodynamic characteristics of the *combustion products* at the same value of F_R. Thus C-2, C-3, and C-4 for C_8H_{16} are accurate, within the limits of reading the curves, with any fuel having a composition near C_nH_{2n}.

On the other hand, the molecular weight of the *unburned* mixture will be affected by the molecular weight of the fuel. This effect will be appreciable when the molecular weight is very different from that of C_8H_{16}. In such cases the molecular weight of the unburned mixture must be computed from eq 3-13.

Goodenough and Baker (ref 4.1) and Tsien and Hottel (ref 4.2) have investigated the effect of a change from C_8H_{18} to $C_{12}H_{26}$ and from C_8H_{18} to C_6H_6, respectively, on the characteristics of the products of combustion. In both cases the differences attributable to fuel composition appeared to be within the probable error of the calculations. This conclusion is in accordance with actual experience, which indicates substantially the same performance with various liquid petroleum products when the relative fuel-air ratio and air density at point 1 are held the same. More extreme differences in fuel composition will, of course, alter the thermodynamic properties sufficiently to cause appreciable differences in the fuel-air cycle. The bibliography for Chapter 3 refers to thermodynamic charts of a number of fuels outside the range of the charts for C_8H_{16}. See especially refs 4.94, 14.2, and 14.6.

www.TechnicalBooksPDF.com

Exhaust-Gas Characteristics of Fuel-Air Cycles

Consider the steady-flow system from inlet receiver i to the exhaust receiver e in Fig 1-2. From expression 1-18, for a unit mass of gas,

$$H_e - H_i = Q - \frac{w}{J} \tag{4-29}$$

where w is the work done by the gases between the two receivers. This work must include the work of inlet and exhaust strokes in the case of a four-stroke engine as well as the indicated work of scavenging (negative) in the case of a two-stroke engine. In the case of fuel-air cycles, Q is taken as zero. For a fuel-air cycle with ideal inlet and exhaust processes,

$$\frac{w^*}{J} = (1 - f)FQ_c\eta + (p_i - p_e)(V_1^* - V_2^*)/J \tag{4-30}$$

COMPARISON OF REAL AND FUEL-AIR CYCLES

Comparison of real cycles and fuel-air cycles is the subject of exhaustive treatment in Chapter 5.

ILLUSTRATIVE EXAMPLES

Example 4-1. Constant-volume fuel-air cycle (Fig 4-1).
Given Conditions:

$$F_R = 1.2, \quad r = 8, \quad f = 0.05, \quad p_1 = 14.7, \quad T_1 = 600$$

Preliminary Computations:

$$F = 1.2 \times 0.0678 = 0.0813$$

$$(1 + F)/m \quad \text{from Fig 3-7} \quad = 0.0355$$

$$m = 1.0813/0.0355 = 30.5$$

www.TechnicalBooksPDF.com

Point 1: On C-1 at $p = 14.7$, $T = 600$, $F_R = 1.2$, $f = 0.05$, read

$$V_1^\circ = 440, \qquad E_1^\circ = 220, \qquad H_1^\circ = 1430$$

Process 1–2: $V_2^\circ = V_1^\circ/8 = 55$. From point 1 follow a line of constant entropy to $V_2^\circ = 55$. This line is parallel to the $F_R = 1.2$, $f = 0.05$ line at the left of C-1. At the intersection of this line with various volume lines, record pressures and plot as in Fig 4-1. At $V_2^\circ = 55$, read

$$T_2 = 1180, \qquad p_2 = 230, \qquad E_2^\circ = 3810, \qquad H_2^\circ = 6200$$

Process 2–3 and Transfer to C-4: Since point 3 is to be read from C-4, we compute values of point 3 for a mass of $(1 + F)$ lb. Thus

$V_2^* = 55 \times 0.0355 = 1.95$. From eq 4-1

$E_3^* = (0.0355 \times 3810) + 0.95(0.0813)(19{,}180) + 0.05(336) = 1622$

On C-4, at $E^* = 1622$ and $V^* = 1.95$, read

$$T_3 = 5030, \qquad p_3 = 1100, \qquad H_3^* = 2012$$

Process 3–4. Expansion: On C-4, follow an isentropic (vertical) line from point 3 to $V^* = 8 \times 1.95 = 15.6$ and read

$$T_4 = 3060, \qquad p_4 = 83, \qquad E_4^* = 969, \qquad H_4^* = 1215$$

The pressures and volumes along the line 3–4 are read and plotted as in Fig 4-1.

Residual Gases: These are assumed to expand isentropically from point 4 to the exhaust pressure. Taking p_e as equal to $p_i = 14.7$ and continuing the isentropic expansion to this pressure, we read, at point 5,

$$T_5 = 2100, \qquad V_5^* = 60, \qquad E_5^* = 700, \qquad H_5^* = 863$$

Work, mep and Efficiency:
From eq 4-2,

$$\frac{w^*}{J} = (1622 - 969) - 0.0355(3810 - 220) = 522 \text{ Btu}$$

From eq 4-3,

$$\text{mep} = \frac{778}{144}\left(\frac{522}{15.6 - 1.95}\right) = 206 \text{ psi}$$

From eq 4-4,

$$\eta = 522/0.95(0.0813)19{,}035 = 0.355$$

Summary of Example 4-1:

Point	p	T	V°	V^*	E°	E^*	H°	H^*
1	14.7	600	440	15.6	220	7.8	1430	51
2	230	1180	55	1.95	3810	135	6200	220
3	1100	5030	55	1.95	—	1622	—	2012
4	83	3060	440	15.6	—	969	—	1215
5	14.7	2100	—	60	—	700	—	863

www.TechnicalBooksPDF.com

$$\frac{w^*}{J} = 522 \text{ Btu} \qquad \frac{1+F}{m} = 0.0355$$

$$\text{mep} = 206 \text{ psi} \qquad m = 30.5$$

$$\eta = 0.355$$

Example 4-1a. Fuel-Air Cycle with Idealized Inlet Process. Same as example 4-1, except that T_1 and f are not given. T_i is given as 600°R, and the cycle is assumed to have the idealized four-stroke inlet process previously described. p_e is given as 14.7.

Estimate of f. The induction process occurs at $p_e/p_1 = 1.0$. From Fig 4-5 (*hh*), at $T_i = 520$, $F_R = 1.20$ and $r = 8$, $f = 0.030$. Correcting this value to $T_i = 600$ from (*ff*) gives

$$f = 0.030(0.045/0.04) = 0.034$$

Estimate of T_5. For the cycle of example 4-1 with $T_1 = 600$, we found that $T_5 = 2100$. Take 2280 as a trial value for the present example.

Computation of T_1. The residual gases mix with the fresh mixture at the constant pressure $p_i = p_1$. For this process

$$H_1^\circ = (1 - f)\, H_m^\circ + f H_5^\circ \dagger$$

where m refers to the fresh mixture. From C-1 at 600°R, $H_m^\circ = 1430$, and at $p_5 = 14.7$, $T_5 = 2280$°R, $H^\circ_5 = 14{,}700$, $V_5^\circ = 1750$

$$H_1^\circ = 0.966(1430) + 0.034(14{,}700) = 1867$$

From C-1, at $F_R = 1.2$, $H_1^\circ = 1867$, read $T_1 = 660$°F, $E_1^\circ = 570$, $V_1^\circ = 490$. At $r = 8$, $V_2 = 490/8 = 61.3$. The actual fraction of residual gas = $61.3/1750 = 0.035$ which is reasonably close to the original assumption. For condition at point 1, take $T_1 = 660$, $f = 0.034$. From this point the cycle is constructed as in example 4-1, with the following results:

Point	p	T	V°	V^*	E°	E^*	H°	H^*
1	14.7	660	490	17.35	570	20.2	1867	66
2	217	1225	61.3	2.17	4100	145	6530	231
3	1000	5150	—	2.17	—	1663(1)	—	2060
4	76	3165	—	17.35	—	997	—	1235
5	14.7	2215	—	64.0	—	730	—	903(2)

$$\frac{w^*}{J} = 541 \text{ Btu for } (1+F) \text{ lbm}$$

$$\text{mep} = 193 \text{ psi}$$

$$\eta = 0.362$$

(1) $E_3^* = 145 + 0.966(0.0813)(19{,}180) + 0.034(336) = 1663.$

(2) $E_5^* = 730$, $H_5^* = 730 + \dfrac{14.7 \times 64 \times 144}{778} = 903.$

†Referring to equation (4–15), $(p_i - p_e) = 0$ and the molecular weight ratios are nearly 1.0.

www.TechnicalBooksPDF.com

From eq 4-12, we compute the residual-gas fraction: $f = 2.17/64 = 0.034$. The computed values of f and T_1 agree well with the estimated values. If this agreement had not been obtained, it would have been necessary to recompute the cycle, using the computed values of T_5 and f, and to repeat this process until agreement with computed and estimated values was established.

The efficiency is little changed from example 4-1, and the mep is nearly in proportion to the air density at point 1, that is, to $(1 - f)/T_1$.

Example 4-2. Same as example 4-1, except that $f = 0.10$. The method is the same as in example 4-1. The results are as follows:

Point	p	T	$V°$	$V*$	$E°$	$E*$	$H°$	$H*$
1	14.7	600	440	15.7	220	7.8	1430	51
2	232	1185	55	1.95	3810	135	6210	220
3	1040	4850	55	1.95	—	1538	—	1915
4	79	3010	440	15.7	—	925	—	1150
5	14.7	2100	—	60	—	675	—	833

$\frac{w^*}{J} = 486$ Btu $\qquad \frac{(1+F)}{m} = 0.0357$

mep = 192 psi $\qquad m = 30.3$

$\eta = 0.348$

As compared to example 4-1 (5% residuals), maximum pressure and mep are lower because of the smaller quantity of fuel-air mixture per unit volume. Efficiency and temperatures are very little changed.

Example 4-3. Same as example 4-2, except that inlet pressure is reduced to $\frac{1}{2}$ atm, 7.35 psia, representing a throttled engine. The method is the same as in example 4-1. The results are as follows:

Point	p	T	$V°$	$V*$	$E°$	$E*$	$H°$	$H*$
1	7.35	600	880	31.4	220	7.8	1430	51
2	115	1170	110	3.92	3780	132	6100	215
3	508	4815	110	3.92	—	1535	—	1904
4	39	2910	880	31.4	—	924	—	1150
5	14.7	2350	—	67	—	768	—	950

$\frac{w^*}{J} = 487$ Btu $\qquad \frac{(1+F)}{m} = 0.0357$

mep = 96 psi $\qquad m = 30.3$

$\eta = 0.348$

www.TechnicalBooksPDF.com

mep and expansion pressures are lower because of larger specific volume. Efficiency and temperatures are little changed over example 4-2.

Example 4-4. Limited-pressure fuel-air cycle, with liquid fuel injected at end of compression.

Given Conditions:

$$F_R = 0.8, \quad r = 16, \quad f = 0.03, \quad p_1 = 14.7, \quad T_1 = 600, \quad p_3/p_1 = 70$$

Preliminary Computations: Before fuel injection, $F_R = F = 0$, $(1 + F)/m$ from Fig 3-7 $= 0.0345$, $m = 1/0.0345 = 29$. (On the chart air with 3% residual gas is indistinguishable from air.)

Point 1: On C-1 at $p = 14.7$, $T = 600$, $F_R = 0$, read

$$V° = 440, \quad E° = 210, \quad H° = 1400$$

Process 1–2: Since $F_R = 0$, $f \cong 0$, follow vertical line to $V_2° = \frac{440}{16} = 27.5$. At this point read

$$p_2 = 675, \quad T_2 = 1702, \quad E_2° = 6100, \quad H_2° = 9455$$

for 1 lbm, $E = 6100(0.0345) = 210$, $H = 326$ †

Fuel Injection: It is assumed that liquid octene is injected at this point to give $F = 0.8 \times 0.0678 = 0.0542$. From expression 4-6,

$$E_2^* = 0.0345 \times 6100 + 0.97 \times 0.0542(19{,}180 - 145) = 1213$$

also,

$$V_2^* = 27.5 \times 0.0345 = 0.948$$

and, from eq 4-8,

$$H_{3A}^* = 1213 + 70 \times 14.7 \times 0.948 \times \tfrac{144}{778} = 1213 + 181 = 1394$$

On C-2, at $p_3 = 70 \times 14.7 = 1030$ and $H_{3A}^* = 1394$, we read

$$V_{3A}^* = 1.75, \quad T_{3A} = 4560, \quad E_{3A}^* = 1056$$

Expansion: From point 3*A* follow line of constant entropy to $V_4^* = 440 \times 0.0345 = 15.2$, reading pressures and volumes to give expansion line of Fig 4-2. At $V_4^* = 15.2$, read, from C-2,

$$p_4 = 70, \quad T_4 = 2690, \quad E_4^* = 495, \quad H_4^* = 690$$

Residual Gas: Continuing the expansion to $p_5 = 14.7$, we read, from C-2,

$$T_5 = 1960, \quad V_5^* = 51, \quad E_5^* = 310, \quad H_5^* = 449$$

Work:

$$\frac{w^*}{J} = H_{3A}^* - p_3 V_3^*/J - E_4^* - (E_2^* - E_1^*)$$

$$= 1394 - 181 - 495 - 0.0345(6100 - 210)$$

$$= 513 \text{ Btu}$$

$$\text{mep} = \tfrac{778}{144} \times 513/(15.2 - 0.948) = 194$$

$$\eta = 513/0.97(0.0542)19{,}035 = 0.512$$

† Note: Strictly speaking, if the charge is to contain $(1 + F)$ lbm after injection, the mass before injection is $(1 + fF)$ lbm. However, the value of fF is so small that the mass before combustion may be taken as 1 pound.

www.TechnicalBooksPDF.com

Example 4-5. Same as example 4-4, except that F_R after injection is 0.6.

Points 1 and 2: These points and pressure p_3 are the same as in example 4-4. $V_1° = 440$ and $V_2° = 27.5$ as before. Since a chart for $F_R = 0.6$ is not available, the chart for $F_R = 0.8$ (C-2) is used, with the assumption that the thermodynamic characteristics *per unit mass* of burned products is the same within the accuracy required.

Fuel Injection:

$$F = 0.6 \times 0.0678 = 0.0407, \qquad V_2^* = 27.5/29 = 0.948$$

$$E_2^* = 0.0345 \times 6100 + 0.97 \times 0.0407(19{,}180 - 145) = 960$$

$$H_{3A}^* = 960 + 181 = 1141 \quad (181 \text{ is from example 4-4})$$

In using the foregoing values with C-2, it must be remembered that the *actual* H^* and E^* values are for 1.0407 lbm of material, whereas C-2 is based on 1.0542 lbm. Thus, to enter C-2, H_{3A}^* is multiplied by $1.0542/1.0407 = 1.012$ and

$$H_{3A} \text{ chart} = 1141 \times 1.012 = 1158$$

The volume values, however, were fixed by the compression process with air only and remain the same as in example 4-4; namely,

$$V_1^* = V_4^* = 15.2 \quad \text{and} \quad V_2^* = V_3^* = 0.948$$

Point 3A: This point is found at the chart values $H = 1158$ and $p_{3A} = 1030$. Here we read $V = 1.48$, $T_{3A} = 3980$. The actual value of V_{3A}^* is $1.48/1.012 = 1.46$.

Expansion: This is followed along a constant entropy line on the chart from $V = 1.48$, $T_{3A} = 3980$ to V_4^*, whose actual value is 15.2, chart value $15.2 \times 1.012 = 15.4$. Volumes along the expansion line are chart volumes divided by 1.012.

Point 4:

$$V = 15.4, \qquad p_4 = 57, \qquad V_4^* = 15.2,$$

$$T_4 = 2090, \qquad E_{\text{chart}} = 360, \qquad E_4^* = 355$$

Point 5:

$$p_5 = 14.7, \qquad T_5 = 1590, \qquad E_{\text{chart}} = 220, \qquad E_5^* = 217$$

Work: From eq 4-8*a*,

$$\frac{w^*}{J} = \left\{1141 - \frac{1030 \times 0.948}{5.4} - 355 - 0.0345(6100 - 210)\right\} = 403 \text{ Btu}$$

$$\text{mep} = 403 \times \tfrac{778}{144}/15.2 - 0.948 = 154 \text{ psi}$$

Efficiency:

$$\eta = 403/0.97(0.0404)19{,}035 = 0.54$$

Example 4-6. Gas-Turbine Cycle (Fig 4-3).

Given Conditions: Fuel is octene, $F_R = 0.25$, $T_1 = 600$, $p_1 = 14.7$, pressure ratio $p_2/p_1 = 6$, no heat exchange.

www.TechnicalBooksPDF.com

Method: For fuel-air ratio of $F_R = 0.25$ or less, C-1 can be used, since the maximum temperature will not exceed 2500°R. For the gas turbine, $f = 0$, $F = 0.25 \times 0.0678 = 0.017$. From Fig 3-5, $m = 29$ before fuel injection and also after combustion.

Compression: This process involves air only. From C-1, at $p = 14.7$, $T = 600$, $f = 0$, $F = 0$, we read

$$V_1° = 440, \quad E_1° = 210, \quad H_1° = 1400$$

Dividing by 29,

$$V_1 = 15.2, \quad E_1 = 7.2, \quad H_1 = 48$$

Following a line of constant entropy (vertical) to $p_2 = 6 \times 14.7 = 88.2$, read

$$T_2 = 995, \quad E_2° = 2200, \quad H_2° = 4180, \quad V_2° = 122$$

Dividing by 29,

$$E_2 = 76, \quad H_2 = 144, \quad V_2 = 4.21$$

Fuel Injection and Burning: At point 2 it is assumed that liquid fuel is injected and burned to equilibrium at constant pressure. From eq 4-9,

$$H_3° = 4180 + (29)0.017(19{,}180 - 145) = 13{,}580$$

On C-1, reading at $p_3 = 88.2$, $H_3° = 13{,}580$, $F_R = 0.25$ gives

$$T_3 = 2175, \quad V_3° = 265, \quad E_3° = 9280$$

Multiplying by 1.017/29 (after burning),

$$V_3* = 9.3, \quad E_3* = 325, \quad H_3* = 477$$

Expansion: Following a line parallel to that for constant entropy at $F_R = 0.25$, from point 3 to $p_4 = 14.7$, read

$$V_4° = 1050, \quad H_4° = 7620, \quad E_4° = 4770, \quad T_4 = 1430.$$

Multiplying by 1.017/29,

$$V_4* = 37, \quad H_4* = 264, \quad E_4* = 164$$

Work and Efficiency: From eq 4-10,

$$\frac{w*}{J} = (477 - 264) - (144 - 48) = 117$$

$$\frac{w*}{V_1} = 117(778)/144(15.2) = 41.5 \text{ psi}$$

$$\eta = \frac{117}{19{,}035 \times 0.017} = 0.37$$

www.TechnicalBooksPDF.com

Table 4-1 compares the results obtained in the foregoing examples.

Table 4-1

Comparison of Fuel-Air Cycles

(Constant Volume and Limited Pressure)

Example	4-1	4-1*a*	4-2	4-3	Air *	4-4	4-5	Air *
Type	CV					LP		
r	8	8	8			16		
F_R	1.2	1.2	1.2			0.8		0.6
f	0.05	0.034	0.10	0.10	0.05			0.03
p_1	14.7	14.7	14.7	7.35		14.7		
p_e	14	14.7	14.7					
T_1	600	660	600					
p_2	230	217	232	115	270	675	675	715
T_2	1180	1225	1185	1170	1380	1702	1702	1820
p_3	1100	1000	1040	508	1836	1030	1030	1030
T_3	5030	5150	4850	4815	9360	—	—	—
V_{3A}	—	—	—	—	—	1.75	1.46	1.73
T_{3A}	—	—	—	—	—	4560	3980	4820
p_4	83	76	79	39	98	70	57	50
T_4	3060	3165	3010	2910	4075	2690	2090	2020
T_5	2100	2215	2100	2350	2355	1960	1590	1440
w/J	522	541	486	487	774	513	403	423
mep	206	193	192	96	316	194	154	161
η	0.355	0.362	0.348	0.348	0.570	0.512	0.54	0.588
Fig No.	4-1				4-1		4-2	4-2

* See Chapter 2.

Example 4-7. Gas-turbine fuel-air cycles have also been computed by using the assumption that the medium after fuel injection has the properties of $(1 + F)$ lbm of air. This assumption is convenient when only air characteristics

www.TechnicalBooksPDF.com

are available, as in ref 3.21. By using this assumption and the same given conditions for example 4-6, the results indicated in Table 4-2 are produced.

Example 4-8. A still simpler method of computing gas-turbine cycles is to assume average values for specific heat of air during compression and expansion. Suggested values when $F_R \cong 0.25$ are $C_p = 0.244$, $k = 1.39$ for compression, and $C_p = 0.265$, $k = 1.35$ for expansion. Results of this assumption for the given conditions, the same as in example 4-6, are listed in Table 4-2.

Example 4-9. Gas-turbine air cycle for the same given conditions. $C_p = 0.24$, $k = 1.4$. (See Chapter 2.) Results are shown in Table 4-2.

It should be noted that methods 4-6 and 4-7 produce the same result within the accuracy of reading C-1. Method 4-8 is a good approximation for computations of gas-turbine fuel-air cycles when thermodynamic data are not at hand.

Table 4-2 compares the gas-turbine cycles computed in examples 4-6 to 4-9.

Table 4-2

Comparison of Gas-Turbine Cycles

($T_1 = 600$, $p_1 = 14.7$, $p_2/p_1 = 6$, $F_R = 0.25$, $V_1 = 15.2$)

Method	Example 4-6 Using C-1	Example 4-7 Using ref 3.21	Example 4-8 $C_p = 0.244$ comp $= 0.265$ exp	Example 4-9 $C_p = 0.24$ $k = 1.4$
T_2	995	994	955	1000
T_3	2200	2187	2155	2080
T_4	1435	1390	1350	1246
V_2	4.21	4.2	4.0	4.2
V_3	9.3	9.2	9.0	8.8
V_4	37	35.0	34.0	31.7
w/V_1	42.7	42	45	58
η	0.37	0.367	0.389	0.503
Fig No.	4-3	—	—	4-3

Example 4-10. Using Fig 4-5, compute the efficiency, mep, and conditions at point 3 of a constant volume fuel-air cycle having the following conditions: $p_1 = 30$ psia, $T_1 = 800°R$, $F_R = 1.2$, $r = 12.5$, $f = 0.025$, $h = 0.04$.

Efficiency (referring to Fig 4-5): $p_1 = 30/14.7 = 2.04$ atmospheres.

From (a), the efficiency at $p_1 = 1.0$, $T_1 = 700$, $f = 0.05$ and $h = 0.02$ is 0.41.

From (c), the correction factor for $p_1 = 2.04$ is 1.0.

From (d), the correction factor for $T_1 = 800$ is 0.995.

From (e), the correction for $f = 0.025$ is 0.998.

From (f), the correction for $h = 0.04$ is 1.0.

www.TechnicalBooksPDF.com

The corrected efficiency is

$$\eta = 0.41(1.0)(0.995)(0.998)(1.0) = 0.408$$

mep: $F = 1.2(0.0678) = 0.0814$. From Fig 3-5, $m_1 = 30.7$. For octene $Q_c = 19{,}035$. Using these values in equation 4-25*a* gives

$$\frac{\text{mep}}{p_1} = \frac{0.503(30.7)}{800}\left[0.0814(19{,}035)0.408\right]$$

$$\left[\frac{0.95}{1.0814 + 0.02(0.975)}\right] = 10.55$$

$$\text{mep} = 30(10.55) = 316 \text{ psi}$$

Conditions at Point 3: From Fig 4-5 (*k*), $p_3/p_1 = 103$. Correction for T_1 from (*m*) = 0.895. Correction for $f = 0.025$ from (*n*) is 1.014. Correction for $h = 0.04$ from (*o*) = 0.978. Corrected p_3/p_1 is

$$(30)103(0.895)(1.014)(0.978) = 91.4 \text{ and } p_3 = 91.4(30) = 2740 \text{ psia}$$

From (*p*) $T_3/T_1 = 7.54$. Correction for $T_1 = 800$ from (*r*) is 1.017. Correction for $f = 0.025$ from (*s*) is 1.014. Correction for $h = 0.04$ from (*t*) is 0.983. Therefore:

$$T_3 = 800(7.54)(1.017)(1.014)(0.983) = 6110°\text{R}$$

www.TechnicalBooksPDF.com

five—— The Actual Cycle

The discussion in this chapter is confined to the events which occur between the beginning of the compression stroke and the end of the expansion stroke. The inlet and exhaust strokes of four-stroke engines and the scavenging process in two-stroke engines are considered in Chapters 6 and 7.

THE ACTUAL CYCLE IN SPARK-IGNITION ENGINES

Since the equivalent constant-volume fuel-air cycle represents the limit which can be approached by spark-ignition engines, it is used as the standard of comparison and discussion in this section.

Figure 5-1A shows, qualitatively, how an actual indicator diagram from a spark-ignition engine differs from that of the *equivalent* fuel-air cycle.

In constructing the equivalent cycle (see Chapter 4) it is taken to coincide in temperature, pressure, and composition at a point, such as x, about midway in the compression stroke. With this assumption, and since the actual compression process is nearly isentropic, the compression lines of the two cycles coincide very closely up to point a, at which ignition causes the pressure of the real cycle to rise sharply.

www.TechnicalBooksPDF.com

After combustion starts the pressure of the real cycle rises along a line such as *a–b*. Point *b* is taken where the expansion line becomes tangent to an isentropic line parallel to that of the fuel-air cycle. Experience shows that in well-adjusted engines point *b* is the point at which the charge becomes fully inflamed and combustion is virtually complete.

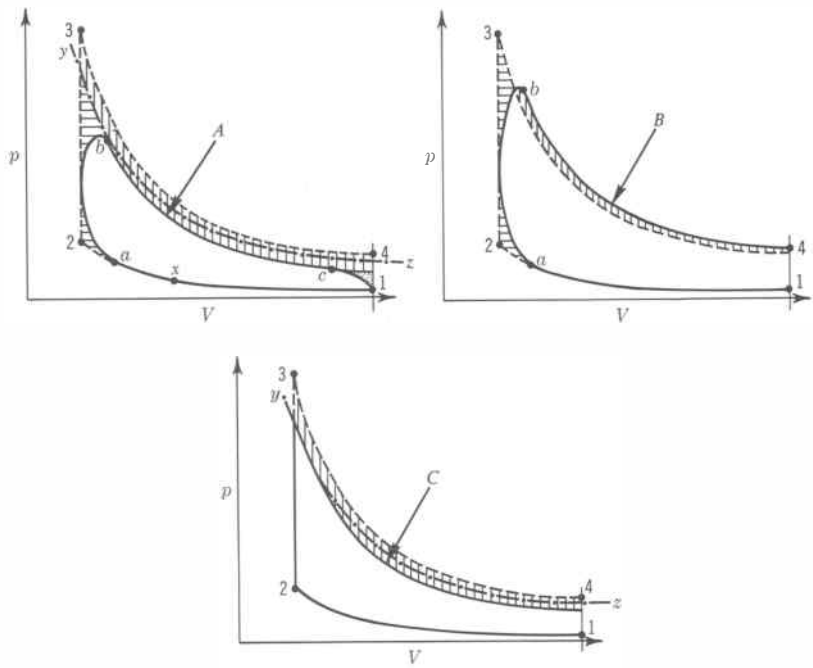

Fig. 5-1. Cycle losses.

- - - - Equivalent fuel-air cycle
A——— Actual cycle
B——— Cycle with time loss only
C——— Cycle with heat loss only
x is point of measurement of pressure temperature and volume
y-z is isentropic through point *b*
▩ exhaust blowdown loss.

As the charge expands, the expansion line falls below the isentropic line, due to heat loss.

At point *c* the exhaust valve starts to open, and the pressure falls rapidly as the piston approaches bottom center.

Possible causes of the observed differences between the actual and the fuel-air cycle include the following:

1. Leakage
2. Incomplete combustion
3. Progressive burning
4. Time losses; that is, losses due to piston motion during combustion

www.TechnicalBooksPDF.com

5. Heat losses
6. Exhaust loss; that is, the loss due to opening the exhaust valve before bottom dead center

Leakage. Except at very low piston speeds, leakage in well-adjusted engines is usually insignificant. Leakage can be estimated by measuring *blow-by*, that is, the mass flow of gases from the crankcase *breather*.

Incomplete Combustion. By this term is meant failure to reach theoretical chemical equilibrium before the exhaust valve opens. Experience shows that with spark-ignition engines there is always some incompletely burned material in the exhaust, probably due to quenching of the combustion process on the relatively cool surfaces of the combustion chamber. In well-designed and well-adjusted engines the resultant loss in efficiency is very small except, perhaps, at light loads and idling. However, the unburned material in the exhaust may be an important cause of "smog" and odor.

Progressive Burning

The details of the combustion process in spark-ignition engines are discussed at length in Vol 2. For present purposes it is necessary to recall the following facts:

1. Normal combustion in spark-ignition engines starts at one or more ignition points and continues by means of moving flame fronts which spread from these points at measurable time rates.
2. Combustion is virtually complete when the flame fronts have passed through the entire charge.
3. The time required for the combustion process varies with fuel composition, combustion-chamber shape and size (including number and position of ignition points), and engine operating conditions, one of the most important of which is engine speed. Fortunately, combustion time varies nearly inversely as speed, so that the crank angle occupied by combustion tends to remain constant as speed varies.
4. Best power and efficiency are obtained when ignition is so timed that points a and b of Fig 5-1 are at substantially the same crank angle from top center. (This means that the cylinder volume at these points is the same.) However, in order to avoid *detonation* (see Vol 2), a later spark timing is often used.

Since the movement of a flame requires a certain amount of time, it is evident that even if the piston remained stationary during combustion different parts of the charge would burn at different times.

www.TechnicalBooksPDF.com

To explain the mechanism of progressive burning, its effect will be computed by using the assumptions of the fuel-air cycle for each infinitesimal portion of the charge. The assumptions are listed below:

1. The piston motion during combustion is negligible
2. At any instant the pressure in all parts of the cylinder is the same
3. Chemical reaction occurs only at the flame front
4. The process is adiabatic for each particle of the charge

Assumptions 1 and 2 are ordinarily made for fuel-air cycles. Assumptions 3 and 4 are useful for simplification of the reasoning and are probably good approximations.

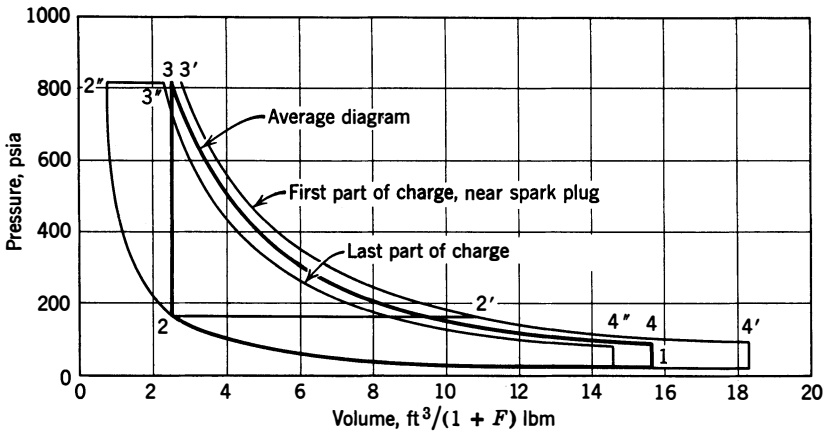

Fig 5-2. Pressure-volume relations of various parts of the charge with progressive burning: fuel-air cycles, $F_R = 1.175$; $T_1 = 600°\text{R}$; $p_1 = 14.7$ psia; $r = 6$.

The average pressures of a constant-volume cycle are represented by diagram 1–2–3–4 in Fig 5-2 (note that the abscissa scale is chart volume). All of the gas in the cylinder is compressed from p_1, V_1 to p_2, V_2; consequently at point 2 it is at a uniform temperature, T_2. At point 2 ignition occurs at some definite point in the cylinder.

As soon as it ignites, the small volume of gas immediately adjacent to the point of ignition is *free to expand* against the unburned gas in the cylinder. If the volume chosen is infinitesimal, it will expand without affecting the general cylinder pressure. As combustion occurs in this small volume, it will expand to point 2′ on the diagram at *constant pressure*. As combustion proceeds, this small volume of gas will be compressed to point 3′ (adiabatically, since no heat interchange is assumed).

www.TechnicalBooksPDF.com

It will then be re-expanded, by the motion of the piston, to the release pressure, point 4′.

If the last part of the charge to burn is now considered, it is seen to be compressed *before combustion* to the maximum cyclic pressure at point 2″. Since its volume is small compared to the total volume of gas, this part of the charge also expands at constant pressure to point 3″, whence it is further expanded to 4″ by the motion of the piston. Similarly, any intermediate small volume of gas will go through a cycle in which combustion takes place at some pressure level intermediate between p_2 and p_3. Thus an actual cycle may be viewed as the resultant of the sum of an infinite number of different cycles in each of which combustion occurs at constant pressure. We also observe that after combustion there is a difference in chart volume, and, therefore, in temperature, between the last part of the charge to burn and the part near the ignition point. Pressures and temperatures can be computed for the various parts of the charge by means of the thermodynamic charts of Chapter 3. On the assumption that the compression ratio is 6, the inlet conditions are $p_1 = 14.7$, $T_1 = 600°\text{R}$, and the fuel-air ratio is 0.0782, the results of such computations are listed in the following table.

Point	p	v^*	T
1	14.7	15.6	600
2	160	2.6	1070
3	810	2.6	4980
2′	160	11.2	4250
2″	810	0.78	1520
3′	810	2.9	5470
3″	810	2.4	4630

T_3', the temperature near the spark plug after combustion is complete, is 840°F higher than T_3'', the temperature at the same instant of the last part of the charge to burn. T_3' minus T_3'' represents the maximum temperature difference which could exist under the assumed conditions. In the actual cycle this temperature difference will be smaller, since both heat transfer and mechanical mixing occur during combustion, and the chemical reaction occurs in a zone of finite thickness. However, there can be no doubt that the actual process is similar to this simplified theoretical process. This similarity was confirmed by Hopkinson (ref 5.22) as early as 1906. In a series of experiments performed in a constant-volume bomb filled with a nine-to-one air-coal-gas mixture

www.TechnicalBooksPDF.com

at atmospheric pressure and temperature, he measured a temperature difference of about 900°F in the gas immediately after combustion. The maximum temperature occurred near the point of ignition while the minimum temperature was in the last part of the charge to burn. Measurements by Rassweiler and Withrow (ref 5.11) in an actual engine yielded the results shown in Fig 5-9 (p. 121) in which the maximum difference in temperature between the two ends of the combustion chamber is about 400°F.*

Calculation of fuel-air cycles with progressive burning show that the mep and efficiency of the cycles are the same, within the accuracy of the charts, as for similar fuel-air cycles with simultaneous burning. For such cycles, of course, the piston is assumed to remain at top center during burning of all parts of the charge.

On the other hand, *piston motion* during burning results in measurable losses, as is shown.

Time Loss, Heat Loss, and Exhaust Loss

In well-adjusted engines the losses due to leakage, incomplete mixing, and progressive burning are too small to be evident or measurable by means of an indicator diagram. On the other hand, the remaining losses, namely, *time* loss, *heat* loss, and *exhaust* loss, can be distinguished and at least approximately evaluated by means of an accurate indicator diagram compared with the diagram for the equivalent fuel-air cycle.

Time Losses. By this term is meant the loss of work due to the fact that the piston moves during the combustion process.

Heat Loss. By this term is meant the loss of work due to heat flow from the gases during the compression and expansion stroke. In most cases heat transfer during the compression stroke up to the point at which combustion starts appears to be a negligible quantity.

The factors which control the total rate of heat flow from the gases to the cylinder walls are discussed at length in Chapter 8. Here we are interested only in the heat which is lost by the gases during the compression and expansion strokes. Since much heat is also transferred to

* The actual difference may have been considerably higher than the measured difference because of experimental limitations. For example, the average temperatures of relatively large volumes of the mixture were measured instead of the temperatures of infinitesimal layers. It was also impossible to make measurements very close to the spark points or in the very last small element of the charge to burn.

www.TechnicalBooksPDF.com

the coolant by the exhaust gases after they leave the cylinder, the total heat flow to the coolant is much greater than the flow with which we are here concerned.

Separation of Time Loss and Heat Loss. Fig 5-1 *B* shows a hypothetical cycle with no heat loss, but with a finite combustion time, and Fig 5-1 *C* shows a cycle with instantaneous combustion, but with heat losses during combustion and expansion. For any cycle from point *a* to point *b*, from eq 1-16,

$$E_b = E_a + Q_{a\text{-}b} - \frac{1}{J}\int_a^b p\, dv \tag{5-1}$$

If no heat is lost between *a* and *b* (as in Fig 5-1 *B*) the pressure at volume *b* and the subsequent expansion line will be higher than the fuel-air-cycle pressure, because less work has been done at volume *b* in the cycle with time loss. The work lost will be the horizontally hatched area minus the vertically hatched area. Finite combustion time always involves a net loss as compared to the fuel-air cycle, which means that the work gained on expansion (vertical hatching) is always less than the work lost (horizontal hatching).

In Fig 5-1 *C* with instantaneous combustion, heat lost during combustion lowers the maximum pressure, and heat lost during expansion causes the pressure to fall faster than along the isentropic line *y-z*. The lost work is given by the vertically hatched area.

In an actual cycle accurate separation of heat loss from time loss requires greater precision in pressure and temperature measurement than has been achieved to date. A useful division of the losses however, is illustrated in Fig 5-1 *A*. Referring to the tangent isentropic line *y-z*, the horizontally hatched area is chiefly due to time loss, and the vertically hatched area is chiefly attributable to heat loss. For convenience, values determined in this way will be designated *apparent* time loss and *apparent* heat loss. In practice, apparent heat loss can be nearly zero (see Fig 5-12) in the case where the actual heat lost during combustion is just sufficient to bring point *b* in Fig 5-1 *B* down to the fuel-

www.TechnicalBooksPDF.com

air-cycle expansion line, and the heat lost during expansion is so small that little departure from the isentropic line is evident.

Exhaust Loss. There is always an appreciable loss due to the fact that the exhaust valve starts to open at a point, such as *c* in Fig 5-1, before bottom center. Such early opening is required in order to minimize the exhaust-stroke loss in four-stroke engines (see Chapter 6) and in order to allow time for scavenging in two-stroke engines. In general, earlier opening is required for two-stroke engines, which gives their p-V diagrams a characteristic shape near bottom center, as shown in Fig 5-7 (p. 118). This question is discussed in more detail in Chapter 7.

PRESSURE AND TEMPERATURE MEASUREMENTS

Quantitative analysis of the differences between the actual cycle and its equivalent fuel-air cycle obviously requires an accurate pressure-volume diagram of the real cycle.

Indicators. For speeds at which most internal-combustion engines run the mechanical type of indicator, familiar in steam-engine practice, is unsatisfactory because of the considerable inertia of its moving parts. Of the many types of high-speed indicator proposed or developed,* your author has found only one, namely, the balanced-pressure type (refs 5.01, 5.04), which is sufficiently accurate to be used for quantitative purposes. The particular balanced-pressure indicator used for most of the diagrams in this book is illustrated by Figs 5-3 and 5-4.

The MIT balanced-pressure indicator is the stroboscopic, or point-by-point, type. The pressure-sensing element is about the size and shape of a spark plug (Fig 5-4). This element is screwed into a hole in the cylinder head. At its inner end it carries a thin steel diaphragm, supported between two heavy perforated disks, called *grids*. The space between the grids is a few thousandths of an inch greater than the thickness of the diaphragm.

In operation, a steady gas pressure, called the *balancing pressure*, is applied to the outer side of the diaphragm, whose inner side is exposed to the cylinder pressure. The balancing pressure is also applied to the piston of the recording mechanism, which sets the recording point at an axial position along the recording drum; this point is determined by the

* See refs 5.0—. There is a number of electrical indicators which give good qualitative results, and pressure-sampling indicators have been used with some success for light-spring diagrams.

www.TechnicalBooksPDF.com

balancing pressure and by the calibration of the spring which restrains the piston motion.

The recording drum rotates with the engine crankshaft and must be connected to it by a torsionally rigid shaft.

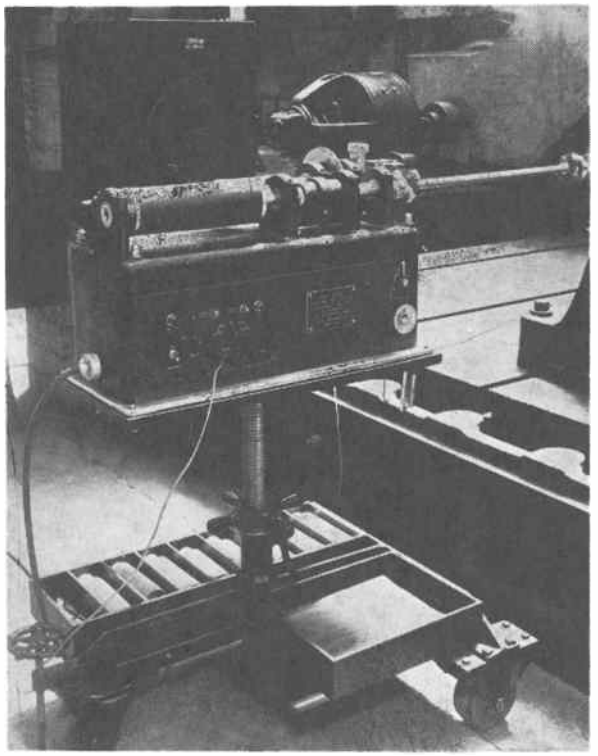

Fig 5-3. The MIT balanced-diaphragm pressure indicator, recording unit. (Manufactured by American Instrument Co, Inc, Silver Spring, Md.)

With a given balancing pressure, the diaphragm will move from one grid to the other when the cylinder pressure reaches the balancing pressure and again when the cylinder pressure drops below the balancing pressure. The crank angle at which these two events occur is recorded by a spark which jumps from the recording point to the recording drum, through the paper on the drum. The spark is caused to jump by an electronic circuit connected to the insulated electrode of the pressure-sensitive unit. (See Fig 5-4.) When the cylinder pressure rises to the balancing pressure the diaphragm moves against the end of the electrode,

www.TechnicalBooksPDF.com

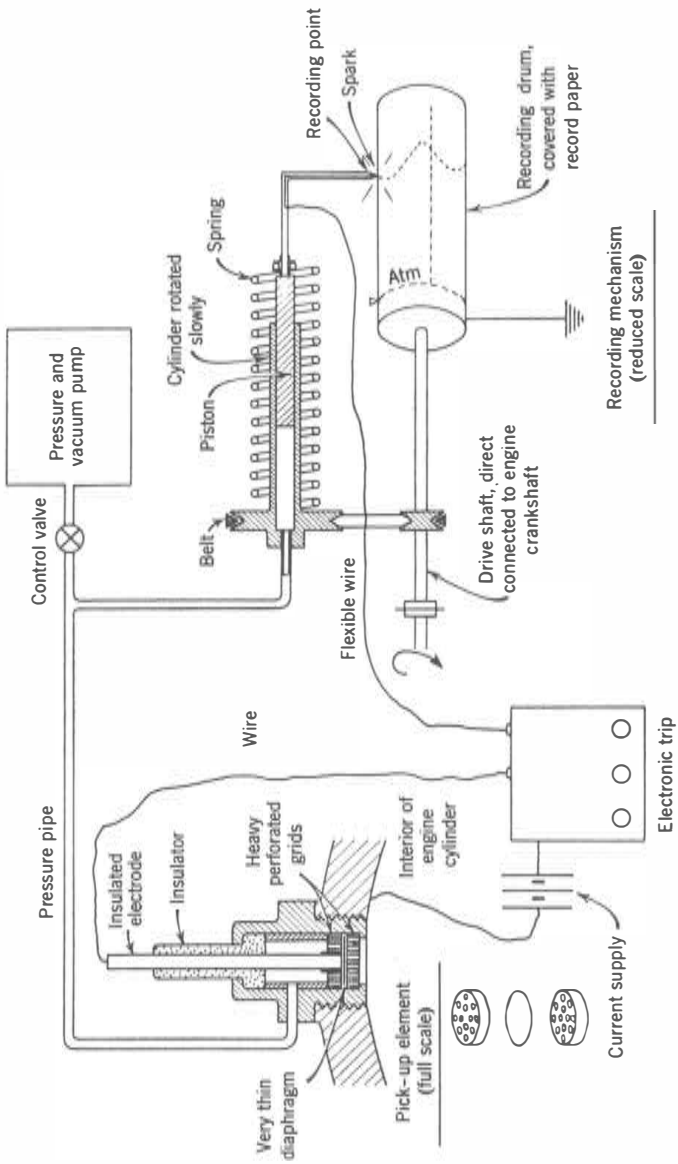

Fig 5-4. Diagram showing arrangement of MIT balanced-diaphragm indicator units.

www.TechnicalBooksPDF.com

thus *grounding* the electrode. When the cylinder pressure falls back through the balancing pressure the diaphragm breaks contact with the electrode. In either case a spark jumps from the recording point through the paper on the recording drum.

It is evident that this indicator records the crank angles at which the cylinder pressure is equal to the balancing pressure. To make a complete pressure-crank-angle curve with this mechanism, it is necessary to vary

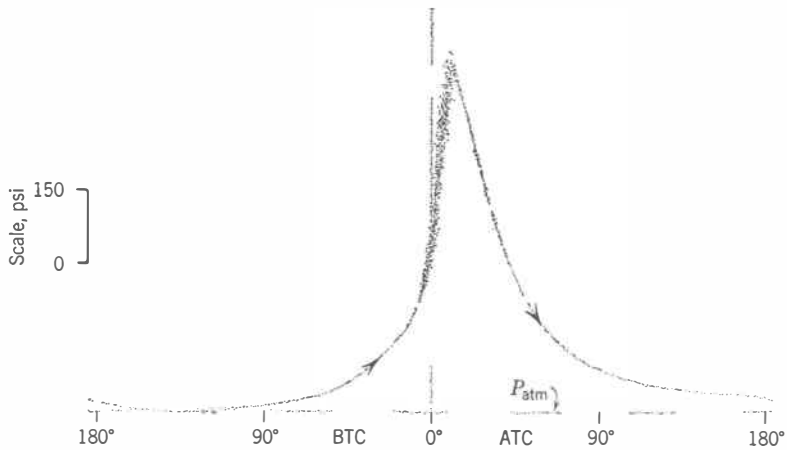

Fig 5-5. Heavy spring indicator card, made with indicator in Figs 5-3 and 5-4: CFR engine, 3¼ x 4½ in; V_d = 37.33 in^3; r = 8.35; iso-octane fuel; F = 0.0782; SA = 20° BTC; N = 1200 rpm; p_i = 14.4 psia; p_e = 15.1 psia; T_i = 175°F.

the balancing pressure over a range slightly greater than the range of pressure in the cylinder.

Figure 5-5 shows a typical record made by this indicator. The record indicates not only the average pressure for a large number of cycles but also shows the range of pressure variation from cycle to cycle and gives an indication of the relative number of cycles which have a given deviation from the average. When the crank-connecting-rod ratio of the engine used is known the record can be converted to pressure-volume coordinates, as illustrated by Fig 5-6.* In such a translation the average pressures of the original record are usually used. Figure 5-7 shows a similarly constructed record for a two-stroke engine.

A limitation of the balanced-pressure indicator is the fact that it cannot measure the pressures of a single cycle. For this purpose various

* A mechanical device has been developed to facilitate this conversion. (See ref 5.05.)

www.TechnicalBooksPDF.com

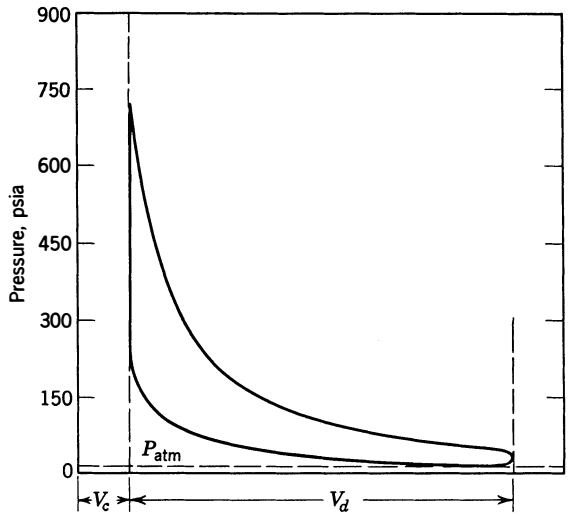

Fig 5-6. Pressure-volume diagram from Fig 5-5: area = 3.79 in^2; mep = 113.7 psia; ihp = 6.43.

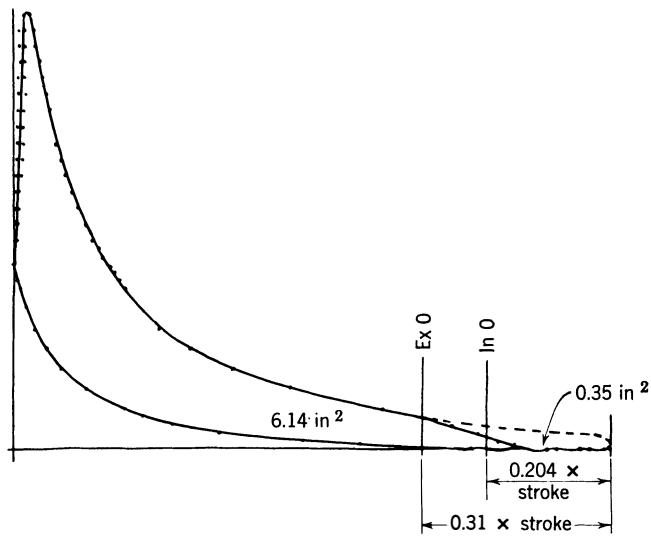

Fig 5-7. Indicator diagram from two-stroke engine (a four-stroke engine having the same expansion curve would follow, approximately, the dashed line): commercial gas-engine, loop scavenged; bore 18 in; stroke 20 in; piston speed 833 ft/min; mep 87.7 psi; $\frac{\text{area two-stroke diagram}}{\text{area four-stroke diagram}} = 0.945$.

www.TechnicalBooksPDF.com

types of electric indicator are generally used. (Refs 5.06–5.092.) Such indicators are very useful for qualitative comparisons, as in fuel testing, and for demonstration purposes, since they will display successive cycles on either p-θ or p-V coordinates on an oscilloscope screen or photographic film. The best ones have sufficient accuracy for most purposes, except for the measurement of indicated mean effective pressure. A study of the accuracy of several types of indicator is reported in ref 5.04.

When well adjusted the accuracy of the balanced-pressure indicator is believed to be within $\pm 2\%$ for heavy-spring diagrams and ± 1 psi for light-spring diagrams.

Temperature Measurements. No instrument as satisfactory as the pressure indicators just described has been developed for measuring cyclic temperatures. However, a very promising method, illustrated in Fig 5-8, is that of measuring instantaneous sound velocity in the gases and using the gas laws to compute the corresponding temperatures. (See ref 5.15.) Temperature measurements by this method are believed accurate to $\pm 20°$F before combustion. After combustion the accuracy is less certain.

Various spectroscopic methods, notably that of sodium-line reversal (refs 5.10–5.12) have also been used.

All methods of temperature measurement require special cylinder heads and elaborate auxiliary apparatus. In every case the measurement gives some sort of a mean temperature in a small part of the charge. At the time of writing, published results of such measurements are limited to a very few types of engine, each operating within a limited range. (See refs 5.13–5.16.)

Figure 5-9 shows temperatures measured by the sodium-line method, and Fig 5-10, by the sound-velocity method. Temperatures of the equivalent fuel-air cycle are given in each case.

The temperatures given in Fig 5-9 were taken across the combustion chamber in three different areas. These measurements show the expected differences due to progressive burning and also indicate that it is possible for local temperatures to exceed the average temperature of the equivalent fuel-air cycle.

Calculations based on the fuel-air cycle have shown that there would be no appreciable loss in efficiency due to the fact that burning is nonsimultaneous, provided that there was no piston motion during the burning process. The loss due to piston motion we have classified as *time* loss.

Figure 5-10 shows temperatures measured by the sound-velocity method in the end-gas zone of the cylinder illustrated in Fig 5-8.

www.TechnicalBooksPDF.com

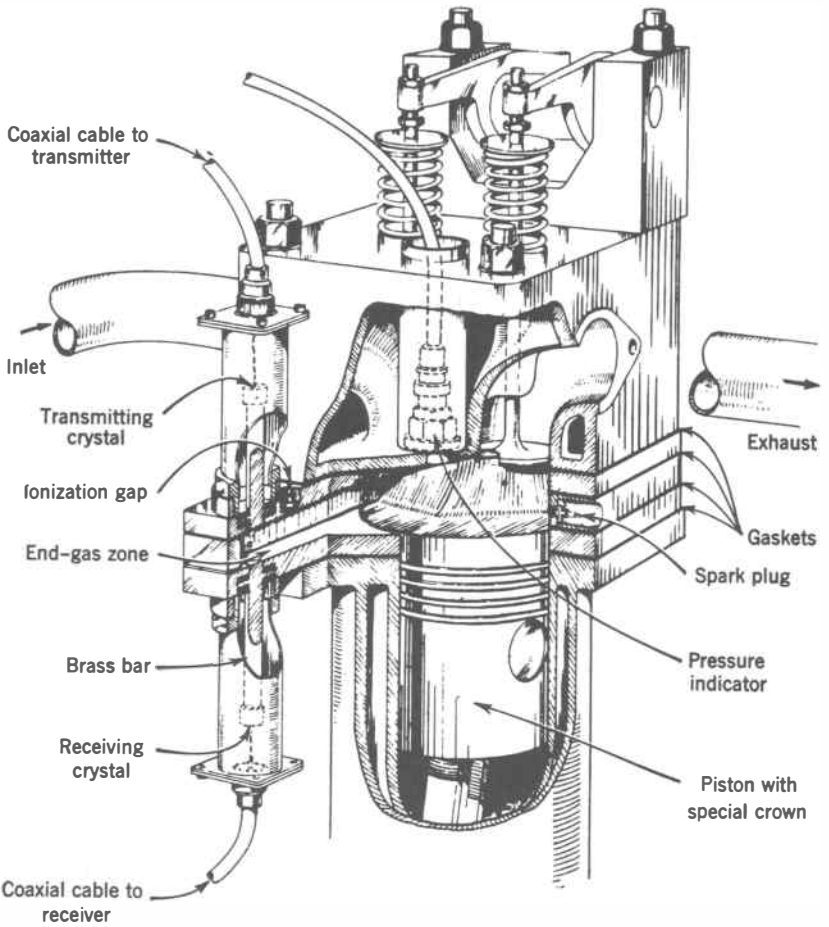

Fig 5-8. Apparatus for measuring sound velocity in cylinder gases: time of transit of a sound pulse from transmitter to receiver is measured electronically. Measurement is in end gas zone. (Livengood et al., ref 5.15)

As would be expected from previous discussion, progressive burning of the first part of the charge carries the end gas to a specific volume considerably smaller than the minimum specific volume of the equivalent fuel-air cycle. Except for this feature, the measured temperatures are remarkably close to those of the fuel-air cycle. (The two cycles were assumed to coincide at point x, Fig 5-10.)

Compression-stroke temperatures of the end gas are thought to be fairly representative of the whole charge, since there is no reason for

www.TechnicalBooksPDF.com

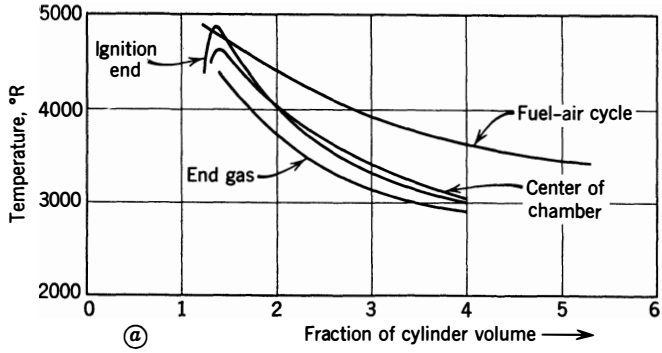

Fig 5-9. Gas temperatures measured by the method of sodium-line reversal: L-head engine, 2.88 x 4.75 in; $r = 4.4$; $T_c = 212°F$; 800 rpm; $F_R = 1.25$, full throttle; Gasoline, 75 ON. (Rassweiler and Withrow, ref 5.11)

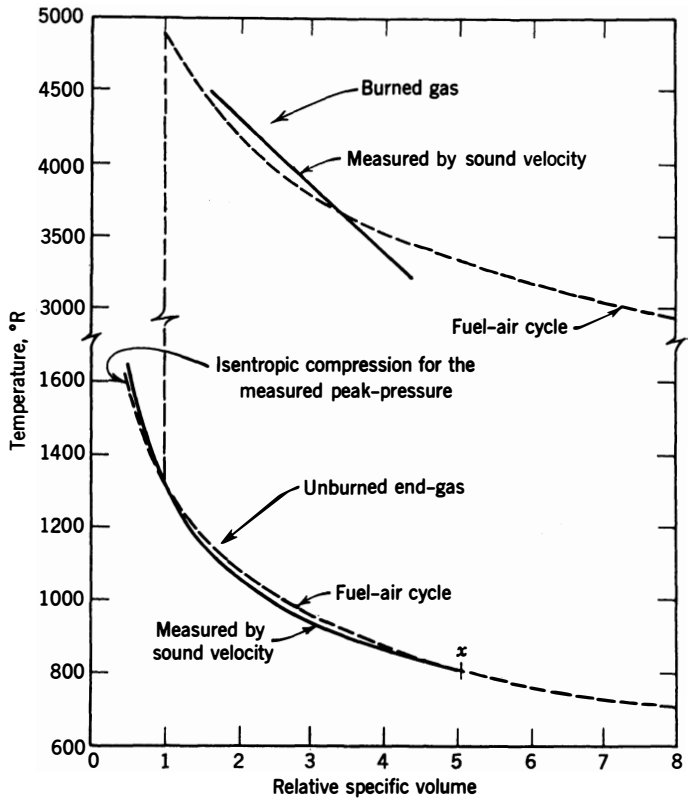

Fig 5-10. Comparison of temperatures in the fuel-air cycle and measurements by sound-velocity method of Fig 5-8: CFR 3.25 x 4.5 in engine; $r = 8$; $F_R = 1.2$; $C_i = 1.9$; $\gamma = 1.0$; $D_i = 1.35$ in; 1500 rpm; 27° SA; $p_i = 16.7$ psi; $p_e/p_i = 0.59$; $T_i = T_c = 620°R$. (Livengood et al., ref 5.16)

www.TechnicalBooksPDF.com

large temperature gradients before combustion starts. On the other hand, it is evident from Fig 5-9 that end-gas temperature after combustion is below the average temperature of the charge. Thus the agreement on the expansion line is probably not so good as it first appears.

The fact that the measured temperature appears to fall faster than the fuel-air cycle temperature on the expansion curve can be taken as due to heat loss.

The sound-velocity apparatus could not measure temperatures for the whole expansion process at the time the data for Fig 5-10 were taken.

QUANTITATIVE ANALYSIS OF LOSSES IN SPARK-IGNITION ENGINES

Figures 5-11 and 5-12 give quantitative comparisons between actual cycles and their equivalent fuel-air cycles. Wherever they were available for points corresponding to x of Fig 5-1, temperature measurements by sound-velocity method have been used to compute residual-gas fraction. When temperature measurements were not available reasonable estimates of f have been made. Figure 5-11 compares an actual cycle from a spark-ignition engine with its equivalent fuel-air cycle. The ratio of mep and efficiency of the actual cycle to that of the fuel-air cycle is 0.80, which is quite typical for cylinders of automotive size running at full load. Of the "lost" work, that is, 0.20 $\times$ the work of the fuel-air cycle, 60% is attributable to apparent heat loss (Fig 5-1), 30% to apparent time loss, and 10% to exhaust blowdown loss.

Figure 5-12 shows a comparison of actual and fuel-air cycles for a large aircraft cylinder running at 2000 ft/min piston speed. The cylinder was air-cooled, and the walls ran at considerably higher temperature than those of the water-cooled cylinder of Fig 5-11. The latter fact, plus the high gas-side Reynolds number at which the engine was operating, may account for the fact that apparent heat loss is nearly zero. This means that the actual heat loss during combustion just offsets the reduced work at point b of the diagram. (See Chapter 8 for the influence of size and wall temperature and Reynolds number on heat flow from gases to cylinder walls.)

Figure 4-9, presented in Chapter 4, gives values for residual-gas fraction of actual cycles measured from sound-velocity determinations at point x, compared with the values shown in Fig 4-5 for fuel-air cycles which use an idealized four-stroke inlet process. Figure 5-13 gives additional determinations of residual fraction by the same method. It is

www.TechnicalBooksPDF.com

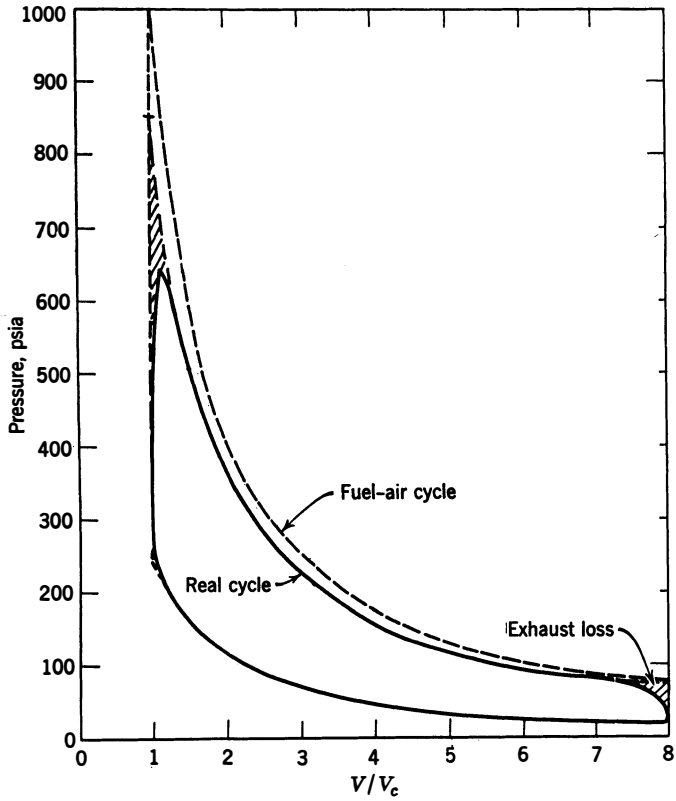

Fig 5-11. Cylinder pressure vs volume for real and equivalent fuel-air cycle:

Item	Actual	Fuel-air	Ratio
mep	143	178	0.80
η_i	0.288	0.360	0.80
isfc	0.498	0.392	1.25
Apparent heat loss 12%			
Apparent time loss 6%			
Exhaust-blowdown loss 2%			

p-V diagram, Run 161, (ref 5.16); $F = 0.079$; $F_R = 1.2$; $M_a = 0.001025$ lbm/cycle; $f = 0.15$; $r = 8$; $T_x = 817°\text{R}$ at $\theta = 270°$; $p_i = 16.6$; $p_e = 9.8$ psia; $T_i = T_c = 620°\text{R}$; 1500 rpm; $Z = 0.48$.

www.TechnicalBooksPDF.com

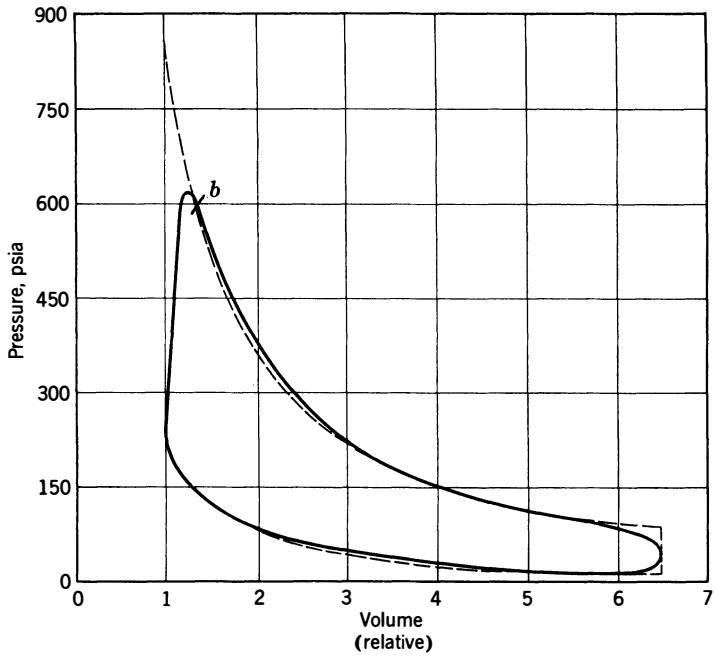

Fig 5-12. Cylinder pressures vs volume for real cycle and equivalent constant-volume fuel-air cycle:

	Fuel-Air Cycle	Real Cycle
mep	185	167
η	0.33	0.298

ratio of mep and efficiency 0.903
apparent heat loss = 0
apparent time loss ratio = 0.08
exhaust blowdown loss ratio = 0.02

Wright aircraft cylinder; 6⅛ x 6⅞ in; r = 6.50; 1710 rpm; F/F_c = 1.175; p_i = 16.1 psia; p_e = 14.7 psia; spark 15° BTC; T_1 = 702°R; f = 0.038; air cons; 0.008 lbm/cycle. (Courtesy Wright Aeronautical Corporation.)

evident that "measured" values are larger than those of the ideal four-stroke inlet process, Fig 4-5, parts *ee* to *hh*, since:

1. The volumetric efficiency of the actual cycle is considerably lower than that of the fuel-air cycle with idealized inlet process. Hence the mass of fresh mixture per unit of cylinder volume is less.

2. In the real cycle the residual gases lose heat rapidly during the exhaust stroke. Hence the density of residuals in the clearance space at

www.TechnicalBooksPDF.com

the beginning of induction is greater than in the idealized case in which heat transfer is taken as zero.

3. The temperature measured in the end-gas zone may not be equal to the average charge temperature. If the temperature in the end-gas zone at point x is less than the average, as might be expected from heat-loss considerations, fictitiously high values of f will result. (See expression 4-27.)

It is evident from the foregoing considerations that the actual value of f may be lower than the measured values of Figs 4-9 and 5-13.

Unless the measured temperature is close to the average temperature of the charge, a rather large error may be introduced in the computation of f. Fortunately, as long as the amount of fresh air and fresh fuel in the cylinder is measurable with reasonable accuracy, a considerable error in estimating f makes an insignificant difference in the fuel-air cycle mean effective pressure and efficiency; hence it has little effect on the ratios of actual to fuel-air cycle characteristics.

Figure 5-13 also shows values of T_1, the temperature at the beginning of the induction process, compared with the value of this quantity for the idealized four-stroke induction process shown in Fig 4-4. Values for T_1

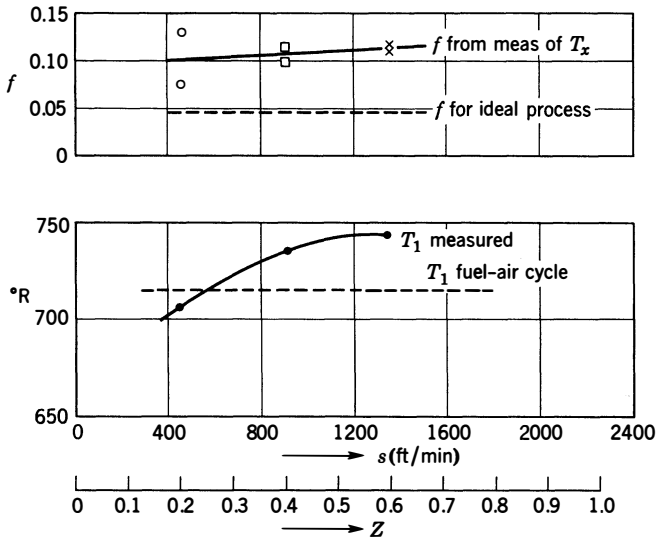

Fig 5-13. f and T_1 from indicator diagrams and gas-temperature measurements (engine of Fig 5-8): $T_c = 200°F$; $T_i = 160°F$; $r = 6$; $F = 0.078$ (iso-octane); $k = 1.345$; $P_e/P_i = 1.03$. (Livengood et al., ref 5.16)

www.TechnicalBooksPDF.com

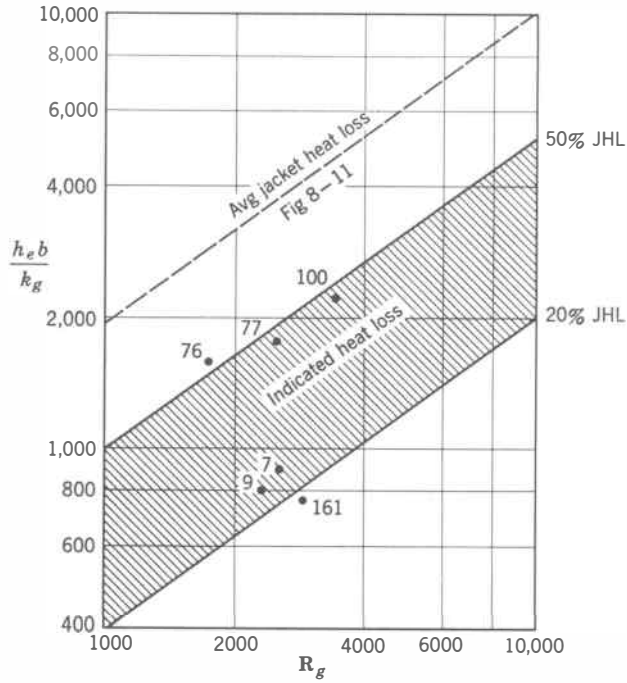

Fig. 5-14. Apparent heat loss vs jacket heat loss:

$\mathbf{R}_g$ is gas-side Reynolds number
$h_e b/k_g$ is engine Nusselt No.
} see Chapter 8

Numbers on test points refer to run numbers in ref 5.16.

were computed from temperature measurements at 60° before top center, assuming that the compression process from point 1 to this point was isentropic.

If we assume that the measured value at x is representative of the whole charge, the fact that T_1 is lower than the fuel-air cycle value at low engine speed may be attributed to heat loss from the residual gases during induction.

Figure 5-14 shows apparent loss as defined in Fig 5-1A, compared with heat delivered to the cooling medium (jacket-heat loss). The coordinates used in this figure are defined and discussed in Chapter 8. These measurements were made from indicator diagrams and do not depend on temperature measurement.

The wide spread in the ratio of indicated heat loss to jacket loss may be due in part to inaccuracy in the indicator diagrams. However, it

www.TechnicalBooksPDF.com

can be explained only partially on this basis. From Fig 5-14 it appears that an estimate of indicated heat loss at 35% of the heat lost to the jackets would represent an average figure for the cylinder of Fig 5-8. Cylinders with more compact combustion chambers should show lower heat-loss ratios.

EFFECT OF OPERATING VARIABLES ON THE ACTUAL CYCLE OF SPARK-IGNITION ENGINES

Figures 5-15–5-20 are p-V diagrams showing effects of major operating variables. Best-power spark timing was used in each case, except when spark timing was the independent variable (Fig 5-15). The definition of "time loss" and "heat loss" suggested by Fig 5-1 are not valid for the later-than-normal spark timings of Fig 5-15.

Figure 5-21 shows ratios η_i/η_0 and Fig 5-22 shows maximum-pressure ratios, actual-to-fuel-air, for a number of other cycles whose diagrams are not shown.

A remarkable feature of all the diagrams in which best-power ignition timing is used is the small variation in η_i/η_0, the ratio of actual efficiency to equivalent fuel-air cycle efficiency. The maximum pressures of the actual cycle compared to those for the equivalent fuel-air cycles also show a remarkably small variation, as indicated by Fig 5-22. The near constancy of these ratios makes it possible to make good estimates of actual efficiencies and maximum pressures from the data on fuel-air cycles presented in Fig 4-5. (See also discussion of performance estimates in Chapter 11.)

Another notable feature of the diagrams is that the apparent time losses appear to be a nearly constant fraction of the imep of the actual cycles, except for the case of non-best-power spark advance (Fig 5-15). Thus it may be concluded that proper adjustment of the spark timing will effectively compensate for normal variations in flame speed.

Since, with the exception noted, time losses account for little variation in efficiency, and since exhaust loss is small in the case of four-stroke engines, the major factor causing variations in four-stroke η_i/η_0 must be heat loss. This fact is made evident by comparing Figs 5-11 and 5-12.

www.TechnicalBooksPDF.com

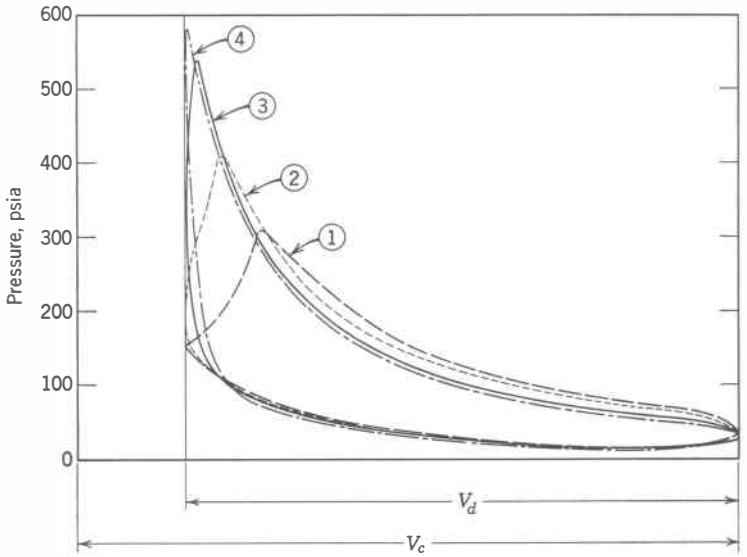

Fig 5-15. Effect of spark advance on p-V diagram:

Curve	SA degrees	Comb Θ	Measured bmep	Measured imep	Measured η_i	Measured η_i/η_0	Motoring imep	Motoring η_i
①	0	40	72	99.0	0.252	0.73	103	0.261
②	13	40	82	109	0.278	0.82	113	0.287
③	26	38	84	109	0.278	0.82	115	0.293
④	39	39	72	99.5	0.253	0.74	103	0.263

CFR engine, 3¼ x 4½ in; $r = 6$; $F_R = 1.13$; $\eta_0 = 0.34$; $p_i = 14.3$ psia; $p_e = 14.75$ psia; $T_i = 130°F$, 1200 rpm. (Sloan Automotive Laboratories, 11/13/47.)

www.TechnicalBooksPDF.com

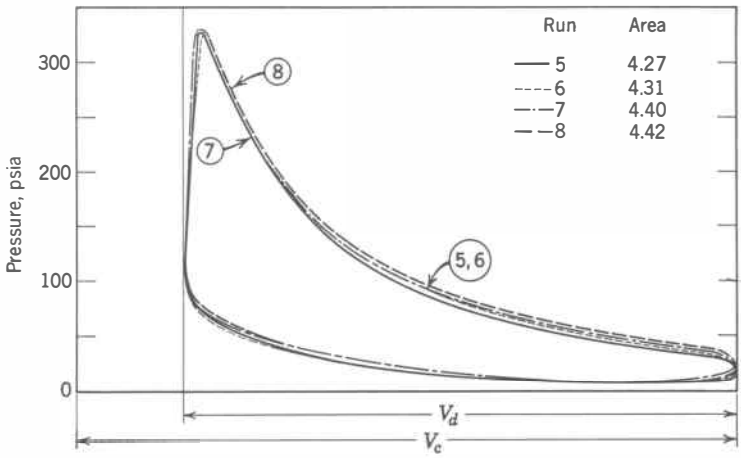

Fig 5-16. Effect of speed on p-V diagram, constant volumetric efficiency:

Curve	p_i in Hga	rpm	s ft/min	SA degrees	Comb Θ	Measured bmep	Measured imep	Measured η_i	Measured η_i/η_0	Motoring imep	Motoring η_i
⑤	22.3	900	675	18	36	56.5	85.4	0.286	0.842	82.8	0.277
⑥	23.3	1200	900	19	39	54.7	86.2	0.288	0.848	83.5	0.280
⑦	28.0	1500	1125	22	40	55.1	88.0	0.294	0.865	88.0	0.294
⑧	28.9	1800	1350	18	38	52.0	89.0	0.298	0.877	87.2	0.294

CFR engine, 3¼ x 4½ in; $r = 6$; $T_i = 150°F$; $F = 0.075$; $F_R = 1.13$; $p_e = 14.75$ psia, bpsa. (Sloan Automotive Laboratories, 3/14/50. Exp. 53, Group 1.)

www.TechnicalBooksPDF.com

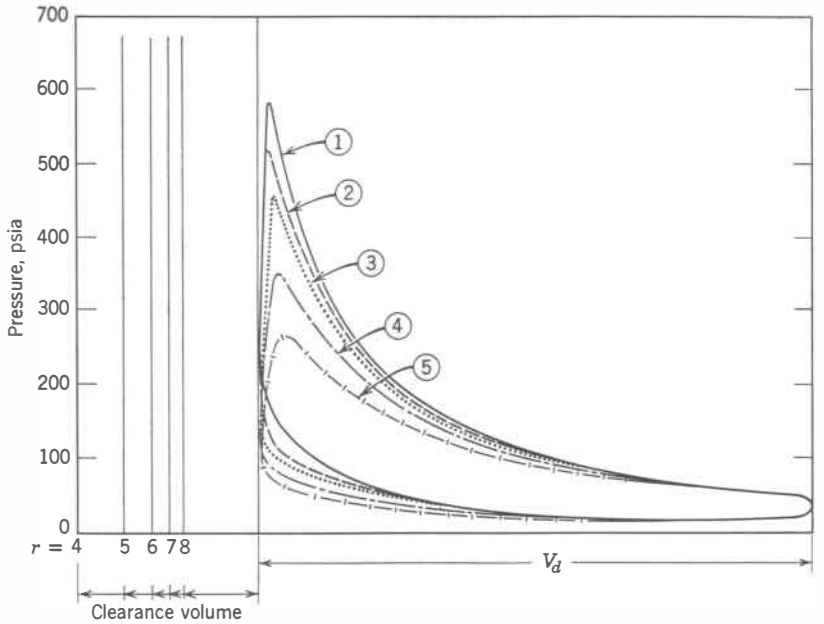

Fig 5-17. Effect of compression ratio on p-V diagram:

Curve	r	SA degrees	Comb θ	Measured bmep	Measured imep	Measured η_i	Measured η_i/η_0	Motoring imep	Motoring η_i
①	8	13	29	80	115	0.309	0.79	113	0.306
②	7	14	31	77	114	0.316	0.86	110	0.303
③	6	15	33	75	105	0.287	0.84	104	0.287
④	5	16	37	69	99	0.269	0.87	97	0.264
⑤	4	17	39	59	88	0.239	0.86	87	0.235

CFR engine, 3¼ x 4½ in; 1200 rpm; p_i = 28 in Hga; p_e = 30.8 in Hga; T_i = 150°F; F_R = 1.13; bpsa. (Sloan Automotive Laboratories, 10/16/51.)

www.TechnicalBooksPDF.com

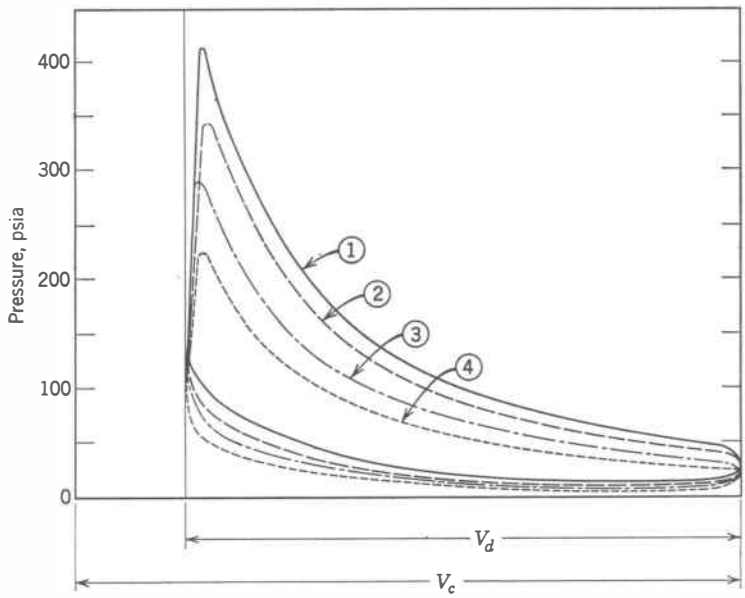

Fig 5-18. Effect of inlet pressure on p-V diagram:

Run	p_i in Hga	SA degrees	Comb Θ	Measured imep	Measured bmep	Measured η_i	Measured η_i/η_0	Motoring imep	Motoring η_i
①	28	19	36	106	74	0.292	0.86	103	0.282
②	24	19.5	38	91	58	0.296	0.87	80	0.286
③	20	26	42	72	39	0.304	0.89	70	0.294
④	16	28	44	53	23	0.278	0.82	55	0.285

CFR engine, 3¼ x 4½ in; $r = 6$; $p_e = 30$ in Hga; $T_i = 150°$F, 1200 rpm; $F_R = 1.13$; bpsa. (Sloan Automotive Laboratories, 3/14/50.)

www.TechnicalBooksPDF.com

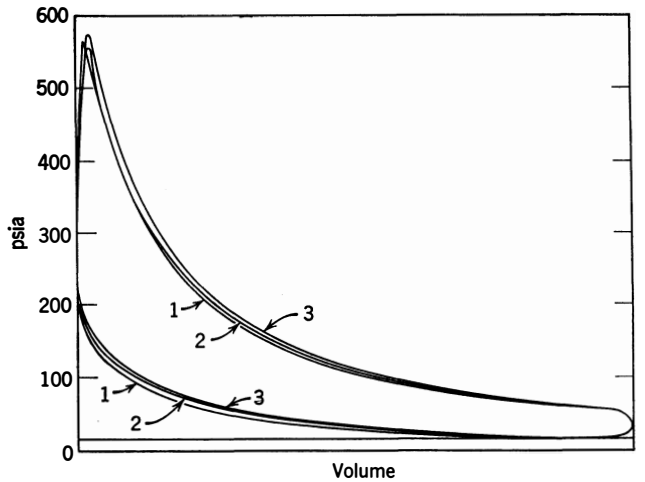

Fig 5-19. Effect of exhaust pressure on p-V diagram with constant mass of fresh mixture per stroke:

Run	p_i	p_e	Motoring Method imep	Motoring Method η_i	Indicator Card imep	Indicator Card isfc	Indicator Card η_i	η_i/η_o	Spark Advance degrees	Comb θ
1	27.1	15	108	0.282	111.7	0.463	0.291	0.83	17.5	24
2	28	28	110	0.286	111.5	0.464	0.290	0.83	17.5	25
3	29.2	45	112	0.292	111.5	0.464	0.290	0.83	17.5	25

CFR engine, 3¼ x 4½ in; $r = 7$; 1200 rpm; $\dot{M}_a = 0.01035$ lb/sec; $F_R = 1.17$; $T_i =$ 180°F; bpsa. Pressures are in inches Hg absolute.

www.TechnicalBooksPDF.com

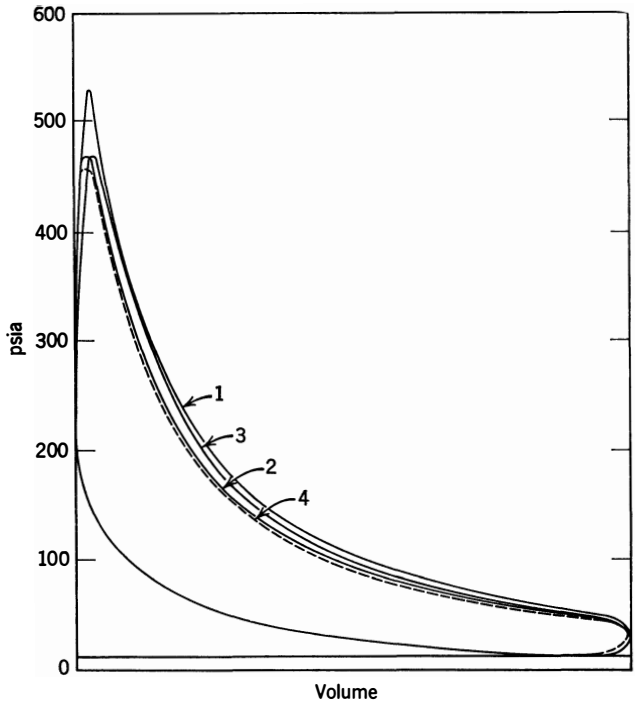

Fig 5-20. Effect of fuel-air ratio on p-V diagram:

Run	F_R	Motoring Method imep	η_i	Indicator Card imep	isfc	η_i	η_i/η_o	Spark Advance degrees	Comb Θ
1	1.17	110	0.294	111	0.453	0.298	0.85	15	33
2	0.80	93.5	0.359	93.5	0.375	0.350	0.83	23	39
3	1.80	101	0.175	102	0.761	0.177	0.83	20	39
4	0.735	87.8	0.358	91	0.363	0.370	0.80	33	58

CFR engine, 3¼ x 4½ in; $r = 7$; 1200 rpm; $p_i = 13.75$ psia; $p_e = 14.8$ psia; $T_i =$ 179°F; bpsa.

www.TechnicalBooksPDF.com

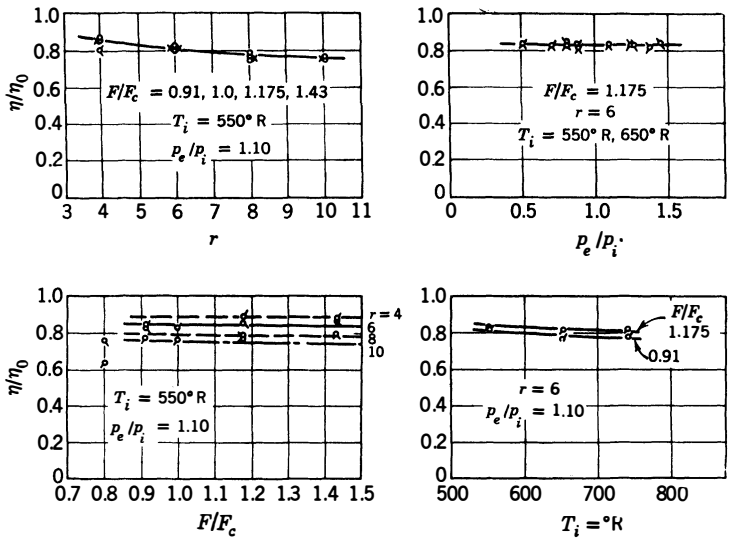

Fig 5-21. Comparison of efficiencies of actual cycles with efficiencies of equivalent fuel-air cycles—spark-ignition engines: η_0 = efficiency of equivalent constant volume fuel-air cycle with octane; η = indicated efficiency of CFR, 3¼ x 4½ in engine, 1200 rpm; fuel, gaseous butane, C_3H_8. (Van Duen and Bartas, ref 5.21)

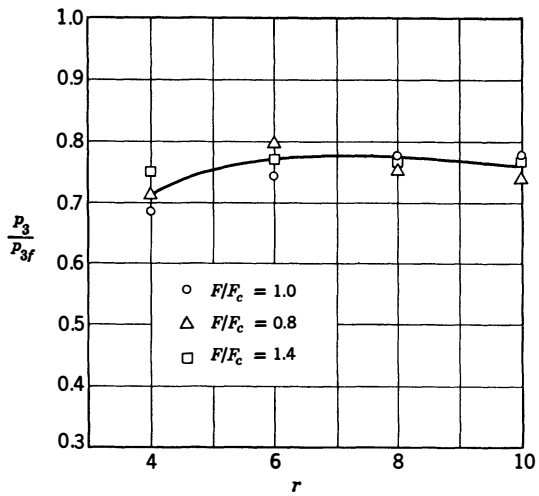

Fig 5-22. Ratio of maximum pressures, actual and fuel-air cycles: p_3 = maximum pressure actual cycle; p_{3f} = maximum pressure, equivalent constant-volume fuel-air cycle with octane; r = compression ratio; CFR engine, 3¼ x 4½ in, 1200 rpm; bpsa; fuel, gaseous butane, C_3H_8. (Van Duen and Bartas, ref 5.21)

www.TechnicalBooksPDF.com

THE ACTUAL CYCLE IN DIESEL ENGINES

The details of the combustion process in Diesel engines are discussed at length in Vol 2. For present purposes the following basic facts are important:

1. There is always a *delay* period, that is, a measurable time between the start of injection and the appearance of a flame or a measurable pressure rise due to combustion.
2. The delay period is followed by a very rapid rise in pressure. If the delay is as long or longer than the injection period, most of the fuel burns during the period of rapid pressure rise.
3. The period of rapid pressure rise is followed by relatively slow combustion, as the remaining unburned fuel finds the necessary oxygen. Except perhaps at light loads, this slow combustion extends over a considerable part, if not all, of the expansion stroke.
4. The crank angles occupied by the delay, the period of rapid pressure rise, and the subsequent period of slow combustion vary with design and operating conditions. At a given engine speed these angles are subject to a certain amount of control by means of injection timing, spray characteristics, and fuel composition.

Experience shows that Diesel engines can be operated with very rapid combustion, that is, with an approach to constant-volume combustion of most of the fuel. This result is obtained when the delay period is long enough so that most of the injected fuel is well mixed and evaporated before combustion occurs. However, such operation is undesirable because of the resultant high maximum pressures and high rates of pressure rise. (See Vol 2.)

In the practical operation of Diesel engines, therefore, the fuel, the injection system, and the operating conditions are chosen to limit rates of pressure rise and maximum pressures to values well below the maximum attainable.

Since the equivalent constant-volume fuel-air cycle represents the maximum output and efficiency obtainable by Diesel engines, as well as by spark-ignition engines, this cycle may properly be used as a basis of comparison for both types of operation. However, in view of the intentional limitation of maximum pressure in most Diesel engines, the equivalent limited-pressure fuel-air cycle is often chosen as the basis of evaluating actual Diesel cycles.

As indicated in Chapter 4, the equivalent limited-pressure fuel-air cycle has the following characteristics in common with the actual cycle

www.TechnicalBooksPDF.com

under consideration:

1. Compression ratio
2. Fuel-air ratio
3. Maximum pressure
4. Charge density at point x, Fig 5-1
5. Charge composition at all points

As compared to the equivalent limited-pressure cycle, the losses of actual Diesel cycles can be classified as follows:

1. Leakage
2. Heat losses
3. Time losses
4. Exhaust loss

Referring to the similar list for spark-ignition engines, we note that two items have been omitted, namely, nonsimultaneous burning and incomplete mixing. These losses may be large in the Diesel engine, but since burning occurs during the mixing process such losses cannot be separated from the time losses.

Quantitatively, all but the time losses in the above list can be considered as equivalent to the corresponding losses in the spark-ignition engines, and the same remarks apply.

Time Losses in Diesel Engines. These losses are much more variable than in spark-ignition engines because they depend so heavily on operating conditions, on the fuel, and on the design of the injection system and combustion chamber. Whereas, in spark-ignition engines, the mass rate of burning starts relatively slowly and accelerates to its highest velocity near the end of the process, in Diesel engines the reverse is true. Due to the fact that the available supply of oxygen decreases as burning progresses, the mixing process, hence the burning process, tends to slow down in the later stages of burning.

If we could measure the mass rate of burning in Diesel engines, plots of this rate against crank angle, under full-load conditions, would probably have the characteristics indicated by Fig 5-23. The difference between an efficient and a less efficient Diesel engine will depend, to a large extent, on how near an approach to the constant-volume fuel-air cycle is achieved.

Temperatures of the Diesel Cycle. From the nature of the injection process it is evident that the temperature in a Diesel cylinder must be extremely nonuniform during the combustion process. Using spectroscopic methods, Uyehara and Myers (refs 5.30–5.301) have measured

www.TechnicalBooksPDF.com

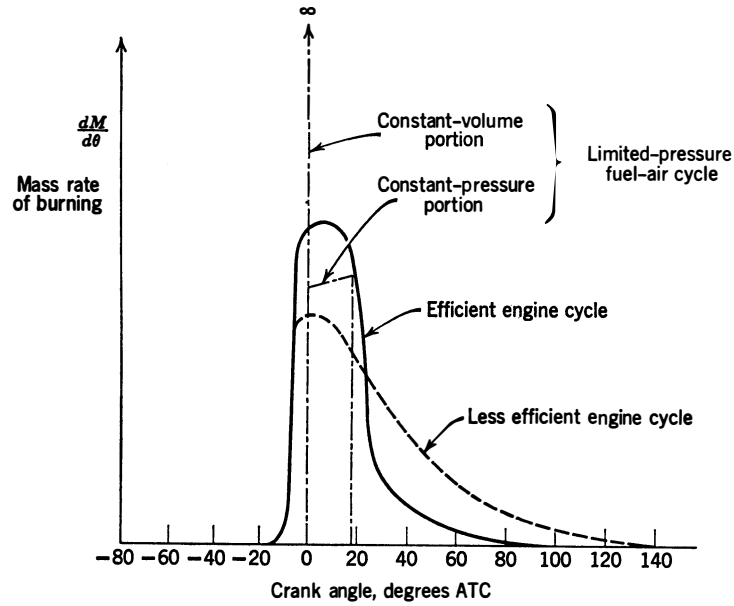

Fig 5-23. Hypothetical mass rate of burning vs crank angle in Diesel engines.

temperatures in the prechamber of a divided-chamber engine. A typical result of this work is given by Fig 5-24. The greater part of the combustion process appears to take place at constant temperature. Changes in fuel quantity per cycle (fuel-air ratio) appear to have little effect on the maximum temperature measured, although changing the fuel quantity does change the crank angle occupied by the constant-temperature portion of the process. This result indicates that what is being measured may be nearer to the maximum flame temperature than to the average temperature. The fact that the measurements of Fig 5-24 were made in the prechamber means that the hottest part of the charge was the one under observation. Maximum theoretical flame temperature for the conditions in this figure was about 4050°R. This figure confirms the fact, previously mentioned, that in Diesel engines combustion may continue during a considerable part of the expansion stroke.

Actual vs Fuel-Air Cycles in Diesel Engines. Unfortunately, no such array of p-V diagrams for Diesel engines, as presented for spark-ignition engines, is available. We must, therefore, be content with a few typical examples only. Figures 5-25 and 5-26 compare indicator diagrams taken from two compression-ignition engines with their equivalent limited-pressure fuel-air cycles.

www.TechnicalBooksPDF.com

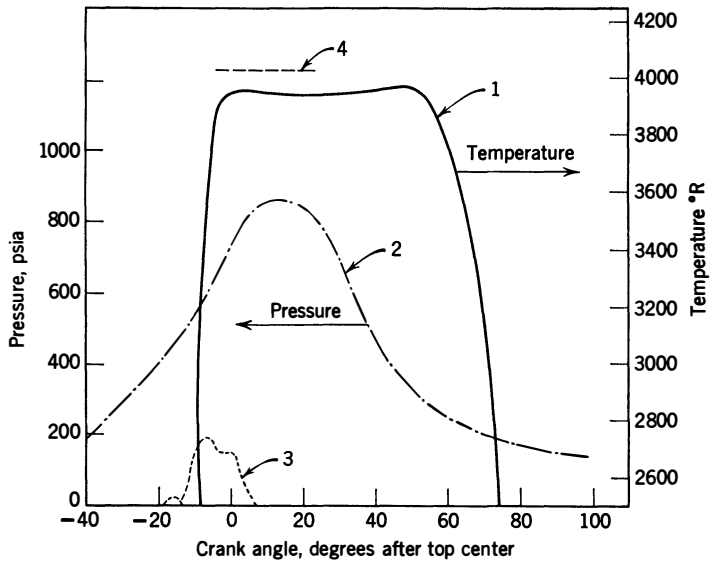

Fig 5-24. Typical temperature-crank-angle curve from the work of Uyehara and Meyers, ref 5.301: 1. Measured gas temperature, in prechamber. 2. Measured pressure in prechamber. 3. Injection-valve lift. 4. Maximum temperature, T_{3a} of equivalent fuel-air cycle.

Fairbanks Morse, 4½ x 6 in, comet head, four-stroke engine; r = 14.5; rpm = 1240; p_i = 14.5 psia; T_i = 550°R; T_c = 594°R; F/F_c = 0.6; fuel, cat. cracked Diesel oil.

Figure 5-25 is taken from a laboratory engine in which the injection system was not optimum. The difference between the fuel-air and actual cycle are thus considerably larger than in most well-developed commercial Diesel engines. In this figure the dotted line shows an isentropic through point c, just before exhaust-valve opening. The fact that the actual expansion line does not meet the dotted line until about one third of the expansion stroke is completed (point q) indicates that combustion is incomplete at point 3 and continues as far as q at a rate sufficient to more than offset heat loss. From point q to point c the combustion rate appears just sufficient to offset heat loss. It is quite possible that combustion was not entirely complete at exhaust-valve opening.

Figure 5-26 shows two diagrams for a well-developed Diesel engine whose actual efficiency approaches that of the equivalent fuel-air cycle much more closely than in Fig 5-25. Here again, however, there is evidence that combustion is not complete until after the expansion stroke is at least one third completed. These diagrams are typical of

www.TechnicalBooksPDF.com

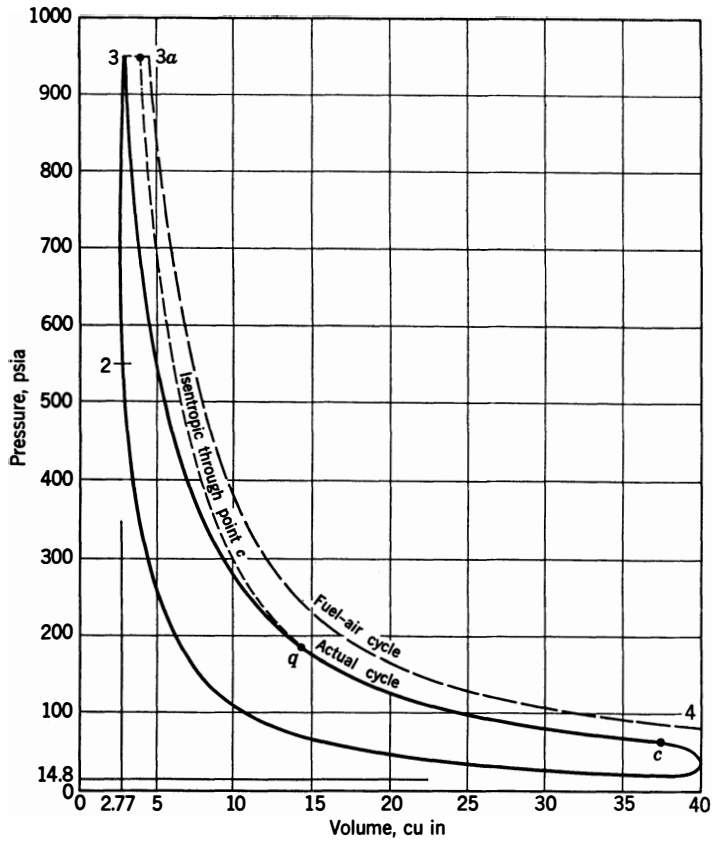

Fig 5-25. Cylinder pressures in a Diesel engine compared with equivalent limited-pressure fuel-air cycle:

	Actual Cycle	Fuel-Air Cycle		Actual Cycle	Fuel-Air Cycle
f	0.0255	0.0255	T_2, °R	—	1650
p_1, psia	—	14.7	T_3, °R	—	—
p_2, psia	—	560	T_{3a}, °R	—	4880
p_3, psia	945	945	T_4, °R	—	3085
p_{3a}, psia	945	945	imep psi	112	182
p_4, psia	—	72	η_i	0.295	0.48
T_1, °R	—	705			

$$\eta_i/\eta_0 = 0.614$$

Single-cylinder Waukesha Comet-Head Diesel engine; $V_d = 37.33$ in^3, $V_c = 2.77$ in^3; $V_t = 40.10$ in^3; $r = 14.5$; 3.25 x 4.50 in; 1000 rpm; $F = 0.0605$; optimum injection timing; air consumption = 39.1 lb/hr; $p_i = 14.4$ psia; $p_e = 14.7$ psia; $p_{atm} = 14.8$ psia; $T_i = 550$°F; area of diagram = 8.35 in^2. (Sloan Automotive Laboratories)

www.TechnicalBooksPDF.com

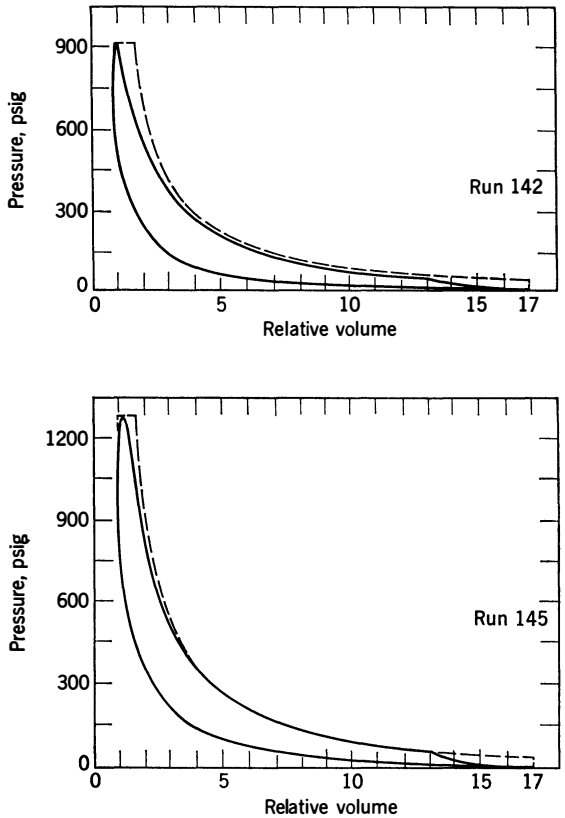

Fig 5-26. Actual Diesel cycles compared with equivalent limited-pressure fuel-air cycles:

Run No.	142 Actual	142 Equivalent	145 Actual	145 Equivalent
R_s	1.00		1.23	
F	0.0375	0.0375	0.039	0.039
f	0.08	0.08	0.06	0.06
M_a' lb/cycle	0.00235	—	0.003	—
imep	103	121	143	171
η_i	0.467	0.548	0.490	0.584
Ratio η_i/η_0	0.852	—	0.838	—
p_i	17.32	—	24.00	—
p_e	14.83	—	14.83	—

GM-71, two-stroke Diesel engine, 4.25 x 5.9 in; r = 17; 1600 rpm. (Crowley et al., ref 5.32)

the best commercial practice and show that late combustion is responsible for a large part of the difference in output and efficiency between limited-pressure fuel-air cycle and the actual Diesel cycle.

Figure 5-27 shows indicated efficiencies of a number of commercial Diesel engines compared with the efficiencies of average equivalent limited-pressure fuel-air cycles. The following general conclusions can be drawn from this figure:

1. The *best* Diesel engines of each type (open chamber four-stroke, open chamber two-stroke, and divided chamber) have about equal indicated thermal efficiencies.
2. Wide ranges of efficiency below that of the best engines are tolerated, especially with divided-chamber types.
3. A ratio between actual and fuel-air cycle efficiency of 0.85–0.90 is attainable.

Heat Loss in Diesel Cycles. For the cycle of Fig 5-25 from the beginning of compression to exhaust-valve opening at c we can write

$$E_c^* - E_1 + (1 - f)F(E_{lg} + E_c) = Q - \int_1^0 p\,dv \qquad (5\text{-}2)$$

This equation assumes combustion to equilibrium at point c, which is probably close to the case for the average Diesel cycle. With an accurate indicator diagram and measurements of temperature at point 1 and c, the cyclic heat loss could be found. However, temperature measurements at point 1 and c are not yet feasible. The definitions of "time loss" and "heat loss" suggested by Fig 5-1 are not applicable to Diesel cycles.

The total heat transferred from the gases to the coolant in Diesel engines is discussed in a later chapter. If it is assumed that the ratio heat-lost-in-working cycle to heat-transferred-to-the-coolant is the same for Diesel engines as for spark-ignition engines, an estimate of cyclic heat loss is possible when a measurement of heat loss to the coolant is available. (See Chapter 8.)

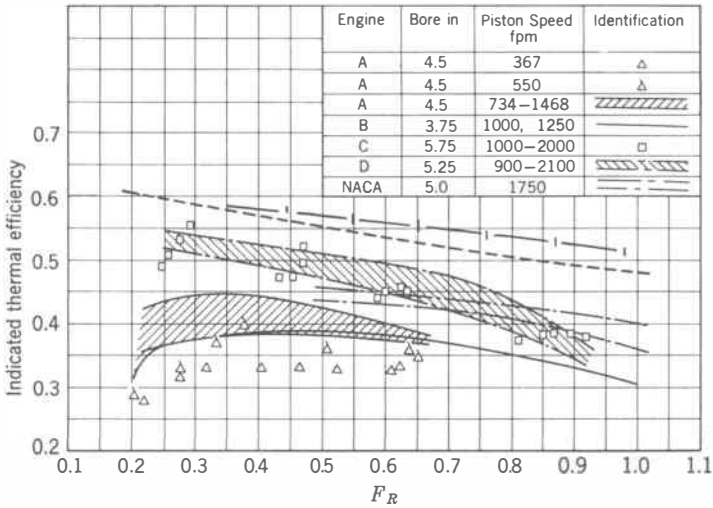

Indicated thermal efficiency vs fuel-air ratio, four-stroke divided-chamber diesel engines

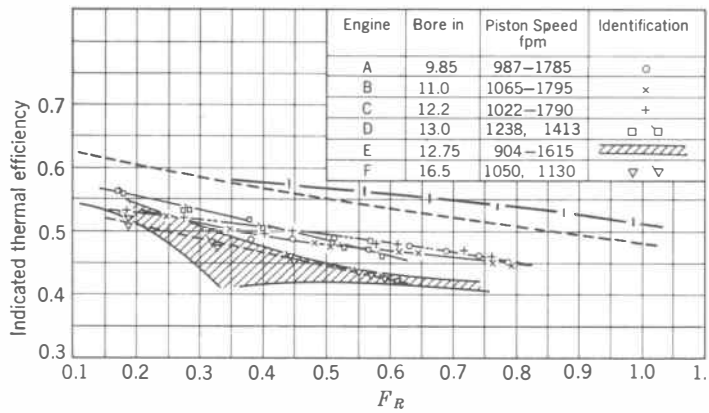

Indicated thermal efficiency vs fuel-air ratio, four-stroke open-chamber diesel engines

Fig 5-27. Indicated thermal efficiency of compression-ignition engines. Computed from manufacturer's data on specific fuel consumption. ---------- is efficiency of limited-pressure fuel-air cycles, $r = 15$ and $p_3/p_i = 70$. —·—·— is efficiency of constant-volume fuel-air cycles at $r = 15$.

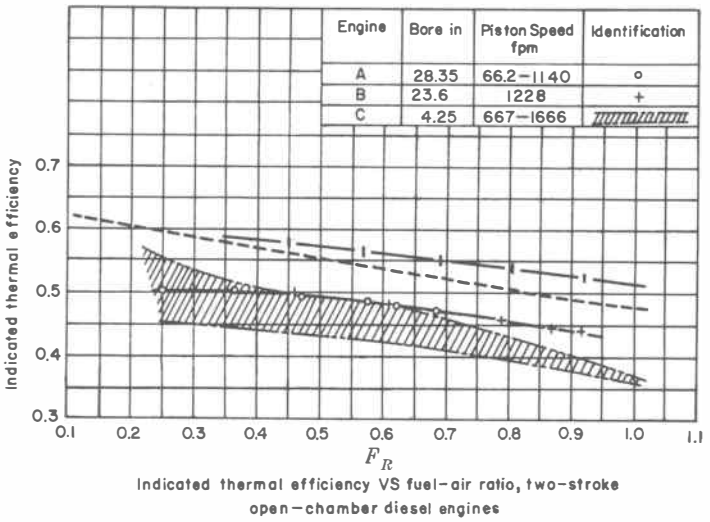

Indicated thermal efficiency VS fuel–air ratio, two-stroke open–chamber diesel engines

Fig 5-27. (*Continued*).

ILLUSTRATIVE EXAMPLES

Example 5-1. Progressive Burning. In Fig 5-9 the measured temperature of an actual cycle is higher than that of the corresponding fuel-air cycle at one point. Is it possible for this to be the case, or do you regard it as probably an experimental error? Explain fully.

Solution: Since temperature measurements of this kind seldom err on the low side, the measured temperature is probably not higher than the actual temperature at this point. The highest measured temperature is that of the gas at the ignition end of the cylinder where the gas has burned at nearly constant volume at almost the compression pressure and then has been compressed to the maximum pressure by subsequent combustion. This measurement corresponds to point 3′ of Fig 5-2, which is seen to be at larger specific volume and therefore at higher temperature than point 3, which represents the fuel-air cycle. The temperature measurement in question is, therefore, not too high to be entirely possible.

Example 5-2. An engine of compression ratio 4.0 has the following conditions at point 1 on the indicator diagram: $T_1 = 750$, $p_1 = 10$, $f = 0.05$, $F_R = 1.0$. By means of the thermodynamic charts, and assuming progressive burning, compute the maximum temperature and pressure and the corresponding chart volume of the following:

(*a*) The average constant-volume fuel-air cycle.

(*b*) A small element of the charge near the spark plug after combustion of the whole charge.

(*c*) A small element of the charge last to burn after combustion.
(*d*) Maximum possible pressure and temperature of end gas in detonation. (Assume end gas burns at constant volume from maximum pressure of the cycle.)

Solution: From C-1,

$$E_1^\circ = 1060, \quad V_1^\circ = 800, \quad V_2^\circ = 800/4 = 200, \quad p_2 = 65,$$

$$T_2 = 1185, \quad E_2^\circ = 3720, \quad H_2^\circ = 6080$$

From Fig 3-7, $(1 + F)/m = 0.03525$ and $V_2^* = 7.05$,

$$E_{S2}^* = 131, \quad H_{S2}^* = 215$$

(*a*) For point 2 of the standard fuel-air cycle from eq 3-31,

$$E_3^* = 131 + 0.95(0.0678)19{,}180 = 131 + 1235 = 1366$$

From C-3 at this value and $V_3^* = 7.05$,

$$p_3 = 280, \quad T_3 = 4960°\text{R}$$

(*b*) For point 3′, the charge burns from point 2 at constant pressure and then is compressed to 280 psia isentropically.

$$H_2' = 215 + 1235 = 1450$$

At this point on C-3 at $p_2 = 65$, $E^* = 1120$, $V^* = 27.5$. Compressing isentropically to $p = 280$ gives $T_3' = 5300$. $V_3' = 7.6$.
(*c*) For point 3″, compress the unburned mixture on C-1 to $p = 280$. Here $H^\circ = 10{,}100$, $T = 1640$, $V^\circ = 63$, $V^* = 2.22$, $H^* = 356$. Burning at constant pressure to 280 psia gives $H_3^* = 356 + 1235 = 1591$, $T'' = 4730$, $V_3^* = 6.7$.
(*d*) In detonation the end gas is compressed to the maximum cyclic pressure (280 psi) and burns at constant volume. On C-1 at $T = 1640$, read

$$E^\circ = 6700, \quad E^* = 6680 \times 0.03525 = 235$$

Combustion occurs at constant volume, $V^* = 2.22$ with $E^* = 235 + 1235 = 1470$.
On C-3 at $V^* = 2.22$, $E = 1470$, read

$$T = 5240, \quad p = 950$$

Tabulating the above results,

Point	3	3′	3″	End
	Average	First	Last	Gas
T	4960	5300	4730	5230
V^*	7.05	7.6	6.7	2.22
p	280	280	280	950

Example 5-3. Losses. Refer to Fig 5-1. Measurements of the indicator diagram of a gasoline engine show the following results:

Point	p	V in^3	Work
a	200	10.4	200
b	800	10.4	ft-lb (a to b)
V_1	—	80	
V_2	—	10	

It is estimated that $f = 0.05$. Air consumption is 0.00243 lbm/cycle and $F_R = 1.2$.

Compute apparent time loss and heat loss between points a and b.

Solution: Use expression 5-1. Molecular weight of unburned mixture from Fig 3-5 is 30.25.

$$F = 0.0678 \times 1.2 = 0.0815$$

$$V_a^\circ = \frac{10.4 \times 30.25}{1728 \times 0.00243} = 75 \text{ ft}^3$$

From Fig 3-9 $(1 + F)/m = 0.03545$, therefore, $V_a^* = V_b^* = 75 \times 0.03545 = 2.66$ ft^3.

From C-1, at $p = 200$, $V^\circ = 75$, read

$$E^\circ = 5200, \qquad T_a = 1383,$$

From eq 3-31,

$$E_a^* = 0.03545(5200) + (0.95)(0.0815)19{,}180 + 0.05(1680 \times 0.2)$$

$$= 185 + 1480 + 17 = 1672$$

From C-4, at $p = 800$, $V^* = 2.66$, $E_b^* = 1600$, $T_b = 5000$. $w = 200$ ft lbf for 0.00243 lbm fresh air. Fresh air in $1 + F$ lbm is 0.95 lbm. Therefore $w^*/J = 200(0.95)/778(0.00243) = 100$ Btu.

From eq 5-1:

$$1600 - 1672 = Q^* - 100$$

$$Q^* = 28 \text{ Btu}$$

$$Q_{a\text{-}b} = 28 \times 0.00243/0.95 = 0.072 \text{ Btu lost between } a \text{ and } b$$

Example 5-4. Actual Engine Performance. Estimate the indicated power and indicated specific fuel consumption of the following engines

Type	Piston Speed ft/min	r	F_R	Fuel	Air For Combustion lb/sec
(a) Automobile	2500	10	1.2	gasoline	0.3
(b) Aircraft	2000	7	1.0	gasoline	5.0
(c) Diesel	1500	15	0.5	light Diesel oil	5.0

Solution: From eq 1-9, power $= J\dot{M}_a FQ_c\eta/K_p$, and eq 1-13, sfc $= 2545/Q_c\eta$.

(*a*) From Table 3-1 for gasoline, $Q_c = 19{,}020$ and $F_cQ_c = 1275$ Btu/lbm. Therefore, $FQ_c = 1275 \times 1.2 = 1530$.

From Fig 4-5, (*a*), the fuel-air cycle efficiency at $F_R = 1.2$, $r = 10$, is 0.38. From Fig 5-21, the ratio actual to fuel-air cycle efficiency is 0.77. Therefore, from eq 1-9, $\eta_i = 0.38(0.77) = 0.29$ and

$$P = \frac{778(0.3)(1530)(0.29)}{550} = 188 \text{ ihp}$$

The indicated specific fuel consumption from eq 1-5 $= 2545/19{,}020(0.29) = 0.46$.

(*b*) The solution is similar to that of (*a*)

$$Q_c = 19{,}020, \qquad FQ_c = 1275$$

$$\eta_i = 0.40(0.80) = 0.32$$

$$P = \frac{778(5)(1275)(0.32)}{550} = 2900 \text{ ihp}$$

$$\text{isfc} = 2545/19{,}020(0.32) = 0.42 \text{ lbm/ihph}$$

(*c*) From Table 3-1 for light Diesel oil, $Q_c = 18{,}250$, $F_cQ_c = 1220$; therefore, $FQ_c = 1220 \times 0.5 = 610$ Btu/lbm. From Fig 4-6, part 2, at $p_3/p_1 = 70$ (average figure), the fuel-air cycle efficiency is 0.56. From Fig 5-27, at $F_R = 0.5$, the average best ratio of actual to fuel-air cycle efficiency is 0.90. Thus the actual efficiency of the best design is $0.56 \times 0.9 = 0.503$.

From eq 1-9,

$$P = \frac{778(5)(610)(0.503)}{550} = 2170 \text{ ihp}$$

and, from eq 1-13,

$$\text{isfc} = 2545/18{,}250(0.503) = 0.277 \text{ lbm/ihp-hr}$$

A more conservative estimate would assume an efficiency ratio of 0.85 rather than 0.90, which would give $P = 2170 \times 0.85/0.90 = 2050$ and isfc $= 0.277 \times 0.90/0.85 = 0.294$.

six — Air Capacity of Four-Stroke Engines

Equation 1-5 of Chapter 1 is reproduced here:

$$P = J\dot{M}_a(FQ_c\eta) \tag{6-1}$$

where P = power developed
J = mechanical equivalent of heat
$\dot{M}_a$ = mass flow of dry air per unit time, or *air capacity*
Q_c = heat of combustion per unit mass of fuel
η = thermal efficiency, which may be indicated or brake, depending upon whether P is defined as indicated or brake power
F = fuel-air ratio

Figure 6-1 shows how the indicated power of a spark-ignition engine remains proportional to air capacity, $\dot{M}_a$, provided there is no change in fuel-air ratio or compression ratio and no departure from optimum spark timing. Under these conditions, indicated thermal efficiency remains substantially constant and indicated power is directly proportional to air capacity. This proportionality has been found to hold good with many types and sizes of spark-ignition engines.

In contrast to spark-ignition engines, in which power output is controlled primarily by varying $\dot{M}_a$, compression-ignition engines are controlled by varying F, which, of course, varies the efficiency. Furthermore, even with a constant fuel-air ratio, the combustion process in

compression-ignition engines may be affected by inlet pressure, inlet temperature, and rpm to an appreciable extent. For these reasons it should not be assumed without experimental verification that indicated efficiency remains constant in a compression-ignition engine, even with the same fuel-air ratio. However, it is obvious that even with this type of engine the maximum power under any given set of conditions is

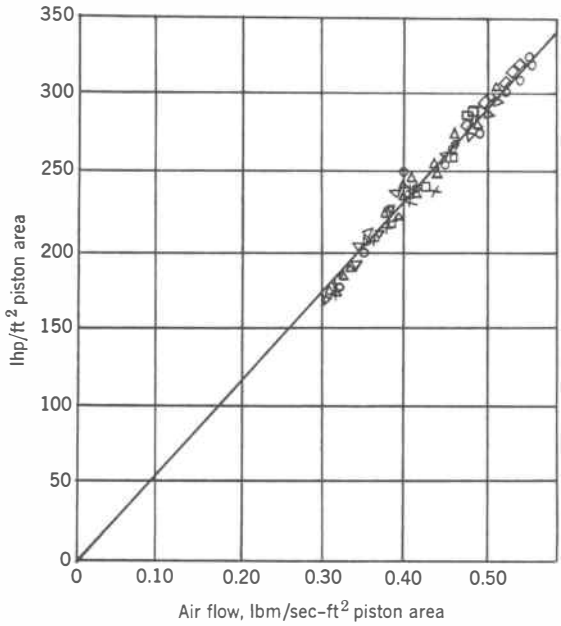

Fig 6-1. Relationship of indicated power and air flow: CFR engine, 3.25 x 4.5 in; $r = 5$; $F/F_c = 1.2$. Different symbols are for different inlet-valve sizes, shapes, and lifts. (Livengood and Stanitz, ref 6.41)

limited by the air capacity as soon as the maximum practicable value of $(FQ_c\eta)$ has been reached. This maximum value is largely determined by the maximum value of F which may be used without difficulties from smoke, excessive deposits of carbonaceous material, or excessive cylinder pressures.

DEFINITIONS

In this study it is convenient to use the following definitions, some of which have already been stated but are repeated here for the sake of emphasis.

Induction Process. The events which take place between inlet-valve opening and inlet-valve closing.

Fresh Mixture. The new gases introduced to the cylinder through the inlet valve. These gases consist of air, water vapor, and fuel in carbureted engines and of air and water vapor only in Diesel and other fuel-injection engines. Subscript i is used in referring to the fresh mixture, and subscript a, in referring to the air in the fresh mixture.

Residual Gases. The gases left in the charge from the previous cycle. Subscript r is used in referring to these gases.

Charge. The contents of the cylinder after closing of all valves; the charge consists of the fresh mixture and the residual gases.

VOLUMETRIC EFFICIENCY

In studying air capacity it is convenient to set up a figure of merit which is independent of cylinder size. Such a figure of merit for the four-stroke cycle is the *volumetric efficiency*, introduced in Chapter 4. In terms of quantities applying to an actual engine, volumetric efficiency is defined as the mass of fresh mixture which passes into the cylinder in one suction stroke, divided by the mass of this mixture which would fill the piston displacement at *inlet density*. Expressed algebraically,

$$e_v = \frac{2\dot{M}_i}{NV_d\rho_i} \tag{6-2}$$

where $\dot{M}_i$ = mass of fresh mixture per unit time
N = number of revolutions per unit time
V_d = total displacement volume of the engine
ρ_i = inlet density

The factor 2 in this equation arises from the fact that in the four-stroke engine there is one cycle for every two crank revolutions. A similar expression applying to two-stroke engines is developed in Chapter 7.

Definition of Inlet Density. Volumetric efficiency is of chief interest as a measure of the performance of the *cylinder assembly* as an air-pumping device. In order to evaluate this quantity, it is necessary to define the inlet density as the density of fresh mixture in or near the inlet port. When ρ_i is determined in this manner the resulting volumetric efficiency measures the pumping performance of the cylinder and valves alone.

As is explained later, it may not always be convenient, or even possible, to measure ρ_i at the inlet port. However, density can always be measured in the atmosphere near the air intake to the engine. When ρ_i is measured at this point the resulting volumetric efficiency measures the flow performance of all the equipment in the system between air intake and cylinder, as well as the pumping performance of the cylinder itself. The volumetric efficiency based on this method of measurement is called the *over-all volumetric efficiency.*

Over-All Volumetric Efficiency. In unsupercharged engines, with small pressure and temperature changes in air cleaner, carburetor, and inlet manifold, over-all volumetric efficiency will not differ greatly from volumetric efficiency based on inlet-port density. Because of convenience in measurement over-all volumetric efficiency is often used in connection with unsupercharged engines.

Over-all volumetric efficiency is of little significance in supercharged engines, since it does not differentiate between supercharger and cylinder performance. It is seldom used in such cases.

Unless otherwise noted, the volumetric efficiencies discussed in this chapter are based on values of ρ_i at the inlet port.

Volumetric Efficiency Based on Dry Air. On account of the close relationship between indicated output and air capacity (see Fig 6-1), it is convenient to express volumetric efficiency in terms of $\dot{M}_a$, the dry air supplied per unit time. Let ρ_a be the mass of dry air per unit volume of the fresh mixture. Since fuel, air, and water vapor all occupy the same volume, it is evident that $\dot{M}_a/\rho_a = \dot{M}_i/\rho_i$.

It is also convenient to substitute mean piston speed and piston area for displacement volume and N in eq 6-2. Making these substitituons in eq 6-2 gives

$$e_v = \frac{4\dot{M}_a}{\rho_a A_p s} \tag{6-3}$$

MEASUREMENTS OF VOLUMETRIC EFFICIENCY IN ENGINES

It is obvious from eq 6-3 that volumetric efficiency can be evaluated for any engine under any given set of operating conditions, provided $\dot{M}_a$ and ρ_a can be measured.

Measurement of Air Capacity. No serious difficulties in measuring $\dot{M}_a$ are involved if suitable air-measuring equipment is available and the air meter is protected from pulsations in air flow by suitable *surge tanks*

located between the engine and the air meter. The ASME sharp-edge orifices (ref 6.01) have been found to furnish a very satisfactory system of air measurement.

Measurement of Inlet Air Density. For mixtures of air, water vapor, and gaseous or evaporated fuel we may use Dalton's law of partial pressures:

$$p_i = p_a + p_f + p_w \tag{6-4}$$

where p_i = total pressure
p_a = partial pressure of air
p_f = partial pressure of fuel
p_w = partial pressure of water vapor

Since each constituent behaves nearly as a perfect gas, we can write

$$\frac{p_a}{p_i} = \frac{p_a}{p_a + p_f + p_w} = \frac{M_a/29}{M_a/29 + M_f/m_f + M_w/18}$$

$$= 1 \Big/ \left(1 + F_i \frac{29}{m_f} + 1.6h\right) \tag{6-5}$$

where M indicates mass, 29 is the molecular weight of air, 18 is the molecular weight of water, and m_f is the molecular weight of the fuel vapor. F_i is the mass ratio of fuel vapor to dry air, and h is the mass ratio of water vapor to dry air at the point at which p_i and T_i are measured.

From the gas law

$$\rho_a = \frac{29p_a}{RT_i} = \frac{29p_i}{RT_i}\left(\frac{1}{1 + F_i(29/m_f) + 1.6h}\right) \tag{6-6}$$

This equation shows that the air density in the mixture is equal to the density of air at p_i and T_i, multiplied by a correction factor which is the quantity in parenthesis.*

Figure 3-1 shows values of h over the usual range of interest. Values of m_f are given in Table 3-1. Figure 6-2 gives values of the correction factor in eq 6-6 for typical fuels over the range of interest.

In Fig 6-2 the curves for octene can be taken as representative for gasoline. In laboratory testing it is unusual to find h in excess of 0.02, and it is usually much smaller. With the usual manifold design, F_i is small. Under these circumstances the correction factor will generally be less than 0.98, which is within the accuracy of measurement in all but

* When pressure is in psia and temperature in °R, $29p/RT$ is equal to $2.7p/T$.

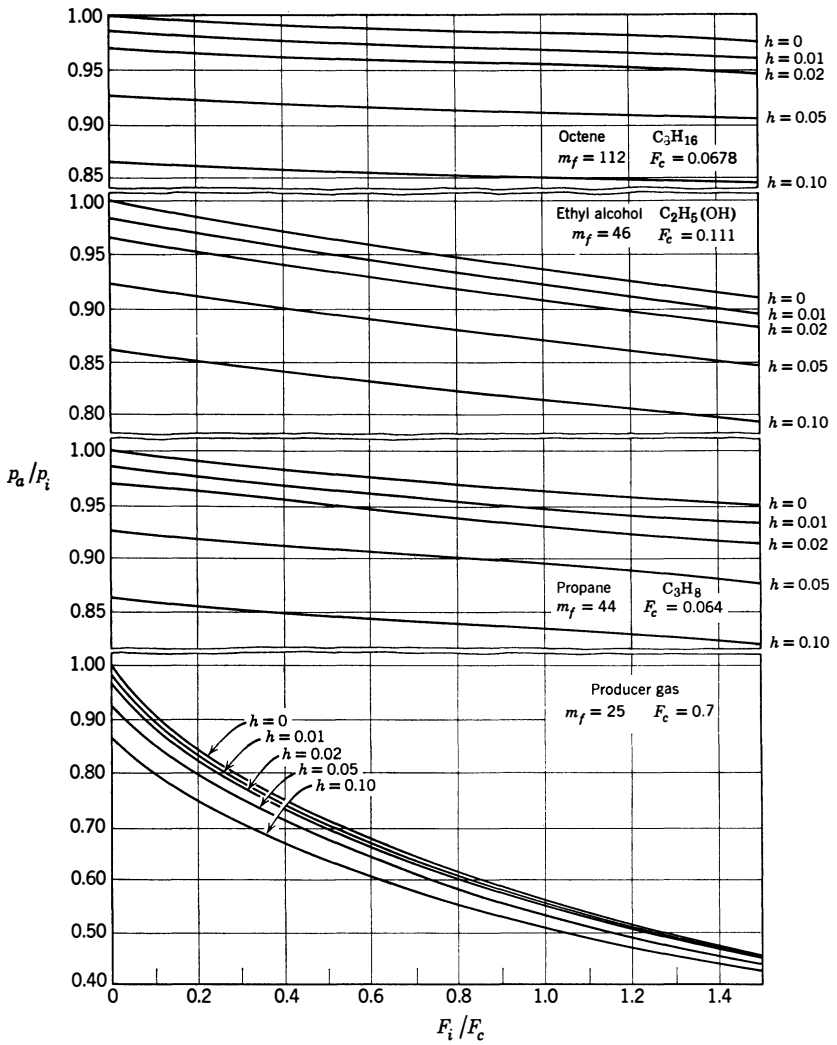

$$\frac{p_a}{p_i} = \frac{1}{1 + F_i \frac{29}{m_f} + 1.6h}$$

Fig 6-2. Ratio air pressure to total pressure in fuel-air-water-vapor mixtures: p_a = air pressure; p_i = total pressure; F_i = mass fuel vapor/mass dry air; h = mass water vapor/mass dry air.

the most carefully conducted engine tests. In the case of Diesel engines F_i is, of course, zero.

In practice, with spark-ignition engines using gasoline and with Diesel engines, the following approximation is quite generally used:

$$e_v \cong \frac{\dot{M}_a}{\left(\frac{29p_i}{RT_i}\right)\left(\frac{A_p s}{4}\right)} \tag{6-7}$$

On the other hand, in regions of high humidity or with carbureted engines using fuels of low molecular weight, Fig 6-2 shows that the correction factor in eq 6-6 should not be ignored.

Figure 6-2 also shows that the use of fuels of light molecular weight in carbureted engines will reduce air capacity considerably because of the reduction in ρ_a at a given inlet pressure.

Measurement of F_i. When the fuel is gaseous at the point at which ρ_i is measured, F_i is equal to the over-all ratio of fuel to air. However, when evaporation of a liquid fuel is incomplete at the point in question there is no simple method of measuring F_i. Since liquid fuel is generally present in the inlet manifold and inlet ports of a gasoline engine, the approximation indicated by eq 6-7 is generally used for such cases.

Measurement of p_i and T_i. The usual pressure fluctuations in an inlet pipe obviously introduce difficulties in measuring p_i and T_i. Also, when liquid fuel is present there is no satisfactory way of measuring T_i, the temperature of the gaseous portion of the mixture.

In the laboratory these difficulties can be overcome by the arrangement suggested in Chapter 1 and shown in Fig 1-2. To represent engines fed with a fuel-air mixture, fuel is introduced in or before the inlet tank, and the temperature in the tank is maintained high enough so that fuel evaporation is complete before the mixture reaches the thermometer which measures T_i. If this thermometer, together with the pressure-measuring connection, is located in the tank, the resultant measurements will give the T_i and p_i specified in the definition of volumetric efficiency. F_i will be equal to the over-all fuel-air ratio.

Although the arrangement just described is feasible for laboratory tests of single-cylinder engines, it is usually inconvenient for multicylinder engines.

In the case of unsupercharged carbureted engines p_i and T_i are most often measured ahead of the carburetor, and the over-all volumetric efficiency is recorded. In the case of supercharged carbureted engines,

when cylinder performance is desired, the following approximations are generally used:

1. p_i is taken as equal to the reading of a manometer connected to some convenient point in the inlet manifold.
2. T_i is taken as equal to the reading of a thermometer in the air stream ahead of the carburetor, unless there is reason to believe that fuel evaporation is substantially complete in the inlet manifold, in which case the reading of a thermometer in the inlet manifold may be used.
3. F_i is ignored, except in the case of carbureted engines using gaseous fuels.

For supercharged engines using cylinder injection or inlet-port injection pressure and temperature readings in the inlet manifold are generally used.

When fewer than three cylinders are connected to a small inlet manifold pressure fluctuations are often so severe that the readings from a pressure gage will not yield the true average pressure. Such situations are to be avoided if accurate evaluations of volumetric efficiency are desired.

VOLUMETRIC EFFICIENCY, POWER, AND MEAN EFFECTIVE PRESSURE

Substituting the value for $\dot{M}_a$ indicated by eq 6-3 in eq 6-1 gives

$$P = \tfrac{1}{4} J A_p s \rho_a e_v (F Q_c \eta) \tag{6-8}$$

for four-stroke engines. Since mep is defined as the work per cycle divided by the piston displacement,

$$\text{mep} = \frac{4P}{A_p s} = J \rho_a e_v (F Q_c \eta) \tag{6-9}$$ *

The mean effective pressure may be indicated or brake, depending on whether η is the indicated or brake thermal efficiency. Equation 6-9 shows that mean effective pressure is proportional to the product of inlet-air density and volumetric efficiency when the product of the fuel-air ratio, the heat of combustion of the fuel, and the thermal efficiency are constant. Thus the relation between the product $\rho_a e_v$ and the mean

* When mep is in psi, ρ_a in lbm/ft^3 and Q_c is in Btu/lbm, the coefficient J in eq 6-9 is 778/144 = 5.4. In eq 6-8, if these units are used and P is in horsepower, s in ft/min, the value of J is 778/33,000 = 1/42.4.

effective pressure is the same as the relation between air capacity, $\dot{M}_a$, and power, as given in eq 6-1.

IDEAL INDUCTION PROCESS

In order to study the real induction process and its volumetric efficiency, it is convenient to consider first an idealized four-stroke induction process.

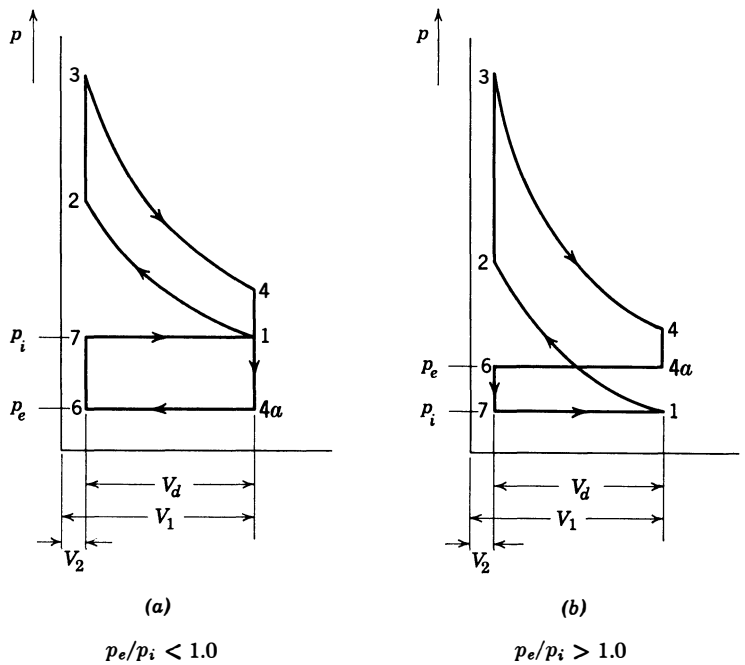

Fig 6-3. Idealized four-stroke inlet process. (See also Fig 4-4)

Let an ideal induction process be defined by the process 6–7–1 in Fig 6-3 and the following assumptions:

1. Both fresh mixture and residual gases are perfect gases with the same specific heat and molecular weight
2. No heat transfer (adiabatic process)
3. Inlet pressure constant = p_i
4. Inlet temperature constant = T_i
5. Exhaust pressure constant = p_e

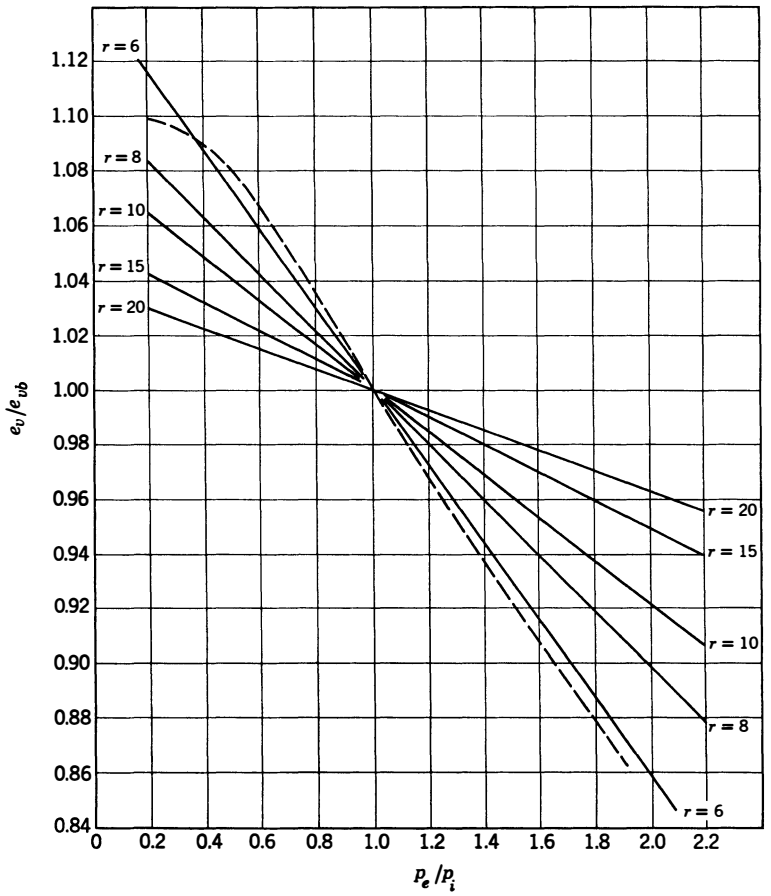

Fig 6-4. Effect of p_e/p_i on volumetric efficiency with small valve overlap: e_{vb} is vol eff when $p_e/p_i = 1.0$

———— is ideal process, $e_v/e_{vb} = 0.285 + \dfrac{r - p_e/p_i}{1.4(r-1)}$

--------- is measured from two aircraft cylinders with $r = 6$. (Livengood and Eppes, ref 6.45)

At point 6 the clearance space above the piston, V_2, is filled with residual gas at temperature T_r and pressure p_e. At this point the exhaust valve closes, and as soon as it is closed the inlet valve opens.

Before the piston starts to move, if $p_i > p_e$, fresh mixture flows into the cylinder, compressing the residual gases to p_i. If $p_i < p_e$, residual gas flows into the inlet pipe until cylinder pressure equals p_i.

The piston then moves from V_2 to V_1 on the inlet stroke, with pressure in the cylinder equal to p_i at all times (line 7–1 in Fig 6-3). If any residual gas was in the inlet pipe, it is returned to the cylinder during this process.

By assuming that the specific heats of fresh mixture and residual gas are the same and by using the laws of a perfect gas, it is shown in Appendix 4 that the volumetric efficiency of this ideal cycle may be expressed as follows:

$$e_{vi} = \frac{k-1}{k} + \frac{r - (p_e/p_i)}{k(r-1)} \tag{6-10}$$

For this process the volumetric efficiency when $(p_e/p_i) = 1$ is evidently equal to unity. Figure 6-4 shows volumetric efficiencies of this cycle for various values of p_e/p_i and r.

Effect of Residual-Gas Temperature. It has often been supposed that volumetric efficiency is reduced by heat transfer between hot residual gases and the fresh mixture when the two gases mix together

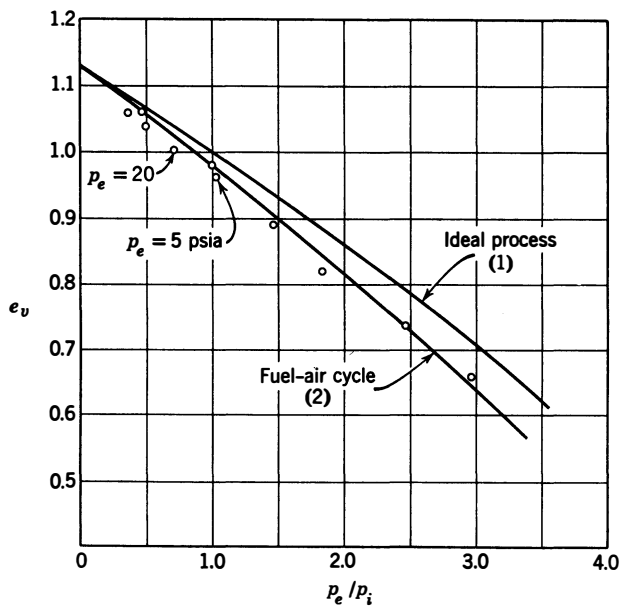

Fig 6-5. Volumetric efficiencies of four-stroke inlet processes. (1) Ideal process with a perfect gas, $r = 6$. (2) Four-stroke fuel-air cycle (see Chapter 4): $r = 6$; $T_i = 600°R$; $p_e = 14.7$ psia except as noted; F_R (fuel-air cycle) = 1.18. (Mehta, ref 6.11)

during the induction process. Therefore, it is interesting to note that the temperatures T_i and T_r do not appear in eq 6-10. The reason that these temperatures do not affect e_v in this idealized process can be visualized by remembering that, with the same specific heat and molecular weight, when the two gases mix at constant pressure the contraction of the residual gas as it is cooled by the fresh mixture equals the expansion of the fresh mixture as it is heated by the residual gas. Thus no change in volume occurs in the mixing process, and no gas moves into or out of the cylinder on this account.

Volumetric Efficiency of Fuel-Air Cycles. It may be recalled from Chapter 4 that the ideal inlet process proposed for the fuel-air cycle is the same as that proposed in this chapter, except for the fact that the assumption of perfect gases with the same specific heat and the same molecular weight is not included. The volumetric efficiency of such cycles is plotted in Fig 4-5 (p. 86). Figure 6-5 compares the volumetric efficiency of fuel-air cycles with that for the ideal induction process of eq 6-10 at $r = 6$.

The difference in volumetric efficiency between the fuel-air curve and that for the present ideal process is the result of the difference in specific heat and molecular weight between fresh and residual gases in the fuel-air cycle. The region of practical interest is that in which p_e/p_i is equal to or less than unity. Here the differences between the two processes are considered negligible.

VOLUMETRIC EFFICIENCY FROM THE INDICATOR DIAGRAM

Before considering the many variables which affect volumetric efficiency in engines, it may be well to examine and to discuss the nature of the induction process as shown by the light-spring indicator diagram.

Figure 6-6 shows a typical light-spring indicator diagram with the inlet valve opening at x and closing at y. In order to develop a reasonably simple expression for volumetric efficiency from the pressure-volume relations shown by such a diagram, it is necessary to make two simplifying assumptions, namely:

1. Fresh and residual gases are perfect gases with the same specific heat and molecular weight.

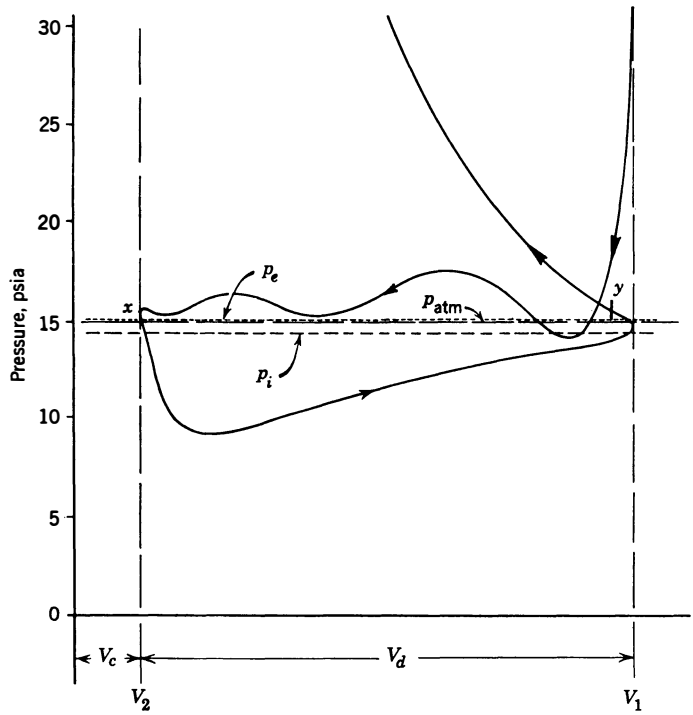

Fig 6-6. Typical light-spring indicator diagram: CFR engine, 3.25 x 4.5 in; r = 8.35; F/F_c = 1.18; s = 900 ft/min; T_i = 175°F; p_i = 14.4; p_e = 15.1 psia; pmep = 4.65 psi. (Sloan Automotive Laboratories.)

2. There is no appreciable flow through the exhaust valve after the inlet valve starts to open.*

For the induction process between inlet-valve opening at x and closing at y, from the general energy eq 1-16, we can write

$$(M_i + M_r)E_y - M_iE_i - M_rE_r = Q - w/J \qquad (6\text{-}11)$$

where M_i = mass of fresh mixture taken in
M_r = mass of residual gas in the cylinder during induction

* Flow through the exhaust valve after the inlet valve opens is possible only when there is an appreciable *overlap angle*, that is, when exhaust closing follows inlet opening by a considerable number of degrees of crank travel. The present discussion and analysis is based on the assumption that the valve overlap is so small that this type of flow is negligible. With the usual cam contours, this assumption is satisfactory for overlap angles of 20° or less.

E_y = internal energy, per unit mass of gas, at the end of the induction process
E_i = internal energy of the fresh mixture, per unit mass, at the start of the process
E_r = internal energy of the residual gases, per unit mass, at the start of the process
Q = net heat transferred to the gases during the process (if the gases lose heat, Q is negative)
w = work done by the gases on the piston, minus the work done by the inlet pressure on the gases; that is,

$$w = \int_x^y p\,dV - p_i e_v V_d \tag{6-12}$$

where p is the instantaneous cylinder pressure during induction and V_d is the displacement volume, $V_1 - V_2$.

As shown in Appendix 4, expressions 6-2, 6-10, and 6-11 can be combined to give the following relation:

$$e_v = \frac{1}{1 + (\Delta T/T_i)} \left\{ \frac{\alpha(k-1)}{k} + \frac{(p_y y/p_i)r - (p_x/p_i)}{k(r-1)} \right\} \tag{6-13}$$

where k = specific-heat ratio of the gases
$\Delta T = Q/C_p M_i$; that is, ΔT is the rise in temperature of the fresh gases which would occur if Q were added to the fresh mixture at constant pressure
r = compression ratio V_1/V_2
$y = V_y/V_1$
α = ratio of actual work on the piston to the product $p_i V_d$; that is,

$$\alpha = \int_x^y p\,dV/p_i V_d \tag{6-14}$$

The quantities, p_i, T_i, V_d, r, and k are fixed by the conditions of operation. All other quantities on the right-hand side of this equation, except ΔT, can be obtained from the indicator diagram. It will be noted that the value of the integral can be obtained by measuring the area under the curve from x to y (Fig 6-6), giving proper attention to algebraic signs. The value of k can safely be taken as 1.4, if the fresh charge is air, or 1.37, if it is a mixture of fuel and air, since the fraction of the residual gas in the charge is usually small.

By comparing eq 6-13 with the corresponding equation for the ideal process eq 6-10, we find that for the ideal process

$$\Delta T = 0, \qquad \alpha = 1, \qquad y = 1, \qquad p_y y/p_i = 1, \qquad p_x/p_i = p_e/p_i$$

Substituting these values in eq 6-13 gives eq 6-10. Taking k as 1.4, eq 6-10 can be written

$$e_{vi} = 0.285 + \frac{r - p_e/p_i}{1.4(r - 1)} \tag{6-15}$$

We have seen from Fig 6-5 that the actual differences in specific heat and molecular weight between the fresh mixture and the residual gases do not seriously affect the validity of eq 6-13, which has been developed on the basis of equal specific heats and molecular weights for these two components. If the specific heat effect is taken to be negligible, this

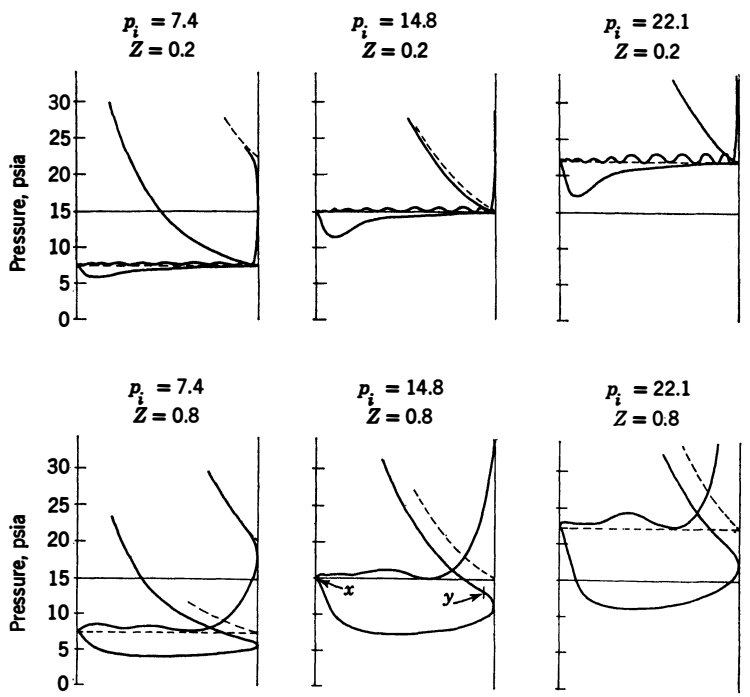

Fig 6-7. Light-spring diagrams with $p_e/p_i = 1$: CFR engine, shrouded inlet valve; bore = 3¼ in; stroke = 4½ in; $r = 6.5$; $D_i = D_e = 1.350$ in; $C_i = 0.18$; $C_e = 0.36$. (Grisdale and French, ref 6.10)

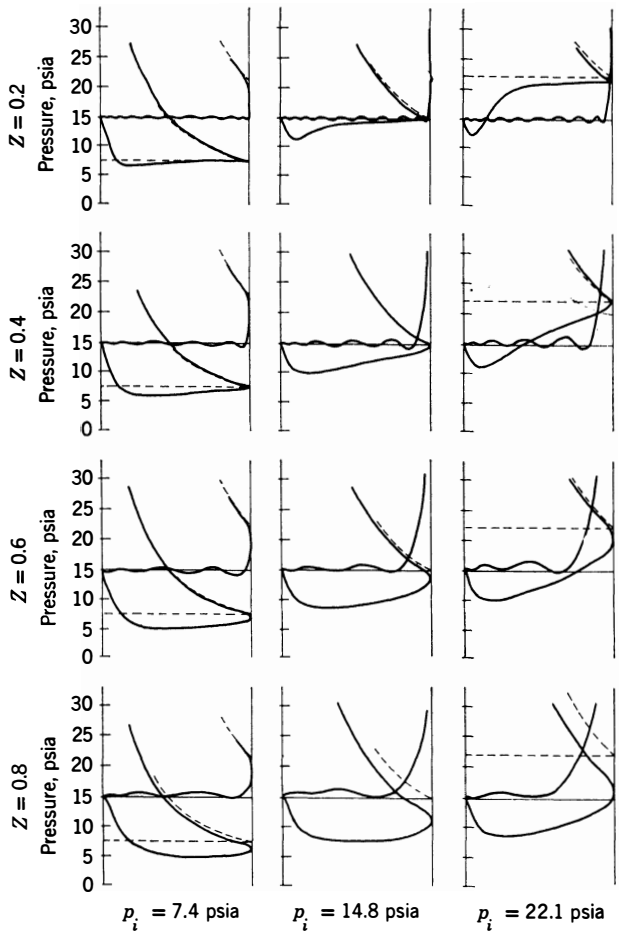

Fig 6-8. Light-spring diagrams with variable ratio of exhaust-to-inlet pressure: Same engine and same conditions as Fig 6-7; p_e = 14.8 psia. (Grisdale and French, ref 6.10)

equation can be quite useful in analyzing real indicator diagrams obtained from engines with small valve overlap, provided the diagrams are accurate.

Since all quantities in eq 6-13 except ΔT can be measured by means of existing equipment, including an accurate indicator, eq 6-13 may be used to evaluate ΔT, as will be explained.

Another quantitative use of eq 6-13 is to determine the relative importance of induction work and pressure effects on volumetric efficiency.

Figures 6-7 and 6-8 show light-spring indicator diagrams made with various values of p_e/p_i for an engine with small valve-overlap angle.

Figure 6-9 shows curves, plotted against the parameter Z. Z is the nominal mach index of the gases flowing through the inlet valve. With a given cylinder and valve design, piston speed is proportional to Z, and the mass velocity, G, increases with increasing Z. This parameter is discussed in detail later.

e_v is the *measured* volumetric efficiency, taken from air-flow measurements made while the indicator diagrams of Figs 6-7 and 6-8 were taken.

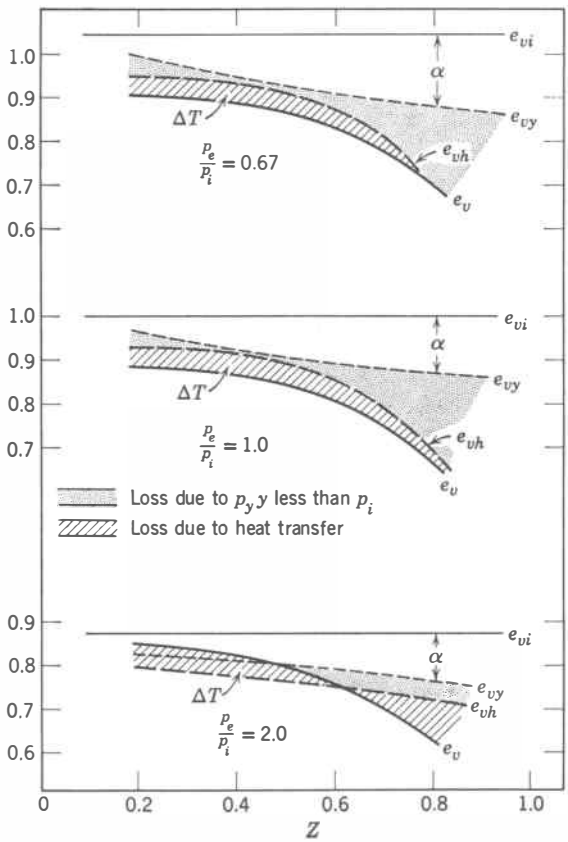

Fig 6-9. Volumetric efficiency vs inlet Mach index: e_{vi} = ideal volumetric efficiency; e_v = measured volumetric efficiency; e_{vh} = volumetric efficiency without heat transfer; e_{vy} = volumetric efficiency without heat transfer and with $p_y y/p_i = 1.0$; α loss due to reduced inlet-stroke work. (From indicator diagrams of Figs 6-7 and 6-8)

e_{vh} volumetric efficiency computed from eq 6-13 with ΔT assumed zero.

e_{vy}, volumetric efficiency computed from eq 6-13 with $\Delta T = 0$ and $p_y y/p_i = 1$.

e_{vi}, volumetric efficiency of the corresponding ideal process, eq 6-10.

EFFECT OF HEAT TRANSFER ON VOLUMETRIC EFFICIENCY

Let it be assumed that the pressures during the inlet process are not affected by the heat transferred to or from the gases during that process. This assumption has been shown to be nearly true over a considerable range of operating conditions (ref 6.32—). Under this assumption, the entire effect of heat transfer is contained in the value of ΔT, and a volumetric efficiency calculated from eq 6-13 setting $\Delta T = 0$ will give the value which would have been obtained without heat transfer. This non-heat-transfer volumetric efficiency is called e_{vh}.

Values of e_{vh} for the indicator diagrams of Figs 6-7 and 6-8 are plotted in Fig 6-9. The difference between e_v and e_{vh}, that is, the *heat-transfer effect*, is the hatched area shown for each set of curves.

In order to explain the trends indicated by the hatched areas of Fig 6-9, it is convenient to consider a simplified model of the induction system, Fig 6-10, which represents a gas flowing through a heated cylindrical tube.

In Appendix 5 it is shown that the rise of temperature of the gas as it flows through the tube can be written

$$\Delta T = C(GD)^{-0.2} \frac{L}{D} \{T_s - T_x\} \tag{6-16}$$

where C = a constant
L = length of jacketed tube
D = tube diameter
G = mass flow of gas divided by tube section area
T_s = mean surface temperature of the tube
T_x = the mean temperature of the gas as it flows through the tube

If the model is a good qualitative representation of the heat transfer process during induction, it can be used to explain the trends shown in Fig 6-9. In considering this figure, it should be remembered that inlet and coolant temperatures and fuel-air ratio were the same for all runs.

In Fig 6-9 the mass flow per unit area increases with increasing Z. In eq 6-16 ΔT decreases as G increases. Thus the model explains the observed fact that the heat-transfer effect grows smaller as gas flow increases.

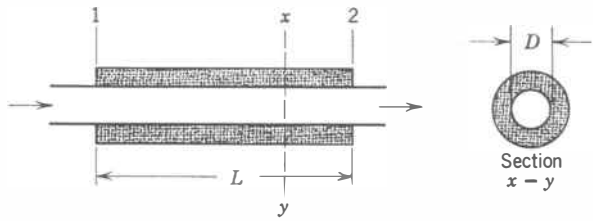

Fig 6-10. Heat-transfer model for a fluid flowing through a heated tube:

$$\Delta T = (T_2 - T_1) = \frac{Kk_c}{\dot{M}C_p}\left(\frac{\rho u D}{\mu g_0}\right)^{0.8} \pi L(T_s - T_x)\mathbf{P}^{0.4} \qquad \text{(A-38)}$$

For gases at moderate temperature:

$$\Delta T = C(GD)^{-0.2}\frac{L}{D}(T_s - T_x) \qquad \text{(A-39)}$$

T_s = tube surface temperature;
T_1 = gas temperature at section 1;
T_2 = gas temperature at section 2;
T_x = mean gas temperature between 1 and 2;
K = a dimensionless coefficient;
k_c = fluid coefficient of conductivity;
$\dot{M}$ = mass flow of fluid per unit time;
C_p = specific heat at constant pressure;
u = fluid velocity;
ρ = fluid density;
μ = fluid viscosity;
g_0 = Newton's law constant;
$\mathbf{P}$ = fluid Prandtl number;
$G = \rho u = 4\dot{M}/\pi D^2$;
C = a near constant for gases at moderate temperatures. (See Appendix 5 for derivation.)

Figure 6-9 shows that the heat-transfer effect is smaller as the value of p_e/p_i grows larger. We have seen in our study of the fuel-air cycle (Chapter 4) that both the fraction of residual gas and its temperature (f and T_5 in Fig 4-5) increase with increasing values of p_e/p_i. In the model this means that T_x increases and ΔT decreases.

Surface Temperature, T_s. The surfaces for heat transfer during induction are the surfaces of the inlet manifold, inlet port, inlet valve,

and cylinder walls. The mean temperature of these parts evidently will vary with fuel-air ratio, coolant temperature, and to some extent with T_i. The design of the engine will also have a strong effect on T_s, especially as between engines in which the inlet manifold is and is not heated by the exhaust gases. Since F, T_c, and T_i were all constant in Fig 6-9, that figure furnishes no information on the results of changing these three quantities.

Pressure Effects Shown by Indicator Diagrams. If we continue to use the assumption that pressures are not affected by heat transfer, it is seen that the difference between the ideal volumetric efficiency, e_{vi}, and the no-heat-transfer volumetric efficiency, e_{vh}, must be due entirely to the following:

1. p_x greater than p_e. In the diagrams of Figs 6-7 and 6-8, p_x seems to be equal to p_e in each case. However, the use of a smaller exhaust valve or the presence of dynamic pressure waves in the exhaust system often results in $p_x > p_e$ and a loss in e_v as compared to e_{vi}.
2. $p_y y/p_i$ less than 1.0. When this is the case the compression line on the indicator diagram falls below the ideal line, which is an isentropic starting at p_i and V_1 (shown dotted in Figs 6-7 and 6-8).

In Fig 6-9, when $p_e/p_i = 2$ and $Z < 0.6$, the heat-transfer effect makes e_v greater than e_{vh}. This relation means that the mean gas temperature, T_x, is less than T_s in this regime and that heat flows from the gases to the cylinder walls, thus improving volumetric efficiency.

In practice, the volumetric efficiency when p_e/p_i is much larger than 1 is of little practical interest, since this situation occurs only in throttled engines in which air capacity is deliberately cut down by reducing p_i.

In real engines the inlet valve always closes after the piston has passed bottom center, and y is therefore always less than 1.0. The object of such timing is to secure a maximum value of $p_y y$ at some particular speed by utilizing dynamic effects. At low engine speeds dynamic effects are small, and the pressure in the cylinder tends to remain at p_i until the valve closes. In this case the fraction $p_y y/p_i = y$, and there is a loss, compared to the ideal process. Another way of visualizing this loss is to see that at low engine speeds the cylinder contents will be pushed back into the inlet manifold between bottom center and the point of inlet-valve closing.

As engine speed is increased from a low value, p_y increases, due to favorable dynamic effects. The value of y, that is, the point of inlet-

valve closing, is chosen to take fullest advantage of dynamic effects at the speed at which maximum torque is desired. In the case of Fig 6-9 minimum $p_y y$ loss occurs at about $Z = 0.5$. As speed is increased still further, p_y falls off with rising speed due to pressure loss through the inlet valve. This falling off is evident in the two top diagrams of Fig 6-9. (Note that the real compression curve is appreciably below the ideal curve at the highest value of Z, that is, the highest speed in Fig 6-8.)

The fact that the $p_y y$ loss appears to be constant when $p_e/p_i = 2.0$ may be due to experimental error. In any case, volumetric efficiency when the engine is throttled to this extent is of little practical interest.

Reduced Inlet-Stroke Work. The remaining loss, that is, the difference between e_{vi} and e_{vy} (Fig 6-9), is due to the fact that α is less than unity. Decreasing α means that the work done on the piston by the gases decreases, thus leaving the gases at a higher temperature at the end of the inlet process than would have been the case had the cylinder pressure been equal to p_i at all times. The fact that α is less than unity is due to the pressure drop through the inlet valve during the suction stroke. It is evident from the indicator diagrams that this pressure drop becomes greater as gas flow increases, and therefore α becomes smaller.

USE OF DIMENSIONAL ANALYSIS IN VOLUMETRIC EFFICIENCY PROBLEMS

The foregoing analysis has shown how the light-spring diagram may be used in the study of volumetric efficiency and has served to show some basic factors which control this important parameter. Unfortunately, in most practical cases accurate light-spring indicator diagrams are not available. An alternative approach, found useful by your author, employs analogy with steady-flow processes, together with the principles of dimensional analysis (refs 11.001–11.007) which are now reasonably well known but have not been extensively used in connection with internal-combustion engines.

From the discussion to this point it is obvious that the process of induction is one involving fluid flow and heat flow. Gravitational forces may be considered negligible.

Appendix 3 gives equations for the flow of a perfect gas through an orifice of area A, without heat transfer. Equation A-15 can be written

in dimensionless form as follows:

$$\frac{\dot{M}}{Aa\rho} = \phi_1(k, p_2/p_1, m) \tag{6-17}$$

		Dimensions
where $\dot{M}$ =	mass flow per unit time	Mt^{-1}
A =	the orifice area	L^2
a =	sonic velocity in entering gas at pressure p_1 and temperature T_1	Lt^{-1}
p_1 =	upstream stagnation pressure	FL^{-2}
T_1 =	upstream stagnation temperature	T
ρ =	density of the gas at p_1 and T_1	ML^{-3}
p_2 =	downstream static pressure	FL^{-2}
k =	specific-heat ratio of the gas	1
m =	molecular weight of the gas	1

ϕ indicates a mathematical function of the variables in parenthesis and means that if values are assigned to all of them a value of the mass flow term is determined.

Since $\dot{M}/A\rho$ is the mean gas velocity through area A, it can be called a *typical velocity* of the flow system and designated by u. Thus the left-hand term of eq 6-17 can be written u/a and is usually called the *Mach index* of the flow system.

The flow of a real gas through a real orifice, without heat transfer, is usually handled by placing a coefficient C before the function sign of eq 6-17. C depends on the design of the whole flow system, including the orifice and the pressure-measuring connections, as well as on the *Reynolds number*, which is defined in Appendix 5. Thus, for a real flow system, we can write

$$\frac{u}{a} = \phi_2\left(\frac{p_2}{p_1}, \frac{uL\rho}{\mu g_0}, k, m, R_1 \cdots R_n\right) \tag{6-18}$$

$R_1 \cdots R_n$ are the *design ratios* of the flow system, that is, the ratios of all pertinent dimensions of the system to the typical dimension L.

In words, eq 6-18 states that the Mach index at a given point in a passage through which a perfect gas flows without heat transfer depends on the ratio of outlet to inlet pressure, the Reynolds number of the system, the specific heat ratio and molecular weight of the gas, and on the shape of the whole flow system, including the pressure-measuring connections.

Let us now add heat transfer to the problem, assuming a system behaving according to expression 8-1 (p. 269). The new variables to be

added are

Symbol	Name	Dimensions
k_c	heat conductivity of gases	$Qt^{-1}L^{-1}T^{-1}$
C_p	specific heat of gases	$QM^{-1}T^{-1}$
T_s	mean temperature of the walls during induction	T
T_x	temperature of gases entering tube	T

The mean gas temperature, T_x in expression 8-1, is dependent on the other variables and therefore need not be included.

The rules of dimensional analysis say that when there are n variables and m fundamental dimensions the number of dimensionless ratios which must be used is $n - m$. Since we have added four variables and two new dimensions (Q and T), two new dimensionless ratios will be required. By choosing these as the Prandtl number of the fluid, $\mathbf{P} = C_p\mu g_0/k_c$ and T_x/T_s, we can write

$$\frac{u}{a} = \phi_3\left(\frac{p_2}{p_1}, \frac{uL\rho}{\mu g_0}, \frac{T_x}{T_s}, \mathbf{P}, k, m, R_1 \cdots R_n\right) \tag{6-19}$$

For purposes of studying its air capacity, an engine may be considered as a gas-flow passage with heat transfer. But the engine has the further complication of moving parts and an internal-combustion process.

Motion of the various parts may be adequately described by adding to the variables in eq 6-19 the crankshaft angular speed, N, and additional design ratios describing all relevant parts.

In the engine the temperature of the walls, corresponding to T_s in eq 6-19, will be controlled by the design, by the coolant temperature, and by the mean temperature of the gases in the cylinder during the cycle. From our study of the fuel-air cycle (Chapter 4) we have seen that cyclic temperatures depend on T_i and on the fuel-air ratio and the compression ratio. (See Fig 4-5.) It is obvious that these temperatures will also depend on the heat of combustion of the fuel.

Therefore, in order to adapt eq 6-19 to an engine, it is necessary to

	Dimensions
substitute p_i for p_1	
substitute p_e for p_2	
substitute T_i for T_x	
replace T_s by T_c, the coolant temperature, and add	
F, the fuel-air ratio	1
Q_c, the heat of combustion	QM^{-1}
N, the crankshaft angular speed	t^{-1}

The compression ratio, r, as well as all other design ratios necessary to describe the gas-flow system, must be included in the design ratios.

Three new variables have been added to eq 6-19. No new dimensions have been added, so that three new dimensionless ratios are required. These will be chosen as follows:

$\frac{4\dot{M}}{A(NL)\rho}$, which is the volumetric efficiency, e_v, when A is the piston area and L is the stroke

T_iC_p/FQ_c

T_cC_p/FQ_c

Since we are chiefly interested in volumetric efficiency, this quantity is set on the left side of the equation, and u/a is transferred to the right. By making the above changes, we can write

$$e_v = \phi_4\left(\frac{u}{a}, \frac{p_e}{p_i}, \frac{uL\rho}{\mu g_0}, \frac{T_iC_p}{FQ_c}, \frac{T_cC_p}{FQ_c}, \mathbf{P}, k, m, R_1 \cdots R_n\right) \quad (6\text{-}20)$$

as applying to the volumetric efficiency of an engine.

Equation 6-20 is still not easy to use because it contains a typical velocity, u, which has not been specifically defined. This velocity can be eliminated from the Reynolds number by replacing it by a. This replacement is permissible under the rules of dimensional analysis, since the ratio u/a is included. By this means u is confined to one argument in eq 6-20.

Another simplification can be made by observing that the values of $\mathbf{P}$, k, and m depend only on the fuel-air ratio and type of fuel. Assuming that the type of fuel is sufficiently identified by its heat of combustion, we can substitute F for $\mathbf{P}$, k, and m.

Thus eq 6-20 can be written in more convenient form:

$$e_v = \phi\left(\frac{u}{a}, \frac{p_e}{p_i}, \frac{aL\rho}{\mu g_0}, \frac{T_iC_p}{FQ_c}, \frac{T_cC_p}{FQ_c}, F, R_1 \cdots R_n\right) \quad (6\text{-}21)$$

where ϕ = a mathematical function

u = characteristic gas velocity

p_i, T_i, ρ, and a = inlet pressure, temperature, density, and sonic velocity, respectively

μ = inlet viscosity

p_e = exhaust-system pressure

T_c = coolant temperature, usually taken as the average between coolant inlet and outlet temperatures

F = fuel-air ratio
Q_c = heat of combustion of the fuel
$R_1 \cdots R_n$ = engine design ratios, which must include the compression ratio and all other ratios necessary to describe the whole gas-flow passage through the engine

The form of the functional relation between e_v and each argument in eq 6-21 must be found by experiment. If the equation is correct, e_v will depend not on the separate variables which make up each argument but on the value of the argument as a whole. For example, when all other arguments are held constant, e_v should have the same value, whether p_e is 10 and p_i, 15, or p_e is 8 and p_i, 12, since the ratio p_e/p_i remains the same.

EFFECT OF OPERATING CONDITIONS ON VOLUMETRIC EFFICIENCY

Inlet Mach Index. For convenience the ratio of the typical velocity to the inlet sonic velocity, u/a, is called the *inlet Mach index.*

From the science of fluid mechanics we know that the controlling velocity in a compressible flow system is the velocity in the smallest cross section. Considering typical engine designs, it appears that the smallest cross section in the inlet flow system is usually the inlet-valve opening.

Since the actual velocity through the inlet valve is a variable and is seldom known, it would be convenient to find a known velocity upon which the actual velocity through the valve depends. If the fluids involved were incompressible, the mean velocity through the inlet valve at any instant would be $A_p s/A_i$, where A_p is the piston area, s is the velocity of the piston, and A_i is the area of the inlet valve opening. The corresponding Mach index is $A_p s/A_i a$.

For the usual cam contours, it might be expected that the mean flow area through the inlet valve will be proportional to $\pi D^2/4$, where D is the valve diameter. In this case A_p/A_i becomes $(b/D)^2$ where b is the cylinder bore.

Figure 6-11 shows e_v plotted against $(b/D)^2 s/a$ for a given engine equipped with inlet valves of various sizes, shapes, and lifts. Inlet temperature, and therefore a, was constant. The poor correlation obtained indicates that the velocity $(b/D)^2 s$ was not controlling.

As a next step it was decided to make flow tests through the valves at various lifts in order to determine their flow coefficients under low-velocity, steady-flow conditions. From these tests a *mean inlet flow co-*

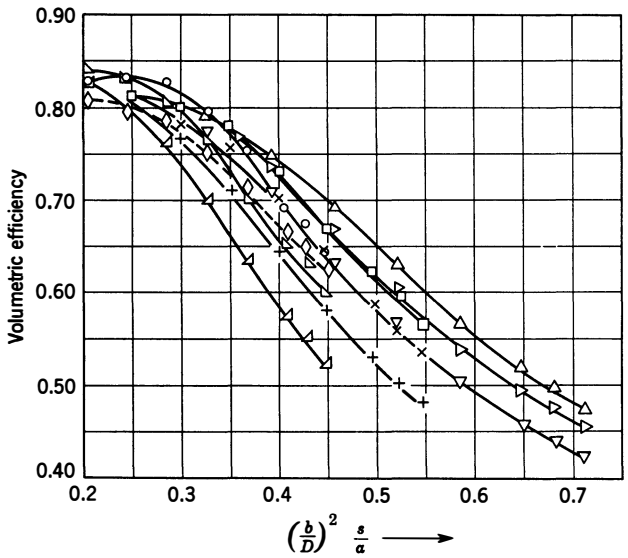

D (in) \ Lift (in) →	0.208	0.238	0.262	Design
1.050	◿	◺	○	A
0.950	+	×	□	A
0.830	▽	▷	△	A
1.050			◊	B

Fig 6-11. Volumetric efficiency with several inlet-valve sizes, lifts, and shapes: b = cylinder bore; D = valve outside diameter; s = mean piston speed; a = velocity of sound at inlet temperature; CFR 3.25 x 4.5 in cylinder; r = 4.92. (Livengood and Stanitz, ref 6.41)

efficient, C_i, was obtained. (See ref 6.40.) As indicated by Fig 6-12, this flow coefficient was computed by averaging the steady-flow coefficients obtained at each lift over the actual curve of lift vs crank angle used in the tests. At each lift the coefficient was based on the area $\pi D^2/4$. It was felt that if this area were multiplied by C_i a better correlation would be obtained.

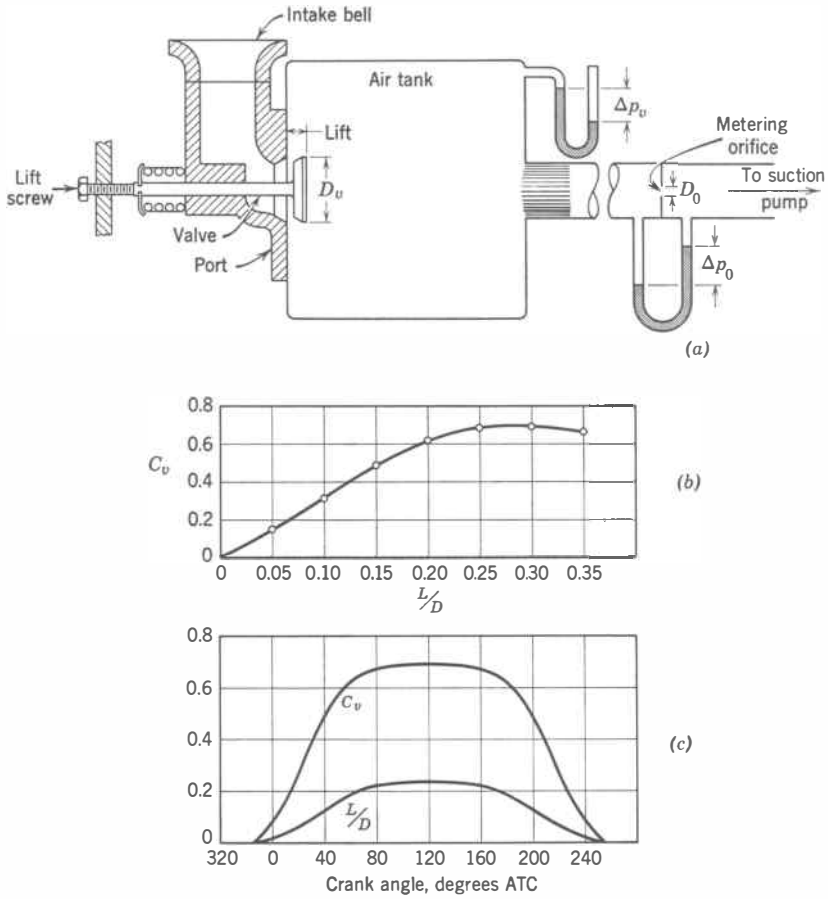

Fig 6-12. Method of measuring inlet-valve flow coefficient: (*a*) Experimental arrangement. For small pressure drops

$$C_v = C_0(D_0/D_v)^2\sqrt{\Delta p_0/\Delta p_v}$$

(*b*) Curve of C_v vs L/D from experimental results; (*c*) Plot of C_v vs crank angle. C_i = mean ordinate of C_v curve. (See also ref 6.40)

Figure 6-13 shows volumetric efficiency plotted against an inlet-valve Mach index defined as

$$Z = \left(\frac{b}{D}\right)^2 \frac{s}{C_i a} \tag{6-22}$$

The plot shows that e_v is a unique function of Z within the limits of measurement of engine operation over a wide range of engine speeds and

of inlet-valve diameters, lifts, and shapes. Valve timing was held constant.

As a further check on the validity of Z as a volumetric-efficiency parameter, Fig 6-14 shows e_v vs Z for a different valve timing and for several different values of p_e/p_i. The test data reduce to a single curve when base values e_{vb} are chosen at a particular value of Z, and other

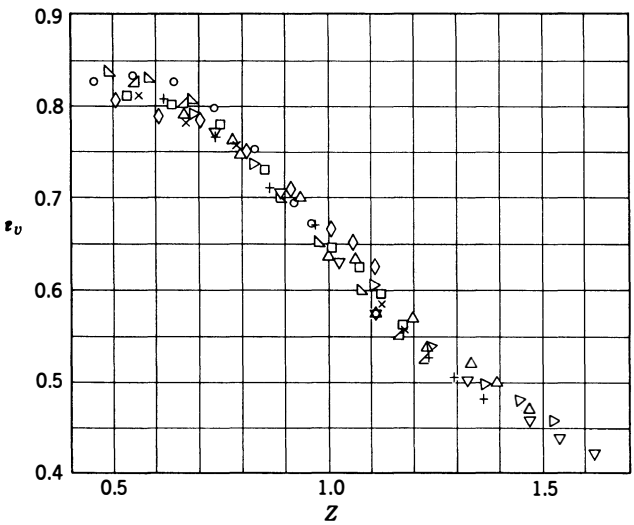

Fig 6-13. Volumetric efficiency vs inlet-valve Mach index. Same data as in Fig 6-11:

$$Z = (b/D)^2 \times s/C_i a$$

C_i = inlet-valve flow coefficient, as determined by method illustrated in Fig 6-12; r = 4.92; valve overlap = 6°; inlet closes 55° late; T_i = 580°R; T_c = 640°R, p_i = 13.5 psia; p_e = 15.45 psia; p_e/p_i = 1.14; F_R = 1.17; inlet pipe zero length. (Livengood and Stanitz, ref 6.41)

values are divided by the appropriate base value. In general, if eq 6-21 is true, this type of correlation should be possible for any of its independent arguments.

From Figs 6-13 and 6-14 we conclude that the velocity ratio Z can safely be used in place of u/a in eq 6-21.

Examination of Figs 6-13 and 6-14 shows that e_v begins to fall off sharply when Z exceeds about 0.6 In Fig 6-9 it is seen that loss due to reduced p_y, which is the dotted area, increases rapidly as Z increases above 0.5. Thus it is evident that as Z exceeds 0.6 the effect of the falling

pressure ratio $p_y y/p_i$ becomes dominant. It may be concluded that when Z exceeds 0.6 the engine is in the range in which volumetric efficiency falls rapidly with increasing speed.

Maximum Z Value. From the foregoing results it is possible to draw the very important conclusion that *engines should be designed, if possible, so that Z does not exceed* 0.6 at the highest rated speed. To assist

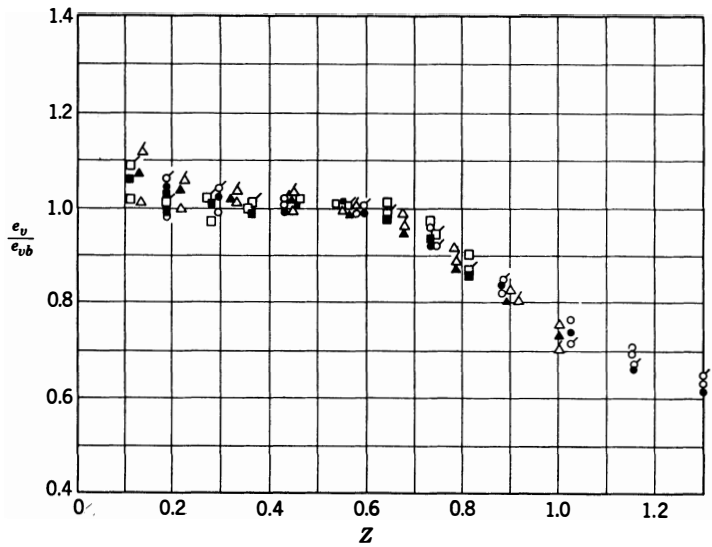

Fig 6-14. Volumetric efficiency vs inlet-valve Mach index: cam No 2; IO, 30°BTC; IC, 60°ABC; EO, 60°BBC; EC, 30°ATC; black symbols, $p_e/p_i = 0.05$; flag symbols, $p_e/p_i = 0.25$; others, $p_e/p_i = 1.0$; $D = 0.830 - 1.05$ in; L/D, 0.198 – 0.25; C_i, 0.365 – 0.445; $s = 367 - 2520$ ft/min; e_{vb} = volumetric efficiency when $Z = 0.5$. (Livengood and Eppes, ref 6.44)

designers in checking this point, typical values of C_i are given in Table 6-1.

An important restriction on the results of Figs 6-13 and 6-14 is that they were obtained with the arrangement shown in Fig 1-2, that is, with a single-cylinder engine connected to large inlet and exhaust receivers by short pipes. In this way pressure pulsations in the inlet and exhaust systems were effectively eliminated. The effect of long inlet piping on volumetric efficiency is discussed later in this chapter.

Similar Engines. In order to explore the effects of cylinder size, there have been built at MIT (refs 11.24, 11.26) three *similar* single-cylinder engines of different size.

Table 6-1

Inlet Mach Indices of Commercial Four-Stroke Engines at Maximum Rating

Name	Model 1958	Service	No. Cylinders, Bore, and Stroke	Maximum Rating, hp-rpm	Inlet Valve Diameter, in	Lift, in	C_i	$\left(\frac{b}{D}\right)^2$	$\frac{s}{a}$	Z
American Motors	Rebel 5820	PA	8—3.5 × 3.25	215—4900	1.787	0.375	0.304	3.85	0.038	0.48
Chrysler	300-D	PA	8—4.0 × 3.91	380—5200	2.00	0.389	0.282	4.0	0.0484	0.685
Plymouth	Fury	PA	8—3.91 × 3.31	290—5200	1.84	0.405	0.319	4.5	0.041	0.578
Ford	Thunderbird	PA	8—4.0 × 3.5	300—4600	2.027	0.399	0.285	3.9	0.0383	0.525
Buick	Century	PA	8—4.125 × 3.41	300—4800	1.875	0.423	0.327	4.85	0.0390	0.578
Chevrolet	Corvette	PA	8—3.875 × 3.0	230—4800	1.72	0.399	0.336	5.1	0.0343	0.521
Studebaker	Golden H	PA	8—3.56 × 3.625	275—4800	1.656	0.359	0.314	4.63	0.0415	0.612
Edsel	Ranger	PA	8—4.047 × 3.5	303—4600	2.025	0.411	0.294	3.97	0.0384	0.518
Willys	F-head (1954)	"Jeep"	6—3.125 × 3.5	90—4200	1.75	0.26	0.19	3.17	0.0352	0.535
Alco	Diesel	LOCO	16—9 × 10.5	2400—1000	4.0(2)	0.94	0.34	5.10	0.025	0.186
Wright	R-1820	Air	9—6.125 × 6.875	1525—2800	3.1	0.625	0.32 *	3.94	0.043	0.53
Pratt and Whitney	2800	Air	18—5.75 × 6.0	2400—2800	2.97	0.70	0.38	3.76	0.037	0.363
Rolls Royce	Merlin (1946)	Air	12—5.4 × 6.0	2200—3000	1.88(2)	0.58	0.49	8.25/2	0.040	0.34
Bristol	Hercules (1946)	Air	18—5.75 × 6.5	2000—2900	sv	—	†	—	0.042	0.52

C_i is estimated, except where noted, as follows:
for auto engines $C_i = 1.45L/D$
for aircraft engines $C_i = 1.60L/D$
* measured value
† measured C_i × port area = 2.1
(2) two inlet valves
PA is passenger automobile
sv is sleeve valve

By *similar engines* (or, more generally, *similar machines*) is meant engines (machines) which have the following characteristics:

1. All design ratios are the same. The MIT similar engines were built from the same set of detail drawings. Only the *scale* of the drawings was different for each engine.
2. The same materials are used in corresponding parts. For example, in the MIT engines all pistons are of the same aluminum alloy and all crankshafts are of the same steel alloy.

Figure 6-15 shows a drawing of these engines and gives their principal characteristics.

From this point on, when the word *similar* is used, it will refer to engines or other structures which differ in size but have the characteristics listed above.

Effect of Reynolds Index. The similar engines at MIT made possible tests under circumstances in which the Reynolds index $aL\rho/\mu g_0$ was the only variable in eq 6-21.

In order that the Reynolds index would be the same at a given piston speed, the engines were run with the same fuel and the same values of p_e, p_i, T_i, T_c, and F. Under these circumstances ρ, μ, and a were the same. Since the engines have the same values of D/b and the same valve design, Z was the same for all three engines at a given piston speed. Figure 6-16 shows e_v vs Z when the engines were run under the indicated conditions.

The data show no significant differences in e_v between the three engines at a given value of Z, in spite of the fact that the Reynolds indices are different in the proportion of 2.5, 4, and 6.

Without heat transfer, the Reynolds index is a measure of the relative importance of inertia and viscous forces, as these factors influence fluid flow. Evidently, differences in viscous forces are too small to affect the flow within the range of Reynolds index represented by these engines.

With regard to heat transfer, it will be recalled from the discussion of the inlet-system-heat-transfer model that ΔT would be expected to vary as Reynolds index to the power -0.2. The ratio $(6/2.5)^{-0.2} = 0.84$. Assuming ΔT for the small engine was 30°R, the quantity $(1 + \Delta T/T_i)$ would be as follows:

$$\text{for } 2\tfrac{1}{2}\text{-in engine} \qquad \left(1 + \tfrac{30}{600}\right) = 1.05$$

$$\text{for 6-in engine} \qquad \left(1 + \frac{0.84 \times 30}{600}\right) = 1.042$$

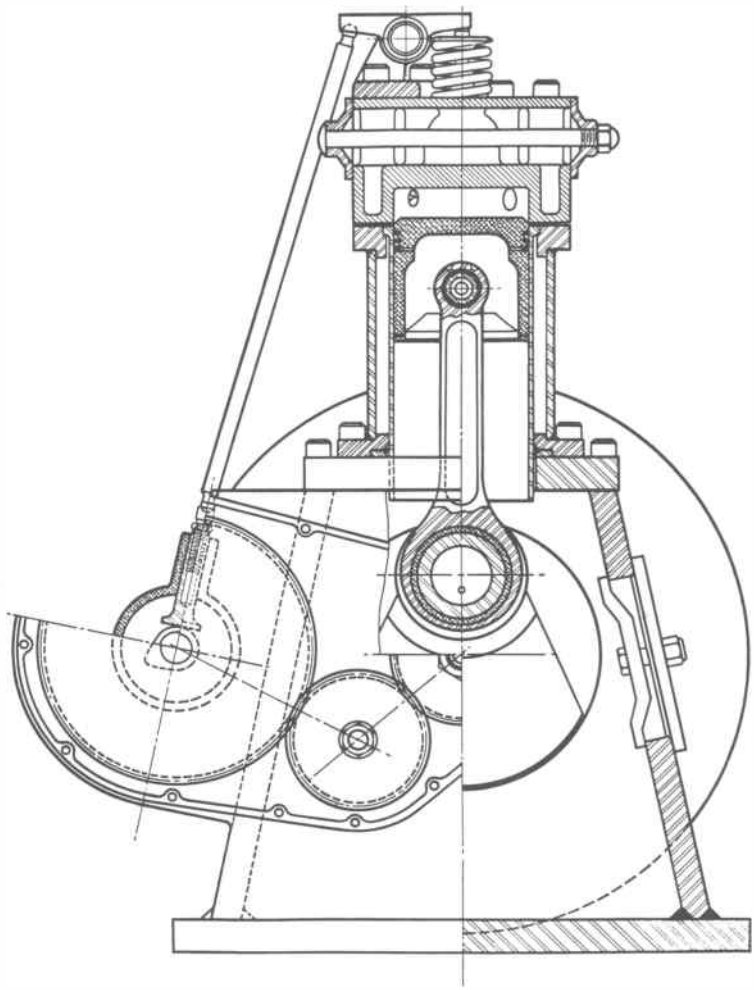

Fig 6-15. MIT similar engines. Lateral cross section for all three engines:

Engine	Bore in	Stroke in	Valves D, in	Valves L, in
Small	2.5	3.0	0.97	0.19
Medium	4.0	4.8	1.55	0.30
Large	6.0	7.2	2.33	0.45

Valve timing:

IO 15°BTC EO 45°BBC
IC 50°ABC EC 10°ATC
overlap 25°

(For further details see ref 11.24)

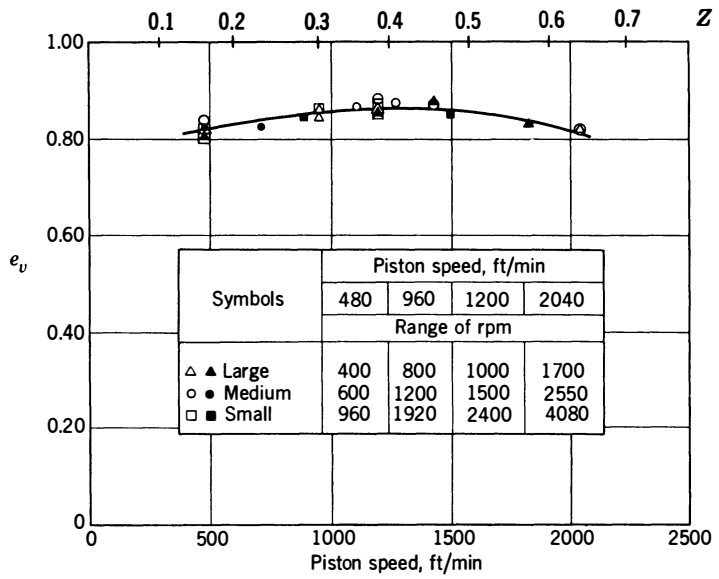

Fig 6-16. Volumetric efficiency vs mean piston speed of the MIT geometrically similar engines under similar operating conditions: $Z = 0.000315 \times$ piston speed; $r = 5.74$, $F_R = 1.10$; $p_i = 13.8$ psia; $p_e = 15.7$ psia; $T_i = 610°R$; $T_c = 640°R$; bpsa. (From refs 11.20, 11.21, 11.22)

A 1% difference in volumetric efficiency is within the limits of accuracy of engine measurements.

Effect of Engine Size. From Fig 6-16 the following important relation can be stated:

Similar engines running at the same values of mean piston speed and at the same inlet and exhaust pressures, inlet temperature, coolant temperature, and fuel-air ratio will have the same volumetric efficiency within measurable limits.

It is possible that the Reynolds index effect might become appreciable in the case of very small cylinders. Some research in this regard would be of interest.

Figure 6-17 shows that the light-spring indicator diagrams of the similar engines are substantially identical at the same value of s and Z. This figure is further confirmation of the general relation stated. The no-heat-transfer volumetric efficiency, computed from eq 6-13, would evidently be the same for these three diagrams.

Engines with Similar Cylinders. Under certain limitations the foregoing considerations can be extended to engines having similar cylinders, even though the number and arrangement of the cylinders may be different.

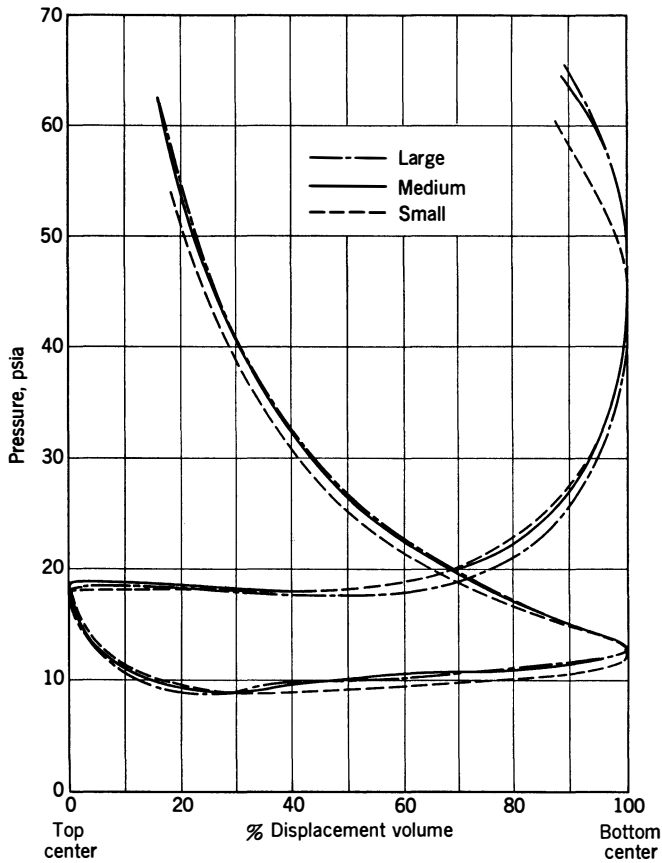

Fig 6-17. Light-spring indicator diagrams from the MIT similar engines: mean piston speed, 2040 ft/min; $Z = 0.642$; $T_i = 150°F$; $T_c = 180°F$; $p_i = 13.8$ psia; $p_e = 15.7$ psia; $F_R = 1.1$; $r = 5.74$. (From refs 11.20, 11.21, and 11.22)

In the first place, it must be remembered that the shape and size of the whole inlet system, from atmosphere to inlet ports, may have a strong effect on volumetric efficiency. The same is true for exhaust systems, although here small departures from similitude usually have only a minor effect in the case of four-stroke engines. Therefore, inlet and exhaust systems, as well as other parts, must be similar, in order that cylinders of different size have the same curve of e_v vs s/c. In Figs 6-16 and 6-17 the inlet and exhaust systems, as well as the engines themselves, were exactly similar.

For a new design the number, and, therefore, the size, of cylinders to

be used for a given power output is an extremely important decision. (See also ref 11.24.) If the cylinders can be manifolded in groups of the same number with the same firing order and essentially similar piping for each group, regardless of cylinder number and arrangements, the relations shown in Fig 6-16 will apply rigorously. The same can be said if the manifolding is such that each cylinder draws and discharges to and from reservoirs where the pressure remains substantially constant and the length and diameter of each individual pipe, between reservoir and cylinder, remains proportional to the bore.

Engines with similar cylinders, but with different manifold designs, will not necessarily have similar curves of volumetric efficiency against piston speed. However, in many cases the effects due to common inlet and exhaust manifolds are small, and the rule that volumetric efficiency among cylinders of similar design is the same at the same mean piston speed is a good first approximation when actual test data are not available.

Effect of p_e/p_i. Experimental values of the ratio e_v/e_{vb} are plotted against p_e/p_i in Fig 6-4 for two engines with $r = 6$ (dashed line). These engines had small valve overlap.

The curve of e_v/e_{vb} follows the theoretical curve for the same compression ratio quite well down to the point where p_e/p_i is about 0.5. For lower values of the pressure ratio the real volumetric efficiency curve has a smaller slope than the theoretical curve. This result is probably due to the fact that as p_e/p_i falls below 0.5 the flow through the inlet valve becomes critical for a considerable portion of the inlet stroke. In the indicator diagrams for $p_e/p_i = 0.67$, in Fig 6-8, it is apparent that the pressure drop across the inlet valve is approaching the critical value at high values of Z.

Because of the good agreement between the actual and theoretical curves for pressure ratios greater than 0.5 the theoretical relation given by eq 6-15 is often used for estimating volumetric efficiency vs p_e/p_i for engines with small valve overlap.

The effects of large valve overlap are discussed in a later section.

Effects of Fuel-Air Ratio and Temperature Changes. In dealing with the next three variables, namely, fuel-air ratio, inlet temperature, and jacket temperature, it is inconvenient to try to hold strictly to the separate dimensional relations indicated by eq 6-21. For example, when F is varied, in order to hold the two arguments containing temperature constant, T_i and T_c would have to be varied in proportion to F. The change in T_i would change the value of a, and therefore piston speed would have to be changed to hold Z constant.

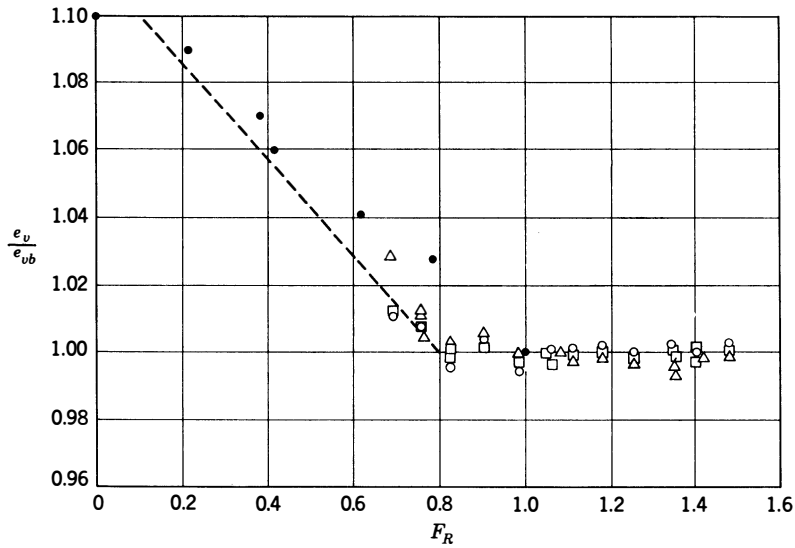

● 5 x 7 in direct-injection Diesel engine; s = 1750 ft/min; T_i = 515°R; T_c = 630°R; F_c = 0.067. (Foster, ref 6.24)

○△□ CFR spark-ignition engine; gaseous fuel-air mixture; F_c = 0.0665, T_i = 560°R to 680°R; T_c = 670°R; s = 750 to 1950 ft/min. (Malcolm and Pereira, ref 6.21)

Fig 6-18. Volumetric efficiency vs fuel-air ratio: e_{vb} is volumetric efficiency when F_R = 1.0.

It is more typical of actual practice, and perhaps of more practical value, to hold engine speed constant and to vary F, T_i, and T_c separately. However, when this procedure is adopted it must be remembered that a change in F, T_i, or Q_c will affect more than one dimensionless ratio in eq 6-21.

Effect of Fuel-Air Ratio on Volumetric Efficiency. Figure 6-18 shows e_v vs fuel-air ratio for a Diesel engine and for a spark-ignition engine supplied with a gaseous fuel-air mixture.

Changing the fuel-air ratio changes the values of F as well as the two arguments containing temperature (eq 6-21). In the spark-ignition engine changing the fuel-air ratio also changes the inlet sound velocity and thus changes Z. Values of a for various fuels and fuel-air ratios are given in Table 6-2.

If Z is not in the range above 0.5, the effect of fuel-air ratio on Z will not cause much change in e_v. The principal effect will be due to changes in the cyclic gas temperatures, as represented by the product FQ_c in eq 6-21.

Table 6-2

Effect of Fuel-Air Ratio on Properties of Octane-Air Mixtures

$\frac{F}{F_c}$	F	m	C_p	$\frac{a}{\sqrt{T}}$	$\left(\frac{a_{mix}}{a_{air}}\right)^2$	$\frac{a_{mix}}{a_{air}}$	$\frac{k-1}{k}$	k
0	0	28.95	0.240	49.0	1.000	1.000	0.286	1.400
0.8	0.0533	30.1	0.248	47.5	0.938	0.9	0.266	1.362
1.0	0.0667	30.4	0.250	47.0	0.921	0.960	0.262	1.353
1.2	0.0800	30.6	0.253	46.7	0.912	0.954	0.256	1.345
1.4	0.0933	30.9	0.254	46.4	0.896	0.947	0.253	1.339
1.6	0.1067	31.2	0.256	46.1	0.883	0.941	0.249	1.330

F_c = chemically correct fuel-air ratio. Units = ft, lbf, lbm, sec, Btu, °R. F = fuel-air ratio, m = molecular weight, C_p = specific heat at constant pressure, a = sonic velocity, k = specific-heat ratio.

In the Diesel-engine operating range both combustion temperatures and residual-gas temperature increase with increasing fuel-air ratio. Referring to the heat-transfer model, eq 6-16, an increase in the fuel-air ratio will increase both T_s and T_x. The effect on T_s is apparently predominant, since e_v falls; that is, ΔT gets larger with increasing fuel-air ratio.

The effect of fuel-air ratio on volumetric efficiency for a spark-ignition engine appears to be negligible except at the lowest fuel-air ratio, and even there it is small. Spark-ignition engines usually operate in the range $0.8 < F_R < 1.4$. In this range residual-gas and combustion temperatures reach a peak at $F_R \cong 1.1$ and decrease as F_R exceeds this value. (See Fig 4-5.) The fact that e_v shows little variation with F for the spark-ignition engine is probably because in this range of fuel-air ratios changes in the temperature difference, represented by $(T_s - T_x)$ in the model, are small.

Effect of Fuel Evaporation on Volumetric Efficiency. The spark-ignition engine of Fig 6-18 was operated with a completely gaseous mixture in the inlet pipe and port. In most commercial spark-ignition engines, on the other hand, the fresh mixture contains a great deal of unevaporated fuel during the inlet process. (See refs 6.3—.)

As we have seen, it is not practicable to measure temperatures in a wet mixture. Therefore, T_i must be measured upstream of the point where fuel is introduced. In this case evaporation of fuel while the inlet valve is open may have an appreciable effect on volumetric efficiency.

For the process of evaporating liquid fuel in air at constant pressure we can write

$$[(1 - F)H_a + (1 - x)FH_L + xFH_G]_2 = [(1 - F)H_a + FH_L]_1 + Q \tag{6-22a}$$

where H = enthalpy per unit mass
F = fuel-air ratio
x = fraction of fuel evaporated
Q = heat added during the process

Subscripts:

1 = before evaporation
2 = after evaporation
a = air
L = liquid fuel
G = gaseous fuel

If the enthalpy of the gaseous part of the mixture is taken as equal to C_pT, and if the value of H_L is assumed to be the same before and after evaporation, the above equation can be written

$$T_2 - T_1 = \frac{xFH_L + Q}{(1 - F + xF)C_p} \tag{6-23}$$

For liquid fuels H_L is a negative number approximately equal to H_{lg} of Table 3-1.

It is evident that if no heat is added to the mixture during the evaporation process its temperature will fall. For complete evaporation of octane at $F_R = 1.2$, 60°F, the drop in temperature when $Q = 0$ would be 44°F.

In applying eq 6-23 to an engine Q is the heat transferred to the charge during induction (Q in eq 6-11) and $(T_2 - T_1)$ is the ΔT of eq 6-13.

As we have seen, it is difficult to evaluate Q, and there is no practicable method of measuring or of predicting x under engine conditions. However, eq 6-23 assists in a qualitative approach to the problem.

The heat-transfer effects shown in Fig 6-9 were obtained with a gaseous mixture. If the fuel had been introduced in liquid form, in the inlet pipe, the effect on ΔT would have depended on the difference between xFH_L and Q. If Q remained unchanged and evaporation was complete before inlet closing, with octane ΔT would be decreased by about 44°F. On the other hand, heat-transfer studies of wet mixtures show that the presence of liquid on the walls tends to increase the rate of heat transfer. Thus it is probable that even with complete evaporation during induc-

tion the reduction in ΔT would be considerably less than 44°F. In actual practice, evaporation is seldom complete before the inlet valve closes.

Effect of Latent Heat of Fuel. Reference to Table 3-1 reveals that the product FH_{lg} is especially high for the alcohols. For example, at the stoichiometric mixture it is 10 Btu per lbm for octene, 40 Btu for ethyl, and 73 Btu for methyl alcohol.

With conventional carburetor-manifold systems it is not usually practicable to use the alcohols alone without adding a great deal of heat to the fresh mixture in order to insure good distribution and evaporation before ignition. (See ref 6.31—.) However, fuels containing large fractions of alcohol are often used in racing in which it is possible, by using multiple carburetors, to take advantage of a good part of the available temperature drop due to evaporation. The maximum temperature drop with ethyl alcohol (when $x = 1$, $Q = 0$ in eq 6-23) is about 170°F and with methyl alcohol, 300°F, at the stoichiometric fuel-air ratio.

Effect of Fuel Injection on Volumetric Efficiency. The injection of fuel in a Diesel engine occurs after induction, and the injection process itself has no direct effect on volumetric efficiency.

In spark-ignition engines a change from a carburetor-manifold system to injection of liquid fuel into the inlet port usually improves air capacity for two reasons:

1. Pressure drop through the carburetor may be eliminated, unless the equivalent of a carburetor is retained for metering purposes. The need for inlet-manifold heating to assist distribution may also be reduced or eliminated entirely. Thus density at the inlet port may be increased.
2. The amount of liquid fuel in contact with the walls of the induction system is reduced; the result is a reduction in Q in eq 6-23. Although x may also be reduced, there is usually a decrease in ΔT and therefore an improvement in volumetric efficiency.

When injection is made directly into the cylinder before inlet-valve closing very little wet fuel may come in contact with the cylinder walls, and Q will be still smaller than in port injection. If injection occurs early in the inlet process, enough fuel may evaporate in the cylinder before inlet-valve closing to cause a considerable improvement in volumetric efficiency over the carburetor-manifold or port-injection arrangements.

Experiments (ref 6.30—) show that volumetric efficiency may be increased about 10% by injection into the cylinder during induction, as compared to carburetion. Inlet-port injection usually affords a lesser, though appreciable, improvement.

Effect of Inlet Temperature. In order to isolate $T_i C_p/FQ_c$ as a variable when T_i is changed, it would be necessary to readjust piston speed to hold Z constant. (The variation in Reynolds index, due to changes in a, could be ignored.) As an alternative, we may explore the effect of variations in T_i, allowing Z to vary as T_i varies. Fortunately, the change in Z is much smaller than the change in T_i, since a varies as $\sqrt{T_i}$.

Figure 6-19 shows the effect of changing T_i on volumetric efficiency for two typical spark-ignition engines. The fact that e_v increases with

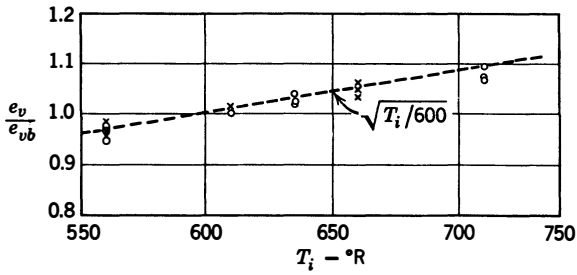

Fig 6-19. Effect of air-inlet temperature on volumetric efficiency: e_{vb} = volumetric efficiency when T_i = 600°R. Tests on two engines—Plymouth 1937 six and Ford 1940 V-8: T_c = 610°R; s = 1000 to 2500 ft/min; $p_e = p_i$ = 13 psia. (Markell and Taylor, ref 6.22)

increasing T_i indicates that the principal effect is a reduction in ΔT (eq 6-13). The higher T_i goes, the smaller the mean difference in temperature between gases and walls and the smaller the temperature rise of the gases during induction.

The fact, shown in Fig 6-19, that e_v varies very nearly as $\sqrt{T_i}$ has been observed in many spark-ignition engines. Since inlet density is proportional to $1/T_i$, the product $\rho_i e_v$, hence the mass flow of air, varies as $1/\sqrt{T_i}$. This relation is now generally accepted as a good approximation, and the output of spark-ignition engines is usually corrected for air temperature changes by assuming that indicated power varies in proportion to $1/\sqrt{T_i}$. (See refs 6.21 and 12.10—.)

In Diesel engines, in practice, the maximum fuel-pump delivery rate is usually set at the factory. When such engines are tested over the usual range in air temperature, at maximum fuel-pump setting, the quantity of fuel per cycle will not change. Thus, although volumetric efficiency varies as in spark-ignition engines, engine output will vary only as the indicated efficiency is changed by the resultant changes in fuel-air ratio and in initial temperature of the cycle. In the usual range

of Diesel-engine operation the change in power due to these causes may be too small to be noticed. (See also Chapter 12.)

On the other hand, if a Diesel engine is rated at its maximum allowable fuel-air ratio, fuel flow should be changed with air flow to hold the fuel-air ratio constant. In this case output will vary with $1/\sqrt{T_i}$, as in spark-ignition engines. (See Chapter 12.)

Effect of Coolant Temperature. Figure 6-20 shows volumetric efficiency vs coolant temperature for two engines.

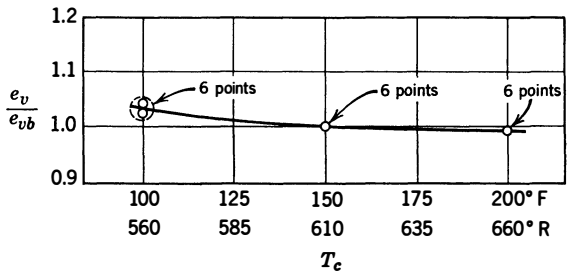

Fig 6-20. Effect of coolant temperature on volumetric efficiency: e_{vb} = volumetric efficiency when T_c = 610°R. Tests on two engines—Plymouth 1937 six and Ford 1940 V-8: T_i = 460 to 610°R; $p_e = p_i$ = 13 psia; s = 2000 ft/min, full throttle. (Markell and Taylor, ref 6.22)

When coolant temperature is changed the chief effect must be a change in the mean wall temperature to which the gases are exposed during induction (T_s in eq 6-16). It would seem that changes in T_c would have negligible effects on the other variables in eq 6-21. If Fig 6-20 is typical, the effect of T_c on volumetric efficiency can be approximated by the relation

$$\frac{e_v}{e_{vb}} = \frac{T_{cb} + 2000}{T_c + 2000} \tag{6-24}$$

EFFECT OF DESIGN ON VOLUMETRIC EFFICIENCY

Design is here taken to mean the geometrical shape of the cylinder, valves, valve gear, and manifold system and the materials of which they are made. Thus assemblies of different size are taken to be of the same design provided all the ratios of corresponding dimensions to the bore remain unchanged and the same materials are used in corresponding parts.

Effect of Design on ΔT. Design affects ΔT largely through its effect on the temperature of the surfaces to which the gases are exposed during induction. Thus designs which minimize the temperatures of inlet manifolds, inlet ports, and inlet valves are desirable from this point of view.

Obviously, exhaust heating of the inlet system is undesirable from the point of view of volumetric efficiency, although it may be necessary for reasons of fuel distribution or evaporation.

Experiments (ref 6.32) have shown that inlet valves and valve seats tend to run at temperatures far above that of the coolant. Therefore, improvement of heat conductivity between these parts and the coolant is effective in reducing ΔT. The same can be said for the conductivity between inner cylinder surfaces and the coolant.

Aside from heat-transfer effects, the design factors having important effects on volumetric efficiency are

1. Inlet-valve size and design, already considered in connection with the Mach index, Z
2. Valve timing
3. Exhaust-valve size and design
4. Stroke-bore ratio
5. Compression ratio
6. Design of inlet system
7. Design of exhaust system
8. Cam-contour shape

Valve timing is discussed under the assumption of constant lift-diameter ratios and, except for the necessary changes in the crank angle between valve opening and valve closing, the same cam contours.

The two features of valve timing which have important effects on volumetric efficiency are *valve-overlap angle* and *inlet-closing angle.* Within the limits of conventional practice, the other valve events have little effect on volumetric efficiency.

Effect of Valve Overlap. From the flow point of view, the cylinder with valve overlap can be represented by a cylinder with no overlap plus a bypass passage between inlet and exhaust pipes.

When volumetric efficiency is based on the total fresh mixture supplied it is evident that with the bypass

$$e_v = e_{vc} + \frac{4CA_b a\phi_1}{A_p s} \tag{6-25}$$

where e_{vc} = volumetric efficiency of the cylinder without bypass
A_b = bypass flow area

C = bypass flow coefficient
A_p = piston area
s = mean piston speed
a = inlet sound velocity
ϕ_1 = compressible-flow function, Fig A-2

When p_e/p_i is less than unity the last term of eq 6-25 has positive values, which means that fresh mixture flows through the bypass into the exhaust pipe. For a given bypass and pressure ratio it is apparent

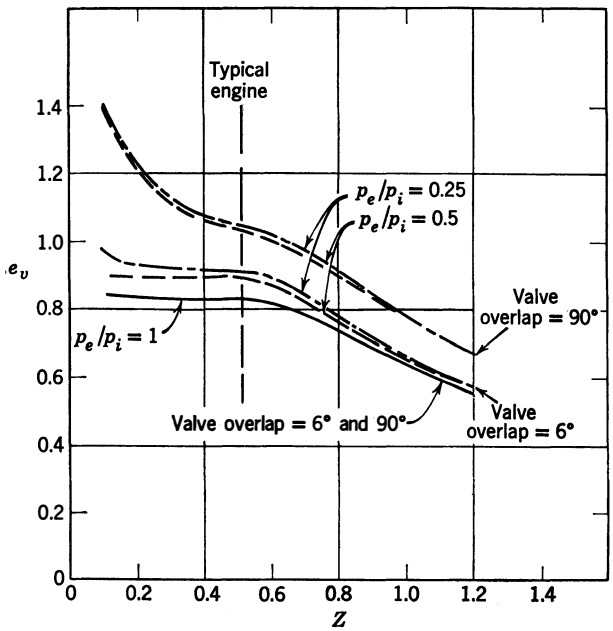

Fig 6-21. Volumetric efficiency vs Z. Various valve-overlap angles and various pressure ratios: CFR engine 3.25 x 4.5 in; r = 4.9. (Livengood and Eppes, ref 6.44)

that the last term of eq 6-25 increases toward infinity as piston speed approaches zero.

When the exhaust pressure is greater than the inlet pressure ($p_e/p_i >$ 1.0) exhaust gas will flow through the inlet bypass into the inlet pipe. The cylinder will then take in a combination of fresh mixture and exhaust gas. To represent this condition, the plus sign in eq 6-25 should be changed to minus, and a should be taken as sound velocity in the exhaust gases. Under these circumstances, e_v approaches zero at low piston

speeds, and the ratio of exhaust gas to fresh mixture in the cylinder increases as s grows smaller or p_e/p_i becomes larger.

The bypass term in eq 6-25 represents, of course, the flow which takes place through a cylinder during the overlap period. An important difference between the engine and the model is the fact that in the engine with p_e/p_i less than one flow during overlap helps to *scavenge*, that is, to sweep out residual gases from the clearance space above the piston. In the process some of the fresh air which flows through during overlap may be trapped in the cylinder, although some always escapes through the exhaust valve.

Figures 6-21 and 6-22 show curves of volumetric efficiency vs Z and vs p_e/p_i with several overlap angles. The trends predicted by eq 6-25 are evident.

Trapping Efficiency. When p_e/p_i is less than unity and fresh mixture flows through during overlap, some of the fresh mixture is lost for combustion purposes. In engines with valve overlap output will be proportional to the air *retained* in the cylinder rather than to that *supplied* to the cylinder. Let the ratio of air retained to air supplied be known as the *trapping efficiency*, Γ. Volumetric efficiency based on air retained is designated as e_v', which is equal to $e_v\Gamma$.

Values of Γ for two overlap angles are given in Fig 6-22. This figure also shows e_v'/e_{v6} vs p_e/p_i at various values of Z. The quantity e_{v6} is the volumetric efficiency of the same engine under the same operating conditions but with 6° overlap. Since the valve lift is extremely small during a 6° overlap period, it can be assumed that there is no flow during that period.

It will be noted that with a 90° overlap appreciable gains in e_v'/e_{v6} are achieved at high values of Z, even when $p_e/p_i = 1.0$. These gains are probably due to the fact that early inlet-valve opening results in larger effective inlet-valve area during the suction stroke, with consequent lower pressure drop through the inlet valve during this time. Thus α in eq 6-13 would be larger.

Value of Valve Overlap. Since spark-ignition engines are controlled by throttling, the effect of overlap when p_e/p_i is greater than one must be considered. We have seen from the model that under this condition the fraction of exhaust gas in the cylinder increases rapidly as speed decreases.

A disadvantage of valve overlap for carbureted engines is that when such engines are supercharged some fuel may be lost during the overlap period. The fraction of fuel lost will be $(1 - \Gamma)$ and the indicated efficiency will suffer accordingly.

The increased residual fraction appears to be unimportant, since modern American passenger cars use overlaps ranging from 20 to 76°,

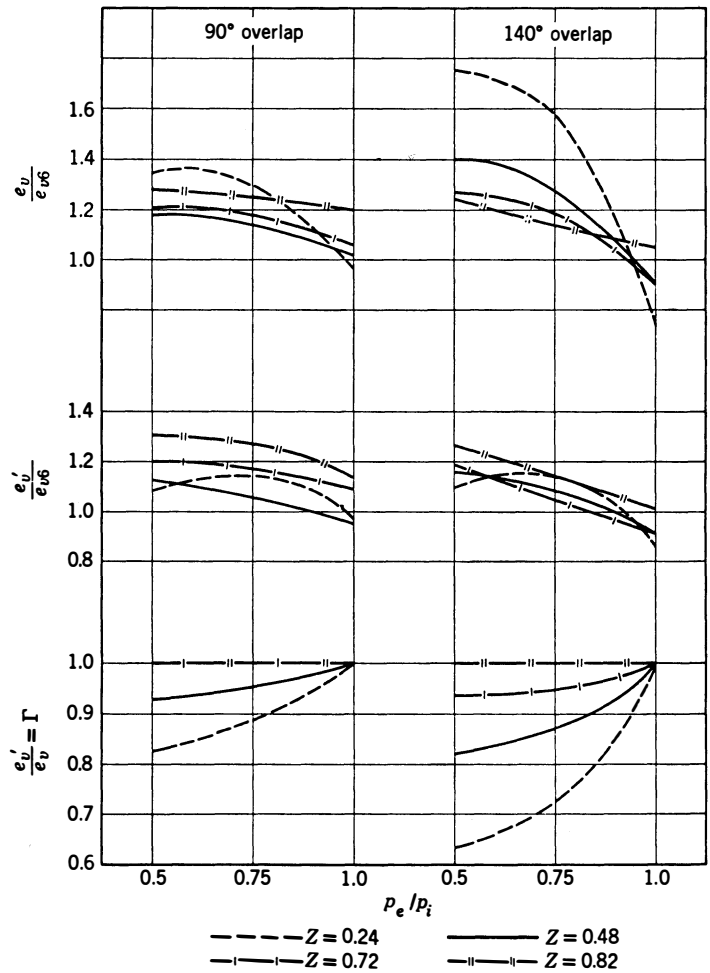

Fig 6-22. Effect of valve overlap on volumetric efficiency: e_{v6} = volumetric efficiency with 6° overlap; e_v' = volumetric efficiency based on air retained. (Faired curves from ref 6.54)

with one example at 102°. These engines, of course, are not supercharged.

Supercharged aircraft engines use considerable overlap in order to achieve high values of $e_v\Gamma$ under take-off conditions. The fuel lost is

unimportant because of the short take-off time. At cruising, p_e/p_i is not much less than one, and little fuel is lost due to overlap.

Engines using fuel injection into the cylinder after all valves are closed can use valve overlap without detriment to efficiency. The combustion fuel-air ratio in such engines will be F/Γ, where F is the over-all ratio of fuel to air.

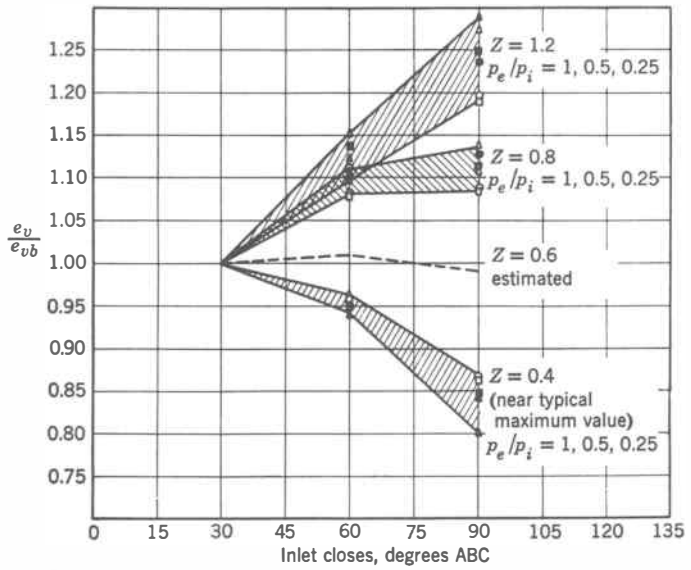

Fig 6-23. Effect of inlet-valve closing on volumetric efficiency: CFR engine, short inlet pipe; e_{vb} = volumetric efficiency when inlet valve closes 30°ABC. (Livengood and Eppes, ref 6.44)

In Diesel engines p_e/p_i is never much greater than unity, hence overlap does not affect idling. Since no fuel can be lost during overlap, it is not surprising to find that a considerable overlap angle is used in many Diesel engines. Largest valve overlaps (up to 150°) are used in turbosupercharged Diesel engines. Here, an important reason for large overlap is to protect the exhaust turbine from excessive temperatures. The fresh air which flows through the cylinder during the overlap period is an effective method of reducing turbine inlet temperature (see also Chapter 10).

Whenever valve overlap is considered for supercharged engines it should be remembered that the power required by the compressor will be increased in direct proportion to the increase in mass flow.

Inlet-Valve Closing. Figure 6-23 shows the effect of inlet-valve closing angle on volumetric efficiency when the inlet pipe is so short that inertia effects are negligible. Figures 6-7 and 6-8 show that for low values of Z the pressure in the cylinder at the end of the inlet stroke is equal to the inlet pressure. Under these circumstances, delaying the effective * inlet-valve closing beyond bottom center allows some fresh mixture to be driven back into the inlet system.

At high values of Z, as Figs 6-7 and 6-8 show, the cylinder pressure may be well below inlet pressure at bottom center. In this case delaying the inlet-valve closing allows more flow into the cylinder up to the time when cylinder and inlet pressures reach equality. Thus the higher the values of Z, the later the inlet-valve should be closed, as shown in Fig 6-23. These effects seem to be independent of p_e/p_i or of valve overlap within the range of these tests.

With long inlet pipes, inlet-valve closing should be timed to take advantage of the inertia of the inlet-gas column as well as of the effects previously noted. This subject is discussed more fully under a subsequent heading.

Exhaust-Valve Capacity. Figure 6-24 shows volumetric efficiency vs Z for three ratios of exhaust-valve flow capacity to inlet-valve flow capacity. This ratio is defined as $(D_e/D_i)^2 \times (C_e/C_i)$ where D_e and C_e have the same definition for the exhaust valve as D_i and C_i have for the inlet valve. (See p. 173.) Thus C_e is the steady-flow coefficient of the exhaust valve and port, averaged over the valve-lift curve. This flow-capacity ratio, which we here call γ, is in the range 0.60 to 1.0 for most engines.

Figure 6-24 shows that enlarging the exhaust valve to 179% of the inlet-valve capacity does not benefit volumetric efficiency even at abnormally high values of Z. The exhaust-valve capacity can be cut even to 50% of inlet-valve capacity without affecting volumetric efficiency over the usual range of Z. However, the effect of a small exhaust valve on the work lost on the exhaust stroke may be considerable, and, in general, exhaust valves of much smaller capacity than 0.60 of the inlet valve are not recommended.

* The word "effective" is used because of the characteristics of poppet-valve lift curves. Because of limitations imposed by the inertia of the valve mechanism valve openings are very small near the opening and closing points. (See Fig 6-29.) Therefore, a delay in inlet-valve closing up to about 20° of crank angle allows very little flow through the valve after bottom center and can be considered to close the valve effectively at bottom center.

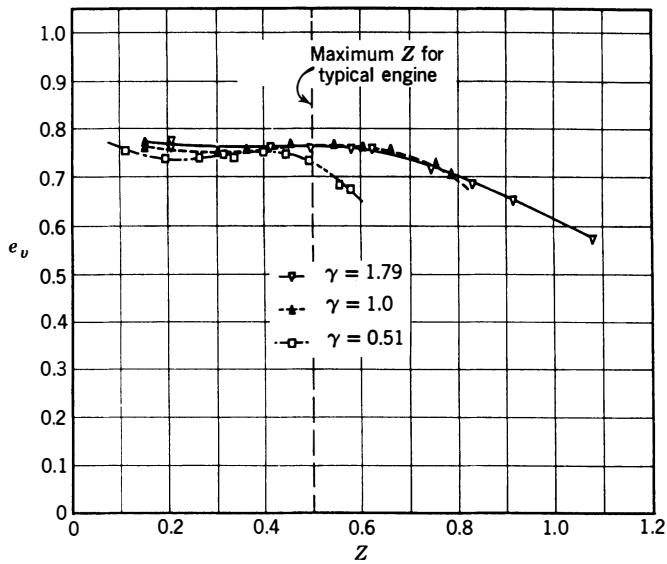

Fig 6-24. Effect of exhaust-to-inlet valve capacity on volumetric efficiency. Inlet closes 66°ABC:

$$\gamma = \left(\frac{D_e}{D_i}\right)^2 \times \left(\frac{C_e}{C_i}\right)$$

where D is valve outside diameter and C is its flow coefficient. (Eppes et al., ref 6.43)

Stroke-Bore Ratio. Let us assume an engine in which the stroke alone is varied. Valves and ports will be unaffected by this change. Since there is no change in valve size or design, Z will be proportional to piston speed. Under conditions in which Z controls, it is evident that volumetric efficiency will be independent of stroke at a given value of piston speed.

Figure 6-25 shows volumetric efficiency vs piston speed for a single-cylinder engine with three different strokes. As predicted, volumetric efficiency is a unique function of piston speed (and Z) where piston speed and stroke are the only independent variables. Here is another relation of great usefulness to the designer which should stimulate new thinking on the question of optimum stroke-bore ratios. The basic aspects of this question have been seriously obscured by the usual decision to hold rpm constant when changes in stroke-bore ratio are made.

In the tests of Fig 6-25 the inlet pipe was so short (less than the bore) that the inertia of the gas column in the pipe had negligible influence on gas flow. With a long inlet pipe, differences in the ratio of pipe length

to stroke would have caused appreciable differences in volumetric efficiency at the same piston speed. However, even with a long inlet pipe, if pipe length is made proportional to the stroke, volumetric efficiency will again be the same at the same piston speed. (See later discussion of inlet-pipe effects.)

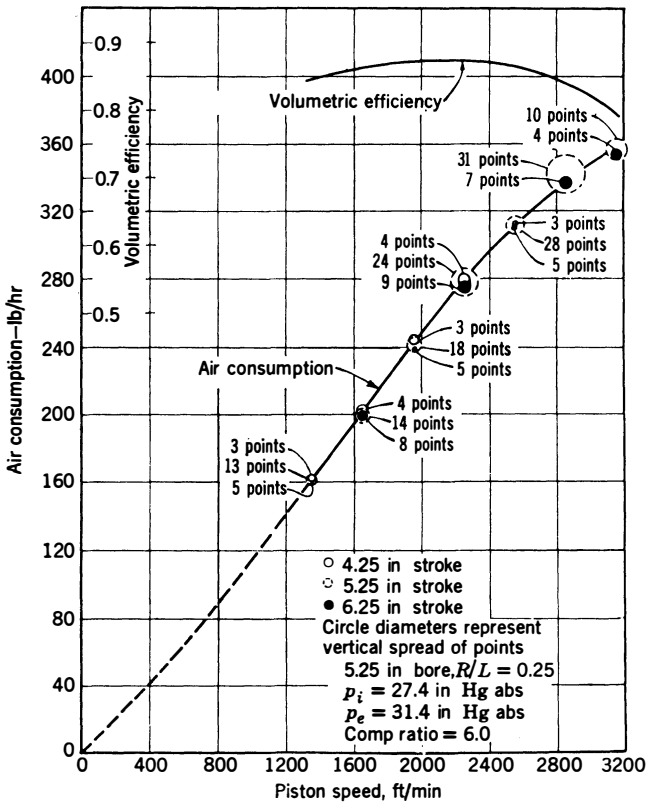

Fig 6-25. Effect of stroke-bore ratio on volumetric efficiency and air consumption. (Livengood and Eppes, ref 6.45)

Effect of Compression Ratio. Work by Roensch and Hughes (ref 6.25) shows that when p_e/p_i is near 1.0 changes in compression ratio have small effect on volumetric efficiency. Figure 6-4 and eq 6-10 show the effect of changing compression ratio when there is a considerable difference between inlet and exhaust pressure and valve-overlap is small. The effect of compression ratio in supercharged engines when overlap is large has not yet been explored.

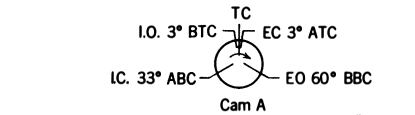
TC
I.O. 3° BTC
EC 3° ATC
I.C. 33° ABC
EO 60° BBC
Cam A

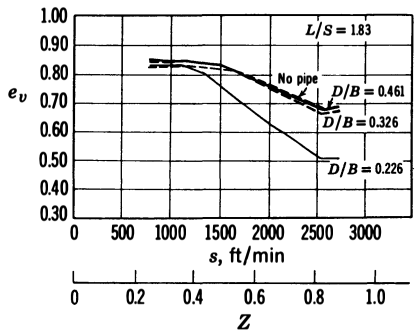
e_v
$L/S = 1.83$
No pipe
$D/B = 0.461$
$D/B = 0.326$
$D/B = 0.226$
s, ft/min
Z

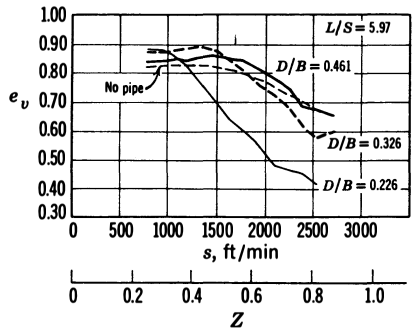
e_v
$L/S = 5.97$
No pipe
$D/B = 0.461$
$D/B = 0.326$
$D/B = 0.226$
s, ft/min
Z

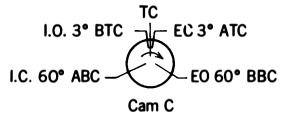
TC
I.O. 3° BTC
EC 3° ATC
I.C. 60° ABC
EO 60° BBC
Cam C

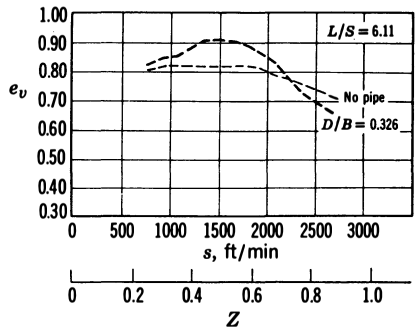
e_v
$L/S = 6.11$
No pipe
$D/B = 0.326$
s, ft/min
Z

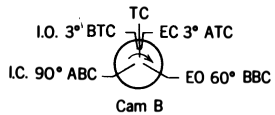
TC
I.O. 3° BTC
EC 3° ATC
I.C. 90° ABC
EO 60° BBC
Cam B

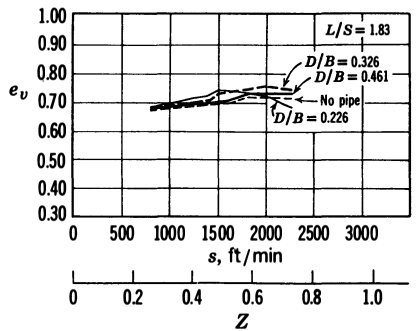
e_v
$L/S = 1.83$
$D/B = 0.326$
$D/B = 0.461$
No pipe
$D/B = 0.226$
s, ft/min
Z

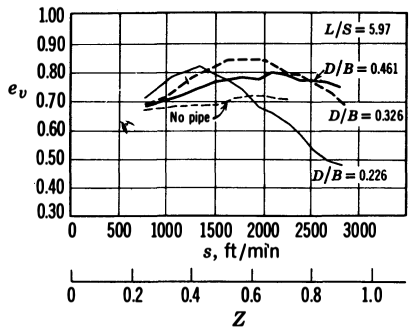
e_v
$L/S = 5.97$
$D/B = 0.461$
No pipe
$D/B = 0.326$
$D/B = 0.226$
s, ft/min
Z

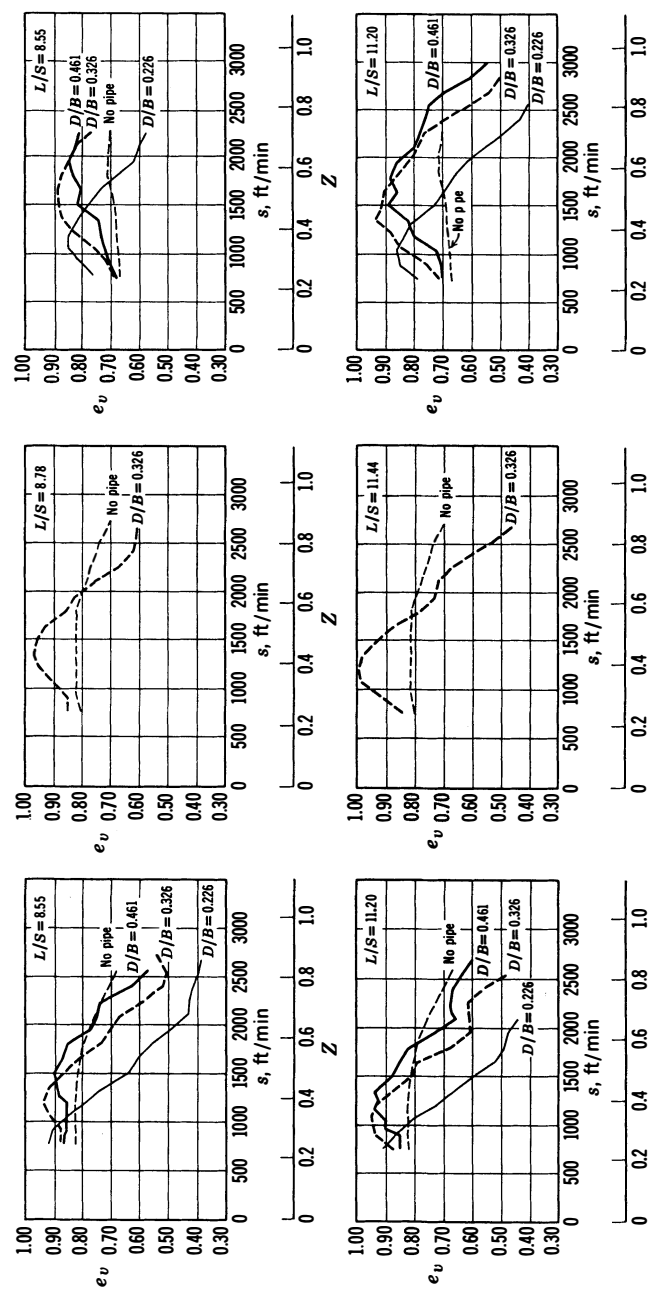

Fig 6-26. Volumetric efficiency as affected by inlet-pipe length and diameter and inlet-valve timing: CFR cylinder, 3½ x 4½ in; $r = 6$; $p_i = 27.4$ in Hga; $p_e = 31.4$ in Hga; $T_i = 100°F$; $F = 0.08$; bpsa. (Taylor et al., ref 6.63)

Fig 6-27. Relative volumetric efficiency as affected by inlet-pipe length and diameter and inlet-valve timing: CFR cylinder, 3¼ x 4½ in; $r = 6$; $p_i = 27.4$ in Hga; $p_e = 31.4$ in Hga; $T_i = 100°F$; $F = 0.08$; bpsa. (Taylor et al., ref 6.63)

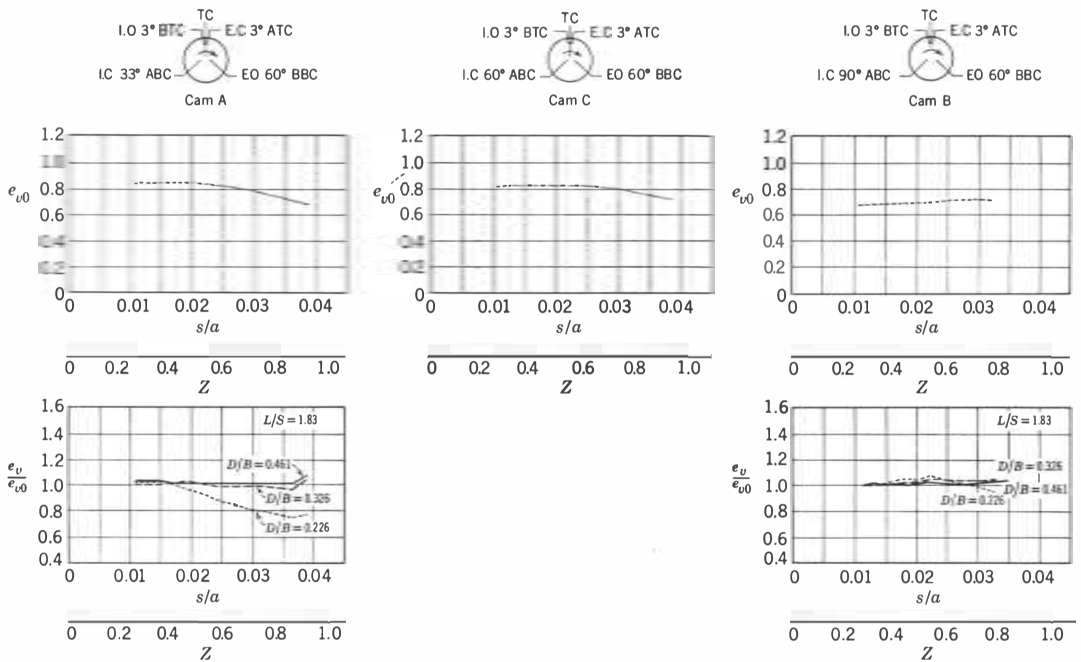

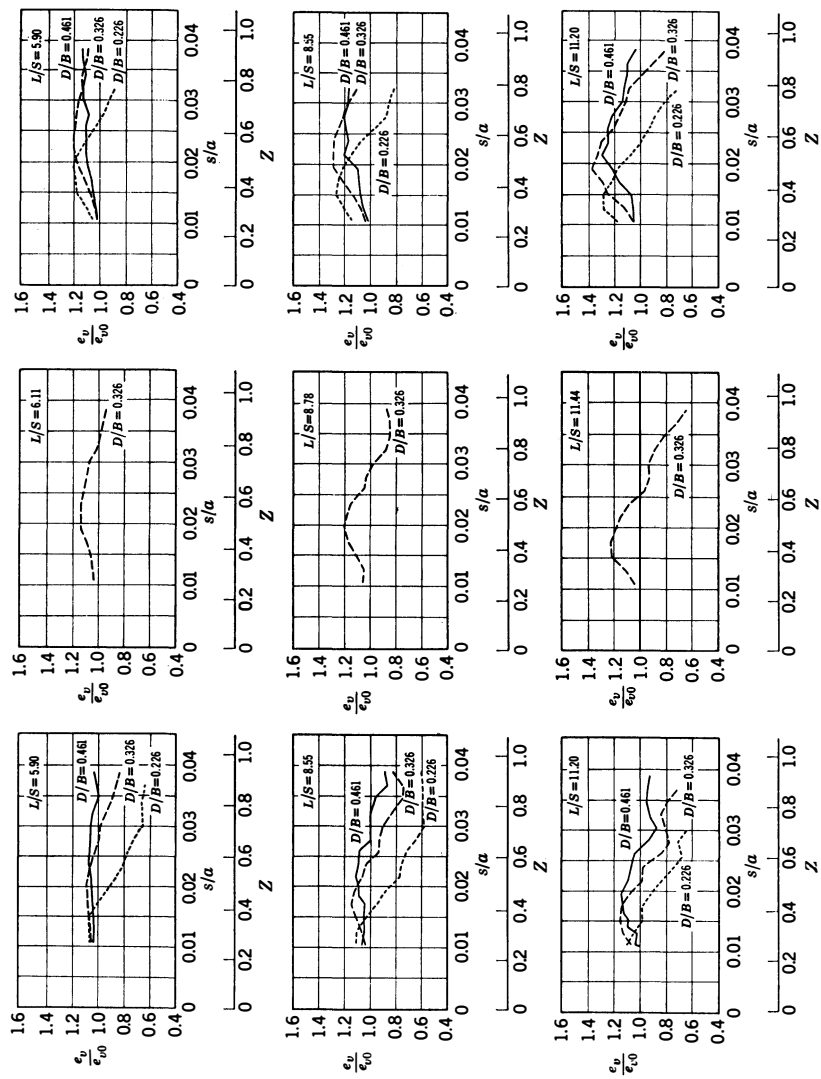
L/S = 5.90
D/B = 0.461
D/B = 0.326
D/B = 0.226
L/S = 6.11
D/B = 0.326
L/S = 8.55
D/B = 0.461
D/B = 0.326
D/B = 0.226
L/S = 8.78
D/B = 0.326
L/S = 11.20
D/B = 0.461
D/B = 0.326
D/B = 0.226
L/S = 11.44
D/B = 0.326
$\frac{e_v}{e_{v0}}$
s/a
Z

Inlet-System Design. It has long been known that high volumetric efficiencies can be obtained at certain speeds by means of long inlet pipes (see ref 6.6—). The effects noted are caused by the inertia and elasticity of the gases in the inlet pipe and cylinder.

Figures 6-26 and 6-27 show the effect of various inlet-pipe lengths and diameters on volumetric efficiency. These tests were made with a single-cylinder engine, with a short exhaust pipe, and with large surge tanks at the end of the inlet and exhaust pipes.

Complete theoretical treatment of the relation of inlet pipe dimensions to cylinder dimensions is beyond the scope of this volume. A comprehensive experimental and analytical treatment of this subject is given in ref 6.63. The following general relations are important:

1. If viscosity effects are assumed negligible and, if similar engines have similar inlet systems, the effects of inlet dynamics on volumetric efficiency will be the same at the same piston speed, other operating variables being held constant. This conclusion also applies to engines of different stroke-bore ratios, provided the cylinder design is otherwise the same and the ratios pipe-diameter-to-bore and pipe-length-to-stroke are held the same. Thus, the curves of Figs 6-26 and 6-27 should apply over the useful range of cylinder size and stroke-bore ratio.

2. The dynamic pressure at the inlet port at the end of induction is the sum of effects caused by "standing" waves which have been set up in the inlet pipe by previous inlet strokes and the effects of the transient wave set up by the induction process.

3. There are no sudden changes in the volumetric efficiency curves at points at which the "organ pipe" frequencies of the inlet pipe are even multiples of the speed of revolution.

4. Long pipes with small ratios of D/B give high volumetric efficiencies at low piston speeds because high kinetic energy is built up in the pipe toward the end of the induction process. At higher piston speeds, the flow restriction offered by small D/B ratios becomes dominant and volumetric efficiency falls.

5. Long pipes with large ratios of D/B show maximum volumetric efficiencies at intermediate piston speeds due to kinetic energy built up in the pipe. At high piston speeds the air mass in such pipes is slow to accelerate, and volumetric efficiency falls off.

6. As pipes become shorter, the maximum gains in volumetric efficiency over that with no inlet pipe grow smaller, but the range of piston speeds over which some gain is made grows wider.

7. Figures 6-26 and 6-27 should be of assistance in selecting the best pipe dimensions for a given type of service.

Multicylinder Inlet Systems. When several cylinders are connected to one inlet manifold, the problem of manifold design becomes complicated, especially if liquid fuel as well as air must be distributed.

In carbureted engines using liquid fuel manifold shape and size is dictated to a considerable degree by the necessity of securing even distribution of fuel. At high piston speeds manifolds may cause appreciable

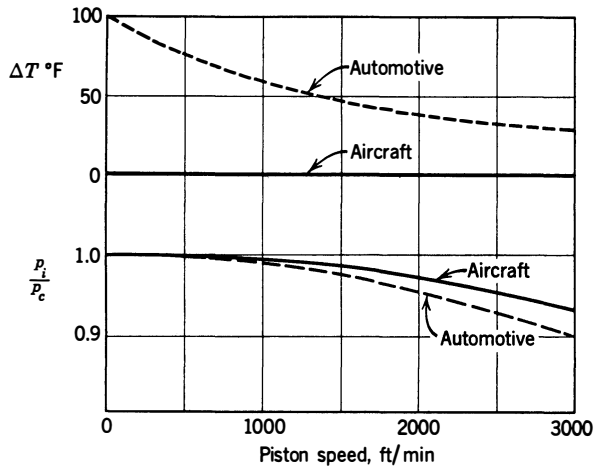

Fig 6-28. Estimated pressure ratio and temperature rise from carburetor inlet to inlet port for aircraft and automotive engines at full throttle, unsupercharged: p_c = pressure ahead of carburetor (absolute); p_i = pressure at inlet port (absolute); ΔT = estimated temperature rise, carburetor inlet to inlet manifold (evaporation of fuel plus heat input). (Based on average values from miscellaneous sources.)

sacrifices in density at the inlet ports. Figure 6-28 may be used for estimating inlet-port density for carbureted engines.

When questions of distribution are not involved the manifold giving highest air capacity will be such that there is no *interference* between cylinders; that is, two or more cylinders will not be drawing from a restricted volume at the same time. Individual inlet pipes leading from each cylinder to the atmosphere, or to a relatively large *header*, are most effective in this respect. With either arrangement, the length and diameter of the individual pipes could be chosen on the basis of Figs 6-26 and 6-27.

Effect of Exhaust-Pipe Length. At a given speed, the length of the exhaust pipe can have an appreciable effect on p_x in eq 6-13 because of its influence on intensity of exhaust-pipe pressure waves and their timing in relation to top center. However, in practice it is found that

the effect of changing exhaust-pipe length on volumetric efficiency is usually small because the effect of changes in p_x on volumetric efficiency is slight. (See eq 6-13.)

Cam Contour. At first glance it might be thought desirable to have a sudden opening and closing of the inlet valve as indicated by the dashed line in Fig 6-29*a*. Such a curve would not only be impossible

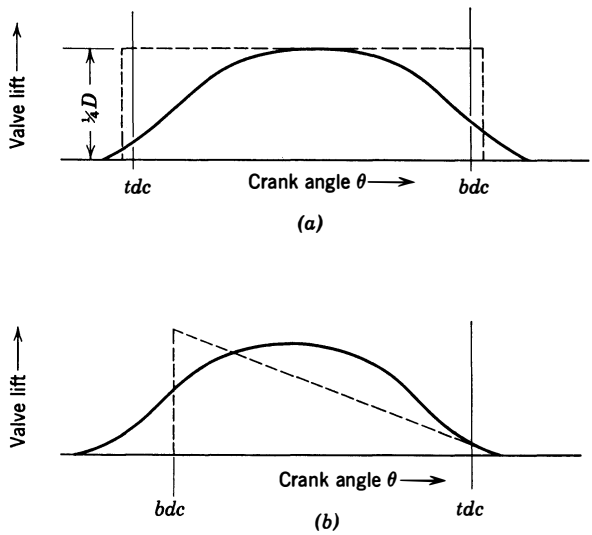

Fig 6-29. Valve opening vs crank angle curves: (*a*) Inlet-valve lift curves, (*b*) exhaust-valve lift curves. Dashed lines show ideal curve, solid lines show practical curve.

mechanically, but it would be quite unnecessary because piston motion is slow near top and bottom centers. In practice, the valve lift curve is similar to that shown by the full line of the figure, and little is gained by attempting to approach more nearly the rectangular pattern.

With the usual form of lift curve, the average flow coefficient, C_i, increases quite slowly as the maximum L/D increases beyond 0.25. (See Fig 6-12.) Because of this fact, and also because of geometric and stress limitations, poppet valves are seldom lifted much beyond $\frac{1}{4}$ of the valve diameter.

In the case of the exhaust valve a sudden opening near bottom center on the expansion stroke (see dashed line of Fig 6-29*b*) would be very desirable in order to minimize the crank angle occupied by the *blowdown angle*, that is, the crank angle between exhaust-valve opening and approach to exhaust-system pressure in the cylinder. After the blowdown

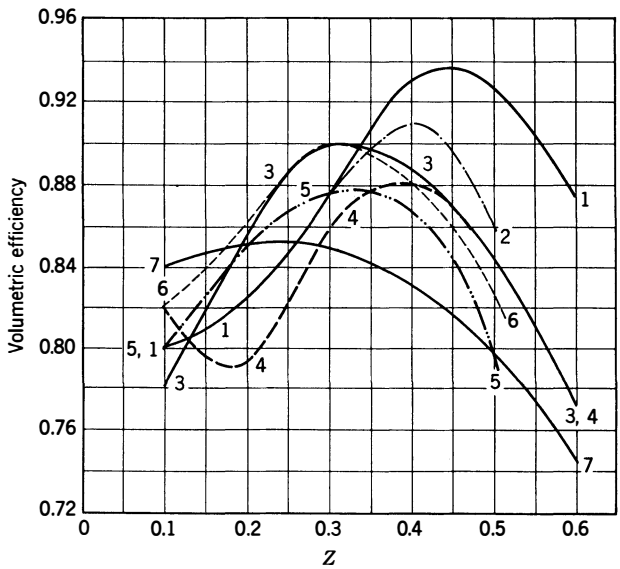

Fig 6-30. Volumetric efficiency of commercial engines vs inlet Mach index:

No.	Engine Type and No. of Cylinders	Carburetor	Bore, in	Compression Ratio
1	PC-8	4-B	4.00	9.5
2	A-1	MT	6.13	6.5
3	PC-8	4-B	3.80	9.0
4	PC-8	4-B	4.00	9.75
5	PC-8	2-B	3.56	7.6
6	PC-8	4-B	3.75	9.0
7	PC-8	2-B	3.19	6.3

Inlet densities (except 2) based on air temperature entering carburetor and manifold absolute pressure. No. 2 single-cylinder test with gaseous mixture; PC = passenger car; A = aircraft; MT = mixing tank; 4-B = four-barrel carburetor; 2-B = two-barrel carburetor. All engines are overhead-valve type except No. 7, which is L-head. Sources are manufacturers' tests except 2 and 7, which were tested at Sloan Automotive Laboratories, MIT. All values corrected to $p_e/p_i = 1.0$.

period the opening could be reduced as indicated. Since such a curve is impossible mechanically, it is compromised in practice, as shown by the full line in the figure, by starting to open the valve well before bottom center.

Because of stress limitations it is not possible to depart very far from the type of lift curve indicated by the full lines in Fig 6-29 when using poppet valves.

Volumetric Efficiency of Commercial Engines. Figure 6-30 shows e_v vs Z for a number of types of commercial engines.

Until the advent of automatic transmissions and the need for a high advertised maximum power, many motor-vehicle engines were designed to have maximum torque at low speeds to give good low-speed performance in high gear. Thus volumetric efficiency at high speeds was sacrificed for high values at low speeds, as shown in curve 7. The chief devices for obtaining this kind of curve are early inlet-valve closing (30° or less ABC; see Fig 6-23) and small valve overlap.

Curves 1 and 3 through 6 represent passenger automobile engines for use with torque converters. In this case high torque is not required below about 1500 rpm, which corresponds to Z values of 0.15 to 0.20. Curves of this kind result from considerable valve overlap and late inlet closing.

Engines which require maximum torque at only one speed can be equipped with valve timing, inlet-pipe dimensions, etc., which are optimum for that particular speed. Aircraft and marine engines as well as constant-speed stationary engines are generally in this class. Curve 2 of Fig 6-30 is an example of this kind.

ESTIMATING AIR CAPACITY

The foregoing discussion and data can be used for estimating the air capacity of new engines or of existing engines under new operating conditions.

The steps in such an estimate are as follows:

1. Select speed and atmospheric conditions under which air capacity is to be maximized.
2. Determine valve diameters and flow coefficients (if not already fixed). For new engines, since a low value of Z is desired, the largest feasible inlet valves are desirable, consistent with exhaust valves of at least 60% of the inlet-valve total area and with good mechanical design.

3. At the chosen value of Z determine a *base volumetric efficiency* from the appropriate figure in this chapter. With short inlet pipes, use Fig 6-16 for values of Z below 0.5 and Fig 6-13 for higher values. With long inlet pipes use e_{vo} from Fig 6-27.

4. Correct the base volumetric efficiency for the special conditions of the problem by means of the following relation:

$$\frac{e_v}{e_{vb}} = \sqrt{T_i/T_{ib}}\left(\frac{T_{cb} + 2000}{T_c + 2000}\right) K_P \cdot K_F \cdot K_{IC} \cdot K_{IP} \qquad (6\text{-}26)$$

where K_P = correction for p_e/p_i from Fig 6-4 or Fig 6-22
K_F = correction for fuel-air ratio, Fig 6-18
K_{IC} = correction for inlet-valve closing Fig 6-23
K_{IP} = correction for long inlet pipe, Figs 6-26 and 27

The first two terms will be recognized as the correction for inlet temperature and coolant temperature.

With valve overlap K_P should be evaluated by means of Fig. 6–22.

ILLUSTRATIVE EXAMPLES

(All pressures are in psia, temperatures in °R, densities in lbm/ft³.)

Example 6-1. Inlet-Air Density. Measurements in the inlet manifold of an engine indicate that half the fuel is evaporated at the point of measurement. The temperature of the gaseous portion of the manifold contents is estimated at 680°R. The manifold pressure is 13.5, and the atmospheric moisture content is 0.02 lbm/lbm air. The over-all fuel-air ratio is 0.08, gasoline being used. Compute the density of air in the manifold.

Solution: From Table 3-1, the molecular weight of gasoline is 113.

$$F_i = 0.08/2 = 0.04$$

From eq 6-5,

$$p_a/p_i = 1/[1 + 0.04\tfrac{29}{113} + 1.6(0.02)] = 0.96$$

From eq 6-6 and footnote on same page,

$$\rho_a = 2.7(13.5)0.96/680 = 0.0515 \text{ lbm/ft}^3$$

Example 6-2. Inlet-Air Density. An engine using producer gas at 1.2 of the stoichiometric ratio has a pressure of 13.5 and temperature of 680 in the manifold after the gas has been introduced. The atmospheric moisture content

is 0.02 lbm/lb air. Compute the inlet air density. Compare the indicated power with that of the same engine using gasoline under conditions of example 6-1.

Solution: From Table 3-1 for producer gas, the molecular weight is 24.7, F_c is 0.700 and lower heat of combustion is 2320 Btu/lbm.

From eq 6-6,

$$\rho_a = \frac{2.7(13.5)}{680}\left(\frac{1}{1 + 0.7(1.2)\frac{29}{24.7} + 1.6(0.02)}\right) = 0.0535(0.496) = 0.0266$$

If we assume the same volumetric efficiency and indicated efficiency, the ratio of indicated power to that using gasoline with the conditions of example 6-1 is

$$\frac{P}{P \text{ (example 6-1)}} = \frac{0.0266(0.7)(1.2)(2320)}{0.0515(0.08)(19{,}020)} = 0.66$$

(Q_c for gasoline from Table 3-1.)

Example 6-3. Indicated Power. Let the four-stroke engine of examples 6-1 and 6-2 have a volumetric efficiency of 0.85. If it has 12 cylinders, 6-in bore, 8-in stroke, and runs at 1500 rpm with indicated efficiency of 0.30, compute the indicated mep and indicated power with gasoline and producer gas.

Solution:

$$A_p = 12(28.2\,*)/144 = 2.35 \text{ ft}^2$$

$$s = 1500(2)\tfrac{8}{12} = 2000 \text{ ft/min}$$

From eq 6-8,

$$\text{ihp (gasoline)} = \frac{778(2.35)(2000)(0.0515)(0.85)(0.08)(19{,}020)0.30}{(4)33{,}000} = 555$$

$$\text{ihp (gas)} = 555(0.66) = 367$$

From eq 6-9,

$$\text{imep (gasoline)} = \tfrac{778}{144}(0.0515)(0.85)(0.08)(19{,}020)0.30 = 108 \text{ psi}$$

$$\text{imep (gas)} = 108(0.66) = 71 \text{ psi}$$

Example 6-4. Inlet Mach Index. A carbureted gasoline engine is operated at $F_R = 1.2$. If fuel injection after the inlet valves close is substituted for the carburetor, and if this lowers the temperature in the inlet manifold from 600°R to 580°R, what will be the new value of Z? What would be the effect on volumetric efficiency?

Solution: From Table 6-2 at $F_R = 1.2$, $a/\sqrt{T} = 46.7$. For air $a/\sqrt{T} = 49$, Z varies inversely as a; therefore,

$$\frac{Z \text{ injection}}{Z \text{ carbureted}} = \frac{46.7\sqrt{600}}{49\sqrt{580}} = \frac{1145}{1180} = 0.97$$

From Fig 6-13, this change would have negligible effect if Z were originally less than 0.5. If Z had been 0.7 or higher, the gain in volumetric efficiency would be about 1%.

* Area of circle with diameter 6.

Example 6-5. Inlet Valve Size. A Diesel engine with a cylinder bore of 4 in has an inlet valve of 1.7 in diameter with steady-flow coefficient of 0.35. If the stroke is 5 in, what is the value of Z at 2000 rpm, $T_i = 560$? Is the inlet-valve diameter adequate, and, if not, how large should it be?

Solution: From Table 6-2, $a = 49\sqrt{560} = 1160$ ft/sec.

From eq 6-22,

$$Z = \left(\frac{4}{1.7}\right)^2 \frac{2000(5)2}{12(1160)60(0.35)} = 0.38$$

According to Fig 6-13, Z is sufficiently low so that no increase in valve size is called for.

Example 6-6. Inlet-Valve Size. A racing engine using a gasoline-alcohol mixture is expected to run with an inlet temperature of about 500°R. It is designed for a piston speed of 4000 ft/min and a cylinder bore of 2.5 in. The maximum inlet-valve flow coefficient is estimated at 0.40. What should be the minimum inlet-valve diameter?

Solution: According to Fig 6-13, Z should not exceed 0.6. With alcohol in manifold, estimate $a = 46.9\sqrt{T} = 46.9\sqrt{500} = 1050$ ft/sec. (See Table 3-1.)

From eq 6-22,

$$0.6 = \left(\frac{2.5}{D}\right)^2 \frac{4000}{1050(60)(0.4)} \quad \text{and} \quad D = 1.3 \text{ in}$$

An inlet-valve of this size is possible with a domed cylinder head.

Example 6-7. Volumetric Efficiency vs Speed. What will be the volumetric efficiency of the three similar engines of Fig 6-16 if all are run at 1500 rpm? Other conditions are the same as in that figure.

Solution: 2.5-in engine, $s = 1500(3)\frac{2}{12} = 750$ ft/min (stroke is 3-in, from Fig 6-15).

From Fig 6-16, $e_v = 0.84$,

$$\text{4-in engine } s = 750\left(\frac{4}{2.5}\right) = 1200 \text{ ft/min}$$

$$e_v = 0.86 \text{ from Fig 6-16}$$

$$\text{6-in engine } s = 750\left(\frac{6}{2.5}\right) = 1800 \text{ ft/min}$$

$$e_v = 0.84 \text{ from Fig 6-16}$$

Example 6-8. Inlet Temperature and Pressure Effects. Estimate the volumetric efficiency of the 6-in bore engine of Fig 6-16 at 10,000 ft altitude, 1500 rpm, with the same ratio of p_e/p_i and the same fuel-air ratio as in Fig 6-16 (see Table 12-1 for altitude data). What will be the reduction in indicated power?

Solution: From Table 12-1, the mean values of temperature and pressure at 10,000 ft are 483°R and 10.10 psia. For a single-cylinder engine no manifold heat is required, and we may assume that inlet temperature equals atmospheric temperature. At 1500 rpm $s = 1800$ ft/min and, from Fig 6-16, $e_v = 0.84$. For the new inlet conditions, using the square-root correction for T_i,

$$e_v = 0.84\sqrt{483/610} = 0.75$$

Since p_e/p_i remains the same, and the change in Z is accounted for by the square-root relation (Fig 6-19), no further correction is necessary. Remembering that indicated power will be proportional to $\rho_a e_v$,

$$\frac{\text{power at 10,000 ft}}{\text{power of Fig 6-16}} = \frac{10.10(600)0.75}{13.8(483)0.84} = 0.81$$

Example 6-9. Inlet-Pipe Dimensions. How much indicated power could be gained by using the best inlet pipe on the 6-in. bore similar engine of Fig 6-16 instead of the very short pipe (*a*) at 1000 rpm and (*b*) at 1800 rpm, and what would be the proper pipe dimensions in each case? The timing of these engines is similar to that of the central column of Fig 6-27.

Solution:

(*a*) At 1000 rpm, $s = \dfrac{1000(7.2)}{6} = 1200$ ft/min, and, from Fig 6-16, $Z = 0.38$. From Fig 6-27, the highest volumetric efficiency at this value of Z is with $L/S = 11.44$ and $D/B = 0.326$ $e_v/e_{v0} = 1.21$. Therefore, gain in power is 21%, with $L = 11.44 \times 7.2/12 = 6.9$ ft and $D = 0.326 \times 6 = 1.96$ in.

(*b*) At 1800 rpm, $s = 1800\ (7.2/6) = 2160$ ft/min and $Z = 0.68$. From Fig 6-27, the highest volumetric efficiency at this value of Z is with $L/S = 6.11$ and $D/B = 0.326$. Figure 6-27 shows $e_v/e_{v0} = 1.08$. Therefore, gain in power is 8%, with pipe $6.11 \times 7.2/12 = 3.67$ ft long and 1.96 in diameter.

Example 6-10. Inlet-Valve Closing. Is the inlet valve closed at the proper time for the similar engines of Figs. 6-15 and 6-16 if they are to run at a piston speed of 2000 ft/min? At 1200 ft/min?

Solution: At these speeds $Z = 2000 \times 0.000315 = 0.63$ and 0.38. Figure 6-23 shows that inlet-valve timing has little effect on volumetric efficiency at $Z = 0.63$. At $Z = 0.38$, the best timing is obviously 30° late. It is concluded that the inlet valve closes too late for best volumetric efficiency for values of Z less than 0.6.

Example 6-11. Exhaust-Valve Size. An aircraft engine which takes off at a piston speed of 3000 ft/min $Z = 0.50$ has an inlet-valve diameter of 3.1 in. What is the smallest diameter of exhaust valve that could be used without serious loss of take-off power?

Solution: Figure 6-24 shows that at $Z = 0.5$ a reduction of the exhaust-valve area to 51% of the inlet-valve area reduces volumetric efficiency 4%, whereas there is no reduction when the valves are of equal diameter. From this it is estimated that the exhaust-valve area could be cut to 75% of the inlet-valve area without appreciable loss. Therefore, minimum exhaust-valve diameter would be $3.1\sqrt{0.75} = 2.68$ in.

Example 6-12. Valve Overlap Effect. A four-stroke supercharged Diesel engine operates under the following conditions: $p_i = 29.4$, $p_e = 22$, $T_i = 700$, $Z = 0.50$, $r = 16$, $F_R = 0.6$, $T_c = 640$, valve overlap 140°, inlet closes 60° late. Estimate volumetric efficiency and $e_v\Gamma$.

Solution: From Fig 6-13 at $Z = 0.5$, read base volumetric efficiency 0.83. The conditions for this value are given in the figure. Fuel-air ratio correction, Fig 6-18, 1.03; inlet temperature correction, Fig 6-19, 1.08/0.98 = 1.1; coolant temperature correction, Fig 6-20, none; valve overlap correction from Fig 6-22

at $Z = 0.50$, $p_e/p_i = 22/29.4 = 0.75$, read $e_v/e_{v6} = 1.28$, $\Gamma = 0.86$. Inlet-closing correction, Fig 6-23, = 0.98.

$$e_v = 0.83(1.03)(1.1)(1.28)(0.98) = 1.18$$

$$e_v\Gamma = (1.18)(0.86) = 1.02$$

Example 6-13. Power Estimate. Assume that the engine of problem 6-12 has 6 cylinders, 4-in bore, 6-in stroke, and runs at 1800 rpm with indicated efficiency 0.45 and mechanical efficiency 0.85, using light Diesel oil. Compute its brake horsepower.

Solution:

$$\rho_i = 2.7 \times 29.4/700 = 0.113$$

$$A_p = (6)12.5/144 = 0.521 \text{ ft}^2$$

$$s = 1800(2)(6)/12 = 1800 \text{ ft/min}$$

From eq 6-3,

$$\dot{M}_a' = 1.02(0.113)(0.521)(1800)/4 = 27.1 \text{ lbm/min}$$

From Table 3-1,

$$F_cQ_c = 1220 \text{ Btu}, \qquad FQ_c = 1220 \times 0.6 = 733$$

From eq 6-1,

$$\text{bhp} = \frac{778}{33{,}000}(27.2)(733)(0.45)(0.85) = 180$$

Example 6-14. Valve Overlap Effect. A supercharged Diesel engine with short inlet pipes runs under the following conditions: $r = 16$, $F_R = 0.6$, $p_3/p_i = 70$, $Z = 0.5$, $T_i = 700°\text{R}$ dry air, $T_c = 640°\text{R}$, $p_i = 2$ atm, $p_e = 1.5$ atm, valve overlap 140°, inlet valve closes 60° late. Estimate the volumetric efficiency, trapping efficiency, and trapped-air volumetric efficiency.

Solution: Take base volumetric efficiency from Fig 6-13 at $Z = 0.5$ as $e_{vb} = 0.83$. Base conditions are given under the figure. Fuel-air ratio correction, Fig 6-18, 1.03. T_i correction, Fig 6-19, 1.08/1.04 = 1.04. T_c correction, Fig 6-20, none (base value same). Inlet-valve timing correction, none (base value nearly the same). Inlet pipe correction, none (base also has short pipe). Valve overlap correction, Fig 6-22, at $p_e/p_i = 1.5/2.0 = 0.75$, $Z = 0.5$, is 1.28. (Valve overlap of base engine was 6°.) The estimated volumetric efficiency is $e_v = 0.83(1.03)(1.04)(1.28) = 1.14$. Trapping efficiency from Fig 6-22 is 0.86, and retained-air volumetric efficiency is $0.86 \times 1.14 = 0.98$.

Example 6-15. Stroke-Bore Ratio. Compute the indicated power of the 4-in bore engine of Fig 6-16 at 2000 rpm, assuming that indicated efficiency is 80% of fuel-air cycle efficiency. Could it give equal power if the stroke were shortened from 4.8 to 4.0 in and, if so, under what conditions?

Solution: From Fig 4-5, part *a*1, at $r = 5.74$, $F_R = 1.10$, fuel-air cycle efficiency is 0.33. Assuming no moisture in the air and all fuel evaporated in inlet pipe, from eq 6-6,

$$\rho_a = \frac{2.7(13.8)}{610}\left(\frac{1}{1 + 1.1(0.0670)(29/113)}\right) = 0.06$$

Fuel characteristics from Fig 3-1:

$$s = 2000 \times 4.8/6 = 1600 \text{ ft/min}, \qquad e_v = 0.85 \quad \text{from Fig 6-16}$$

$$FQ_c = 0.0670(1.1)19{,}020 = 1400 \text{ Btu}$$

$$A_p = \text{area of 4-in circle} = 12.6 \text{ in}^2$$

From eq 6-8,

$$\text{bhp} = \frac{778(12.6)(1600)(0.06)(0.85)(1400)(0.33)(0.80)}{33{,}000(4)(144)} = 15.5 \text{ hp}$$

With a 4-in stroke, Fig 6-25 shows that the engine could attain the same power at the same piston speed but the rpm would have to be increased to 2000(4.8)/4 = 2400.

seven—— Two-Stroke Engines

The distinguishing feature of the two-stroke method of operation is that every outward stroke of the piston is a working, or expansion, stroke. Such operation is made possible by the fact that the pumping function is not carried out in the working cylinders but is accomplished in a separate mechanism called a *scavenging pump.* It must be remembered, however, that for a given output a definite air capacity is always required and that the two-stroke engine must take into its cylinders at least as much air, per unit time, as its four-stroke equivalent to achieve the same output.

Figure 7-1 shows several types of two-stroke cylinder. The principles on which they operate are the same in spite of the differences in mechanical design and arrangement. These engines all have *ports* which are uncovered by the piston near bottom center. In Fig 7-1*a* and *b* these ports are at one end of the cylinder only but are divided into two groups, one group for inlet and the other for exhaust. In (*c*) and (*d*) the inlet ports are opened by one piston and the exhaust ports by another. In (*e*) and (*f*) there are valves at the head end of the cylinder in addition to the piston-controlled ports. Cylinders with inlet and exhaust ports at one end, such as types (*a*) and (*b*), are often called *loop-scavenged,* whereas cylinders with inlet and exhaust ports at both ends are said to be *through-scavenged.* For convenience, these terms are used here. In the following discussion the word *ports* is used to indicate the inlet and exhaust openings, even though in some cases, such as (*e*), the openings may actually be controlled by valves.

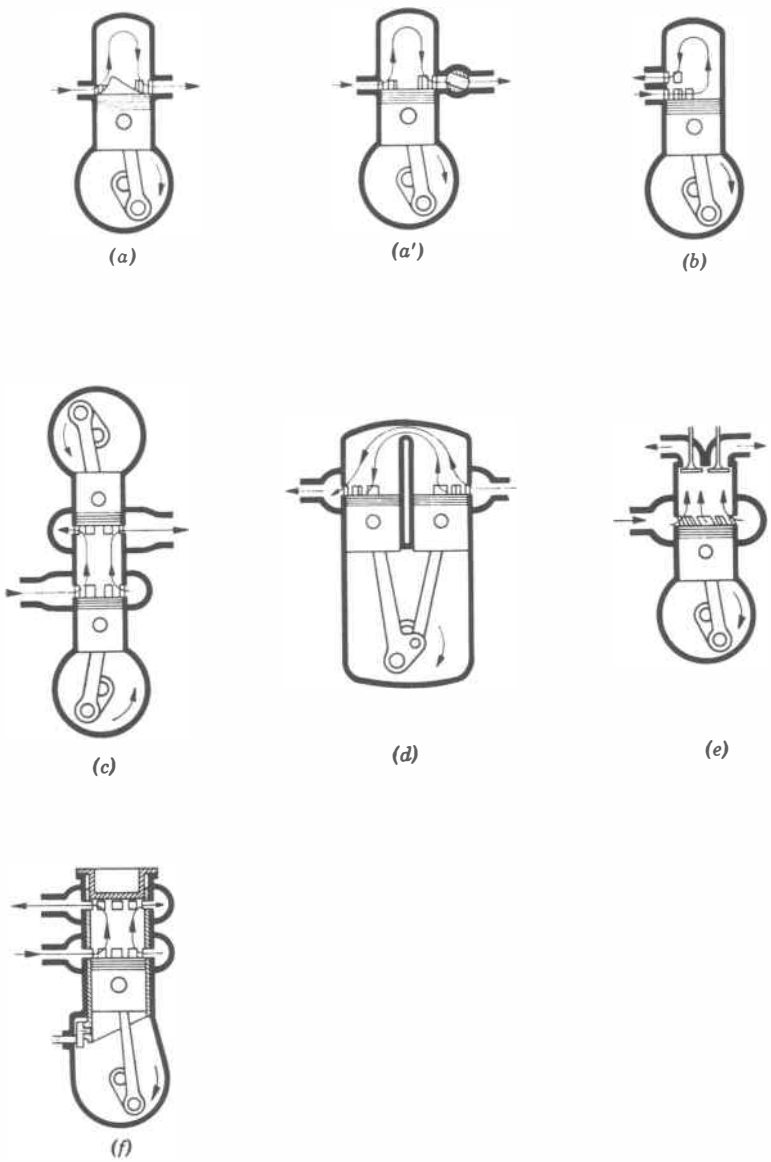

Fig 7-1. Two-stroke cylinder types: (*a*) conventional loop-scavenge; (*a'*) loop-scavenge with rotary exhaust valve; (*b*) reverse-loop scavenge; (*c*) opposed-piston; (*d*) U-cylinder; (*e*) poppet-valve; (*f*) sleeve-valve.

In all commercial two-stroke engines air, or a fuel-air mixture, is supplied to the inlet ports at a pressure higher than exhaust-system pressure by means of a scavenging pump. The operation of clearing the cylinder of exhaust gases and filling it more or less completely with fresh mixture is called *scavenging.*

THE SCAVENGING PROCESS

Figure 7-2 shows a light-spring pressure-crank-angle diagram taken from a two-stroke engine. After the exhaust ports open the cylinder pressure falls rapidly in the *blowdown process.* The *blowdown angle* is

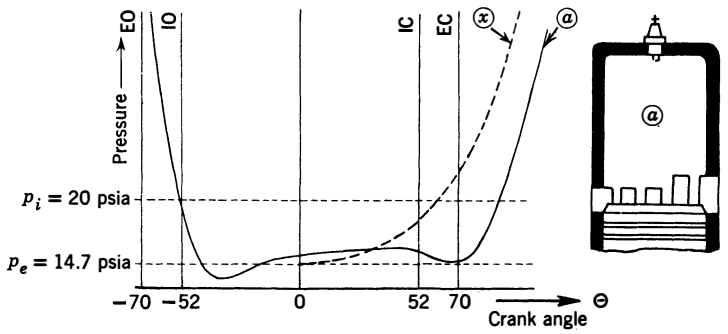

Fig 7-2. Light-spring indicator diagram for a two-stroke engine: (*a*) 4.5 x 6.0 in loop-scavenged type (*a*) cylinder, piston speed 30 ft/sec, $r = 7.0$, $R_s = 1.4$; (*x*) adiabatic compression from p_e at bottom center. (Ref 7.19)

defined as the crank angle from exhaust-port opening to the point at which cylinder pressure equals exhaust pressure.

After the blowdown process the cylinder pressure usually falls below exhaust pressure for a few degrees because of the inertia of the gases.

Soon after the exhaust ports begin to open the inlet ports open, and, as soon as the cylinder pressure falls below the scavenging pressure, fresh mixture flows into the cylinder. This flow continues as long as the inlet ports are open and the inlet total pressure exceeds the pressure in the cylinder.

While gases are flowing into the inlet ports exhaust gases continue to flow out of the exhaust ports, a result of their having been started in this direction at high velocity during the blowdown period and because the fresh mixture flowing in through the inlet ports eventually builds up a pressure in the cylinder which exceeds the exhaust-system pressure.

The crank angle during which both inlet and exhaust ports are open is called the *scavenging angle*, and the corresponding time, the *scavenging period.*

Either the inlet ports or exhaust ports may close first, depending on the cylinder design. The merits of these two possibilities are discussed later. In any case, after all ports are closed, the cycle proceeds through compression, combustion, and expansion, as in the four-stroke engine.

Figure 7-3 shows typical pressure-volume diagrams for a two-stroke engine. In all such engines the exhaust ports must open well before

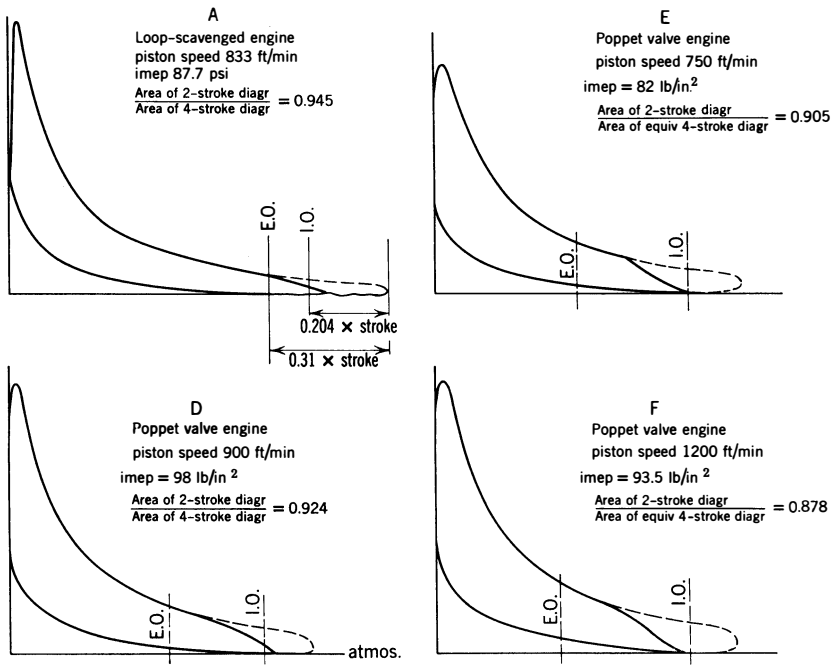

Fig 7-3. Indicator diagrams from two-stroke engines: Dotted lines show estimate of corresponding four-stroke diagram.

Configuration	Cylinder	Exhaust Lead°	CA_e/CA_i
A	18 x 22 in gas engine loop scav	0	—
D	3¼ x 4½ in poppet valves	7	1.25
E	3¼ x 4½ in poppet valves	14	1.25
F	3¼ x 4½ in poppet valves	21	1.25

(A—manufacturer's data D–F—Taylor et al, ref 7.23)

bottom center in order that the cylinder pressure be substantially equal to the exhaust-system pressure before the piston reaches bottom center and so that excessive blow back of unburned gases into the inlet system can be avoided. This characteristic makes two-stroke indicator diagrams easy to recognize.

As in four-stroke engines, the inlet ports of a two-stroke engine may be supplied with air alone, the fuel being injected into the cylinders later, or the inlet gases may consist of a carbureted mixture of air and fuel. The term *fresh mixture* is assumed to refer to the material introduced through the inlet ports in either case.

IDEAL SCAVENGING PROCESSES

In the ideal scavenging process the fresh mixture would push the residual gases before it without mixing or exchanging heat with them, and this process would continue until all the burned gases had been replaced with fresh mixture, at which point the flow would cease.

Assuming that the exhaust ports remain open during the whole scavenging process and that they offer no restriction to flow, the ideal process fills the cylinder at bottom center with fresh mixture at *inlet temperature* and *exhaust pressure.* As in the four-stroke engine, we define inlet temperature and pressure and exhaust pressure as the values which would be measured in large tanks connected to the inlet and exhaust ports. (See Fig 1-2.)

It will be noted that in the idealized scavenging process described not only is the cylinder completely filled with fresh mixture, but also no fresh mixture escapes from the exhaust ports, and thus all of the mixture supplied remains to take part in the subsequent combustion and expansion.

In actual engines, of course, the fresh mixture mixes and exchanges heat with the residual gases during the scavenging process, and some portion of the fresh mixture is usually lost through the exhaust ports. However, although actual two-stroke engines never realize the ideal scavenging process, they can approach it in varying degrees as design and operating conditions permit. Consideration of this ideal scavenging process makes it possible to define several terms which are useful in measuring the effectiveness of the actual scavenging process.

COMPRESSION RATIO

Except where otherwise noted, compression ratio for two-stroke engines is defined in the same way as for four-stroke engines, that is, maximum cylinder volume divided by minimum cylinder volume, and the symbol r is used as before. In much of the literature on two-stroke engines compression ratio is defined as the ratio of cylinder volume at port closing to cylinder volume at top center. This definition is given in an attempt to allow for the fact that the ports of a two-stroke engine do not close until the piston has traveled a considerable distance from bottom center. The same argument could, of course, be made in the case of four-stroke engines in which the inlet valve closes well past bottom center. In both cases such a definition ignores dynamic effects. In deciding on the compression ratio to be used it may be necessary to allow for the fact that the ports close late, but for purposes of analytical discussion it is more convenient to use the definition based on total cylinder volume, as in four-stroke engines.

It is evident by reference to the indicator diagrams (Fig. 7-3) that the area near the *toe* is appreciably less than it would be with the normal exhaust-valve timing used on four-stroke engines. It is also evident that the indicated efficiency of a two-stroke engine will generally be less than that of a four-stroke engine of the same compression ratio, based on the definition of compression ratio used here. However, use of the other definition would entail a corresponding efficiency difference in the opposite direction.

TWO-STROKE DEFINITIONS AND SYMBOLS

In general, the same system of symbols is used as in the case of four-stroke engines:

$\dot{M}$ = mass flow per unit time supplied to the engine
M' = mass retained in cylinder after ports close
Γ = the trapping efficiency, that is, the ratio mass retained in cylinder to mass supplied
$\dot{M}'$ = $\dot{M}\Gamma$, mass retained per unit time
F = fuel-air ratio based on fuel and air supplied to engine
F' = ratio of fuel to fresh air trapped in the cylinder. This fuel-air ratio may be called the *combustion fuel-air ratio*
F' = F/Γ in injection engines
F' = F for engines scavenged with a fuel-air mixture

η = indicated thermal efficiency based on fuel supplied
η' = indicated thermal efficiency based on fuel retained
$\eta' = \eta$ for injection engines
$\eta' = \eta/\Gamma$ for engines scavenged with a fuel-air mixture
p = absolute pressure
T = absolute temperature

Subscripts used with p and T are i, referring to conditions in the inlet receiver, and e, referring to conditions in the exhaust receiver. (It is assumed that these receivers are sufficiently large so that velocities are negligible.)

Subscripts used with $\dot{M}$ and $\dot{M}'$ are a, fresh air, f, fresh fuel, i, fresh mixture, c, cylinder contents or *charge*, and r, residual gases.

V_d is displacement volume, and V_c is total cylinder volume = $V_d\,[r/(r-1)]$, in which r is the compression ratio.

ρ is density = pm/RT in the case of a gas, in which R is the universal gas constant and m molecular weight.

Scavenging Ratio. The mass of fresh mixture supplied in the ideal scavenging process would be that which would just fill the cylinder at bottom center with fresh mixture at inlet temperature and exhaust pressure. A definition of the *scavenging ratio* as the ratio of mass of fresh mixture supplied to the ideal mass results in the following expression:

$$R_s = \dot{M}_i/NV_c\frac{p_e m_i}{RT_i} \tag{7-1}$$

in which R_s is the scavenging ratio and N is the revolutions per unit time.

By analogy with eqs 6-2 and 6-3,

$$R_s = \dot{M}_a/NV_c\,\rho_s \tag{7-2}$$

in which ρ_s is the density of dry air in the inlet mixture at T_i and p_e and $\dot{M}_a$ is the mass flow of dry air to the engine per unit time.

By analogy with eq 6-6,

$$\rho_s = \frac{29p_e}{RT_i} \times \left(\frac{1}{1 + F_i(29/m_f) + 1.6h}\right) \tag{7-3}$$

where F_i = mass ratio of gaseous fuel to dry air upstream from the inlet ports
h = mass fraction of water vapor in the inlet air

Values of the term in parenthesis are given in Fig 6-2.

For injection engines F_i is zero. For carbureted engines using a liquid petroleum fuel the factor in parenthesis, as in four-stroke engines, lies between 0.95 and 0.99 and is usually taken as equal to unity. Thus, except in carbureted engines using unusual fuels,

$$R_s \cong \frac{\dot{M}_a}{NV_c} \times \frac{RT_i}{29p_e} \tag{7-4}$$

This definition of scavenging ratio is used hereafter unless otherwise noted.

Scavenging Efficiency. In the ideal scavenging process the mass of fresh mixture retained in the cylinder would be $V_c p_e m_i / RT_i$. If *scavenging efficiency* is defined as the ratio of mass of mixture retained to the ideal mass retained,

$$e_s \cong \frac{\dot{M}_a'}{NV_c} \times \frac{RT_i}{29p_e} \tag{7-5}$$

A combination of eqs 7-4 and 7-5 gives

$$e_s = \Gamma R_s \tag{7-6}$$

where Γ is the trapping efficiency.

In subsequent discussion involving scavenging efficiency expression 7-5 is used. It should be remembered, however, that in carbureted engines using fuels of light molecular weight the right-hand side of expression 7-5 should be divided by the quantity in parenthesis in expression 7-3.

Relation of Power and Mean Pressure to R_s and e_s. A combination of eqs 7-4 and 7-5 and eq 1-5 gives

$$P = JR_s NV_c \rho_s F Q_c \eta \tag{7-7}$$

$$= Je_s NV_c \rho_s F' Q_c \eta' \tag{7-8}$$

If we divide these equations by NV_d, remembering that $V_c = V_d [r/(r-1)]$, we may write

$$\text{mep} = JR_s \rho_s F Q_c \eta \left(\frac{r}{r-1}\right) \tag{7-9}$$

$$= Je_s \rho_s F' Q_c \eta' \left(\frac{r}{r-1}\right) \tag{7-10}$$

A comparison of eq 7-10 with the corresponding equation for four-stroke engines, eq 6-9, makes it apparent that by the use of cylinder

volume instead of piston displacement the imep of a two-stroke engine will be $r/(r-1)$ times that of a four-stroke engine operating with the same combustion fuel-air ratio, the same thermal efficiency based on fuel retained, and with $\rho_i e_v'$ of the four-stroke engine equal to $\rho_s e_s$ of the two-stroke engine.

RELATIONSHIP OF SCAVENGING RATIO AND SCAVENGING EFFICIENCY

Figure 7-4*a* shows e_s vs R_s for ideal scavenging. In this case the scavenging efficiency equals scavenging ratio at all points, and Γ is unity.

A second hypothetical relationship of considerable interest is based on the assumptions that the fresh mixture mixes completely with the resid-

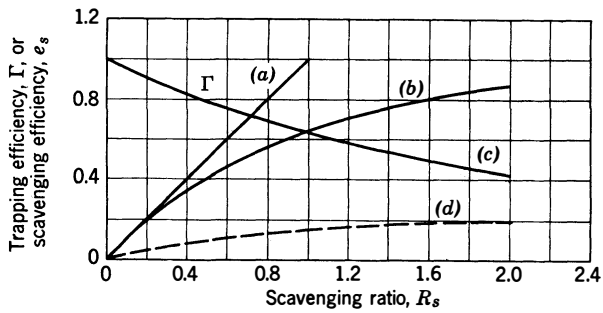

Fig 7-4. Theoretical relationships between scavenging efficiency, trapping efficiency, and scavenging ratio: (*a*) e_s with perfect scavenging; (*b*) e_s with perfect mixing, $e_s = 1 - \epsilon^{-R_s}$; (*c*) Γ with perfect mixing; (*d*) e_s with complete short circuiting.

ual gases as it enters the cylinder, that the residual gases are at the same temperature and have the same molecular weight as the fresh mixture, and that the piston remains at bottom center during the scavenging process.

Let x be the volumetric fraction of fresh mixture in the cylinder at any instant, v the volume of fresh mixture which has flowed into the cylinder up to that instant, and V_c the maximum cylinder volume. If cylinder pressure is assumed constant and equal to the exhaust pressure and all volumes measured at this pressure, then, for a given time, the volumetric increase in fresh mixture in the cylinder is equal to the volume of fresh mixture which has flowed in, minus the volume of fresh mixture which has escaped. In mathematical terms this relationship

may be expressed as

$$V_c\,dx = dv - x\,dv \tag{7-11}$$

or

$$dx = \frac{(1 - x)\,dv}{V_c} \tag{7-12}$$

Integration of this equation gives

$$x = 1 - \epsilon^{-(v/V_c)} \tag{7-13}$$

where ϵ is the base of natural logarithms. By definition, x is the *scavenging efficiency*, and v/V_c, the *scavenging ratio*. Therefore, under this set of assumptions,

$$e_s = 1 - \epsilon^{-R_s} \tag{7-14}$$

and

$$\Gamma = \frac{1 - \epsilon^{-R_s}}{R_s} \tag{7-15}$$

Figure 7-4*b* and *c* shows e_s and Γ vs R_s for the above relations.

There is a third possibility in scavenging which must be considered, and that is the case in which the fresh mixture might flow through the cylinder and out of the exhaust ports in a separate stream without mixing with the residual gases or pushing them out. This process is called *short-circuiting.* In this case only a little fresh mixture would be trapped, and the scavenging efficiency at any value of the scavenging ratio would be very low. (See Fig 7-4*d*.)

In two-stroke engines the scavenging process partakes of all three of the hypothetical processes described. In other words, there is some pushing out of the residuals without mixing, some mixing, and some short-circuiting in all real engines.

MEASUREMENT OF SCAVENGING RATIO AND SCAVENGING EFFICIENCY

Scavenging ratio is measurable, provided an air meter can be used in the inlet system and provided inlet pressure and temperature and exhaust pressure can be measured. The best method of insuring accurate measurements of these pressures and temperatures is by the use of large inlet and exhaust tanks or receivers. Large inlet and exhaust receivers are usually used with two-stroke engines except in the case of those using the crankcase as a scavenging pump. In measuring inlet temperature care must be exercised to see that the thermometer is not placed where

it will be influenced by exhaust gas blowing back through the inlet ports or by radiation through the inlet ports while they are open.

Scavenging Efficiency Measurements. Even with accurate measurements of air consumption, inlet temperature, and exhaust pressure, measurement of scavenging efficiency is difficult because there is no convenient way of determining what portion of the fresh mixture remains in the cylinder after the scavenging process. Many methods of measuring scavenging efficiency have been proposed. (See refs 7.1—.) Of these, your author has found only two which yield reliable results and are reasonably easy to apply.

Indicated Mean Effective Pressure Method. This method (ref 7.10) applies only to spark-ignition engines scavenged with a homogeneous, gaseous, fuel-air mixture of known composition. In using this method, expression 7-10 is employed. For a given engine test J, ρ_s, F', and Q_c are known, and imep is measured from an indicator card or from brake hp and friction hp tests. (See Chapter 9.) The remaining unknowns are e_s and η_i'.

The most reliable method of estimating η_i' is to operate a four-stroke engine of nearly the same cylinder size, with the same compression ratio and the same operating conditions, and to measure its indicated thermal efficiency based on the compression and expansion strokes only. It is then assumed that η_i' for the two-stroke engine will be equal to x times the indicated efficiency of the four-stroke engine, where x is the correction factor accounting for the smaller area of the toe of the two-stroke diagram. (See Fig 7-3.) x can be measured by comparing the two-stroke and four-stroke indicator diagrams. It usually lies between 0.85 and 0.95 and can safely be taken as 0.90 when measurements are not available.

In order that η_i' of the two-stroke engine equal η_i for the four-stroke engine (except for the correction factor above suggested), the two engines must have the same compression ratio and fuel-air ratio, and the following conditions must be fulfilled:

1. The fuel-air ratio used should be near that for maximum imep, both to reduce errors in measurement of imep and to reduce the influence of differences in residual-gas content on efficiency.
2. The four-stroke engine should not have a large valve-overlap angle, since escape of fresh mixture during the overlap period would affect the efficiency of the four-stroke engine to an unknown extent.
3. Best-power spark advance should be used in all cases.
4. The two engines should have nearly the same cylinder dimensions and should be run at the same piston speed and jacket temperatures.

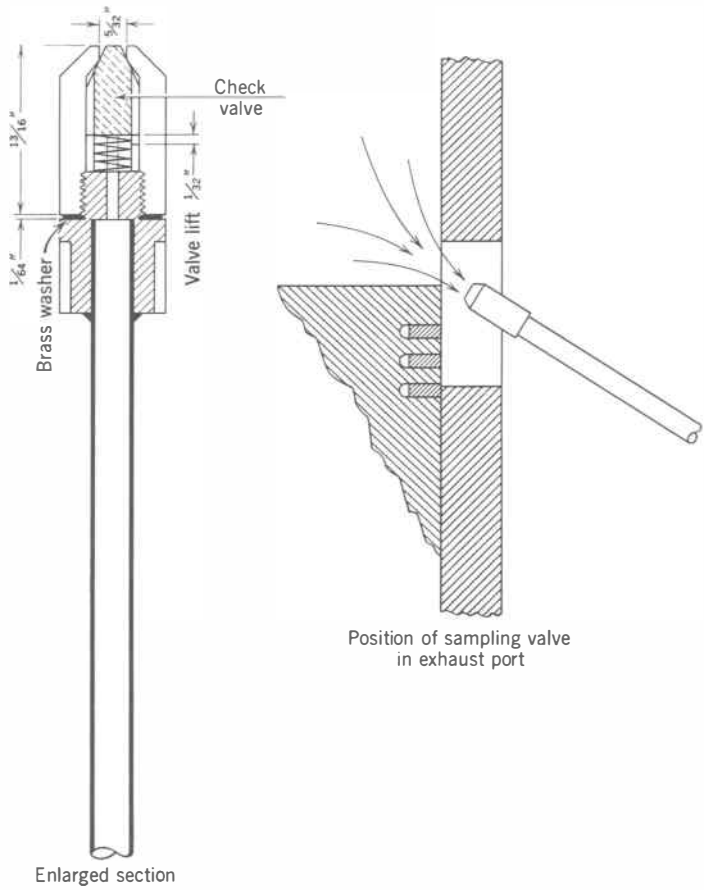

Fig 7-5. Exhaust-blowdown sampling valve. (Developed at Sloan Automotive Laboratories, MIT.)

In the absence of a suitable comparative test on a four-stroke engine it may be assumed with reasonable assurance that η_i' for a two-stroke engine scavenged with a homogeneous gaseous fuel-air mixture will be 0.80 times the corresponding fuel-air-cycle efficiency, provided optimum spark timing is used and the fuel-air ratio is near that for maximum imep.

Example 7-1, at the end of this chapter, gives an illustration of the application of this method to a practical problem.

Gas-Sampling Method. This method (ref 7.11) applies to Diesel engines and also to spark-ignition engines in which the fuel is injected after the ports close. In engines of these types the scavenging efficiency

can be computed from a measurement of the mass of fuel supplied and chemical analysis of a sample of the gases which were in the cylinder near the end of the expansion process.

The gas sample may be taken by means of an impact tube of the type shown in Fig 7-5. This instrument consists of a small tube whose open end carries a check valve. The tube is placed in the exhaust port facing the exhaust-gas stream at the point at which it first emerges from the exhaust-port opening. The tube opening is thus exposed to a total pressure about equal to the cylinder pressure during the early part of the exhaust process. The tube is connected to a small receiving tank with a bleed valve to atmosphere. This valve is adjusted to hold the pressure in the tank well above the scavenging pressure. Thus the check valve closes before the cylinder pressure falls to scavenging pressure, and no fresh gases enter the sampling tube during the scavenging process. In taking a sample the gases are allowed to flow through the sampling system long enough to make sure that it is well purged before the contents are analyzed. Analysis may be made with the usual Orsat apparatus or its equivalent.

Figure 7-6 shows the relation of exhaust-gas composition to fuel-air ratio for four-stroke engines with small valve overlap. For two-

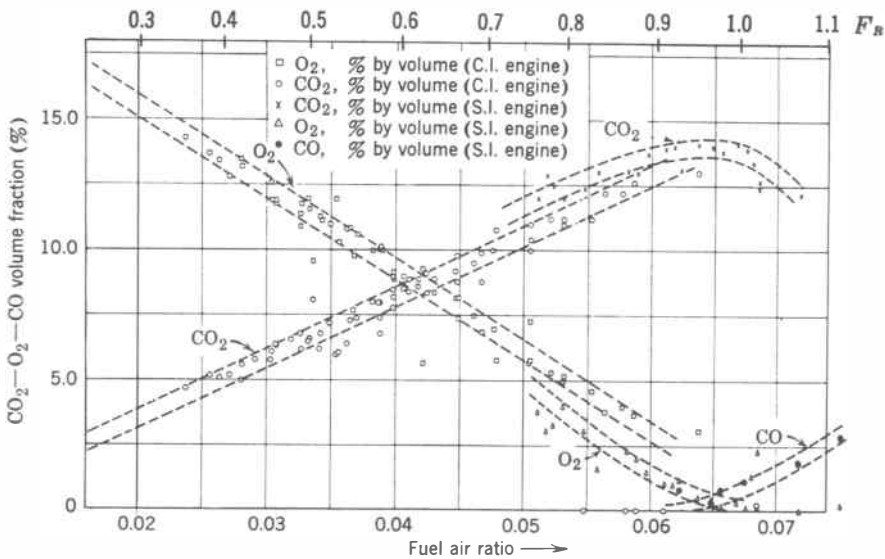

□ ○ Diesel engine, ref 7.21, 7.162
× △ • Spark-ignition engine, ref 7.16

Fig 7-6. Composition of exhaust gases from four-stroke engines.

stroke engines the combustion fuel-air ratio is determined by applying the gas-analysis results to this figure. The mass of air retained per unit time is obviously equal to the mass of fuel supplied per unit time divided by the combustion fuel-air ratio. Thus the missing term in eq 7-5 is supplied.

Example 7-2 at the end of this chapter shows how the gas sampling method can be used in a practical case.

Tracer-Gas Method. This method (ref 7.12) is based on the use of small quantities of a gas which are assumed to burn completely at combustion temperatures but not to burn at temperatures below those prevailing in the cylinder when the exhaust ports open. The tracer gas must be easy to identify qualitatively and quantitatively by chemical analysis. Suppose such a gas is thoroughly mixed with the fresh mixture. Then

$$e_s = \Gamma R_s = \frac{x - y}{x} R_s \tag{7-16}$$

where x is the mass fraction of tracer gas in the inlet air and y is the mass fraction of unburned tracer gas in the exhaust gases. x can be measured by measuring the inflow of tracer gas, y can be obtained by chemical analysis of the exhaust gases, and R_s by measurement of the mass flow of air and fuel through the engine. The latter measurement is also necessary in order to obtain x. The chief objection to this method is uncertainty of the assumption that none of the tracer gas burns after the exhaust ports open and that none escapes burning before the ports open. There appears to be no easy way, in practice, to verify this assumption.

Model Tests. Estimates of the comparative scavenging efficiency of various cylinder and port arrangements have been made by means of cylinder models. (See refs 7.13–7.14.) In such tests the model cylinder, with closed ports, is filled with a gas containing no free oxygen (CO_2 is usually used). A simulated scavenging process is then carried out with air. The composition of the resulting mixture is then measured by chemical analysis.*

A good simulation of the actual scavenging process might be obtained with a model in which the pressure in the cylinder, before scavenging, was adjusted to be the same at exhaust-port opening as that in the corresponding engine, thus simulating the blowdown process. The piston-travel vs time during scavenging would also have to reproduce engine conditions. However, most such tests have been carried out with atmospheric pressure in the cylinder and with slow piston motion. It is

* Obviously the cylinder may be filled with air and scavenged with CO_2 with equally useful results.

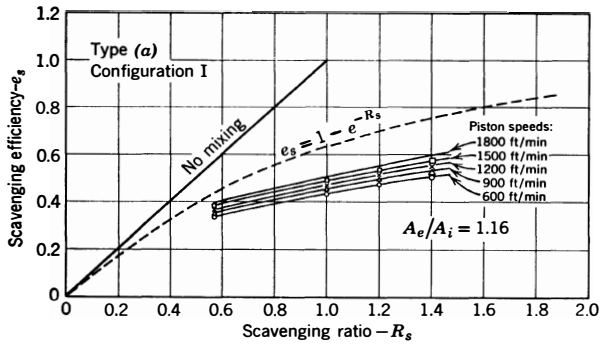

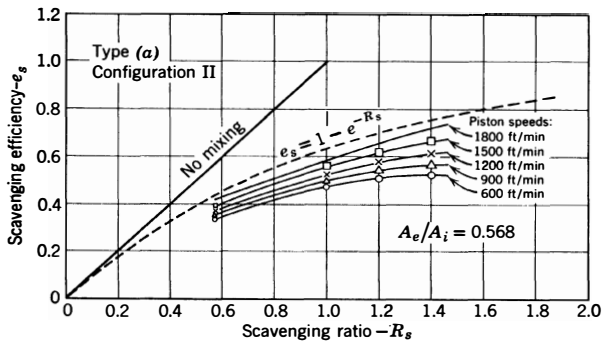

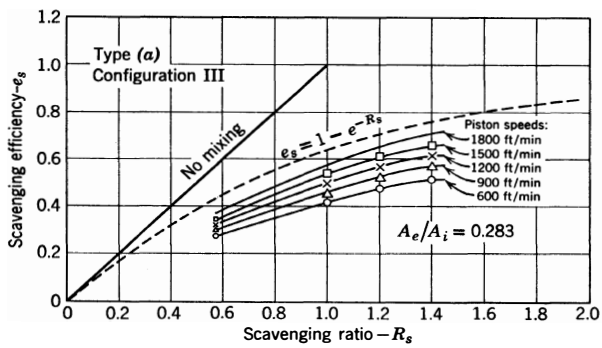

Fig 7-7. Scavenging efficiency vs scavenging ratio, loop-scavenged engine: 3¼ x 4½ in cylinder; type (*a*); $r = 5.43$.

Configuration	Timing, Degrees IO	EO	IC	EC	$(CA)_i/A_p$	$(CA)_e/A_p$	$(CA)_e/(CA)_i$	C, $R_s = 1.2$	
I	56	62	56	62	0.0384	0.048	1.25	0.026	Taylor et
II	56	62	56	62	0.0384	0.0231	0.604	0.024	al., ref
III	56	62	56	62	0.0384	0.0125	0.326	0.017	7.23

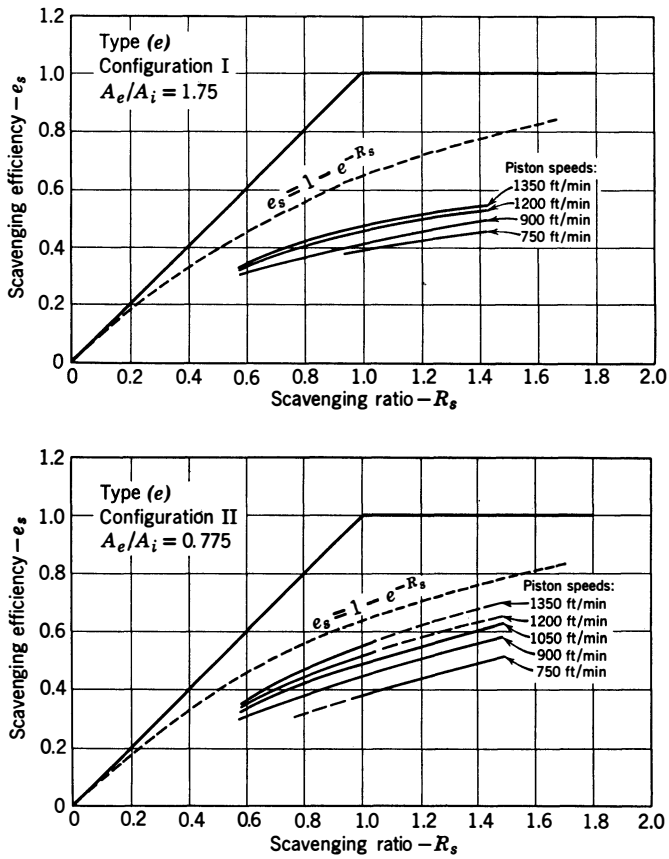

Fig 7-8. Scavenging efficiency vs scavenging ratio, through-scavenged engine with symmetrical timing: 3¼ x 4½ in cylinder; type (*e*); r = 5.8.

Configuration	Timing, Degrees IO	EO	IC	EC	$(CA)_i/A_p$	$(CA)_e/A_p$	$(CA)_e/(CA)_i$	C, R_s = 1.2
I	57	88*	57	88*	0.0386	0.050	1.29	0.023
II	57	88*	57	88*	0.0386	0.0233	0.601	0.016

* Because of the nature of the poppet-valve opening curve, Fig 6-29, this timing is effectively equivalent to the 62-degree exhaust timing in Fig 7-7. (Taylor et al., ref 7.23)

obvious that under such conditions experiments of this kind can at best yield only comparative data. However, such tests may be helpful in the early stage of development of a new two-stroke cylinder.

Results of Scavenging Efficiency Tests

On account of difficulties in measurement, few data are available on the scavenging efficiency of two-stroke engines in actual operation, and many of the published data are of doubtful accuracy. In Figs 7-7, 7-8,

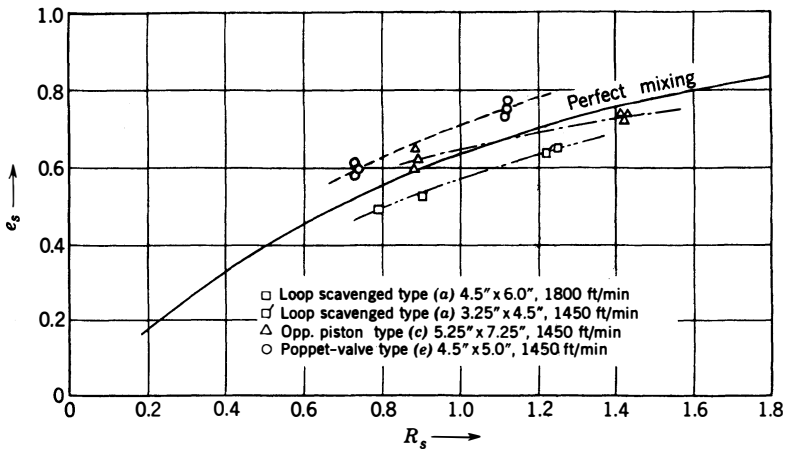

Fig 7-9. Scavenging efficiency vs scavenging ratio for three cylinder types. (Houtsma et al., ref 7.21)

and 7-9 the plotted points were obtained, under the author's direction, by careful use of the imep or the gas-sampling method, with the engine at full-load operation in each case.

Figure 7-7 shows scavenging efficiency vs scavenging ratio for a loop-scavenged engine of type (*a*), Fig 7-1, with several different exhaust-port arrangements.

Figure 7-8 shows scavenging efficiency vs scavenging ratio for a cylinder of type (*e*), Fig 7-1, with two porting arrangements.

Figure 7-9 shows scavenging ratio vs scavenging efficiency for several commercial two-stroke Diesel engines.

It will be noted that all the curves have the same general shape as the curve for perfect mixing. This fact, together with some high-speed motion pictures of the scavenging process made by Boyer et al. (ref 7.15), indicates that there is much mixing and little "piston" action in the actual scavenging process. When a curve lies generally below

the curve for complete mixing, considerable short-circuiting is indicated.

The differences in the curves of Figs 7-7–7-9 due to differences in design and operating conditions are taken up later in this chapter.

TWO-STROKE ENGINE FLOW COEFFICIENT

Although the relation of scavenging efficiency to scavenging ratio is a highly important characteristic of a two-stroke engine, the power required to attain a given scavenging ratio is a factor of nearly equal importance.

The power to scavenge is, of course, a function of mass flow of the fresh charge and the pressure at which this charge has to be delivered to the inlet ports. For purposes of analysis it is convenient to consider the ports as they form a flow passage between the inlet and exhaust receivers during the scavenging process.

As explained in Appendix 3, the mass flow of a gas through an orifice between two large reservoirs may be expressed as

$$\dot{M} = ACa\rho\phi_1 \tag{7-17}$$

where A = the orifice area, or a given reference area
C = the orifice flow coefficient, that is, the ratio of the actual mass flow to the ideal flow through the reference area under the same conditions (see Appendix 3)
a = the speed of sound in the gas in the upstream reservoir
ρ = the density in the upstream reservoir
ϕ_1 = the function of k and p_2/p_{01}, shown in Fig A-2, for $k = 1.4$. This function is a constant when p_2/p_1 is less than the critical value ($= 0.578$ when $k = 1.4$)

Equation 7-17 can be applied to the flow through a two-stroke cylinder mounted between large inlet and exhaust tanks, as in Fig 1-2. To use expression 7-17, p_{01} is taken as p_i, and p_2, as p_e. In this case it is convenient to take the piston area as the reference area. C can then be evaluated from measurements of mass flow, inlet pressure and temperature, and exhaust pressure. On the other hand, if C is known or can be estimated, the mass flow can be computed for any given inlet conditions and exhaust pressure, and the power required to scavenge can also be evaluated.

For use with a two-stroke engine in operation, eq 7-17 may be combined with eq 7-1 as follows:

$$R_s = \frac{A_p C a_i \rho_i}{N V_c \rho_s} \phi_1 \tag{7-18}$$

where A_p is the piston area, C is the flow coefficient based on the piston area, and a_i and ρ_i are, respectively, the speed of sound and the density of the gases in the inlet receiver. Other symbols remain as before.

For NV_c we may substitute $[r/(r-1)](sA_p/2)$ where s is the mean piston speed. For ρ_i/ρ_s we can substitute p_i/p_e, since both densities are measured at the same temperature. These substitutions reduce eq 7-18 to

$$R_s = 2C\left(\frac{r-1}{r}\right)\left(\frac{a_i}{s}\right)\left(\frac{p_i}{p_e}\right)\phi_1 \tag{7-19}$$

Figure 7-10 gives solutions for this equation for conditions representative of engine performance. Values of ϕ_1 are shown in Fig A-2.

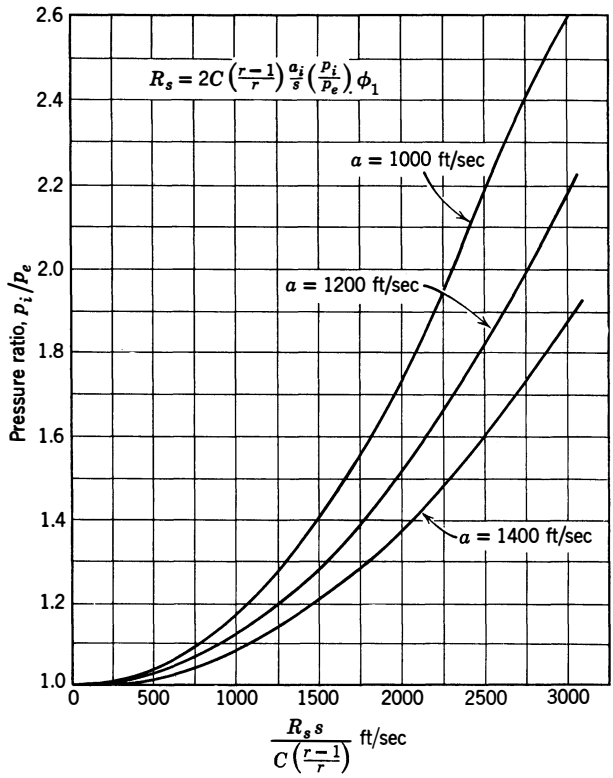

Fig 7-10. Pressure ratio required for scavenging: C = engine flow coefficient; R_s = scavenging ratio; s = piston speed (ft/sec); r = compression ratio; a = inlet sound velocity; p_i = inlet pressure; p_e = exhaust pressure; ϕ_1 = compressible flow function.

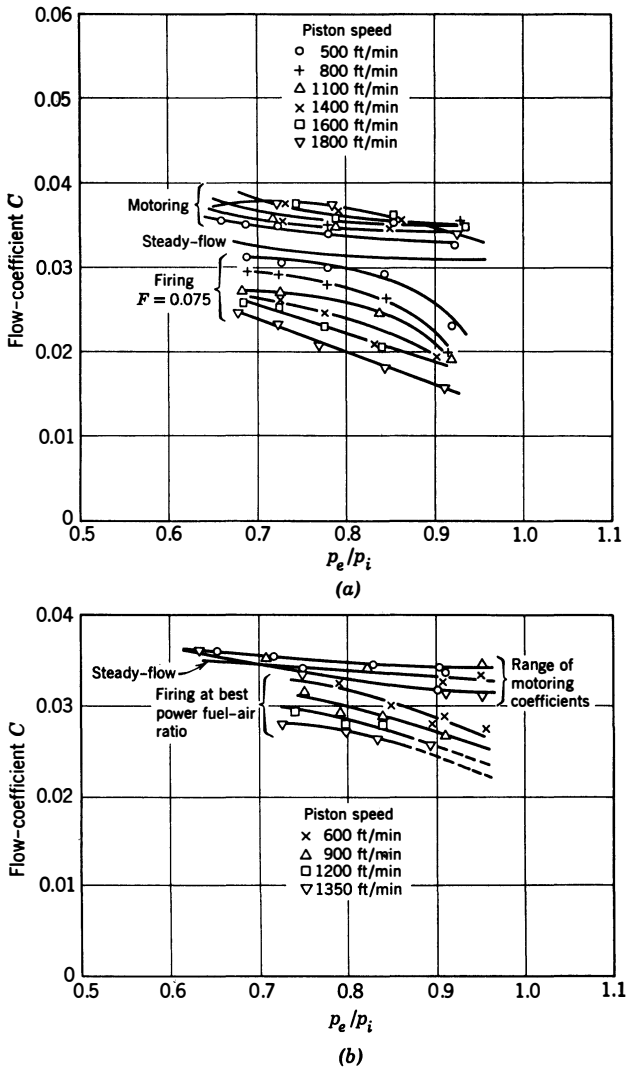

Fig 7-11. Flow coefficients of two loop-scavenged cylinders: (*a*) Type (*a*) 4.5 x 6.5 in, $A_i/A_p = 0.277$, $A_e/A_p = 0.396$, A_e/A_i 1.43; (*b*) Type (*a*) 3.25 x 4.5 in, $A_i/A_p = 0.26$, $A_e/A_p = 0.302$, A_e/A_i 1.16. (Toong and Tsai, ref 7.4)

It is evident that eq 7-19 is an explicit solution of an equation similar to 6-21 in Chapter 6, except that scavenging ratio has been substituted for volumetric efficiency. Like volumetric efficiency, scavenging ratio is

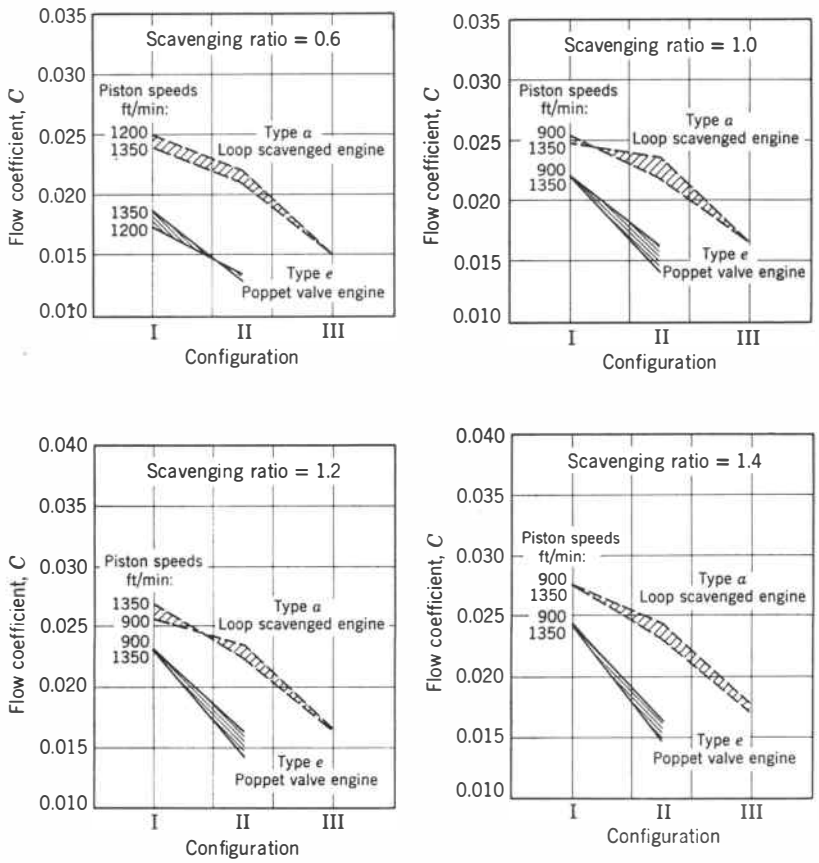

Fig 7-12. Flow coefficients of engines of Figs 7-7 and 7-8. Values of C_eA_e/C_iA_i: I, 1.25 loop, 1.29 pv; II, 0.60 loop and pv; III, 0.33 loop only (ref 7.23).

a function of u/a_i, r, (p_e/p_i), and design,* but in this case the function is determined when a value has been assigned to C.

Figures 7-11, 7-12, and 7-13 show measured values of C for several engines under various operation conditions. These values were deter-

* The effect of Reynolds index is included in the value of C when the latter is determined by experiment. This effect is probably very small within the range of interest here.

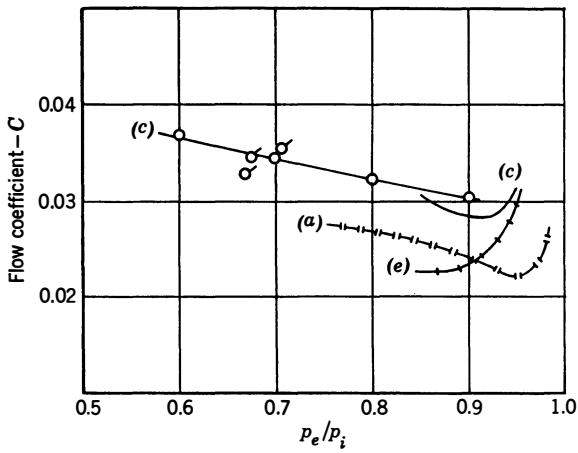

Curve	Engine	Type	A_i/A_p	A_e/A_p	A_e/A_i	Piston speed ft/sec	Ref.
–♂–♂–	Junkers airplane	*(c)*	0.30	0.415	1.38	42	7.32
———	Commercial	*(c)*				17–25	7.21
—+—+—	Commercial	*(e)*	0.40	0.17	0.43	24	7.21
⊢⊢⊢⊢	Experimental	*(a)*	0.215	0.25	1.16	20	7.21

♂ indicates motoring tests
A_i is maximum inlet-port area
A_e is maximum exhaust-port area
A_p is piston area
(a) loop-scavenged type
(c) opposed-piston type
(e) poppet exhaust-valve type

Fig 7-13. Flow coefficients of commercial two-stroke engines.

mined by measuring $\dot{M}_i$, p_i, T_i, and p_e with the engine in operation, or motoring, and solving eq 7-19 for C.

It is apparent that C varies with design and with operating conditions. In order to explain these variations, it is convenient to consider a simplified model consisting of two orifices in series. (See Fig 7-14.) The orifices are considered to be separated by a reservoir large enough to make the approach velocity to the second orifice negligibly small.

The abscissa scale of Fig 7-14 is the ratio $(CA)_2/(CA)_1$, that is, the ratio of the flow capacity of the downstream orifice to that of the upstream orifice. The ordinate scale is the ratio of flow through the system to the flow which would be obtained through the upstream orifice alone at the same over-all pressure drop and thus is equal to C/C_1 where C is the flow coefficient of the two-orifice system based on the upstream orifice area. Flow coefficients are defined by eq 7-17. The graph shows the

effect of adding a second orifice downstream, on the flow which would be obtained at the same over-all pressure drop through the first orifice alone.

Effect of p_e/p_i on Flow Coefficient. It is evident, assuming that C_1 is constant, that when the flow-capacity ratio of the two orifices lies between 0.5 and 2 (as in most two-stroke engines) the flow coefficient of the system decreases as p_2/p_1 increases. This relation accounts for the fact that C decreases with increasing p_e/p_i in Figs 7-11–7-13.

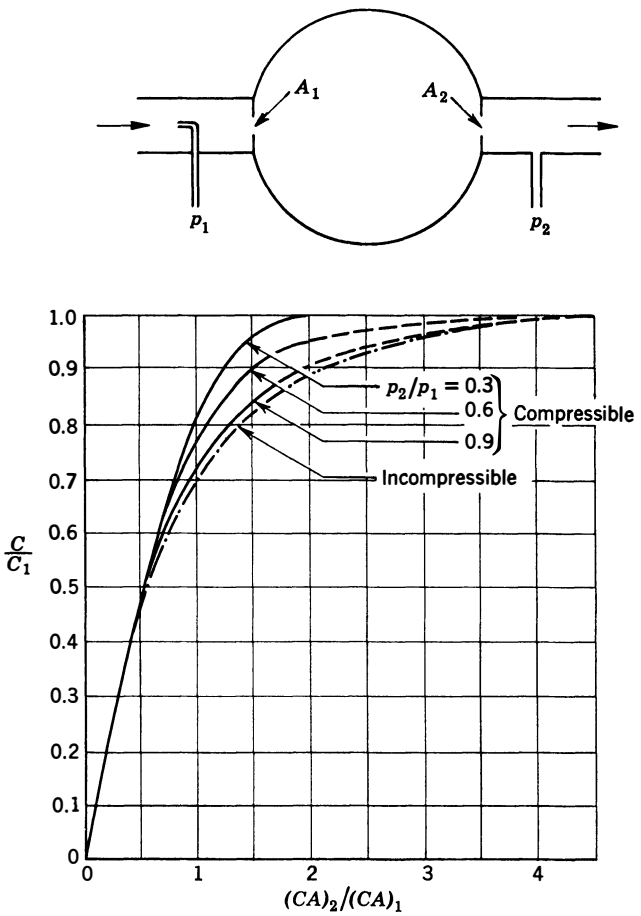

Fig 7-14. Flow through two orifices in series: $(CA)_1$ = area of upstream orifice × its flow coefficient; $(CA)_2$ = area of downstream orifice × its flow coefficient; C = system coefficient based on A_1; C_1 = flow coefficient of A_1 alone; velocity ahead of A_2 assumed very small.

The flow coefficient may also be influenced by the assistance which blowdown gives to the scavenging process, sometimes known as the "Kadenacy" effect. (See ref 7.5.) Although this effect is relatively unimportant at low values of p_e/p_i, where flow through the cylinder is rapid, it may be important when p_e/p_i approaches 1.0 and the flow due to this pressure ratio becomes small. This effect is shown by the sharp upward turn of several of the curves in Fig 7-13 at high values of p_e/p_i. However, since scavenging ratio is usually very low when p_e/p_i is more than 0.85, values of C in the region where p_e/p_i exceeds 0.85 are of academic interest only.

Effect of Piston Speed on *C*. In general, Figs 7-11–7-13 show decreasing values of C with increasing piston speed. In a firing engine the fact that the coefficient falls off with increasing speed is due chiefly to increase in the blowdown angle, which leaves a decreasing crank angle available for flow of fresh gases into the cylinder.

The motoring tests of Fig 7-11 show no consistent variation with piston speed. The differences that do appear at the different speeds must be due to inertia effects.

The effects of design on flow coefficient are discussed later in this chapter.

EFFECTS OF OPERATING CONDITIONS ON SCAVENGING RATIO

Effect of T_i on Scavenging Ratio. The velocity of sound in a perfect gas is given by the relation

$$a = \sqrt{kRT/m} \ * \tag{7-20}$$

where k = specific-heat ratio
R = universal gas constant
T = absolute temperature
m = molecular weight

Thus, for a given value of C, s, and p_e/p_i, eq 7-19 shows that scavenging ratio will vary directly with the square root of T_i. Tests made with an engine of type (*a*), Fig 7-1, show that this relationship holds in practice. (See ref 7.60.)

Effect of T_c on Scavenging Ratio. The jacket temperature T_c would affect scavenging ratio only as it affects C through heat transfer

* For dry air, $a = 49\sqrt{T}$ when a is in ft/sec and T in °R.

to the gases during scavenging. Since the amount of heat transferred to and from the flowing gases during the scavenging process is probably quite small, except at low speeds, it is probable that changes in jacket temperature have little effect on C over the usual operating range. Experiments are needed to confirm this supposition.

Effect of Fuel-Air Ratio. As we have seen, fuel-air ratio affects exhaust pressures and temperatures and, therefore, has a marked effect on the blowdown process. Changes in fuel-air ratio also change the sonic velocity slightly. (See Tables 3-1 and 6-2.)

Reference 7.60 shows that the effect of fuel-air ratio on the flow coefficient is small in a spark-ignition engine scavenged by a homogeneous fuel-air mixture. In compression-ignition engines, in which the range of useful fuel-air ratios is much greater, the effect of fuel-air ratio on the flow coefficient may be more important. Experimental data are needed to confirm this supposition.

POWER TO SCAVENGE

The power requirement of a scavenging pump is discussed in some detail in Chapter 10. From eqs 10-8 and 7-2,

$$\text{cmep} = JR_s\rho_s C_p T_1 (Y_c/\eta_c)\left(\frac{r}{r-1}\right) \qquad (7\text{-}21)\ *$$

where cmep = the engine mep required to drive the compressor
J = the mechanical equivalent of heat
C_p = the specific heat of air at constant pressure (0.24 Btu/lb °F)
T_1 = the compressor inlet temperature (usually atmospheric)
$Y_c = [(p_i/p_1)^{(k-1)/k} - 1]$ (7-22)
p_1 = compressor inlet pressure
k = the specific-heat ratio $(k-1)/k = 0.285$ for air
η_c = the compressor adiabatic efficiency

From eq 7-19

$$p_i/p_e = \frac{sR_s[r/(r-1)]}{2Ca_i\phi_1} \qquad (7\text{-}23)$$

* Values of Y_c vs pressure ratio are plotted in Fig 10-2, page 364.

The above relation shows that p_i/p_e and cmep, with given values of R_s and s, decrease rapidly with increasing flow coefficient. The importance of a large flow coefficient, especially at high piston speeds, is evident from these relations.

Figure 7-10 gives solutions for eq 7-23 over the useful range.

DESIGN OF TWO-STROKE CYLINDERS

It is evident from the foregoing discussion that from the point of view of effective scavenging the design objective should be to secure high values of scavenging efficiency and flow coefficient at the desired operating conditions. At the same time, the port design must not sacrifice too great a portion of the expansion stroke to the scavenging process. (See Fig 7-3.) Since these requirements conflict with each other to a considerable extent, the design of a two-stroke cylinder involves considerable compromise.

The principal variables at the command of the designer which affect the scavenging process may be classified as follows:

General Parameters

1. Stroke/bore
2. Port area/piston area
3. Exhaust-port area/inlet-port area
4. Port timing, that is, port-area vs crank angle

Detail Design

1. Cylinder size
2. Cylinder type
3. Detail design of ports and valves

Stroke-Bore Ratio. In regard to scavenging efficiency it seems probable that for thorough scavenging there should be less mixing as the stroke gets longer.

For loop-scavenged engines it would seem that very long strokes would tend to increase mixing, whereas very short strokes would lead to excessive short-circuiting. Whether these effects are important within the practical limitations of engine design has not yet been determined.

The effect of stroke-bore ratio on the ratio of port area to piston area

is easy to predict if a few reasonable assumptions are made. For piston-controlled ports, if the fraction of stroke devoted to porting is fixed, the ratio of port height to stroke is constant. The total width of a set of ports, on the other hand, will be proportional to the cylinder circumference and to the fraction of this circumference devoted to porting. Let us assume rectangular ports with height = $k_1 \times$ stroke. Let the aggregate width of a set of ports be $(k_2 k_3 \pi b)$ where k_2 is the fraction of the cylinder circumference occupied by the whole set and k_3 is the ratio port width to port-plus-bridge width. Then,

$$\frac{\text{port area}}{\text{piston area}} = \frac{A}{A_p} = \frac{(k_1 \text{ stroke})(k_2 k_3 \pi \text{ bore})}{\text{bore}^2\, \pi/4}$$

$$= 4k_1 k_2 k_3 \times \frac{\text{stroke}}{\text{bore}} \tag{7-24}$$

It is evident that, with piston-controlled ports, A/A_p tends to be proportional to the stroke-bore ratio.

For poppet valves, on the other hand, the ratio A/A_p is independent of either stroke or bore and depends only on detail design. It is difficult to secure a value of A/A_p higher than 0.40 with poppet valves.

Port Area/Piston Area. Equation 7-19 and Fig 7-10 show that in order to avoid high scavenging pressure ratios at high piston speeds flow coefficients must be large. For example, suppose that with $R_s = 1.2$, $r = 16$, $a = 1200$ ft/sec the pressure ratio p_i/p_e is to be limited to 1.5. From Fig 7-10, $R_s s/C(r-1)/r$ must not exceed 1950. Thus when

$$s = 15 \text{ ft/sec}, \qquad C \geqq 0.0087$$

$$s = 30 \text{ ft/sec}, \qquad C \geqq 0.0174$$

$$s = 45 \text{ ft/sec}, \qquad C \geqq 0.026$$

Obviously, with a given shape and timing of the ports, C increases with increasing port area. In order to secure a port area large enough for satisfactory values of C at high piston speeds, the port height may have to be large.

On the other hand, as the height of ports increases, an increasing portion of the piston stroke is given over to the scavenging and blowdown processes, with consequent reduction in stroke available for compression and expansion. Thus there is always a conflict between the need for a high flow coefficient and the requirement for minimizing the fraction of stroke devoted to porting.

Table 7-1

Two-Stroke Engine Porting

Engine	Type Fig 7-1	Bore in	Stroke in	Port Timing, degrees EO BBC	IO BBC	EC ABC	IC ABC	Max Port-Area Piston-Area in	ex	A_e/A_i	Source of Data	$\frac{A_r}{A_p}$	s	$\frac{A_r}{A_p \times S} \times 10^3$
MIT exp E ports	a	4.5	6	65	54	65	53	0.252	0.249 0.161 0.114	0.99 0.637 0.450	ref 7.19	0.178 0.136 0.104	—	—
MIT(CFR) Conf I	a	3.25	4.5	62	56	62	56	0.23	0.29	1.26	Fig 7-20	0.18	—	—
Diesel *	c	5.25	7.25	62	45	62	66	0.22	0.30	1.36	Mfg inst book	0.177	1450	0.122
Automotive Diesel	e	4.25	5	96 (86)	49	60 (50)	49	0.401	0.170	0.421	Mfg drawing	0.157	1500	0.105
Automotive Diesel	a	4.1	4.1	83	67	83	67	0.242	0.235	0.97	Mfg drawing	0.169	1500	0.113
Junkers * Jumo 207 aircraft	c	4.14	6.3	71	53	71	75	0.296	0.410	1.38	ref 7.32	0.240	2630	0.091
S. I. gas engine	e	16	16	75 (70)	45	40 (35)	45	0.290	0.231	0.80	Mfg drawing	0.181	853	0.212
Diesel engine	a	18	27	66	44	66	44	0.372	0.338	0.91	Mfg letter 9/21/54	0.250	1250	0.200
Diesel * engine	c	8.13	10	56	40	56	64	0.256	0.229	0.90	Mfg letter 9/21/54	0.171	1200	0.142

A_e = max exhaust-port area, in^2
A_i = max inlet-port area, in^2
A_r = max reduced port area = $1/\sqrt{1/A_i^2 + 1/A_e^2}$

A_p = piston area, in^2
s = piston speed, ft/min
S = stroke, in
* Timing based on exhaust shaft

Only a limited number of design data are available to indicate optimum port heights for various types of cylinder. Reference 7.19 showed that in a loop-scavenged cylinder of type *a* (Fig 7-1), running at 1800 ft/min piston speed, the optimum heights for the particular port configuration chosen were 0.15 × stroke for inlet and 0.24 × stroke for exhaust.

With port height fixed, it would appear desirable to use the largest inlet-port areas which are feasible without interfering with structural strength or satisfactory operation of the piston rings. Port areas used in a number of successful commercial engines are given in Table 7-1 and Fig 7-20.

Exhaust-Port to Inlet-Port Area Ratio. Figure 7-15 shows the results of tests on a loop-scavenged engine when exhaust-port area was varied while inlet-port area and port timing remained unchanged. The corresponding flow coefficients are shown in Fig 7-12.

The improvement in scavenging efficiency when C_eA_e/C_iA_i was reduced from 1.2 to 0.6 is marked except at the lowest piston speed (600 ft/min). Little further gain is obtained by reducing the ratio to 0.326, although the flow coefficient is markedly reduced.

The explanation for the trend shown in Fig 7-15 is that the cylinder pressure at the end of scavenging tends to build up toward the inlet pressure as exhaust ports are made smaller, and when the scavenging ratio is held constant by increasing p_i/p_e scavenging efficiency improves. On the other hand, it is evident from the discussion of flow through two orifices in series that with a given inlet-port area the flow coefficient will decrease as the area of the exhaust ports is reduced. Here, again, the requirements for high flow coefficient and high scavenging efficiency are in conflict.

Net indicated mean effective pressures corresponding to Fig 7-15 were measured as follows:

Loop-Scavenged Engine of Fig 7-15, R_s = 1.4

(Taylor et al, ref 7.23)

Configurations	$\frac{C_eA_e}{C_iA_i}$	Net imep *	
		s = 1350 ft/min	s = 750 ft/min
I	1.250	86	82
II	0.604	95	84
III	0.326	91	85

* Net imep = measured imep minus cmep computed from eq 7-21 with compressor efficiency 0.75.

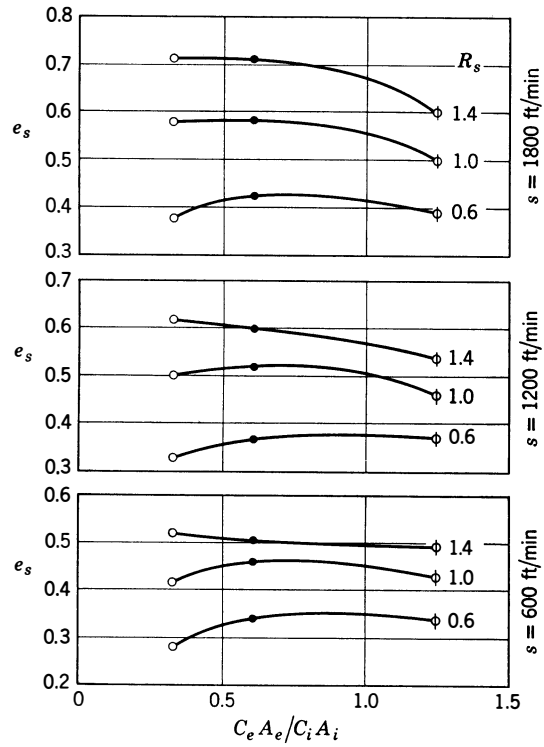

Fig 7-15. Effect of exhaust-port/inlet-port capacity, loop-scavenged cylinder.

Configuration	A_i/A_p	A_e/A_p	A_e/A_i	C_iA_i/A_p	C_eA_e/A_p	C_eA_e/C_iA_i	mean value of C (R_s = 1.0)
ϕ I	0.26	0.303	1.17	0.0384	0.048	1.25	0.026
• II	0.26	0.148	0.57	0.0384	0.023	0.604	0.022
○ III	0.26	0.074	0.28	0.0384	0.0125	0.326	0.016

(Taylor et al, ref 7.23)

It is evident that the gains in scavenging efficiency shown by Fig 7-15 when the area ratio is reduced from 1.25 to 0.6 are accompanied by significant gains in net imep. However, when the area ratio is reduced to 0.326 the reduced flow coefficient increases cmep enough to reduce net imep except at the lowest piston speed.

Similar gains made by reducing the area ratio from 1.29 to 0.601 in the poppet-valve cylinder of Fig 7-8 were also observed when sym-

metrical timing was used. (See ref 7.23.) No tests are yet available in which the area ratio was varied with unsymmetrical timing.

Port area ratios in practice (Fig 7-20 and Table 7-1) are seen to vary over an extremely wide range. It is unlikely that the optimum ratio has been used in each case.

Figure 7-16 shows port-area ratios and flow coefficients as a function of the circumferential angle occupied by the inlet ports for a loop-scavenged cylinder with fixed port heights. To attain an exhaust-to-inlet port ratio of 0.6, the inlet ports should occupy 67% of the cylinder circumference, under the assumptions used. This design will reduce the flow coefficient to 80% of the possible maximum value.

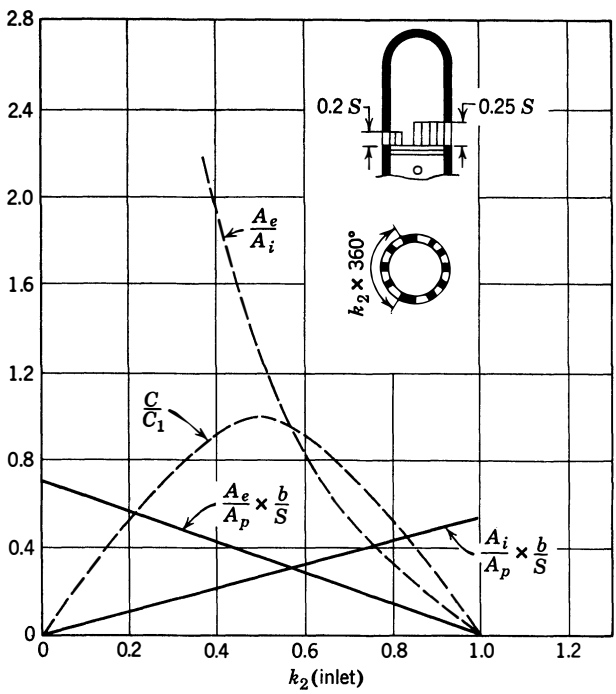

Fig 7-16. Effect of circumferential port distribution on loop-scavenged cylinder characteristics: k_2 = fraction of circumference occupied by inlet ports; $1 - k_2$ = fraction of circumference occupied by exhaust ports. Port width = 70% of available circumference. Height of ports 0.20 × stroke inlet and 0.25 × stroke exhaust; A_i = max inlet port area; A_e = max exhaust port area; A_p = piston area; C = cylinder flow coefficient calculated from Fig 7-14, assuming $p_e/p_i = 0.6$ and inlet-port flow capacity is 1.3 times exhaust-port flow capacity for same area; C_1 = flow coefficient when $k_2 = 0.5$.

Port-Timing. It is evident that the timing of piston-controlled ports is fixed by their axial dimensions, their location in the cylinder, and by the crank-rod ratio.

Loop-scavenged cylinders without auxiliary valves must have *symmetrical* timing; that is, both inlet and exhaust events must be evenly spaced from bottom center.

Experiments to determine best timing of loop-scavenged cylinders are reported in refs 7.10–7.23. When studying this work, it should be remembered that the results will depend to a considerable extent on the detail design of the porting.

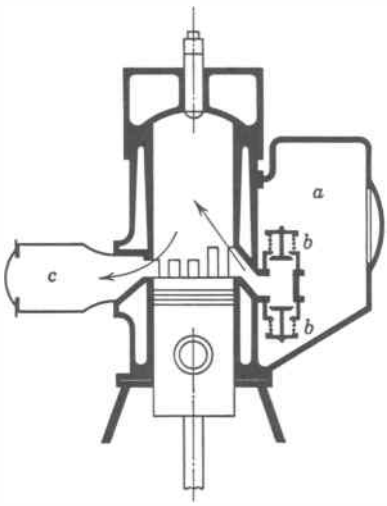

Fig 7-17. Loop-scavenged cylinder with nonreturn valves between inlet receiver and inlet ports: a = inlet receiver; b = nonreturn valves; c = exhaust receiver. Inlet ports are higher than exhaust ports. One-way valve prevents inlet opening until end of blowdown. Inlet ports close later than exhaust ports.

Because the exhaust ports must always open *before* the inlet ports open, the disadvantage of symmetrical timing is that the exhaust ports must also close *after* the inlet ports close. With such timing, there may be some escape of fresh mixture to the exhaust system which could be avoided if the exhaust ports closed earlier. Furthermore, if the exhaust ports close first, there is a better chance for the cylinder pressure to build up to a value higher than the exhaust pressure during the subsequent period before the inlet ports close.

Unsymmetrical timing can be achieved with loop-scavenged cylinders either by making the inlet ports higher than the exhaust ports and inserting nonreturn valves in the inlet passage (Fig 7-17) or by using a mechanically operated auxiliary valve in the exhaust port (Fig 7-1a′).

Figure 7-18 shows light-spring p-θ diagrams taken on a reverse-loop type of cylinder with and without an auxiliary exhaust valve. The increase in cylinder pressure at port closing when the auxiliary valve is used is quite pronounced (21%). The increase in retained air may have been less, however, if the exhaust gases were not so well purged with the earlier exhaust closing.

It is important to note that this experiment was made at a modest piston speed (1100 ft/min). At much higher piston speeds the advantage of the auxiliary valve will decrease because of the shorter period of time between exhaust and inlet closing.

Figure 7-19 shows the effects of unsymmetrical timing with a poppet-exhaust-valve cylinder. These data show that considerable gains in scavenging efficiency can be made by unsymmetrical timing, as compared to the best symmetrical timing. The net indicated mean effective pressures * at s = 1200 ft/min were as follows:

Configurations	Exhaust-Port Advance, Degrees	Net imep, psi	
		$R_s = 1.4$	$R_s = 1.0$
II	0	94	84
IV	7	96	81
V	14	102	90
VI	21	102	86

(Hagen and Koppernaes, ref 7.22)

In the tests covered by Fig 7-19 unsymmetrical timing was tried only with exhaust/inlet capacity ratio = 1.29. Tests with smaller values of this ratio would be of considerable interest.

Figure 7-20 shows three cases of unsymmetrical timing used in commercial practice. The *advance* of the exhaust ports (crank angle between mid-port opening of the exhaust and inlet ports) varies from 8 to 18° of crank travel. It is considered unlikely that the optimum ratio is used in every case.

Porting of Commercial Engines. Figure 7-20 and Table 7-1 show porting characteristics of a number of commercial two-stroke cylinders. When comparing these data it should be remembered that the bore-stroke ratio and the service requirements are not the same for each case. However, it seems safe to conclude that the wide differences revealed are due in large measure to uncertainty as to where the optimum design lies. Evidently further research is needed before two-stroke cylinder design can be completely rationalized.

The work recently done under the author's direction and summarized in Figs 7-7–7-15 and Fig 7-19 (see also refs 7.19–7.24) should be of assistance in connection with this problem.

* Net imep is taken as measured imep, less mep required to scavenge with a pump efficiency of 0.75.

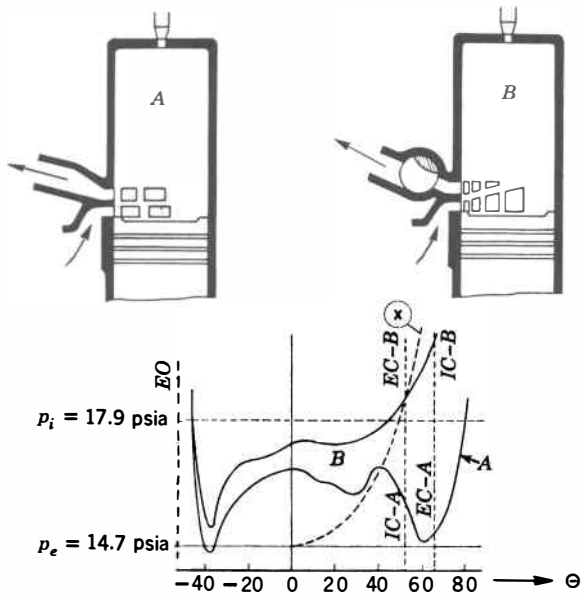

Fig 7-18. Effect of auxiliary exhaust valve.

Curve	Bore, in	Stroke, in	s, ft/min	r	R_s	Reference
A	20.4	26.5	1100	15	—	7.33
B	20.4	26.5	1100	15	—	7.33
x	adiabatic compression from p_e at bdc					

Reduced Port Area. This parameter has been used in estimating relative flow coefficients when measurements of C are not available.

If ideal incompressible flow (expression A-24) is assumed through two orifices in series (Fig 7-14), and if the velocity at each orifice entrance is low, the mass flow through the two orifices will be equal to the mass flow through a single orifice whose area is defined as follows:

$$A_r = \frac{1}{\sqrt{1/A_1^2 + 1/A_2^2}} \tag{7-25}$$

For convenience, A_r is called the *reduced area.*

In two-stroke engines A_r can be computed for each crank angle, and a curve of A_r can be plotted against crank angle, as in Fig 7-20.

The shaded areas of Fig 7-20 show reduced port area divided by piston area, which is designated by the symbol Λ. With a given design of ports

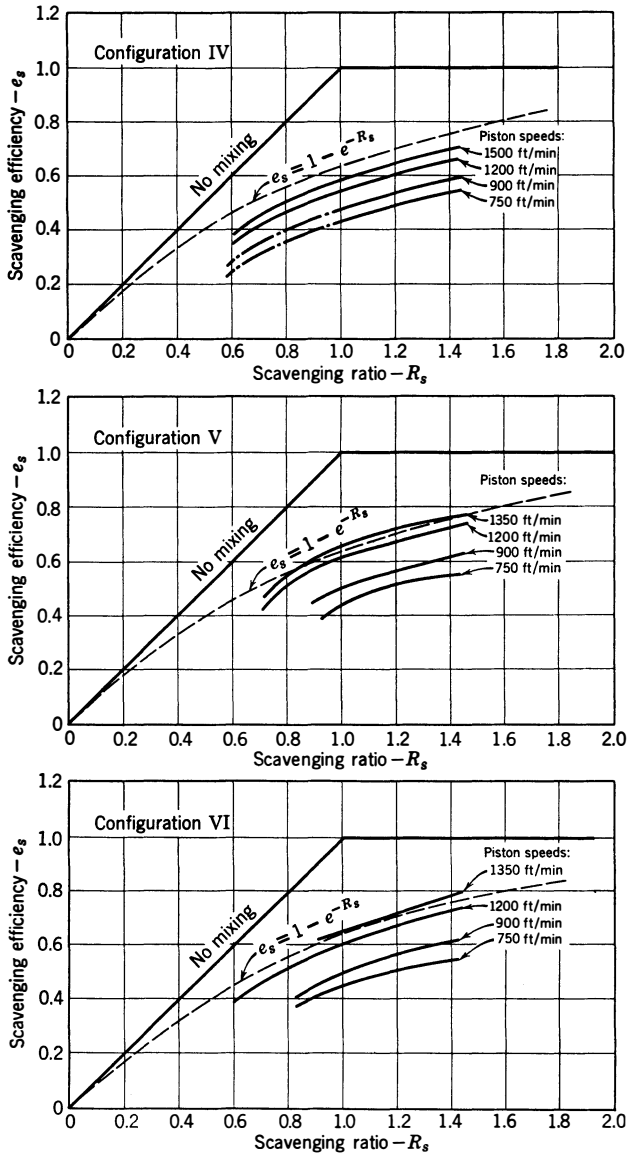

Fig 7-19. Effect of unsymmetrical timing: 3¼ x 4½ in engine; type (*e*), Fig 7-1; r = 5.8.

Configuration	Timing, Degrees IO	EO	IC	EC	C, $R_s = 1.2$	All Configurations
IV	57	95	57	81	0.023	$(CA)_i/A_p = 0.0386$
V	57	102	57	74	0.023	$(CA)_e/A_p = 0.050$
VI	57	109	57	67	0.0225	$(CA)_e/CA_i = 1.29$
						(Taylor et al, 7.23)

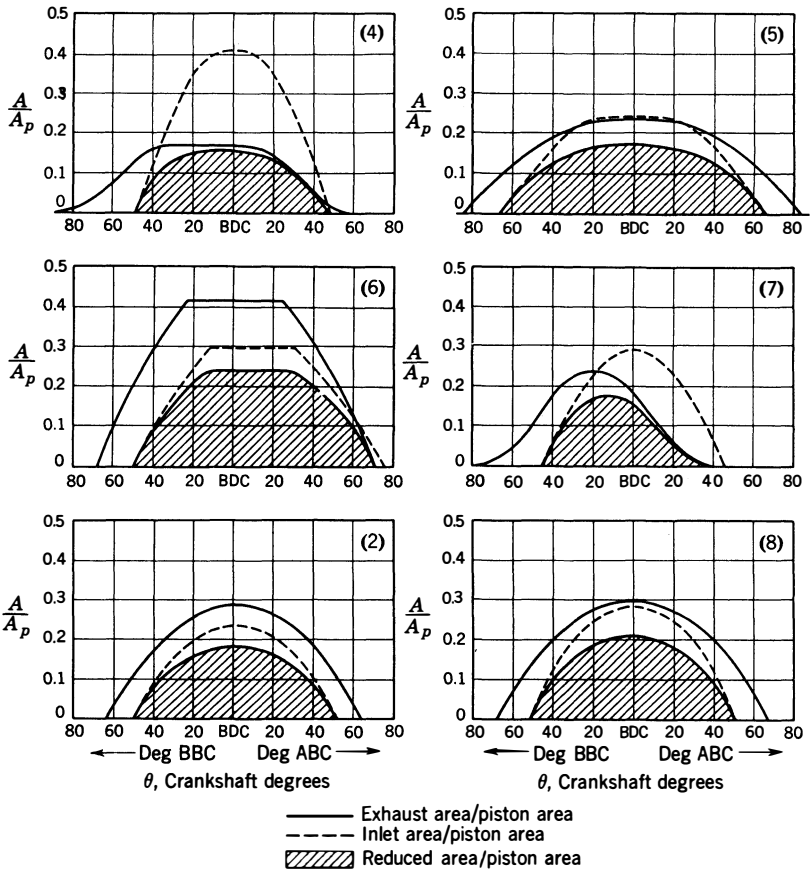

Fig 7-20. Porting of commercial engines.

Engine	Bore × Stroke, inches	Type	Λ	Rated piston speed,* ft/sec
(4) Automotive Diesel	4.25 × 5.00	Poppet valves	0.115	25
(5) Automotive Diesel	4.10 × 4.10	Loop-scav	0.168	25
(6) Junkers Aircraft Diesel	4.14 × 6.30	Opp Piston †	0.219	44
(7) Spark-ignited gas engine	16 × 16	Poppet valves	0.09	14
(2) CFR experimental	3.25 × 4.50	Loop-scav	0.131	30
(8) Spark-ignited gas engine	18 × 20	Loop-scav	0.156	14

* At continuous rating. † Valve diagram based on exhaust crankshaft. Λ is total reduced area/piston area. Reduced area is shaded in diagrams.

and at a given set of operating conditions, the flow coefficient C should be nearly proportional to Λ, and, therefore, this quantity is useful in the absence of measured values of C.

Another useful value employed in two-stroke practice is the value of A_r based on the *maximum* values of A_i and A_e.

Effect of Cylinder Size. It has already been shown (Chapter 6 and ref 6.2) that for comparable fluid-flow conditions cylinders of similar design should run at the same piston speed. Neglecting the probable small effects of Reynolds number (see Chapter 6), C should also be independent of size among cylinders of the same design. Equation 7-19 shows that when s/a_i is the same similar two-stroke cylinders will have the same scavenging ratio at the same inlet and exhaust conditions, regardless of size. The curves of e_s vs R_s should also be little affected by size, provided the design is unchanged. Thus the indicated mep of two-stroke cylinders at the same values of F, s/a_i, and p_e/p_i should be nearly independent of cylinder size, as in four-stroke cylinders. (See Chapter 6.)

CHOICE OF CYLINDER TYPE

Geometric considerations show that cylinder type has a very strong influence on the maximum feasible values of the ratio port area to piston area and also on the ratio exhaust-port area to inlet-port area. Table 7-2 shows limitations on these ratios for the various cylinder types shown in Fig 7-1. This table is based on typical values of k_1, k_2, and k_3, so that the figures are comparable.

It is evident from Table 7-2 that type (b) cylinder has the smallest potential ratios of port area to piston area. Thus this type is suitable only for long-stroke engines running at low piston speeds.

The port-area ratios of loop-scavenged cylinders depend on how much circumference is devoted to inlet and exhaust ports. Fig 7-16 illustrates these relationships for type (a) cylinders.

Port-area-to-piston-area ratios of the opposed-piston and U-cylinder engines are smaller than might at first be expected because each set of ports must serve two pistons.

The poppet-valve type of cylinder can have a large ratio of inlet port to piston area. For high-speed operation the exhaust-port area in this type may be limited by stress considerations. Poppet valves for two-stroke engines must open and close in about 120° of crank angle, whereas four-stroke engines allow over twice this value.

Table 7-2

Maximum Port-Area Ratios for Various Two-Stroke Cylinder Types (See Fig 7-16)

Cylinder Type (See Fig 7-1)	No Pistons Served	Inlet Ports: Fraction of Cylinder Circumference k_2	Inlet Ports: A/A_p	Inlet Ports: A/A_p S/b = 1.2	Exhaust Ports: Fraction of Cylinder Circumference k_2	Exhaust Ports: A/A_p	Exhaust Ports: A/A_p S/b = 1.2	$\frac{A_e}{A_i}$	$\frac{A_e}{A_i}$ in Practice
(*a*) and (*a'*) loop	1	0.6	$0.34S/b$	0.41	0.4	$0.28S/b$	0.34	0.83	0.97 1.21 0.91
(*b*) Reverse loop	1	0.6	$0.25S/b$	0.30	0.6	$0.21S/b$	0.25	0.83	
(*c*) and (*d*) o.p. and U	2	1.0	$0.28S/b$	0.34	1.0	$0.35S/b$	0.42	1.24	1.38 0.90 1.36
(*e*) Poppet valves	1	1.0	$0.56S/b$	0.67	*	0.36	0.36	0.54 $S/b = 1.2$	0.42 0.80
(*f*) Sleeve valve	1	1.0	$0.40S/b$	0.48	all	$0.50S/b$	0.60	1.25	—

Assumptions: Port area/piston area = $4k_1k_2k_3S/b$.

* Four poppet valves, each with i.d. 0.3 × bore. S = stroke, b = bore. For inlet ports $k_1 = 0.20$ except (*b*) where $k_1 = 0.15$. For exhaust ports $k_1 = 0.25$ except (*b*) where $k_1 = 0.125$. $k_3 = 0.7$ except for (*f*) where $k_3 = 0.5$.

Table 7-2 indicates that the sleeve-valve type could be made with the largest port areas for a given timing and stroke-bore ratio, but this type is mechanically complex and has not been used commercially.

Effect of Type on Scavenging Efficiency. It has often been claimed that the flow path in loop-scavenged engines tends to give more mixing

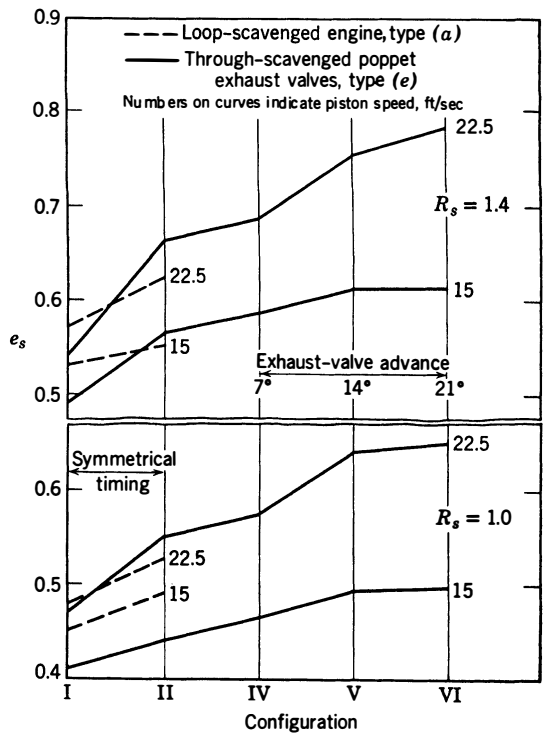

Fig 7-21. Effect of porting on scavenging efficiency.

Type	Configuration	$(CA)_i/A_p$	$(CA)_e/A_p$	Timing IO	EO	IC	EC	C, R_s = 1.2	r
(a)	I	0.0384	0.048	56	62	56	62	0.026	5.43
(e)	I	0.0386	0.050	57	88	57	88	0.023	5.8
(a)	II	0.0384	0.0231	56	62	56	62	0.024	5.43
(e)	II	0.0386	0.0233	57	80	57	80	0.016	5.8
(e)	IV	0.0386	0.050	57	95	57	81	0.023	5.8
(e)	V	0.0386	0.050	57	102	57	74	0.023	5.8
(e)	VI	0.0386	0.050	57	109	57	67	0.0225	5.8

3¼ x 4½ in cylinders (Taylor et al, ref 7.23)

and short-circuiting than that in through-scavenged types. Figure 7-21 shows the results of tests made under the author's direction with cylinders of these two types having the same effective port area, the same bore and stroke, and the same port timing (configurations I and II in the figure). Under these circumstances there is evidently little to choose between the two types as measured by their scavenging efficiency vs scavenging-ratio curves or by their comparative indicated mean pressure. The stroke-bore ratio used in these tests was 1.39. It is possible that opposed-piston engines, having much greater ratios of passage length to passage diameter than 1.39, might show an advantage in respect to mixing and short-circuiting.

Through-scavenged cylinders usually have unsymmetrical timing, whereas loop-scavenged cylinders are seldom so equipped. The results shown in Figs 7-19 and 7-21 would indicate that better performance, when it has been observed for through-scavenged cylinders, is due almost entirely to the use of unsymmetrical port timing. It would be interesting to add a rotary exhaust valve (type *a'*, Fig 7-1) to the loop-scavenged cylinder of Fig 7-21 and to determine whether, so equipped, it could equal the performance indicated by configurations V and VI of the poppet-valve cylinder.

Figure 7-12 indicates a lower flow coefficient for the through-scavenged cylinder than for the loop-scavenged cylinder, even when their port areas and steady-flow port coefficients were equal. Pending further testing on this point, it seems probable that this anomaly is a result of experimental error.

General Remarks on Cylinder Type

Loop Scavenging. More two-stroke engines use type (*a*) cylinders than any other type because of the simplicity of their mechanical design. Under comparable operating conditions this type gives lower mep and, therefore, lower specific output than those with unsymmetrical timing; but it may give *higher output per unit weight and bulk* because of the absence of the extra parts required to achieve unsymmetrical timing and because the absence of such parts may make higher piston speeds feasible.

Much work has been done to improve the scavenging efficiency of type (*a*) cylinders because of their inherent mechanical simplicity. Published work is indicated by refs 7.1—. Although much work remains to be done in this field, the following general relations seem to be established:

For type (*a*) cylinders it is necessary to direct the incoming air so that it follows an axial path close to the inlet side of the cylinder wall on its way toward the cylinder head. This objective can be accomplished either by a properly designed deflector on the piston or by inlet ports designed to direct the air toward the side of the cylinder away from the exhaust ports (see refs 7.13, 7.14, 7.19.)

With supercharging, and at high piston speeds, the specific output of loop-scavenged cylinders can be very high indeed, as evidenced by the published performance of the Napier Nomad experimental aircraft engine. (See ref 7.35 and Fig 13-10.)

Reverse-Loop Scavenging. Excellent scavenging efficiency is claimed for type (*b*) (ref 7.33), but few convincing measurements are presented in the literature. One obvious disadvantage of this type is the limitation on port area (Table 7-2). However, for long-stroke engines operating at low piston speeds, this arrangement has proved satisfactory and has been used for a long time by at least one prominent manufacturer of large Diesel engines, both with and without auxiliary exhaust valves. (See Fig 7-18.)

As we have seen, the addition of auxiliary valves gives the advantages of unsymmetrical timing to loop-scavenged cylinders. Whether this improvement justifies the added mechanical complication depends on particular circumstances. At present, the commercial use of these devices is confined to large cylinders running at low piston speeds.

Opposed-Piston Type. Type (*c*), Fig 7-1, can have both excellent scavenging efficiency and high flow coefficients, as indicated by Figs 7-9 and 7-13, thus leading toward high mean effective pressures. Here the problem is to decide whether the increased specific output outweighs the disadvantage of the required mechanical arrangement. In general, this type is very attractive when high specific output is important and is quite widely used in locomotive and submarine engines. It was the basis of the only successful Diesel aircraft engine (ref 7.32) which, incidentally, holds the world's record for high specific output of Diesel engines (see Fig 13-10, Junkers engine).

Type (*d*), Fig 7-1, is not well adapted for use with Diesel engines because the necessarily high compression ratio may involve a serious restriction to air flow at the junction of the two cylinder bores. Such arrangements have had a very limited use in small European spark-ignition engines.

The Poppet-Valve Type. Type (*e*), fig. 7-1, can show excellent performance, as suggested by the high scavenging efficiency curve in Fig 7-9.

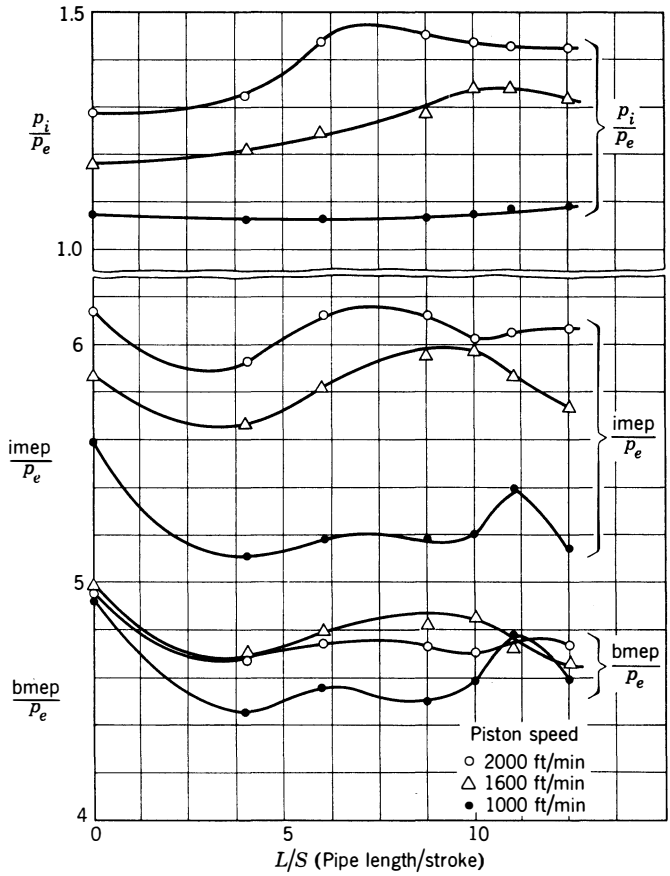

Fig 7-22. Effect of exhaust-pipe length on two-stroke, type (*a*) engine performance. MIT loop-scavenged cylinder, 4½ x 6 in: $r = 7$; $T_i = 618°R$; $T_c = 610°R$. Scavenged with gaseous fuel-air mixture: $F = 0.078$; $F_R = 1.175$; $p_e = 14.18$ psia; pipe diameter = 2 in = 0.444 × bore. Scavenging ratio = 0.90, held constant by adjusting inlet pressure. (From Cockshutt and Schwind, ref 7.53)

Here, again, the gain in specific output may not mean a gain in output per unit of bulk and weight, especially if speed is limited by the poppet-valve gear.

Type (*f*) seems to have no commercial application, probably on account of mechanical considerations.

Effect of Inlet and Exhaust-System Design. Figure 7-22 summarizes the results of tests in which exhaust-pipe length was varied over a wide range with a type (*a*) cylinder (Fig 7-1). Scavenging ratio was

held constant at 0.90. In this case zero exhaust pipe gave lower required scavenging pressure and higher power than any other pipe used.

Other research in this field (ref 7.50) has indicated that a favorable effect can be obtained by proper utilization of the pressure waves set up in a long exhaust pipe. Apparently this favorable effect occurs when the timing of the pressure waves in the exhaust pipe is such that exhaust pressure is low during the first part of the scavenging process and high at the end of the process. The high pressure acts effectively to close the exhaust port early and thus act as an auxiliary exhaust valve. This effect is the subject of a patented exhaust-pipe design.

In earlier tests made under the author's direction stronger effects of long exhaust pipes have been encountered. In one case exhaust pulsations were so strong that a speed could be found at which the engine would run without using the scavenging pump. It is obvious that in such cases flow through the cylinder is induced by the exhaust blowdown. On the other hand, several cases have been encountered in which the unfavorable effects of an exhaust pipe prevented satisfactory operation over a wide speed range. Kadenacy (refs 7.51, 7.52) claimed to have developed exhaust-pipe designs which would give a workable scavenging ratio over a considerable range of speed without the use of a scavenging pump. However, experimental data to prove this contention are lacking, and commercially available two-stroke engines are invariably supplied with scavenging pumps and in most cases with very short exhaust pipes.

Figure 7-23 shows how scavenging ratio varied with speed for an engine of type (*f*) with inlet and exhaust pipes of appreciable length. As in four-stroke engines, such curves are a function of the phase relation between the valve events, the piston motion, and the pressure waves set up in the pipes.

For two-stroke engines which have to run over a wide range of speed long pipes are not usually practicable, as might be inferred from Figs 7-22 and 7-23. The need to eliminate unfavorable dynamic effects accounts for the relatively short exhaust passages combined with large-diameter inlet and exhaust manifolds of many two-stroke engines. The diameter of these manifolds is often greater than the cylinder bore. Another solution of this problem is to use manifolds such that the exhaust from one cylinder acts as a "jet pump" with respect to other cylinders. (See ref 7.54.)

Engines equipped with centrifugal scavenging pumps will be more sensitive to the effect of pressure waves in the inlet and exhaust system

than those equipped with displacement pumps, since, in the latter case, the quantity of air flowing through the pump is not seriously affected by the pump discharge pressure.

The sensitivity of the two-stroke engine to dynamic effects and to exhaust back pressure is a considerable disadvantage, since the exhaust system is a part of the installation not always under the direct control of the engine manufacturer.

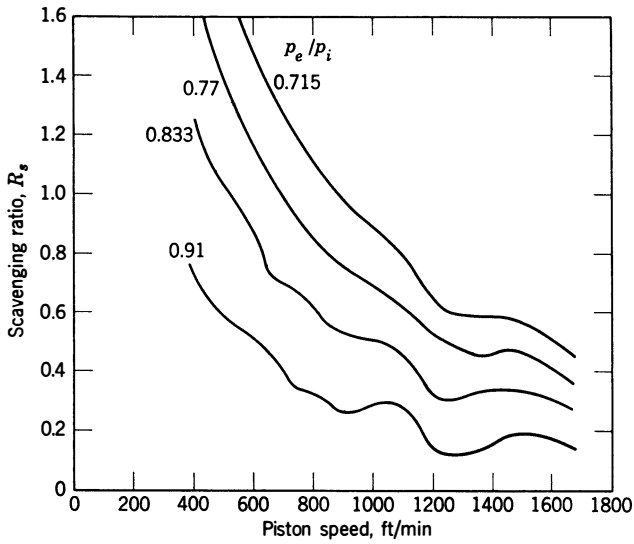

Fig 7-23. Scavenging ratio vs piston speed with inlet and exhaust pipes of lengths several times the bore: Type (f) cylinder, 4.74 x 5.0 in; r = 6.75. (Sloan Automotive Laboratories.)

SCAVENGING PUMPS

The performance of a two-stroke engine depends heavily on the characteristics of the compressor used as a scavenging pump. Figure 7-24 shows the important types in current use.

Displacement Pumps. In this class are included crankcase scavenging, piston, and Roots types. As shown in Chapter 10, the mass flow of air delivered by such pumps, or compressors, may be written

$$\dot{M}_a = N_c D_c \rho_1 e_c \tag{7-26}$$

where $\dot{M}_a$ = the mass of air delivered per unit time
N_c = the compressor revolutions per unit time

D_c = the compressor displacement per revolution
ρ_1 = the compressor inlet density (which is usually the atmospheric density)
e_c = the compressor volumetric efficiency

By combining eq 7-26 with eq 7-2, the scavenging ratio will be

$$R_s = \left(\frac{N_c}{N}\right)\left(\frac{D_c}{V_c}\right)\left(\frac{p_1}{p_e}\right)\left(\frac{T_i}{T_1}\right)e_c \qquad (7\text{-}27)$$

where V_c is the maximum cylinder volume.

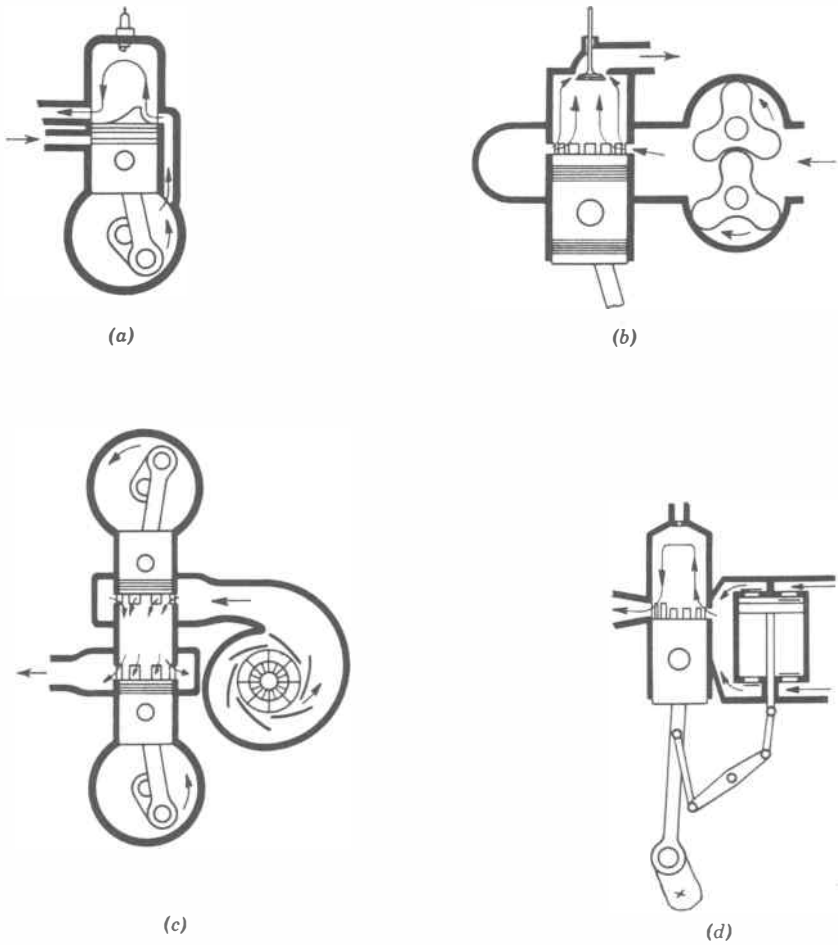

Fig 7-24. Scavenging-pump types: (*a*) crankcase; (*b*) Roots; (*c*) centrifugal; (*d*) piston.

For crankcase-scavenging $N_c/N = 1.0$ and $D_c/V_c = (r - 1/r)$, in which r is the compression ratio. For most two-stroke engine operation $p_1/p_e \cong 1.0$. Thus, for crankcase scavenging,

$$R_s \cong \left(\frac{r-1}{r}\right)\frac{T_i}{T_1}\,e_c \tag{7-28}$$

T_i/T_1 is the temperature ratio across the pump and is dependent on pressure ratio and pump efficiency. It is evident that the scavenging ratio of this type will always be considerably less than unity, especially since the volumetric efficiency of such pumps is usually low.

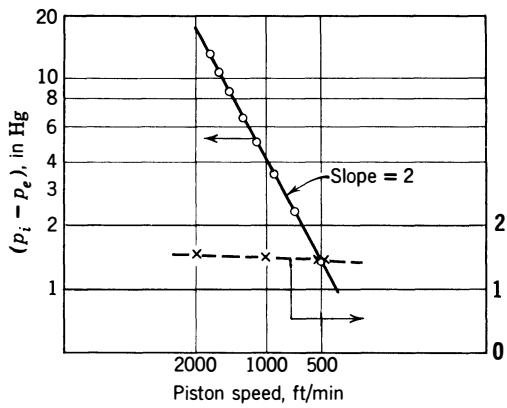

Fig 7-25. Scavenging ratio and pressure difference vs speed (log-log plot): GM-71 engine, type (*e*); 4.25 x 5.0 in; $r = 16$; Roots blower. (Shoemaker, ref 7.30)

Both eq 7-27 and eq 7-28 show that with a given engine and displacement pump R_s will be proportional to $[(T_i/T_1) \times e_c]$. As speed increases, T_i rises, due to the higher pressure ratio through the pump, whereas e_c usually falls off. With displacement pumps of good design, the result is that R_s remains nearly constant over the usual running range.

An important characteristic of displacement pumps is that their volumetric efficiency, and, therefore, the mass of air delivered per unit time, is not seriously reduced even by considerable increases in their outlet pressure. Thus scavenging ratio tends to remain constant even though ports may become partially clogged with deposits. Also, the addition of restrictions on the exhaust system, such as mufflers, will have

a small effect on scavenging ratio. Such restrictions, of course, increase the pressure ratio across the pump and the power required to scavenge.

Centrifugal Pumps. As explained in Chapter 10, with a centrifugal scavenging pump, the mass flow is heavily influenced by the engine and exhaust system resistance. Fortunately, when a centrifugal pump is geared to an engine the conditions are such that the pressure ratio varies very nearly as the rpm squared. Figure 7-25 shows that this relation is just what the engine requires for a constant scavenging ratio. Thus the centrifugal-type scavenging pump is very satisfactory, *provided* the resistance of the flow system is not sharply altered by carbon deposits in the ports, a restricted exhaust, or by long exhaust piping which may develop adverse pressure waves at certain speeds. More detailed discussion of compressor characteristics may be found in Chapter 10.

CHOICE OF SCAVENGING RATIO

When a displacement compressor is geared to a particular engine with a fixed ratio, the scavenging ratio is established within narrow limits by the size and design of the compressor and the ratio compressor-to-engine speed (see eq 7-27). With a centrifugal compressor, a similar situation exists as long as the flow resistance is not altered by such items as mufflers, air cleaners, long exhaust pipes, or carbon deposits in the ports. Thus scavenging ratio is a quantity which may be chosen, within limits, by the designer.

The value of the optimum scavenging ratio depends heavily on the engine flow coefficient and piston speed. Figure 7-26 shows specific output and fuel consumption of a two-stroke Diesel engine computed with realistic assumptions as to fuel-air ratio, indicated efficiency, scavenging efficiency, compressor efficiency, and friction. Two values of the flow coefficient are assumed, namely, 0.03, which is about the maximum found in current practice (see Fig 7-13), and 0.04, which might be attainable under favorable circumstances.

General conclusions to be drawn from Fig 7-26 are as follows:

1. A high flow coefficient becomes increasingly important as piston speed increases.
2. Fuel economy decreases rapidly as piston speed is increased above 1000 ft/min, with flow coefficients of 0.03 or less.

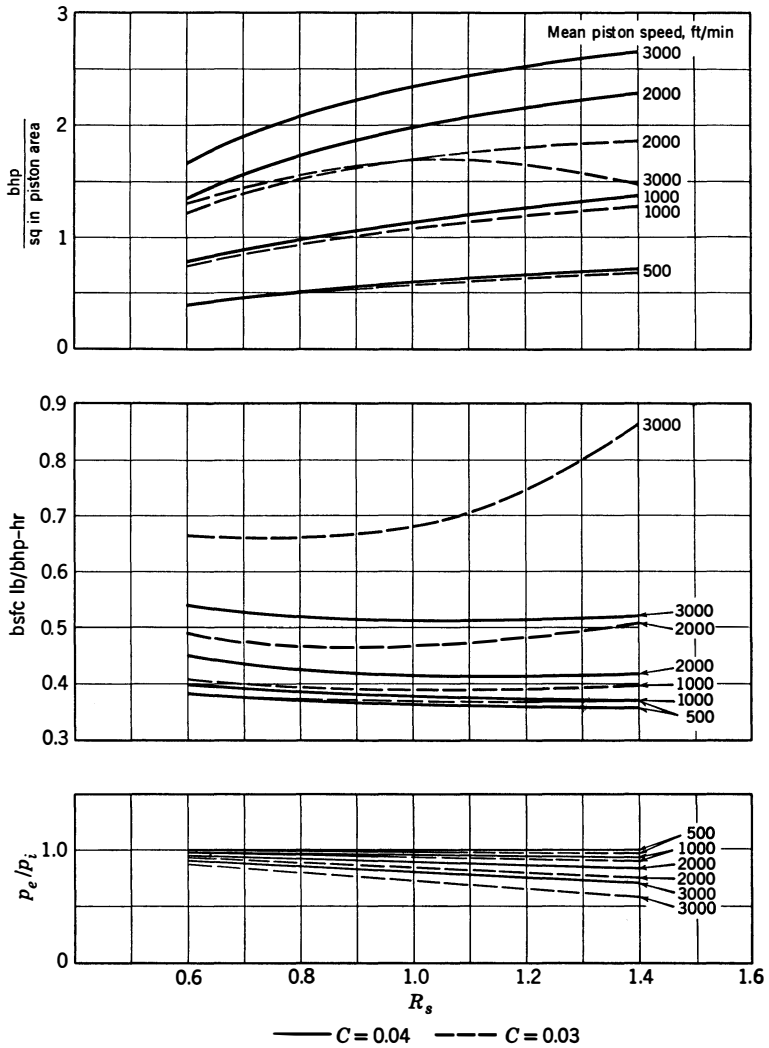

Fig 7-26. Performance of two-stroke Diesel engines: $r = 16$; $F = 0.0402$; $F/F_c = 0.06$; $Q_c = 18{,}500$ Btu/lbm; $T_a = 520°R$; $p_a = p_e = 14.7$ psia; $k = 1.4$; $\eta_p = 0.75$; $\eta_i = 0.43$; $e_s = 1 - e^{-R_s}$. Scavenging pump is driven from crankshaft.

For this particular example, the optimum scavenging ratios are evidently as follows:

Piston Speed	Optimum R_s, $C = 0.03$	Optimum R_s, $C = 0.04$
500	1.4 or greater	1.4 or greater
1000	1.4 or greater	1.4 or greater
2000	0.9 for economy	1.2 for economy
	1.4 for output	1.4 for output
3000	0.8 for economy	1.1 for economy
	1.0 for output	1.4 for output

In practice, scavenging ratios higher than 1.4 are seldom used. Many two-stroke engines are designed for scavenging ratios near 1.2.

The material in this and the subsequent chapters can be used to estimate the optimum scavenging ratio for any given engine, provided the flow coefficient is known. (See Illustrative Examples 12-12 and 13-5.)

SUPERCHARGING TWO-STROKE ENGINES

For a given cylinder design, Figs 7-7, 7-8, and 7-9 show that as scavenging ratio is increased beyond about 1.4 the gain in scavenging efficiency is small. We have also seen that the power required to scavenge increases rapidly with increasing scavenging ratio. Thus, if an attempt is made to *supercharge* a two-stroke engine by raising p_i/p_e above the value required for a normal scavenging ratio, fuel consumption increases and a point may be reached at which net power output reaches a peak. (See Fig 7-26.)

With fixed values of e_s vs R_s and a given value of C, the only feasible way to achieve large gains in output is by increasing *the exhaust pressure and the inlet pressure together.* If this is done in such a way that the pressure ratio p_e/p_i and the engine inlet temperature T_i are held constant, R_s will not vary but ρ_s will increase in direct proportion to p_e.

The necessity for increasing exhaust pressure immediately suggests the use of an exhaust-driven compressor to furnish the necessary increase in inlet pressure. Several arrangements are possible:

1. Retention of the engine-driven compressor and the addition of an exhaust-driven compressor to furnish air at increased pressure to the scavenging pump inlet. (See refs 13.06, 13.09.)

By this method, an existing two-stroke engine may be supercharged by the simple addition of a turbo-compressor in the manner customary for four-stroke engines.

2. The entire pressure rise from atmosphere to p_i can be assigned to a single compressor. If the exhaust blowdown is used to help drive the turbine (see Chapter 10), and if the efficiencies of turbine and compressor are high, it may be possible to use a free turbo-compressor unit, that is, one not geared to the engine. (See ref 13.08.) In many cases, however, the turbine has insufficient power to drive the compressor at all required speeds and loads, and the turbo-compressor unit has to be geared to the crankshaft. (See ref 13.22.) When this arrangement is used and turbine power exceeds compressor power the excess power is added to that from the engine.*

Two-stroke engines have been built with all of the above systems, and a number are in commercial operation. (See ref 13.00—.) The principal question remaining is concerned with the degree of supercharging which may be feasible in a given service without unduly sacrificing reliability and durability. For further discussion of supercharging and its relation to engine performance see Chapters 10 and 13.

ILLUSTRATIVE EXAMPLES

Example 7-1. Measurement of Scavenging Efficiency, imep Method. A single-cylinder two-stroke carbureted gasoline engine of $3\frac{1}{4}$-in bore and $4\frac{1}{2}$-in stroke with compression ratio 8 is running at 2500 rpm when the following measurements are made:

indicated power	23 hp
fuel-air ratio	0.08
T_i	620°R
p_e	14.8 psia

Compute the scavenging efficiency.

Solution: Displacement = 37 in^3, $V_c = 37(8)/7 = 42.3$ in^3. From Table 3-1, Q_c is 19,020 Btu/lbm, $F_c = 0.067$, $F_R = 0.08/0.067 = 1.2$.

From eq 7-3, if air is dry,

$$\rho_s = \frac{2.7(14.8)}{620}\left(\frac{1}{1 + 0.08(29/113)}\right) = 0.063 \text{ lbm/ft}^3$$

From Fig 4-5, fuel-air cycle efficiency is 0.36, actual efficiency estimated as 0.80(0.36) = 0.288, based on air retained in cylinder.

* In some cases, however, the turbo-compressor unit is geared to the engine by a "free-wheeling" coupling, so that when turbine power becomes sufficient, it drives the compressor faster than it would be driven with a fixed gear ratio.

From eq 7-8,

$$23 = \frac{778}{33{,}000} e_s \frac{2500(42.3)}{1728} (0.063)(0.08)(19{,}020)0.288$$

$$e_s = 0.57$$

Example 7-2. Scavenging Efficiency by Exhaust-Blowdown Analysis. A two-stroke Diesel engine of 5-in bore, 6-in stroke, $r = 15$, is running at 1800 rpm when the following measurements are made:

fuel flow	16 lbm/hr
inlet-air temperature	530°R
exhaust pressure	14.9 psia

An analysis of the exhaust-blowdown gases by means of a probe similar to that of Fig 7-5 yields the following results:

CO_2	7.5% by vol
O_2	9% by vol

Compute the scavenging efficiency.

Solution: From Fig 7-6,

$$F = 0.04, \qquad \dot{M}_a' = 16/0.04 = 400 \text{ lbm/hr}$$

$$V_c = 118(15)/14 = 126 \text{ in}^3, \qquad \rho_s = 2.7(14.9)/530 = 0.076$$

From eq 7-5,

$$e_s = \frac{(400)(1728)}{1800(126)60(0.076)} = 0.67$$

Example 7-3. Relation of Scavenging Efficiency to Mean Effective Pressure. Compute the mean effective pressure of the engine of example 7-2, assuming that the maximum pressure is limited to 70 times the inlet pressure.

Solution: From Fig 4-6 (1), the fuel-air cycle efficiency at $r = 16$, $F/F_c = 0.91$, and $p_m/p_i = 70$ is 0.49. F/F_c for this engine is $0.04/0.067 = 0.6$. Correcting for this ratio from Fig 4-6 (2) gives a fuel-air cycle efficiency of $0.49(0.54/0.49) = 0.54$. Estimated indicated efficiency is $0.85(0.54) = 0.46$. For light Diesel oil, $Q_c = 18{,}250$ Btu/lbm (Fig 3-1).

From eq 7-10,

$$\text{imep} = \tfrac{7}{14}\tfrac{7}{4}\tfrac{8}{4}(0.67)(0.076)(0.04)(18{,}250)0.46(\tfrac{15}{14}) = 99 \text{ psi}$$

Example 7-4. Scavenging Pressure, Scavenging Ratio, and Engine Flow Coefficient. If the engine of example 7-1 had a pressure of 17 psia at the inlet ports and the flow coefficient were 0.03, compute the air consumption and the scavenging ratio.

Solution: $p_e/p_i = 14.8/17 = 0.87$, $p_i/p_e = 1.15$. From Fig A-2 (Appendix 3), $\phi_1 = 0.397$ and $p_i/p_e(t_1) = 0.457$. $s = 2500(4.5)\frac{2}{12} = 1875$ ft/min $= 31$ ft/sec. From Table 6-2, for the mixture $F/F_c = 0.08/0.0675 = 1.2$, molecular weight $= 30.6$ and $a = 46.7\sqrt{620} = 1160$ ft/sec. Piston area $= 8.3/144 = 0.0577$ ft^2.

$$\rho_i = \frac{17(144)30.6}{1545(620)} = 0.0782 \text{ lbm/ft}^3$$

From eq 7-17,

$$\dot{M}_a = 0.0577(0.03)(1160)(60)(0\ 0782)0.397/1.08 = 3.46 \text{ lbm/min}$$

From eq 7-2,

$$R_s = 3.46/2500 \left(\frac{42.3}{1728}\right) 0.063 = 0.90$$

Another method of determining R_s would be by the use of Fig 7-13 as follows. At pressure ratio 1.15 and sound velocity 1260, the value of the parameter is 1160 ft/sec. Thus

$$R_s s/C \left(\frac{r-1}{r}\right) = 1160$$

$$R_s = 1160(\tfrac{1800}{60})(0.03)\tfrac{7}{8} = 0.90$$

Example 7-5. Engine Flow Coefficient. It is desired to operate a two-stroke Diesel engine at 2500 ft/min piston speed and not to exceed a scavenging pressure of 5 psi above atmospheric. Compression ratio is 17. It is estimated that the inlet temperature will be 60°F above atmospheric. If the scavenging ratio is to be 1.0, what flow coefficient is required?

Solution: If we assume that sea-level conditions are standard,

$$p_i = 14.7 + 5 = 19.7, \qquad T_i = 520 + 60 = 580°\text{R}, \qquad p_e/p_i = 0.747$$

$$\rho_i = 2.7(19.7)/580 = 0.0918, \qquad a_i = 49\sqrt{580} = 1180 \text{ ft/sec}$$

From Fig A-2,

$$\phi_1 = 0.512$$

From eq 7-19,

$$1.0 = 2C \left(\frac{16}{17}\right) \frac{1180(60)}{2500} \left(\frac{19.7}{14.7}\right) 0.512$$

$$C = 0.0273$$

Example 7-6. Compressor mep. Compute the compressor mean effective pressure required for the engine of example 7-5, with a compressor efficiency of 0.75.

Solution:

$$p_2/p_1 = 19.7/14.7 = 1.34, \qquad Y_c = 1.34^{0.285} - 1 = 0.087$$

$$\rho_s = 2.7(14.7)/580 = 0.0685$$

From eq 7-21,

$$\text{cmep} = \frac{778}{144}(1)(0.0685)(0.24)(580)\frac{0.087}{0.75}\left(\frac{17}{16}\right) = 6.35 \text{ psi}$$

Example 7-7. Compressor mep. Plot compressor mep required vs mean piston speed for a two-stroke engine with $C = 0.025$, under standard atmospheric conditions, with compressor efficiency of 0.75, $R_s = 1.2$, $r = 15$.

Solution:

$$\rho_s = 2.7(14.7)/T_i = 39.7/T_i$$

From eq 7-21,

$$\text{cmep} = \frac{778}{144}(1.2)(39.7)(0.24)(520)\left(\frac{15}{14}\right)\frac{Y_c}{T_i(0.75)} = 45{,}800\ Y_c/T_i$$

s ft/sec	$\frac{R_s s}{C(r/r-1)}$	p_i/p_e from Fig 7-13 at $a = 1200$	Y_c	$T_i = 520\times\left(1+\frac{Y_c}{\eta}\right)$	cmep psi
10	450	1.03	0.01	527	0.9
20	900	1.12	0.03	541	2.5
30	1350	1.23	0.06	562	4.9
40	1800	1.43	0.11	596	8.5
50	2250	1.66	0.15	624	11.1

a has been taken as constant at 1200 ft/sec, whereas it actually varies as $49\sqrt{T_i}$. However, the error involved is small.

Example 7-8. Cylinder Type. Compute the piston area required for 100 indicated horsepower at 1500 ft/min piston speed for the following Diesel cylinder types at standard sea-level conditions, scavenging ratio 1.2:

	Type (Fig. 7-1)	C (Fig 7-12)	e_s at $R_s = 1.2$ (Fig 7-9)
a	conventional loop scav.	0.028	0.65
b	loop scav. with ex. valve	0.020 (est)	0.67
c	opposed piston	0.030	0.70
e	poppet valve	0.024	0.75

For all cylinders $F' = 0.04$, $\eta' = 0.45$, $r = 16$, compressor efficiency 0.75.
Solution:

$$\frac{R_s s}{C(r/r-1)} = \frac{1.2(25)15}{16C} = \frac{28.1}{C}$$

From Fig 7-13, p_i/p_e is obtained and tabulated below (assuming $a = 1160$ ft/sec). Corresponding values of Y_c are tabulated below. $T_i = 520(1 + Y_c/0.75)$ and $\rho_s = 2.7(14.7)/T_i$. Both are tabulated.

$$F'Q_c\eta' = 0.04(18{,}250)0.45 = 329 \text{ Btu/lbm}$$

Using eq 7-8 and remembering that $NV_c = \frac{r}{r-1}A_p s/2$,

$$A_p = \frac{2(100)(33{,}000)(15)(144)}{778(16)(1500)(329)e_s\rho_s}\text{ in}^2 = 2.32/e_s\rho_s \quad \text{(see tabulation)}$$

Type	p_i/p_e	p_e/p_t	Y_c	T_i	ρ_s	A_p in^2
a	1.15	0.87	0.041	548	0.0724	49.4
b	1.22	0.82	0.058	560	0.0708	49.0
c	1.14	0.88	0.038	546	0.0725	45.7
e	1.16	0.86	0.043	550	0.0721	42.9

Example 7-9. Effect of Cylinder Type on Performance. If the engines of example 7-8 are to have 4 cylinders each, with stroke 1.2 × bore, compute the bore, stroke, and rpm of each engine.* If mechanical efficiency is 0.8 and the compressor is gear driven, compute the brake horsepower of each. Compute the specific fuel consumption at the given power.

Solution:

$$\text{bore}^2 = 4A_p/4\pi \quad \text{(see table)}$$

$$\text{stroke} = (1.2)\ \text{bore} \quad \text{(see table)}$$

$$\text{rpm} = 1500(12)/\text{stroke}\ (2) \quad \text{(see table)}$$

From eq 7-21,

$$\text{cmep} = \frac{778}{144}(1.2)(0.24)(520)\frac{Y_c\rho_s}{0.75} = 1080Y_c\rho_s$$

Taking the latter values from example 7-8, cmep is tabulated below. Compressor horsepower is $\dfrac{\text{cmep}\ (A_p)s}{2 \times 33{,}000}$ and this is tabulated below. The brake horsepower is 100 × 0.8 minus the compressor horsepower, as tabulated.

From eq 1-12,

$$\text{isfc} = \frac{2545}{18{,}020(0.45)} = 0.312$$

$$\text{bsfc} = \text{isfc}\ (100)/\text{bhp} \quad \text{(tabulated below)}$$

Type	Bore, in	Stroke, in	rpm	cmep	chp	bhp	bsfc
a	3.96	4.75	1895	3.2	3.6	76.4	0.409
b	3.95	4.74	1900	4.47	5.0	75.0	0.416
c	3.82	4.59	1960	2.98	3.1	77.9	0.401
e	3.70	4.45	2020	3.35	3.2	77.8	0.401

It may be noted that at this moderate piston speed the differences in size, output, and fuel economy between the four types is small, provided the assumptions are realistic, which they are believed to be.

* In the case of type (*c*) four cylinders is interpreted as four pistons.

Example 7-10. Scavenging-Pump Types. Compute the performance of engine (*a*) of example 7-9 if it were fitted with a crankcase type of scavenging pump whose volumetric efficiency was 0.7.

Solution: From eq 7-28, assuming atmospheric temperature is 520°R,

$$R_s \cong \frac{15}{16}\left(\frac{T_i}{520}\right) 0.7 = 0.00134T_i$$

Estimate T_i as 540°R, $a = 49\sqrt{540} = 1140$ ft/sec. Then $R_s = 0.00134(540) = 0.725$.

$$R_s s/C(r - 1/r) = 0.725(1500)/60(0.028)0.94 = 690$$

From Fig 7-13, $p_i/p_e = 1.04$. $Y_c = 0.0113$ and with compression efficiency 0.75,

$$T_i = 520\left(1 + \frac{0.0113}{0.75}\right) = 546°\text{R}$$

T_i was estimated at 540°R. Correcting for the new value,

$$R_s = 0.00134(546) = 0.732$$

At this point, Fig 7-9 indicates $e_s \cong 0.47$.

Indicated power of engine (*a*) in example 7-9 was 100 hp. Correcting this value for the new values of T_i and e_s gives

$$\rho_s = 0.0724\left(\tfrac{546}{548}\right) = 0.0723$$

$$\text{ihp} = 100\left(\frac{0.0724}{0.0723}\right)\frac{0.47}{0.65} = 72$$

$$\text{cmep} = \tfrac{778}{144}(0.724)(0.732)0.24(520)0.0113/0.75 = 0.54$$

$$\text{bhp} = 72(0.8) - 0.54 = 57 \text{ hp}$$

To equal the brake power of the type (*a*) engine with separate scavenging pump at $R_s = 1.2$, the piston area would have to be increased in the ratio $76.4/57 = 1.34$ and the bore with four cylinders to $3.96\sqrt{1.34} = 4.6$ in.

Heat Losses — eight

We have seen in Chapter 5 that the loss of heat from the working medium during the compression and expansion strokes accounts for reductions in power and efficiency up to about 10% of the power and efficiency of the equivalent fuel-air cycle.

In addition to the heat transferred from the working fluid during the compression and expansion strokes, a significant amount is transferred to the cylinder structure, thence to the cooling medium, during the exhaust process. Piston friction is also a source of a measurable amount of heat flow. Thus the total heat flow handled by the cooling system is much greater than the heat which flows from the gases during the working cycle.

It is the purpose of this chapter to discuss the question of heat flow in engines, both qualitatively and quantitatively, as it affects, and is affected by, operating conditions, cylinder design, and cooling-system capacity.

GENERAL CONSIDERATIONS

In the external-combustion power plant, examples of which are the steam engine, the steam turbine, and the closed-cycle gas turbine, heat must be added to the working fluid to bring it up to its maximum temperature. This being the case, at least a part of the surface of one heat exchanger must run at an even higher temperature. The physical

strength of the material of the heat exchanger at this temperature thus limits the maximum cyclic temperature.

In the internal-combustion power plant, on the other hand, exchange of heat is not an essential part of the cycle. For example, many internal-combustion turbines operate with an almost negligible amount of heat exchange. In this case parts of the combustion chamber and turbine must operate near the maximum cyclic temperature, and limitations on this temperature are imposed by strength considerations.

In the reciprocating internal-combustion engine, however, the temperature of the working fluid in the combustion chamber varies with time so rapidly that, with the required wall thicknesses, the surface temperature would never equal the maximum cyclic temperature even in the absence of external cooling. However, without cooling, the maximum cyclic temperature would still be limited by structural considerations, and therefore reciprocating internal-combustion engines are always provided with cooling systems to control the temperatures of the cylinders, pistons, valves, and associated parts.

Sources of Heat Loss. The cooling process involves flow of heat from the gases whenever gas temperature exceeds wall temperature. Another cause of heat flow to various engine parts is friction. As is well known, mechanical or fluid friction raises the temperature of the lubricant and the parts involved, with the result that heat flows to the cooler surrounding parts and from there to the coolant.

Heat losses, both direct and from friction, obviously reduce the output and efficiency compared to those of the corresponding fuel-air cycle. The study of engine heat losses is important not only from the point of view of efficiency but also for cooling-system design and, perhaps most important of all, for an understanding of the effect of heat flow on the operating temperatures of engine parts.

PROCESSES OF HEAT TRANSFER

For purposes of this discussion, the following definitions of the usual heat-transfer processes are used.*

Conduction is the process of heat transfer by molecular motion through solids and through fluids at rest. This is the mechanism by which heat flows through the engine structure.

Radiation is the process of heat transfer through space. It takes place not only in vacua but also through solids and fluids which are transparent

* For a more complete discussion of the mechanism of heat flow see ref 8.01.

to wavelengths in the visible and infrared range. A small fraction of the heat transferred to the cylinder walls from the hot gases flows by this process.

Convection is the process of heat transfer through fluids in motion and between a fluid and a solid surface in relative motion. This type of heat transfer involves conduction as well as bulk motion of the fluid.

Natural Convection is the term used when the fluid motion is caused by differences in density in a gravitational field.

Forced Convection is the term used to designate the process of heat transfer between a fluid and a solid surface in relative motion, when the motion is caused by forces other than gravity. *Most of the heat which flows between the working fluid and the engine parts and between the engine parts and the cooling fluid is transferred by this process.*

Heat Transfer by Forced Convection

Since forced convection accounts for the major part of the heat which flows from the gases to the engine parts, a somewhat detailed consideration of this process is advisable at this point.

Experiments in Forced Convection. Most of the quantitative work on heat transfer by forced convection has been done with fluids flowing steadily through tubular passages, arranged as shown in Fig 8-1. For the general case of a fluid flowing through such a tubular passage an equation of the following form has been used to correlate test results

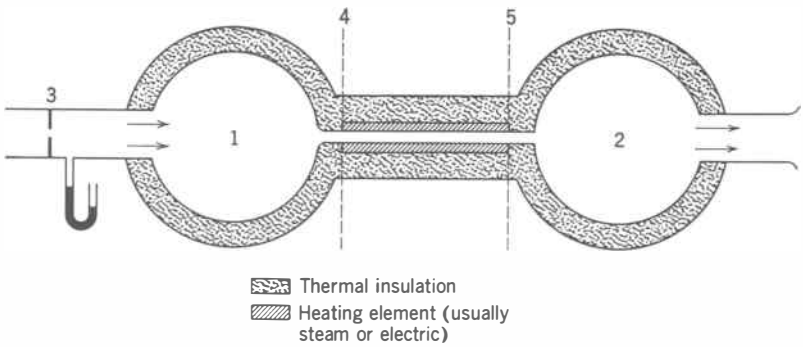

Fig 8-1. Typical apparatus for measuring heat flow between a surface and a moving fluid:

1 Inlet reservoir
2 Outlet reservoir
3 Orifice for measuring mass flow
4–5 Tubular test section

over a wide range of experiments:

$$\frac{hL}{k} = C\left(\frac{GL}{\mu g_0}\right)^n \left(\frac{C_p \mu g_0}{k}\right)^m \tag{8-1}$$

where h = the coefficient of heat transfer, that is, the heat flow per unit time per unit area, divided by a mean difference in temperature between the fluid and the surface of the passage
L = a characteristic dimension of the passage
k = the fluid coefficient of heat conductivity
G = the mass flow of gas per unit time, divided by the cross-sectional area of the test passage
μ = the fluid viscosity
C_p = the fluid specific heat at constant pressure
g_0 = the force-mass-acceleration constant
C, n, and m = dimensionless numbers which depend on the geometry of the flow system and on the regime of flow

The fraction $(GL/\mu g_0)$ is the *Reynolds number* of the flow system. Strictly speaking, a Reynolds number has significance only when it is

Table 8-1

Viscosity, Prandtl Number, and Thermal Conductivity of Water

(For similar characteristics for gases see Fig 8-12)

Temperature °F	Viscosity * μ lbf sec ft^{-2} $\times 10^6$	Viscosity * μg_o lbm sec^{-1} ft^{-1} $\times 10^4$	Thermal Conductivity † Btu/sec ft °F $\times 10^4$	Prandtl † No
250	4.0	1.28	1.18	1.10
200	6.4	2.06	1.12	1.86
180	7.25	2.34	1.11	2.13
160	8.36	2.70	1.08	2.50
140	9.82	3.16	1.06	3.00
120	11.70	3.77	1.03	3.70
100	14.30	4.60	1.01	4.55
80	18.00	5.80	0.98	5.90

* From International Critical Tables, Vol 5.
† From McAdams, ref 8.01.

applied to systems of similar shape, in which case the typical dimension L can be taken as any dimension of the system, usually a diameter of the flow passage. With similar systems, all other dimensions are proportional to L.

The fraction hL/k is often called the *Nusselt number*, since Nusselt

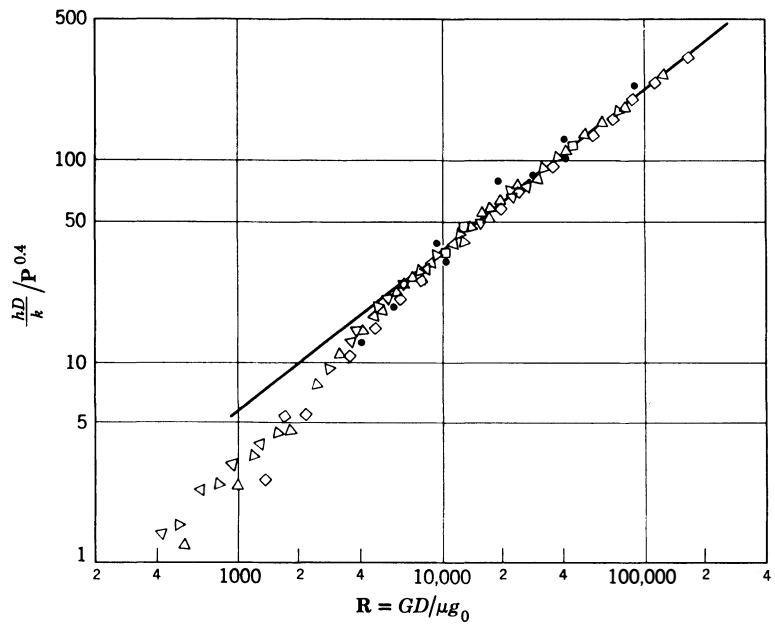

Fig 8-2. Nusselt number/Prandtl number vs Reynolds number for heated tubes. Various wall and gas temperatures: T_{sg} = 672 − 1749°R; T_g = 563 − 770°R; k, **P**, and μ are evaluated at T_{sg}; T_{sg} = tube surface temperature; T_g = mean fluid temperature (bulk); **P** = Prandtl number; μ = viscosity. All test points are for air, except black dots, which are for water. ——— $hD/k = 0.023(\mathbf{R})^{0.8}(\mathbf{P})^{0.4}$ (Warren and Loudermilk, ref 8.12)

(ref 8.20) was a pioneer in the use of this dimensionless parameter. Like the Reynolds number, it contains the characteristic dimension L and can be applied with rigor only to systems having similar geometry.

The fraction $(C_p\mu g_0/k)$ will be recognized as the *Prandtl number* of the fluid. For ordinary gases, this number is nearly constant and equal to 0.74. For liquids, the Prandtl number varies with composition and temperature. Values of this number together with other thermal characteristics for water are given in Table 8-1.

The practical value of expression 8-1 depends on the observed fact that the coefficient C and the exponents m and n tend to remain constant

over a wide range of experimental conditions, for a given shape of the flow passage, and provided proper average values are chosen for the fluid characteristics and the mean fluid and wall temperatures.

In practice, the surface temperature of the passage is measured at several points and averaged. The fluid temperature is measured in large insulated tanks at the entrance and exit of the test section (Fig 8-1), and the mean gas temperature is computed from these measurements. (See refs 8.1—.)

The best correlations are obtained when the fluid characteristics are taken at the mean surface temperature of the walls, or at a temperature which is half way between this temperature and the mean temperature of the entering and leaving fluid. (See ref 8.12.)

Figure 8-2 shows correlations of measurements of heat transfer coefficients in passages of uniform circular cross sections, based on eq 8-1 for air and for water. The typical dimension, L, was taken as the diameter of the passage. It is evident that at Reynolds numbers above 10,000 expression 8-1, with constant values of C, n, and m, represents the average results quite well for both fluids. The dispersion of points is normal even for the most careful heat-transfer measurements.

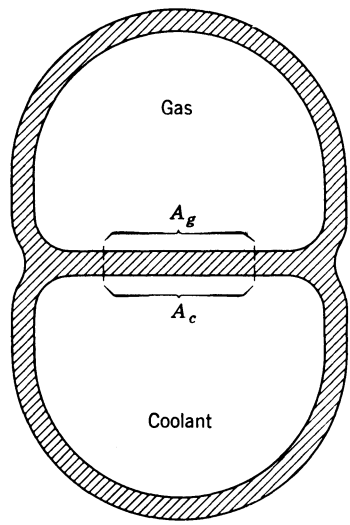

Fig 8-3. Heat exchange through a common wall section. Cross-sectional view, with flow normal to plane of drawing.

Heat Exchanger

As a next step in our analysis let us take two passages with a common wall, as illustrated in Fig 8-3. Let it be assumed that a hot gas flows through one passage and a cooler fluid, which may be a gas or a liquid, flows through the other.

Let the subscript g apply to the gas and the subscript c apply to the coolant or fluid in the other passage. Let it be assumed that we can identify a section of the common wall between the passages such that all the heat which passes into this section from its surface, the area A_g on the gas side, passes out from the area A_c on the coolant side. In other words, let it be assumed that the net flow of heat through the dashed-line boundaries of the wall section shown in Fig 8-3 is zero.

The following symbols are used in this analysis:

$\dot{Q}$ = the quantity of heat which flows, per unit time, through the surfaces A_g and A_c
T_c = the mean temperature of the coolant passing over the area in question
T_g = the mean temperature of the gas passing over the area in question
T_{sg} = the mean surface temperature of the area A_g
T_{sc} = the mean surface temperature of the area A_c
k_w = the conductivity coefficient of the material of the wall section (dimensions $Qt^{-1}L^{-1}$)
h = a heat-transfer coefficient, as already defined
t = the thickness of the wall between A_g and A_c

For the heat flow from the gas to the area A_g we can write

$$\dot{Q}/A_g = h_g(T_g - T_{sg}) \tag{8-2}$$

Heat flow through the wall will be by conduction. With a uniform wall thickness, if heat flow is normal to the surfaces, we can write

$$\dot{Q}/A_g = \frac{k_w}{t}(T_{sg} - T_{sc}) \tag{8-3}$$

Finally, for the heat flow from wall to coolant,

$$\dot{Q}/A_c = h_c(T_{sc} - T_c) \tag{8-4}$$

Equations 8-2, 8-3, and 8-4 are evidently three simultaneous equations which express the heat flow in question. They can be combined to yield several useful expressions in the consideration of heat flow in engines.

1. *Heat flow per unit area of inner surface:*

$$\frac{\dot{Q}}{A_g(T_g - T_c)} = \frac{1}{1/h_g + t/k_w + A_g/h_cA_c} \tag{8-5}$$

2. *Inner (hot) surface temperature:*

$$\frac{T_{sg} - T_c}{T_g - T_c} = \frac{t/k_w + A_g/h_cA_c}{1/h_g + t/k_w + A_g/h_cA_c} \tag{8-6}$$

3. *Temperature difference across the tube wall:*

$$\frac{T_{sg} - T_{sc}}{T_g - T_c} = \frac{t/k_w}{1/h_g + t/k_w + A_g/h_cA_c} \tag{8-7}$$

Having developed these relations * for the system shown in Fig 8-3, let us see how they can be used in connection with problems of heat flow in internal-combustion engines.

Heat Transfer in Engines

The process of heat-flow between the working fluid and the cooling medium of an engine can be approached by means of the assumption that it is analogous to the heat flow process in the heat-exchanger previously described. The differences in detail between the engine and the heat exchanger may be listed as follows:

1. An appreciable fraction of the heat transferred to the cylinder walls and exhaust system is by radiation rather than by conduction.
2. The rate of fluid flow on the gas side is unsteady.
3. The geometry of the flow system is irregular and changes periodically as the crankshaft rotates.
4. Gas temperatures vary widely with position in the system and change periodically with crankshaft position.
5. Conductivity of the walls varies with location and with the amount of oil, carbon, or other deposits on the inside and outside surfaces.
6. The surface temperatures on both the gas and coolant sides vary from point to point in an irregular manner, and there is a small, but appreciable, variation of these temperatures with time (or crank angle).
7. Some of the heat transferred to the cylinder barrel is due to piston friction.
8. Heat flows along the cylinder walls from hotter to cooler points.

These considerations would indicate that analysis of heat flow in engines is a problem of formidable proportions. Fortunately, by the use of the heat-exchanger relations, together with appropriate approximations, a method which gives useful results may be developed. First, however, it is necessary to discuss the above items in more detail.

Radiation. Under the conditions existing in an engine cylinder it would appear that radiation can play an appreciable part in the heat transfer process only during combustion and expansion, that is, when the gases are inflamed.

Investigations of the radiation from engine combustion flames (refs 8.2—) have shown that the emissivity of the flame varies, both in total

* Note that the assumption of uniform wall thickness and heat flow normal to the surfaces makes areas A_g and A_c equal. However, it is convenient to carry the ratio A_g/A_c in the above equations for later reference.

intensity and in wavelength distribution, with time, with fuel-air ratio, with fuel composition, and with the amount of detonation present. Measurements indicate that radiation may account for 1 to 5% of the heat loss in engines. Although the probable error in such measurements is considerable, it seems safe to conclude that radiation accounts for only a small portion of the heat transferred from the gases to the engine parts. If this is true, no serious quantitative error will be introduced if the heat transferred by radiation is assumed to be included in a hypothetical convection process.

Geometry. The *shape* of the gas and coolant flow systems in an engine is so complex that theory cannot predict in detail the flow patterns or temperature patterns involved. However, experience with steady-flow systems has shown that with proper choice of mean values systems with irregular but similar geometry can be correlated by means of equations of the type developed for tubular passages. This experience leads to the hope that for a given cylinder, or for a series of similar * cylinders, equations similar to those developed for tubular passages will be found useful.

Temperatures. The variation of temperature with time and position can be handled by defining each temperature as a *mean effective temperature*, that is, the equivalent steady, uniform temperature which would result in the observed rate of heat flow over the same surface area. Methods of estimating such temperatures are discussed later. For the present only the definition is important.

Heat of Friction. Some of the heat which flows from the cylinder barrel is caused by piston friction. In the heat-transfer equations which follow it is assumed that $\dot{Q}$ includes only heat transferred from the gases. Obviously, friction will not have an appreciable influence on the heat transferred to cylinder parts other than the barrel.

BASIC ENGINE HEAT-TRANSFER EQUATIONS

Bearing in mind the definitions and limitations already discussed, let us assume that relations 8-1–8-7 can be applied to the heat-flow process from the gases to the coolant of an internal-combustion engine in the following manner:

Let the area A_g represent a part of the cylinder-wall surface exposed to the hot gases, such as a portion of the inside surface of the cylinder head. Let A_c represent an area on the coolant side so chosen that it

* Similar cylinders have the same shape and use the same materials for corresponding parts. For a more complete discussion of similitude see Chapter 11.

transmits to the coolant only the heat received by A_g. Let t be the average length of the heat-flow path between A_g and A_c, and let k_w be the average coefficient of conductivity of the path. Let the typical length be the bore, b, and let the Prandtl number be a constant for both gases and coolant. The latter assumption is true for the gases and when air is used as the coolant. It is also true for a given liquid coolant over the small range of temperature used in a given practical case.

With these assumptions we can write an equation similar to 8-1:

$$\frac{hb}{k} = K\mathbf{R}^n \tag{8-7a}$$

The above relation applies to the gas side or coolant side of a given section of the cylinder. K in either case is $C\mathbf{P}^m$, where C is a dimensionless coefficient similar to C in eq 8-1 and $\mathbf{P}$ is the appropriate Prandtl number.

Equations corresponding to 8-5, 8-6 and 8-7 may then be written as follows:

1. *Heat flow per unit area of surface:*

$$\frac{\dot{Q}}{A_g(T_g - T_c)} = \frac{k_g/b}{1/(K\mathbf{R}^n)_g + tk_g/bk_w + [k_g/(kK\mathbf{R}^n)_c](A_g)/(A_c)} \tag{8-8}$$

2. *Inner (hot) surface temperature:*

$$\frac{T_{sg} - T_c}{T_g - T_c} = \frac{tk_g/bk_w + [k_g/(kK\mathbf{R}^n)_c](A_g)/(A_c)}{1/(K\mathbf{R}^n)_g + tk_g/bk_w + [k_g/(kK\mathbf{R}^n)_c](A_g)/(A_c)} \tag{8-9}$$

3. *Temperature difference across wall:*

$$\frac{T_{sg} - T_{sc}}{T_g - T_c} = \frac{tk_g/bk_w}{1/(K\mathbf{R}^n)_g + tk_g/bk_w + [k_g/(kK\mathbf{R}^n)_c](A_g)/(A_c)} \tag{8-10}$$

In these equations,

$\dot{Q}$ = the heat flowing per unit time through the areas, A_g and A_c
T_g = the mean effective gas temperature over the surface A_g
T_{sg} = the mean temperature of that surface
T_c = the mean coolant temperature over the surface A_c
T_{sc} = the mean temperature of that surface
$\mathbf{R}$ = the *local* Reynolds number, $(Gb/\mu g_0)$, G being measured at the flow cross section adjacent to the area in question, on the gas and coolant sides respectively
k_g = the gas coefficient of conductivity
k_c = the coolant coefficient of conductivity

It will be noted that, in order to obtain the fraction on the right side of the equality sign, in each case the numerator and denominator in the

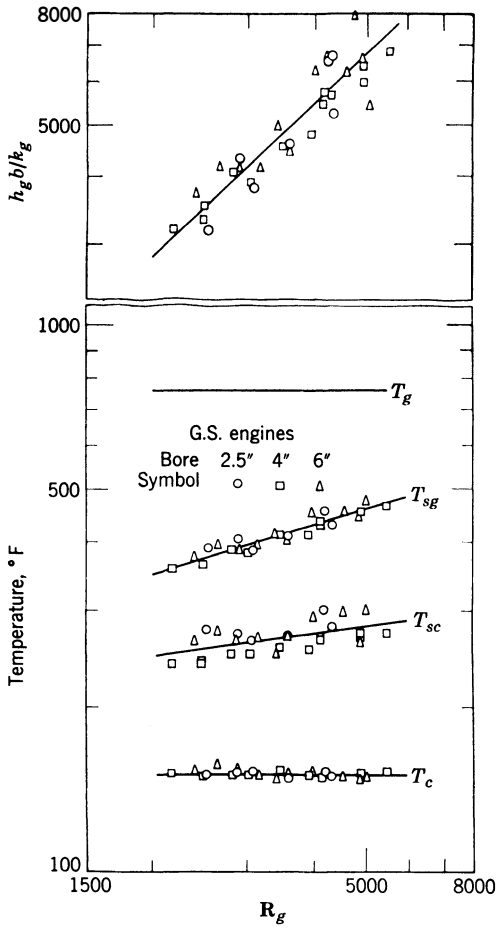

Fig 8-4. Gas-side heat transfer coefficient and cylinder-head surface temperatures vs gas-side Reynolds number for three similar engines. For description of engines see Fig 6-15. T_i = 634°R; F_R = 1.17; T_c = 630°R. (Toong et al., ref 8.47)

heat-exchanger equations, eqs 8-5, 8-6, and 8-7 have been multiplied by the fraction k_g/b.

Validity of Eqs 8-8 to 8-10. Figure 8-4 shows measured values of $h_g b/k_g$, T_{sg}, and T_{sc} plotted against gas-side Reynolds number for the three geometrically similar engines at MIT. (See refs 8.42–8.44.)

For these tests T_{sg} and T_{sc} were measured at corresponding points near the gas-side surface and coolant-side surface of the cylinder heads. T_g and T_c were held constant. h was the heat transferred per unit time to the cylinder-head coolant, divided by $A_p(T_g - T_{sg})$.

Coolant-side Reynolds and Prandtl numbers were constant and the same for all three engines. The cross-sectional area used in computing Reynolds numbers was the piston area, and the typical dimension was the bore, b.

For the similar engines t/b is constant. so that the only variables beside gas-side Reynolds number were h, T_{sg}, T_{sc}, and the bore.

Allowing for the unavoidable inaccuracies of heat-transfer measurements, Fig 8-4 shows satisfactory agreement with the theoretical relations.

Another support for the validity of eqs 8-8–8-10 is that the ratio of A_g to piston area obtained by substituting measured values of $\dot{Q}$, T_{sg}, and T_{sc} in these equations turned out to be nearly the same ($= 2.0$) for each test point shown in Fig 8-4. (See ref 8.43.)

Work by the NACA along similar lines also gives confirmation of the validity of the heat-exchanger equations as applied to internal-combustion engines. (See refs 8.3—.)

Another confirmation was obtained by Ku (ref 8.45) who exposed a water-cooled heat collector in the combustion chamber of an engine in operation. This work showed that the heat transfer coefficient between gases and heat-collector surface followed a relation similar to expression 8-1 with $n \cong 0.5$.

In all the foregoing work the values of n for both gas and coolant have been found to lie in the range of 0.5–0.9.

General Implications of Engine Heat-Transfer Equations

Having established their validity, but without attempting to assign particular values to the terms of eqs 8-8–8-10, we find it possible to use these relations to draw important conclusions regarding engine heat flow and wall temperatures. These equations are arranged to show effects on the three primary desiderata in engine heat-flow and cooling, namely:

1. *Heat loss per unit area*, $\dot{Q}/A_g$. From considerations of engine efficiency and cooling-system capacity, it is evidently desirable to hold this quantity to a minimum.

2. *Inner surface temperature*, T_{sg}. This temperature is limited by considerations of strength and durability of the material and, in the case of

the cylinder bore and valve stems, by the necessity of maintaining a bearing surface free from excessive friction and wear.

3. *Temperature difference between hot and cool surfaces,* $(T_{sg} - T_{sc})$. It may be shown (refs 8.5—) that with a given pattern of temperature distribution the stresses due to thermal expansion in a solid body of a given material are proportional to the *difference in temperature* between two points in the body.* This relation holds true for bodies of different size, provided their shape, material, and pattern of temperature distribution remain the same. By applying these fundamental relations to the case of an engine cylinder, we may assume, as a working approximation, that the pattern of temperature distribution is dependent chiefly on shape and material. If this is the case, for a given design using given materials, we may conclude that stresses due to thermal expansion will be proportional to $(T_{sg} - T_{sc})$. Thus it may not always be advisable to reduce hot-surface temperature by methods which, at the same time, increase the difference in temperature between the hot and cold surfaces.

Effect of Engine Output. As we have seen, maximum power output of an engine occurs when the rate of gas flow is maximum (maximum G_g) and when the fuel-air ratio is that for maximum power. In chapters 4 and 5 we have seen that the fuel-air ratio for maximum power is also nearly that which gives maximum combustion and expansion temperatures and therefore has the maximum probable value of T_g in the foregoing equations. From these considerations and from eqs 8-8–8-10 it is obvious that maximum heat flow, $\dot{Q}/A_g$, and maximum values of T_{sg} and $(T_{sg} - T_{sc})$ will generally occur at maximum engine output. Maximum output is, therefore, the condition of primary interest in any discussion of heat losses and cooling.

It would be desirable to establish maximum output from considerations other than cooling. With good design, this is usually possible, unless very high specific outputs are desired, as in supercharged engines or with very large cylinders. In such cases, in spite of careful design, temperatures may set a limit on the maximum output allowable.

Local Temperatures. Let us assume that a particular cylinder is being operated at given values of fuel-air ratio, coolant temperature, and mass flow of gas and coolant. Under these conditions, expressions 8-9 and 8-10 show that both T_{sg} and $(T_{sg} - T_{sc})$ will be high where local values of T_g, $\mathbf{R}_g$, and the fraction t/k_w are large. Locations in which

* For a given shape and temperature pattern thermal stress is a function of the elastic modulus, Poisson's ratio, coefficient of thermal expansion, and a typical temperature difference.

such conditions prevail are the following:

1. *A poppet exhaust valve.* T_g is high because much of the surface is exposed to the gases during exhaust, as well as during combustion and expansion. Gas velocity, and therefore local Reynolds number, is especially high during the exhaust process. The relative path from hot surface to coolant, t, is long, and k_w is low, both because of the material and configuration of the valve and because heat received by the valve must pass from one part to another at the valve seat and valve-stem surface.

It is evident that the poppet exhaust valve presents serious cooling difficulties. Fortunately, however, design and materials have been developed so that exhaust valves can be allowed to operate at surface temperatures up to 1400°F (1860°R). Figure 8-5 shows measured exhaust-valve temperature plotted against $\mathbf{R}_g$ for an aircraft engine.

2. *Exhaust-port bridges on two-stroke engines.* These operate with values of gas temperature and gas velocity similar to those of the poppet exhaust valve. However, they are limited to much lower surface temperatures because they form part of the piston bearing surface. Fortunately, for a given bore the path length is smaller than in the case of the poppet exhaust valve. With liquid cooling, there is the possibility of circulating coolant through the bridges, but, with air cooling, exhaust-port bridges may present serious cooling problems unless cylinder size is kept small.

3. *Piston crown.* Unless the piston crown is directly cooled by a liquid, it is evident that the heat-flow path from the center of the crown to the nearest cooled surface (the outer cylinder wall surface) will be long and the effective value of t/k_w will be large.

4. *Spark-plug points.* These obviously have especially large values of t/k_w. On the other hand, they can be allowed to run very hot, the limiting temperature usually being that which causes pre-ignition.

Effect of Cylinder Size. Equations 8-8–8-10 and also Fig 8-4 indicate that when cylinders of similar design, but of different size, are run at the same gas and coolant temperatures and the same gas and coolant Reynolds numbers $\dot{Q}/A_g$ will be inversely proportional to the bore and temperatures at corresponding points will be the same. Under such conditions, gas flow and power output would be proportional to the bore, and heat loss per unit mass of gas would be the same for all sizes. Such operation would place a large handicap on big cylinders, since their weight and volume per unit of power output would increase as b^2.

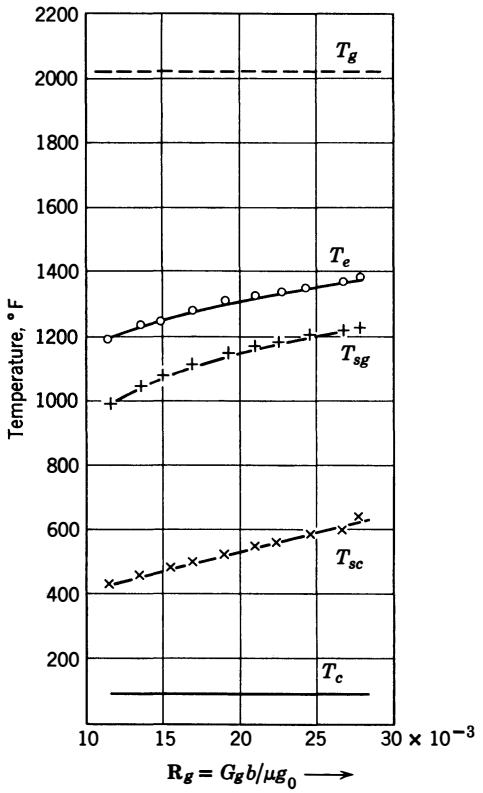

Fig 8-5. Exhaust-valve temperature vs gas-side Reynolds number: T_g = from Fig 8-9, curve (*c*); T_e = reading of thermocouple in exhaust pipe; T_{sg} = temperature of exhaust-valve face; T_{sc} = temperature of exhaust-valve guide at its mid-section; T_c = coolant temperature (80°F); 6⅛ x 7 in air-cooled cylinder; $F = 0.08$; 2200 rpm. (Sanders et al., ref 8.381)

In practice, for a given type of service, cylinders of different size tend to be operated at the same mean piston speed, the same inlet and exhaust pressures, and the same gas and coolant temperatures. (See Chapter 11.) Under these circumstances, G will be the same and the Reynolds number will be proportional to the bore. Since n is less than one, it is evident that under these circumstances $\dot{Q}/A_g$ decreases as bore increases, T_{sg} increases as bore increases, $T_{sg} - T_{sc}$ increases as bore increases. Figure 8-6 confirms these conclusions.

Cooling Problems with Large Cylinders. From the foregoing considerations it is evident that in practice large cylinder size could involve serious problems due to high surface temperatures and large tem-

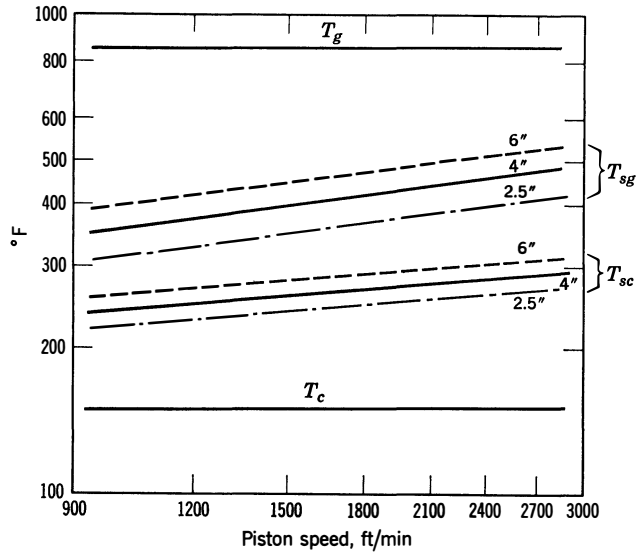

Fig 8-6. Cylinder-head surface temperatures of three similar engines vs piston speed: p_i = 14.0 psia; T_i = 150°F; p_e = 14.0 psia; F = 0.078; F/F_c = 1.175; bpsa; T_c = 150°F; h_c constant.

$(T_{sg} - T_{sc})$ at 1800 ft/min { 6-in cylinder, 180°F; 4-in cylinder, 140°F; 2½-in cylinder, 125°F

(Replotted from Fig 8-4)

perature differences. The effect of increased cylinder size is most quickly felt in the case of surfaces for which the heat path is relatively long. Examples are the exhaust valve and the piston crown, already mentioned.

To avoid excessively high temperatures and thermal stresses, the detail design of cylinders is changed as size increases. Figure 8-7 shows how structures such as the exhaust valve, cylinder head, and piston crown can be modified to insure an acceptable value of t/k_w while still retaining the necessary structural strength. The general method is to separate the structural components from the heat-transferring wall and therefore avoid the necessity of increasing the wall thickness in proportion to the bore.

Even with the use of all these expedients, however, when very large cylinders are used, as in some marine and stationary Diesel engines, G_g and T_g may have to be limited in order to avoid excessive temperatures. Such conditions are accomplished by limiting the mean piston speed

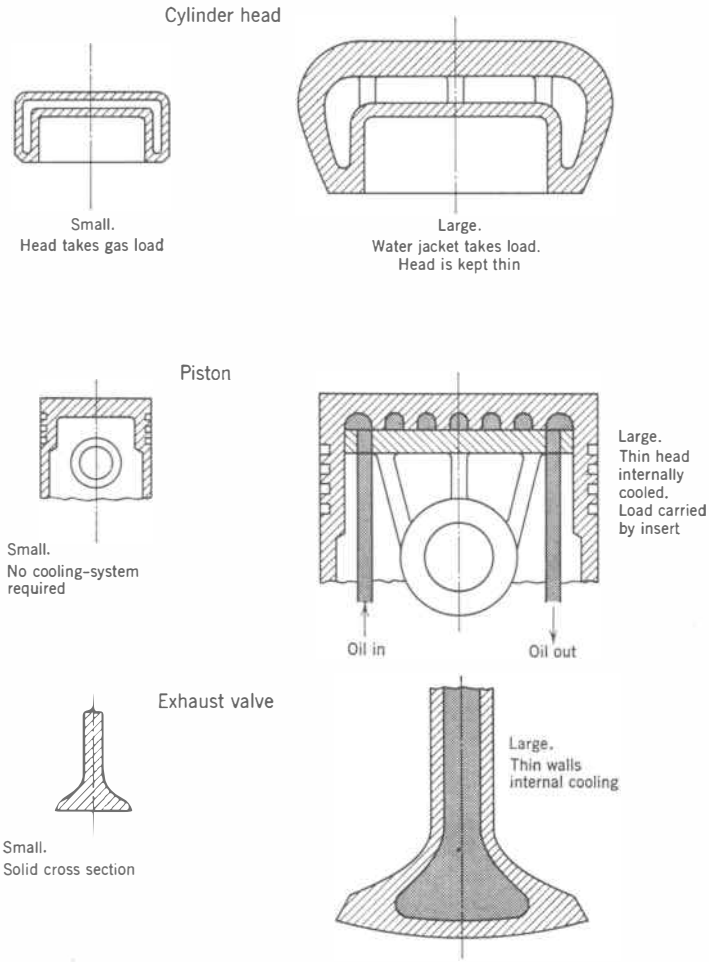

Fig 8-7. Changes in design to avoid high thermal stress as cylinder-bore increases.

(which limits G_g) and by using low fuel-air ratios to limit T_g. Thus eqs 8-8–8-10 show one important reason why the specific output * of engines with very large cylinders tends to be lower than that for engines with smaller cylinders designed for the same type of service. (See Chapter 11.)

Use of High Conductivity Materials. From the point of view of minimizing T_{sg} and $(T_{sg} - T_{sc})$, the use of materials of high conductivity, which thus increases the value of k_w, is attractive. This effect ac-

* Specific output is defined as power per unit piston area. See Chapter 11 for a full discussion.

counts for the popularity of aluminum as a piston material and as a cylinder-head material for air-cooled cylinders. However, it must not be assumed that aluminum should always be used, since it has disadvantages in respect to strength (especially at high temperatures), coefficient of expansion (three times that of iron or steel), and hardness.

Effect of Design Changes on Temperature and Temperature Difference. To give some idea of magnitudes applying to the foregoing discussion, Table 8-2 shows estimated effects on T_{sg} and on

Table 8-2

Effect of Changes in Heat-Flow Parameters on T_{sg}

Surface	Base Value	Lower T_c by 100°F	Decrease B 50%	Decrease t/bk_w 50%
		T_{sg} °F		
Exhaust valve	1354 *	1312	1348	1022
Iron cylinder head	478 †	408	468	366
Aluminum cylinder head	326 †	241	310	270

* T_{sg} when $T_g = 2230$, $T_c = 200$, $G_g^{0.5}b^{-0.5}t/k_w = 50$ } see eqs
† T_{sg} when $T_g = 1180$, $T_c = 180$, $G_g^{0.65}b^{-0.35}t/k_w = 5$ } 8-8–8-10
$B = (K\mathbf{R}^n A)_g/(K\mathbf{R}^n A)_c$

$(T_{sg} - T_{sc})$ of arbitrary changes in T_c, h_g/h_c, A_g/A_c, and t/k_w, for the case of a poppet exhaust valve, an iron cylinder head, and an aluminum cylinder head. Reduction in t/k_w is effective in each case. On the other hand, it is important to note that the exhaust-valve temperature is not at all sensitive to changes in the other variables. This characteristic will hold for other points at which the local values of t/k_w are large; this includes the spark-plug points and the crown of a piston not directly cooled by oil or water.

Quantitative Use of Engine Heat-Flow Equations

Evaluation of Mean Gas Temperature. Quantitative use of eqs 8-8–8-10 requires evaluation of the mean gas temperature, T_g. One

possibility of determining T_g is by operating an engine in such a way as to measure typical values of $\dot{Q}$ vs T_{sg}, under circumstances in which h_g and T_g are known or believed to remain constant, and then to solve eq 8-2 for T_g.

This method has been followed in tests made under the author's direction. T_{sg} was varied by varying the coolant temperature, in which case T_g and h_g should not change. The results are given graphically in Fig

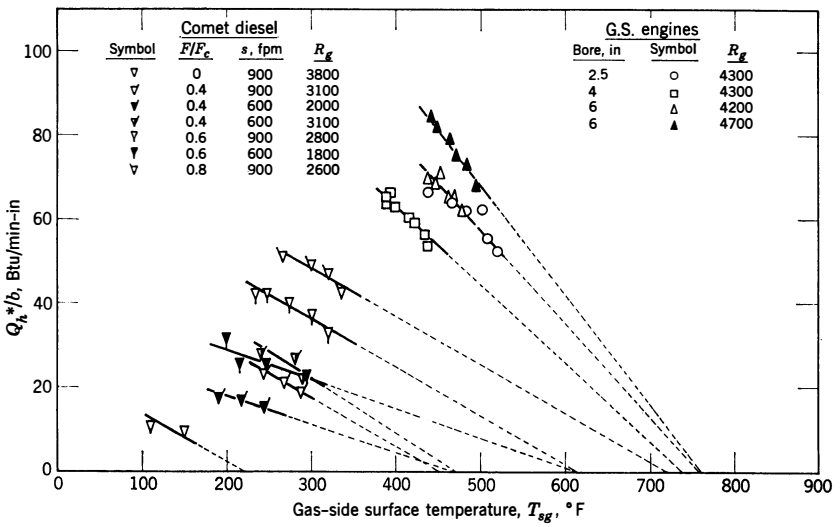

Fig 8-8. Method of evaluating T_g: Q_h^* is heat flow to cylinder-head coolant per unit time; b is cylinder bore. (Toong et al., ref 8.47)

8-8. The plotted points are based on measurements of $\dot{Q}$, from the cylinder head only, together with readings of a thermocouple embedded in the cylinder head near its inner surface. The solution for T_g for each group of points is given by the intercept of the dotted line on the horizontal axis. The main uncertainty of this method is whether the point chosen for measuring T_{sg} is typical for the portion of the cylinder in question, in this case the whole cylinder head.

The curves of Fig 8-9 have been determined by the method shown in Fig 8-8, or by methods similar in principle. (See references.) The shape of each curve is as expected from the variations of cyclic temperatures with fuel-air ratio discussed in Chapter 4. It is evident that the value of T_g obtained depends on where the measurement of T_{sg} is made. Correlations of engine heat-loss data which appear later in this chapter

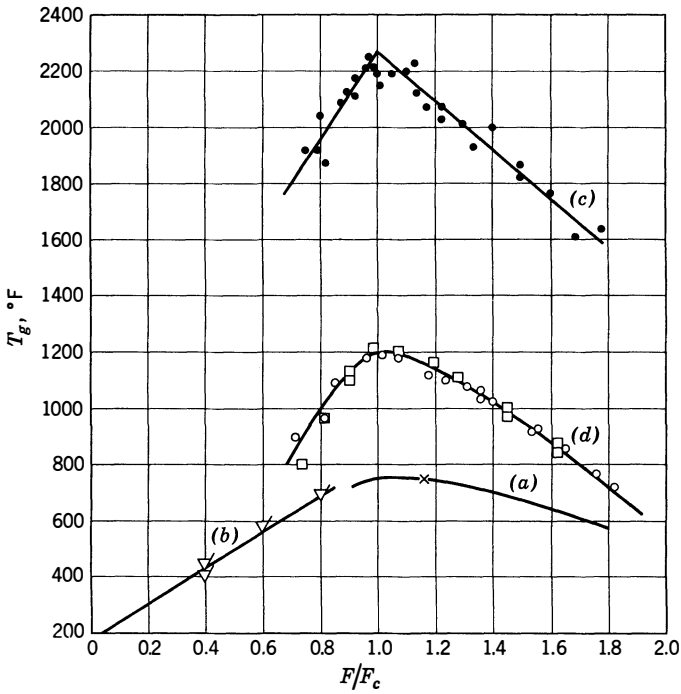

Fig 8-9. Mean effective gas temperatures vs fuel-air ratio: T_i = 80°F; P_e = 14.7 psia.

Curve	Engine	Part	Cooling	Reference
(*a*)	aircraft	cyl	L	8.36
(*b*)	Diesel	cyl	L	8.46
(*c*)	aircraft	ex valve	A	8.35
(*d*)	aircraft	head	A	8.34
×	SIM *	head	L	8.43

* Three MIT similar engines, ref 8.43. For other values of T_i, $T_g = T_{g80} + 0.35 (T_i - 80)$.

indicate that curves (*a*) and (*b*) give a good approximation of the mean effective gas temperature vs fuel-air ratio for the whole cylinder assembly for most types of engine with normal atmospheric exhaust pressure.

Correction of T_g for Inlet Temperature. It is apparent that T_g will vary with the inlet temperature, other things remaining the same. To correct the values of T_g given in Fig 8-9 to values of T_i, other than

80°F, ref 8.37 shows that the following relation may be used:

$$T_g = T_{g80} + 0.35(T_i - 80) \tag{8-11}$$

All temperatures are in °F. T_{g80} is the value of T_g from Fig 8-9.

Correction of T_g for Exhaust Pressure. Reference 8.36 shows that T_g increases somewhat with increasing exhaust pressure, other operating variables remaining the same. Figure 8-10 can be used when exhaust pressure is not equal to 1 atm.

Operating variables other than fuel-air ratio and exhaust pressure seem to have minor effects on T_g. The fuel-air-ratio effect follows from our knowledge of cycle temperatures, discussed in Chapter 4. The increasing value of T_g with increasing p_e is due to the higher average temperature of residual gases and exhaust gases as their expansion ratio after leaving the cylinder decreases. (See Fig 4-5, *i*3.)

Coolant Temperature. In practice, the coolant is circulated at a sufficiently rapid rate so that its rise in temperature as it passes through the engine is not large (20°F for liquid cooling and 50–100°F for air cooling are typical values at rated power). The arithmetic mean of the inlet and outlet temperatures is usually taken as the coolant temperature, T_c.

Coolant Prandtl Number. Work by the NACA (ref 8.37) shows that the value of m in eq 8-1 is about 0.35 for engines. (See Table 8-1 for values of the Prandtl number.)

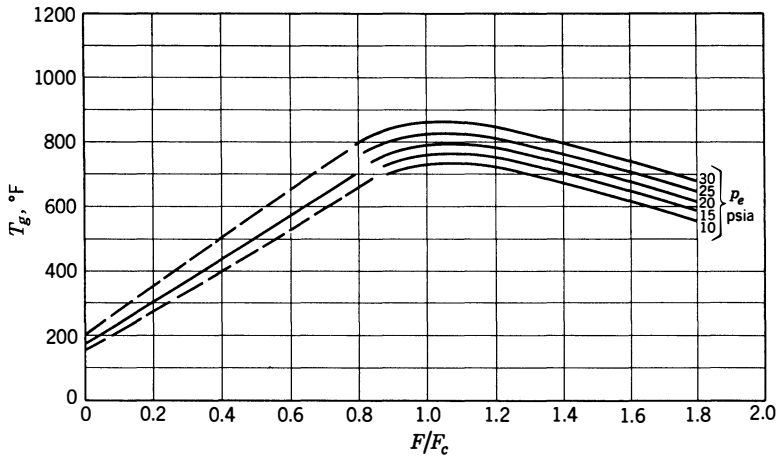

Fig 8-10. Mean gas temperature vs fuel-air ratio and exhaust pressure, $T_i = 80$°F. Solid lines from ref 8.36 and Fig 8-9, dashed lines estimated. For other values of T_i, $T_g = T_{g80} + 0.35\,(T_i - 80)$.

Surface Temperatures. As we have seen, temperatures near, but not at, the gas-side and coolant-side surfaces can be measured by means of thermocouples. To obtain an average over any considerable portion of the cylinder assembly requires a considerable number of such couples. In much of the work on engine cooling T_{sg} and T_{sc} have each been measured at a single point (as in the work illustrated by Figs 8-4 and 8-8). With this method, values of the coefficients and exponents in eqs 8-8–8-10 and of the heat transfer coefficients on the gas and coolant side will depend on the location of the points chosen for measuring the surface temperatures.

Surface Areas. In the case of the whole cylinder, or an isolated cylinder head, areas corresponding to A_g and A_c can be measured. Except for these two cases, accurate evaluation of A_g and A_c is not usually practicable. However, the ratio A_g/A_c can be computed from the equations when values of the other variables have been established. (See ref 8.43.)

Heat Conductivity and Heat-Path Length. These quantities are difficult to evaluate except for thin walls of considerable extent, such as a section of cylinder head or cylinder wall.

Heat Transfer Coefficient. Obviously, values of h_g and h_c determined from eqs 8-8–8-10 will be valid only within the limitations on evaluating the other terms in these equations. References 8.30–8.47 report evaluations based on particular methods of defining T_g and the surface temperatures.

Heat Flow. Quantitative confirmation of eq 8-8 is obviously limited to conditions under which $\dot{Q}$ can be measured. This measurement is possible for a whole cylinder, or engine, by taking measurements of all the heat lost (to coolant, oil, and atmosphere) and subtracting the heat of friction. Wherever cylinder heads are separately cooled, measurement of heat flow to the head coolant gives values of $\dot{Q}$ free from friction effects and from heat escaping to the oil. Data of this kind may be found in refs 8.20–8.491. Especially valuable in this respect is ref 8.47.

OVER-ALL HEAT-TRANSFER COEFFICIENT

In most practical cases data sufficient to evaluate the coefficients in eqs 8-8–8-10 are not available. However, when interest centers on the total quantity of heat which is given up by the gases, rather than on local values of heat flow and temperature, the simplified approach which follows has proved very useful.

Let us define an over-all engine heat-transfer coefficient by the following relation:

$$h_e = \frac{\dot{Q}}{A_p(T_g - T_c)} \tag{8-12}$$

Let it further be assumed that h_e can be expressed in a manner analogous to that of eq 8-1:

$$\frac{h_e b}{k_g} = \phi \left(\frac{Gb}{\mu g_0}\right)_g = \phi \mathbf{R}_g \tag{8-13}$$

In the above equations,

$\dot{Q}$ = heat lost from the gases per unit time
A_p = piston area (chosen, for convenience, as the reference area)
T_g = mean effective gas temperature
T_c = mean coolant temperature
μ = gas viscosity, measured at T_g
b = cylinder bore
k_g = gas conductivity measured at T_g
G = gas flow per unit time divided by the piston area
ϕR_g = a function of the gas-side Reynolds number

From eq 8-8 we see that $\dot{Q}$, and, therefore, h_e, will also be a function of t/k_w and the coolant-side Reynolds number. However, within the usual range of engine design and operation these variables appear to have only a limited influence.

Figure 8-11 shows $h_e b/k_g$ against $\mathbf{R}_g$ for a large number of engines, including many different types, over a wide range of piston speed, fuel-air ratio, and inlet density. Cylinder bores range from $2\frac{1}{2}$ to 28 in. Values for T_g were obtained from curves (*a*) and (*b*) of Fig 8-9. Viscosity and conductivity for the gases were taken as the value for air at temperature T_g. Values of T_g, μ, and k used are plotted in Fig 8-12 vs F/F_c.

Values of $\dot{Q}$ for Fig 8-11 were obtained from measurements of heat to the coolant, plus heat to the oil, minus heat of friction, wherever these data were available. In many cases only heat to the coolant was given. In these cases it was assumed that heat to the oil equaled the heat of friction, that is, $\dot{Q}$ was taken as the heat to the coolant only.

From Fig 8-11 it appears that the following expression represents the average quite well:

$$\frac{h_e b}{k_g} = 10.4 \left(\frac{Gb}{\mu g_0}\right)_g^{0.75} \tag{8-14}$$

The dispersal of the points about the average is little greater than for

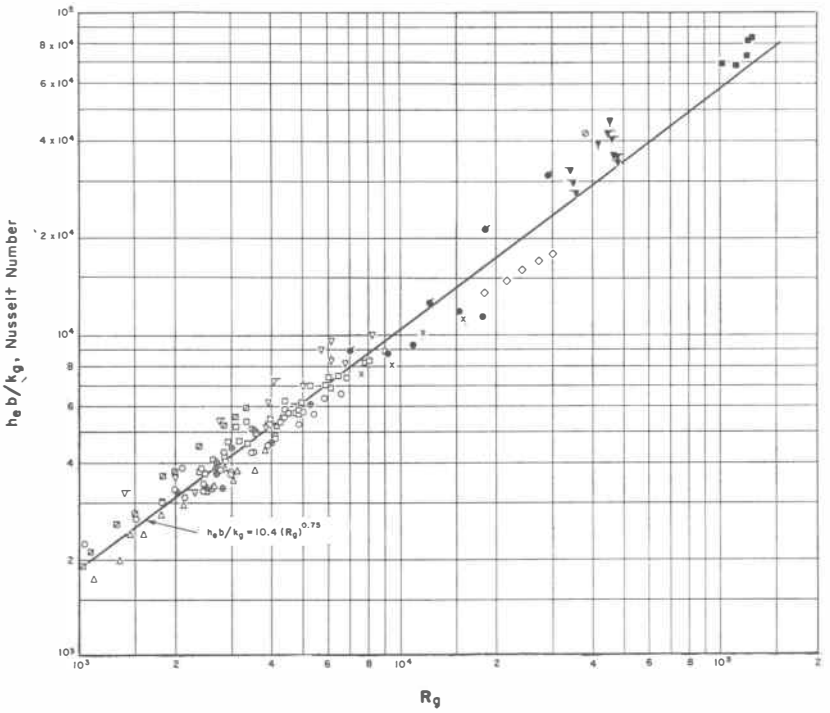

KEY TO SYMBOLS

SYMBOL	TYPE	MODEL	CYCLE	S I OR DIESEL	BORE IN.	STROKE IN.	SOURCE OF DATA
△	GS	2-1/2"	4	S I	2.5	3	Smith et al., M I T Thesis, 1952
○	GS	4"	4	S I	4.0	4.8	Botter and Consever, M I T Thesis, 1954
□	GS	6"	4	S I	6.0	7.2	
●	CFR	4 - Stroke	4	S I	3.25	4.5	Meyers and Goelzer, M I T Thesis, 1948
●	CFR	Loop Scav.	2	S I	3.25	4.5	
◇	Aircraft	Rolls Royce V-12	4	S I	5.4	6.0	Povolny et al, NACA TN 2069, April, 1950
▼	COM	Loop Scav.	2	D	6.25	9.0	Manufacturer's Curves
▼	COM	Loop Scav.	2	D	8.5	11.5	" "
▼	COM	OP	2	D	8.13	10.75	" "
▼	LOCO	OP	2	D	8.13	10.75	" "
◀	TRUCK	Pop. Valve	2	D	4.25	5.0	" "
⊠	CFR	Comet Head	4	D	3.25	4.5	Lundholm and Steingrimsson, M I T Thesis, 1954
■	MAR	Loop Scav.	2	D	28.3	47.3	Sulzer Tech. Review, No. 2, 1935
▽	AUTO	V-8	4	S I	3.56	3.6	Manufacturer's Curves
▽	AUTO	6 - Cyl.	4	S I	3.56	3.6	" "
▽	AUTO	V-8	4	S I	3.8	3.5	" "
▽	TRUCK	V-8	4	S I	3.5	3.1	" "
⊗	LOCO	12 - Cyl.	4	D	8.13	10	Manufacturer's Letter
x	Aircraft	Air Cooled	4	D	6.13	6.88	NACA TR-683

Fig 8-11. Engine over-all Nusselt number vs gas-side Reynolds number for commercial engines.

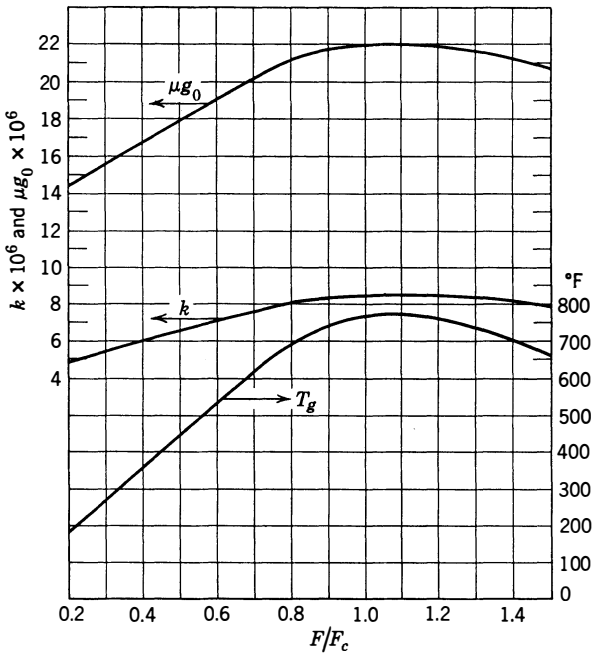

Fig 8-12. Mean effective gas temperature, viscosity, and conductivity vs fuel-air ratio. T_g plotted for T_i = 80°F (curve *a–b* Fig 8-9). For other values of T_i add $0.35(T_i - 80)$. k is in Btu/sec ft°F for air at T_g. μg_0 is in lbm/sec ft for air at T_g.

heat-transfer experiments with steady flow in tubes, when the work of different experimenters is included. (See refs 8.1—.) It is interesting to note that Fig 8-11 does not show a significant separation between two-stroke and four-stroke engines.

A combination of eqs 8-14 and 8-12 gives

$$\frac{\dot{Q}}{A_p} = 10.4 \frac{k_g}{b} (T_g - T_c) \mathbf{R}_g^{0.75} \tag{8-15}$$

Expression 8-14 makes possible a reasonably accurate prediction of engine heat loss whenever fuel-air ratio and mass flow are known or can be estimated.

For a given engine operating at a given fuel-air ratio eq 8-15 can be written

$$\frac{\dot{Q}}{A_p} = K_e G_g^{0.75} (T_g - T_c) \tag{8-16}$$

where $K_e = (10.4 k_g/b)(b/\mu g_0)^{0.75}$.

Ratio of Heat Loss to Heat of Combustion. This ratio is of interest in heat-balance computations. The heat of combustion of the fuel per unit piston area per unit time can be expressed as

$$\dot{Q}_f/A_p = G_g Q_c \left(\frac{F}{1+F}\right) \tag{8-17}$$

where F is the fuel-air ratio and Q_c is the heat of combustion per unit mass fuel.

Dividing expression 8-16 by 8-17 gives

$$\frac{\dot{Q}}{\dot{Q}_f} = \frac{K_e G_g^{-0.25}(T_g - T_c)(1+F)}{FQ_c} \tag{8-18}$$

Ratio of Heat Loss to Power. From the definition of efficiency, power is equal to $J\dot{Q}_f \eta$.

Therefore,

$$\frac{J\dot{Q}}{P} = \frac{\dot{Q}}{\dot{Q}_f \eta} \tag{8-19}$$

The power, P, and the efficiency, η, may be indicated or brake values, as desired. Generally, indicated values of $J\dot{Q}/P$ are given wherever possible, since the indicated efficiency tends to remain constant over wide ranges of engine operation. Brake values can be computed by dividing by the mechanical efficiency. The brake values are of considerable practical importance because, by their use, the conditions for minimum heat loss for a given power output can be determined.

EFFECT OF OPERATING VARIABLES ON HEAT LOSS TO COOLANT

The heat dissipated by an engine can be expressed as follows:

$$\dot{Q}_t = \dot{Q} + P_m/J \tag{8-20}$$

$$= \dot{Q}_j + \dot{Q}_o + \dot{Q}_r \tag{8-21}$$

where $\dot{Q}_t$ = total heat dissipated per unit time
$\dot{Q}$ = heat lost by the gases
P_m = power lost in mechanical friction
$\dot{Q}_j$ = heat to the coolant radiator
$\dot{Q}_o$ = heat to the oil radiator (if any)
$\dot{Q}_r$ = heat escaping directly from the engine, sometimes called "radiation"

The distribution of the total heat flow between jacket cooling, oil cooling, and direct cooling varies with design and with the arrangement of the cooling system. When engines have no separate oil radiator $\dot{Q}_o$ is zero, and both $\dot{Q}_j$ and $\dot{Q}_r$ are larger than they would be if a separate oil radiator were installed. In general, most small gasoline engines use no oil radiator, and the oil is cooled partly by the jacket water (or air) and partly by direct loss from the engine.

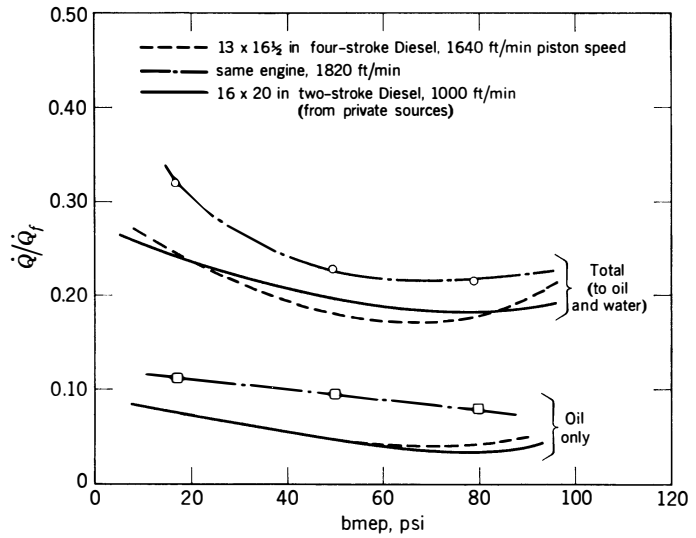

Fig 8-13. Heat loss of two Diesel engines.

In gasoline engines of high specific output, such as aircraft and tank engines, separate oil coolers are always used. This practice is also general for Diesel engines in which the pistons are cooled by special oil circulation or spray systems.

Figure 8-13 shows $\dot{Q}_j$ and $\dot{Q}_o$ for a Diesel engine with oil cooling of the piston.

The curves presented to show the effect of engine variables on heat loss are in most cases based on measurements of $\dot{Q}_j$ only. However, they can be taken as giving the *relative* effect of the same variables on the heat lost from the gases, $\dot{Q}$. The principal uncertainty here is that frictional heat may change this relation.

Piston Speed and Inlet Pressure. As shown in Chapters 6 and 7, these two variables chiefly affect gas flow, G *, with little effect on in-

* From this point on the symbol G refers to gas flow per unit time per unit piston area, with or without the subscript g.

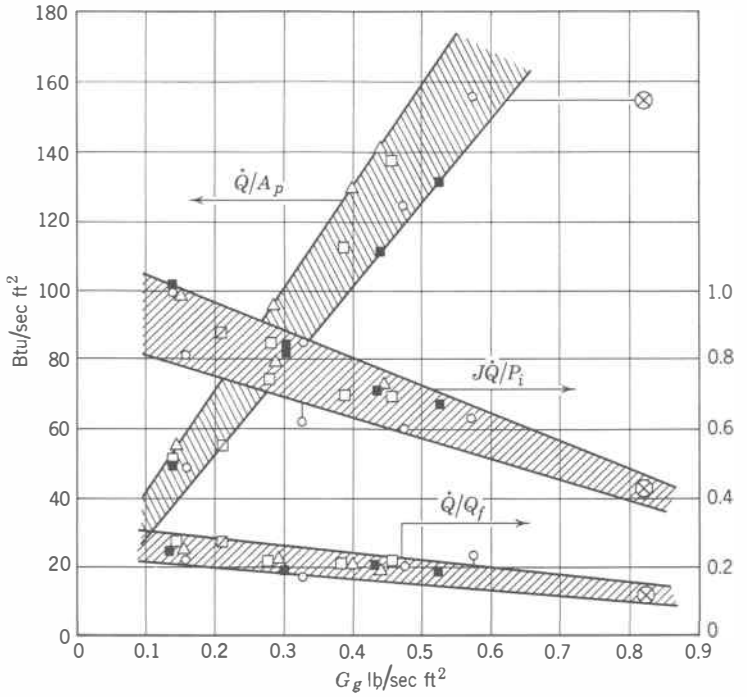

Symbol	Type	No. Cyl.	Bore, in.	Stroke, in.	r	s, ft/min	T_c, °F
■	Auto	8	3.63	3.1	7.5	517-2070	180-185
□	Truck	8	3.5	3.1	7.2	517-2070	
△	Auto	6	3.56	3.6	7.0	600-2160	
○	Auto	8	3.8	3.5	8.0	583-2330	
⊗	Aero*	12	5.4	6.0	6.0	2700	
⊠	CFR †	1	3.25	4.5	8.0	900	

*from Fig. 8-20 †from Fig. 8-18. Remainder from Mfr's tests

Fig 8-14. Heat to water jackets of spark-ignition engines.

dicated efficiency over the usual range of operation (provided fuel-air ratio is held constant). With P_i proportional to G, both $J\dot{Q}/P_i$ and $\dot{Q}/\dot{Q}_f$ will vary as G^{n-1}.

Figure 8-14 shows heat transfer parameters plotted against G for typical spark-ignition engines.

Effect of Exhaust Pressure. When exhaust pressure is the only independent variable both gas flow and T_g are affected. Figure 8-10 shows the relation of T_g to exhaust pressure for a four-stroke spark-ignition engine, and Fig 8-15 shows the effect of p_e on jacket heat losses when mass flow was held constant by appropriate variations in the inlet pressure. In two-stroke engines exhaust pressure cannot be varied in-

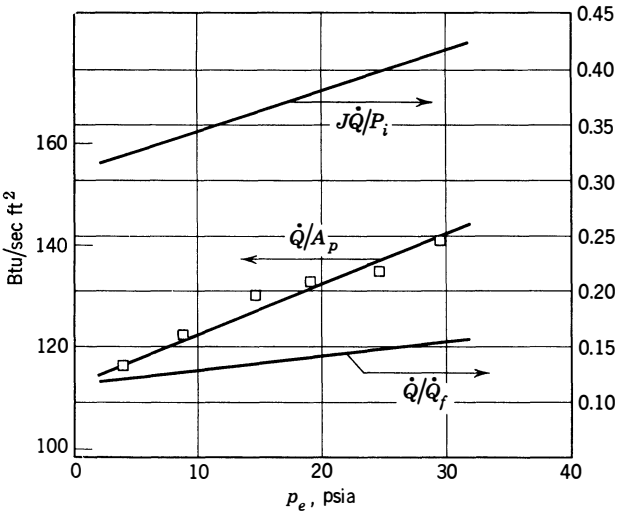

Fig 8-15. Effect of exhaust pressure on heat loss: liquid-cooled aircraft engine, 12 cyl 5.4 x 6.0 in; $r = 6$; $F/F_c = 1.2$; $T_i = 150°F$; $p_i = 16.7$ to 22.1 psia; $T_c = 240°F$; $G_g = 0.785$ Btu/sec ft^2; $h_e = 0.24$ Btu/sec ft^2°F; $A_p = 1.91$ ft^2; $s = 2400$ ft/min. (Povolny et al., ref 8.36)

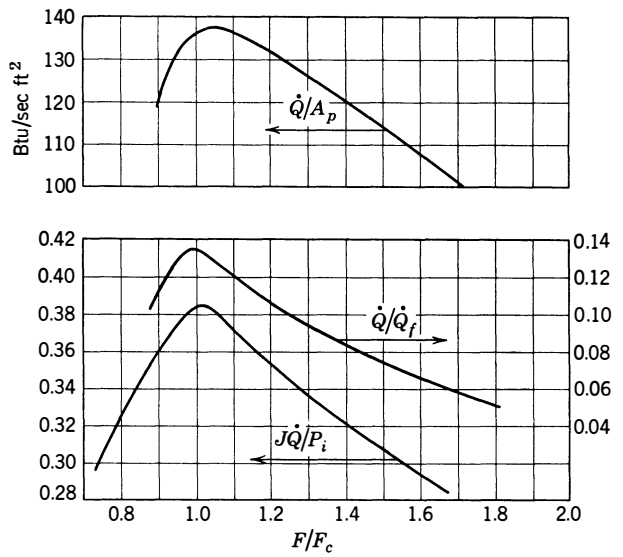

Fig 8-16. Effect of fuel-air ratio on heat loss. Same engine as Fig 8-15: $p_i = 18.7$ to 19.7 psia; $p_e = 14.3$ psia; $T_i = 118°F$; $T_c = 240°F$; $G_g = 0.88$ lbm/sec ft^2; $h_e = 0.25$ Btu/sec ft^2°F. (Povolny et al., ref 8.36)

dependently of inlet pressure without large effects on G and on engine output. (See Chapter 7.)

Effect of Fuel-Air Ratio (Fig 8-16). Here there are three important influences, namely, the resultant changes in T_g, in F, and in efficiency.

The effect on $\dot{Q}/\dot{Q}_f$ curve reflects simultaneous changes in T_g and rate of fuel flow. The shape of the $J\dot{Q}/P_i$ curve is the result of the latter change and the change in efficiency. The latter curve shows why both rich and lean mixtures are effective in reducing engine temperatures at a given power output.

In unsupercharged engines the choice of fuel-air ratio is usually dictated by power requirements rather than by heat-loss and temperature considerations. On the other hand, with supercharged engines, advantage can be taken of the low ratios of $J\dot{Q}/P_i$ characteristic of rich and lean mixtures, since the required power can be obtained by the proper choice of supercharger capacity. The following table illustrates this point:

		Typical Values of F_R	
Type	Regime	Unsupercharged	Supercharged
Aircraft	take-off	1.2	1.4
Aircraft	cruise	1.0	0.8
Diesel	rated	0.6	0.4–0.5

The notion that *engines overheat with lean mixtures* is probably derived from the fact that the carburetors of many gasoline engines are set to give F_R about 1.2. Figure 8-16 shows that if the carburetor is adjusted to give $F_R \cong 1.0$ and the same power is developed overheating may result.

Effect of Spark Advance (Fig 8-17). Increasing spark advance increases the time during which the cylinder walls are exposed to hot gases. Thus advancing the spark effectively increases T_g and $\dot{Q}/A_p$. $\dot{Q}/\dot{Q}_f$ follows the same trend because the denominator is constant.

The curve of $J\dot{Q}/P_i$ reflects changes in efficiency as well as changes in T_g.

Compression Ratio (Fig 8-18). Although not strictly an operating variable, compression ratio is here classed as such because changes in compression ratio can easily be made in spark-ignition engines. Here the principal variables are T_g and efficiency. T_g decreases as compression ratio increases on account of the lowering of exhaust temperatures.

(See Fig 4-5, $h1$, $i1$.) This decrease in T_g reduces $\dot{Q}/A_p$ and $\dot{Q}/\dot{Q}_f$, since the denominator in each case remains constant. $J\dot{Q}/P_i$ decreases faster than the other two parameters because η_i increases as compression ratio increases. The effectiveness of a high compression ratio in reducing heat flow at a given power output is apparent in Fig 8-18. It should be

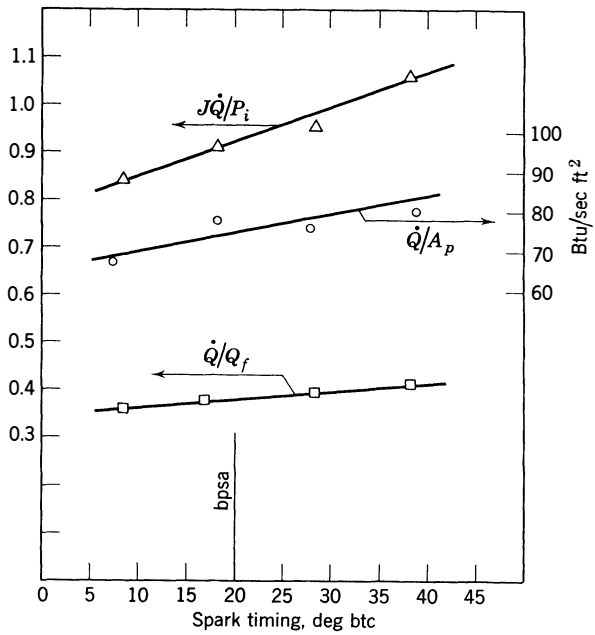

Fig 8-17. Effect of spark timing on heat loss: CFR liquid-cooled engine; $r = 6$; $s = 900$ ft/min; $p_i = 14.2$; $p_e = 14.8$ psia; $F/F_c = 1.2$; $T_c = 170°$F. (Sloan Automotive Laboratories)

remembered, however, that this reduction in heat flow is confined chiefly to those parts exposed to the exhaust gases and that heat flow through the cylinder head may actually increase because of the increased maximum temperatures. (See Fig 4-5, $g1$.)

Effect of Detonation. Experiments to date on the effect of detonation on heat loss to the cooling medium are fragmentary and have yielded conflicting results. This is due in part to the technical difficulties involved in heat measurements of this kind and in part to the fact that in most of these experiments the intensity of detonation has been controlled by an independent variable, such as spark advance or

fuel-air ratio, which itself has had a pronounced effect on the heat loss. However, such experiments generally agree on the following points:

1. The temperature of spark plugs, or of a thermal plug in the cylinder head, increases with increasing intensity of detonation.
2. Severe detonation sustained over long periods often results in burning of aluminum pistons and cylinder heads in a region which appears to be adjacent to the detonating zone.

There is some uncertainty regarding the apparent effect of detonation on the rate of heat transfer to the cooling medium: some experiments (ref 8.6) show a negligible effect, whereas others indicate a significant increase. After rather exhaustive study of such tests, supplemented by general experience with engines in operation under controlled conditions, your author has come to the conclusion that *detonation by itself increases the total heat loss by a small amount*, often within the experimental error of heat-loss measurements. The increases in gas temperature and pressure associated with detonation are of very short duration and these increases are confined chiefly to the detonating portion of the charge. On the other hand, nearly all spark plugs contain

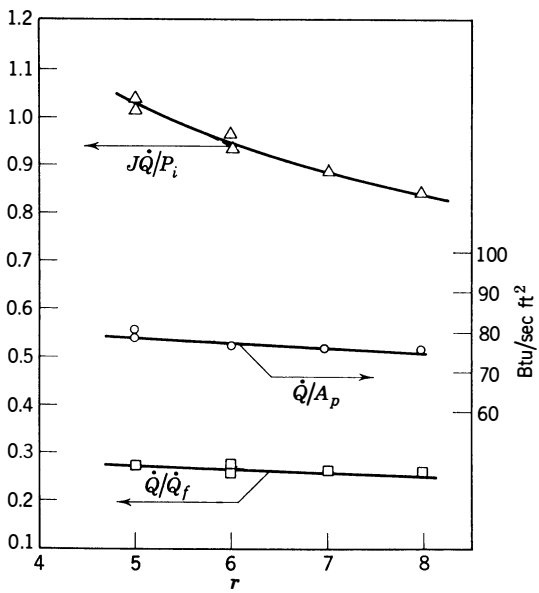

Fig 8-18. Effect of compression ratio on heat loss: CFR engine 3.25 x 4.5 in; 900 ft/min; p_i = 14.2; p_e = 14.7 psia; $\dot{G}_g$ = 0.21 lbm/sec ft^2; T_i = 120°F; F/F_c = 1.13; bpsa. (Sloan Automotive Laboratories)

a small cavity behind the ignition points, and it is apparent that a rapidly fluctuating pressure will cause rapid flow of gases in and out of this cavity. Thus the gas velocity with respect to the ignition points will be increased, and the rate of heat transfer at this point will be increased accordingly.

The local erosion of aluminum pistons and cylinder heads, which sometimes occurs with severe and long-continued detonation, is probably caused by high local heat transfer due to the high density and temperature which exist together in the detonating portion of the charge. Thus, even though detonation may not markedly increase the total heat transfer, there may be very pronounced increases in the rate of heat transfer in certain local areas because of higher local temperatures and increased relative velocity.

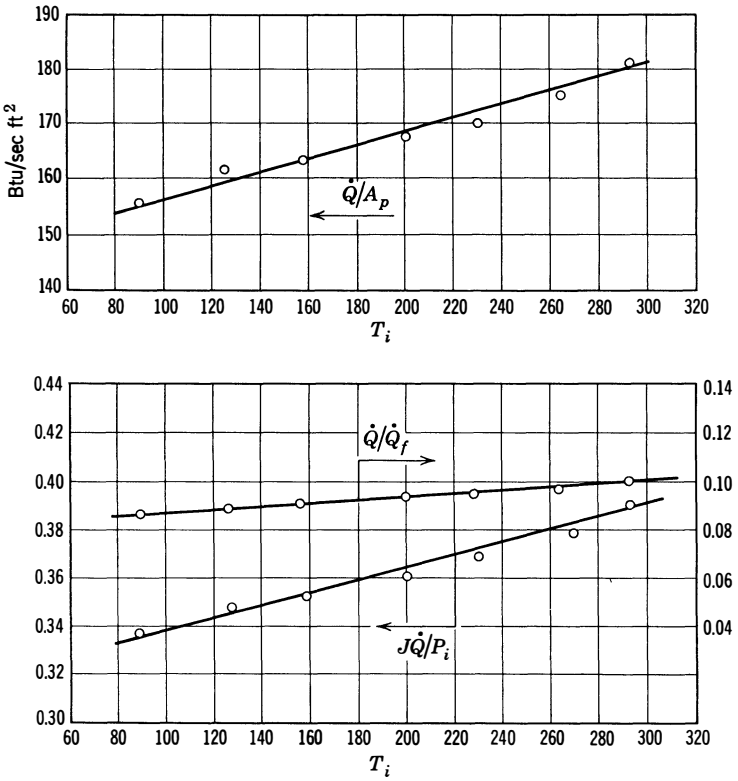

Fig 8-19. Effect of inlet temperature on heat loss with constant air flow. Same engine as Fig 8-15; p_i = 22.1 to 27 psia; p_e = 14.3 psia; s = 2400 ft/min; T_c = 240°F; F_R = 1.2; G_g = 2.68 lbm/sec ft². (Povolny et al., ref 8.36)

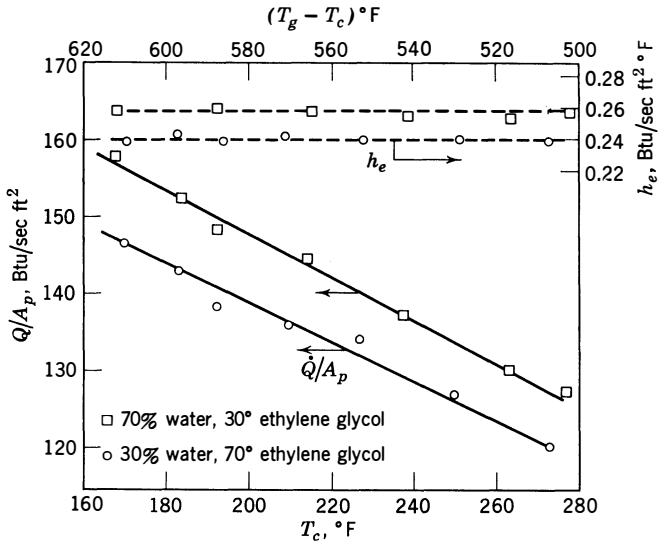

Fig 8-20. Effect of coolant temperature and coolant composition on heat loss: 12-cyl liquid-cooled aircraft engine, 5.4 x 6 in; s = 2700 ft/min; 950 ihp; F/F_c = 1.2; G_g = 0.823 lbm/sec ft²; T_i = 138°F; p_i = 17 psia; T_g = 180°F; A_p = 1.91 ft²; $\dot{G}_c$ = 15 lbm/sec ft². (Povolny et al., ref 8.36)

Large increases in rate of heat transfer to the cooling system which might be attributed to detonation are probably due to *pre-ignition* which often accompanies detonation. In such cases detonation causes the spark plug points or carbon deposits to overheat to such an extent that there is early ignition and an increase in heat loss similar to that caused by an advanced spark. The increase in $\dot{Q}/A_p$ with detonation, shown in Fig 8-18, is probably explainable in this manner.

Inlet Temperature. If mass flow is held constant, an increase in T_i increases T_g, and thus the heat-flow parameters will increase with increasing T_i, as shown in Fig 8-19. As indicated by expression 8-11, T_g appears to increase about 1° for each 3° increase in T_i. If, instead of mass flow, p_i is held constant, changes in T_i will affect the mass flow as well as T_g. (See Chapters 6 and 7.) Since these two influences oppose each other, the effect of T_i on $\dot{Q}$ is small under such circumstances.

Coolant Temperature. As we have seen, $\dot{Q}$ is directly proportional to $(T_g - T_c)$, so that if T_g can be estimated the effect of T_c on heat flow is easily predicted. Figure 8-20 shows the expected trend. Since effects of T_c on mass flow and power are small, the changes in $\dot{Q}/\dot{Q}_f$ and $J\dot{Q}/P_i$ are proportionately the same.

Coolant Composition. We have already discussed the general effects of changing from liquid cooling to air cooling. As regards liquid coolants, they almost always have a water base, with various amounts of antifreeze added as necessary. Aircraft engine coolants may consist of as much as 50% ethylene glycol in water. Within the range from pure water to this mixture, the change in thermodynamic characteristics is appreciable and will have measurable, though small, effect on the heat-flow parameters. Figure 8-20 shows that increasing the fraction of

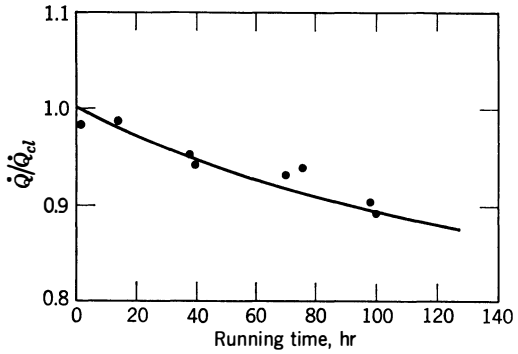

Fig 8-21. Effect of deposits on heat loss: $\dot{Q}$ = heat to jackets per unit time; $\dot{Q}_{cl}$ = heat to jackets per unit time, clean engine. (Tests run by DuPont Company under laboratory conditions giving rapid deposit accumulation. Automobile engine.)

glycol in the coolant reduces heat loss to the jackets. This effect is accounted for by the lower Prandtl number and coefficient of conductivity of glycol as compared with water. Thus an increase in the glycol content reduces k_c in eqs 8-8–8-10. Reference 8.36 gives additional data on the effects of coolant composition.

Engine Deposits. Carbon deposits inside the cylinder and deposits such as lime in the water jackets decrease the effective values of k_w and tend to decrease $\dot{Q}$. Because of their poor heat conductivity the surfaces of deposits may reach temperatures considerably higher than that of the clean surface at the same point. Since heat flow decreases, the actual wall-surface temperatures, T_{sg} and T_{sc}, also decrease. Figure 8-21 gives an example of the effect of deposit build-up on heat loss. From this figure it appears that the effects of deposits may be large, especially when engines are run for long periods of time without cleaning, as in the case of road vehicles.

Sometimes carbon deposits take the form of scaly projections from the cylinder walls or piston. For the exposed end of such deposits the ef-

fective values of t/k_w are very high, and, therefore, these projections run at high temperatures and may cause pre-ignition.

Temporary Methods of Controlling Engine Cooling. For short-time operation very rich mixtures may be used to reduce heat flow and, therefore, reduce cylinder temperatures at a given engine output. Figure 8-16 shows this effect, which is generally used for take-off condi-

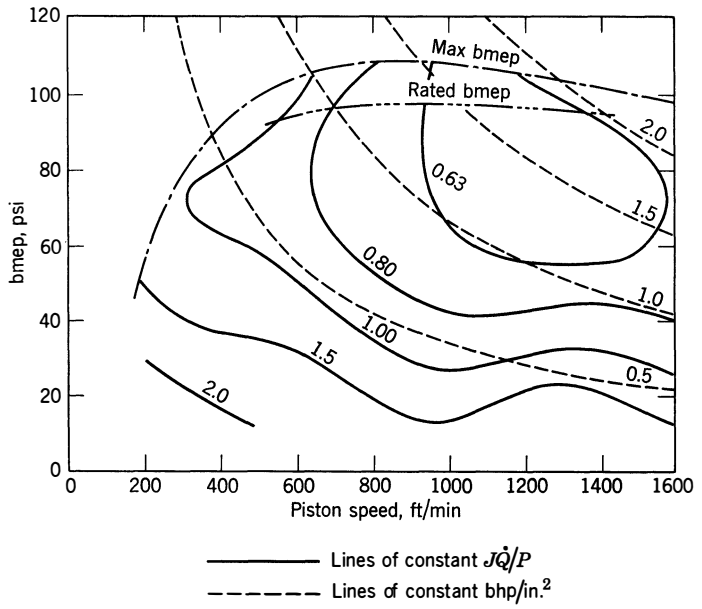

Fig 8-22. Heat loss map for a Diesel engine: Junkers 1-cyl; two-stroke opposed-piston engine; 3.15 x 2 x 5.9-in, piston area = 15.5 in^2. (Englisch, ref 8.27)

tions in aircraft engines, unless water injection is used. Injection of water, or water-alcohol mixture, into the inlet system reduces T_g considerably.

Heat Rejection Map. Figure 8-22 shows $J\dot{Q}/P$, where P is the brake power, over the entire useful range of speed and load for a two-stroke Diesel engine. Such a "map" is very useful for purposes of cooling-system design, but few engine builders have published such information. Another very important use for such data is to indicate how to run an engine so as to minimize heat loss at a given power output. For example, for minimum heat loss at 1.0 hp/in^2 piston area, the engine of Fig 8-22 should be operated at 1100 ft/min piston speed and bmep = 60 psi. The trends shown in Fig 8-22 are attributable to the changes in fuel-air ratio,

mass flow, and mechanical efficiency, which accompany changes in speed and load in this type of engine. The large values of $J\dot{Q}/P$ at light loads are due to low mechanical efficiency.

Distribution of Heat Loss Over the Cylinder. Information on this subject has been obtained from tests made on a 5 x $5\frac{1}{2}$ in single-cylinder engine. (See ref 8.40.) The water jacket was divided into compartments comprising the cylinder barrel up to the top of piston travel, the cylinder head, and the exhaust-port, exclusive of the valve seat. The results are shown in Table 8-3.

Table 8-3

Distribution of Heat Flow to Various Parts of the Cylinder

	Fraction of Total Heat Flow to Coolant	
Part of Cylinder	Including Piston Friction	Not Including Piston Friction
Head and valve seats	0.50–0.55	0.57–0.63
Barrel	0.27–0.32	0.16–0.18
Exhaust port	0.17–0.22	0.20–0.25

From tests on a 5 x $5\frac{1}{2}$ in cylinder with water jackets divided as indicated. (Goldberg and Goldstein, ref 8.40.)

Previous tests had shown that no measurable amount of heat was transmitted from the intake port to the cooling water. Some idea of the importance of the exhaust process, in transmitting heat to the jackets, may be formed by noting that *all* of the exhaust-port heat came from this source, plus a portion of that collected by the cylinder head, especially through the exhaust-valve seat.

Since in this particular engine there was no special provision for cooling of the piston, we may assume that the heat of piston friction was taken up by the coolant and appears in the jacket heat. An estimate of the piston friction indicates that approximately half of the heat rejected to the cylinder barrel came from piston friction. This being the case, the distribution of heat lost from the gases would be that given by the second column of Table 8-3. From these results it appears that about 50% of the heat rejected to the coolant was transferred from the gases during the compression, combustion, and expansion strokes, where efficiency would be influenced.

Heat Loss and Efficiency Loss

Figure 5-14 in Chapter 5 shows that the heat loss during the compression and expansion strokes was 20 to 50% of the heat lost to the jackets. If these limits are taken as typical, the effect of heat loss on indicated efficiency can be roughly estimated from Fig 8-11.

Further research is needed to explore the variation of the ratio of heat loss during compression and expansion to jacket-heat loss for types of cylinder other than the one used as a basis for Fig 5-14.

Control of Engine Heat Loss

If given values of T_g and G_g are assumed, it is apparent that the requirements for cooling and for minimizing heat loss are generally in conflict because lowering of the surface temperatures always results in increased heat loss.

Considering the whole cylinder, there is one method of reducing $\dot{Q}$ which does not affect temperatures, namely, a reduction of the area exposed to the hot gases. In four-stroke engines overhead-valve arrangements are attractive from this point of view. In two-stroke designs the opposed-piston arrangement, Fig 7-1*c*, affords the smallest surface area for a given bore and stroke. On the other hand, some of the combustion chambers which are especially resistant to detonation have large areas for heat transfer, and many successful compression-ignition chambers contain small throats through which hot gases pass at high velocity. Wherever such designs are used it is because gains to be made in other respects are considered to justify the greater heat losses involved.

As we have seen, much of the heat rejected to the coolant may come from the exhaust system, including the exhaust ports and jacketed portions of the exhaust manifolds. Although reduction in these cooled areas reduces heat to be handled by the cooling system, it obviously does not contribute to improved efficiency. Wherever the supply of low temperature coolant is plentiful, as in marine installations, there may be no reason to minimize cooled surface areas other than those of the combustion chamber.

Choice of Coolant Temperature. The only practical advantages of a low coolant temperature are reduced hot-surface temperatures and improved volumetric efficiency. (See Chapter 6.) On the other hand, a low coolant temperature increases jacket loss, temperature stresses, and, if a radiator must be used, the required radiator size. With liquid coolants, the usual compromise is to carry the coolant outlet temperature

comfortably below the boiling point.* If it is important to minimize radiator capacity, high-boiling-point liquids may be used. (See discussion under radiator design.)

With air cooling, the mass flow of coolant used must be a compromise between the advantages of small temperature difference across the cylinder and power required to circulate the coolant, which can easily become excessive if the cooling system is improperly designed.

RADIATOR AND FIN DESIGN

It is not within the scope of this book to deal in detail with the design of radiators. It may be of interest, however, to outline some basic considerations, since they are closely related to the foregoing material.

The term *radiator* is here used to designate the heat exchanger used for transferring heat from a liquid coolant to the atmosphere. The heat-exchanging passages are formed by an assembly of sheets or tubes, called a *core*, which contains many similar passages for air flow, the walls of which also form the passages to carry the coolant. Heat flow to the air is chiefly by forced convection.

For the heat flow from radiator to air (from eq 8-1), assuming that μ Prandtl number and k_c are constant, we can write

$$\dot{Q} = A_r K_r G^n L^{n-1} (T_r - T_a) \tag{8-22}$$

where K_r = a coefficient, depending on the core design and the viscosity and thermal conductivity of the cooling air
A_r = radiator surface area
T_r = average temperature of the radiator surface
T_a = air temperature
L = typical length of the core section
G = mass flow of air per unit flow area

Selection of an appropriate *core* design fixes the value of K_r, L, and n. $\dot{Q}$ is the engine jacket loss, determined from tests or from such data as have already been presented in this chapter. With $\dot{Q}$, K_r, n, and L determined, it is evident that increasing values of T_r will reduce the value required for the remaining variable, $(G)^n A_r$. This is the reason that pressurized radiators or high-boiling-point liquids, such as ethylene-glycol solutions, are used when it is important to minimize radiator size

* Many modern installations are designed to carry a pressure somewhat above atmospheric, in order to raise the boiling point in the cooling system.

and air-flow requirements, as in aircraft. The surface temperature, T_r, will always be lower than the coolant temperature (see expression 8-10), but the drop between T_r and the coolant temperature can be minimized by using material of high conductivity for the core and making the path through this material, between coolant and air, as short as possible, that is, by minimizing t/k_w in expression 8-10. In radiators in which the coolant and air are separated only by thin copper sheets T_r can be taken as equal to the mean coolant temperature.

Having selected a core design and having determined the minimum working value of $(T_r - T_a)$, it is evident from eq 8-22 that

$$\dot{Q} = KA_rG^n \tag{8-23}$$

where K is a constant depending on values selected for K_r, L, and $(T_r - T_a)$.

Power Required to Cool. By assuming incompressible flow, we may use Bernoulli's theorem to express the power required to force air through a radiator. Thus

$$P_r = C_rA_rG^3/\rho^2 \tag{8-24}$$

where P_r = power required to force air through the radiator
C_r = a coefficient depending on core design, including the ratio between flow area and surface area
ρ = the air density

Dividing eq 8-24 by eq 8-23 gives

$$\frac{P_r}{\dot{Q}} = \frac{C_rG^{3-n}}{K\rho^2} \tag{8-25}$$

Since n for radiators usually lies between 0.7 and 0.8, the ratio of power required to heat dissipated decreases as the air velocity through radiator decreases. However, if a given quantity of heat must be dissipated, it is evident from eq 8-23 that A_rG^n must be constant, that is, the size of the radiator must be increased as G decreases. How far this process can be carried depends on particular circumstances. In a stationary installation it would be possible to make the radiator so large that the mass flow required would be furnished by natural convection. In most applications, however, it is more economical to use a more moderate radiator size, together with some forced circulation.

In the case of aircraft, motion through the air is used to furnish power for air circulation through the radiator. The power consumed in this way can be large in the case of fast airplanes, unless velocity through the

radiator is much less than the flight velocity. (See refs 8.8—.)* In the case of road vehicles, the vehicle motion is used, but radiator size is limited, and a fan is usually necessary to provide adequate cooling at low vehicle speeds.

Finning of Air-Cooled Cylinders. With reference to eqs 8-8–8-10, the value of the coefficient of conductivity k_c with air is about $\frac{1}{25}$ of k_c with water at the temperatures at which these fluids are commonly used. In order to compensate for this difference, the area A_c is drastically increased by the use of fins on the outer surface of the cylinder. The overall ratio A_c/A_g is near 1.2 for liquid-cooled cylinders, but it is usually between 5 and 20 for air-cooled cylinders, the latter value being used for high-output air-cooled cylinders which run at very high values of G_g. The increased value of A_c/A_g, together with the generally lower coolant temperature, makes possible values of T_{sg} and T_{sc} in air-cooled cylinders comparable with the corresponding values of liquid cooling.

In air-cooled engines the radiator consists of the cylinder outer (finned) surfaces, together with the *cowling* and *baffling* necessary to conduct the air to and over the finned surfaces. Equations 8-8–8-10 can be applied to this problem by taking T_c as the mean temperature of the cooling air and t as the average path length from the gas side to the surface of the fins.

The basic principles are the same for the air-cooled type of radiator as for the liquid-cooled type, but with air cooling there is the additional restriction that the radiator must be part of the cylinder and therefore is subject to serious restrictions in size and shape. Again, however, a large surface area with a small value of G_c is the way to minimize power required to cool.

Obviously, the largest cooling area for a given cylinder will be attained by using the largest practicable number of fins of the greatest practicable depth; but the number of fins must not be so great that the flow passages between them become unduly restricted. Also, as the fins become deeper and thinner, the ratio t/k_w becomes greater. Fin material of high conductivity is obviously desirable from this point of view.

Research in the field of fin design indicates that the greatest values of fin depth and the greatest number of fins deemed practicable from considerations of cost, manufacturing difficulties, etc, are usually none too great from the point of view of economical cooling. (See reports by the United States National Advisory Committee for Aeronautics.)

* With careful design of the flow passages, including the radiator, the *drag* of an airplane radiator may be zero or even negative. In the latter case the heat added to the stream of cooling air provides thrust through a *ramjet* effect. (See ref 8.8.)

HEAT LOSSES IN GAS TURBINES

In most present or proposed gas turbines it has not been considered practicable to provide much cooling for the nozzles or blading, and these parts, therefore, must be designed to run at substantially the stagnation temperature of the gases which surround them. These conditions have imposed a limit on the maximum gas temperature which may be used, and this limit in turn sets a limit on the maximum fuel-air ratio.

The stagnation temperature must, of course, be computed by using the *relative* velocity between the gas and the part in question. As an illustration, let us assume a single-stage impulse turbine with *no cooling* and the following characteristics:

Stagnation temperature before nozzle	2000°R
Absolute velocity of gas issuing from nozzle	2200 ft/sec
Velocity of gas relative to rotating blades	1200 ft/sec

The nozzle temperature would be 2000°R without cooling.

The true temperature of the gas issuing from the nozzle would be

$$T = 2000 - \frac{2200^2}{2g_0JC_p} = 2000 - 403$$

$$= 1597°\text{R}$$

The blade temperature, T_b, without cooling, would be

$$T_b = 1597 + \frac{1200^2}{2g_0JC_p} = 1597 + 120 = 1717°\text{R}$$

In actual practice a limited amount of cooling is always present. As a minimum, it is necessary to cool the bearings. In addition to cooling by conduction through the metal, the blades and nozzles may transfer considerable heat by direct radiation to cooler parts.

The relatively small amount of cooling required by gas turbines is an important practical advantage of this type of prime mover, especially for use in aircraft.

The effects of size on heat flow and temperature gradients are similar to these effects in reciprocating engines, since, due to stress limitations, turbines of varying size are run at nearly the same *linear* velocities of the blades and therefore at nearly the same values of G_g.

ILLUSTRATIVE EXAMPLES

Example 8-1. Local Heat Flow. Compute the heat flux through the cylinder head of the 4-in bore engine (Figs 8-4, 8-6) at 1800 ft/min piston speed at the point where T_{sg} and T_{sc} were measured. The head is made of cast iron and is 0.655 in thick at this point.

Solution: Figure 8-6 shows that at 1800 ft/min for this engine $T_{sg} = 400°F$, $T_{sc} = 260°F$. The conductivity of cast iron is $7.8(10)^{-3}$ Btu/ft sec °F. Therefore, $\frac{\dot{Q}}{A} = \frac{7.8(10)^{-3}(400 - 260)12}{0.655} = 20$ Btu/sec ft^2 of head area at the point of measurement.

Example 8-2. Local Temperature. Estimate the temperature of the exhaust-valve face of an aircraft cylinder 6-in bore and stroke of design similar to that of Fig 8-5 running under the following conditions: 2000 rpm, $F = 0.0675$, inlet temperature 620°R, inlet pressure 30 psia, volumetric efficiency 1.0.

Solution:

$$\text{piston displacement} = 170 \text{ in}^3 = 0.0985 \text{ ft}^3, \qquad \rho_i = \frac{2.7(30)}{620} = 0.13 \text{ lbm/ft}^3$$

$$\dot{M} = \frac{2000(0.0985)0.13(1.0)}{2(60)} = 0.214 \text{ lbm/sec}$$

$$\text{bore} = 6 \text{ in} = 0.5 \text{ ft}$$

$$\text{piston area} = 28.4 \text{ in}^2 = 0.197 \text{ ft}^2$$

From Fig 8-12, at $F/F_c = 1.0$, $\mu g_0 = 22(10)^{-6}$, and $k = 8.3(10)^{-6}$,

$$\mathbf{R}_g = \frac{0.214(0.5)}{0.197(22)(10)^{-6}} = 24.6(10)^3$$

In Fig 8-5 T_g for the exhaust valve is 2100°F at $F/F_c = 0.08/0.067 = 1.2$. Figure 8-12 indicates that there is very little change in T_g from $F_R = 1.2$ to $F_R = 1.0$. Therefore, T_g is taken as 2100° at $T_i = 80°F = 540°R$. The present T_i is 620°R, and the correction indicated is $0.35(620 - 540) = 28°F$. The estimated T_g is $2100 + 28 = 2128°F$. Returning to Fig 8-5 at $\mathbf{R}_g = 24.6(10)^3$, T_{sg} is given as 1200°F with $T_g = 2100$. The estimated valve temperature is therefore $1200 + 28 = 1228°F$.

Example 8-3. Limits on Size. It is desired to run an engine with cylinders similar to those of Fig 8-4 at a piston speed of 2000 ft/min supercharged to 2 atm inlet pressure; other conditions are the same as in Fig 8-4. What is the largest cylinder bore feasible without design changes if the gas-side cylinder-head temperature is not to exceed 500°F? (See Figs 6-15 and 6-16 for particulars regarding the engine.)

Solution: With the inlet pressure increased to 2 atm, $p_e/p_i = 0.5$. At $r = 5.74$, Fig 6-5 shows the volumetric efficiency correction to be about 1.07. Figure 6-16 shows volumetric efficiency at $p_e/p_i = 1$ and 2000 ft/min to be 0.81. By definition, $G = \dot{M}_a(1 + F)/A_p$ and $\dot{M}_a = A_p s \rho_i e_v/4$. Therefore,

$$G = s\rho_i e_v(1 + F)/4 \qquad \rho_i = 2.7(29.4)/634 = 0.125 \text{ lbm/ft}^3$$

From Fig 8-12, $\mu g_0 = 21.8(10)^{-6}$. Therefore,

$$\mathbf{R}_g = \frac{2000(0.125)(0.81)(1.079)b}{4(60)21.8(10)^{-6}} = 4.18(10)^4 b$$

From Fig 8-4, T_{sg} reaches 500 when Reynolds index reaches 8000. Therefore,

$$b = \frac{8000}{41{,}800} = 0.192 \text{ ft} = 2.3 \text{ in}$$

If larger cylinders are desired, the head design must be changed along the lines indicated by Fig 8-7.

Example 8-4. Heat to Jackets. Estimate the heat flow to the jackets of an 8-cylinder automobile engine of 3.75-in bore, 3.5-in stroke, fuel-air ratio 0.08, developing 200 hp with indicated thermal efficiency 0.30, $T_i = 100°\text{F}$, $T_c = 180°\text{F}$. Compute $\dot{Q}/A_p$, $\dot{Q}/\dot{Q}_f$, and $J\dot{Q}/P_i$.

Solution: From eq 1-13,

$$\text{sac} = 2545/0.08(19{,}020)0.30 = 5.67 \text{ lbm/hp-hr}$$

$$F_R = 0.08/0.067 = 1.2$$

$$\dot{M}_a = 200(5.67)/3600 = 0.315 \text{ lbm/sec}$$

$$\dot{M}_g = 0.315(1.08) = 0.34 \text{ lbm/sec}$$

From Fig 8-12, $\mu g_0 = 21.8(10)^{-6}$, $k = 8.3(10)^{-6}$, $T_g = 760°\text{F}$ at $T_i = 80°\text{F}$. Therefore,

$$T_g = 760 + 0.35(100 - 80) = 767°\text{F}$$

$$\text{piston area} = 86.7 \text{ in}^2 = 0.603 \text{ ft}^2$$

$$\text{bore} = 3.75/12 = 0.313 \text{ ft}$$

$$\mathbf{R}_g = 0.34(0.313)/0.603(21.8)10^{-6} = 8.1(10)^3$$

From Fig 8-11, the Nusselt number is $8.8(10)^3$. Therefore,

$$h_e = 8.8(10)^3(8.3)(10)^{-6}/0.313 = 0.234 \text{ Btu/sec ft}^2 \text{ °F}$$

$$\dot{Q} = h_e A_p(T_g - T_c)$$

$$\dot{Q} = 0.234(0.603)(767 - 180) = 82.5 \text{ Btu/sec}$$

$$\dot{Q}/A_p = 82.5/0.603 = 137 \text{ Btu/sec ft}^2$$

$$\dot{Q}_f = 200(5.67)(0.08)19{,}020/3600 = 480 \text{ Btu/sec}$$

$$\dot{Q}/\dot{Q}_f = 82.5/480 = 0.172$$

$$J\dot{Q}/P_i = 82.5 \times 60/200(42.4) = 0.585$$

Compare these results with Fig 8-14 at $G_g = 0.34/0.603 = 0.564$ lb/sec ft^2.

Example 8-5. Heat to Jackets, Air-Cooled Engine. Estimate heat loss of the Continental 1790 in^3 gasoline tank engine operating at 800 bhp, $F_R = 1.2$,

$T_i = 80°F$, $T_c = 125°F$. 12 cylinders, 5.75×5.75 in $= 1790$ in^3. Compression ratio is 6.5. Compute also $\dot{Q}/A_p$, $\dot{Q}/Q_f$, and $J\dot{Q}$/brake power.

Solution: Fuel-air cycle efficiency at $r = 6.5$, $F_R = 1.2$, is 0.32, estimating indicated efficiency as 0.85 times fuel-air, and mechanical efficiency 0.85, gives brake efficiency $= 0.32(0.85)0.85 = 0.23$.

From eq 1-13 sac $= 2545/19{,}020(0.08)0.23 = 7.3$ lb/bhp-hr.

$$\dot{M}_a = 800(7.3)/3600 = 1.62 \text{ lbm/sec}$$

$$\dot{M}_g = 1.62(1.08) = 1.75 \text{ lbm/sec}$$

$$\text{bore} = 5.75/12 = 0.477 \text{ ft}$$

$$\text{piston area} = 12(26)/144 = 2.15 \text{ ft}^2$$

At $F_R = 1.2$, Fig 8-12 shows $T_g = 760$, $\mu g_0 = 21.8(10)^{-6}$ and $k = 8.3(10)^{-6}$. By definition,

$$\mathbf{R}_g = 1.75(0.477)/(2.15)(21.8)(10)^{-6} = 1.78(10)^4$$

From Fig 8-11, Nusselt No. $= 1.1(10)^4$,

$$h_e = 1.1(10)^4(8.3)(10)^{-6}/0.477 = 0.192 \text{ Btu/sec ft}^2 \text{ °F}$$

$$\dot{Q} = 0.192(2.15)(760 - 125) = 262 \text{ Btu/sec}$$

$$\dot{Q}/A_p = 262/2.15 = 122 \text{ Btu/sec ft}^2$$

$$\dot{Q}_f = 1.62(0.08)19{,}020 = 2470 \text{ Btu/sec}$$

$$\dot{Q}/Q_f = 262/2470 = 0.106$$

$$J\dot{Q}/P_b = 262(60)/42.4(800) = 0.464$$

Compare with Fig 8-14 at $G_g = 1.75/2.15 = 0.815$.

Example 8-6. Heat to Jackets of Diesel Engine. The engine of example 8-5 is also built as a supercharged Diesel engine with the same bore, stroke, and numbers of cylinders. In this form it is rated at 700 bhp at 2200 rpm with $r = 17$ and $F_R = 0.6$. Estimate heat to cooling air and heat-loss parameters at 120°F air temperature.

Solution: From Fig 4-6, fuel-air cycle efficiency is 0.55 and brake efficiency is estimated at $0.55(0.85)(0.85) = 0.40$. Fuel-air ratio $= 0.6 \times 0.067 = 0.04$. For light Diesel fuel from Table 3-1, $Q_c = 18{,}250$, $F_c = 0.067$.

$$\text{sac} = 2545/0.04(18{,}250)0.40 = 8.7 \text{ lbm/bhp-hr}$$

$$\dot{M}_a = 700(8.7)/3600 = 1.69 \text{ lbm/sec}$$

$$\dot{M}_g = 1.69(1.04) = 1.76 \text{ lbm/sec}$$

At $F_R = 0.6$ in Fig 8-12, $T_g = 560°F$. Correcting T_g for $T_i = 120°F$ gives $560 + 0.35(120 - 80) = 574°F$. $\mu g_0 = 19.2(10)^{-6}$ and $k = 7.1(10)^{-6}$. Then $\mathbf{R}_g = 1.76(0.477)/2.15(19.2)(10)^{-6} = 2.04(10)^4$.

From Fig 8-11, Nusselt No. = $1.7(10)^4$.

$$h_e = 1.7(10)^4(7.1)(10)^{-6}/0.477 = 0.253 \text{ Btu/sec ft}^2\,^\circ\text{F}$$

$$\dot{Q} = 0.253(2.15)(577 - 120) = 248 \text{ Btu/sec}$$

$$\dot{Q}/A_p = 248/2.15 = 115 \text{ Btu/sec ft}^2$$

$$\dot{Q}_f = 1.69(0.04)18{,}250 = 1230 \text{ Btu/sec}$$

$$\dot{Q}/Q_f = 248/1230 = 0.202$$

$$J\dot{Q}/P = 248(60)/42.4(700) = 0.501$$

Example 8-7. Heat Exchanger. A steady-flow air cooler is made of very thin copper tubes 12 in long and $\frac{1}{4}$ in in diameter. The coolant is water which surrounds the tubes, entering at 80°F and leaving the heat exchanger at 90°F. Air enters the tubes at 200°F and flows through them at a rate of 160 lbm/min/ft^2 of cross-sectional tube area. Compute the exit temperature of the air and the effectiveness of the cooler. Viscosity times g_0 for air at 80°F is $12.1(10)^{-6}$ lbm/sec ft, and its conductivity, $4.5(10)^{-6}$ Btu/ft sec °F.

Solution: Since the tubes are thin and have a high conductivity, it may be assumed that the mean surface temperature on the air side is equal to the mean water temperature, that is, 85°F. The heat-transfer coefficient may be computed from eq 8-1, using the tube diameter as the typical dimension.

$$\frac{hd}{k} = C\left(\frac{Gd}{\mu g_0}\right)^n (\mathbf{P})^m$$

$$\frac{Gd}{\mu g_0} = \frac{160(0.25)10^6}{60(12)12.1} = 4.58(10)^3$$

The Prandtl number of air is 0.74. By including $(\mathbf{P})^m$ in the coefficient C, McAdams (ref 8.00) gives C as 0.026 and n as 0.8. Therefore,

$$\frac{h(0.25)10^6}{12(4.5)} = 0.026(458{,}000)^{0.8}, \qquad h = 19(10)^{-4} \text{ Btu/sec ft}^2\,^\circ\text{R}$$

The heat transfer area for 1 ft^2 of flow area is $4\pi DL/\pi D^2 = 4L/D = 4(12)/0.25 = 192$ ft^2.

The air temperature drop:

$$C_p\dot{M}\,\Delta T = hA(T_1 - T_s)$$

$$\Delta T = \frac{19(10)^{-4}(60)(192)(200 - 85)}{0.24(160)} = 65.5^\circ\text{F}$$

$$\text{exit air temperature} = 200 - 65.5 = 134.5^\circ\text{F}$$

$$\text{effectiveness} = \frac{200 - 134.5}{200 - 85} = 0.57$$

Friction, Lubrication, and Wear —— nine

Under the general heading of *friction* it is convenient to include those items which account for the difference between the indicated and brake output of an engine. In an internal-combustion engine this difference always includes power absorbed by *mechanical friction*, that is, friction due to relative motion of the various bearing surfaces. In addition to mechanical friction, the difference between indicated and brake power may also include the following:

Pumping power, defined as the net work per unit time done by the piston on the gases during the inlet and exhaust strokes. By this definition, pumping power is zero in two-stroke engines.

Compressor power, that is, power taken from the crankshaft to drive a scavenging pump or supercharger. In unsupercharged four-stroke engines, or in engines in which the supercharger is separately driven, this power is zero.

Auxiliary power—the power required to drive auxiliaries, such as oil pump, water pump, cooling fan, and generator.

The above items may be classed as "losses" because each one contributes to a reduction in the useful output of the engine.

Turbine power. In some engines an exhaust turbine has been geared to the crankshaft. (See Chapters 10, 13.) In such cases the power developed by the turbine will add to the brake power of the engine and could be classed as a "negative" friction loss.

Friction Mean Effective Pressure. It is often convenient to express the differences between brake and indicated output in terms of mean effective pressure, that is, power divided by engine displacement per unit time. Using this definition, we can write*

$$\text{bmep} = \text{imep} - \text{mmep} - \text{pmep} - \text{cmep} - \text{amep} + \text{tmep}$$

$$= \text{imep} - \text{fmep} \qquad (9\text{-}1)$$

In this equation, as before, imep includes the work of the compression and expansion strokes only, and bmep is the brake mean effective pressure, that is, net shaft work per unit time divided by the power-stroke displacement per unit time.

mmep = that part of the indicated mean effective pressure used to overcome mechanical friction

pmep = the mean effective pressure of the exhaust stroke, minus the mean effective pressure of the inlet stroke, and is zero in two-stroke engines

cmep = that part of the indicated mean effective pressure used to drive a supercharger or scavenging pump

amep = that portion of the indicated mean effective pressure used in driving the auxiliaries

tmep = the power delivered to the crankshaft by an exhaust turbine divided by the power-stroke displacement per unit time; in other words, the mean effective pressure added by the turbine

fmep = the difference between indicated and brake mep, called *friction mean effective pressure.*

In cases in which a supercharger is driven by an exhaust turbine, without mechanical connection of either component to the crankshaft system, cmep = tmep. The effect on engine output of such a system depends on its influence on inlet temperature and pressure and on exhaust pressure. Such systems are discussed in Chapter 13.

Mechanical Efficiency. Since there are so many kinds of friction losses, this term has been used with a great many different meanings. Its use in this discussion is confined to the ratio bmep/imep, one which varies widely with design and operating conditions. It is evidently zero under idling conditions and can even be greater than unity when an exhaust-driven turbine is geared to the crankshaft. In practice, the range of variation of mechanical efficiency is so great that typical values cannot be given unless design details and operating conditions are

* See page 521 for calculation of these quantities.

specified in rather complete detail. For these reasons mechanical efficiency is not a convenient parameter.

Friction of Gas Turbines. Strictly speaking, the friction of gas turbines includes aerodynamic friction as well as the mechanical friction of the bearings and the loss due to driving the auxiliaries. However, since it is very difficult to separate aerodynamic friction from the other internal losses, the term friction is usually reserved for the sum of the bearing losses and auxiliary loss. These losses are often a much smaller fraction of the brake output than in reciprocating engines.

MECHANICAL FRICTION

Since this type of friction is common to all types of engine, it is dealt with first.

Types of Mechanical Friction. The friction associated with engine bearing surfaces may be divided into four classes:

1. *Hydrodynamic*, or *fluid-film*, friction
2. *Partial-film* friction
3. *Rolling* friction
4. *Dry* friction

The last type is unimportant in engines because some lubricant nearly always remains between the rubbing surfaces, even after long periods of disuse.

Fluid friction is associated with surfaces entirely separated by a film of lubricant, in which case the friction force is due entirely to lubricant *viscosity*. As is shown later, the bearing surfaces in engines which contribute importantly to friction operate in the fluid-film regime most of the time. Therefore, this type of friction is the principal component of the mechanical friction losses in an engine.

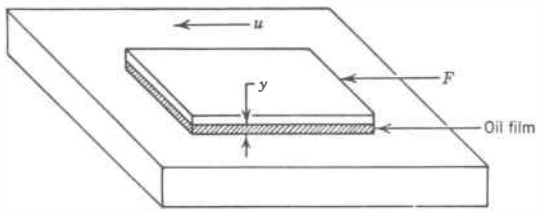

Fig 9-1. Definition of viscosity: $F/A = \mu(u/y)$; A = area of plate; F = force to move plate with velocity u; y = thickness of film of lubricant; μ = film viscosity $[FL^{-2}t]$.

The *viscosity* of a fluid is defined as the shearing force per unit area required to produce a velocity gradient of unit value. Figure 9-1 represents a thin layer of liquid between two plates. If one of the plates is moved at a constant velocity u, a force, F, will be required to overcome the frictional resistance of the fluid. The layer of fluid adjacent to this plate will also have the velocity u, whereas the layer adjacent to the

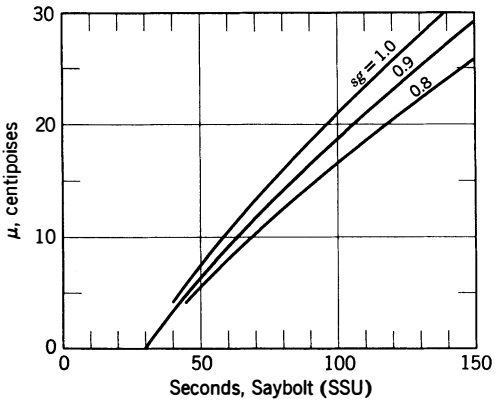

Fig 9-2. Conversion from Saybolt viscosity to centipoises. From 32 to 35 sec Saybolt is 1 to 2 centipoises. Above 150 sec, $\mu = 0.22 \times \text{sg} \times \text{sec Saybolt}$. sg = specific gravity of liquid. (*Theory of Lubrication*, Hersey, Wiley, 1938, pp 30–31.)

stationary plate will have zero velocity. For this arrangement, $F/A = \mu(du/dy)$.

If the distance between the plates is small, as in most bearings, the velocity varies linearly between the plates, and we may write

$$\frac{F}{A} = \mu\left(\frac{u}{y}\right) \tag{9-2}$$

where F = force required to move the plate
A = area of the moving plate
u = velocity of the moving plate
y = perpendicular distance between plates

μ is, by definition, the viscosity of the fluid. The usual absolute unit of viscosity is the *poise*, which has the dimensions dyne seconds per square centimeter,* or $FL^{-2}t$ in fundamental units.

* 1 poise = 2.09×10^{-3} lb sec/ft^2
1 centipoise = 2.09×10^{-5} lb sec/ft^2
See Fig 9-2 and Table 9-1 for other conversion data.

Table 9-1

Viscosity Conversion

One centipoise, dyne sec/100 cm^2 =
1.02×10^{-4} kg sec/m^2
2.09×10^{-5} lbf sec/ft^2
1.45×10^{-7} lbf sec/in^2
2.42×10^{-9} lbf min/in^2

For ordinary oils the viscosity is found to be nearly independent of the rate of shear, du/dy, to decrease rapidly with increasing temperature, and, at high pressures, to increase with pressure. (See ref 9.12.) The effect of oil composition on viscosity is discussed later in this chapter.

Theory of Fluid Friction. In the case of rubbing surfaces completely separated by a film of fluid, application of dimensional analysis leads to useful results. (See refs 9.0—.) Let the dependent variable be the coefficient of friction, f, which is the ratio of frictional force, in the direction of motion, to load between the moving elements normal to the motion. It is apparent that this force will depend on the following variables:

Variable	Symbol	Dimensions
Viscosity of fluid	μ	$FL^{-2}t$
Relative velocity of surfaces	u	Lt^{-1}
Load	W	F
Typical dimension	L	L
Shape of the surfaces, as defined by the design ratios	$R_1 \cdots R_n$	0

If we have included all the relevant variables, we can write

$$\phi_1(f, \mu, u, W, L, R_1 \cdots R_n) = 0 \tag{9-3}$$

where ϕ_1 indicates a function of the terms in parenthesis. This expression may be rearranged by using dimensionless ratios:

$$\phi_2\left(f, \frac{\mu u L}{W}, \quad R \cdots R_n\right) = 0 \tag{9-4}$$

If we take L^2 to be the typical area, we can define the unit pressure, p,

on the bearing as W/L^2. Using this definition, and solving for f, gives

$$f = \phi_3\left(\frac{\mu u}{pL}, R_1 \cdots R_n\right) \tag{9-5}$$

Bearing Deflection. Since the oil film in most bearings is very thin, small changes in the shape of the bearing surfaces may have appreciable effect on bearing friction. Therefore, eq 9-5 is strictly true only if deflections under load are negligibly small or if the design ratios refer to the bearing in its deflected state.

Partial-Film Friction. When rubbing surfaces are lubricated, but there is also contact between the surfaces, they are said to operate in the *partial-film* regime. Engine bearing surfaces must operate in this regime in starting. However, in normal engine operation there appears to be very little metallic contact except between the piston rings and cylinder walls. It has been shown (ref 9.41) that even these parts operate without metallic contact except for a brief moment at the end of each stroke when the piston velocity is nearly zero. Another piece of evidence indicating that engine bearings operate normally in the fluid-film regime is the fact that lubricants which have been found to reduce partial-film friction have no measurable effect on engine friction.

Thus partial-film friction, like dry friction, is of little importance as a contributor to engine friction.* Readers who are interested in this subject will find appropriate references in the bibliography at the end of this book.

Rolling Friction. This is the type of friction associated with ball and roller bearings and with cam-follower and tappet rollers. These bearings have a coefficient of friction which is nearly independent of load and speed. The frictional force is due partly to the fact that the roller is continuously "climbing" the face of a small depression in the track created by the contact surfaces as they deflect under the load. (See refs 9.35—.)

JOURNAL BEARINGS

Journal bearings are defined as bearings in which a circular cylindrical shaft, the contact surface of which is called the *journal*, rotates against a cylindrical surface, called the *bushing*. Journal bearings are termed *partial* when the bearing surface is less than a full circumference.

* This type of friction, however, may be an important contributor to wear.

The rotary motion may be continuous or oscillatory. Unless otherwise mentioned, this discussion is confined to full (360°) bearings with continuous rotation. A great deal of theoretical and experimental work has been done on the subject of journal bearings. (See refs 9.0— and 9.2—.) Here we confine the treatment to those aspects which are helpful in the study of engine friction.

Let us consider an idealized bearing consisting of an exactly cylindrical shaft and journal. The clearance space between them is filled with lubricant, the surfaces do not deflect under load, and there are no oil holes, grooves, or other interruptions in the bearing surfaces. In this case the geometry can be completely described by the ratios L/D and C/D, in which L is the bearing length, D is the journal diameter, and C is the diametral clearance, that is, the difference between the bushing inside diameter and the journal outside diameter. Take the typical length as D: the relative velocity, u, is proportional to DN where N represents the revolutions per unit time, and the parameter $\mu u/pL$ in eq 9-5 can be written in the more familiar form $\mu N/p$. The unit pressure p is taken as the load, W, divided by the *projected area*, DL. Thus for ideal journal bearings eq 9-5 can be written

$$f = \phi_4\left(\frac{\mu N}{p}, \frac{D}{C}, \frac{L}{D}\right)$$

In theoretical work with journal bearings it has been found convenient to rearrange the above expression as follows:

$$f\left(\frac{D}{C}\right) = \phi_5\left[\frac{\mu N}{p} \times \left(\frac{D}{C}\right)^2, \frac{D}{C}, \frac{L}{D}\right] \tag{9-6}$$

The quantity $[\mu N/p]\,(D/C)^2$ is called the *Sommerfeld variable* and is widely used in plotting the performance of both theoretical and actual bearings. The symbol S will be used for this quantity.

Petroff's Equation. A useful further simplification is the assumption that the journal runs concentric with the bearing. The tangential frictional force of such a bearing can be computed directly from the definition of viscosity. In this case referring to eq 9-2, $u/y = u/\frac{C}{2}$, and we can write

$$F/A = \mu 2\pi DN/C \tag{9-7}$$

where F is the tangential force and A is the area of the bearing surface, πDL.

If the load on this bearing is taken as W, $f = F/W$ and $p = W/DL$. Dividing both sides of eq 9-7 by W gives

$$f = 2\pi^2 \left[\frac{\mu N}{p} \times \frac{D}{C} \right]$$

or

$$f\left(\frac{D}{C}\right) = 19.7 \left[\frac{\mu N}{p} \times \left(\frac{D}{C}\right)^2 \right] \tag{9-8}$$

The foregoing expression is a form of *Petroff's equation* and is useful because the friction of real bearings approaches the Petroff value at high values of $\mu N/p$.

Friction of Real Journal Bearings. Figures 9-3 and 9-4 show measured values of $f(D/C)$ vs S for real journal bearings with steady unidirectional load. These results come from test bearings in which the structure was very stiff, hence deflections were minimized. Petroff's values are included in several cases for comparison.

Important conclusions which have been drawn from such work are the following:

1. The linear portion of such curves represents the zone of hydrodynamic operation. The point at which the curves depart from linearity, as S decreases, indicates the beginning of metallic contact and *partial-film* operation. This point may be called the *transition* point.

2. Effects due to bearing materials, oil composition, load, speed, etc, appear only in the partial-film region. This result confirms the validity of eq 9-6.

3. In the hydrodynamic region the coefficient of friction of real journal bearings is of the form

$$f = f_0 + f_1 \left(\frac{\mu N}{p}\right) \tag{9-9}$$

in which the values of f_0 and f_1 depend on the geometry of the bearing, including the shape and location of oil grooves and holes.

Although not strictly a question of friction, the following relations are of interest and importance in bearing design and operation.

4. Because of the fact that oil viscosity decreases with increasing temperature operation at values of S above the transition point tends to be *stable*, whereas the reverse is true for operation at values of S below the transition point. This conclusion can be explained by noting that increased friction means increased heat generation and higher oil temperature. In the stable region anything which increases the work of friction lowers the oil viscosity and prevents f from increasing indefi-

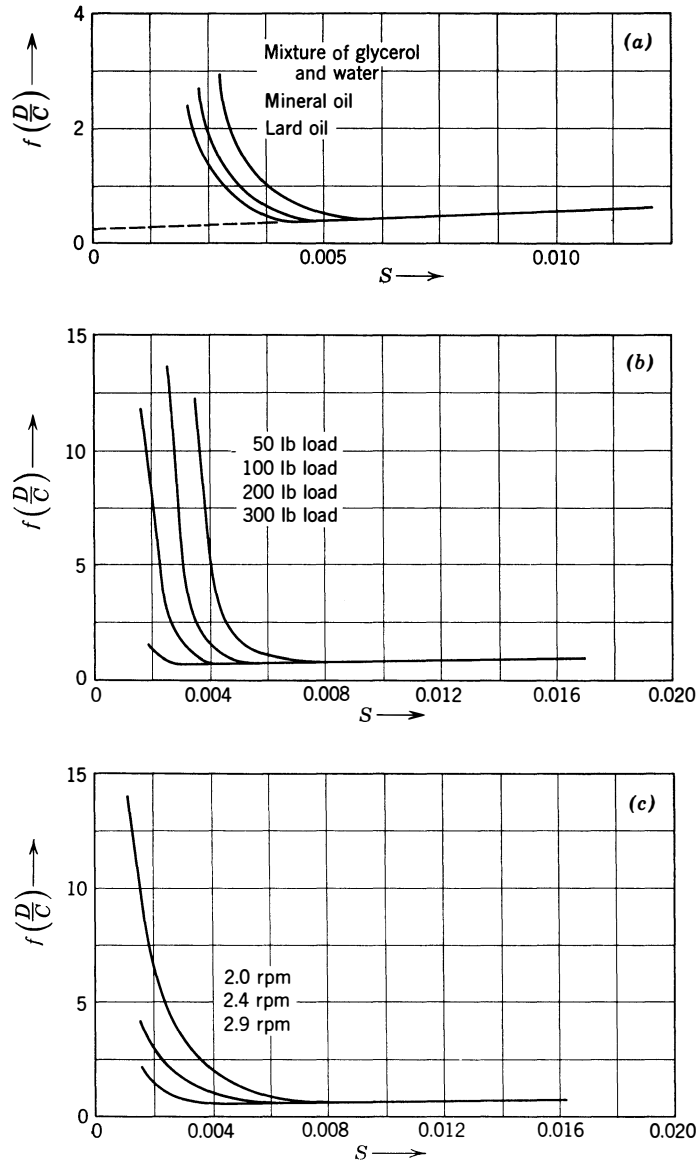

Fig 9-3. Coefficients of friction vs Sommerfeld variable for journal bearings at low values of S:

$$S = \left(\frac{\mu N}{p}\right)\left(\frac{D}{C}\right)^2$$

(*a*) Different lubricants: $D/C = 359$ (ref 9.24). (*b*) Different loads: $D/C = 1100$; $L/D = 1$ (ref. 9.20). (*c*) Different speeds: $D/C = 100$; $L/D = 1$ (ref 9.20).

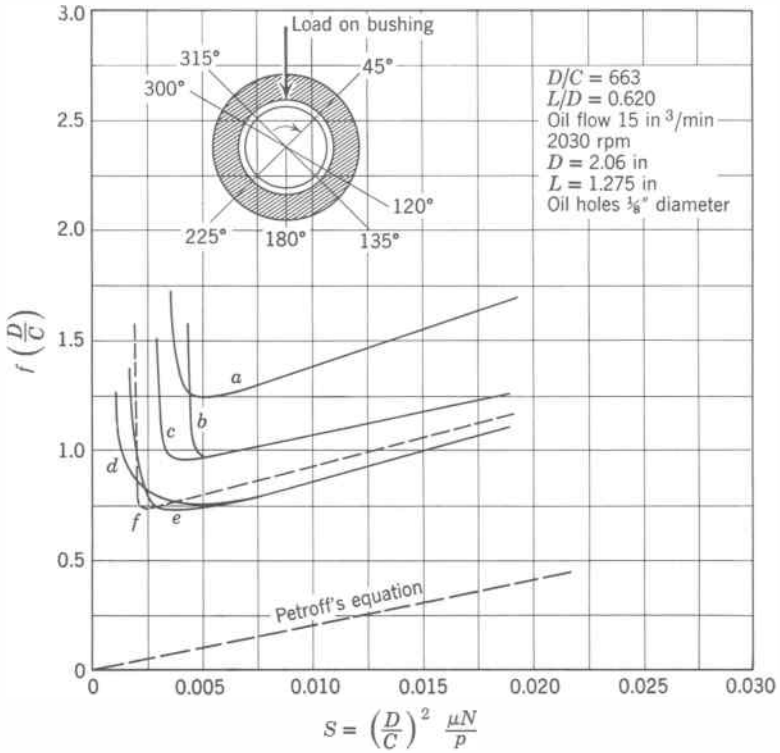

Fig 9-4. Effect of oil supply geometry on journal-bearing performance, steady unidirectional load. Oil feed under pressure into (*a*) circumferential groove in bushing; (*b*) 4 holes in bushing of 45°, 135°, 225°, and 315° from load; (*c*) 2 holes in bushing at 120° and 300° from load; (*d*) axial groove at feed hole in bushing, ⅛ in wide, 180° from load, ½ length of bushing; (*e*) 1 hole in bushing, 180° from load; (*f*) 1 hole in shaft, rotating with shaft. Center of hole or groove always lies in center plane of bearing. (McKee, refs 9.21 and 9.22)

nitely. In the unstable region an increase in the work of friction lowers μ, decreases S, and *increases* f. The increase in f leads to further heating, and so on to complete bearing failure, unless a point is reached at which the heat is dissipated with sufficient rapidity to prevent further increase in temperature.

5. Grooves, oil holes, and similar interruptions in the bearing surfaces in the region of high oil-film pressure * increase friction and move the transition point toward higher values of S. (See Fig 9-4.)

* This region lies between $+90°$ and $-90°$ of circumference measured from the point of load application on the *bearing*, except close to the *ends* of the bearing where the pressure is always small. (See ref 9.25.)

6. Work on the subject of bearing deflection (refs 9.24—) has shown that structural deflections *may* be helpful but are usually harmful. A type of deflection leading to serious increase in friction is lack of parallelism of the journal and shaft axes.

Oscillating Journal Bearings. Present fluid-film theory (ref 9.26) does not account for the fact that oscillating bearings, such as piston pins and knuckle pins, can carry extraordinarily heavy loads without apparent rupture of the film. Apparently these bearings operate most of the time in the hydrodynamic region, for otherwise wear caused by surface contact would be much more serious than it proves to be in service (see later discussion of wear). One reason why such bearings are successful may be that the average linear velocity is very low, hence the rate of heat generation is small.

The friction of oscillating bearings will depend on the parameters of eq 9-5 plus the angle of oscillation. The velocity u would ordinarily be taken as the average surface speed of the bearing. Few experimental data are available concerning the friction of such bearings. In engines these bearings normally oscillate through such small angles that their total contribution to engine friction must be small.

Sliding Bearings (refs 9.3—). Figure 9-5 represents a flat slider moved over a lubricated plane surface by the horizontal force F applied

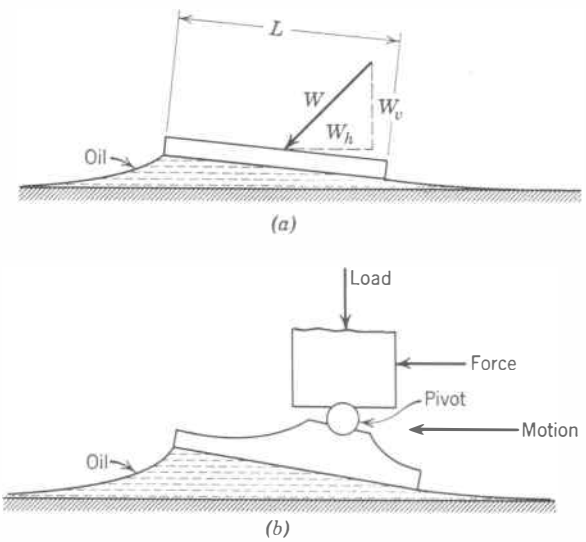

Fig 9-5. (*a*) Action of a plane slider under constant load and at constant velocity. (*b*) Michel or Kingsbury type bearing element, using the principle of the plane slider.

at the same point as the vertical load W_v. If the point of load application is behind the center of the slider, with reference to the direction of motion, the slider will take up a sloping position as indicated to form a wedge-shaped oil film as it moves over the lubricated surface. Similar action will result from a slider which has its leading edge slightly curved upward like the runner of a sled, even though the load is applied at or ahead of the center of the slider. Expression 9-5 again applies, and the

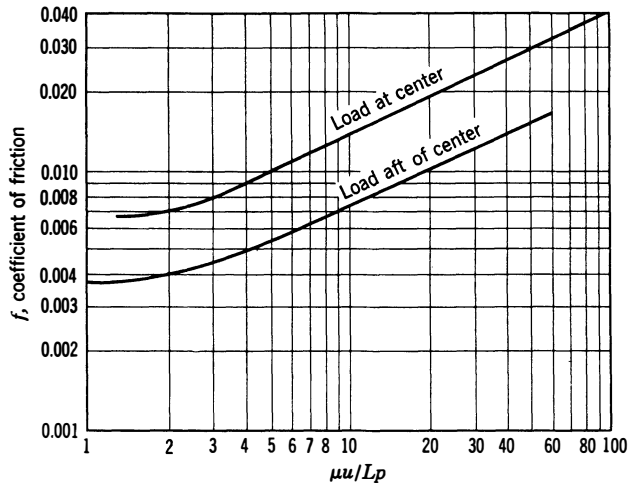

Fig 9-6. Coefficients of friction of slider bearings. (Fogg, ref 9.33)

coefficient of friction depends on the design ratios of the slider, and on the parameter $\mu u/pL$, where L is the slider length.

Figure 9-6 shows results of experiments on sliders. In the fluid-film region the coefficient of friction follows an expression of the form

$$f = f_0 + f_1 \left(\frac{\mu u}{Lp}\right)^{1/2} \tag{9-10}$$

MECHANICAL FRICTION OF ENGINES

From the foregoing discussion it is evident that mechanical engine friction must consist chiefly of the friction of journal and sliding bearings operating in the fluid-film regime.

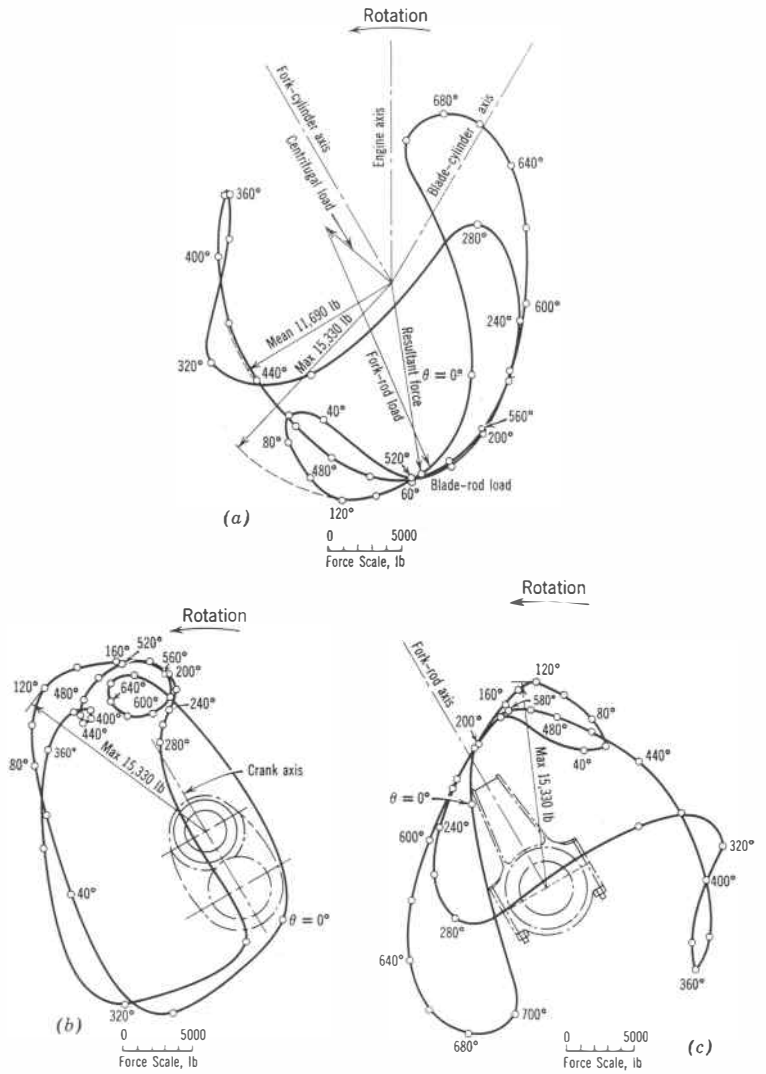

Fig 9-7. Bearing-load diagrams: (*a*) Polar diagram showing the magnitude of the resultant force on the crankpin of the Allison V-1710 engine and its direction with respect to the engine axis. Engine speed, 3000 rpm; imep, 242 psi. (*b*) Polar diagram showing the magnitude of the resultant force on the crankpin of the Allison V-1710 engine and its direction with respect to the crank axis. Engine speed, 3000 rpm; imep, 242 psi. (*c*) Polar diagram showing the magnitude of the resultant force on the crankpin bearing of the Allison V-1710 engine and its direction with respect to the fork-rod axis. Engine speed, 3000 rpm; imep, 242 psi. (*Courtesy of NACA*)

Journal-Bearing Friction. The main differences between journal bearings in engines and the bearings represented by Figs 9-3 and 9-4 is that in the principal engine bearings, loads vary with time both in direction and magnitude. These loads can be computed from the indicator diagram and from the weights and dimensions of the moving parts. Reference 9.03 gives methods of computation and some data from typical engines. Figure 9-7 is an example of the crankpin bearing loading for one particular engine.

The subject of the effect of load variation on journal-bearing friction has received considerable theoretical treatment (ref 9.26) but does not yet give a completely satisfactory explanation of bearing behavior in engines. For example, theory indicates that when loads vary sinusoidally at a frequency equal to $\frac{1}{2}$ the journal rpm the oil film will rupture, and the result will be high friction and wear. However, in four-stroke engines a large component of the load varies at $\frac{1}{2}$ journal speed, yet very heavy loads are carried.

Another important difference between engine bearings and those represented in the foregoing figures is that, in general, the supporting structure in engines is more flexible and distortions are, therefore, relatively greater. Some data on the effect of distortion on bearing friction are given in refs 9.24 and 9.241.

In spite of these differences, the general behavior of journal bearings in engines appears to be similar to that of the test bearings of Figs 9-3 and 9-4 and the same basic laws appear to apply, although absolute values of the coefficients are undoubtedly different. For example, in the absence of serious distortion the coefficient of friction of engine bearings must be a function of $\mu u/pL$ in which u and p are *average* values of the linear speed and the unit load.

Piston Friction. Observation of piston behavior by means of glass cylinders (refs 9.40—) has shown that qualitatively, at least, a trunk piston behaves like a pivoted plane slider. The piston tilts in such a way that on the loaded side the oil film at the leading edge is nearly always thicker than at the trailing edge. These tests also showed that the quantity of lubricant between the piston and the cylinder wall is normally insufficient to fill the entire space between the piston and the cylinder wall. The complete oil film is on the loaded side only and extends for a limited distance on either side of the plane perpendicular to the crankshaft through the cylinder center line. Under these circumstances, as with a plane slider, it is evident that the average oil-film thickness between piston and cylinder wall varies with load and speed.

In order to assist in building up the oil film, piston skirts are sometimes

relieved slightly at each end to give a *sled-runner* effect. Although this alteration may assist the process, it is evidently not essential, since most successful pistons are not so designed. The very small amount of wear normally experienced on piston skirts is an indication that lubrication of this surface is for the most part in the complete-film region. What small wear there is usually occurs in a manner to create a sled-runner effect.

Piston Ring Friction. Piston rings are of two kinds—*compression rings* designed to seal against gas pressure and *oil rings* designed to limit the passage of oil from the crankcase to the combustion space.

In compression rings the force between the piston ring and the cylinder wall is due partly to the elasticity of the ring and partly to the gas pressure which leaks into the groove between the ring and the piston. Experiments have shown that the gas pressure in the top ring groove is nearly cylinder pressure, with less-than-cylinder pressure in the second ring groove and very little in the third (ref 9.47). Oil rings generally have their ring grooves *vented* by holes drilled into the piston interior, and therefore no gas pressure can build up in their grooves. In this case the pressure of the ring surface on the cylinder walls is due entirely to ring elasticity.

Because of their spring action piston rings press against the cylinder walls at all times; that is, there is no period without load. Theoretically, under these circumstances, hydrodynamic lubrication can exist only if (*a*) the sliding surface of the ring operates at an angle to the cylinder wall, or (*b*) the corners of the ring are rounded. However, even with rings whose corners are apparently sharp there is enough rounding and tilting so that piston rings normally operate without metallic contact except very near top and bottom of the stroke. (See ref 9.41.) Here the velocity is so low that this contact involves much less friction and wear than might at first be anticipated.

Antifriction Bearings. The friction of ball and roller bearings (ref 9.35) and of such parts as tappet rollers is due in part to local deflection of the track, or *race*, which causes a slight ridge ahead of the roller, plus some local sliding which takes place in the interface between roller and race. Contrary to popular belief, the coefficient of friction of antifriction bearings is not much lower than that of well-lubricated journal bearings operating at normal values of S. Unless flooded with oil, the friction coefficient of antifriction bearings is nearly independent of of oil viscosity, and it is therefore evident that such bearings will have much lower friction in starting and at low oil temperatures than corresponding journal bearings. Unfortunately, this characteristic is of

little advantage in reciprocating engines because most of the friction in starting is due to pistons and piston rings. When antifriction bearings are used in engines it is because of characteristics not connected with friction. For example, ball and roller bearings do not require force-feed lubrication and take up less axial space than corresponding journal bearings.

Since journal bearings in turbines normally have to run at very high values of S, hence high values of f, there is considerable advantage in using antifriction bearings in gas turbines. Here the low starting friction of such bearings is an important advantage, especially since gas turbines require rather high rpm for starting.

Mechanical Friction mep

The most convenient measure of mechanical friction, as already suggested, is in terms of mean effective pressure.

The power, P_m, absorbed by mechanical friction in an engine may be expressed as

$$P_m = Fs = Wfs \tag{9-11}$$

and the mean effective pressure as

$$\text{mmep} = \frac{(2 \text{ or } 4)P_m}{A_p s} = \frac{(2 \text{ or } 4)Wf}{A_p} \tag{9-12}$$

where F = a force which, multiplied by the piston speed will give the observed power, P_m
s = mean piston speed
f = a mean coefficient of friction
W = a mean load, such that $W = F/f$
A_p = the piston area

The numbers 2 and 4 are to be used for two-stroke and four-stroke engines, respectively.

It is apparent that mechanical friction mean effective pressure in a given engine varies directly with the product Wf. Although we cannot evaluate these quantities separately, the conception is useful for purposes of explaining experimental results.

The average loads on the bearing surfaces of any engine must be of the following types:

1. *Fixed loads* include loads due to gravity, to piston-ring tension, and to spring tension on glands, oil seals, etc.

2. *Inertia loads* proportional to mass $\times$ (piston-speed)^2.

3. *Gas loads* which can be taken to consist of a fixed mean load due to compression and expansion without firing, plus a load nearly proportional to the imep.

Measurement of Mechanical Friction mep

The mechanical friction mep of an engine can be measured by measuring indicated and pumping mep with an indicator and the bmep by means of a dynamometer, auxiliaries * being removed or separately driven. Since the result is a difference which is usually small compared to either quantity measured, the measurements must be very accurate. This method is the only one available for measuring mechanical friction with the engine in normal operation, but it has been little used on account of the scarcity of accurate indicators and the amount of work involved, especially in multicylinder engines, in which each cylinder must be indicated for each condition of operation.

The commonest method of measuring friction is by *motoring*, that is, by determining the power required to drive a nonfiring engine by an outside source of power.

In two-stroke engines, with auxiliaries removed, the motoring power is due to mechanical friction, except the very small work done to make up the heat lost during compression and expansion of the air in the cylinder. Cylinder pressures are those due to this compression and expansion process.

To measure mechanical friction in four-stroke engines the pumping loss must be eliminated. This may be accomplished by one of the following means:

1. Cylinder heads or valves are removed. In this case there is no gas-pressure load on the pistons.

2. Valves are kept closed. In this case there is compression and expansion of air during each revolution, but the average cylinder pressure is near atmospheric, due to leakage.

3. The engine is not altered, but an estimated or measured pumping mep is subtracted from the motoring mep.

* Usually only the important power-absorbing auxiliaries, such as compressor or scavenging pump, fan, and generator, are removed. The power absorbed by water and oil pumps is usually considered part of the mechanical friction. In most cases the power absorbed by these pumps is relatively small.

The obvious objection to all motoring methods is that the engine is not firing, and therefore neither pressures on nor temperatures of the bearing surfaces are representative of conditions under normal operation. The amount of error which these differences involve will appear as the discussion proceeds.

Finally, friction may be measured by means of especially designed apparatus, several examples of which are included in the subsequent discussion.

In presenting the results of friction measurements the method used, together with comments on its probable significance and accuracy, is given in each case.

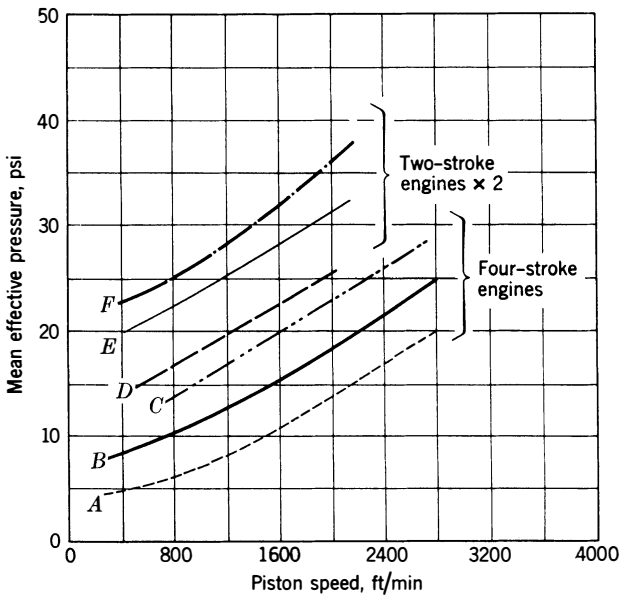

Curve	Type	Cycle	No. cyls	Bore, in	Stroke, in	p_i, psia	imep, psi	Method	Reference
———	Automotive	4	6	3⅛	4¾	—	0	a	9.561
—·—·—	Automotive	4	6	3⅛	4¾	—	240*	a	9.561
- - - -	Aircraft	4	12	5.5	6	—	0	a	9.703
— —	Test	2	1	4.5	6	14.7	0	b	7.34
———	Test	2	1	4.5	6	22.7	0	b	7.34
—•—	Diesel	2	6	4.25	5	—	0	b	7.30

* 60 psi steady pressure on pistons. See table page 332.

Fig 9-8. Mechanical fmep of several engines. Methods: (*a*) motoring without cylinder heads or valves; (*b*) motoring with compression and expansion of air. Jacket temperature normal in all cases (150–180°F). Oil viscosity unknown.

Figure 9-8 shows the experimental data available to your author on the mechanical friction mep of typical engines. The method by which each curve was obtained is indicated below the figure. The mep plotted for the two-stroke engines is doubled so as to be comparable with that of four-stroke engines. In both cases mep is normally computed on the basis of the firing strokes only.

The greater friction of the two-stroke engines shown in Fig 9-8 is due to the following factors:

1. The two-stroke engines were motored with cylinder heads in place, hence with gas loads during each revolution. Cylinder pressures are especially high in the Diesel engine, curve *F*, which has a compression ratio of 16. The four-stroke engines were motored without any cylinder pressure, except in the case of curve *C*, which had a steady pressure of 240 psi in the cylinders.
2. Two-stroke engines have longer and heavier pistons and usually have more piston rings than corresponding four-stroke engines. Thus the inertia loads and ring loads are generally higher.

Based on the power stroke only, the two-stroke engines have mechanical friction mep quite comparable with that of four-stroke engines, which indicates that their actual friction forces are nearly double those of corresponding four-stroke engines.

Distribution of Mechanical Friction. Figure 9-9 is computed from motoring tests made on two quite different engines. Mechanical friction was measured by motoring with auxiliaries removed and valves closed. Piston friction was taken as mechanical friction minus twice the friction measured with pistons and rods removed. If this assumption is accepted, the results indicate that piston friction accounts for $\frac{3}{4}$ of the mechanical friction in the average multicylinder engine.

Effect of Cylinder Pressure. Since the curves of Fig 9-8 were not made with normal cylinder pressures, it is of interest to explore the effect of cylinder pressure on mechanical friction. Interesting information in this connection is provided by M. Taylor. (See ref 9.561.) In this work motoring friction of a six-cylinder engine was measured with a steady pressure on the pistons. For this purpose the valves were removed and the openings to the atmosphere of the inlet and exhaust manifolds were closed so that a constant air pressure could be applied to the space above the pistons. Figure 9-10 shows that mechanical friction increases with increasing steady pressure on the pistons.

Allowing for the fact that the high pressures in an engine cycle occur near top center where piston motion is slow, your author has estimated

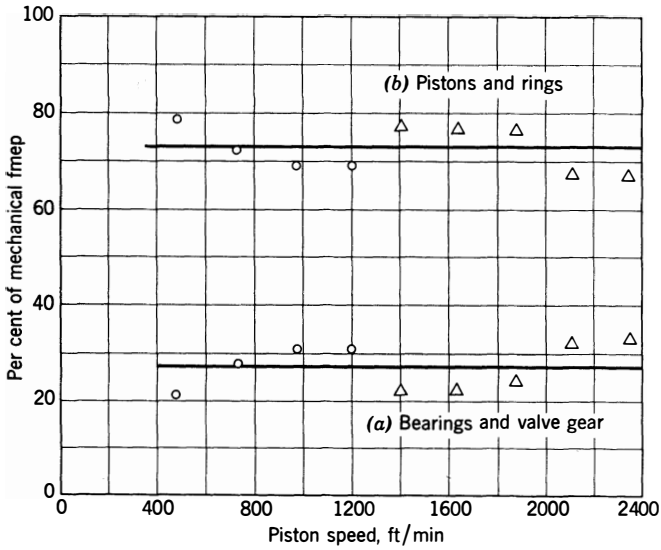

Fig 9-9. Distribution of mechanical friction:

○ Chrysler 6-cyl auto engine, 3⅛ x 4¾ in (Sloan Automotive Laboratories)
△ Liberty V-12 aircraft engine, 5 x 7 in (U.S. Air Force)
(*a*) Based on motoring mep without rods and pistons × 2
(*b*) Based on motoring mep, valves closed, minus mep (*a*)

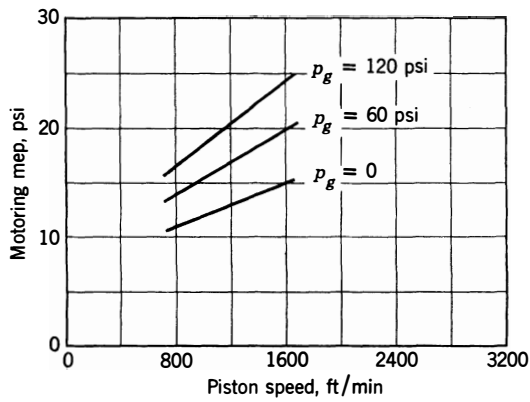

Fig 9-10. Effect of a constant gas pressure on mechanical friction. Results of motoring tests on Chrysler 6-cyl engine with valves removed and air pressure applied to closed inlet and exhaust manifolds. p_g = steady gas pressure on pistons.

that, in the case of four-stroke spark-ignition engines, the steady pressure which would have an effect on friction equivalent to that shown in Fig 9-10 would be about one fourth of the mean effective pressure. Correspondingly, for four-stroke Diesel engines, the equivalent steady pressure will be about half the mean effective pressure. For two-stroke engines, the equivalent steady pressure will be twice those of the corresponding four-stroke types. Thus the effect of changes in mean effective pressure on friction can be estimated from Fig 9-10 by means of the following table:

Engine Type	To Obtain Equivalent Steady Pressure Multiply imep by
Four-stroke SI	0.25
Two-stroke SI Four-stroke Diesel	0.5
Two-stroke Diesel	1.0

Effect of Oil Viscosity. Figure 9-11 shows mechanical friction mep plotted against nominal oil viscosity at jacket temperature. Since oil-pan temperature was not changed, it is probable that the oil viscosity in the journal bearings was nearly constant. Thus the effects shown must be due chiefly to changes in piston friction. The fact that the curves tend to become horizontal at the higher viscosities is partly due to the square root relation for sliders. (See expression 9-10.) Observations with glass cylinders (refs 9.41–9.421) show that pistons operate with an oil film covering only part of the piston. The fact that oil is supplied to the pistons by throw-off from the rods introduces the possibility that the oil film becomes smaller in area as viscosity increases. Such a reduction in film area would tend to offset the greater shearing resistance of the film as viscosity increases. However, most engines operate in the range in which oil viscosity has a marked effect on friction.

Piston and Ring Friction. A method recently used to study piston friction (ref 9.48) employed a special engine with a cylinder sleeve free to move axially against a stiff spring (Fig 9-12). By measuring the very small axial motion of the barrel, piston friction forces have been measured directly under actual operating conditions.

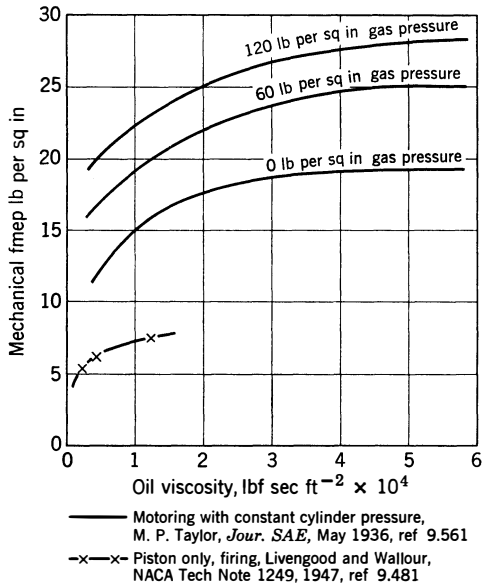

Fig 9-11. Effect of oil viscosity on engine friction.

Figure 9-13 shows friction force vs piston position for a typical set of operation conditions. The following features are notable:

1. The average force of friction on the compression and exhaust strokes is nearly the same.
2. The average force of friction on the power stroke (15 lbf) is about twice that on the suction stroke (7 lbf).
3. Forces tend to be high just after top and bottom centers, probably because these are the points where the piston rings have metallic contact with the cylinder walls.
4. The force is not zero at top and bottom centers. This is probably due to deflection of the engine parts such that piston velocity does not reach zero exactly at the top and bottom center positions of the crank.

Figure 9-14 shows the effect of several operating variables on piston-friction mep, as measured in diagrams such as those of Fig 9-13. These curves show that:

1. Piston friction mep increases with increasing oil viscosity in a manner similar to that shown in Fig 9-11.

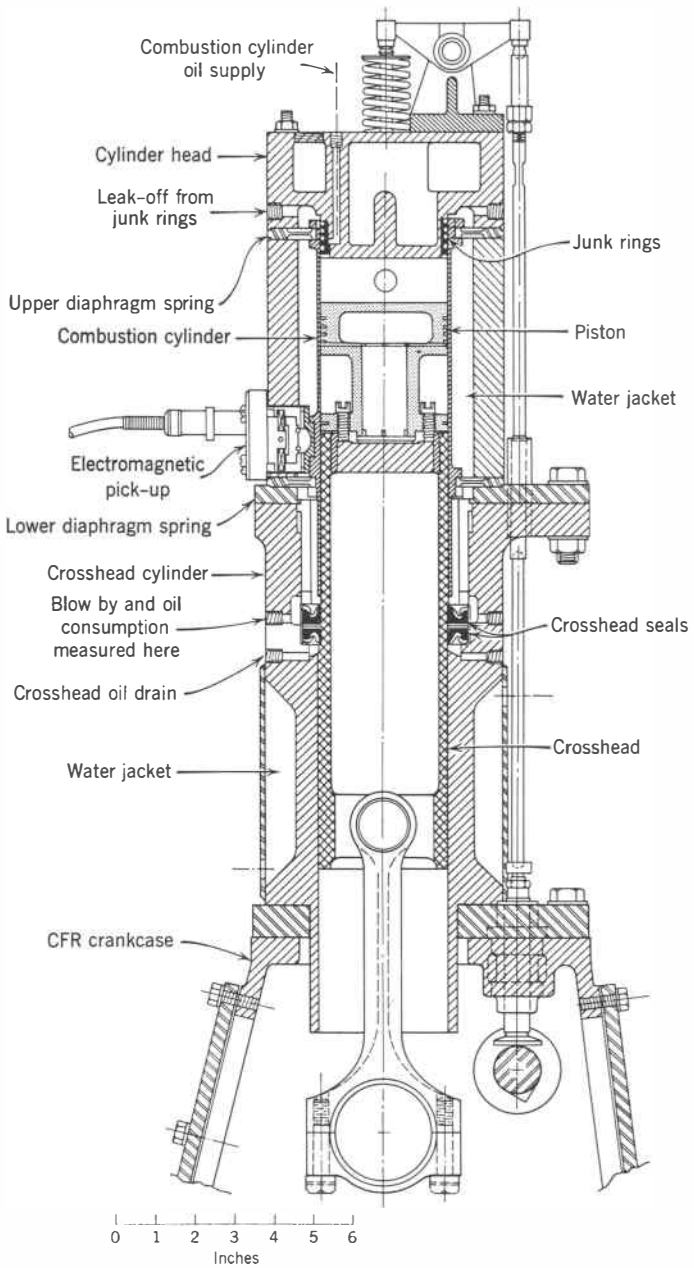

Fig 9-12. Friction-research engine with spring-mounted cylinder barrel: 3.25 in bore; 4.50 in stroke; $r = 5.05$; can be used with or without crosshead. (Livengood and Wallour, ref 9.481)

2. Piston friction mep increases with increasing piston speed, as already indicated by Figs 9-8–9-10.

3. Piston friction mep increases with increasing imep. The increase is about 3 lb for 100 lb increase in imep, which is nearly the same as predicted by means of the table on page 332 and the tests of Fig 9-10.

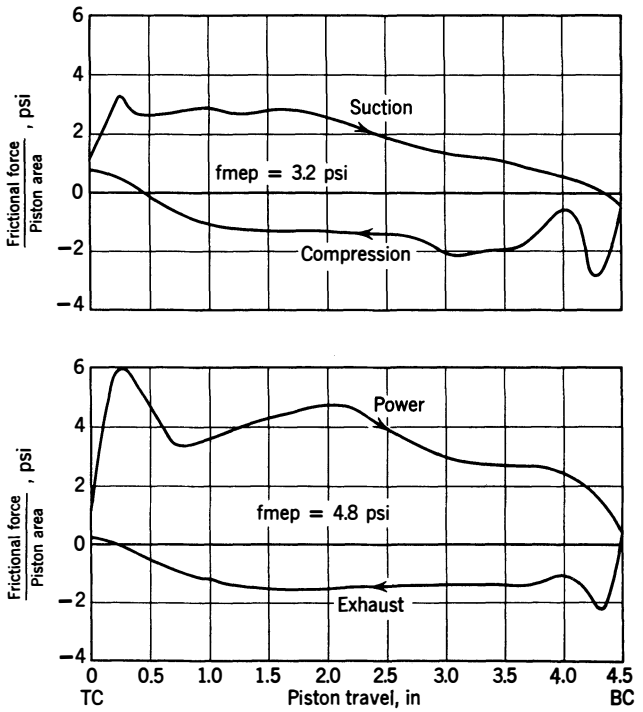

Fig 9-13. Piston-friction diagrams. Engine of Fig 9-12 without crosshead; piston speed 900 ft/min; bmep 85 psi; T_c = 180°F; oil temp 180°. (Leary and Jovellanos, ref 9.48)

For the runs shown by dashed lines in Fig 9-14, the piston was guided by a cross-head in such a way that only the rings came in contact with the cylinder sleeve. Under these conditions the friction of the rings only was about 80% of the friction of the whole piston assembly. From this result it seems safe to conclude that the greater part of piston friction under operating conditions is caused by the piston rings.

Effect of Design on Mechanical Friction. A striking feature of Fig 9-8 is the relatively low mechanical friction of the aircraft engine, compared to the others. The important features which contribute to

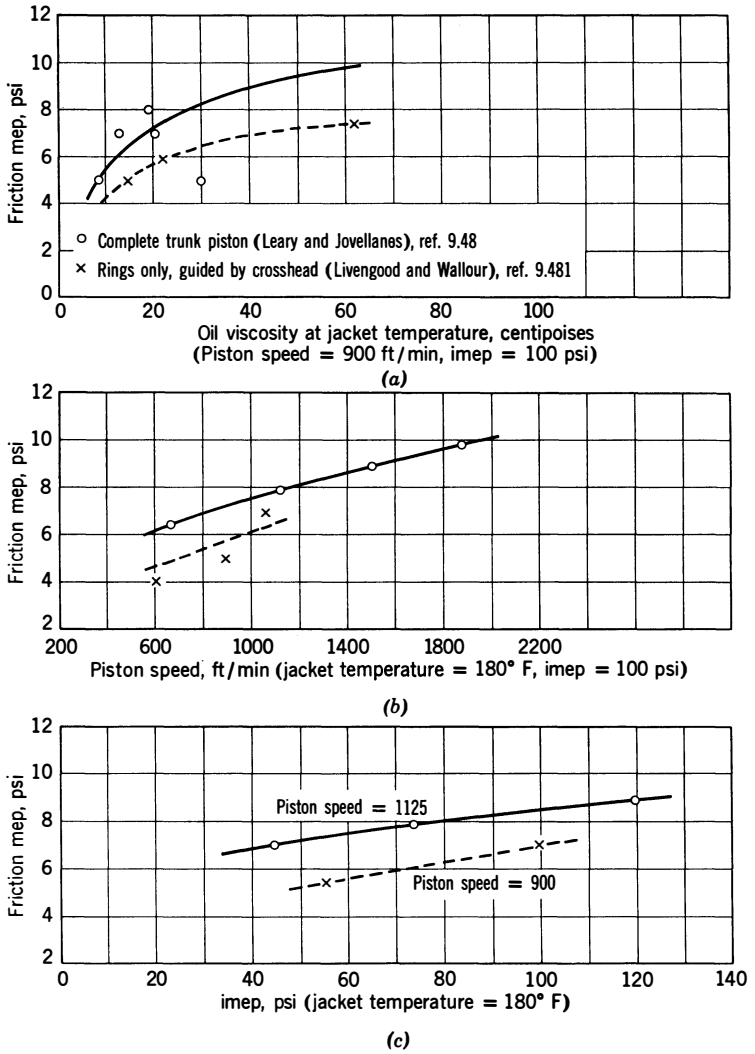

Fig 9-14. Piston and piston-ring friction. (Engine of Fig 9-12)

this result appear to be the following:

1. Light reciprocating parts, which minimize inertia loads.
2. Large piston-to-cylinder clearances, which limit the extent of the piston oil film.
3. Short pistons, with the nonthrust surfaces cut away.

4. Few piston rings and light ring pressure.
5. Low D/C ratios of the journal bearings. (See eq 9-8.)

In general, the differences between curves A and C and between curves F and D of Fig 9-8 are due to the combined effects of the foregoing items listed. When a low engine noise level is required, as in automobiles,

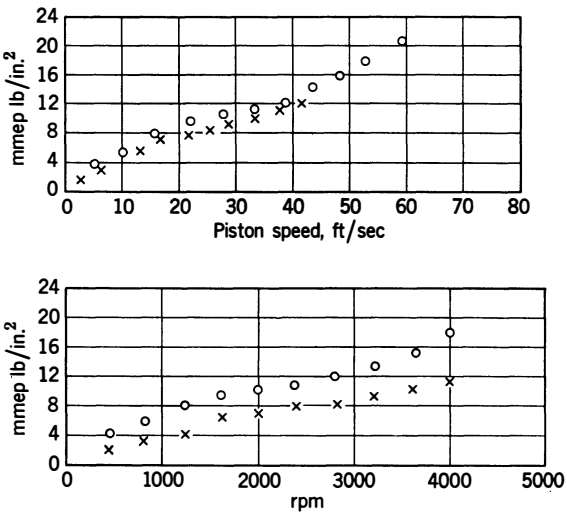

Fig 9-15. Effect of stroke-bore ratio on mechanical friction. Automobile engines with cylinder heads removed:

Symbol	No. cyl	Bore, in	Stroke, in	S/b
O	6	3.31	4.75	1.43
X	8	3.38	3.25	0.96

(Hardig et al., ref 9.713)

piston and bearing clearances must be minimized, and thus requirements for low friction are in conflict with those for low noise level.

Stroke-Bore Ratio. In recent years the stroke-bore ratio has been reduced to 1.00 or even less in many automobile engines, and claims have been made that this change reduces friction mep.

Figure 9-15 shows the results of mechanical-friction tests on two automobile engines with almost the same bore. It is evident that mechanical friction mep is nearly independent of the stroke at a given piston speed. (See also Fig 9-28.) At the same rpm, of course, mmep is larger

for the engine with the longer stroke. This relation is the basis for the claim of "less friction" for small stroke-bore ratios.

Effect of Engine Size on Mechanical Friction. It is readily shown (see Appendix 7) that in similar engines running at the same piston speed and imep unit pressures will be the same; therefore, W/A_p in eq 9-12 will be the same in such engines. Since piston speed is constant, it follows that for constant $\mu u/Lp$ the ratio μ/L must be constant. It is thus

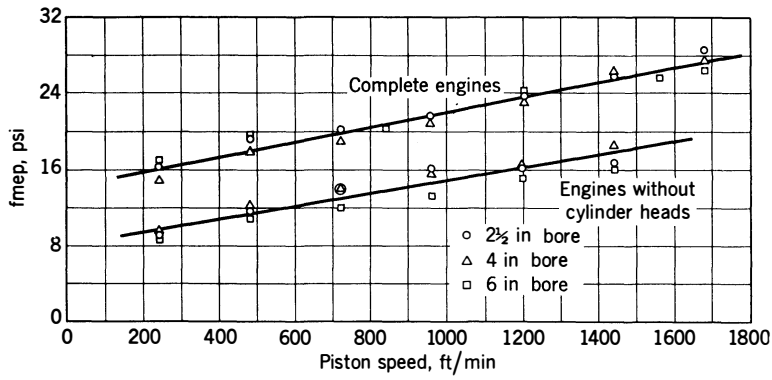

Fig 9-16. Motoring friction mep of MIT similar engines. Jacket water temperature 150°F in, 180°F out. Oil viscosities at 250°F proportional to bore. (Aroner and O'Reilly, ref 9.582)

evident that if the viscosity in oil films is held proportional to the bore the friction coefficients in similar engines should be the same at the same piston speed. Friction forces will then be proportional to bearing *areas*, and the *mechanical friction mep should be the same regardless of size.*

Figure 9-16 shows motoring friction mep vs piston speed, obtained by motoring, for the three geometrically similar engines at MIT. (See Fig 6-15.) The oil viscosity was chosen to be proportional to the bores at 250°F. The figure shows that friction mep at a given piston speed is nearly the same for the three engines. A slight tendency toward reduced fmep with increasing bore might be read from the curves made without cylinder heads. If this is not experimental error, it could be attributed to the fact that the oil-film temperatures on the cylinder walls are higher as the bore becomes larger due to heat-flow considerations explained in Chapter 8.

PUMPING MEP IN FOUR-STROKE ENGINES

Pumping mep of Ideal Cycles. The pumping mep of four-stroke cycles with ideal inlet and exhaust processes, as described in Chapter 6, is evidently $(p_e - p_i)$.

Pumping mep of Real Cycles. Typical light-spring diagrams have already been shown (Figs 6-7 and 6-8) and discussed from the point of

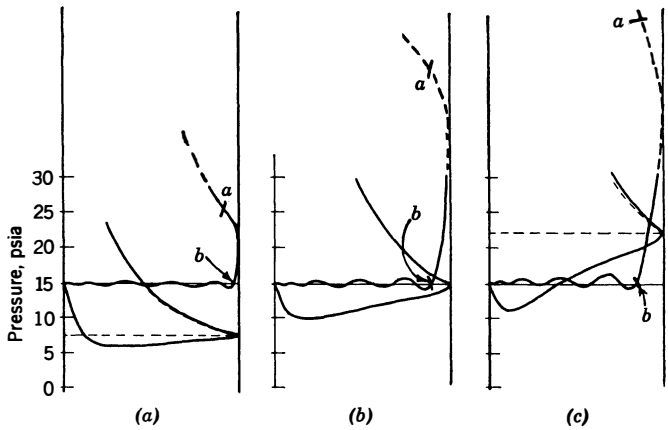

Fig 9-17. Light-spring diagrams: *a–b* is the exhaust blowdown process; CFR 3.25 x 4.5 in engine:

	(*a*) Throttled	(*b*) Normal	(*c*) Supercharged
Inlet pressure, psia	7.4	14.8	22.1
Exhaust pressure, psia	15.0	15.0	15.0
Inlet-valve Z factor	0.4	0.4	0.4
Approx mean piston Speed ft/min	2200	2200	2200

(Grisdale and French, ref 9.61)

view of their relation to air capacity. Figure 9-17 shows additional light-spring diagrams.

For convenience, discussion of the pumping work is divided into separate discussions of the exhaust stroke and the inlet stroke.

Exhaust Stroke

Exhaust Blowdown. As we have seen in Chapter 6, it is necessary to open the exhaust valve before bottom center on the expansion stroke in order to get the cylinder pressure down to the exhaust-system pressure, if possible early in the exhaust stroke. At bottom center the cylinder pressure is usually still considerably higher than the exhaust-system pressure, but, as the exhaust stroke proceeds, the pressure falls rapidly and at some point arrives at, or approaches very closely, the exhaust-system pressure, p_e. The process from bottom center to the point at which cylinder pressure reaches or closely approaches p_e (process a–b in Fig 9-17) is called the *blowdown.* A considerable part of this process may be, and usually is, in the *critical range* in which the ratio of p_e to cylinder pressure is below about 0.54 * and the gas velocity in the smallest flow cross section is the velocity of sound in the gases at that point. Since exhaust-gas temperatures are high, the gas velocity through the valve opening is very high during the critical portion of blowdown.

Since the speed of the gases through the exhaust valve is independent of piston speed during the critical part of blowdown, the process occupies an increasing number of crank degrees as piston speed increases. This trend is clearly shown in Figs 6-7 and 6-8.

Exhaust Process After Blowdown. In many cases, at the end of the blowdown process, the inertia of the exhaust gases causes the pressure to fall below p_e. In such cases the cylinder pressure will fluctuate at a frequency dependent on the design of the exhaust system as well as on the operating conditions.

In the absence of appreciable dynamic effects the exhaust stroke mep can be quite accurately predicted from the equations of fluid flow through an orifice, provided the area and flow coefficient of the exhaust valve as a function of crank angle are known, together with the rpm, cylinder pressure, and density at the time of exhaust-valve opening and the pressure in the exhaust system. For an example of such an analysis see ref 6.42. Unfortunately, such calculations are extremely laborious, and in most practical cases the necessary data on which they must be based are not available.

Figures 6-7 and 6-8 were made from an engine in which γ, the ratio of exhaust-valve flow capacity to inlet-valve flow capacity, was abnormally large (about 2.0) because the inlet valve was *shrouded* † for 180°. In engines with the more normal value of γ (0.60–1.00), near the end of the

* Taking k as 1.35 for the exhaust gases, the critical pressure ratio is 0.542.

† The *shroud* closes part of the flow area in order to create air swirl in the cylinder.

exhaust stroke, there may be an appreciable rise in pressure due to the fact that the flow area is being restricted by the closing of the exhaust valve.

Ratio of Exhaust mep to Ideal Exhaust mep. The ratio of actual exhaust work to theoretical exhaust work is equal to mep_e/p_e, where mep_e is the mean pressure during the exhaust stroke. Assuming a steady exhaust-system pressure, we can say, from our knowledge of the laws of fluid flow, that the cylinder pressures during the exhaust process will be a function of the following:

p_e = exhaust-system pressure
p_0 = pressure at exhaust-valve opening
T_0 = temperature at exhaust-valve opening
s = mean piston speed
d_e = diameter of the exhaust valve
C_e = mean flow coefficient of the exhaust valve
b = cylinder bore

We have seen that the pressure and temperature at exhaust-valve opening is chiefly dependent on the volumetric efficiency, the fuel-air

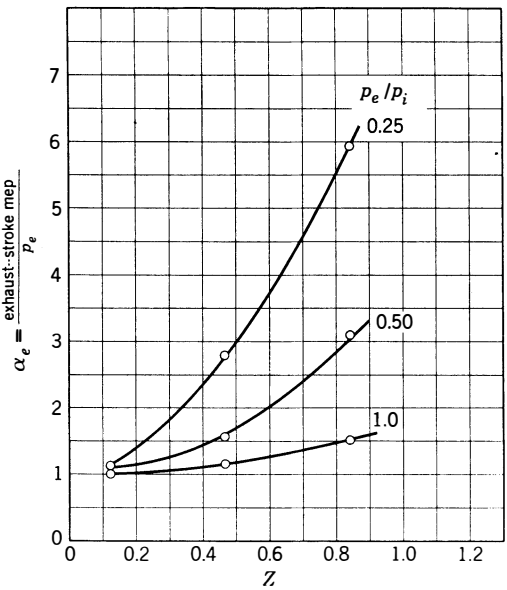

Fig 9-18. Ratio of exhaust-stroke mep to exhaust pressure: CFR engine, 3¼ x 4½ in, $r = 4.9$; $T_i = 580°\text{F}$; $p_e/p_i = 1.0$, 0.5, and 0.25; $\gamma \cong 1.2$. (From indicator diagrams taken by Livengood and Eppes in connection with ref 6.44)

ratio, and the compression ratio. Taking the volumetric efficiency as a function of p_e/p_i and the inlet-valve Mach index Z (see Chapter 6), for four-stroke engines, we can write

$$\alpha_c = \text{mep}_e/p_e = \phi\left(\frac{p_e}{p_i}, Z, F, r, \gamma, R_1 - R_n\right) \tag{9-13}$$

where γ is $(D_e/D_i)^2 \times (C_e/C_i)$, the ratio of exhaust-valve area $\times$ flow coefficient to the same product for the inlet valve. The cylinder bore and piston speed are included in the value of Z, and the valve timing in the design ratios.

Figure 9-18 shows mep_e/p_e plotted against Z for a number of tests on spark-ignition engines running at constant values of F, r, and the design ratios. At low values of Z, $\alpha_e \cong 1$ as would be expected from Figs 6-7 and 6-8. These curves were made with γ, the exhaust/inlet-valve flow capacity near 1.0. Smaller values of γ would increase α_e at given values of Z and thus increase the exhaust-stroke loss.

Inlet Stroke

The curve of cylinder pressure vs cylinder volume during the inlet stroke can also be quite accurately predicted from compressible flow

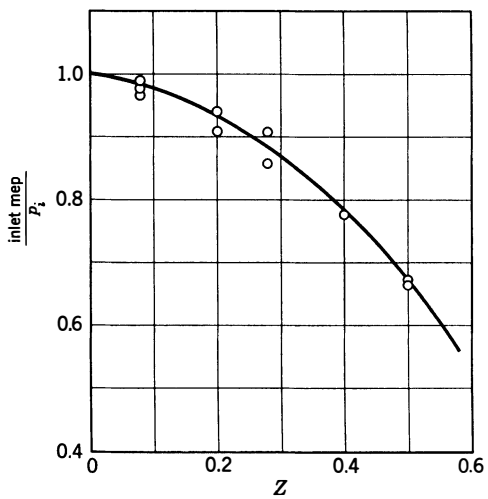

Fig 9-19. Ratio of inlet-stroke mep to inlet pressure: CFR engine 3¼ x 4½ in; r = 4.9; T_i = 580°F; p_e/p_i = 1.0, 0.5, and 0.25; $\gamma \cong 1.2$. (From indicator diagrams taken by Livengood and Eppes in connection with ref 6.44.)

equations under the same limitations stated for the exhaust process. An illustration of this method is also available in ref 6.42. Again, however, the method is laborious, and adequate data are seldom available. In general we can predict that the ratio of inlet-stroke mep to inlet pressure will be a function of those factors which were found in Chapter 6 to affect volumetric efficiency. If heat-transfer effects are assumed to be negligible, the prevailing influences will be p_e/p_i, the inlet-valve Mach index, and the design ratios, including γ. Thus we may write

$$\alpha_i = \frac{\text{mep}_i}{p_i} = \phi\left(\frac{p_e}{p_i}, Z, \gamma, R_1 \cdots R_n\right) \tag{9-14}$$

Curves of mep_i/p_i are shown in Fig 9-19. Because of pressure losses through the inlet valve, mep_i/p_i decreases with increasing values of Z.

As in the case of the exhaust process, the actual mep is close to the ideal mep at low values of Z. These curves can be taken to have more general validity than those for the exhaust mep (Fig 9-18) because the inlet process is not greatly affected by subsequent events in the cycle.

Pumping mep. This quantity is defined as the net work done by the piston during the inlet and exhaust strokes, divided by the piston

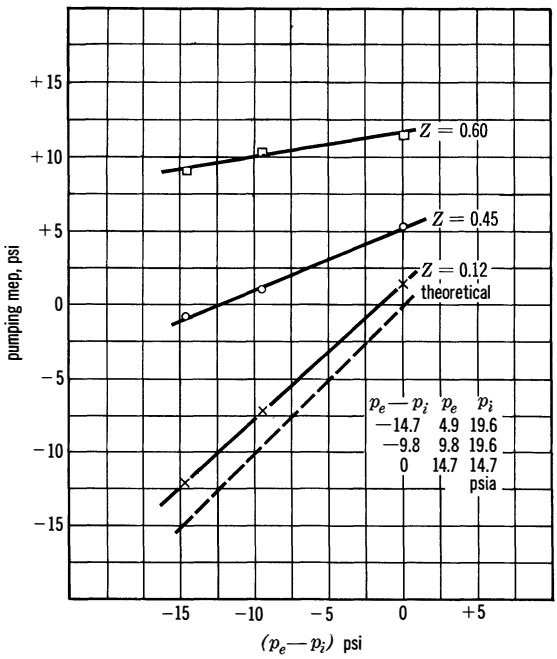

Fig 9-20. Pumping mep vs $(p_e - p_i)$. CFR $3\frac{1}{4}'' \times 4\frac{1}{2}''$ single-cylinder engine. $T_i = 120°\text{F}$, $T_c = 180°\text{F}$, $r = 4.9$, $\gamma \cong 1.2$. (Livengood and Eppes, ref 6.44.)

displacement. Also,

$$\text{pmep} = \text{exhaust mep} - \text{inlet mep} \tag{9-15}$$

Except in the case of highly supercharged engines at low piston speeds, the exhaust mep is higher than the inlet mep. Figure 9-20 shows pmep vs $(p_e - p_i)$ for a typical four-stroke engine.

Effect of Engine Size on Pumping Losses. As we have seen in Chapter 6, similar four-stroke engines running at the same piston speed and same inlet and exhaust conditions have nearly identical indicator diagrams. Under these conditions, pmep will be the same, and the power of pumping will be proportional to the square of the characteristic dimension.

Effect of Design on Pumping Loss. From the foregoing discussion and from the discussion of the light-spring indicator diagrams in Chapter 6 it is evident that many of the factors which lead toward high air capacity also lead toward reduced pumping loss. Among such factors are increased valve opening areas, increased valve flow coefficients, and increased exhaust-and-inlet-system passage areas.

It appears from ref 6.43 that at high values of Z a small value of γ (less than 1.0) may cause high pumping loss. Thus exhaust valve size should not be too small from this point of view as well as for good volumetric efficiency. (See Chapter 6.)

On the other hand, there are some factors tending toward increased air capacity which also increase pumping loss. Figure 9-21, for example,

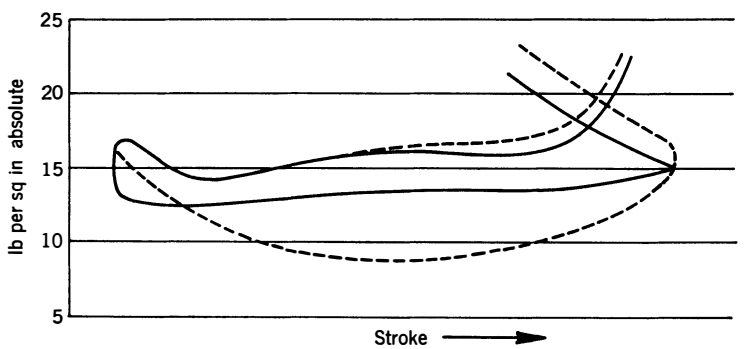

Fig 9-21. Effect of inlet-pipe length on the pumping diagram. (Sloan Automotive Laboratories)

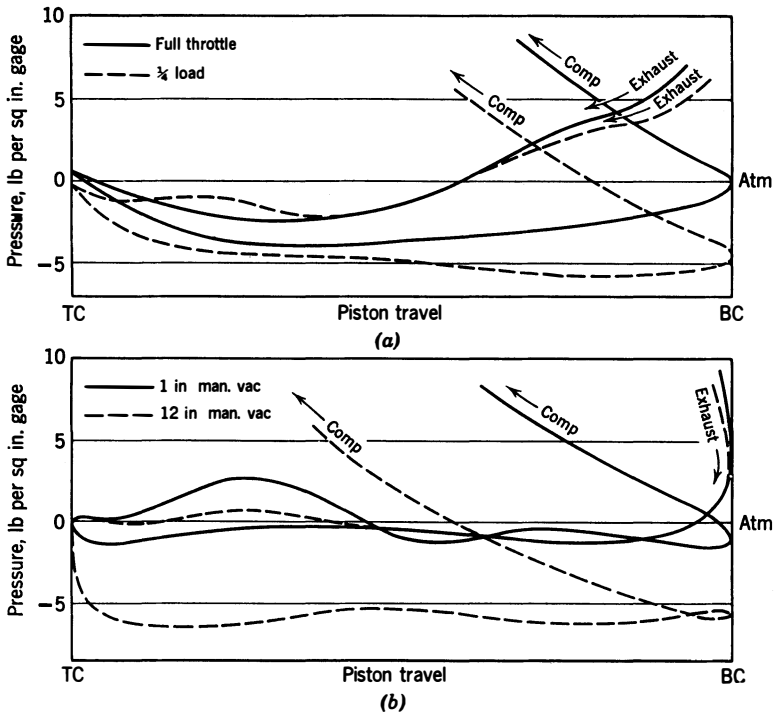

Fig 9-22. Effect of throttling on pumping diagram: (*a*) Single-cylinder engine, short inlet pipe; (*b*) six-cylinder engine, normal manifold. Both engines, 1200 rpm, p_e = 14.7 psia. (Sloan Automotive Laboratories)

shows how a change in inlet-pipe length may increase pumping loss while also increasing volumetric efficiency. Although the inlet loss is increased by the longer pipe, the air capacity is increased by the higher pressure at the end of the inlet stroke.

Figure 9-22 compares throttled and unthrottled pumping diagrams for two different engines. The single-cylinder engine, shown at (*a*) had only a small volume of intake pipe between the inlet valve and the throttle. Thus, during the time that the inlet valve is not open, atmospheric pressure is restored in the inlet pipe by flow through the throttle opening. In this case the throttled cycle starts with atmospheric pressure in the inlet pipe at the beginning of the inlet stroke.

In the multicylinder engine, Fig 9-22*b*, the gases in the inlet manifold are held at nearly constant pressure by the suction for six cylinders. In this case, cylinder pressure is low throughout most of the inlet stroke. A single-cylinder engine with a large tank between throttle and inlet

valve would show a similar effect. Conversely, the pumping diagram for the multicylinder engine would resemble that of the single-cylinder engine if individual throttles were used at the inlet port of each cylinder. Obviously, under throttled conditions, the number of cylinders connected to one inlet manifold and the volume of the inlet manifold between throttle and inlet ports will affect the pumping loss.

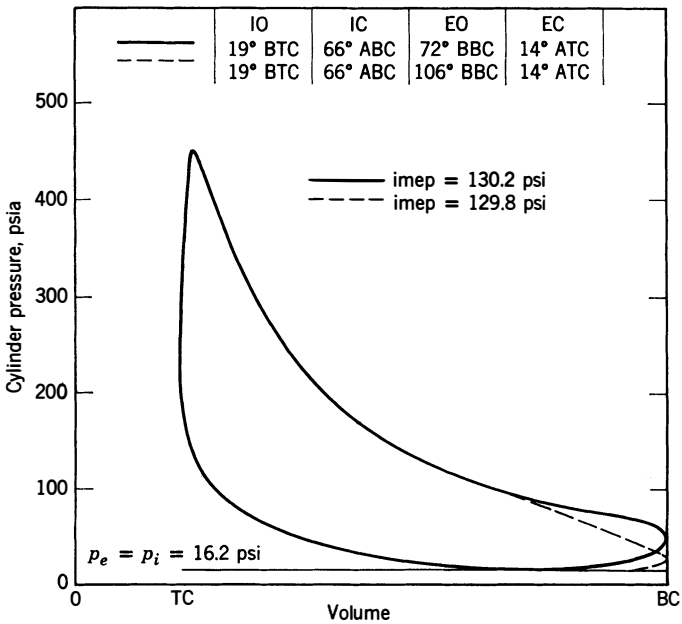

Fig 9-23. Effect of exhaust-valve opening angle on indicator diagram. Single-cylinder variable timing engine, $5\frac{3}{16}$ x 5.5 in; r = 5.5. (From diagrams taken at Sloan Automotive Laboratories by Livengood and Eppes, ref 6.43)

Effect of Exhaust-Valve Opening on Pumping mep. Figure 9-23 shows the effect on the indicator diagram of varying the crank angle of exhaust-valve opening. It is obvious from this figure that opening the exhaust valve earlier reduces exhaust-stroke mep at the expense of reducing the imep. The effect on over-all engine performance is small because there is little effect on volumetric efficiency, and the reduction in imep is almost exactly equal to the reduction in exhaust-stroke mep. Most four-stroke engines use an exhaust-valve-opening angle which divides the pressure drop during blowdown about equally between the expansion and exhaust strokes.

If blowdown is completed well before top center on the exhaust stroke, the exhaust-valve opening angle will have little effect on the inlet process. On the other hand, the time of exhaust-valve closing may affect cylinder pressure both during the latter part of the exhaust process and the early part of the inlet process. Since it is desirable to minimize cylinder pressure at the end of exhaust from considerations of air capacity as well as for minimizing exhaust mep, the exhaust-valve closing point should be delayed as far after top center as is consistent with valve-overlap limitations.

Exhaust System. In the exhaust system, design changes which reduce exhaust losses generally tend to increase air capacity because they tend to lower the residual-gas pressure at the time of inlet-valve opening. (See Chapter 6.) Exceptions to this statement might include the case in which a long exhaust pipe would lower the average cylinder pressure during exhaust while increasing the cylinder pressure at inlet-valve opening.

Effect of Fuel-Air Ratio. In spark-ignition engines variations in fuel-air ratio are generally within the range in which the effect on pumping losses is small. In compression-ignition engines increasing fuel-air ratio means increasing cylinder pressure at the time of exhaust-valve opening, hence greater exhaust-stroke mep. At the same time, the imep increases, so that the effect on the ratio of pumping mep to imep is small.

THE MOTORING TEST ON FOUR-STROKE ENGINES

As we have already indicated, most of the published data on the friction of engines has been obtained by motoring the complete engine, holding the operating temperatures as nearly as possible the same as while firing. In an attempt to simulate firing conditions motoring tests are usually made soon after a firing run. Figure 9-24 shows that the readings thus obtained stabilize about one minute after ignition cut-off.

Attention has already been invited to the fact that bearing loads and oil-film temperatures are not the same when motoring and firing. Motoring tests of four-stroke engines are generally made without alteration of the engine and therefore include pumping work as well as mechanical friction. Figure 9-25 compares typical light-spring diagrams, motoring and firing. It is evident that, although the inlet-stroke diagrams are nearly the same, the exhaust-stroke diagrams are quite different. The differences are due to the absence of blowdown and the much lower tem-

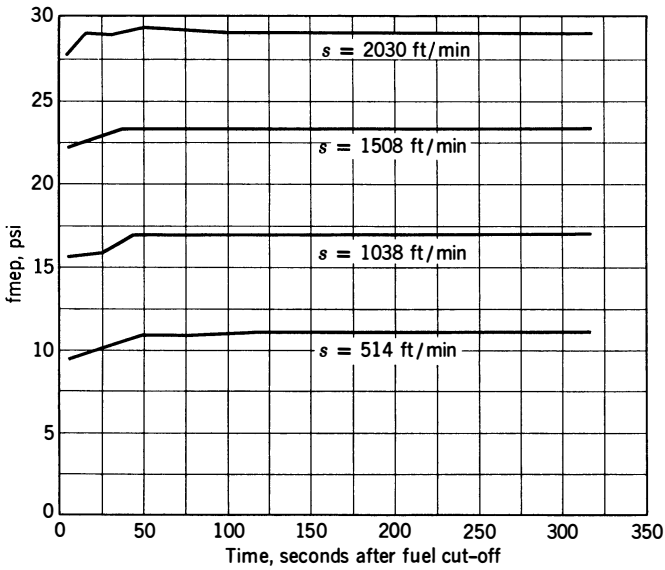

Fig 9-24. Effect of time of reading on motoring friction: 8-cyl, 3.75 x 3.25 in engine; $r = 8$. (Courtesy of General Motors Corporation)

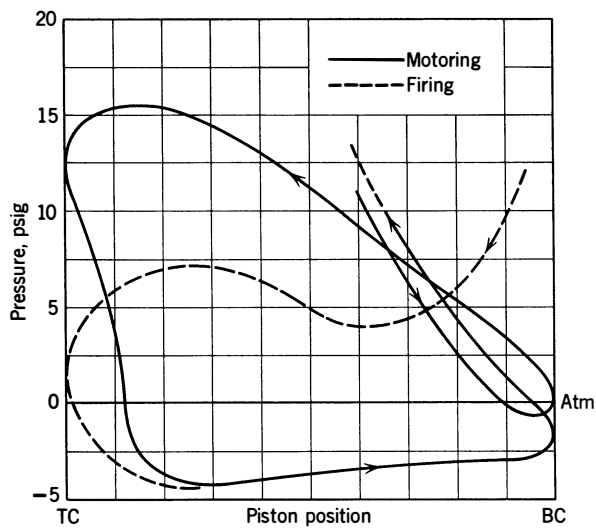

Fig 9-25. Light-spring indicator diagrams, motoring and firing. Automobile engine running at peak of power curve: 2700 rpm; pumping mep firing = 9 psi; motoring = 13.5 psi. (McLeod, ref 9.51)

perature of the exhaust gas during the motoring process. The drop in temperature means that both density and Mach number are higher and the pressure difference therefore greater during the latter part of the motoring exhaust process. As a result, exhaust mep tends to be higher in motoring than in firing.

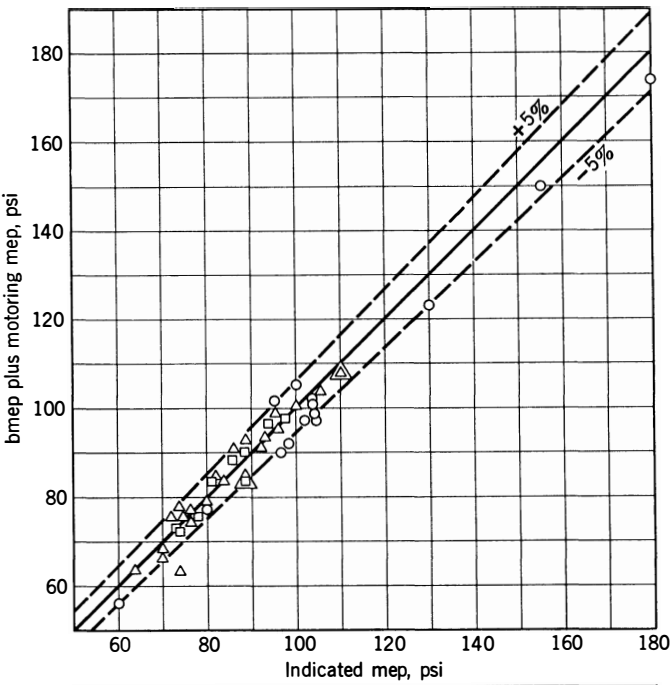

Symbol	Engine	Cycle	Piston speed	r	ref
○	CFR standard	4	300–3150	7	9.52
□	CFR loop scav.	2	600–1500	5.4	7.22
△	CFR through scav.	2	750–1200	5.8	7.22

Single-cylinder engines, 3¼" x 4½"

Fig 9-26. Comparison of bmep plus motoring mep with indicated mep.

Oddly enough, careful tests indicate that for unsupercharged engines, motoring *friction* is usually quite close to the difference between bmep and imep obtained from indicator diagrams. Figure 9-26 shows imep measured by an accurate indicator (5.03, 5.04) compared with the sum of measured bmep and motoring mep for both two- and four-stroke engines. If the motoring test was accurate, the points would lie on the 45° line. Actually, the maximum error is little more than 5% of the

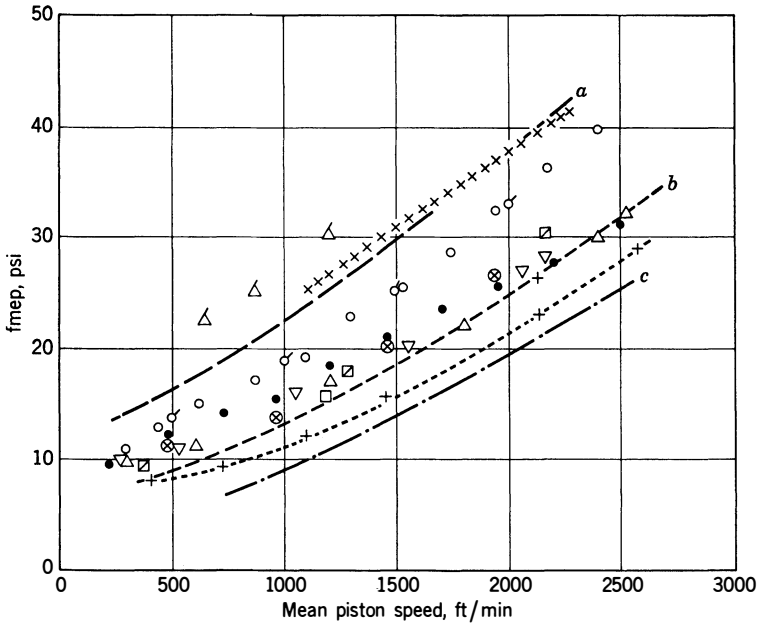

Symbol		Year	Bore	Stroke	Reference
△	Off-highway Diesel	1942	4.5	5.5	9.730
a — —	U.S. passenger cars (max)	1938	—	—	1.10
b - - - -	U.S. passenger cars (min)	1938	—	—	1.10
c —·—	Aircraft engine, V-12	1943	5.5	6	9.703
○	U.S. passenger car, V-8	1949	3.81	3.38	9.57
⊗	U.S. passenger car, V-8	1952	3.81	3.38	9.710
△	U.S. passenger car, 6	1952	3.56	3.60	9.711
▽	U.S. passenger car, V-8	1951	3.50	3.10	9.712
●	U.S. passenger car, V-8	1952	3.38	3.25	9.713
□	Marine Diesel*	1952	11.8	17.7	9.731
♂	Automotive Diesel	1940	3.75	5.0	9.732

*From indicator cards – all others motoring.

+ -------	U.S. passenger car	1946	3.25 x 4.38	9.57
⊠	U.S. passenger car	1946	3.19 x 3.75	9.57
× × × × ×	1.25″ x 1.25″ overhead-valve test engine			9.74
p_e/p_i	1.0 in all cases			

Fig 9-27. Friction mean effective pressure of four-stroke engines.

imep and the probable error much less than 5%. If Fig 9-26 is representative, the motoring test would give a probable error in fmep of about ±7% at mechanical efficiency 0.70 and ±20% at mechanical efficiency 0.90. Although such errors may seem large, they are no larger than the variation in motoring-friction readings obtained in practice under supposedly identical operating conditions.

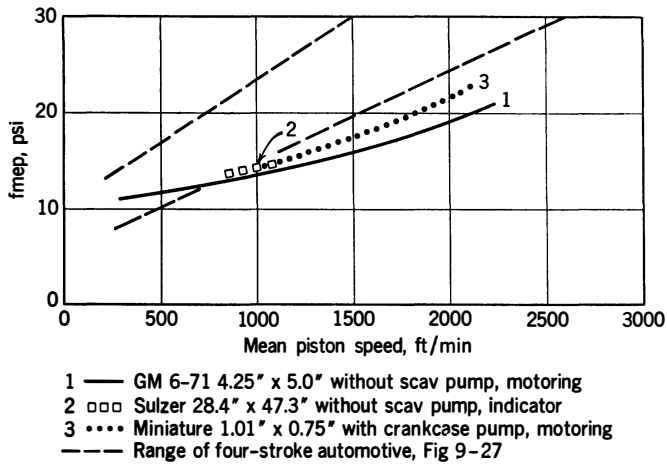

Fig 9-28. Friction mep of two-cycle engines:

1 Shoemaker, ref 7.30.
2 Sulzer Technical Review, ref 7.31.
3 Salter et al., ref 9.74.

Thus it appears that the motoring (without auxiliaries) test is a reasonably good measure of mmep + pmep for unsupercharged four-stroke engines and of mmep for unsupercharged two-stroke engines. When an electric dynamometer is available it is certainly the most convenient method.

Figures 9-27 and 9-28 give, respectively, the results of motoring tests on a considerable number of four-stroke and two-stroke engines. These data show a wide range in values of four-stroke friction depending on design. No aircraft or passenger-car types are included in the two-stroke engines, and the range is much smaller. Figure 9-28, which includes engines with 1.1 to 28.4 in bore, demonstrates convincingly the dependence of friction on piston speed rather than on rpm.

The motoring-test results shown in Fig 9-27 were made with exhaust and inlet pressures nearly equal. Furthermore, the good agreement

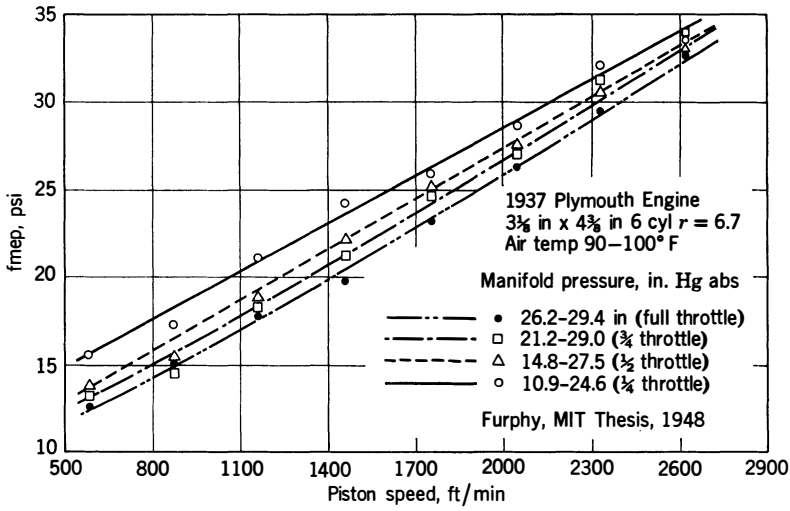

Fig 9-29. Effect of throttling on motoring friction of a four-stroke automobile engine. Exhaust pressure was 30 in Hg absolute. (Furphy, ref 9.714)

shown in Fig 9-26 between motoring and firing results applies only to engines operating with imep near 100 psi. Thus, with four-stroke engines, when p_e and p_i are not nearly equal, or in either type when imep is greatly different from 100 psi, the data shown in Figs 9-27 and 9-28 should be modified as explained under *Friction Estimates*.

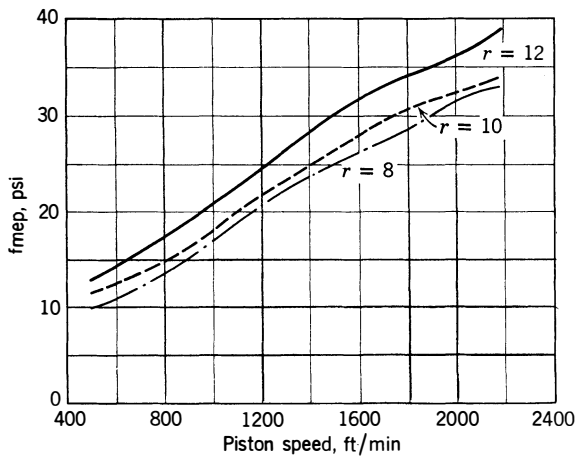

Fig 9-30. Effect of compression ratio on motoring friction: 8-cyl, 3.75 x 3.25 in automobile engine without auxiliaries. (Roensch, ref 9.57)

Effect of Throttling on Motoring Friction. Figure 9-29 shows motoring mep of an automobile engine with various throttle settings. These effects are qualitatively predictable from Figs 9-18 and 9-19.

Effect of Compression Ratio on Motoring Friction. Figure 9-30 shows an appreciable increase in motoring friction with increasing compression ratio. The higher cylinder pressures, perhaps together with more heat loss at the higher ratios, account for this trend. However, the absolute values of the increases in fmep seem high in view of the cylinder pressure effects shown in Fig 9-10. Further study of this effect would be desirable.

FRICTION ESTIMATES

In order to estimate friction mep for a new design, or for an existing design under new operating conditions, it is necessary to refer to friction measurements for the type of engine in question.

Friction measurements by means of indicator diagrams are rare, and in most cases the basic data must come from the results of motoring tests such as those of Figs 9-27 and 9-28. It has been shown that motoring-test results are a reasonably accurate measure of mechanical-plus-pumping friction when imep is in the range of 100 psi and, in the case of four-stroke engines, when p_e/p_i is nearly 1.0. Thus in estimating friction for supercharged or throttled engines, in which these conditions do not hold, suitable correction factors must be applied to motoring-test data.

Since, in four-stroke engines, the motoring test includes pumping mep, usually with p_e and p_i both near one atmosphere, a correction must be made when these conditions do not apply. Figure 9-31 shows results of a limited number of motoring tests in which p_e and p_i have been varied. The results, for a given value of γ, appear to correlate fairly well on the basis of the empirical relation:

$$\text{fmep} = \text{fmep}_0 + x(p_e - p_i)$$

where fmep is the sum of mechanical and pumping mep with the new values of p_e and p_i and fmep_0 is the motoring mep determined when p_e and p_i are one atmosphere, as was the case for Fig 9-27. Figs 9-18, 9-19, and 9-20 indicate that x should be a function of Z, and this appears to be the case, as indicated by Fig 9-31.

The results of tests with varying pressure on the pistons, shown in Fig 9-10, indicate that friction mep increases with imep. Since the motoring tests correlate with firing friction when imep is in the neighbor-

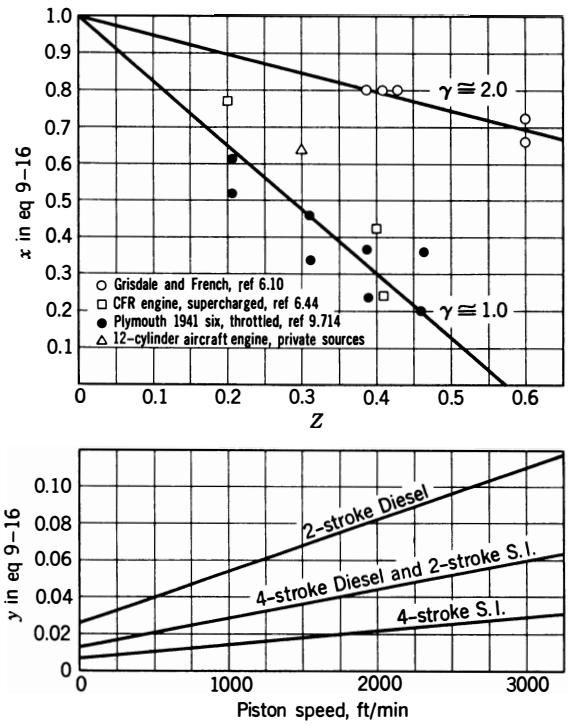

Fig 9-31. Motoring test correction factors: fmep = $\text{fmep}_0 + x(p_e - p_i) + y(\text{imep} - 100)$. y taken from Fig 9-10, x from motoring tests. (See **Fig 6.24** for γ.)

hood of 100 psi, the effect of a departure from this value can be expressed as follows:

$$\text{fmep} = \text{fmep}_0 + y(\text{imep} - 100)$$

where fmep_0 is the result of motoring tests with p_e and p_i near one atmosphere. Values of y, computed on the basis of Fig 9-10, are given in Fig 9-31. Finally, the estimated sum of mechanical and pumping friction mep can be expressed as follows:

$$\text{fmep} = \text{fmep}_0 + x(p_e - p_i) + y(\text{imep} - 100) \qquad (9\text{-}16)$$

where for four-stroke engines fmep_0 is the result of a motoring test at the required piston speed with p_e and p_i near one atmosphere. Since there is no pumping work within the cylinders of two-stroke engines, x is taken as zero for this type. Illustrations of the use of the foregoing relation are given in the examples for this chapter and also for Chapters 12 and 13.

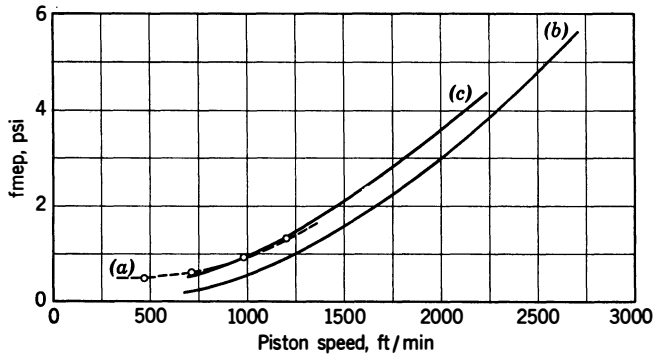

Fig 9-32. Auxiliary friction: (*a*) 1937 Chrysler 6, 3⅛ x 4¾ in, fan only; (*b*) 1948 Cadillac 8, 3½ x 4½ in, fan and water pump; (*c*) 1949 Cadillac 8, 3 3/16 x 3⅝ in, fan and water pump. [(*a*) Sloan Automotive Laboratories; (*b*), (*c*), Roensch, ref 9.57]

Auxiliary Friction. Figure 9-32 gives such data as the author has been able to find on the subject of "friction" due to auxiliaries.

Compressor and Turbine Power. This subject is treated in detail in Chapter 10.

WEAR

The subject of wear of moving parts is a complex one. Basic research in this field is just beginning, and it is not proposed to treat this subject in detail here. However, there is one aspect of wear with respect to engines which can be treated theoretically in such a way as to point out some trends of great practical significance. Since this particular subject has received very little attention, it is covered briefly in the discussion which follows.

Effect of Cylinder Size on Wear

Experience shows that the chief causes of wear in engines are foreign matter, corrosion, and, in some cases, direct metallic contact.

It can be safely assumed that the depth of corrosive wear per unit time is independent of size. However, the depth of wear which can be tolerated is proportional to the size of the part in question. Thus for similar engines we can define *wear damage* as d/L, where d is the depth of wear and L is the typical dimension. It is evident that the larger the cylinder bore or bearing diameter, the less the damage from corrosive wear in a given time.

The wear due to abrasives is a function of the concentration of abrasive material in the oil and the ratio of its average particle size to the bearing clearances. Here, again, large engines will have a great advantage, since, presumably, concentration and particle size are independent of cylinder size.

Finally, in cases in which contact wear may be a factor there is much experimental evidence to indicate that the depth of contact wear on rubbing surfaces tends to be proportional to the product of unit load and distance traveled and inversely proportional to the hardness of the material. If these relations are assumed, we can write

$$d = \frac{Ktpu}{h} \tag{9-17}$$

where d is the depth of wear, t is time, p is unit pressure, u is relative velocity of the surfaces, and h is the hardness of the surface in question. K is a coefficient, depending on materials, lubrication, surface finish, etc. In similar machines using the same materials and running at the same linear velocities and unit pressures for the same length of time it is evident that d will be a constant. Thus the *wear damage* per unit time is expressed by the relation

$$\frac{d}{L} = \frac{Ktpu}{hL} \tag{9-18}$$

The equation indicates that for constant unit pressure, velocity, and hardness, contact wear damage in a given time is inversely proportional to the characteristic dimension.

Thus, for all types of wear, engines with large cylinders and large bearings have a theoretical advantage over engines in which these parts are small. In actual practice, of course, wear depends heavily on particular conditions of operation. No reliable data on the effect of size on wear have been taken under otherwise comparable operating conditions. General experience indicates that large cylinders tend to have longer life than small ones, but this result may be influenced in part by the fact that large engines are generally used under conditions relatively free from dust and with excellent systems of oil filtration.

ILLUSTRATIVE EXAMPLES

Example 9-1. Petroff's Equation. Estimate the power and mep lost in the crankshaft and rod bearings of an 8-cylinder automobile engine 4-in bore, 3.5-in stroke, running at 4000 rpm. The bearing dimensions are as follows:

	No	Length	Diameter	Clearance
Main bearings	5	1.5	2.7	0.003
Rod bearings	8	1.0	2.5	0.003

The oil viscosity is $5(10)^{-5}$ lbf sec/ft^2, and the arrangement of oil feed holes is similar to arrangement *e* of Fig 9-4.

Solution: Since the bearing loads are not given, use Petroff's equation (9-7):

For Main Bearings:

$$D/C = 2.7/0.003 = 900, \quad N = \tfrac{4000}{60} = 66.7 \text{ rps}$$

$$F/A = 5(10)^{-5}2\pi(66.7)900 = 18.9$$

$$\text{torque} = \frac{18.9(5)2.7\pi(1.5)1.35}{144 \times 12} = 0.94 \text{ lbf ft}$$

For Rod Bearings:

$$D/C = 2.5/(0.003) = 833$$

$$F/A = 5(10)^{-5}2\pi(66.7)833 = 17.4$$

$$\text{torque} = \frac{17.4(8)2.5\pi(1.0)1.25}{144 \times 12} = 0.79 \text{ lbf ft}$$

Power Loss:

$$P = \frac{2\pi(0.94 + 0.79)66.7}{550} = 1.32 \text{ hp}$$

$$\text{engine displacement} = 352 \text{ in}^3$$

$$\text{mep} = 1.32(550)/\left[\frac{352(66.7)}{12 \times 2}\right] = 0.74 \text{ psi}$$

Example 9-2. Journal-Bearing Friction. If the average load on the main bearings of problem 9-1 is 3000 lbf and on the rod bearings, 3500 lbf, and if the bearings are lubricated as in curve *e* of Fig 9-4, estimate the power and mep lost in friction.

Solution:

For Main Bearings:

$$p = \frac{3000}{2.7(1.5)} = 740 \text{ psi}$$

$$S = 5(10)^{-5}66.7(900)^2/740(144) = 0.0256$$

from Fig 9-4 curve *e*, $f\left(\frac{D}{C}\right) = 1.3$ and $f = 1.3/900 = 0.00145$

$$F = 5(3000)0.00145 = 21.8 \text{ lbf}$$

$$\text{torque} = 21.8(2.7/2 \times 12) = 2.45 \text{ lbf ft}$$

For Rod Bearings:

$$p = 3500/2.5(1.0) = 1400$$
$$S = 5(10)^{-5}66.7(833)^2/1400(144) = 0.0115$$

from Fig 9-4 curve e, $f\left(\frac{D}{C}\right) = 0.75$

$$f = 0.75/833 = 0.0009$$
$$F = 8(3500)0.0009 = 25.2 \text{ lbf}$$
$$\text{torque} = 25.2(2.5/2 \times 12) = 2.62 \text{ lbf ft}$$

Power Loss:

$$P = \frac{2\pi(2.45 + 2.62)66.7}{550} = 3.86 \text{ hp}$$

engine displacement = 352 in^3:

$$\text{mep} = 3.86(550)/\frac{352(66.7)}{12 \times 2} = 2.17 \text{ psi}$$

Example 9-3. Estimate of Piston Friction. Experiments have shown that the oil film between piston and cylinder wall covers about $\frac{1}{4}$ of the piston surface and has a thickness of about $\frac{1}{10}$ the piston clearance. With oil of $5(10)^{-5}$ lbf sec/ft^2 viscosity, estimate the power lost in piston friction (not including the rings) for an 8-cylinder engine with 4-in bore, 3.5-in stroke, at 4000 rpm. Pistons are 3 in long and have skirt clearance of 0.010 in.

Solution: Assuming friction is due only to shearing of the oil film, use definition of viscosity eq 9-2.

$$F = A\mu(u/y)$$

$$\text{Average velocity } u = 4000[(2)3.5/12(60)] = 39 \text{ ft/sec}$$

$$F = 8\left(\frac{4\pi\frac{3}{4}}{144}\right) 5(10^{-5}) \left(39\Big/\frac{0.001}{12}\right) = 122 \text{ lbf}$$

$$\text{Power loss} = \frac{122(39)}{550} = 8.6 \text{ hp}$$

which gives a loss in mep of 4.8 psi. This estimate confirms attempts at measurement which indicate that piston friction is chiefly due to the rings, and not much of it is attributable to the piston itself.

Example 9-4. Distribution of Friction. A four-stroke Diesel engine with 8 cylinders 10 x 12 in shows 1000 brake hp and 1300 indicated hp at 1500 rpm. The auxiliaries driven by the engine absorb 18 hp, and the indicator diagram shows 40 hp due to inlet and exhaust pumping work. Estimate the power and mep lost due to (*a*) pistons and rings and (*b*) bearings and valve gear.

Solution: The mechanical friction power is evidently $1300 - 1000 - 18 - 40 = 242$ hp.

displacement of engine = 7520 in^3

$$\text{mmep} = 242(33{,}000)\Big/\frac{7520}{2 \times 12}(1500) = 17 \text{ psi}$$

According to Fig 9-9, 27% of mechanical friction is due to bearings and valve gear and 73% to pistons and rings. Therefore,

	hp	mep
Loss due to pistons and rings	176	12.4
Loss due to bearings, etc	66	4.6
Total mechanical loss	242	17

Example 9-5. Effect of Gas Pressure. Estimate the mechanical friction mep of the engine of Fig 9-10 if it is operated as a four-stroke spark-ignition engine at 1600 ft/min with imep = 150 psi.

Solution: From Fig 9-10 and the table on page 332, the equivalent steady pressure is $150 \times 0.25 = 37.5$ psi. Reading Fig 9-10 at this pressure and at 1600 ft/min gives mmep = 18 psi.

Example 9-6. Effect of Gas Pressure. Estimate mechanical friction mep of the engine of Fig 9-10 if operated as a four-stroke Diesel engine at 1600 ft/min piston speed and imep = 150 psi.

Solution: From Fig 9-10 and the table on page 332, the equivalent steady pressure is $150 \times 0.5 = 75$ psi. Reading Fig 9-10 at this pressure and at 1600 ft/min gives mmep = 21 psi.

Example 9-7. Effect of Stroke-Bore Ratio. An automobile engine of 4-in bore and 4-in stroke operating at 4000 rpm shows a mechanical friction mep of 20 psi. If the stroke is shortened to 3.5 in, estimate the friction (*a*) at the same rpm and (*b*) at the same piston speed.

Solution: At the same rpm, the piston speed is reduced from $4000(4)\frac{2}{12} = 2670$ ft/min (44.5 ft/sec) to 2330 ft/min (39 ft/sec). If we assume that the curve is parallel to that of Fig 9-15 (upper figure), fmep at 39 ft/sec = 17 psi. At the former piston speed (44.5 ft/sec), the fmep will be the same as before (20 psi), but the rpm will be increased to $4000(4)/3.5 = 4570$.

Example 9-8. Pumping Loss. An unsupercharged four-stroke engine operates under the following conditions:

$$Z = 0.4, \quad \gamma = 1.2, \quad p_i = 13.8, \quad p_e = 15.0 \text{ psia}$$

(*a*) Estimate the pumping mep; (*b*) estimate the pumping mep if the engine is to be operated supercharged at 20% higher speed with $p_i = 28$, $p_e = 15$.

Solution:

(*a*) From Fig 9-18, $\alpha_e = 1.1$ and, from Fig 9-19, $\alpha_i = 0.76$. Therefore, from eq 9-15,

$$\text{pmep} = 15(1.1) - 13.8(0.76) = 6.0 \text{ psi}$$

(*b*) At $Z = 0.4 \times 1.2 = 4.8$ and $p_e/p_i = \frac{15}{28} = 0.54$; from Fig 9-18, $\alpha_e = 1.6$ and, from Fig 9-19, $\alpha_i = 0.68$. Therefore, from eq 9-15,

$$\text{pmep} = 15(1.6) - 28(0.68) = 5 \text{ psi}$$

As a check, Fig 9-20 shows pmep/p_i = 0.16. Using this relation,

$$\text{pmep} = 28(0.16) = 4.5 \text{ psi}$$

Both results are within limits of accuracy of such estimates.

Example 9-9. Four-Stroke Friction Estimate. Estimate fmep for a supercharged four-stroke automotive Diesel engine operating under the following conditions:

$$p_i = 40 \text{ psia}, \qquad p_e = 15 \text{ psia}, \qquad s = 2000 \text{ ft/min}, \qquad Z = 0.4$$

imep = 200. Inlet and exhaust valves have nearly equal areas.

Solution: From Fig 9-27, the unsupercharged fmep is estimated at 30 psi. From Fig 9-31, x is 0.3 and y is 0.044. Then, from eq 9-16,

$$\text{fmep} = 30 + 0.3(15 - 40) + 0.044(200 - 100) = 26.9 \text{ psi}$$

Example 9-10. Four-Stroke Friction Estimate. A four-stroke supercharged Diesel engine is designed to operate under the following conditions, with $Z = 0.5$, $\gamma = 1.0$.

imep	180 psi
rpm	1000
p_i	37 psia
p_e	30

The bore is 9 in and the stroke, 12 in, with 9 cylinders. All auxiliaries are separately driven. Estimate the brake mep, brake hp, and mechanical efficiency.

Solution:

$$\text{piston speed} = 1000(12)\tfrac{2}{12} = 2000 \text{ ft/min}$$

$$\text{piston area} = (9)63.5 \text{ (area 9-in circle)} = 571 \text{ in}^2$$

$$p_e/p_i = \tfrac{30}{37} = 0.80$$

From Fig 9-27, the fmep measured by motoring with $p_e/p_i \cong 1.0$ is estimated at 33 psi. From Fig 9-31, $x = 0.14$ and $y = 0.044$. Then, from eq 9-16,

$$\text{fmep} = 33 + 0.14(30 - 37) + 0.044(180 - 100) = 35 \text{ psi}$$

$$\text{bmep} = 180 - 35 = 145$$

$$\text{mech eff} = \tfrac{145}{180} = 0.805$$

$$\text{bhp} = (145)571(\tfrac{2000}{4})/3300 = 1260$$

Example 9-11. Friction Estimate, Two-Stroke Engine. If the Diesel engine of example 9-9 were to be designed as a two-stroke engine operating at imep = 140, with other conditions the same, estimate the brake mep, brake power, and mechanical efficiency. Scavenging pump takes 23 mep.

Solution: From Fig 9-28, the motoring fmep at 2000 ft/min is estimated at 19 psi. For two-stroke engines x is zero and y, from Fig 9-31, is 0.082. From

eq 9-16,

$$\text{fmep} = 19 + 0.082(140 - 100) + 23 = 45.3 \text{ psi}$$

$$\text{bmep} = 140 - 45.3 = 94.7 \text{ psi}$$

$$\text{bhp} = (94.7)571(\tfrac{2000}{2})/33{,}000 = 1635 \text{ bhp}$$

$$\text{mech eff} = 94.5/140 = 0.675$$

Example 9-12. Effect of Throttling, Four-Stroke Engine. Estimate the mechanical efficiency of an automobile engine under the following conditions:
(*a*) Full throttle, $s = 2500$ ft/min, $Z = 0.4$, imep = 165, $p_i = 14.0$, $p_e = 17.5$ psia.
(*b*) Throttled to $s = 1000$ ft/min, imep = 45, $p_i = 8.0$, $p_e = 15.0$ psia.
Solution:
(*a*) From Fig 9-27, motoring mep = 32. From Fig 9-31, $x = 0.3$ and $y = 0.022$. Then, from eq 9-16,

$$\text{fmep} = 32 + 0.3(17.5 - 14.0) + 0.022(165 - 100) = 36.4$$

$$\text{mech eff} = (165 - 36)/165 = 0.78$$

Solution:
(*b*) At 1000 ft/min, $Z = 0.4 \times \frac{1000}{2500} = 0.16$. From Fig 9-27, motoring mep = 14. From Fig 9-31, $x = 0.7$ and $y = 0.014$.

$$\text{fmep} = 14 + 0.7(15 - 8) + 0.014(45 - 100) = 18.1$$

$$\text{mech eff} = (45 - 18)/45 = 0.60$$

Example 9-13. Effect of Compression Ratio, Four-Stroke Engine. If the engine of example 9-12 had a compression ratio of 8, estimate the mechanical efficiency at 2500 ft/min full throttle, with a compression ratio of 12.
Solution: If we assume that the increase in thermal efficiency is proportional to air-cycle efficiency, the new imep may be estimated from Fig 2-4 as follows:

$$\text{imep} = 165(0.63)/0.57 = 182$$

From Fig 9-30, we estimate the increase in friction mep from $r = 8$ to $r = 12$ at 6 psi, and the new motoring fmep is 33 + 6 = 39 psi. From eq 9-16,

$$\text{fmep} = 39 + 0.3(17.5 - 14.0) + 0.022(185 - 100) = 42$$

$$\text{mech eff} = (182 - 42)/182 = 0.77$$

Compressors, Exhaust Turbines, Heat Exchangers —— ten

All two-stroke engines use some kind of compressor, though in many cases the compressor is formed by the crank chambers and is scarcely noticeable, externally. All large aircraft engines, as well as many Diesel engines, use compressors for supercharging. In many cases an exhaust turbine drives the compressor or adds power to the shaft. Heat exchangers are often used in the inlet flow passages. Such equipment has become an integral part of many commercial internal-combustion power plants.

IDEAL COMPRESSOR

The ideal compression process is usually taken as a reversible adiabatic compression from p_1, an initial steady pressure, to p_2, a steady delivery pressure. If pressures and temperatures are measured in large surge tanks in which velocity is zero (Fig 10-1), from eq 1-16

$$w_{ca} = J(E_2 - E_1)_a + p_2v_2 - p_1v_1 = J(H_2 - H_1)_a \qquad (10\text{-}1)$$

w_{ca} is the shaft work per unit mass,* E and H are internal energy and

* For convenience in working with compressors we are considering work *supplied* and heat *lost* to have positive signs.

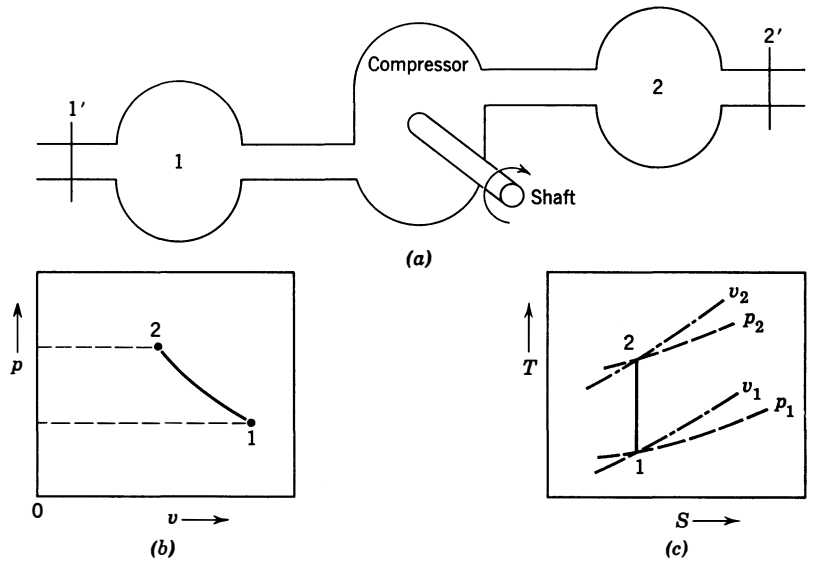

Fig 10-1. Ideal compression process: (*a*) Flow system. 1 and 2 are surge tanks with velocity $\cong 0$. (*b*) *p-v* diagram. *v* is specific volume. (*c*) *T-S* diagram. *S* is entropy.

enthalpy per unit mass, and v is specific volume. The subscript a indicates that the process is reversible and adiabatic.

If the gas handled is assumed to be a perfect gas, eq 10-1 can be written

$$w_{ca} = JC_{p1}T_1Y_c \tag{10-2}$$

where

$$Y_c = \left(\frac{p_2}{p_1}\right)^{(k-1)/k} - 1 \tag{10-3}$$

Since power is work per unit time, we can write for an ideal compressor using a perfect gas

$$P_{ca} = J\dot{M}C_{p1}T_1Y_c \tag{10-4}$$

where P_{ca} is the power of an ideal compressor and $\dot{M}$ is the mass flow delivered by the compressor per unit time.

If the pressures, temperatures, and enthalpies in the foregoing equations are measured in passages in which the velocity is considerable, instead of in large tanks, their *stagnation* values should be used. (See Appendix 3.) In the subsequent discussion it is assumed that this procedure is followed.

Equation 10-4 is generally used as indicating ideal performance for air compressors or compressors handling dry gases.

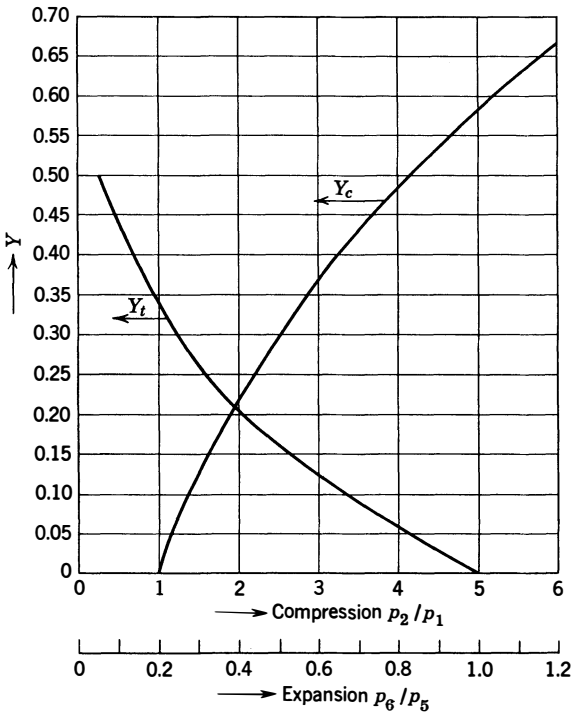

Fig 10-2. Adiabatic compression and expansion factors:

$$Y_c = (p_2/p_1)^{0.285} - 1 \qquad (k = 1.4,\ C_p = 0.24)$$
$$Y_t = 1 - (p_6/p_5)^{0.256} \qquad (k = 1.343,\ C_p = 0.27)$$

p_1 = compressor inlet pressure; p_2 = compressor outlet pressure; p_3 = turbine inlet pressure; p_4 = turbine exhaust pressure.

For air at temperatures below 1000°R, k may be taken as 1.4, $(k - 1)/k = 0.285$.

Values of Y_c vs p_2/p_1 for $k = 1.4$ are given in Fig 10-2. Values of k for fuel-air mixtures are given in Tables 3-1 and 6-2.

REAL COMPRESSORS

In a real compressor the process is neither reversible nor adiabatic. For such a process, using eq 1-18 as a basis, we may write

$$P_c = J(\dot{M}(H_2 - H_1) - \dot{Q}) \qquad (10\text{-}5)$$

where H_1 and H_2 are the enthalpies measured before and after compression and $\dot{Q}$ is the heat lost by the compressor per unit time.

For the relatively high flow rates used in engine practice $\dot{Q}$ is usually small enough to be neglected. If $\dot{Q}$ is negligible and the gas handled by the compressor is assumed to be a perfect gas,

$$P_c = J\dot{M}C_{p1}(T_2 - T_1) \tag{10-6}$$

The efficiency of compressors is usually defined as the ratio of adiabatic shaft power to actual shaft power. If eq 10-4 is divided by eq 10-6,

$$\eta_c = \frac{T_1 Y_c}{T_2 - T_1} \tag{10-7}$$

so that

$$P_c = J\dot{M}C_{p1}T_1 Y_c/\eta_c \tag{10-8}$$

and

$$T_2 = T_1(1 + Y_c/\eta_c) \tag{10-9}$$

For compressors used with engines eqs 10-6–10-9 are sufficiently accurate for engineering purposes and are generally accepted as valid in this field.

COMPRESSOR TYPES

Compressor types may be classified as follows:

1. *Displacement types* (Fig 10-3)
   - *Reciprocating*
     - (*a*) Piston (including the crankcase compressors used with two-stroke engines)
     - (*b*) Oscillating vane
   - *Rotating*
     - (*c*) Roots
     - (*d*) Lysolm
     - (*e*) Rotating vane
2. *Dynamic types* (Fig 10-4)
   - (*a*) Centrifugal (or radial flow)
   - (*b*) Axial
   - (*c*) Combined radial and axial

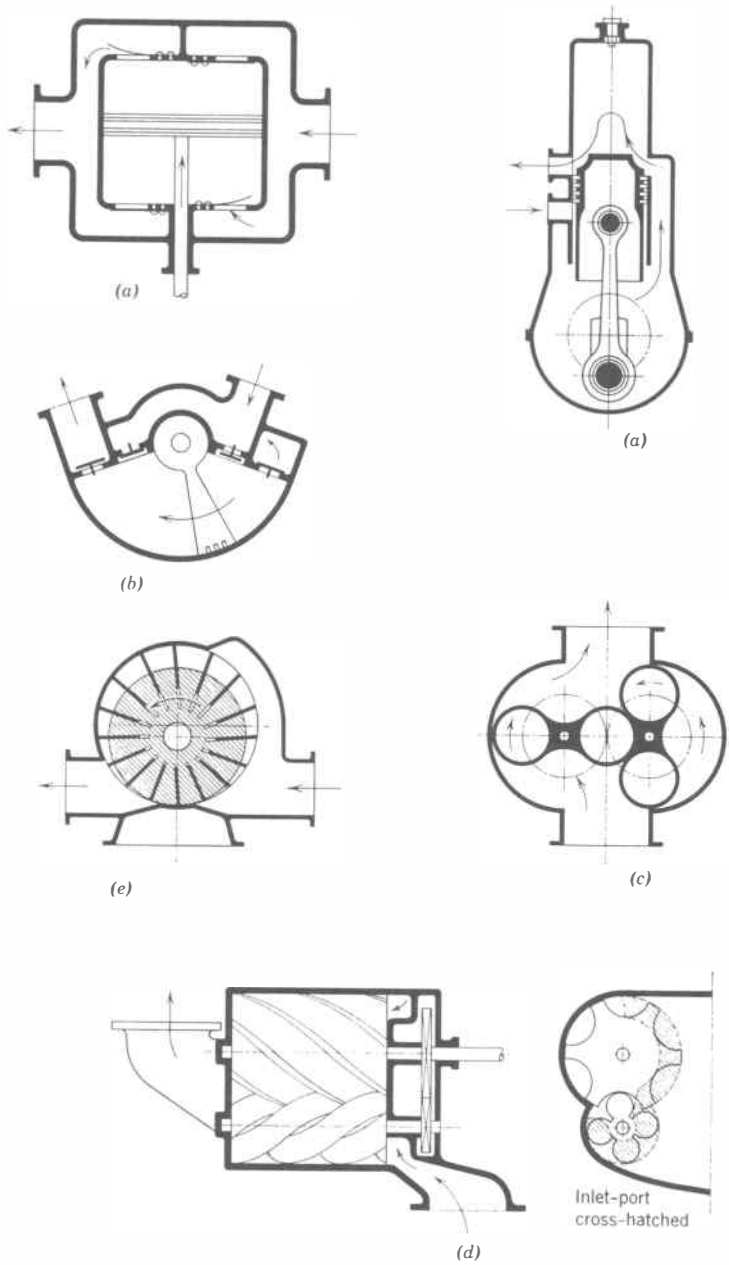

Fig 10-3. Displacement compressors. *Reciprocating:* (*a*) normal piston type (*left*); (*a*) crankcase type (*right*); (*b*) oscillating-vane type. *Rotating:* (*c*) Roots type; (*d*) Lysholm; (*e*) vane type.

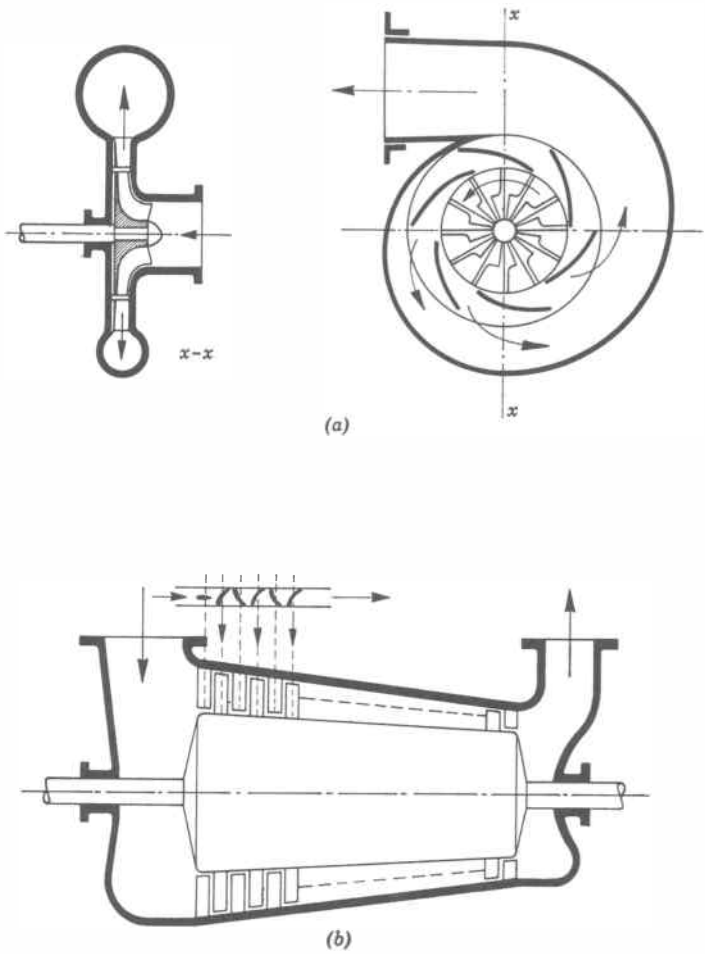

Fig 10-4. Dynamic compressors. (*a*) centrifugal; (*b*) multistage axial.

The types most frequently used with internal-combustion engines are

1*a*. Both crankcase and normal types
1*c*. Roots type
2*a*. Centrifugal type

When axial or combined types are used they are invariably of several stages.

COMPRESSOR CHARACTERISTICS

The problem of compressor performance can be handled in a manner similar to that used for air capacity of four-stroke engines, that is, by starting with the equation for ideal adiabatic flow of a perfect gas through a fixed orifice. Equation A-23 (see Appendix 3) can be written in general terms as follows:

$$\frac{\dot{M}}{\dot{M}^*} = \phi\left(\frac{p_2}{p_1}, k\right)$$

For a compressor, retaining the assumption of a perfect gas and assuming heat flow to be negligible, it is necessary to add arguments containing the speed of shaft rotation, the Reynolds index, and the design ratios. Thus we may write

$$\frac{\dot{M}}{\dot{M}^*} = \phi_1\left(\frac{p_2}{p_1}, k, \frac{ND}{a}, \frac{\dot{M}}{D\mu g_0}, R_1 \cdots R_n\right) \tag{10-10}$$

where N = angular velocity of the compressor shaft
D = a typical dimension, taken as the rotor diameter or piston diameter as the case may be
p_1 = inlet stagnation pressure
p_2 = delivery pressure
a = sound velocity based on inlet stagnation temperature
μ = inlet gas viscosity
$\dot{M}^*$ = the ideal *critical*, or *choking*, flow with the given inlet conditions, assuming the throat area to be $\pi D^2/4$.

Thus, from eq A-22,

$$\dot{M}^* = \frac{\pi D^2}{4} a\rho\sqrt{(2/k+1)^{(k+1)/(k-1)}}$$

where ρ is inlet stagnation density.

For air with $k = 1.4$,

$$\dot{M}^* = 0.578(\pi D^2/4)a\rho \tag{10-11}$$

From experience with four-stroke engines (Fig 6-16), it seems safe to assume that Reynolds number effects will be small. If we confine the problem to air as the fluid medium, k may be considered constant over

the compressor range. Thus the foregoing equation can be written

$$\frac{\dot{M}}{\dot{M}^*} = \phi_2\left(\frac{p_2}{p_1}, \frac{s}{a}, R_1 \cdots R_n\right) \tag{10-12}$$

where ND has been replaced by s, the rotor tip velocity or the mean piston speed.

If this equation is correct, dimensionless performance parameters other than $\dot{M}/\dot{M}^*$ will depend on the same variables, and we may write

$$\eta_c = \phi_3\left(\frac{p_2}{p_1}, \frac{s}{a}, R_1 \cdots R_n\right) \tag{10-12a}$$

$$e_c = \phi_4\left(\frac{p_2}{p_1}, \frac{s}{a}, R_1 \cdots R_n\right) \tag{10-12b}$$

where η_c is compressor efficiency and e_c is compressor volumetric efficiency, $\dot{M}/NV_d\rho$. Here V_d is the displaced volume per revolution and ρ, the compressor inlet air density.

If these equations are correct, experiments should show that $\dot{M}/\dot{M}^*$, η_c, and e_c are unique functions of p_2/p_1 and s/a for air compressors.

COMPRESSOR PERFORMANCE CURVES

Figure 10-5 gives comparative performance characteristics of typical examples of several compressor types. The curves are plotted on the basis of eq 10-12.

Flow Capacity. In interpreting Fig 10-5 it may be noted that $\dot{M}/\dot{M}^*$ is a measure of the flow capacity of each type in relation to its rotor (or piston) area. It is evident that in the useful range the flow capacities per unit rotor (or piston) area are highest for the dynamic types. Efficiencies given in Fig 10-5 are based on shaft power, except in the reciprocating compressor, in which efficiency is based on indicator diagrams.

One thing not shown by Fig 10-5 is the fact that piston compressors can give excellent indicated efficiencies in the range of pressure ratios between 1 and 2. Thus, if friction is small, this type of compressor may be quite efficient for scavenging two-stroke engines. This matter is discussed further under "choice of compressor type."

Pressure Ratio. Figure 10-5 shows that only the piston-type compressor is suitable for pressure ratios greater than about 4 in a single

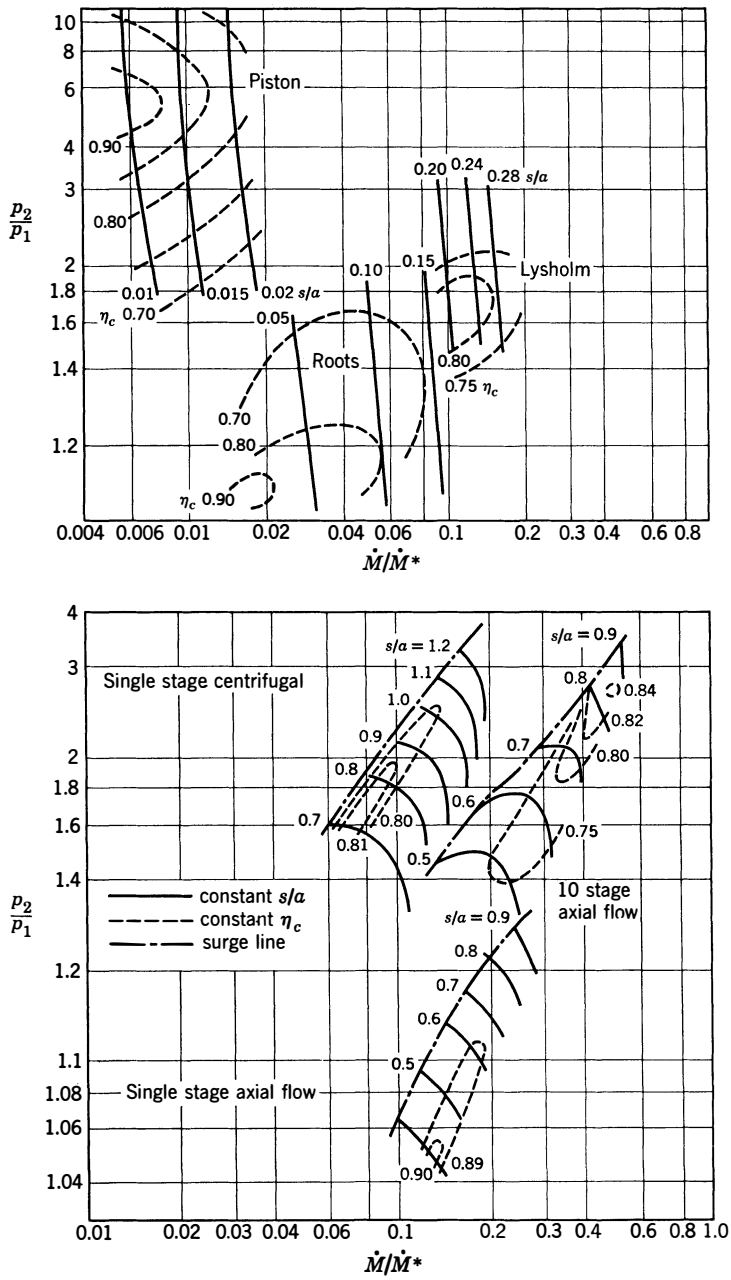

Fig 10-5. Comparative performance of compressors.

stage. The axial and centrifugal types lend themselves especially well to multistage construction.

Individual Performance Curves. Figures 10-6, 10-7, and 10-9 show performance curves of three of the more important compressor types used

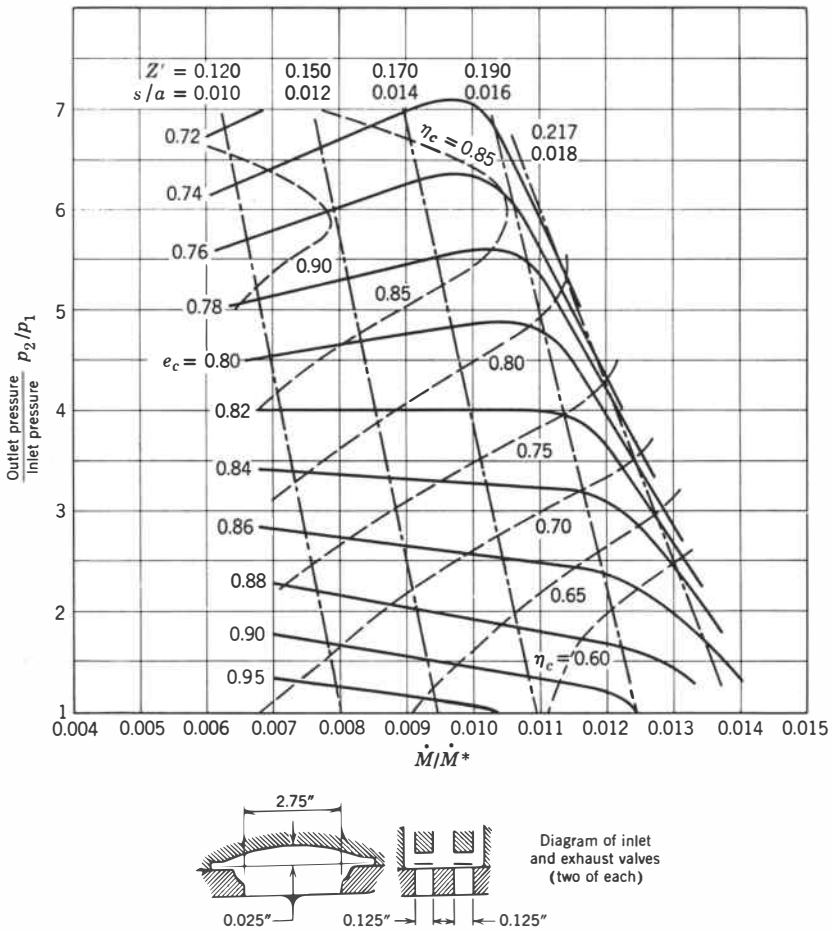

Fig 10-6. Performance of a piston compressor with automatic valves: $Z' = (A_p/A_v)s/a$; $\dot{M}^* = 0.578\ A_p \rho a$; $e_c = \dot{M}/NV\rho$; A_p = piston area; A_v = valve area (length × width of ports); a = inlet sound velocity; $\dot{M}$ = mass flow of air; $\dot{M}^*$ = critical mass flow; N = angular velocity of shaft; p_1 = inlet pressure; p_2 = outlet pressure; s = mean piston speed; V = piston displacement per revolution; ρ = inlet density; η = compressor efficiency; 1 cyl, single-acting compressor; 3.25-in bore; 4.5-in stroke; 5.65% clearance volume; $A_p/A_v = 12.08$. Compressor has automatic valves, per diagram. (Costagliola, ref 10.10)

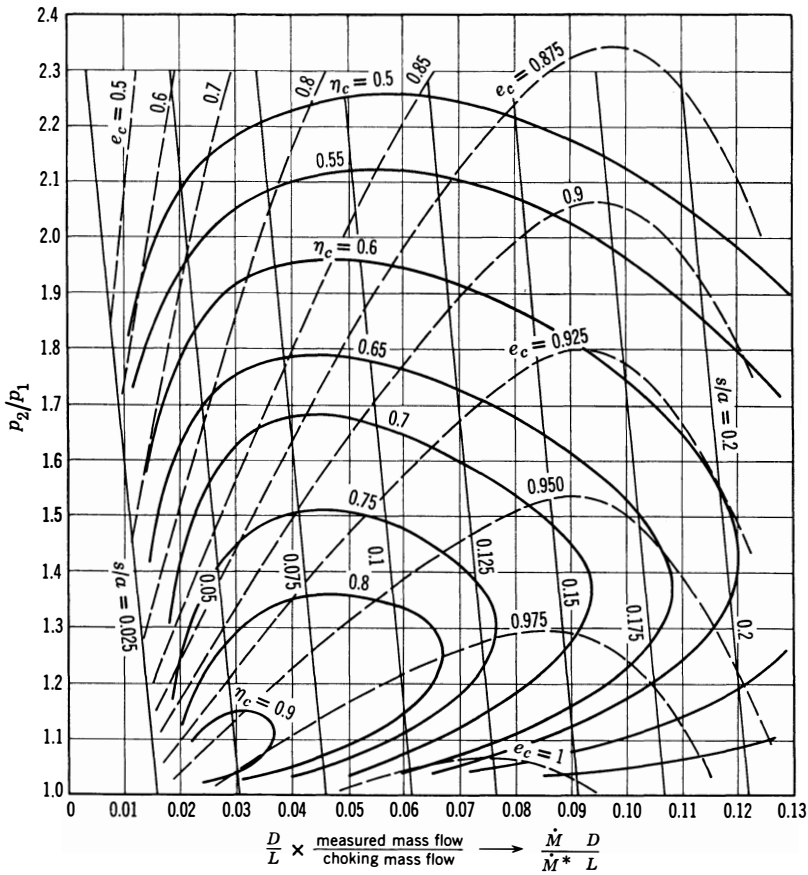

Fig 10-7. Roots compressor characteristics: $\dot{M}^* = 0.578\ (\pi D^2/4)\rho a$; $e_c = \dot{M}/NV\rho$; a = inlet sound velocity; D = rotor diameter; L = rotor length; $\dot{M}$ = mass flow; $\dot{M}^*$ = choking mass flow; N = angular speed of shaft; p_1 = inlet pressure; p_2 = delivery pressure; $s = \pi DN$; V = displaced volume per revolution; ρ = inlet density. (Ware and Wilson, ref 10.23, tables I-V)

with engines. These curves are similar to those of Fig 10-5 but are on a larger scale and contain additional information.

For *displacement type* compressors (Figs 10-6 and 10-7) the *volumetric efficiency* is a useful parameter. This quantity is defined in the same way as for four-stroke engines, namely,

$$e_c = \dot{M}/N_c V_c \rho \tag{10-13}$$

where e_c = compressor volumetric efficiency
$\dot{M}$ = mass flow per unit time
N_c = revolutions per unit time of the compressor shaft
V_c = compressor displacement volume in one revolution
ρ = gas density at compressor inlet.

Substituting eq 10-11 in eq 10-13 gives

for rotary displacement compressors

$$e_c = 1.42 \left(\frac{\dot{M}}{\dot{M}^*}\right) \frac{D^3/V_c}{s/a} \tag{10-14}$$

and for piston compressors

$$e_c = 1.156 \left(\frac{\dot{M}}{\dot{M}^*}\right) \frac{1}{s/a} \tag{10-14a}$$

Lines of constant e_c are given in Figs 10-6 and 10-7.

Figures 10-5, 10-6, and 10-7 show that a special characteristic of displacement-type compressors is small variation of mass flow as pressure ratio varies, speed (s/a) being constant. The reason for this characteristic is explained by noting in eq 10-14 that, with a given speed, displacement, and inlet density, $\dot{M}$ varies only with the volumetric efficiency of the compressor. Since the change in volumetric efficiency with pressure ratio is small (see Figs 10-6 and 10-7), the mass flow changes little at constant speed. As we shall see, this characteristic is very desirable when the resistance to flow of the system is not accurately predictable or when this resistance may change under service conditions.

RECIPROCATING COMPRESSORS

The reciprocating compressor with automatic valves (Fig 10-3*a*) is in common use as a scavenging pump for large and medium-sized two-stroke Diesel engines. It is also a very widely used mechanism for pumping fluids in many other applications. In spite of its wide use, very little basic information on this type of machine is available in the literature (refs 10.1—). Therefore, it seems appropriate to give it some special attention here.

By analogy with the four-stroke reciprocating engine (Chapter 6), it would seem that the inlet and outlet valves of a compressor will have a powerful influence on compressor performance. If an adequate outlet-valve area is assumed, it would appear, again by analogy with the four-

stroke engine, that an important parameter affecting the performance of reciprocating compressors would be a Mach index based on the inlet valves, similar to the factor Z of Chapter 6. We may recall from that chapter that

$$Z = \frac{s}{a} \times \frac{A_p}{A_i C_i} \tag{10-15}$$

where s = mean piston speed
a = inlet sound velocity
A_p = piston area
A_i = nominal inlet-valve area
C_i = inlet-valve mean steady-flow coefficient based on the nominal valve area.

Little information is available in the literature concerning the flow coefficients of automatic valves. Furthermore, because these valves are opened by pressure difference the flow coefficient probably varies considerably with speed and pressure ratio. However, when valves of a given design are used it may be assumed that C_i does not change with the number or size of valves of a given design. In this case the above parameter may be simplified to

$$Z' = \frac{s}{a} \times \frac{A_p}{A_i} \tag{10-16}$$

Figure 10-6 shows curves of constant Z' as well as the other quantities already mentioned. This figure is the result of tests made on a small (3.25 x 4.5 in) compressor at the Sloan Laboratories, MIT, and represents the only data available to your author in which speed and pressure ratio have been varied over a wide range. Most published data on reciprocating compressors cover only design-point values. Whether or not Fig 10-6 can be taken as representative of the performance of piston compressors, generally, remains a question which can be answered only when similar test data on other piston compressors become available.

Use of Fig 10-6 in Compressor Design. Let it be assumed that this figure gives a good indication of the indicated performance of piston-type compressors having these characteristics:

1. Inlet-valve area = exhaust-valve area
2. Small clearance volume (6% or less of the piston displacement)
3. Steady pressures at the compressor inlet and discharge

From the figure it may be seen that for high volumetric and thermal efficiency at a given pressure ratio Z' should be kept below 0.19. Increasing the ratio valve-area-to-piston-area should increase the piston speed at which satisfactory performance can be obtained.

Valve Stresses. Among similar mechanical systems impact stresses are proportional to velocity of impact. From this relation it may be deduced that stresses in the reed valves will be proportional to the product (valve length $\times$ rpm). Therefore, the smaller the valves, the higher the rpm at which they will perform without breakage or serious wear. The valves used in the compressor of Fig 10-6 are said to have satisfactory life up to 1500 rpm. Therefore, any valve of this design should be satisfactory in this respect when (valve length $\times$ rpm) does not exceed 372 ft/min.

Over-All Efficiency. Over-all efficiency of this type of compressor will be its indicated efficiency multiplied by its mechanical efficiency, the latter being equal to $(\text{imep} - \text{fmep})_c/\text{imep}_c$. The indicated mean effective pressure in the compressor cylinder can be computed from the following expression, obtained by dividing both sides of eq 10-8 by $N_c V_c$:

$$\text{imep}_c = J\rho e_c C_{p1} T_1 Y_c/\eta_c \tag{10-17}$$

This indicated mep is not to be confused with cmep in expressions 10-25 and 10-26, which is the engine mep required to drive the compressor.

The friction mep will depend on piston speed and on the design of the compressor. Few data on compressor friction appear to be available. On piston compressors used for scavenging two-stroke engines, rings have sometimes been omitted in order to minimize friction. However, this device is evidently practicable only when pressure ratios are so low that leakage past the piston is relatively small.

Crankcase Compressors. These are piston-type compressors with special limitations due to the fact that they are combined with the crankcase and piston of an engine. In practice, such compressors must have a large ratio of clearance volume to displacement volume. Because of this limitation such compressors cannot give satisfactory efficiencies except at low pressure ratios. Automatic inlet valves are often used, although it is also common to find inlet ports controlled by the piston skirt (Fig 10-3) or by a rotating valve driven by or incorporated in the crankshaft. Outlet ports are always piston-controlled.

Except for a brief test made under the author's direction (ref 10.12),

no test data on crankcase compressors have been found. The test referred to, made on a relatively small engine, showed volumetric efficiencies of the order 0.50–0.60 when delivering through the cylinder.

The attractive features of this type of compressor are

1. Mechanical simplicity and low cost
2. No friction losses need be charged to the compressor
3. Little space or weight is added by the compressor

Such compressors would seem worthy of more scientific attention and development than they appear to have had up to this time.

Oscillating-Vane Type. This type (Fig 10-3) should have characteristics similar to those of the normal piston compressor. It has been used occasionally for scavenging two-stroke engines. The chief disadvantage would seem to be the difficulties associated with sealing against leakage between vane and casing.

Roots Compressor (Fig 10-3*c*). The mechanical simplicity of this type is very attractive. However, it suffers from the fact that compression is accomplished by back flow from the high pressure receiver, and not only the fresh charge of air but also the air which has flowed back into the rotor space must be delivered against the outlet pressure.

The shaft work required to deliver a volume V of gas against a constant pressure p_2 from an inlet pressure p_1 is

$$w_a = V(p_2 - p_1) \tag{10-18}$$

An ideal Roots compressor would have no leakage and the volume delivered would be the displaced volume. Under these circumstances,

$$P_c = ND_c(p_2 - p_1) \tag{10-19}$$

giving a diagram of pressure against volume as shown by the solid lines of Fig 10-8. Under these circumstances, from eqs 10-4 and 10-13,

$$\eta_{cr} = \frac{Je_v\rho C_{p1}T_1Y_c}{p_2 - p_1} \tag{10-20}$$

where η_{cr} is the ideal Roots efficiency, which can also be written

$$\eta_{cr} = \frac{Je_vmC_{p1}}{R}\left\{\frac{(p_2/p_1)^{0.285} - 1}{(p_2/p_1) - 1}\right\} \tag{10-21}$$

where m is the molecular weight of the gas and R, the universal gas constant.

It is evident from the above expression that efficiency of an ideal Roots

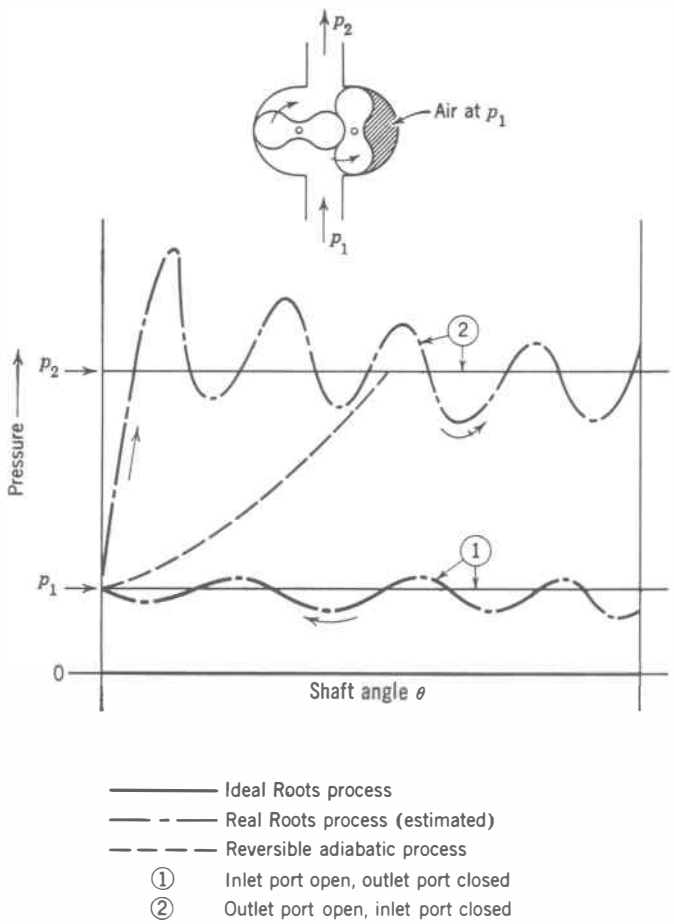

Fig 10-8. Pressure vs shaft-angle diagrams for a Roots compressor. Diagram refers to pressures in the space indicated by cross hatching.

compressor falls rapidly as p_2/p_1 increases. Figure 10-7 shows this trend. An actual Roots compressor has leakage losses which increase with increasing pressure ratio, and pressure fluctuations as indicated by the real curve of Fig 10-8. Table 10-1 compares actual with ideal Roots efficiencies for an exceptionally well-designed compressor.

Table 10-1

Ideal and Actual Roots-Compressor Efficiencies

p_2/p_1	η_{cr} $e_v = 1.0$ (1)	From Fig 10-7 at $\dot{M}/\dot{M}^* = 0.06$ e_v	η_c	η_{cr} (2)	$\frac{\eta_c}{\eta_{cr}}$ (3)
1.0	1.0	—	—	—	—
1.2	0.937	0.97	0.79	0.900	0.878
1.4	0.920	0.96	0.77	0.882	0.872
1.6	0.835	0.95	0.74	0.795	0.930
1.8	0.805	0.935−	0.71	0.752	0.945
2.0	0.765	0.917	0.675	0.700	0.964

(1) From expression 10-21; (2) (column 2) × (column 3); (3) (column 4)/(column 5).

Lysolm and Rotating Vane Compressors (refs 10.3—). These displacement types can be built to compress the gas to delivery pressure before the outlet ports open. Thus their indicated efficiencies can be better than those of the Roots type under similar conditions. However, their mechanical complications, compared to the Roots type or the dynamic compressors, have prevented their extensive commercial use.

Centrifugal and Axial Compressors. These types are so well covered in the literature (refs 10.4—) that their treatment here will be confined to problems in connection with their use as compressors or superchargers for engines.

Figure 10-9 shows characteristic curves of a single-stage centrifugal compressor. As shown by Fig 10-5, these curves are similar in character to those of axial compressors.

It may be noted from Figs 10-5 and 10-9 that the curves of constant s/a are not nearly vertical, as in the case of displacement compressors. Furthermore, as $\dot{M}/\dot{M}^*$ is reduced at constant s/a, the curves end at a *surge line*. To the left of this surge line the pressure pulsates severely, and performance becomes quite unsatisfactory. It can also be noted that if the operating point at a given speed is at the flow for maximum efficiency, a small decrease in mass flow will throw the machine into surge.

From the above considerations it is evident that if dynamic-type compressors are to be used care must be exercised to see that the mass flow is not decreased in service to the point at which surge is encountered. An exception to this statement may be made for the case in which the

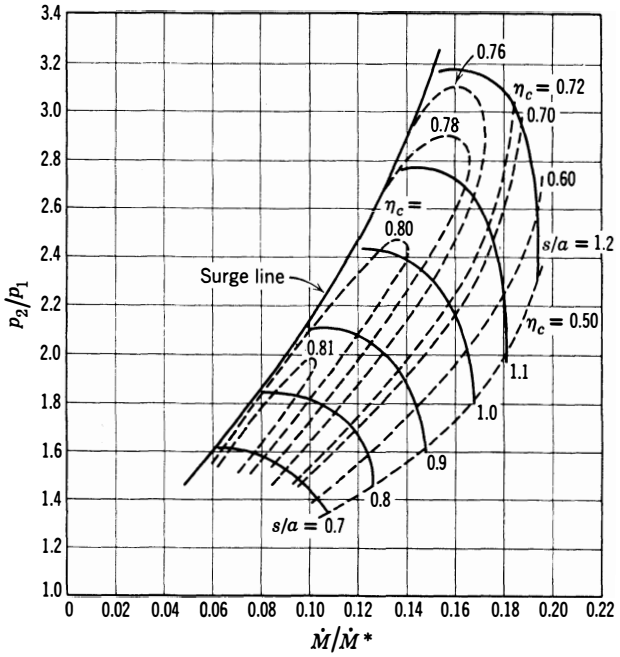

Fig 10-9. Typical centrifugal compressor characteristics: $\dot{M}^* = 0.578\ (\pi D^2/4)\rho a$; a = inlet sound velocity; D = rotor diameter; $\dot{M}$ = mass flow; $\dot{M}^*$ = choking mass flow through impeller area; N = revolutions per unit time of shaft; p_1 = inlet pressure; p_2 = delivery pressure; $s = \pi DN$; ρ = inlet density. (Campbell and Talbert, ref 10.40)

air supply is controlled by a throttle, as in supercharged spark-ignition engines. When the throttle is closed far enough to reduce the inlet-manifold pressure below atmospheric, surge may occur in the compressor. However, since the compressor is now not being usefully employed, the surge may be tolerable under these conditions.

With systems whose flow characteristics are known, it is not difficult to choose the size and speed of the compressor for a given regime of operation. Unfortunately, in the case of engines the flow characteristics may be altered by deposits on the ports or valves or by a change in exhaust piping or exhaust silencer. When such changes are not under the control of the engine manufacturer the use of dynamic-type compressors has serious disadvantages. Some allowance can be made for reduced flow by setting the operating point well to the right of the surge line. However, as indicated by Figs 10-5 and 10-9, a considerable sacrifice in efficiency may be necessary.

In spite of these disadvantages, the centrifugal type compressor is widely used for the following reasons:

1. It operates at rotational speeds appropriate for direct drive by an exhaust turbine.
2. It is relatively simple, small, and cheap to manufacture.
3. It can have very good efficiency in the range of pressure ratios from 1.5 to 3.0 where many superchargers are designed to operate. (See Chapter 13.)

Axial Compressors. In order to furnish pressure ratios appropriate for use with engines, multiple stages must be used. As indicated by Fig 10-5, maximum efficiency can be higher than that of a single-stage centrifugal type. However, the higher cost of the axial type, together with the fact that it does not lend itself so well to operation over a wide range of operating conditions, has caused most engine designers to prefer the centrifugal type.

COMPRESSOR-ENGINE RELATIONS

In practice, under normal operating conditions, the compressor supplies all the air used by the engine. Under these conditions, the mass flow through the compressor can be expressed as a function of engine characteristics:

For four-stroke engines

$$\dot{M} = \frac{A_p s}{4} \rho_a e_v (1 + F_i) \tag{10-22}$$

For two-stroke engines

$$\dot{M} = \frac{A_p s}{2} \rho_s R_s \left(\frac{r}{r-1}\right) (1 + F_i) \tag{10-23}$$

$\dot{M}$ is the mass flow of gas per unit time through the compressor. F_i is ratio of gaseous fuel to air in the compressor and is zero for Diesel engines and for spark-ignition engines in which the compressor is upstream from the carburetor or injector. The other symbols are defined in Chapters 6 and 7 and should be familiar to the reader.

In eq 10-22 e_v is the engine volumetric efficiency, which should not be confused with the compressor volumetric efficiency, e_c, used in eqs 10-12–10-14 and in eq 10-17.

In work with engines it is convenient to express the compressor power requirement in terms of engine mean effective pressure. Let compressor mean effective pressure be defined as

$$\frac{\text{cmep}}{\text{imep}} = \frac{\text{compressor power}}{\text{indicated engine power}} \tag{10-24}$$

From this definition, dividing compressor power (eq 10-8) by engine displaced volume per unit time gives the compressor mean effective pressure. Performing this operation for four-stroke engines,

$$\text{cmep} = J\rho_i e_v (C_{p1} T_1 Y_c / \eta_c) \tag{10-25}$$

For two-stroke engines $e_v\rho_i$ is replaced by $\rho_s R_s(r/r - 1)$.

In engine computations it is also convenient to determine the ratio of compressor mep to engine imep. Dividing eq 10-25 by eq 6-9 and performing a similar operation for two-stroke engines gives, for both four-stroke and two-stroke engines,

$$\frac{\text{cmep}}{\text{imep}} = \frac{1 + F_i}{Q_c F' \eta_i'} \left\{ \frac{C_{p1} T_1 Y_c}{\eta_c \Gamma} \right\} \tag{10-26}$$

The use of this equation is demonstrated in the Illustrative Examples at the end of this chapter.

ENERGY AVAILABLE IN THE EXHAUST

Figure 10-10 illustrates a constant-volume fuel-air cycle. If the expansion line is continued reversibly and adiabatically to point 5, where the exhaust pressure is p_e, the work done by $(1 + F)$ lbm of gas between points 4 and 5 is $E_4^* - E_5^*$. (See Chapters 3 and 4.) For a repetitive process it would be necessary to discharge $(1 - f)$ $(1 + F)$ lbm of the gas from an exhaust receiver at pressure p_5, so that the net work available from the process 4-5-5a would be

$$\begin{aligned} w_{ba}^* &= J(1 - f)\,(E_4^* - E_5^*) - p_5(V_5^* - V_4^*) \\ &= J(1 - f)\,(H_4^* - H_5^*) - V_4^*(p_4 - p_5) \end{aligned} \tag{10-27}$$

where H_5^* is the enthalpy of $(1 + F)$ lbm after reversible adiabatic expansion from H_4^* to p_5. The foregoing is the additional work which would be available from a perfect turbine which expanded the gases from 4 to 5 without losses and discharged the gases at p_5.

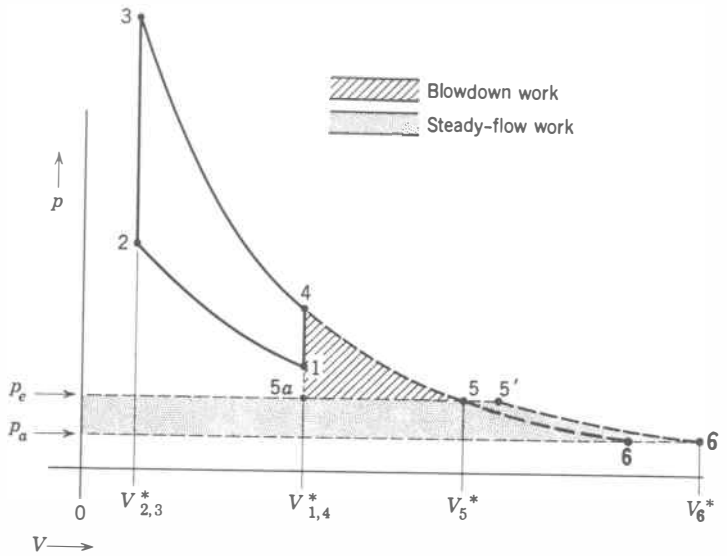

Fig 10-10. Work available from idealized exhaust processes. (Steady-flow work area assumes no blowdown work. If ideal blowdown work is used, remaining steady-flow work would be an extension of the 4–5 expansion line.)

If the exhaust gases are considered perfect gases,

$$H_4^* - H_5^* = (1 + F)C_{p4}T_4Y_{tb} \tag{10-28}$$

where

$$Y_{tb} = 1 - \left(\frac{p_5}{p_4}\right)^{(k-1)/k} \tag{10-29}$$

(See Fig 10-2.)

In all these relations the process 4-5 is reversible and adiabatic. For convenience, the process 4-5-5*a* is called the *blowdown process*.

If the gases were discharged from successive cycles into a tank at the steady pressure p_5, additional work could be obtained by allowing the gas to flow from the tank through another turbine to atmospheric pressure, p_6. The work available from a reversible adiabatic turbine would be

$$w_{sa}^* = J(1 - f)(H_5^* - H_6^*) \tag{10-30}$$

where w_{sa}^* is the reversible adiabatic work obtainable when the cylinder contains $(1 + F)$ lbm of gas. H_6^* is the enthalpy after reversible adiabatic expansion from point 5 to atmospheric pressure.

If the exhaust gas can be considered a perfect gas:

$$H_5^* - H_6^* = (1 + F)C_{p5}T_5Y_{ts} \tag{10-31}$$

where

$$Y_{ts} = 1 - (p_6/p_5)^{(k-1)/k} \tag{10-32}$$

(See Fig 10-2.)

A turbine designed to operate on this process is called a *steady-flow* turbine.*

EXHAUST TURBINES IN PRACTICE

In practice, exhaust turbines may be designed to operate as blowdown turbines, or as steady-flow turbines, or they may be designed to use part blowdown energy and part steady-flow energy.

Steady-Flow Turbines

For this type a number of cylinders are manifolded together to deliver exhaust gas directly to a turbine *nozzle box* which acts as a receiver and is expected to hold a reasonably steady pressure during operation.

From eqs 10-31 and 10-32 the power of such a turbine can be written

$$P_{ts} = J\dot{M}_a(1 + F)C_{pe}T_eY_t\eta_{ts} \tag{10-33}$$

where η_{ts} is the efficiency of the steady-flow turbine, which is defined as the ratio of actual turbine power to the reversible adiabatic power. C_{pe} is the specific heat of the exhaust gases at constant pressure.†

Exhaust Temperature. If conditions at point 4 and the heat flow during the exhaust process were known, or measurable, the temperature in the exhaust receiver could be computed. However, in any actual installation these data are seldom available. Therefore, it is necessary to resort to measured values of T_e in order to make use of eq 10-33. Figure 10-11 gives available data on temperatures measured at the turbine inlet for typical installations.

† For purposes of computation, the characteristics of exhaust gases from internal-combustion engines can be taken as follows:

$$C_{pe} = 0.27 \text{ Btu/lbm°R}, \qquad k_e = 1.343$$

$$m_e = 29 \qquad a_e = 48\sqrt{T_e} \text{ ft/sec} \qquad T \text{ in °R}$$

$$\dot{M}_e^* = 0.58(CA)a_e\rho_e \text{ in consistent units}$$

$$= 0.522(CA)p_e/\sqrt{T_e} \text{ in ft-lb-sec-°R system}$$

* If the gases discharge to p_5 without passing through a blowdown turbine, the temperature in the receiver will be higher than p_5 and the steady-flow turbine will operate between p_5' and p_6' as indicated in Fig 10-10.

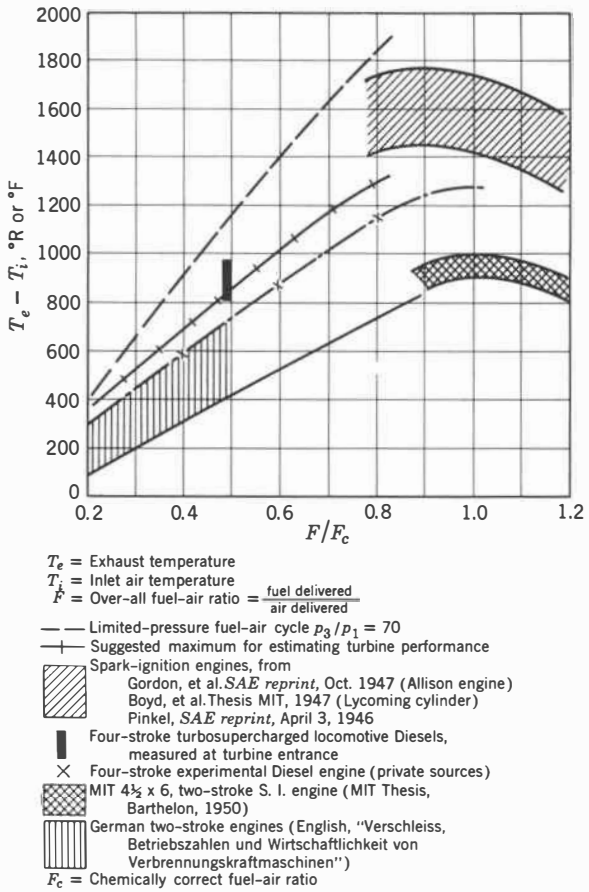

Fig 10-11. Exhaust temperatures.

Exhaust Pressure. In order to scavenge two-stroke engines, their exhaust pressure must be less than their scavenging pressure. The pressure ratio across the engine is established by the required scavenging ratio and the engine flow coefficient. (See Chapter 7.) If the inlet pressure and exhaust/inlet pressure ratio is known, p_e is determined.

In four-stroke engines there is no fixed limit on exhaust pressure. However, with a given inlet pressure, there is an optimum pressure ratio which gives maximum power of turbine-plus-engine and also one which gives best fuel economy. References 13.12 and 13.15 show the optimum p_e/p_i ratio to be nearly 1.0 for typical cases.

For turbines which drive the compressor only, the turbine power must equal the compressor power. In this case the exhaust pressure is fixed

by compressor requirements. This question is taken up later in this chapter.

Efficiency of Steady-Flow Turbines. Figure 10-12 shows performance curves for an axial-flow single-stage impulse turbine of the type generally used as an engine-exhaust turbine. Radial-flow turbines are also frequently used. (For their characteristics see refs 10.83–10.87.)

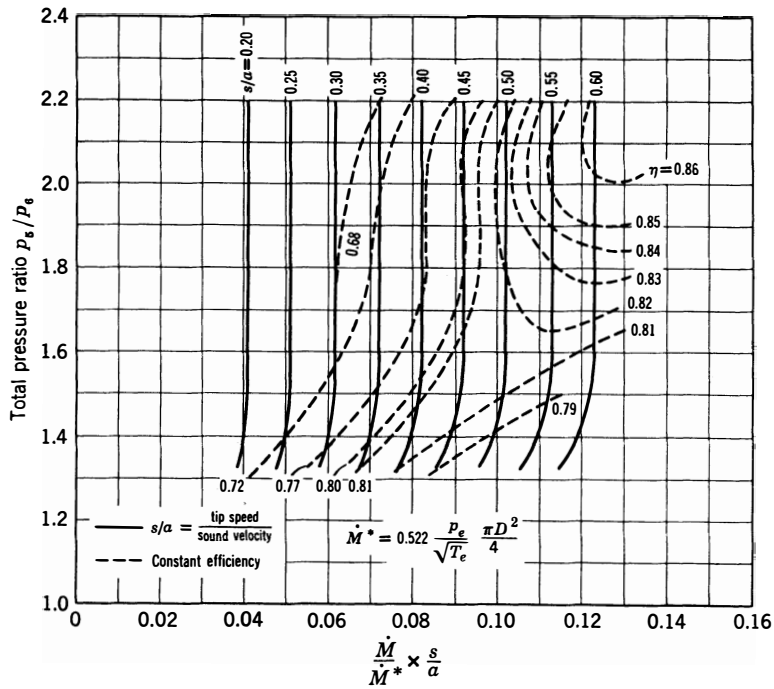

Fig 10-12. Typical steady-flow turbine characteristics (single stage, free vortex type).

Steady-Flow Turbine Performance. Having determined proper values for p_e, p_a, T_e, and η_{ts}, we can compute the power available from a steady-flow exhaust turbine from eq 10-33. Example 10-4, as well as some of the examples of Chapter 13, illustrates such computations.

Blowdown Turbines

A blowdown turbine is a turbine designed to utilize as much as possible of the blowdown energy (4-5-5*a*) shown in Fig 10-10. In order to accomplish this result, the turbine nozzles must be supplied through separate exhaust pipes from each cylinder, or from each group of three

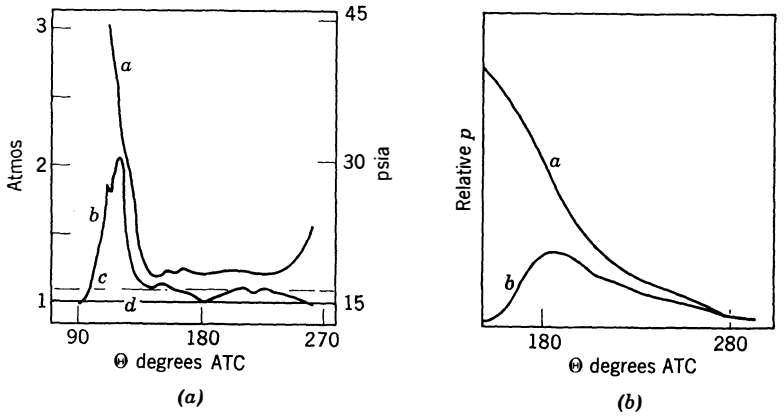

Fig 10-13. Pressure vs crank angle curves with blowdown turbines: *a* cylinder pressure; *b* pressure before nozzle; *c* inlet pressure; *d* exhaust pressure. (*a*) two-stroke engine, ref 10.74; (*b*) four-stroke engine, ref 10.75.

cylinders or less. The pipes have a diameter near that of the exhaust ports, and there is no surge tank nor its equivalent between cylinder and turbine nozzle box. For multicylinder engines each turbine has separate nozzle boxes, each of which is served by not more than three cylinders. The arrangement must be such that one blowdown process will not overlap another and thus interfere with proper blowdown action. The maximum desirable number of cylinders on a single exhaust pipe is three, provided their exhaust processes are equally spaced in terms of crank angle. Thus three four-stroke cylinders with 250° exhaust openings will overlap their exhaust openings only 10°, and three two-stroke cylinders with 120° exhaust opening will have no overlapping.

Blowdown turbines will also act, in part, as steady-flow turbines if the nozzle area is so small that the pressure in the nozzle box is always higher than atmospheric. When this is the case the action of the turbine may be considered as *blowdown* to the minimum nozzle-box pressure and as *steady-flow* from that pressure to atmospheric. In such cases the turbine may be called a *mixed flow* type.

In practice, it is difficult to realize more than a modest fraction of the theoretical blowdown energy for the following reasons:

1. The unsteady nature of the flow through the turbine
2. Pressure losses in the exhaust valve or ports
3. Heat losses between exhaust valve and turbine

Figure 10-13 shows typical curves of cylinder pressure and pressure at turbine nozzle vs crank angle. Nozzle pressure has a sharp rise soon

after blowdown starts, followed by falling and usually fluctuating pressure, as illustrated.

Several fundamental limitations of the blowdown arrangement may be noted:

1. The volume of the pipe should be small in relation to the cylinder volume in order to minimize loss of kinetic energy between exhaust port and turbine nozzle. (See ref 10.76.)
2. Pipe area should be small in order to minimize heat loss. In other words, pipes should be as short as possible.
3. The larger the exhaust valve in relation to the nozzle and the more quickly it opens, the less the pressure loss between cylinder and nozzle and the higher the mean pressure at the nozzle entrance.
4. For a given cylinder pressure at exhaust-valve opening, the smaller the nozzle, the greater the crank angle occupied by blowdown.

Computation of Blowdown Turbine Power. Because of the many unknown losses involved it is difficult to compute actual blowdown turbine characteristics and their effects on engine behavior. Thus most of the quantitative information available is the result of experiments which have generally approached the problem from the point of view of exhaust-gas kinetic energy rather than from the thermodynamic relations indicated by eqs 10-27–10-33.

For steady flow of a perfect gas through a nozzle we have seen from Appendix 3 that the mass flow depends on the nozzle area, the pressure ratio, the upstream density and sonic velocity, and the specific-heat ratio of the gas. Since velocity in the nozzle is mass flow divided by $C\rho A$, we may write

$$\frac{\dot{M}}{C_n A_n a \rho} = \frac{u}{a} = \phi\left(\frac{p_e}{p_4},\ k,\ R_1 \cdots R_n\right)$$

In order to eliminate p_4, we may substitute $\dot{M}a/C_nA_ng_0$ as a variable and write

$$\frac{u}{a} = \phi\left(\frac{p_e C_n A_n g_0}{\dot{M} a},\ k,\ R_1 \cdots R_n\right) \tag{10-34}$$

where u = velocity through the nozzle
a = upstream sonic velocity
p_e = downstream pressure
C_nA_n = nozzle area times flow coefficient
$\dot{M}$ = mass flow
k = specific-heat ratio
$R_1 \cdots R_n$ = design ratios

Viscosity effects (Reynolds number) are omitted as being unimportant in the high-velocity range under consideration.

If we assume that the same relations hold for the blowdown process in the engine, where u, a, and $\dot{M}$ represent *average* values, we could expect the mean nozzle velocity to be a function of $p_e C_n A_n g_0/M_a(1+F)a$.

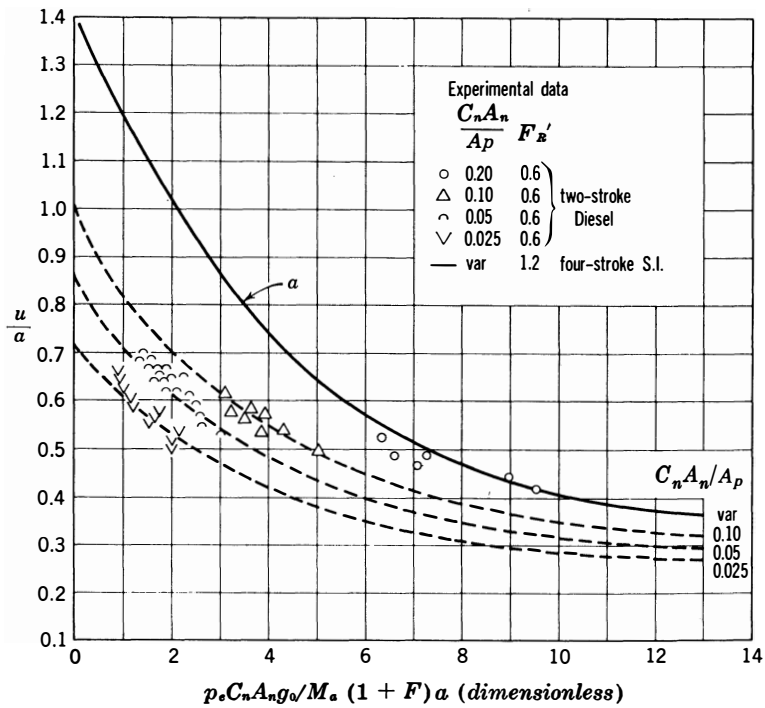

Fig 10-14. Blowdown turbines, nozzle velocity ratio vs blowdown parameter. (*a* from Pinkel, ref 10.61, four-stroke aircraft cylinders. Other data from Witter and Lobkovitch, ref 10.68.) A_p is piston area of *one* cylinder.

This relation has been found valid, as illustrated in Fig 10-14. For this figure, the mean nozzle velocity was computed from the measured thrust on a plate placed opposite the nozzle exit. (See refs 10.68, 10.70.) If we assume that the average velocity u has been determined, the power of a blowdown turbine can be written

$$P_{tb} = \eta_{kb}\left(\frac{\dot{M}_a(1+F)u^2}{2g_o}\right) \tag{10-35}$$

η_{kb} is the *kinetic* efficiency of the turbine, that is, the ratio of measured turbine power to the theoretical power at velocity u. For blowdown turbines of good design $0.75 > \eta_{kb} > 0.70$, according to ref 10.70.

Nozzle Area. From the foregoing discussion it is evident that a very critical problem in fitting a blowdown turbine to an engine is the flow capacity (flow area $\times$ flow coefficient) of the nozzles connected to one group of cylinders. If this area is too large, little energy will be captured, and, if it is too small, flow through the whole compressor-engine-turbine system will be too restricted.

Figure 10-14 indicates that with a given mass flow the smaller the nozzle area, the greater the turbine output. However, it is evident that for a given output the exhaust pressure, hence all cylinder pressures during the cycle, must rise as nozzle area decreases. The optimum nozzle area, which depends on engine type and operating conditions, is discussed more fully in Chapter 13. Nozzle-area to piston-area ratios between 0.05 and 0.10 are generally used for blowdown turbines in practice. (See Table 13-3.) Area ratios below 0.05 usually involve nozzle pressures which never go down to atmospheric pressure and therefore turn the turbine into a *mixed-flow* type.

Comparison of Blowdown and Steady-Flow Turbines

Figure 10-15 compares the performance of steady-flow and blowdown turbines applied to a four-stroke Diesel engine with $F_R' = 0.6$ and $p_e/p_i = 1.0$. Quantitatively, such curves vary with the type of engine and its operating regime, but for comparing the various turbine types Fig 10-15 may be considered typical.

The figure shows that the output of the pure blowdown turbine exceeds that of the steady-flow turbine up to a compressor pressure ratio of 1.2, above which the steady-flow turbine is clearly superior in output. Below a pressure ratio of 1.2 the blowdown turbine has enough power to drive the compressor and the advantage of operating with a lower mean exhaust pressure than a corresponding steady-flow unit. Thus the blowdown turbine is widely used with installations operating at low compressor-pressure ratios.

Mixed-Flow Turbines. Curve 5 of Fig 10-15 shows the turbine output obtainable under the assumed conditions by using a turbine of the mixed-flow type. The nozzle areas have been selected so that the minimum pressure in the nozzle box equals the inlet pressure, as in the case of the steady-flow turbine. The design change required to achieve this result would be to provide separate exhaust piping from each group

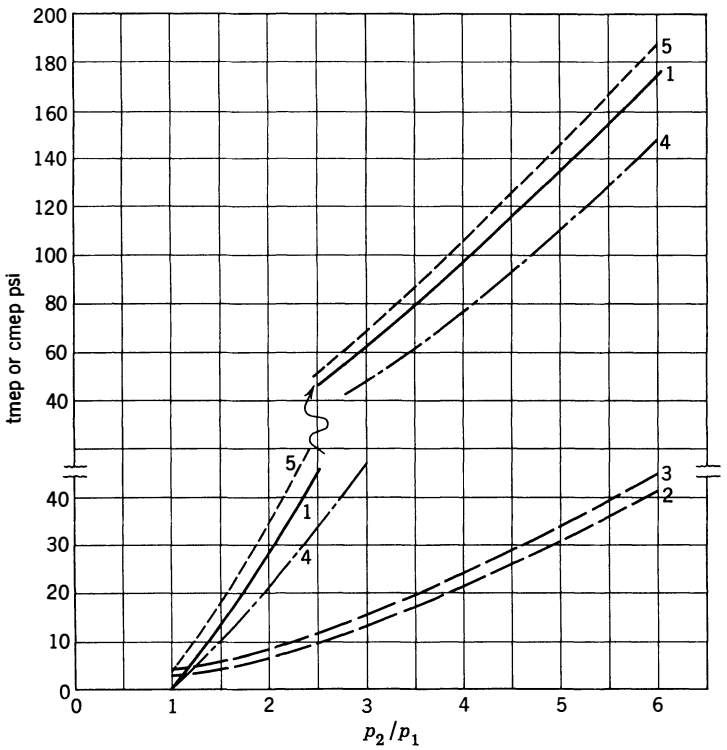

Fig 10-15. Blowdown and steady-flow turbine performance:

1 Steady-flow only
2 Blowdown, $CA_n/A_p = 0.10$
3 Blowdown, $CA_n/A_p = 0.05$
4 Compressor mep
5 Blowdown plus steady flow, $CA_n/A_p = 0.10$

Computed from Fig 10-14 (Diesel curves) and eqs 10-33–10-39: engine, four-stroke Diesel; $F_R' = 0.6$; $e_v = 0.85$ at $T_i = 560°\text{R}$; $p_e/p_i = 1.0$; compressor, $\eta_c = 0.75$; aftercooler, $C_c = 0.75$, 3% pressure drop; p_1 = atmospheric pressure; p_2 = compressor-delivery pressure. Blowdown turbine when used alone operates down to atmospheric pressure. When used with steady-flow turbine, it operates down to $p_e = p_i = 0.97p_2$. $\eta_{kb} = 0.70$. Steady-flow turbine operates between $p_e = p_i$ and atmosphere. $\eta_{ts} = 0.80$.

of three or less cylinders whose firing is evenly spaced and to divide the turbine-nozzle box into separate compartments, each serving one group of cylinders. In this case the exhaust piping and nozzle compartments act as the necessary reservoir for the steady-flow portion of the process.

Many commercial exhaust turbines used in the range of compressor-pressure ratios from 1.2 to 3.0 are the mixed-flow type. For very high pressure ratios the relative gain by using the mixed-flow type would seldom justify the added complication of separate exhaust pipes and multiple turbine-nozzle boxes.

TURBINE-ENGINE COMBINATIONS

By analogy with expression 10-26, we can write

(*a*) For steady-flow turbines (from eq 10-33)

$$\frac{\text{tmep}_s}{\text{imep}} = \frac{(1 + F)}{Q_c F' \eta_i'} \left\{ \frac{C_{pe} T_e Y_t \eta_t}{\Gamma} \right\} \tag{10-36}$$

(*b*) For blowdown turbines (from eq 10-35)

$$\frac{\text{tmep}_b}{\text{imep}} = \frac{(1 + F)}{Q_c F' \eta_i'} \left\{ \frac{u^2 \eta_{kb}}{2 g_0 J \Gamma} \right\} \tag{10-37}$$

Thus the relations between engine and turbine performance are established once we know the operating conditions for the engine and $T_e \eta_t$ or $u^2 \eta_{kb}$ for the turbine. Examples following this chapter and Chapter 13 illustrate the use of the foregoing relations.

Turbo-Supercharger Performance. For the turbo-supercharger compressor and turbine power must be equal, hence their mep must be equal. For a steady-flow turbine setting cmep from eq 10-26 equal to tmep from eq 10-36 gives

$$\frac{C_{p1} T_1 Y_c (1 + F_i)}{(1 + F) C_{pe} T_e Y_t \eta_{ts} \eta_c} = 1 \tag{10-38}$$

and for the blowdown turbine

$$\frac{C_{p1} T_1 Y_c (1 + F_i) 2 g_0 J}{(1 + F) u^2 \eta_{kb} \eta_c} = 1 \tag{10-39}$$

From these equations proper values of the pressure ratio across the steady-flow turbine or the proper value of u (hence, nozzle area) for the blowdown turbine can be determined. (See examples 10-4–10-7.)

AFTERCOOLERS

The performance of compressor-engine combinations can often be improved by inserting a cooler between the compressor and the engine inlet.

The temperature drop through an aftercooler is usually expressed in terms of *effectiveness*, defined as the ratio between the measured temperature drop and the maximum possible temperature drop, which would bring the cooled fluid to the coolant temperature. Thus

$$C_c = \frac{T_1 - T_2}{T_1 - T_w} \tag{10-40}$$

where T_1 = entrance stagnation temperature
T_2 = exit stagnation temperature
T_w = coolant entrance temperature
C_c = the cooler effectiveness

Obviously, an effectiveness of unity would require an infinitely large cooler. Under circumstances in which cooling is worthwhile an effectiveness of 0.6 to 0.8 usually keeps cooler size within reasonable limits.

The use of a cooler inevitably involves a pressure loss. For estimating purposes it can be assumed that well-designed coolers will involve a loss of 2–3% of the entering absolute pressure.

Whether or not an aftercooler is desirable depends chiefly on space limitations and on whether or not a good supply of coolant is available. Air-cooled aftercoolers are sometimes used in aircraft but are not often considered worthwhile for land vehicles which have to operate in warm climates. Water-cooled aftercoolers are particularly attractive for marine installations and for stationary installations which have a copious supply of cooling water.

References 10.9— give design information for the types of heat-exchanger used for aftercooling. Example 10-8 shows the effect of an aftercooler on inlet density, and several examples following Chapter 13 show the effect of an aftercooler on engine performance.

COMPRESSOR DRIVES

Compressor drive arrangements used in practice may be classified as follows:

1. Electric drive
2. Mechanical drive
3. Exhaust-turbine drive

Electric Drive. This method has been used in some marine and stationary installations of large engines. An advantage of this system is that one or two compressors can be made to serve several engines. Disadvantages are the cost and bulk of the electrical equipment, including motors and controls. This type of drive is attractive only where electric current is available for purposes other than compressor drive.

Mechanical Drive. This method is generally used for unsupercharged two-stroke engines and frequently for supercharging four-stroke engines to moderate pressure ratios. Mechanical drive with a single fixed ratio is the usual way of driving displacement compressors. Because of their limited operating range (Fig 10-5) dynamic compressors often require more than one ratio of compressor-to-engine speed.

References 10.5— show design details of typical mechanical drives for compressors used for supercharging. One problem common to most such drives is the possibility of torsional vibration of the compressor rotor against the rotating mass of the engine. Often some form of flexible or friction-type coupling is required in order to reduce the resonant frequency of this vibration to a point below the operating range, or to damp the vibratory motion.

In two-speed arrangements the design is further complicated by the problem of shifting speeds during operation.

Exhaust-Turbine Drive. This method of driving superchargers is popular for both two- and four-stroke engines. The reasons for this popularity are because this type of drive has these advantages:

1. It affords higher over-all power-plant efficiencies than other types of drive.
2. It is mechanically very simple when turbine and compressor are mounted on the same shaft.
3. It can be added to existing engines or changed without altering the basic engine structure.

The reason for higher over-all efficiency is that with this type of drive the loss in engine power due to increased exhaust pressure is usually smaller than the power which would be required to drive the compressor mechanically.

The reason for mechanical simplicity is that if a centrifugal compressor is used it can be designed to run at the same shaft speed as a single-stage

turbine, since the compressor and turbine both handle substantially the same mass flow with comparable pressure ratios. Therefore, these machines usually consist of a single-stage compressor and single-stage turbine mounted on the same shaft. (See refs 10.01–10.04.)

Displacement compressors, on the other hand, cannot be run at turbine speeds and therefore would require gearing between turbine and compressor. Such combinations are not used commercially.

The possibility of adding an exhaust-driven supercharger to an existing unsupercharged engine depends on whether or not the engine can be operated at an inlet pressure above atmospheric. In spark-ignition engines inlet pressure is usually limited by detonation, and in Diesel engines, by stresses due to peak cylinder pressure. The question of whether or not supercharging is advisable in any particular case is discussed more fully in Chapter 13.

The disadvantages of exhaust-turbine drive can be summarized as follows:

1. It requires special exhaust piping, which runs at high temperature.
2. It is attractive only in connection with dynamic compressors.
3. It usually has an acceleration lag, as compared to the engine.
4. It may be more expensive and may require more maintenance than other types of drive.

COMPRESSOR-ENGINE-TURBINE COMBINATIONS

When an exhaust turbine is used its power output may be employed separately from the engine to drive a compressor, or it may be geared to the engine crankshaft so as to add its power to that of the engine. Combinations of this kind are discussed in Chapter 13.

ILLUSTRATIVE EXAMPLES

In computing compressor and turbine performance, the following assumptions will be made:

For Air Compressors: $C_p = 0.24$ Btu/lbm °R, $k = 1.4$, $m = 29$, $a = 49\sqrt{T_1}$ ft/sec, with T in °R. $\dot{M}^* = 0.578 A a_1 \rho_1$ in consistent units, or $\dot{M}^* = 0.53 A p_1/\sqrt{T_1}$ in the ft-lb sec °R system. A is $\pi D^2/4$ where D is rotor diameter.

For Exhaust Turbines: $C_{pe} = 0.27$ Btu/lbm°R, $k = 1.34$, $m = 29$, $a_e = 48\sqrt{T_e}$ ft/sec, with T_e in °R. $\dot{M}^* = 0.58 A a_e \rho_e$ in consistent units, or $\dot{M}^* = 0.522 A p_e/\sqrt{T_e}$ in the ft-lb sec °R system. A is $\pi D^2/4$ where D is rotor diameter.

Example 10-1. Roots Compressor. A Diesel engine runs at 1500 rpm and uses 20 lbm of air/min at an inlet pressure of 1.5 atm. Select the size and speed-ratio required for a Roots supercharger, when ambient air conditions are 560°R and 14.7 psia. Determine the power required to drive the compressor.

Solution: From Fig 10-7, at $p_2/p_1 = 1.5$, maximum efficiency (0.755) occurs at $\dot{M}D/\dot{M}^*L = 0.47$, $s/a = 0.08$. Compute: $a_i = 49\sqrt{560} = 1160$ ft/sec, $\rho_1 = 2.7(14.7)/560 = 0.071$ lbm/ft^3. Then,

$$\frac{\dot{M}D}{\dot{M}^*L} = \frac{(20/60)D}{0.578(\pi D^2/4)0.071(1160)L} = 0.047$$

Let $D/L = 1$, and solving for D,

$$D = 0.435 \text{ ft} = 5.22 \text{ in}$$

$$s/a = \frac{\pi(0.435)N}{1160} = 0.08, \quad N = 68 \text{ rps} = 4080 \text{ rpm}$$

Thus a Roots supercharger for maximum efficiency will have the following characteristics: $D = 5.22''$, $L = 5.22''$, $N = 4080$ rpm, gear ratio $= 4080/1500 = 2.72$, and efficiency $= 0.755$.

Power Required: From Fig 10-2,

$$Y_c = 0.125$$

From expression 10-8,

$$P_c = \frac{778}{33{,}000} \times 20 \times 0.24 \times 560 \times 0.125/0.755 = 10.5 \text{ hp}$$

Example 10-2. Centrifugal Compressor. Determine the rotor diameter, gear ratio, and power for a centrifugal compressor to serve the engine of example 10-1.

Solution: From Fig 10-9, at pressure ratio 1.5, best efficiency will be at $\dot{M}/\dot{M}^* = 0.066$, $s/a = 0.65$, $\eta_c = 0.81$.

From previous example $\rho_1 = 0.071$, $a_1 = 1160$. Therefore,

$$\dot{M}/\dot{M}^* = (20/60)/0.578(\pi D^2/4)0.071(1160) = 0.066$$

$$D^2 = 0.135 \text{ ft}^2, \quad D = 0.368 \text{ ft} = 4.4 \text{ in}$$

$$N = 12(0.65)1160(60)/4.4\pi = 39{,}400 \text{ rpm}$$

Gear ratio $= 39{,}400/1500 = 26.2$. Power (from previous example) $= 10.5(0.755/0.81) = 9.8$ hp

Example 10-3. Piston Compressor. A 5000-hp, 9-cylinder, two-stroke Diesel engine requires piston-type scavenging pumps running at engine speed, which is 150 rpm. The engine uses 1000 lbm of air/min with a scavenging

pressure of 4 psi gage. Determine the size of the compressor cylinders and the power required by the compressor with ambient air at 70°F, 14.7 psia.

Solution: The pressure ratio of the compressor will be $(14.7 + 4)/14.7 = 1.27$. From Fig 10-6, an efficiency of 70% can be obtained by operating at $Z' = 0.11$, $M/M^* = 0.0073$, $e_c = 0.95$. $a_1 = 49\sqrt{530} = 1130$ ft/sec.

It should be possible to design the compressor so that its inlet-valve area can be $\frac{1}{8}$ its piston area. Therefore,

$$Z' = \frac{s}{a} \times 8 = s \times \tfrac{8}{1130}/60 = 0.000118\, s \text{ ft/min}$$

$$s = 0.11/0.000118 = 930 \text{ ft/min}$$

Since $s = 2SN$, the stroke of the compressor will be

$$\text{stroke} = \frac{930}{2 \times 150} = 3.10 \text{ ft}$$

$$\rho_1 = 2.7(14.7)/530 = 0.075$$

and from the definition of volumetric efficiency,

$$A_p = 2(1000)/0.95(0.075)930 = 30.2 \text{ ft}^2$$

If 9 double-acting cylinders are used, arranged as in Fig 7-24*d*, the piston area of each cylinder would be $30.2/18 = 1.68$ ft^2 and the piston diameter, 1.46 ft.

If a compressor in a single unit is preferred, 1 double-acting cylinder can be used, with a piston diameter of 4.38 ft.

Example 10-4. Steady-Flow Turbo-Supercharger. A four-stroke Diesle engine having 8 cylinders of 7.25-in bore requires an inlet pressure of 2 atm from an exhaust-driven centrifugal supercharger. The trapped fuel-air ratio is 0.75 × stoichiometric with $\Gamma = 0.8$. The air consumption is 100 lb/min at standard atmospheric conditions. No aftercooler is used.

Determine the characteristics of a steady-flow compressor-turbine unit and the required turbine-nozzle area. Assume that compressor and turbine have the characteristics shown in Figs 10-9 and 10-12.

Compressor: From Fig 10-9, select the compressor operating point at $p_2/p_1 = 2.0$, $M/M^* = 0.10$, $s/a = 0.86$, $\eta_c = 0.81$, Y_c (Fig 10-2) $= 0.22$, $\rho_1 = 0.0765$.

$$a = 49\sqrt{520} = 1120 \text{ ft/sec}$$

Air flow through compressor $= \frac{100}{60} = 1.67$ lb/sec.

$$\frac{M}{M^*} = 0.10 = \frac{1.67}{0.578(\pi D^2/4)1120(0.0765)}$$

$$D^2 = 0.43 \text{ ft} \qquad D = 7.88 \text{ in}$$

Since $s/a = 0.86$, the speed of the compressor should be

$$N_c = \frac{12 \times 1120 \times 60 \times 0.86}{7.88\pi} = 28{,}000 \text{ rpm}$$

The compressor outlet temperature is computed from expression 10-9:

$$T_2 = T_1 + T_1 Y_c/\eta_c = 520 + 520 \times 0.22/0.81 = 661°\text{R}$$

Since there is no cooling, the engine inlet temperature T_i is equal to T_2.

Turbine: From Fig 10-11, the exhaust temperature at $F_R = 0.75(0.80) = 0.6$ is 1000°F above inlet temperature. Therefore,

$$T_e = 661 + 1000 = 1661°\text{R}$$

and

$$a_e = 48\sqrt{1661} = 1960 \text{ ft/sec}$$

As a trial value, take η_{ts} as 0.80. Using eq 10-38,

$$\frac{0.24 \times 520 \times 0.22}{1.041 \times 0.27 \times 1661 \times Y_t \times 0.81 \times 0.80} = 1$$

$Y_t = 0.09$ and, from Fig 10-2, $p_6/p_5 = 0.68$, $p_5/p_6 = 1/0.68 = 1.47$.

Refer to Fig 10-12; at this pressure ratio the efficiency is 0.80 or better between $s/a = 0.38$ and 0.44.

From Fig 10-12 at $p_5/p_6 = 1.47$ and η_t maximum, read $s/a = 0.44$.

$$\frac{\dot{M}}{\dot{M}^*}\frac{s}{a} = 0.087. \qquad \text{Then} \quad \frac{M}{M^*} = 0.087/0.44 = 0.198$$

$$\frac{\dot{M}}{\dot{M}^*} = \frac{1.67 \times 4\sqrt{1661}\,(1.041)(0.68)}{0.522 \times \pi D^2 \times 14.7} = 0.198$$

from which $D^2 = 40.4$, $D = 6.35$ in.

$$N_t = \frac{12 \times 1960 \times 60 \times 0.44}{6.35\pi} = 31{,}200 \text{ rpm}$$

In order to mount the turbine directly on the compressor shaft, it must be run at the compressor speed of 28,400 rpm. In this case

$$s/a = 0.44 \times \frac{28{,}400}{31{,}200} = 0.40$$

and

$$\frac{M}{M^*}\frac{s}{a} = 0.198 \times 0.40 = 0.079$$

This value is also in the range in which turbine efficiency is 0.80 or better, and therefore the design is balanced. The engine exhaust pressure will be $14.7 \times 1.47 = 21.6$ psia.

Turbine Nozzle Area: At pressure ratio 1/1.47 and $k = 1.34$, the value of ϕ_1 in eq A-17 is computed as follows:

$$\phi_1 = \sqrt{\frac{2}{0.34}\left(0.68^{\frac{2}{1.34}} - 0.68^{\frac{2.34}{1.34}}\right)} = 0.555$$

$$\rho_5 = 2.7(14.7)1.47/1661 = 0.035 \text{ lbm/ft}^3$$

From eq A-15,

$$C_nA_n = \dot{M}/a_e\rho_e\phi_1$$

$$= \frac{100(1.04)144}{60(1960)0.035(0.555)} = 6.55 \text{ in}^2$$

$$C_nA_n/A_p = 6.55/8(41.3) = 0.0198$$

Example 10-5. Blowdown Turbo-Supercharger. Determine nozzle size and exhaust-manifold pressure for a blowdown turbine for the engine of example 10-4. Assume the kinetic efficiency of the turbine is 0.70 and that the engine has the following characteristics in addition to those given in example 10-4: Q_c = 18,000, $\eta_i' = 0.40$.

Solution: The principal uncertainty in exhaust-turbine calculations, especially for blowdown turbines, is the exhaust-gas temperature. Without heat loss, the blowdown process starts at the stagnation temperature of the cylinder gases at exhaust opening and falls nearly isentropically as the gases expand during blowdown. In the actual case, heat loss is large during the blowdown process, and there is no good way of estimating temperatures actually entering the turbine. As an estimate on the conservative side, it is recommended that the estimating curve of Fig 10-11 be used for both steady-flow and blowdown turbines.

$$F' = 0.067(0.75) = 0.05 \qquad F = 0.05(0.80) = 0.04$$

Required Turbine Output: The required value of cmep/imep is computed from eq 10-26 as follows:

$$Q_cF'\eta_i' = 18{,}000(0.05)0.40 = 360$$

From eq 10-26 using values from example 10-4,

$$\frac{\text{cmep}}{\text{imep}} = \frac{1}{360}\left\{\frac{0.24(520)0.22}{0.81(0.8)}\right\} = 0.118$$

The value of $\text{tmep}_b/\text{imep}$ must therefore be 0.118.

Required Nozzle Velocity: In ft-lb-sec units $2g_0J = 64.4(778) = 50{,}000$. Using eq 10-39, we have

$$\frac{0.24(520)(0.22)50{,}000}{1.05(0.70)(0.81)} = u^2$$

and $u^2 = 2{,}320{,}000$, $u = 1525$ ft/sec.

From example 10-4, $a_e = 1960$ ft/sec so that $u/a = 1525/1960 = 0.78$.

From Fig 10-14, this value can be obtained with $C_nA_n/A_p = 0.10$ when the value of the abscissa parameter is 1.1 or less. Since C_nA_n/A_p is based on one cylinder, with $A_p = 41$ in^2,

$$C_nA_n = 4.1 \text{ in}^2 = 0.0285 \text{ ft}^2$$

From example 10-4, gas flow for one cylinder will be $(1.041)100/8(60) = 0.218$ lbm/sec. From these data, the abscissa value for Fig 10-14 is

$$\frac{14.7(144)0.0285(32.2)}{0.218(1960)} = 4.54$$

at which point $u/a = 0.51$ which is too low. A nozzle half as large would still give a parameter of 2.27 and $u/a = 0.58$. Thus, it is not possible to achieve a

compressor-compression ratio of 2.0 with a pure blowdown turbine of 0.70 kinetic efficiency. This can also be inferred from an examination of Fig 10-15.

Example 10-6. Mixed-Flow Turbo-Supercharger. Determine the characteristics of a mixed-flow turbine to drive the compressor of examples 10-4 and 10-5.

Solution: The objective of using a mixed-flow turbine will be to lower the mean exhaust pressure. From example 10-4, the required exhaust pressure for a steady-flow turbine is 1.47 atmospheres. The mixed-flow turbine should be able to operate with a considerably lower mean exhaust pressure.

It is not possible to determine the exact nozzle size required without a detailed analysis of the flow process through the exhaust valve and turbine. However, an approximation of the nozzle size and turbine performance can be obtained as follows:

Nozzle Area: For the blowdown turbine with an 8-cylinder engine, two cylinders will be connected to each nozzle. Thus, the flow through each nozzle will be $(1.041)100/4 \times 60 = 0.434$ lb/sec. With an average exhaust temperature entering the blowdown nozzles of 1661°R (from example 10-4), the area required to pass this amount of gas will depend on the pressure ratio across the nozzles, which varies with crank angle. An approximation can be made by assuming trial values for the effective inlet pressure of the steady-flow portion of the process.

For a trial, assume that the steady-pressure portion of the turbine operates at a pressure ratio of $1/1.25 = 0.80$, and that the temperature entering the steady-pressure element is 1500°R.

From Fig A-2 (page 505), $\phi_1 = 0.475$. Density $\rho = 2.7(14.7)1.25/1500 = 0.033$ and $a = 48\sqrt{1500} = 1860$ ft/sec. From eq A-15,

$$C_n A_n = \frac{0.434}{0.033(1860)0.475} = 0.0148 \text{ ft}^2 = 2.14 \text{ in}^2$$

and

$$C_n A_n / A_p = 2.14/41 = 0.052$$

Actually, the nozzles will be somewhat smaller than this. Assume a value $C_n A_n / A_p = 0.05$ for use with Fig 10-14. Note that the total nozzle area for the engine is $4(2.14) = 8.56$ in^2 which is appreciably larger than the 6.55 in^2 required for the steady-flow turbine of example 10-4.

Blowdown Performance: The parameter for Fig 10-14 is based on a flow of $0.475/2 = 0.238$ lb/sec from one cylinder. Its value is $(14.7 \times 1.25 \times 144) \times 0.05(32.2)/0.238(1860) = 9.62$. From Fig 10-14, $u/a = 0.315$ and $u = 0.315(1860) = 586$ ft/sec. From eq 10-37,

$$\frac{\text{tmep}_b}{\text{imep}} = \frac{1.041}{360}\left(\frac{(586)^2 0.70}{0.80(50{,}000)}\right) = 0.0174$$

Steady-Flow Performance: From Fig 10-2, $Y_t = 0.06$ and from eq 10-36,

$$\frac{\text{tmep}_s}{\text{imep}} = \frac{1.041}{360}\left(\frac{0.27(1500)0.06(0.81)}{0.80}\right) = 0.071$$

The total turbine output is represented by the sum of the two outputs so that,

$$\frac{\text{tmep}}{\text{imep}} = 0.0174 + 0.071 = 0.0884$$

The required value from example 10-5 was 0.118, so we have underestimated the required steady-flow pressure. Trial values higher than pressure ratio 1.25 should be tried until a value is found that gives the required tmep/imep. The resulting estimate would require experimental verification as to nozzle size and performance of the turbine.

Example 10-7. Mixed-Flow Geared Turbine. Using Fig 10-15, compare the engine output at $p_2/p_1 = 2.5$ with a geared-in mixed-flow turbine with the output when a mixed-flow turbine is used for a free turbo-supercharger. Use engine data given with Fig 10-15 with the following additional data: $\eta_t = 0.48$, $T_w = 540°\text{R}$, $\text{fmep}_0 = 20$, $s = 1800$ ft/min, $Z = 0.30$, $\Gamma = 1.0$. With turbo-supercharger $p_e/p_t = 0.75$ and $e_v' = 0.88$.

Solution: From eq 6-9, $\text{imep} = \frac{778}{144}\rho_t 0.85(18{,}000)(0.6)(0.067)(0.48) = 1593\rho_t$. From Fig 10-2, $Y_c = 0.30$ and $T_2 = 560(1 + 0.30/0.75) = 785°\text{R}$. From eq 10-40, $T_t = 785 - 0.75(785–540) = 601°\text{R}$; $p_t = 14.7(2.5)0.97 = 35.6$ psia; $\rho_t = 2.7(35.6)/601 = 0.16$ lbm/ft^3; imep $= 1593(0.16) = 255$ psi. This is the imep when $p_e/p_t = 1.0$ as assumed in Fig 10-15.

With Turbo-supercharger: imep $= 255(0.88/0.85) = 264$. From eq 9-16, fmep $= 20 + 0.47(35.6)(0.75 - 1) + 0.04(270 - 100) = 23$; isfc $= 2545/0.48(18{,}000) = 0.295$; bmep $= 264 - 23 = 241$; bsfc $= 0.295\ (264/241) = 0.324$.

With Geared Supercharger: According to Fig 10-15, at $p_2/p_1 = 2.5$, the tmep of a mixed-flow supercharger will be 52 psi. The compressor mep, from eq 10-26 is

$$\text{cmep} = \frac{255}{18{,}000(0.040)0.48}\left(\frac{0.24(560)0.30}{0.75}\right) = 40 \text{ psi}$$

From eq 9-16, fmep $= 20 + 0.04(261 - 100) = 26.2$; bmep $= 255 - 40 - 26.2 + 52 = 241$; bsfc $= 0.295(255/241) = 0.312$.

The performance with the geared system would be significantly improved with a higher compressor efficiency. From Fig 10-9, this could have been 0.80 in which case, cmep $= 40(0.75/0.80) = 37.5$; bmep $= 241 + (40 - 37.5) = 243.5$; bsfc $= 0.295(255/243.5) = 0.309$.

Example 10-8. Aftercooler. The compressor of example 10-1 is equipped with a water-cooled aftercooler of 0.70 effectiveness. The cooling-water temperature is 80°F. Pressure loss through the cooler is 2%. Compute the engine-inlet density as compared with no cooling.

Solution: The temperature drop through the cooler is computed as follows:

$T_2 = 560 + 560 \times 0.125/0.81 = 647°\text{R}$; $T_w = 460 + 80 = 540°\text{R}$.

From eq 10-40,

$$0.70 = \frac{647° - T_t}{647° - 540}, \qquad T_t = 592°\text{R}$$

$$p_t = 14.7 \times 1.5 \times 0.98 = 21 \times 0.98 = 20.6 \text{ psia}$$

The inlet density with cooling compared to the inlet density without cooling is

$$\frac{20.6}{21.0} \times \frac{647}{592} = 1.07$$

eleven — Influence of Cylinder Size on Engine Performance

Basic to a fundamental understanding of engine performance is an appreciation of the influence of cylinder size. In order to isolate the effects of size, it is necessary to use the concept of *mechanical similitude*, to which frequent reference has already been made. This concept was introduced and defined in Chapter 6, and cylinder-size effects have been discussed in connection with several aspects of engine operation. References 11.10–11.44 discuss the influence of cylinder size in detail.

In a group of cylinders of different size, but of similar design and the same materials of construction, the effects of cylinder size may be summarized as follows:

1. Stresses due to gas pressure and inertia of the parts * will be the same at the same crank angle, provided (*a*) mean piston speed is the same, (*b*) indicator diagrams ($p - \theta$) are the same, and (*c*) there is no serious feed-back of vibratory forces from the crankshaft or other parts of the engine structure. In good design practice this should be true. Theoretical proof of these relations is given in Appendix 7.

2. When inlet and exhaust conditions and fuel-air ratio are the same, similar cylinders will have the same indicator diagrams at the same piston speed (Fig 6-16) and the same friction mean effective pressure. (See

* The parts of a cylinder assembly are taken to include cylinder, piston, connecting rod, and valve-gear parts which pertain to that particular cylinder.

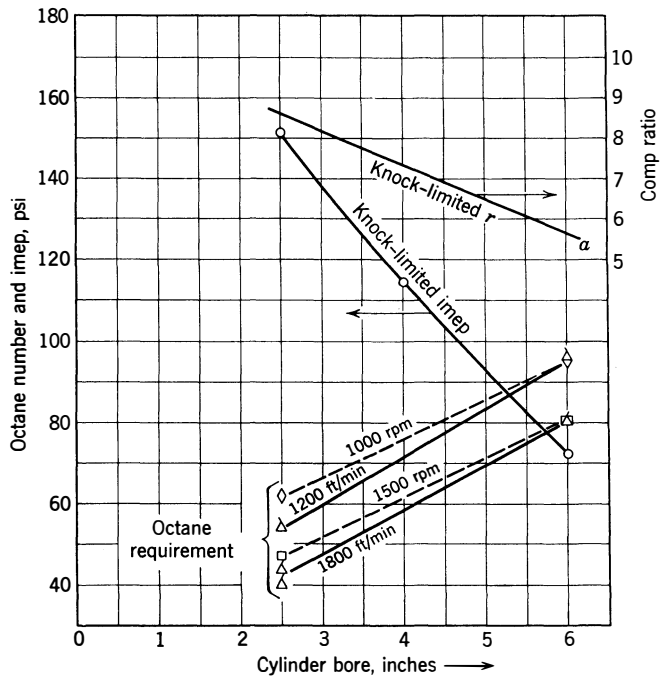

Symbol	Comp ratio	Fuel	Piston speed	Inlet temp °F	rpm	Source
a	var	*	1500	180	var	ref 11.44
○	5.74	72 ON	1200	180	var	ref 11.23
△	5.74	var	1200	160	var	ref 11.43
◁	5.74	var	1800	160	var	ref 11.43
□	5.74	var	var	160	1000	ref 11.43
◇	5.74	var	var	160	1500	ref 11.43

Fig 11-1. Effect of cylinder bore on detonation. MIT similar engines with spark ignition: $F_R = 1.2$; $T_c = 170$°F. For klimep curve, $p_e = 15.7$. For other curves $p_i = 12.1$, $p_e = 15.5$ psia. * 82.5 ON at $s = 1000$, 71 ON at $s = 2000$ ft/min

Fig 9-15.) Under these conditions brake power is proportional to bore squared or to *piston area.* (See also ref 11.6.)

3. Since the weight of a cylinder is proportional to the bore cubed or to the total piston displacement, when the mean pressure and piston speed are the same, the weight per horsepower increases directly with the bore.

4. Unless design changes are made to keep heat-flow paths short, the temperatures of the parts exposed to hot gases will increase as cylinder size increases. (See Fig 8-6 and ref 11.30.)

5. With spark-ignition, as the cylinder bore increases the tendency to detonate increases, and therefore fuels of increasing octane number, or reduced compression ratios, are required, as shown in Fig 11-1. (See refs 11.41–11.44.)

6. In Diesel engines, as cylinder bore increases, because of reduced speed of revolution it becomes easier to control maximum cylinder pressures and maximum rates of pressure rise. Consequently, fuels of lower ignition quality can be used.

7. In both types, as cylinder bore increases, wear damage in a given period of time decreases; that is, the engine lasts longer between overhauls or parts replacement. (See ref 11.36.)

8. With the same fuel, fuel-air ratio, and compression ratio, efficiency tends to increase with increasing cylinder size due to reduced direct heat loss.

Experience to date with the MIT similar engines shows that they behave approximately in accordance with the foregoing "rules." An exception is rule 7, regarding wear, which has not yet been verified by measurements but which is undoubtedly true at least in a qualitative sense.

SIMILITUDE IN COMMERCIAL ENGINES

In practice, the greatest differences in cylinder design are caused by the differing requirements of various types of service. Within each service category, however, a surprising degree of similitude in cylinder design is found. Thus the principles governing similar designs can be used to obtain qualitative comparisons of engine design and performance within a given category.

CYLINDER-SIZE EFFECTS IN PRACTICE

Since ratings constitute the only easily available data on the output of commercial engines, the rated power and rated speed have to be used in any over-all study of cylinder-size effects in practice. In considering the data here presented, it should be remembered that the rating of an engine is partly a subjective decision, based on the manufacturers' estimate of what the engine will be able to do with adequate reliability and durability.

Partly because of detonation limitations and partly because of restrictions imposed by automotive and aircraft service, spark-ignition

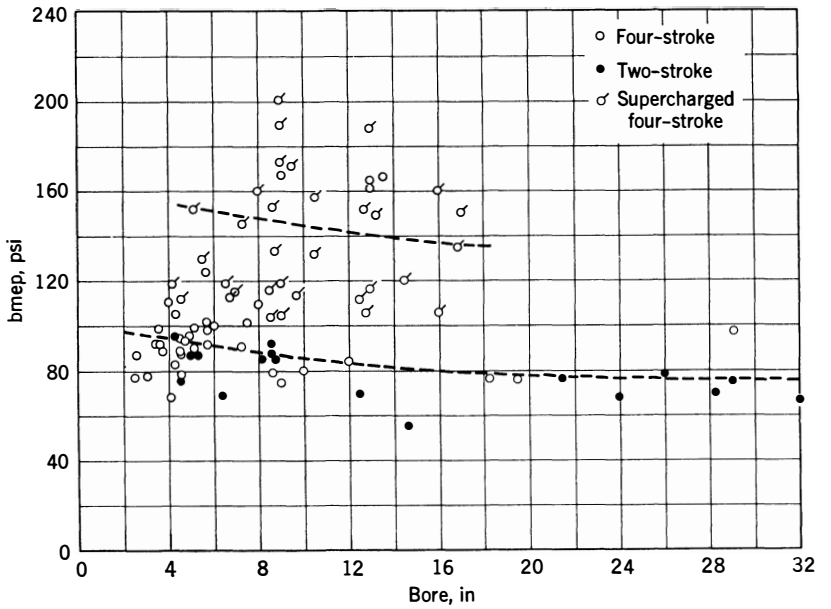

Fig 11-2. Rated bmep vs bore of Diesel engines. (Data from *Diesel Power* April 1954.)

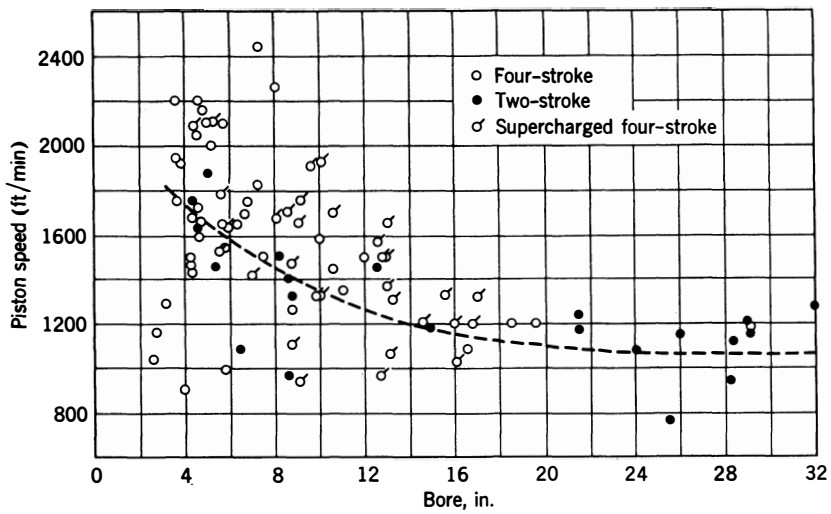

Fig 11-3. Rated piston speed vs bore of Diesel engines. (Data from *Diesel Power* April 1954.)

engines for a given purpose are designed within a small range of cylinder size.* Effects of cylinder size are, therefore, likely to be somewhat obscured by design variations.

Diesel engines, on the other hand, are built in a wide range of cylinder sizes, and for a given type of service the cylinder designs used are quite similar. Therefore, data obtained from Diesel engine ratings should tend

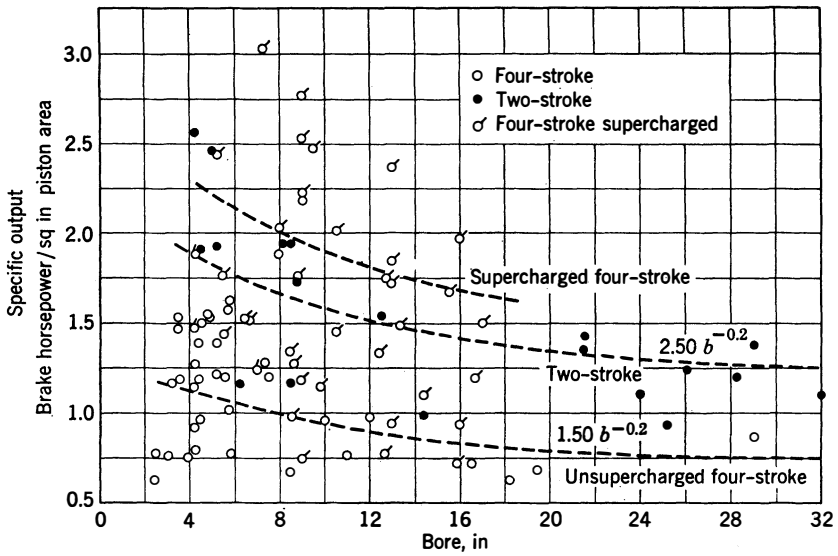

Fig 11-4. Brake horsepower per sq in piston area vs bore of Diesel engines. (Data from *Diesel Power* April 1954.)

to reflect the effects of size which have been shown to hold for similar cylinder designs.

Figures 11-2, 11-3, and 11-4 show rated bmep, piston speed, and specific output of US Diesel engine plotted vs bore. It is evident from these plots that mean values of bmep, piston speed, and specific output all tend to fall as bore increases. These trends are easily explained:

1. Small cylinders are generally used in automotive applications in which high output in proportion to size and weight is very important.

2. In general, large cylinders are used only in services in which there is great emphasis on reliability, durability, and fuel economy. This emphasis encourages low ratings in terms of bmep and piston speed.

* An exception is the case of very large stationary gas engines, which are essentially converted Diesel engines.

3. Stresses due to temperature gradients increase with increasing cylinder size (Chapter 8) unless gas temperatures are reduced. This relation leads toward lower fuel-air ratios, hence lower rated bmep as the bore increases.

4. Extensive development work, and especially destructive testing, become less practicable as cylinder size increases. With little development testing, both bmep and piston-speed ratings must be low in order to insure proper reliability.

5. With increasing cylinder size, it becomes necessary to build up such elements as crankcases, crankshafts, and cylinders out of many parts fastened together, whereas, with small cylinder sizes, one-piece construction is generally used. Since built-up construction is less rigid than one-piece construction, lower ratings are called for.

The foregoing factors appear sufficient to account for the fact that average rated bmep and piston speed grow smaller as cylinder size increases. In spite of this fact, rated power is much more nearly proportional to piston *area* than to piston *displacement*, as indicated by Table 11-1.

Table 11-1

Ratio of Rated Power to Piston Area and Piston Displacement

(From Fig 11-4)

	Highest Rating		Mean Rating		Lowest Rating	
Bore, in	hp/in^2	hp/in^3	hp/in^2	hp/in^3	hp/in^2	hp/in^3
29	1.38	0.041	1.2	0.035	0.87	0.025
4	2.6	0.55	1.6	0.34	0.75	0.16
Ratio 4/29 in	1.9	13.4	1.33	9.7	0.86	6.4

(Bore-stroke ratio taken as 0.85 in each case.)

Minimum Ratings. It is interesting to note from Figs 11-2–11-4 that minimum values of bmep, piston speed, and specific output are independent of the bore over the whole range. Presumably, the lowest ratings at each bore size are for services in which long life and great reliability are important. Apparently, for this type of service the appropriate values are near bmep = 80 psi, s = 1000 − 1200 ft/min, and P/A_p = 0.75. A question of efficiency probably enters the choice of

piston speed because engines designed for long life are generally used when low fuel consumption is very important. In Chapter 12 it is shown that the piston speed for highest efficiency lies near 1200 ft/min.

Weight vs Cylinder Size. Similar engines will, of course, have weights proportional to their piston displacements. Figure 11-5 shows that commercial engines tend to conform to this relationship. If power is proportional to piston area, for similar cylinders weight per horsepower increases in direct proportion to the bore. Figure 11-5 shows a real trend in the expected direction. Weights lying far above the average

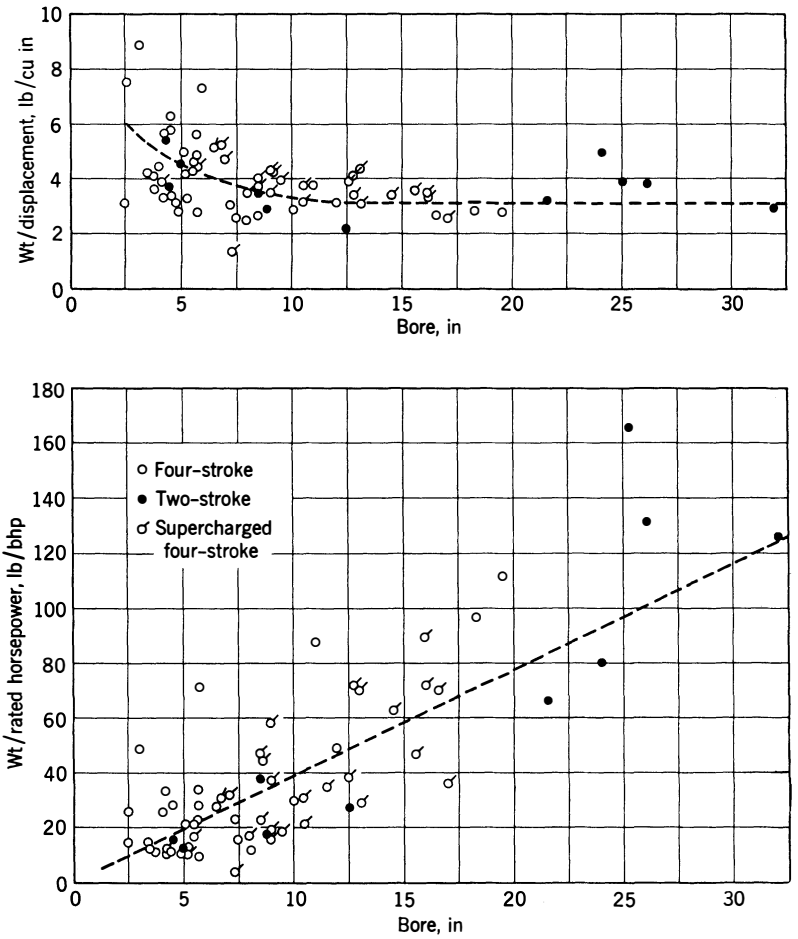

Fig 11-5. Weight per unit displacement and weight per brake horsepower vs bore of Diesel engines. (Data from *Diesel Power* April 1954.)

curve apply largely to obsolescent designs. Designs lying well below the average might be questioned as to their reliability and durability.

EFFECT OF CYLINDER SIZE ON EFFICIENCY

Figure 11-6 shows such data as your author has been able to obtain regarding the effects of cylinder size on thermal efficiency and on specific fuel consumption.

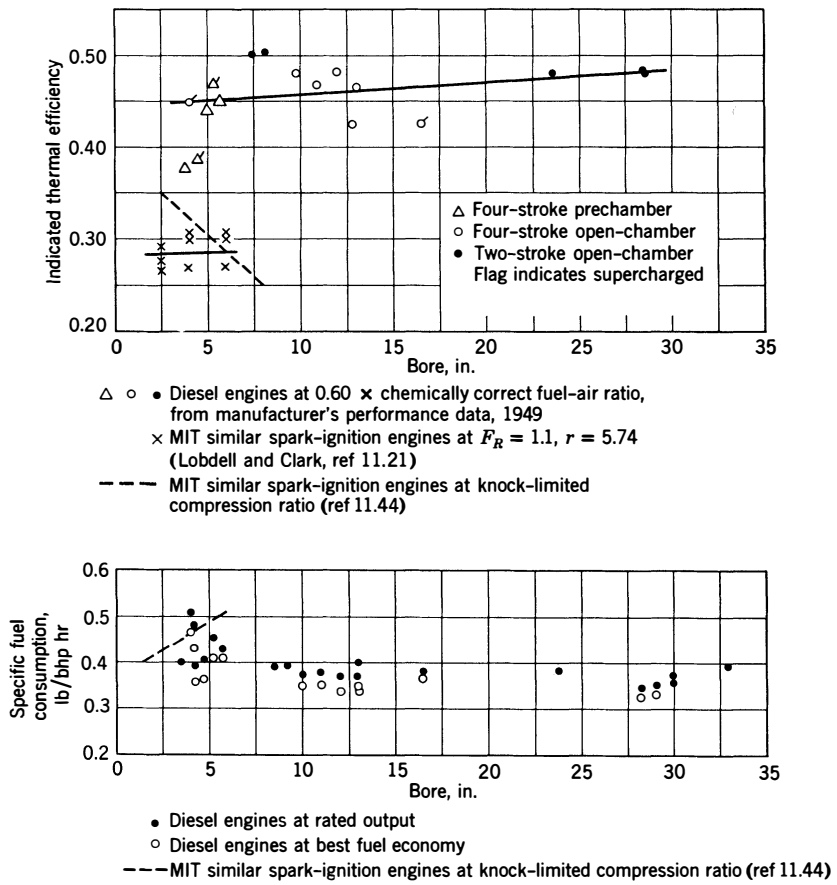

(b)

Fig 11-6. Efficiency and economy vs cylinder bore.

In the case of Diesel engines, if we consider the most economical engines of each size, these data do not indicate a trend toward higher efficiency or improved fuel economy as cylinder bore increases. A possible explanation is that as cylinders are made larger the maximum cylinder pressures are reduced and rates of pressure rise are also lowered. Both of these trends tend to reduce cyclic efficiency and, therefore, to offset the smaller relative heat losses of larger cylinders.

With reference to the data on spark-ignition engines, one curve is taken from measurements on the three MIT similar engines at the same compression ratio and the other is computed from that curve on the assumption that knock-limited compression ratio is used with a given fuel. Evidently, when advantage is taken of the increase in compression ratio which the lower octane requirements of small cylinders allow (ref 11.44), indicated efficiency will not suffer as cylinder size decreases down to $2\frac{1}{2}$-in bore.

Very Small Cylinders. Tests on cylinders of less than 2-in bore (ref 11.35) usually show very poor brake thermal efficiency. This trend can be explained as follows:

1. Very small cylinders have high relative heat loss. (See Chapter 8.)
2. Very small cylinders are used only in services in which fuel economy is relatively unimportant, such as lawnmowers, outboard motors, and model airplanes.
3. Very small cylinders are usually carbureted, with very short inlet manifolds. Therefore, at a given gas velocity the time for mixing of fuel and air is very short. There is evidence that much of the fuel which is supplied by the carburetor in such engines goes through unevaporated and unburned.
4. Because of low cylinder-wall temperatures (giving high ratios of oil viscosity to bore) and generally careless detail design, very small engines may have abnormally high friction mep.*
5. The effective Reynolds number corresponding to gas flow in such engines may be so low that viscous forces add an appreciable increment to the forces resisting gas flow.

It is evident that many of the foregoing characteristics of very small engines should be subject to improvement through careful study and development.

* That this is not always the case is shown by Fig 9-27.

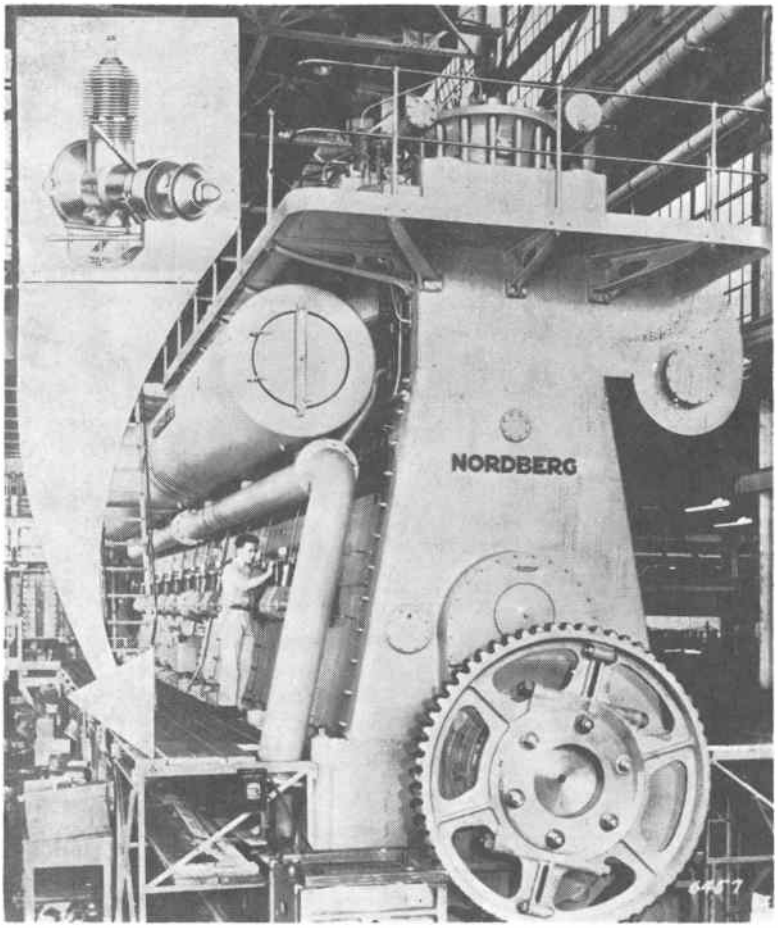

Fig 11-7. Comparison of large Diesel engine with a model airplane engine:

Per Cylinder		Model	Diesel
Bore	in	0.495	29.0
Stroke	in	0.516	40.0
Displacement	in^3	0.10	26,500
bhp		0.136	710
rpm		11,400	164
bmep	psi	47	66
Piston speed	ft/min	980	1,100

See Table 11-2 for further details.

EXTREME EXAMPLE OF SIZE EFFECTS

Figure 11-7 shows the largest and smallest engines for which reliable data are available to the author. Table 11-2 shows the main character-

Table 11-2

Comparison of a Large Diesel Engine with a Model-Airplane Engine

(Both engines are two-stroke, loop-scavenged types. Model-airplane engine has crankcase compression.)

	Model-Airplane Engine	Large Diesel Engine	Ratio Small to Large
Extensive Characteristics			
Bore, in	0.495	29	0.017
Stroke, in	0.516	40	0.013
Displacement (1 cyl), in^3	0.10	26,500	3.8×10^{-6}
Power per cylinder, hp	0.136 *	710 †	1.9×10^{-4}
Rotational speed, rpm	11,400 *	164 †	69.5
Weight per cylinder, lb	0.26	78,300	3.3×10^{-6}
Power per cubic inch, hp/in^3	1.36	0.027	50.3
Comparable Characteristics			
Brake mean pressure, psi	47	66	0.71
Mean piston speed, ft/min	980	1100	0.89
Specific output, bhp/in^2	0.71	1.075	0.66
Weight/displ., lb/in^3	2.6	2.94	1.29

* From tests at MIT.

† Manufacturer's rating.

istics of these two engines. In *extensive* characteristics, that is, dimensions, power, and weight, these engines are poles apart. However, when examined from the point of view of factors controlled by stresses and air capacity, namely, bmep, piston speed, power/piston-area, and weight/displacement, their characteristics are quite comparable. It is obvious that the designs are very different in detail, but there is enough basic similarity so that the size effects predicted by theory are verified in a striking manner.

IMPLICATIONS OF CYLINDER-SIZE EFFECTS

It is apparent that the use of small cylinders is a very powerful method of reducing engine size and weight for a given power output, especially in the case of spark-ignition engines in which the efficiency can be improved at the same time by increasing the compression ratio. In practice, this relationship has not always been fully appreciated, although the use of multicylinder engines, or more than one engine in aircraft and ships, is a tacit admission of its validity. (See refs 11.50–11.53.)

Sacrifices which have to be made when the size of cylinders is reduced and the number of cylinders is increased include the following:

1. In the case of Diesel engines, more expensive fuel may be required.
2. A larger number of parts will have to be serviced.
3. The life of wearing parts will be shorter.
4. A reduction gear may be required because of the increased rpm.
5. If only one engine is used, it may be necessary to use complicated cylinder arrangements such as the multirow radial.

If, as cylinder size is reduced, the number of *engines* is increased rather than the number of cylinders per engine, the following additional advantages may be realized:

6. Possibility of varying the load by cutting in or cutting out appropriate units, thus allowing those in operation to run at ratings where efficiency is high.
7. Greater plant reliability because the failure of one engine does not reduce power to zero.
8. Possibility of continuous maintenance without shutting down the whole plant.
9. More convenient maintenance because of small size of parts.
10. Possibility of savings in cost due to adaptability of small parts to automatic production. Figure 11-8 gives some data on costs vs cylinder size.

On the other hand, use of more than one engine introduces the following disadvantages in addition to Nos. 1–4:

11. A transmission system (either electric, hydraulic, or mechanical) is required if the power is to be taken from fewer shafts than there are engines.

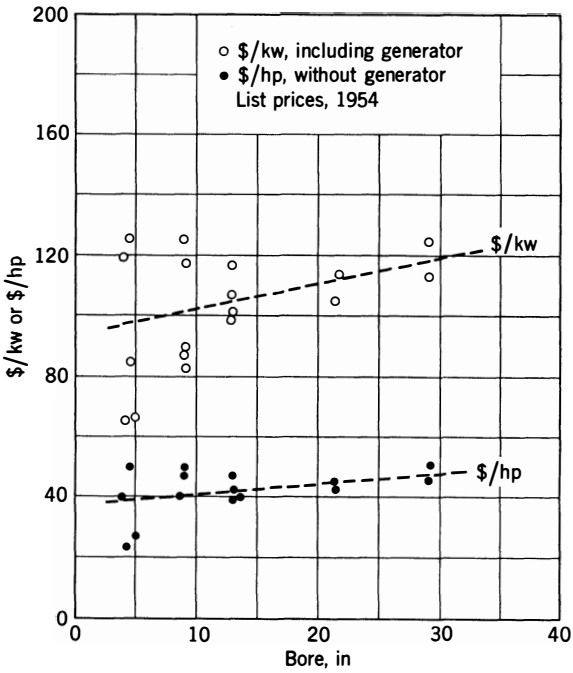

Fig 11-8. Approximate cost of Diesel engines in the United States, in 1954. (Based on dealers' retail quotations in the Boston area.)

12. Problems of control of the relative outputs of the various engines are introduced.

Item No 11 indicates that the use of a number of small engines in place of one large engine is particularly attractive when each engine can be connected to its own separate load, or when electric power is to be generated, because in such cases the problem of connecting the units is minimized. Examples in practice are:

Diesel-engine generating stations
Diesel-engine or gas-engine pumping stations
Multiengine Diesel locomotives
Multiengine airplanes
Multiengine ships

In the latter category is an interesting example of a multiengine installation with eight engines geared to two shafts (ref 11.52). (See also ref 11.53.)

ILLUSTRATIVE EXAMPLES

Example 11-1. Relation of Size and Weight to Bore. A passenger-automobile engine has the following characteristics: 8 cylinders, 4-in bore, $3\frac{1}{2}$-in stroke, max rating 250 hp at 5000 rpm, comp ratio 7.2, weight 550 lb, over-all length 38 in, width 30 in, height 30 in.

By using the same detail design in a 12-cylinder Vee engine with the same maximum output at the same stress level, compute the weight and dimensions. Assume that the angle between cylinder blocks remains at 90°.

Solution: At the same stress level, the 12-cylinder engine will operate at the same mep and piston speed and will therefore have the same total piston area. Bore $= 4\sqrt{\frac{8}{12}} = 3.26$ in. Weight $\sim$ displacement, which is proportional to piston area $\times$ stroke. Since stroke is proportional to bore,

$$\text{weight} = 550 \times 3.26/4.0 = 448 \text{ lb}$$

Width and height will be proportional to bore:

$$\text{width} = (30 \text{ in})3.26/4.0 = 24.5 \text{ in}$$

$$\text{height} = (30 \text{ in})3.26/4.0 = 24.5 \text{ in}$$

Length will be proportional to number of cylinders $\times$ bore:

$$\text{length} = (38 \text{ in})(\tfrac{12}{8})3.26/40 = 46.5 \text{ in}$$

Example 11-2. Relation of Bore to Knock-Limit. Example 11-1 was solved on the assumption of no change in compression ratio. However, Fig 11-1 shows that the compression ratio with the smaller bore could be raised from 7.2 to 7.9 with a corresponding increase in indicated efficiency from a fuel-air cycle value of 0.34 to 0.35 at $F_R = 1.2$. Thus, with the same fuel, the 12-cylinder engine could give greater power by a factor of $0.35/0.34 = 1.03$, or its bore could be decreased by $1/\sqrt{1.03} = 0.985$ to $0.985(3.26) = 3.2$ in. The resultant weights and dimensions would be

$$\text{width} = (30 \text{ in})3.2/4.0 = 24 \text{ in}$$

$$\text{height} = (30 \text{ in})3.2/4.0 = 24 \text{ in}$$

$$\text{length} = (38 \text{ in})(\tfrac{12}{8})3.2/4.0 = 45.6 \text{ in}$$

$$\text{weight} = 550 \times 3.2/4 = 440 \text{ lb}$$

Figure 11-1 shows that with the further decrease in bore from 3.26 in to 3.2 in the compression ratio could be raised to give a slightly increased output and efficiency, but the increment is within the limit of accuracy of the estimate.

Example 11-3. Effect of Cylinder Size, Automobile Engines. Estimate the weight, length, and relative fuel economy of 6-cylinder and 4-cylinder engines to give the same output as the 8-cylinder engine of example 11-1, using the same fuel.

Solution: If the engines run at the same compression ratio and piston speed, the cylinder bores required will be

$$4\sqrt{\tfrac{8}{6}} = 4.62 \text{ in for 6-cylinder engine}$$

$$4\sqrt{\tfrac{8}{4}} = 5.65 \text{ in for 4-cylinder engine}$$

Reading from Fig 11-1, the knock-limited compression ratio at these bores would be 6.7 and 5.8. At $F_R = 1.2$, the corresponding fuel-air-cycle efficiencies from Fig 4-5 are 0.33 and 0.315. To equal the power of the 8-cylinder engine, the bores will have to be enlarged so that the product of piston area and efficiency is the same as that of the eight.

For the 6-cylinder engine:

$4.62\sqrt{0.35/0.33} = 4.75$ in

Knock limited r at this bore (Fig 11-1) = 6.6

Fuel-air efficiency at this ratio is so close to 0.33 that no further correction is necessary.

For the 4-cylinder engine:

$5.65\sqrt{0.35/0.315} = 5.95$ in

Knock-limited r (Fig 11-1) = 5.6

Fuel-air efficiency at this ratio is 0.31 so that a further enlargement of the bore is required.

$5.95\sqrt{0.315/0.31} = 6.0$ in at which bore the knock-limited r is 5.6 and fuel-air-cycle efficiency is 0.31 as required. The following tabulation can now be made:

No Cylinders	Bore	r	Fuel-Air Eff	bsfc at Full Power (1)	Length in (2)	Weight lbm (3)
12	3.20	7.9	0.35	0.53	45.6	440
8	4.00	7.2	0.34	0.547	38.0	550
6	4.75	6.6	0.33	0.563	67.7	652
4	6.00	5.5	0.31	0.600	57.0	825

(1) Fuel-air eff by 0.85(0.80), $Q_c = 19{,}000$, eq 1-12.

(2) 38 (no cylinders in line/4) (bore/4).

(3) 550 (bore/4).

Example 11-4. Multiple vs Single Diesel Engines. A freight ship is propelled by a 12-cylinder direct-drive Diesel engine of 30-in bore giving 10,000 hp and weighing 120 lb/bhp. The engine is 25 ft high, 8 ft wide and 45 ft long. It has been suggested that 8-cylinder engines of 12-in bore be substituted, with gearing to the propeller shaft. The gearing is estimated to weigh 20% as much as the engines and to add 15% to the floor space of the engine to which it is connected. Estimate the new dimensions and floor area required, assuming the smaller engines operate at the same stress level.

Solution: For the same output at the same piston speed and mep, the number of 12-in bore cylinders required will be $12(\frac{30}{12})^2 = 75$. Since there may be some loss in the gears, take 10 8-cylinder engines or 80 12-in cylinders.

Total engine weight = $10{,}000(120)(\frac{12}{30})(\frac{80}{75}) = 512{,}000$ lbm, compared with 1,200,000 lbm for the single engine. To this must be added 20% for the gears so that the total weight of engines and gears will be 614,000 lbm. The height of the engines will be $25(\frac{12}{30}) = 10$ ft, which will allow two more useful decks over the engine room. The floor area covered by the engines plus gears will be $15(\frac{80}{75}) = 16\%$ greater than that of the single engine because floor area is proportional to piston area with engines of similar design.

Example 11-5. Multiple vs Single Diesel Engines. The 1958–1959 Diesel engine catalog shows the Cleveland (GM) model 12-498 marine engine rated at 2100 hp supercharged, with 12 cylinders 8.75″ x 10.5 in. The engine weighs 39,000 lbm and is 5.33 ft wide and 16.1 ft long.

Compute the weight and floor area required for the same total output from Detroit (GM) Diesel model 6-71 supercharged engines rated at 235 hp each, for marine duty, and each 3.04 ft wide, 5.7 ft long and weighing 2740 lbm.

Solution: Number of 6-71's required $\frac{2100}{235} = 9$. Total weight 9(2740) = 24,500 lbm. Floor area 9(3.04)5.7 = 156 ft^2, compared with 5.33(16.1) = 86 ft^2 for the single engine. The single large engine, being of Vee type, occupies less floor area than the same power in 6-cylinder in-line engines. If the in-line engines were made in Vee type, the floor area would be nearly the same as that occupied by the single large engine.

Example 11-6. Comparative Stresses. The large engine of example 11-5 has 12 cylinders, 8.75 x 10.5 in, and is rated at 2100 hp at 850 rpm. The 6-71 engines have 6 cylinders, 4.25 x 5.0 in, and are rated at 235 hp at 1800 rpm for commercial marine purposes. Which engine has the higher stresses due to inertia forces and which has higher stress due to gas loads?

Solution: If engines are of similar design (and they are nearly so), inertia stresses will be approximately proportional to piston-speed squared. For the Cleveland 12-498,

$$s = 850(10.5)\tfrac{2}{12} = 1485 \text{ ft/min}$$

For the Detroit 6-71,

$$s = 1800(5.0)\tfrac{2}{12} = 1500 \text{ ft/min}$$

The inertia stresses, therefore, are nearly the same. Gas loads will be nearly proportional to the indicated mep. If we assume that mechanical efficiency is the same, imep will be proportional to bmep. For the Cleveland Diesel, piston area = 12(60) = 720 in^2. Therefore,

$$\text{bmep} = \frac{(2100)33{,}000(2)}{720(1485)} = 130 \text{ psi}$$

For the Detroit Diesel, piston area = 6(14.2) = 85.2 in^2,

$$\text{bmep} = \frac{(235)33{,}000(2)}{85.2(1500)} = 121 \text{ psi}$$

The larger engine (Cleveland 12-498) appears to carry slightly higher stress due to gas pressure. However, the stress levels are surprisingly close in these two engines.

Example 11-7. Aircraft Application. A typical large reciprocating aircraft engine has 18 cylinders of about 6-in bore and stroke and is rated for take-off at 3500 hp at bmep = 250 psi, piston speed = 3000 ft/min. The compression ratio is 7.0, and the weight close to 1.0 lbm per take-off horsepower. How much weight could be saved by using 4 x 4 in cylinders at the same inertia-stress level, supercharged to the same detonation level with the same fuel? How many cylinders would be required?

Solution: Figure 11-1 shows that the ratio of knock-limited imep between a 4-in and 6-in cylinder is $\frac{115}{72} = 1.6$. For the same inertia-stress level, the same piston speed would be used. The weight per bhp will be proportional to the stroke and inversely proportional to the mep. Therefore,

$$\text{weight/bhp of 4-in cylinder} = 1.0\left(\frac{4}{6}\right)\left(\frac{1}{1.6}\right) = 0.42 \text{ lbm/hp}$$

Comparative weights of the engines using 6 x 6 in and 4 x 4 in cylinders are

$$3500 \times 1.0 = 3500 \text{ lbm} \quad \text{for 6-in bore}$$

$$3500 \times 0.42 = 1470 \text{ lbm} \quad \text{for 4-in bore}$$

The number of cylinders required for the 4-in bore engine would be

$$18(\tfrac{6}{4})^2/1.6 = 25$$

Example 11-8. The General Motors Corporation makes two lines of nearly similar Diesel engines, one with cylinders of 4.25-in bore and 5.0-in stroke and one with cylinders 3.875-in bore and 4.5-in stroke. A 6-cylinder engine of the larger size gives 218 bhp at 2200 rpm with a brake specific fuel consumption of 0.412 lbm/bhp-hr. Estimate the power, rpm, and bsfc of the smaller engine at the same piston speed.

Solution: At the same piston speed, the brake mean effective pressure should be the same and the power will be proportional to piston area. Therefore,

$$\text{bhp (small engine)} = 218\left(\frac{3.875}{4.25}\right)^2 = 180 \text{ bhp}$$

The rpm will be inversely as the stroke:

$$\text{rpm (small engine)} = 2200\left(\frac{5.0}{4.5}\right) = 2440$$

And, since efficiency should not be affected within this small range of bore (see Fig 11-5), the bsfc of the smaller engine should be the same, namely 0.412.

The manufacturer's data on these engines (ref 11.6, Fig 32) confirms these computations.

The Performance of Unsupercharged Engines —— twelve

Under the heading of engine performance may be listed the following factors, all of which are important to the user of an internal-combustion engine:

1. Maximum power (or torque) available at each speed within the useful range (*a*) for short-time operation and (*b*) for continuous operation.
2. Range of speed and power over which satisfactory operation is possible.
3. Fuel consumption at all points within the expected range of operation.
4. Transient operation and control.
5. Reliability, that is, relative freedom from failure in operation.
6. Durability, that is, maximum practicable running time between overhaul and parts replacement.
7. Maintenance requirements, that is, ratio of overhaul time to operating time, and costs of overhaul in relation to first cost and to other operating costs.

Only items 1, 2, and 3 are considered in detail here, since the others do not fall within the scope of this volume. This omission, however, is not intended to minimize the great importance of items 4 through 7 for most types of service.

DEFINITIONS

For the purposes of this discussion the following definitions are used:

Absolute Maximum Power. The highest power which the engine could develop at sea level with no arbitrary limitations on speed, fuel-air ratio, or throttle opening.

Maximum Rated Power. The highest power which an engine is allowed to develop in service.

Normal Rated Power. The highest power specified for continuous operation.

Rated Speed. The rpm at rated power.

Load. Ratio of power (or torque) developed to normal rated power (or torque) at the same speed.

Speed. The revolutions per unit time of the crankshaft.

Piston Speed. Distance traveled by one piston in a unit time.

Torque. The turning effort at the crankshaft.

Automotive Engines. Engines used in passenger automobiles, buses, and trucks.

Industrial Engines. Engines used for quasi-stationary purposes, such as portable electric-power generation, pumping, farm machinery, and contractors' machinery.

Marine Engines. Engines used for ship and boat propulsion.

Stationary Engines. Engines intended for permanent installation at one location.

Smoke Limit. The maximum fuel-air ratio which can be used without excessive exhaust smoke.

BASIC PERFORMANCE MEASURES

The engineer interested in new design, or in appraising existing-engine performance, needs data in a form which will furnish qualitative comparisons. The discussion up to this point indicates that from the point of view of over-all engine performance the following measures of performance will have comparative significance within a given category, assuming that reliability, durability, and maintenance are satisfactory for the given type of service.

I. At maximum rating points:

Mean Piston Speed

This quantity measures comparative success in handling the loads due to inertia of the parts and the resulting vibratory stresses.

Brake Mean Effective Pressure

In unsupercharged engines this quantity is generally not stress limited. It then reflects the product of volumetric efficiency, brake thermal efficiency, and fuel-air ratio at the rating point. In supercharged engines it indicates the degree of success in handling gas-pressure loads and thermal loading.

Specific Output or Power per Unit Piston Area

This affords a measure of the designer's success in utilizing the available piston area regardless of cylinder size. This quantity is, of course, proportional to the product of bmep and piston speed.

Weight per Unit of Power

This quantity indicates relative economy in the use of materials.

Total Engine Volume per Unit of Power

This quantity indicates relative economy in engine space requirements.

II. At all speeds at which the engine will be used with full throttle or with maximum fuel-pump setting:

Maximum bmep

III. At all useful regimes of operation and particularly in those regimes in which the engine is run for long periods of time:

Brake Thermal Efficiency, or

Brake Specific Fuel Consumption and Heating Value of Fuel

COMMERCIAL ENGINE RATINGS

Commercial engine ratings usually indicate the highest power at which the manufacturer believes his product will give satisfactory economy, reliability, and durability under service conditions.

Figure 12-1 shows ratings of commercial engines on the basis of bmep, piston speed, and power per unit of piston area. Since stresses play such a large part in limiting these ratings, it is not surprising to find them falling into groups according to service type.

Maximum Power Ratings. Since structural failure in engines is nearly always due to metal fatigue, the rated bmep and piston speed can be higher for short-time than for long-time operation. Thus the take-off ratings of the aircraft engines are at much higher bmep and piston speed than can be used for continuous operation.

The only engines of Fig 12-1 which are rated at their absolute maximum output are US passenger-automobile engines and two-stroke out-

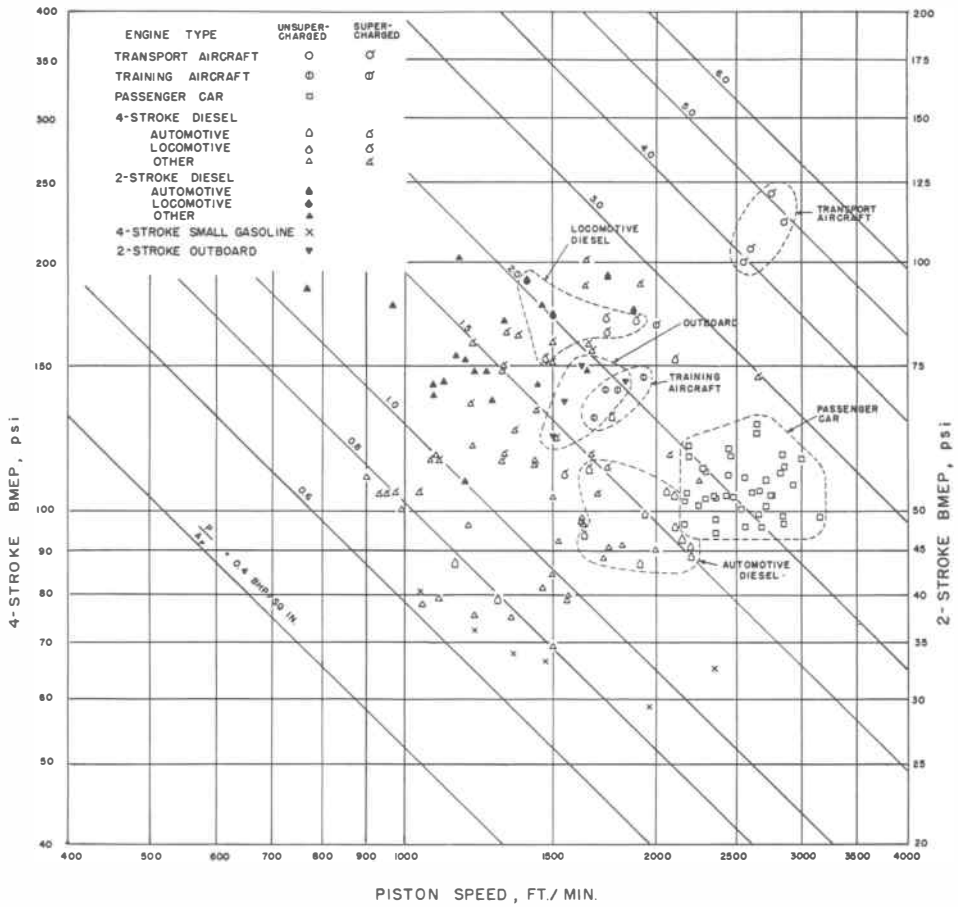

Fig 12-1. Rated brake mean effective pressure, piston speed, and power per sq in piston area. Published rating, 1954 (*Automotive Industries, Diesel Power*). Aircraft-engine ratings are maximum ratings (except take-off) at either sea level or rated altitudes. Diesel and small gasoline engine ratings are continuous maximum; others are maximum.

board engines. In both these cases air capacity tends to approach its peak at a piston speed below that at which inertia stresses become critical. In passenger-car engines the rating is usually based on the highest available power determined on the test-bed without muffler, fan, or air cleaner. Thus rated power is even higher than can be obtained in service (ref 12.2). In passenger automobiles maximum power is seldom used in actual service, and this system of rating is valuable chiefly for sales purposes and as a measure of *relative* engine ability.

In outboard engines the system of crankcase scavenging (Chapter 7) causes the power to peak at piston speeds well below the speed at which inertia stresses become critical. In supercharged aircraft engines the highest or *take-off* rating is limited entirely by considerations of mechanical and thermal stresses.

The maximum, or overload, ratings of Diesel engines are usually based on a fuel-air ratio giving a moderately smoky exhaust. Even these overload ratings are well below the absolute maximum, which occurs at fuel-air ratios so high as to give serious trouble on account of smoke and deposits.

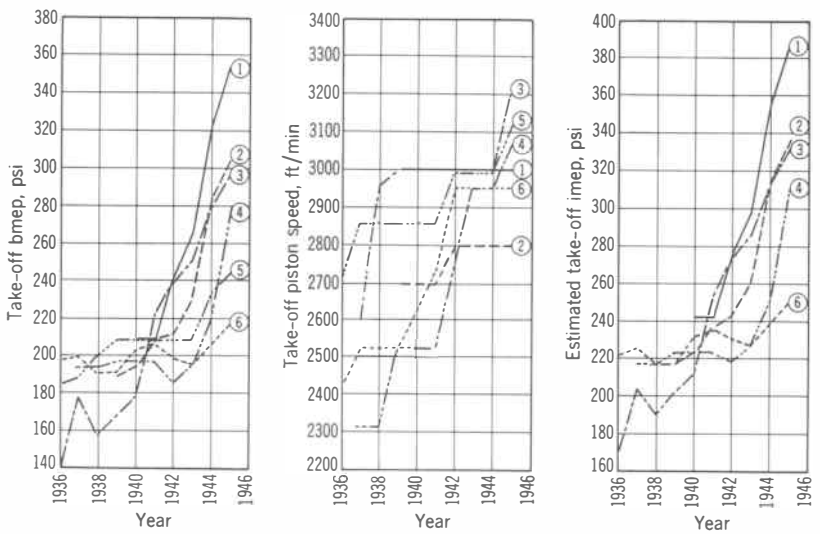

Fig 12-2. Development in United States aircraft engines, 1936–1945:

① Packard Rolls-Royce V1650
② Pratt & Whitney R-2800
③ Allison V-1710
④ Wright R-3550
⑤ Wright R-1820
⑥ Wright R-2600

(From Army Air Force Letter TSEPP-5: EAW: jds, 2-11-46)

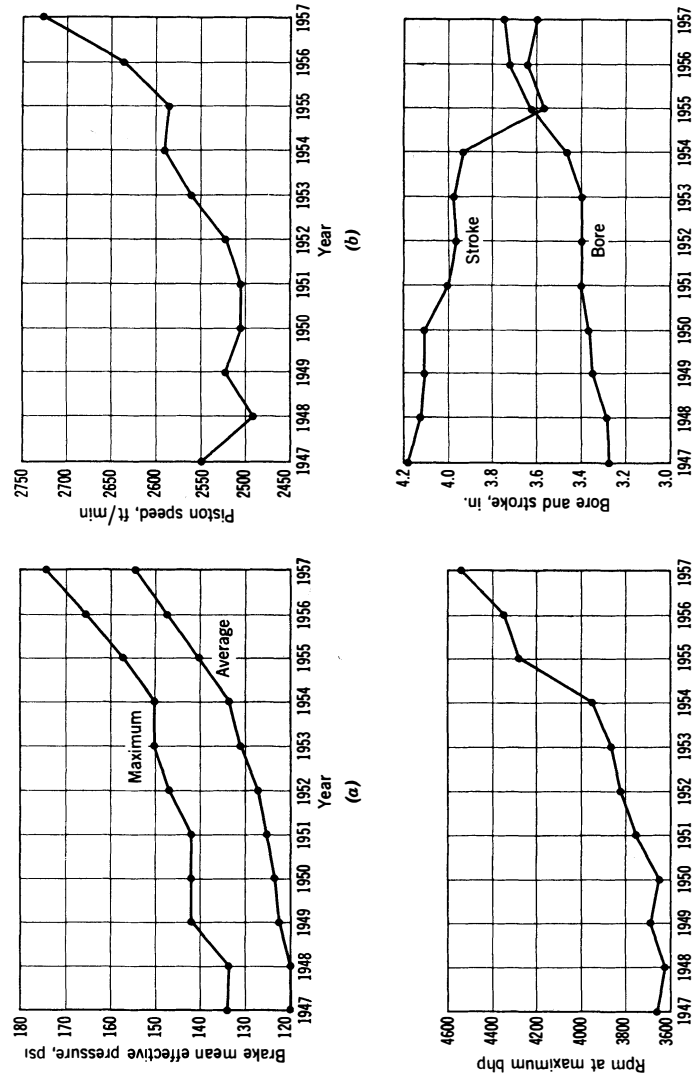

Fig 12-3. Performance vs time, United States automobile engines: (*a*) average and maximum brake mean effective pressure; (*b*) average engine piston speed at maximum brake horsepower rating; (*c*) average engine revolutions per minute at maximum brake horsepower rating; (*d*) average engine bore and stroke measurements. (The Texas Co., ref 12.34) Since 1957 average values have not changed significantly except for bore and stroke, which are slightly smaller in 1985.

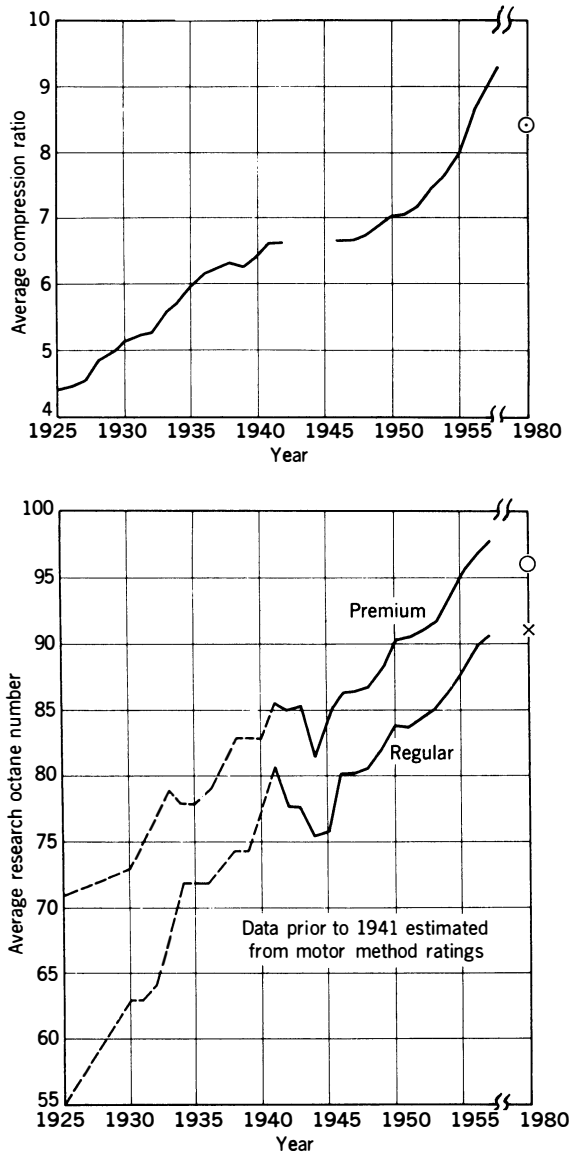

Fig 12-4. Trends in compression ratio and automotive-fuel octane number in the United States. (Bartholomew et al., ref 12.48) ⊙: Average compression ratio, 1980. O Unleaded premium, 1980. X: Unleaded regular, 1980.

Overload, take-off, or absolute maximum ratings are seldom limited by questions of fuel-economy, since the fraction of total operating time at which such outputs are employed is always small.

Effect of Development Time on Engine Ratings

Effect of Development Time on Power Ratings. Figures 12-2 and 12-3 show rated mep and piston speed vs year of manufacture for US aircraft and passenger-car engines. These figures bring out the strong influence of development time on the characteristics of an engine model which is constantly improved as a result of an energetic development program, involving both engine and fuel, carried out concurrently with production and service experience. Rapid improvement in aircraft engines has been shown particularly in wartime when the work has been heavily underwritten by government funds. Since it takes at least four years to bring a new engine model from the design to the production stage, the designer of a new model must take into account the expected improvement of existing competitive models in setting his specifications and objectives.

In general, the increases in piston speed shown in Figs 12-2 and 12-3 have been made possible by improved detail design, whereas the improvements in bmep and bsfc are due partly to improvement in design and partly to increased octane number of the available fuel (Fig 12-4). These two factors have allowed compression-ratio to increase, as shown in this figure.

BASIC PERFORMANCE EQUATIONS FOR UNSUPERCHARGED ENGINES

Unsupercharged engines are defined as including four-stroke engines without compressor or exhaust turbine and two-stroke engines which exhaust directly to the atmosphere. The performance of supercharged engines is covered in Chapter 13. Basic performance equations for all types of engines are summarized in Appendix 8.

From previous definitions, for a change from conditions 1 to conditions 2, we can write:

$$\frac{P_2}{P_1} = \frac{\text{imep}_2 - \text{fmep}_2}{\text{imep}_1 - \text{fmep}_1} \times \frac{s_2}{s_1} \tag{12-1}$$

where P is brake power output and s is piston speed.

When speed is constant, power becomes proportional to bmep, and we write

$$\frac{\text{bmep}_2}{\text{bmep}_1} = \frac{\text{imep}_2 - \text{fmep}_2}{\text{imep}_1 - \text{fmep}_1} \tag{12-2}$$

In the case of unsupercharged four-stroke engines, we have seen from Chapter 9 that, for a given engine, fmep remains substantially constant at a given speed. Two-stroke unsupercharged engines include a gear-driven blower. Equation 10-25 indicates that compressor mep will vary with $\rho_s R_s T_1$, assuming that pressure ratio and compressor efficiency remain constant. However, in most two-stroke engines at constant speed, variations in cmep are so small that it can be considered a constant without serious effect on brake performance. Therefore, when conditions at constant engine speed are under consideration it will be assumed that for two-stroke engines

$$\text{fmep} = \text{mmep} + \text{cmep} = \text{constant} \tag{12-2a}$$

From the definitions of indicated mean effective pressure in Chapters 6 and 7, *for a given four-stroke engine:*

$$\frac{\text{imep}_2}{\text{imep}_1} = \frac{(\rho_a e_v \Gamma)_2}{(\rho_a e_v \Gamma)_1} \frac{(F' \eta_i')_2}{(F' \eta_i')_1} = R_i \tag{12-3}$$

and for a given two-stroke engine:

$$\frac{\text{imep}_2}{\text{imep}_1} = \frac{(\rho_s R_s \Gamma)_2}{(\rho_s R_s \Gamma)_1} \frac{(F' \eta_i')_2}{(F' \eta_i')_1} = R_i \tag{12-4}$$

Combining eqs 12-1 and 12-2 with either eq 12-3 or 12-4 gives

$$\frac{\text{bmep}_2}{\text{bmep}_1} = \frac{R_i - \dfrac{\text{fmep}}{\text{imep}_1}}{1 - \dfrac{\text{fmep}}{\text{imep}_1}} \tag{12-5}$$

From eq 1-6,

$$\text{isfc}_2/\text{isfc}_1 = \eta_{i1}/\eta_{i2} \tag{12-6}$$

and for any condition,

$$\text{bsfc} = \text{isfc}\left(\frac{\text{imep}}{\text{bmep}}\right) \tag{12-7}$$

EFFECT OF ATMOSPHERIC CONDITIONS ON PERFORMANCE

Under this heading we will examine effects of variations in temperature, pressure, and humidity and also the combination of changes in these factors which occurs with changing altitude. From eq 6-6

$$\frac{\rho_{a2}}{\rho_{a1}} = \frac{T_{i1}}{T_{i2}} \left[\frac{p_{i2}[1 + F_i(29/m_f) + 1.6h]_1}{p_{i1}[1 + F_i(29/m_f) + 1.6h]_2} \right] \tag{12-8}$$

where ρ_a = density of dry air in inlet manifold
T_i = inlet temperature
p_i = inlet pressure
F_i = inlet fuel-vapor to dry-air ratio
h = moisture content, mass water vapor to mass dry air
m_f = molecular weight of fuel

A similar equation can be written for two-stroke engines by substituting ρ_s for ρ_a and p_e for p_i.

When atmospheric conditions change let it be assumed that engine speed remains constant.

It seems reasonable to assume that when atmospheric conditions are the only variable the pressure and temperature in the inlet manifold will be proportional to atmospheric pressure and temperature and that the ratio of water vapor to dry air will remain the same in the inlet manifold as in the atmosphere. Under this assumption we may write, for a change from condition 1 to condition 2,

$$\frac{\rho_{a2}}{\rho_{a1}} = \frac{B_2}{B_1} \times \frac{T_1}{T_2} \frac{[1 - F_i(29/m_f) - 1.6h]_1}{[1 - F_i(29/m_f) - 1.6h]_2} \tag{12-9}$$

where B = barometric pressure
T = atmospheric temperature

Effects of Changes in Atmospheric Pressure and Temperature

For this discussion it is assumed that F_i and h and p_e/p_i remain constant while barometric pressure and atmospheric temperature change. In Diesel engines F_i is zero in all cases. In carburetor engines the changes in F_i due to atmospheric changes should be small after the engine is well warmed up. Three cases are considered.

Case 1. Combustion fuel-air ratio is held constant while atmospheric pressure and temperature change, and detonation is not involved. This case approximates the operation of spark-ignition engines at a constant throttle setting and of Diesel engines in which the fuel-pump control is adjusted to hold fuel-air ratio constant.

With p_e/p_i and fuel-air ratio constant, indicated thermal efficiency and trapping efficiency can be assumed constant. Under these conditions it has been shown in Chapters 6 and 7 that $\rho_a e_v$ and $\rho_s R_s$ vary nearly in proportion to $1/\sqrt{T_i}$. Therefore, under the assumed conditions, the value of R_i in eqs 12-5 and 12-7 can be written

$$R_i = \frac{B_2}{B_1}\sqrt{T_1/T_2} \tag{12-10}$$

Effects of atmospheric temperature changes on measured engine performance are shown in Fig 12-5. This figure shows that for multicylinder aircraft engines at fixed throttle and in the absence of a detonation limit, bmep is nearly proportional to $1/\sqrt{T_i}$. This relation indicates that fmep/imep was small and that, possibly, fuel distribution improved with increasing temperature enough to compensate for the friction effect indicated by eq 12-5.

Types other than aircraft engines show a larger reduction in bmep, with increasing T_i, because of their higher ratio of fmep to imep. This trend would be expected from the foregoing equations.

Figure 12-5 also indicates that Diesel engines operated with constant fuel-air ratio show the same trends as spark-ignition engines when allowance is made for their higher friction mep as compared to aircraft engines. (See Chapter 9.)

Case 2. Diesel Engines at Constant Fuel-Pump Setting. At constant engine speed this setting gives a constant rate of fuel flow. Under these conditions fuel-air ratio varies inversely as the mass flow of air, and from eq 12-10 the combustion fuel-air ratio will be proportional to $(B_1/B_2)(\sqrt{T_2/T_1})$.

Since the rate of fuel flow remains constant, the effect on indicated power must be, by definition, affected only by the resulting change in indicated thermal efficiency, and for this case

$$\frac{\text{imep}_2}{\text{imep}_1} = \frac{(\dot{M}_f \eta_i)_2}{(\dot{M}_f \eta_i)_1} = \frac{(\eta_i)_2}{(\eta_i)_1} = R_i \tag{12-11}$$

Figure 12-5 shows a curve for a Diesel engine operated under these con-

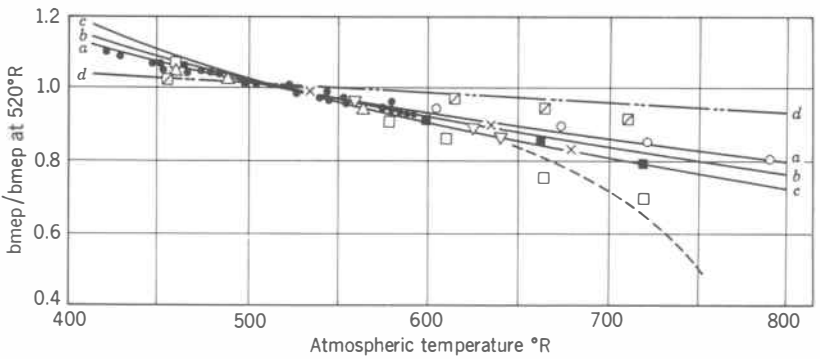

Test results from spark-ignition engines:

- • Wright aero engines, no detonation (ref 12.178)
- ○ Liberty-12 aero engine, no detonation (ref 12.12)
- △ Hispano Suiza aero engine, no detonation (ref 12.13)
- ▽ CFR one-cylinder engine, no detonation (Sloan Labs)
- ——— Pratt and Whitney aero engine, knock-limited (ref 12.174)

Test results from Diesel engines:

- ■ Multicylinder four-stroke engine, (ref 12.181)
- □ One-cylinder four-stroke engine, constant F (ref 12.180)
- ▨ One-cylinder four-stroke engine, constant fuel flow (ref 12.180)
- × Four-stroke sleeve-valve cylinder (ref 12.184)

All data at constant speed, constant barometer.
Throttle setting constant except ———
Fuel-air ratio constant except curve d

Fig 12-5. Effect of atmospheric temperature on engine output:

Theoretical curves

a bmep $\sim 1/\sqrt{T}$
b from eqs 12-5 and 12-10, fmep/imep $\doteq$ 0.15 at 520°R
c from eqs 12-5 and 12-10, fmep/imep = 0.30 at 520°R
d from eqs 12-5 and 12-11 for Diesel engines at constant pump setting, fmep/imep = 0.80 at 520°R

ditions and compares it with results calculated from eq 12-11 with indicated efficiency proportional to fuel-air-cycle efficiency (curve *d*).

Case 3. Detonation Limited. In a spark-ignition engine, when atmospheric temperature or pressure increases to the point at which detonation appears, it is necessary to close the throttle or retard the spark as temperature increases. The resulting curve of bmep vs T_i depends on the character of the fuel used and on details of design and

operation. If the engine is air-cooled, the increase in atmospheric temperature will raise cylinder-wall temperatures also, and the detonation limit may be reached at a lower temperature than would be the case in a liquid-cooled engine with thermostat-controlled coolant temperature. (See refs 12.41–12.45, 12.185, 1.10; also Chapter 6 and Vol 2 of this series.)

Atmospheric Pressure Effects

For the small changes in atmospheric pressure encountered at a given altitude the use of expressions 12-5, 12-7, 12-10, and 12-11 gives results very close to measured engine performance.

Case 1. From eq 12-10 it is evident that when barometric pressure is the only variable and indicated efficiency remains constant $R_i = B_2/B_1$. General experience shows that this assumption holds very well for engines at constant speed with constant fuel-air ratio and fixed throttle opening. (See refs 12.10–12.184.)

Case 2. In Diesel engines at fixed fuel rate the shape of the curve is predicted by eq 12-11, using the variation of efficiency with fuel-air ratio shown in Fig 5-27.

Case 3. As barometric pressure increases if detonation appears, the throttle must be closed or the spark retarded to limit inlet pressure. The shape of the imep vs B curve will depend on particular circumstances, including the type of fuel. (See refs 12.177, 12.186, 12.188, 12.36–12.40.)

Effects of Atmospheric Humidity

Humidity Effects—Spark-Ignition Engines. The effects of humidity on the performance of spark-ignition engine are complicated by the fact that, in general, a change in humidity affects all of the following factors:

1. Inlet-air density
2. Combustion fuel-air ratio
3. Indicated thermal efficiency
4. Volumetric efficiency
5. Detonation limits

The inlet-air density effect is easily calculated from eq 12-8, assuming that h is the only variable.

The effect on combustion fuel-air ratio in carburetor engines depends, of course, on carburetor behavior. From Appendix 3, expression A-15,

it is evident that the mass flow of gas through a carburetor at a given pressure drop will depend on the density, molecular weight, and specific heat ratio of the gas. The changes in these characteristics of air as the humidity changes are given in Fig 3-2. Application of these relations to expression A-16 gives a curve which is approximated closely by the relation

$$\frac{F_2}{F_1} \cong \left(\frac{1 + 1.6h_2}{1 + 1.6h_1}\right)^{3/2} \tag{12-12}$$

The indicated thermal efficiency will, of course, vary with the fuel-air ratio, but it will also be affected by the influence of water vapor on thermodynamic characteristics of the gases before and after combustion. Thermodynamic data (Fig 3-2) show that water vapor increases specific heat and therefore reduces fuel-air-cycle efficiency. It is also known that water vapor slows down combustion and increases time losses unless the spark is properly advanced as humidity increases (ref 12.185).

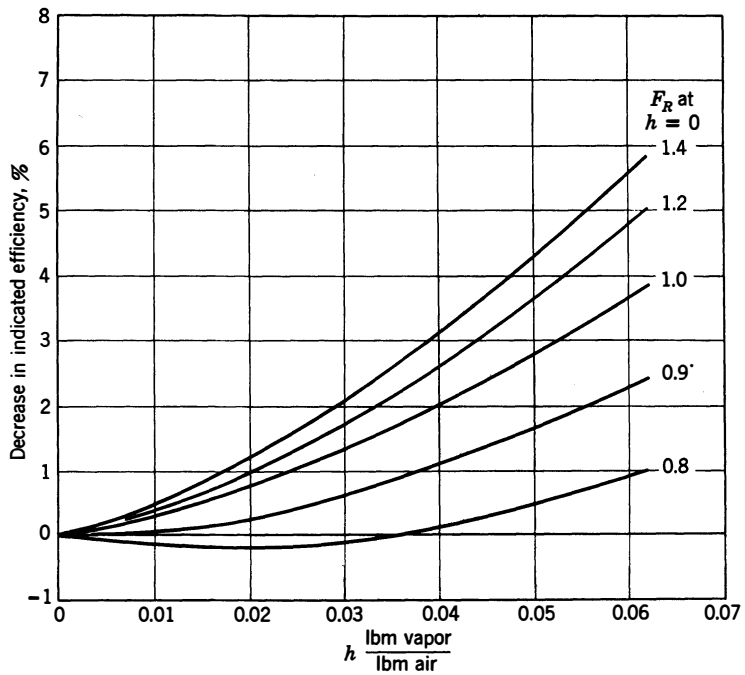

Fig 12-6. Effect of humidity on indicated efficiency: carbureted spark-ignition engine with constant inlet pressure and temperature, constant spark timing, constant carburetor adjustment, *no detonation*. (Based on data in ref 12.189. Courtesy Curtiss-Wright Corporation, Wright Aeronautical Division.)

Volumetric efficiency is affected by the change in sound velocity caused by humidity changes. However, over the usual range, this effect is so small as to be negligible.

Figure 12-6 is based on measured values of indicated thermal efficiency vs humidity, without readjustment in carburetor setting or spark timing, under conditions in which *detonation was not involved.* The drop in efficiency as humidity increases could be somewhat reduced by readjustment of carburetor and spark timing, but such readjustments are never made in practice as a function of varying humidity. Since fuel flow remains constant as humidity varies (and Δp across the carburetor does not change appreciably), the effect of humidity on indicated mep will be the same as the effect on efficiency. Thus, by means of Fig 12-6 and eqs 12-5 and 12-7 the effect of humidity on brake performance can be predicted, provided detonation does not appear.

Effect of Humidity on Detonation. When spark-ignition engines are run near the detonation limit humidity seems to act as a knock suppressor. Figure 12-7 shows octane requirement vs h for an automobile engine using commercial fuel.

If fixed spark timing is assumed, in order to take advantage of the knock-suppressing aspect of increasing humidity, it is necessary to be able to increase the inlet pressure by opening the throttle. Opening the

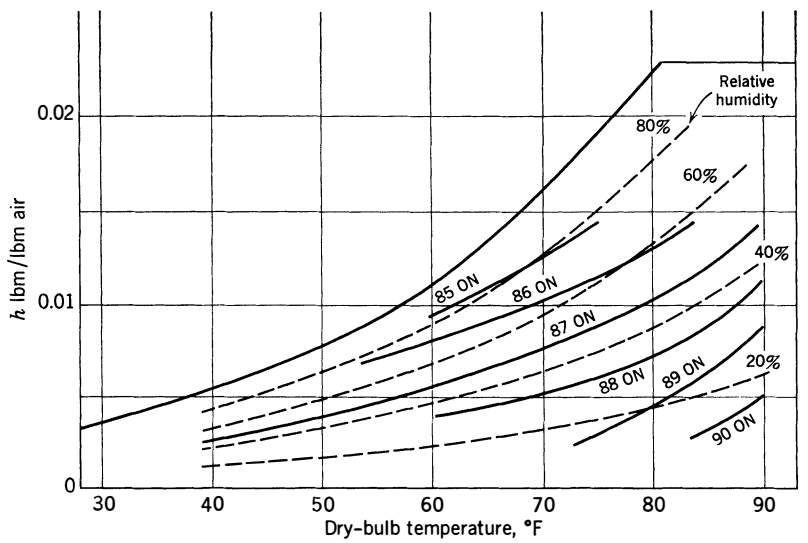

Fig 12-7. Octane-number requirement vs atmospheric humidity. Typical passenger-car engine using commercial fuel. (Potter et al., ref 12.188)

throttle, of course, is possible only if it is not fully open at the lower value of humidity. This situation generally prevails in the case of supercharged aircraft engines at low altitudes but not with most other types. With unsupercharged engines, it is generally not possible to take advantage of the antiknock value of increased humidity, in which case the full-throttle performance is affected as shown in Fig 12-6.

Diesel Engines. Since the fuel-pump setting is never changed as a function of humidity, and since detonation is not involved, the only change would be in efficiency, due to change in dry fuel-air ratio and thermodynamic characteristics. Although no test data appear to be available, it seems safe to conclude that at the low fuel-air ratios used for Diesel engines humidity has little effect on indicated efficiency and therefore little effect on performance.

EFFECT OF ALTITUDE ON ENGINE PERFORMANCE

The question of the effect of altitude on engine performance is of importance when engines are to be operated in mountainous regions and, of course, in aircraft. *Standard* altitude conditions, based on average atmospheric conditions in the United States are given in Table 12-1. Since barometric pressure at a given height varies from day to day, *altitude*, for aeronautical purposes at least, is usually defined by the barometric pressure rather than by the exact height above sea level. Thus a barometric pressure of 20.58 in Hg is taken as 10,000 ft altitude, whatever the actual height above sea level happens to be. Altitudes defined in this way are called *pressure altitudes*.

Since temperature at a given pressure varies according to the weather, and since engine power varies with temperature, the temperature range to be normally expected at a given pressure altitude is of interest. Figure 12-8 shows temperature range vs altitude for the United States.

Figure 12-9 shows curves of bmep vs altitude for a number of engine types with the standard temperatures of Table 12-1. Generally, the effects shown are predictable on the basis of eqs 12-1–12-11. There is an extensive literature on the subject of altitude effects, for which see refs 12.10–12.189.

In Diesel engines a fixed fuel rate can be maintained only over a moderate range of altitude, if excessive smoke and deposits are to be avoided. Actually, if the maximum allowable fuel-air ratio is used at sea level, this ratio must be maintained as altitude increases, and the

Table 12-1

Standard Atmosphere Table

Alt ft	t °F	T °R	a ft/sec	$\frac{\rho}{\rho_o}$	$\sqrt{\rho/\rho_o}$	p in Hg	p lb/sq in	ρ lb/ft^3	$\mu \times 10^7$ $\frac{\text{lb sec}}{\text{ft}^2}$
0	59.0	518.4	1118	1.0000	1.0000	29.92	14.70	0.07651	3.66
1,000	55.4	514.8	1114	0.9710	0.9854	28.86	14.17	0.07430	
2,000	51.8	511.3	1110	0.9428	0.9710	27.82	13.66	0.07213	
3,000	48.3	507.7	1106	0.9151	0.9566	26.81	13.17	0.07001	
4,000	44.7	504.1	1103	0.8881	0.9424	25.84	12.69	0.06794	
5,000	41.2	500.6	1098	0.8616	0.9282	24.89	12.22	0.06592	3.58
6,000	37.6	497.0	1094	0.8358	0.9142	23.98	11.77	0.06395	
7,000	34.0	493.4	1091	0.8106	0.9003	23.09	11.34	0.06202	
8,000	30.5	489.9	1087	0.7859	0.8865	22.22	10.90	0.06013	
9,000	26.9	486.3	1082	0.7619	0.8729	21.38	10.50	0.05829	
10,000	23.3	482.7	1078	0.7384	0.8593	20.58	10.10	0.05649	3.50
11,000	19.8	479.1	1074	0.7154	0.8458	19.79	9.72	0.05474	
12,000	16.2	475.6	1071	0.6931	0.8325	19.03	9.35	0.05303	
13,000	12.6	472.0	1067	0.6712	0.8193	18.29	8.99	0.05136	
14,000	9.1	468.5	1063	0.6499	0.8062	17.57	8.64	0.04973	
15,000	5.5	464.9	1059	0.6291	0.7932	16.88	8.30	0.04814	3.43
16,000	1.9	461.3	1055	0.6088	0.7803	16.21	7.97	0.04658	
17,000	−1.6	457.8	1051	0.5891	0.7675	15.56	7.65	0.04507	
18,000	−5.2	454.2	1047	0.5698	0.7549	14.94	7.34	0.04359	
19,000	−8.8	450.6	1042	0.5509	0.7422	14.33	7.04	0.04216	
20,000	−12.3	447.1	1038	0.5327	0.7299	13.75	6.76	0.04075	3.34
21,000	−15.9	444.5	1034	0.5148	0.7175	13.18	6.48	0.03938	
22,000	−19.5	439.9	1030	0.4974	0.7053	12.63	6.21	0.03806	
23,000	−23.0	436.4	1026	0.4805	0.6932	12.10	5.94	0.03676	
24,000	−26.6	432.8	1022	0.4640	0.6812	11.59	5.69	0.03550	
25,000	−30.1	429.2	1017	0.4480	0.6693	11.10	5.46	0.03427	3.24
26,000	−33.7	425.7	1013	0.4323	0.6575	10.62	5.22	0.03308	
27,000	−37.3	422.1	1008	0.4171	0.6458	10.16	4.99	0.03192	
28,000	−40.9	418.5	1004	0.4023	0.6343	9.72	4.77	0.03078	
29,000	−44.4	415.0	999	0.3879	0.6228	9.29	4.56	0.02968	
30,000	−48.0	411.4	995	0.3740	0.6116	8.88	4.36	0.02861	3.14
31,000	−51.6	407.8	991	0.3603	0.6002	8.48	4.17	0.02757	
32,000	−55.1	404.3	987	0.3472	0.5892	8.10	3.98	0.02656	
33,000	−58.7	400.7	982	0.3343	0.5782	7.73	3.80	0.02558	
34,000	−62.3	397.2	978	0.3218	0.5673	7.38	3.62	0.02463	
35,000	−65.8	393.6	973	0.3098	0.5566	7.04	3.45	0.02369	
36,000	−67.0	392.4	972	0.2962	0.5442	6.71	3.30	0.02265	3.01
37,000	−67.0	392.4	972	0.2824	0.5314	6.39	3.14	0.02160	
38,000	−67.0	392.4	972	0.2692	0.5188	6.10	2.99	0.02059	
39,000	−67.0	392.4	972	0.2566	0.5066	5.81	2.85	0.01963	
40,000	−67.0	392.4	972	0.2447	0.4950	5.54	2.72	0.01872	3.01

Condensed from Standard Atmosphere—Tables and Data. Technical Note No. 218, NACA, 1940. Diehl, Walter S.

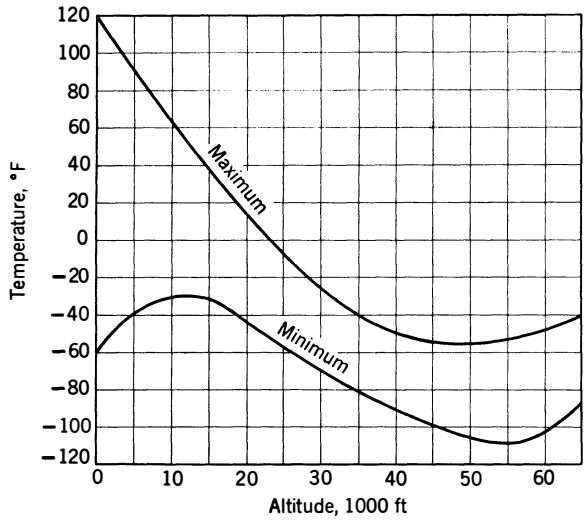

Fig 12-8. Approximate temperature range vs altitude. (Adapted from Byers, *General Meteorology*, McGraw-Hill, 1944.)

power and fuel economy curves will vary in the same way as in spark-ignition engines. (See Fig 12-9.)

Specific Fuel Consumption vs Altitude. In spark-ignition engines, with proper adjustment of spark timing and at a given fuel-air ratio, indicated specific fuel consumption remains nearly constant over wide ranges of inlet density, provided distribution is not affected. If wet fuel is distributed in a multicylinder inlet manifold, the lowering of inlet temperature as altitude increases may have an adverse effect on indicated efficiency, causing a larger reduction in power than would be obtained with constant indicated efficiency. For this reason many aircraft engines use fuel injection to the individual cylinders.

A similar situation may be present in Diesel engines because of the fact that the spray geometry, hence the mixing process, varies with charge density. Therefore, if the injection system is designed for best results at sea level, there may be a reduction in indicated thermal efficiency as altitude increases, even though fuel-air ratio is held constant. This effect would cause power and fuel economy to fall off more rapidly with increasing altitude than in comparable spark-ignition engines. However, the effects of altitude on distribution and on mixing should be small in well-designed engines, and the assumption of constant indicated efficiency will give a good approximation to actual results in most cases.

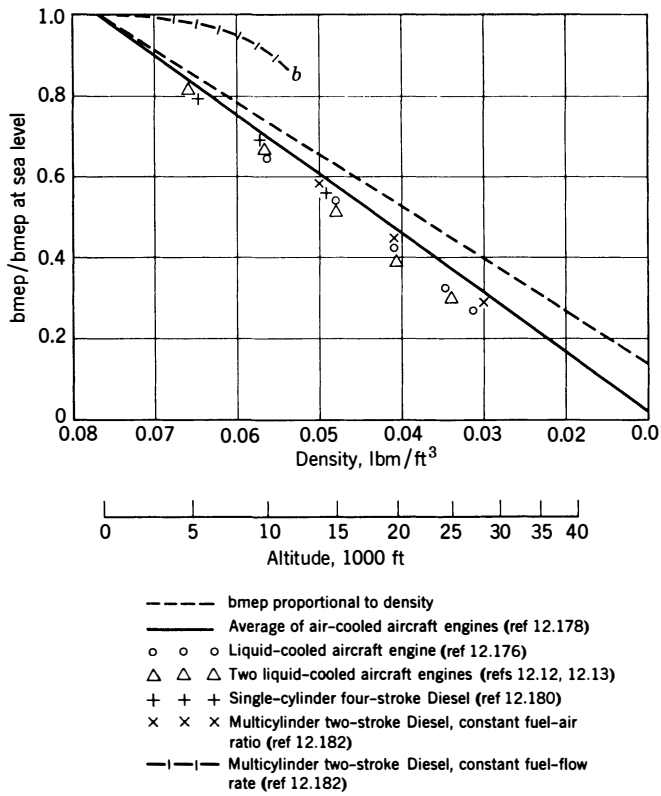

Fig 12-9. Effect of altitude on engine power. Constant speed, full throttle, constant coolant temperature, constant fuel-air ratio except curve *b*. Temperatures standard (Table 12-1).

When altitude changes involve limits imposed by detonation or gas-pressure stresses, indicated mep must be controlled by suitable manipulation of the throttle or fuel-pump control. Under these circumstances, fuel economy vs altitude characteristics are complex functions of fuel and engine characteristics, plus the maker's judgement on what constitutes safe and reliable operation.

Sample calculations of the effect of altitude on performance are given in the Illustrative Examples at the end of this chapter.

EFFECT OF FUEL-AIR RATIO ON PERFORMANCE

In Chapters 4 and 5 we saw the profound effect of fuel-air ratio on indicated output and efficiency, and in Chapters 6 and 7 we saw its much smaller effects on air capacity.

If it is assumed that the air capacity effect can be neglected, we can write from eq 12-3 or 12-4

$$\frac{\text{imep}_2}{\text{imep}_1} = \frac{(F'\eta_i')_2}{(F'\eta_i')_1} = R_i \tag{12-13}$$

where F' is the combustion fuel-air ratio and η_i' is the indicated efficiency based on fuel retained.

It has been shown in Chapter 5 that well-designed engines, either spark-ignition or Diesel, will give 0.80 to 0.90 times the corresponding fuel-air cycle efficiency. (See Figs 5-21 and 5-27.) Figure 12-10 shows the product $F\eta$ for fuel-air cycles taken from Figs 4-5 and 4-6.

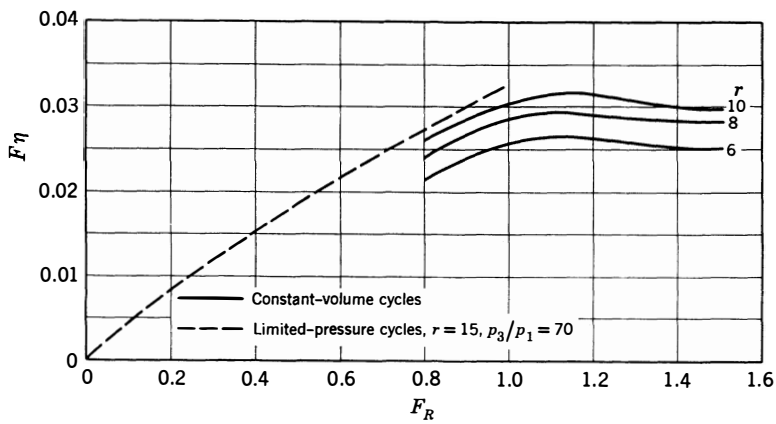

Fig 12-10. Product $F\eta$ for fuel-air cycles. (From Figs 4-5 and 4-6)

It is thus possible, by means of the foregoing equations, to predict the effect of fuel-air ratio on engine performance, provided the friction mep is properly estimated. Chapter 9 has furnished data for friction estimates.

Figures 12-11 and 12-12 compare results computed by means of eqs 12-5, 12-7 and 12-13 with the results of actual engine tests. The assumptions used are given below the figures.

For a spark-ignition engine it is evident in Fig 12-11 that the calculated results agree with the measured results to a very satisfactory degree, except perhaps at $\frac{1}{4}$ load, where small errors in estimating fmep will give

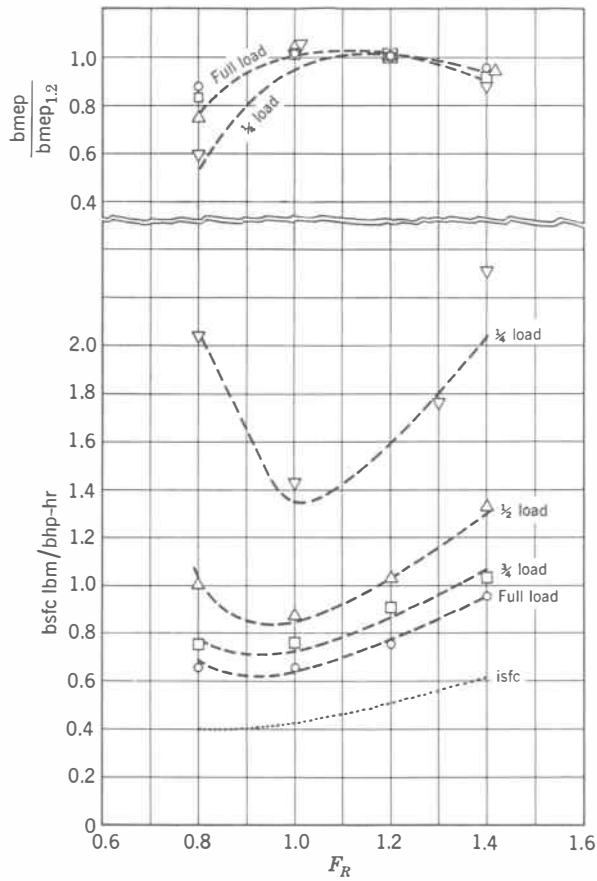

Fig 12-11. Effect of fuel-air ratio on the performance of a spark-ignition engine. ---------- calculated from eqs 12-5, 12-7, and 12-13. Test points are from Fawkes et al., ref 12.30.

large errors in specific fuel consumption. In this case actual measurements of imep and friction mep at full load, $F_R' = 1.2$, were available and were used as the basis of the estimate. The indicated efficiency was taken as 0.80 × fuel-air-cycle efficiency. (See Fig 5-21.)

In Fig 12-12 measurements of fmep and imep also were available. Values of these quantities at $F_R' = 0.6$ were used to establish the base

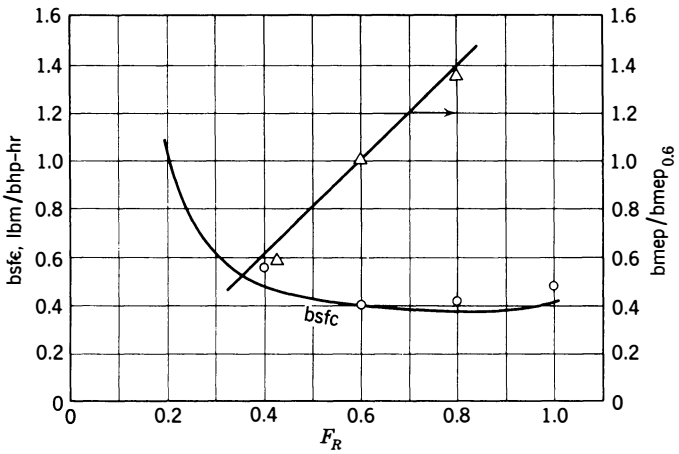

Fig 12-12. Effect of fuel-air ratio on the performance of a Diesel engine.

——— Computed from eqs 12-5, 12-7 and 12-13
$r = 15$, $p_3/p_1 = 70$, $\eta_i = 0.85 \times \eta_{fa}$
fmep/imep = 0.29 at F_R 0.6

o △ Single-cylinder four-stroke Diesel engine,
$r = 15$, fmep/imep = 0.29 at $F_R = 0.6$, (Whitney, ref 12.51)

value of fmep/imep for the calculations. Indicated efficiency was taken as 0.85 of the efficiency of the limited-pressure cycle. (See Fig 5-27.) The results show that indicated efficiency of the actual engine falls somewhat below 0.85 of the fuel-air cycle efficiency except at $F_R' = 0.6$. Values of F_R' above 0.8 are seldom used in practice.

Figure 12-13 shows combustion fuel-air ratios used in practice for spark-ignition and Diesel engines.

In spark-ignition engines the fuel-air ratio for highest power at each throttle setting is at $F_R' = 1.1$, as in the fuel-air cycle. (See Fig 4-5.) At full load the best brake economy in this case occurs at $F_R' = 0.9$. As load decreases, because fmep remains constant, the best economy point increases toward $F_R' = 1.1$ at zero load. The differences between indicated fuel economy and brake fuel economy are, of course, due to the influence of fmep, illustrated by eq 12-7. In spark-ignition engines control of output is achieved by throttling and by changing fuel-air ratio. (The latter control is usually built into the carburetor.) Thus when maximum power is desired F_R' must be at least 1.1. In practice, 1.2 is a more typical full-load value, used in order to allow for imperfect distribution and variations in carburetor performance. At less than full load, the best-economy fuel-air ratio, or more often a slightly higher ratio, is used to allow for variations in carburetion and distribution.

In supercharged aircraft engines the power used for take-off is well above the limits of continuous operation, and for this condition very rich mixtures are used to control cylinder temperatures and detonation.

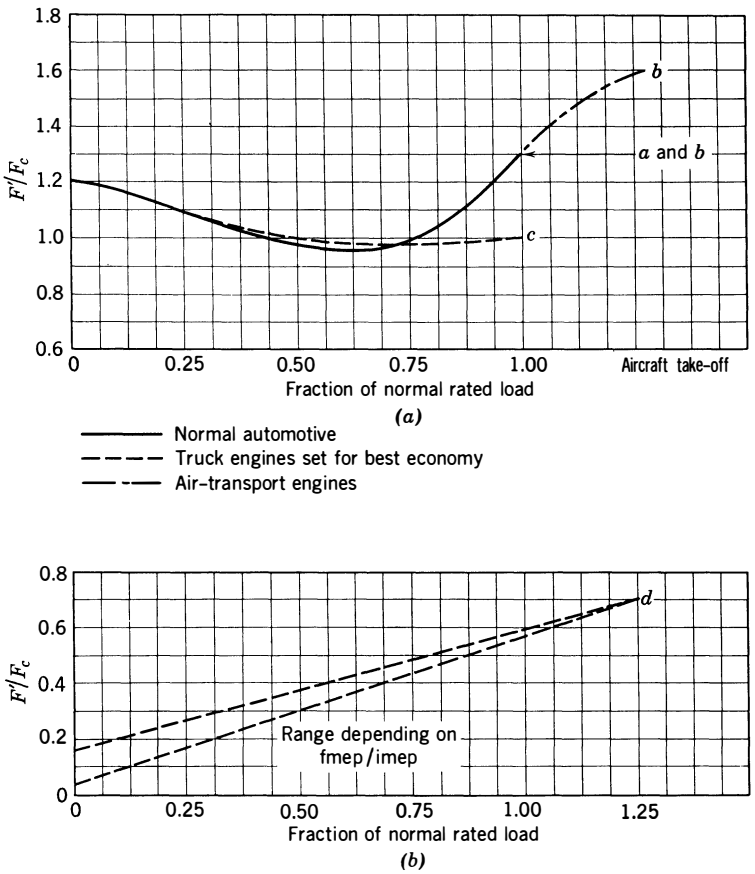

Fig 12-13. Combustion fuel-air ratios normally used in engine operation. Upper graph is for spark-ignition engines. Lower graph is for Diesel engines.

Water-alcohol injection may be used in place of such rich mixtures, in which case the fuel-air ratio is held at about $F_R' = 1.3$ for take-off. The carburetors of some gasoline engines used in trucks are set so that the fuel-air ratio cannot exceed about $F_R' = 1.0$ (curve *c*, Fig 12-13). The reason for this limitation is to conserve fuel (in competition with Diesel engines). In this case maximum engine output is sacrificed for the sake of fuel economy.

More detailed discussion of the question of fuel-air requirements of spark-ignition engines may be found in refs 1.10 and 12.3— and in Vol 2 of this series.

In Diesel engines the maximum allowable combustion fuel-air ratio is that above which smoke and deposits exceed allowable limits. This point is seldom above $F_R' = 0.7$ and is often as low as $F_R' = 0.5$, depending on design and on the type of service. When fuel economy and long life between overhauls are very important, the rating point may be below $F_R' = 0.5$. In most cases operation above $F_R' = 0.6$ is considered overload operation and is limited to short periods. Best economy usually occurs near $F_R' = 0.5$ unless friction mep is large, as in the engine of Fig 12-12.

EFFECT OF SPARK TIMING ON PERFORMANCE

The effect of a change only in spark timing on engine performance must rest on its influence on indicated thermal efficiency. In this case, therefore, the variable in eqs 12-3 and 12-4 will be η_i'.

Figure 12-14 shows that variations in spark timing, from that for maximum power, have the same percentage effect on brake mep at all loads and speeds. This correlation makes it possible to predict the effect of a given departure from best-power spark advance on both output and fuel economy. (See Illustrative Example 12-9.)

Generally, the purpose of using a spark timing other than that for best power is either to control detonation or to make it unnecessary to readjust the spark as a function of engine operating conditions.

A retarded spark is, within limits, a powerful means of controlling detonation. Thus, if the spark is retarded under conditions in which detonation is imminent, it is possible to use a higher compression ratio than would be permissible if the spark were always set for highest power. In this case best-power spark timing can be used under conditions in which detonation is not imminent, and better over-all fuel economy is obtained than with a lower compression ratio. Specifically, engines run most of the time at part throttle, as in road vehicles, use this system of detonation control. How effective it can be is illustrated in the next section under compression-ratio effects.

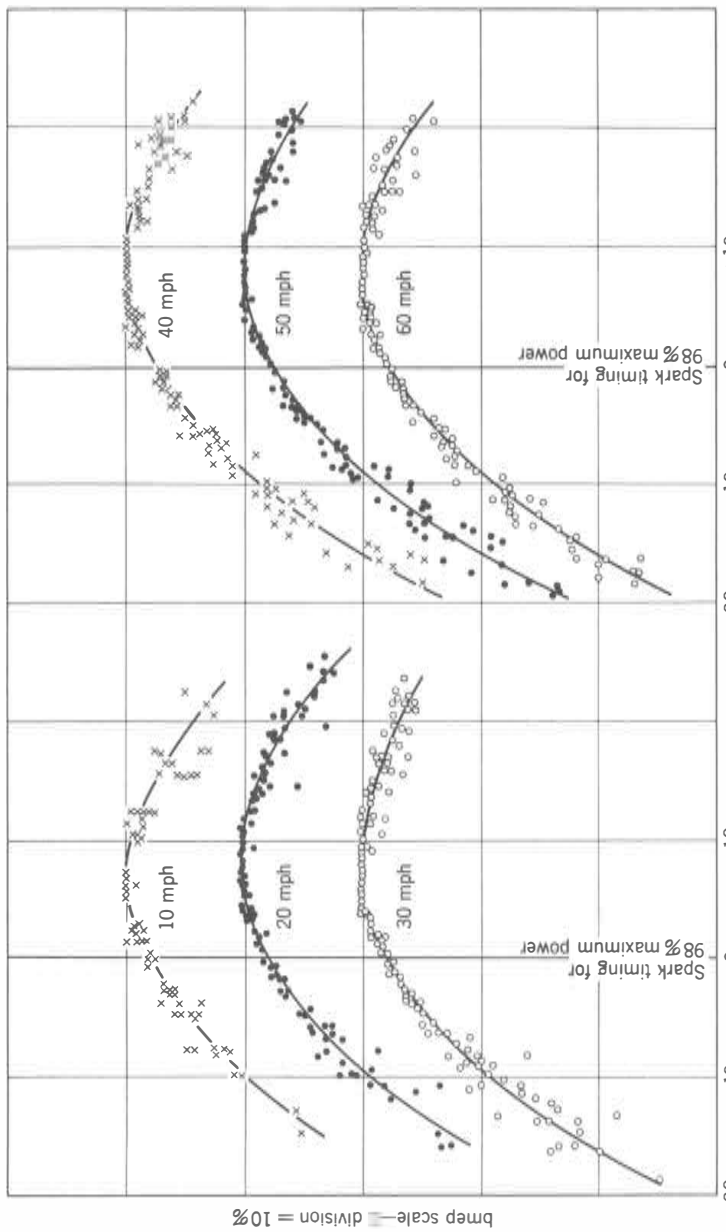

Fig 12-14. Effect of spark timing on bmep for a number of US passenger-car engines (Barber, ref 12.41)

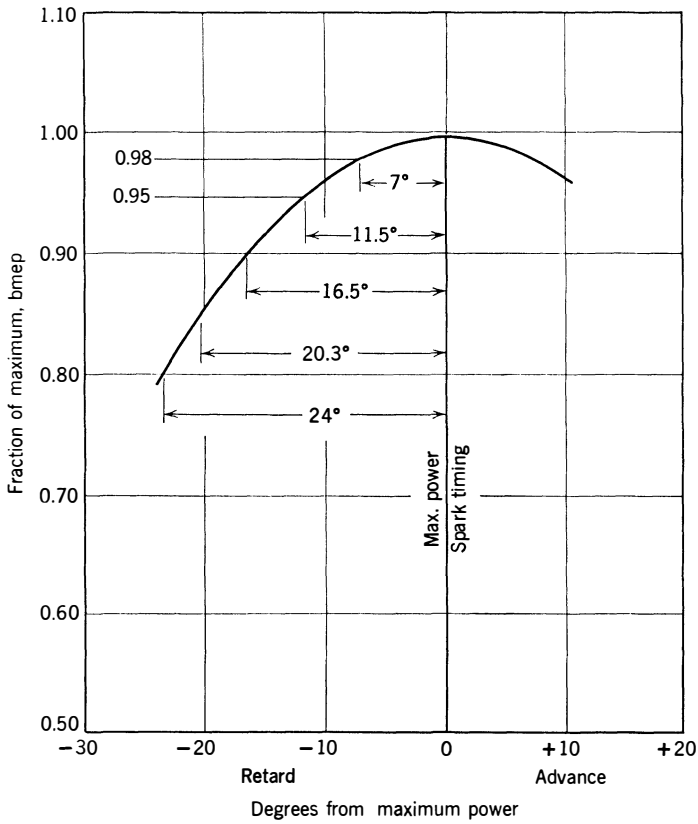

Fig 12-14. Correlation for all speeds and loads

EFFECT OF COMPRESSION RATIO ON PERFORMANCE

Chapter 6 shows that compression ratio has only a small effect on the volumetric efficiency of four-stroke engines. The same is true of the effect of compression ratio on friction (Chapter 9). Thus, in the case of four-stroke engines, the effect of compression ratio comes purely from its influence on thermal efficiency, η_i'.

In the case of two-stroke engines (eq 12-4), since scavenging ratio is based on total cylinder volume, scavenging pump capacity would have to be changed in proportion to $(r - 1)/r$ in order to hold the scavenging

ratio constant. If this is done, R_i for two-stroke engines will be proportional to $\eta_i[r/(r-1)]$.

Four-Stroke Engines with No Detonation. Curve *b* of Fig 12-15 shows the effect of a compression ratio increase from 7.3 to 19 on the performance of an automobile engine using nondetonating fuel. Curve (*a*) shows the performance of the same engine computed from eq 12-5

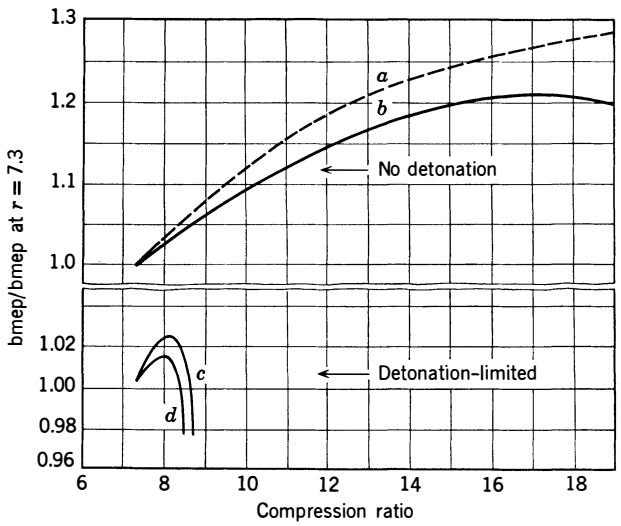

Fig 12-15. Effect of compression ratio on brake output and efficiency. Four-stroke spark-ignition engine: (*a*) from eq 12-5, $\eta_i = 0.85 \times$ fuel-air-cycle efficiency at $F_R = 1.2$; fmep/imep = 0.12 at $r = 7.3$; (*b*) no detonation, ref 12.49; (*c*) spark advanced to incipient detonation, fuel *B*, ref 12.42; (*d*) spark advanced to incipient detonation, 85 ON reference fuel, ref 12.42.

with the assumption that indicated efficiency remains proportional to fuel-air-cycle efficiency. As already shown in Fig 5-21, the ratio indicated efficiency to fuel-air-cycle efficiency decreases as compression ratio rises. Probably the fact that the combustion chamber grows more attenuated and has an increasing surface-to-volume ratio accounts for this decrease in efficiency ratio. At a ratio of 19 the combustion chamber is a very thin disk, which probably means reduced flame speed and increased heat loss as compared to the situation with a lower compression ratio. Probably the shape of curves such as (*b*) of Fig 12-15 will vary appreciably with the details of combustion-chamber design. The peak of brake output at $r = 17$ should not be considered typical until more extensive test results on a number of different engines are available.

Four-Stroke Engines, Detonation Limited. With most fuels, the power output at the borderline of detonation can be maintained for a considerable increase in compression ratio by properly retarding the spark. Figure 12-15 shows that for a particular engine and two fuels, which are knock-limited to 7.3 compression ratio with best-power spark advance, compression ratio can be raised to 8 or more without power loss if the spark is properly retarded. Between ratio 7.3 and 8 a small gain in maximum power is even possible. Quantitatively, such curves vary with engine design, operating conditions, and fuel composition, but, qualitatively, the knock-limited curves of Fig 12-15 are typical. If an automatic spark-timing control is used, as in most automotive spark-ignition engines, the benefits of a high compression ratio can be realized by advancing the spark whenever detonation is not imminent, as may be the case at part throttle or at high speeds.

Two-Stroke Engines. Test results, such as those given in Fig 12-15, do not appear to be available for two-stroke spark-ignition engines. However, the use of eq 12-4 combined with 12-5 and 12-7 should give reliable results, assuming actual indicated efficiency 0.80 times fuel-air efficiency.

Effect of Compression Ratio in Diesel Engines. Within the range used, variations in compression ratio have small effect on efficiency, as indicated by Fig 4-6. Equations 12-5 and 12-7, suitably used, should give reliable results.

CHARACTERISTIC PERFORMANCE CURVES

Methods of Presentation of Performance Data. To the user of a given engine, curves of power, torque, and fuel consumption per unit time covering the useful range of speed and load are usually sufficient. However, such curves do not lend themselves readily to critical analysis or to comparison with other engines as to quality. For our purposes, therefore, it is useful to present performance data on the basis of more generalized parameters, such as bmep, bsfc, piston speed, and specific power output (that is, power output per unit of piston area). As we have seen, these measures are reasonably independent of cylinder size and so are directly comparable between different engines, even though cylinder size may be quite different.

Figures 12-16, 12-17, and 12-18 show curves of bmep, bsfc, and specific output at sea level vs piston speed for typical engines over their useful range. These curves were made with the normal adjustments recom-

mended by the manufacturer and with normal operating temperatures.

Generally speaking, all of these engines show a region of lowest specific fuel consumption (highest efficiency) at a relatively low piston speed

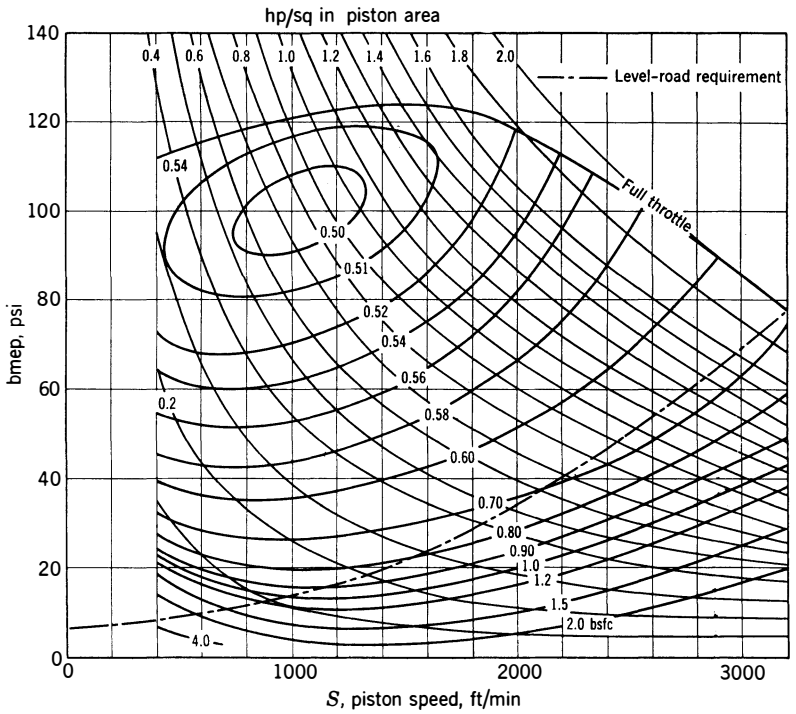

Fig 12-16. Performance map of a typical US passenger-car engine as installed. (Author's estimate from accumulated test data.)

with a relatively high bmep. This region is evidently the one in which the product of indicated and mechanical efficiency is highest.

Moving from the region of lowest bsfc along a line of constant piston speed, mechanical efficiency falls off, as bmep is reduced, because imep decreases while fmep remains nearly constant (Chapter 9). As bmep is increased from the highest efficiency point along a line of constant piston speed, fuel-air ratio increases at such a rate that the indicated efficiency decreases faster than mechanical efficiency increases.

Moving from the region of highest efficiency along a line of constant bmep, friction mep rises as piston speed increases (Chapter 9), and indicated efficiency remains nearly constant. In spark-ignition engines,

moving toward lower piston speed, although friction mep decreases, indicated efficiency falls off because of poor fuel distribution and increased relative heat losses (Chapter 8).

In Diesel engines, as speed is reduced from the point of best economy along a line of constant bmep, the product of mechanical and indicated efficiency appears to remain about constant down to the lowest operating speed. The reduction in fmep with speed is apparently balanced by a reduction in indicated efficiency due to poor spray characteristics at very low speeds.

Attention is invited to the ratio of power at the normal rating point to power at the point of best economy. The ratios of power and economy at these points are a measure of the compromise between the need for high specific output and low fuel consumption in any particular service. The following comparison is interesting:

		Best Economy			SO	Ratio SO at BE
Fig	Type	bmep	s	SO	Max	SO Max
12-16	Passenger car	100	1050	0.8	2.0	0.40
12-17	Four-stroke Diesel	85	1150	0.7	1.7	0.41
12-18	Two-stroke Diesel	80	1000	1.2	2.4	0.50

SO = specific output. BE = best economy. Max = maximum. s = piston speed, ft/min.

It is surprising that among such different types the best-economy point should occur at so nearly the same piston speed and the same ratio of power output to maximum output.

In Fig 12-16 a typical curve of bmep required vs piston speed for level-road operation in high gear is included. As passenger automobiles are now built, it is not possible to run on a level road at constant speed anywhere near the regime of best fuel economy. This penalty is accepted in order to achieve high acceleration and good hill-climbing ability in high gear and to make very high speeds possible. The use of much higher ratios of wheel speed to engine speed would improve fuel economy at the expense of more complicated transmissions and more frequent gear shifts. *Overdrive* is a step in this direction. For a more complete discussion of this subject, see refs 12.70–12.72.

In heavy vehicles, such as trucks, buses, and railroad locomotives, the power-weight ratio is much lower than in passenger cars. In this

type of service average-trip speed is limited more by engine output than by legal speed limits. Since short trip time is of great economic importance, the tendency is to operate these engines most of the time near their point of maximum output rather than maximum economy.

In large aircraft cruising fuel economy is of such great importance that the point of best economy is usually chosen for the cruising regime.

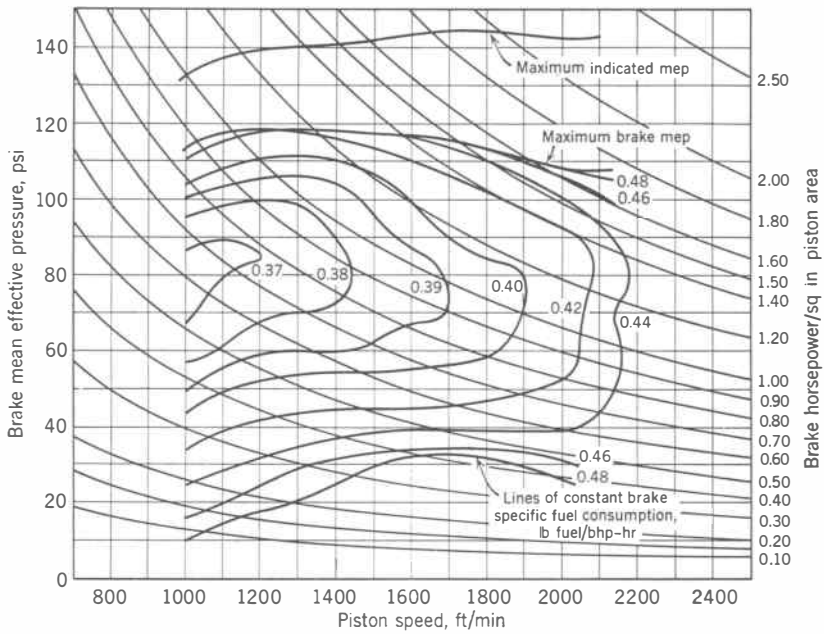

Fig 12-17. Performance curves of a four-stroke prechamber Diesel engine, 5¾ x 6 in (Manufacturer's test, November 1947)

Adjustable pitch propellers make this choice possible. At take-off, fuel economy is of little importance because the time in which take-off power is used is so very short. Figure 12-13 shows how fuel-air ratio is adjusted to attain maximum rated output in take-off and climb and best fuel economy during cruise operation.

Large stationary and marine engines are usually rated at one speed, and no maps, such as Figs 12-16–12-18, appear to be available. In both of these services, however, good fuel economy at or near the engine rating is usually of great importance. Thus such engines tend to be rated at piston speeds and mean effective pressures nearer to the region of best economy than engines for road and rail service.

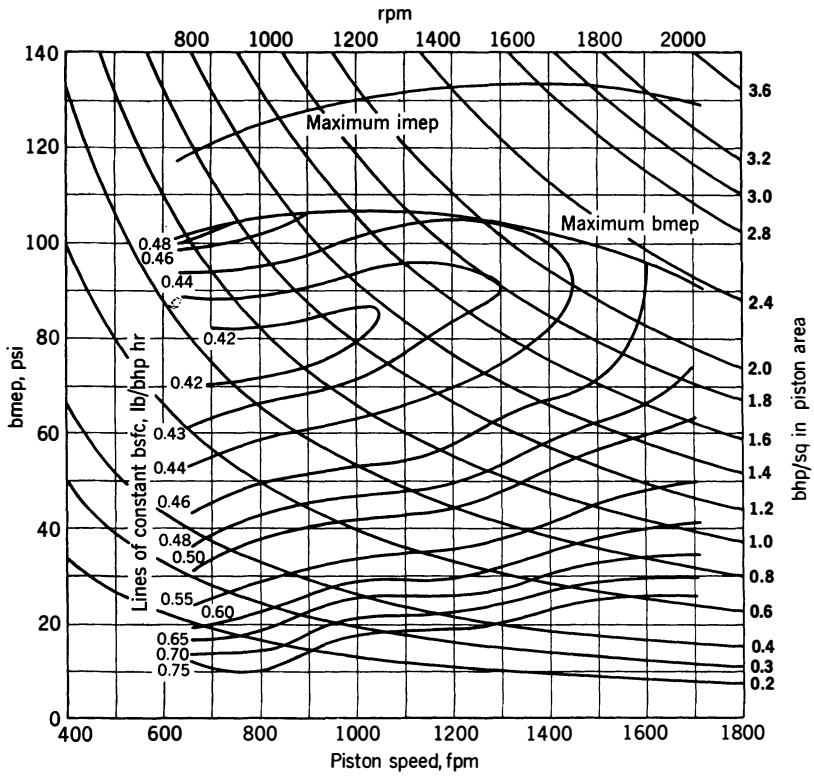

Fig 12-18. Performance curves of a two-stroke, open-chamber Diesel engine, 4¼ x 5 in; $r = 16$. (Manufacturer's test, 1947)

ILLUSTRATIVE EXAMPLES

Example 12-1. Development Time. In designing an automobile engine to be in production in 1961, what values for compression ratio and mean piston speed would be specified? What fuel octane number?

Solution: By projecting the piston-speed curve of Fig 12-3, one might estimate that to be competitive the 1961 rated piston speed should be not less than 3000 ft/min. From Fig 12-4, the compression ratio for 1961 should be not less than 11.0, and the expected octane numbers, 105 for premium fuel and 97 for regular grade.

Example 12-2. Engine Rating. In designing a four-stroke automotive Diesel for 1962, what values of bmep and piston speed should be aimed for?

Solution: The 1962 four-stroke automotive Diesel should be supercharged. Figure 12-1 shows average values for four-stroke supercharged Diesels of bmep =

150, $s = 1500$ ft/min in 1954. By 1962 one would expect these averages to reach bmep = 175 and $s = 1800$. The design for 1962 to be competitive, should have bmep and piston speed not less than these values.

Example 12-3. Effect of Atmospheric Pressure and Temperature, Spark-Ignition Engine. An 8-cylinder automobile engine of 4-in bore, $3\frac{1}{2}$-in stroke, $r = 8.3$ gives 300 bhp at $F_R = 1.2$, 4500 rpm, bsfc = 0.55 with atmospheric conditions 60°F, barometer 29.92 in Hg, dry air. Estimate the power and bsfc under the following conditions:

(*a*) Barometer 29.0 temperature 120°F
(*b*) Barometer 30.5 temperature 20°F

Solution:

$$\text{Piston speed} = 4500(3.5)\tfrac{2}{12} = 2620 \text{ ft/min}$$

$$\text{Piston area} = 8(12.6) = 101 \text{ in}^2$$

$$\text{bmep} = 300(33{,}000)4/2620(101) = 150 \text{ psi}$$

From Fig 9-27, motoring fmep = 35 psi.
From eq 9-16 and Fig 9-31,

$$\text{fmep} = 35 + 0.019(150 - 100) = 36 \text{ psi}$$

From eq 12-10,

(*a*)
$$R_i = \frac{29.0}{29.92}\sqrt{\frac{520}{580}} = 0.92$$

From eq 12-5,

$$\text{bmep} = 150\left[\frac{0.92 - \frac{36}{150}}{1 - \frac{36}{150}}\right] = 134$$

$$\text{bhp} = 300(134/150) = 268$$

Using eq 12-7, we have

$$\text{isfc} = 0.55(150/186) = 0.443$$

$$\text{bsfc} = 0.443\left(\frac{0.92(186)}{134}\right) = 0.565$$

(*b*)
$$R_i = \frac{30.5}{29.92}\sqrt{\frac{520}{480}} = 1.06$$

$$\text{bmep} = 150\left[\frac{1.06 - \frac{36}{150}}{1 - \frac{36}{150}}\right] = 162, \text{ bhp} = 300(162/150) = 324$$

$$\text{bsfc} = 0.443\left(\frac{1.06(186)}{162}\right) = 0.54$$

Example 12-4. Effect of Humidity. Estimate the power and bsfc of the engine of example 12-3 if the humidity had been 80% under conditions (*a*) and 50% under conditions (*b*).

Solution: (*a*) From Fig 3-1, $h = 0.55$. Fig 6-2 shows that at $F_R = 1.2$ the dry air density is decreased in the ratio 0.90/0.98 = 0.92. Fig 12-6 shows that indicated efficiency is decreased by 4%. Therefore, the decrease in indicated power due to humidity is 0.92 (0.96) = 0.883. In example 12-3(*a*), R_t was 0.92. Therefore, the new value of R_t is 0.92 (0.883) = 0.812 and from eqs 12-5 and 12-7, $\text{bmep}_2 = 150\left(\frac{0.812 - 0.193}{1 - 0.193}\right) = 115$, $\text{bhp}_2 = 300(115/150) = 230$, $\text{imep}_2 = 115 + 35 = 150$, $\text{bsfc}_2 = 0.443(150/115) = 0.575$.

(*b*) From Fig 3-1, $h = 0.0011$. From Fig 6-2, decrease in ρ_a is from 0.98 to 0.96. Fig 12-6 shows that efficiency decrease is negligible. R_t in (*b*) of example 12-3 R_t was 1.06. Therefore, R_t for this example is 1.06 (0.96/0.98) = 1.04. From eqs 12-5 and 12-7, $\text{bmep}_2 = 150\left(\frac{1.04 - 0.193}{1 - 0.193}\right) = 158$, $\text{bhp}_2 = 300$ (158/150) = 318, $\text{imep}_2 = 158 + 36 = 194$, $\text{bsfc}_2 = 0.443(194/158) = 0.545$.

Example 12-5. Effect of Humidity. An aircraft engine gives 3000 hp at take off with standard sea-level barometer, air temperature 100°F, humidity zero. Mechanical efficiency is 0.90 and $F_R = 1.4$. Estimate take-off power with saturated air.

Solution: From Fig 3-1, $h = 0.040$ at 100°F saturated. From Fig 6-2, reduction in dry-air density is from 0.98 to 0.92. From Fig 12-6 indicated efficiency will be 0.97 of dry-air value. Therefore,

$$R_t = (0.92/0.98)0.97 = 0.91$$

At mechanical efficiency 0.90, $\text{fmep}/\text{imep}_1 = 0.10$. From eq 12-5:

$$\text{bhp}_2 = 3000(0.91 - 0.10)/1 - 0.10 = 2430$$

Example 12-6. Effect of Altitude, Spark-Ignition Engine. An unsupercharged airplane engine gives 125 hp, bsfc = 0.50 at sea level, $F_R = 1.1$, barometer = 29.92 in Hg, temperature 60°F, humidity 40%. Mechanical efficiency under these conditions is 0.80. Estimate power at 10,000 ft, humidity zero, temperature average.

Solution: From Table 12-1 at 10,000 ft, barometer = 20.58 in Hg, temp = 483°R. From Fig 3-1, h at sea level = 0.0047. From Fig 12-6, this humidity at $F_R = 1.1$ reduces indicated efficiency a negligible amount.

$$R_i = \frac{20.58(1 - 0)}{29.92(1 - 1.6(0.0047))}\sqrt{\frac{520}{483}} = 0.71$$

$$\text{bhp} = 125\left(\frac{0.71 - 0.20}{1 - 0.20}\right) = 80$$

$$\text{isfc} = 0.50(0.80) = 0.40$$

$$\text{bsfc} = 0.40\left[\frac{0.71(125/0.80)}{80}\right] = 0.554$$

Example 12-7. Effect of Atmospheric Changes, Diesel Engine at Fixed Pump Setting. A Diesel engine with $r = 15$ gives 1000 bhp, bsfc = 0.38, with $F_R = 0.6$, barometer 29.8 in, temp 60°F, humidity 60%. Mechanical efficiency is 0.82. Estimate its power and fuel economy with the same fuel-pump setting at 5000 ft altitude, normal temperature and pressure, humidity 30%.

Solution: Since fuel-flow remains the same, any change in power will be due to a change in efficiency. From Table 12-1 the standard conditions at 5000 ft are temperature 41°F, barometer 24.89 in. The new value of F_R will be inversely as the dry air flow. From Fig 3-1, h at sea level = 0.007 and at 5000 ft = 0.0007; then,

$$F_R = 0.6\left[\frac{29.8[1 - 1.6(0.007)]}{24.89[1 - 1.6(0.0007)]}\sqrt{\frac{520}{501}}\right] = 0.74$$

From Fig 4-6, the fuel-air cycle efficiency at $r = 15$, $p_3/p_i = 70$ (average value) is 0.54 at $F_R = 0.6$, and 0.52 at $F_R = 0.74$. If the indicated efficiency remains proportional to the fuel-air cycle efficiency, R_i from eq 12-11 = 0.52/0.54 = 0.964. At 0.82, mechanical efficiency fmep/imep$_1$ = 0.18; then from eq 12-5,

$$\text{bhp} = 1000\left[\frac{0.964 - 0.18}{1 - 0.18}\right] = 957$$

Since fuel flow remains constant, bsfc will be inversely proportional to bhp, and

$$\text{bsfc} = 0.38(1000/957) = 0.397$$

Example 12-8. Effect of Fuel-Air Ratio. A two-stroke Diesel engine of 8-in bore and 10-in stroke, $r = 15$, gives 1200 bhp, 0.36 bsfc at 1000 rpm, bmep = 100 psi, $F_R' = 0.6$. Estimate the power when the fuel rate is reduced 50% at the same speed. Scavenging pump requires 6 mep.

Solution: Piston speed = $1000(10)\frac{2}{12} = 1665$ ft/min.

From Fig 9-27, motoring friction mep is estimated at 18 psi. Friction plus scavenging is, therefore, 18 + 6 = 24 mep. Fuel-air cycle efficiency, from Fig 4-6, is 0.54 at $F_R = 0.6$ and 0.59 at $F_R = 0.3$.

$$\text{imep}_1 = 100 + 24 = 124,\ \text{isfc}_1 = 0.36(100/124) = 0.29$$

$$R_i = 0.3(0.59)/0.6(0.54) = 0.546,\ \text{imep}_2 = 124(0.546) = 67.6$$

$$\text{bmep}_2 = 100\frac{0.546 - 24/124}{1 - 24/124} = 43.6,\ \text{bhp}_2 = 1200\frac{43.6}{100} = 524$$

$$\text{bsfc}_2 = 0.29(0.59/0.54)(67.6/43.6) = 0.491$$

Example 12-9. Effect of Spark Advance. An automobile engine with $r = 7$, $F_R = 1.0$ gives 100 bmep at 2000 ft/min piston speed, best-power spark advance, without detonation. The fuel consumption is 0.50 lbm/bhp-hr. To increase the compression ratio to 8.5 without detonation requires the spark to be retarded 10°. Estimate the power and fuel economy under these conditions.

Solution: At $F_R = 1.0$, Fig 4-5 gives fuel-air cycle efficiency as 0.405 at $r = 7$ and 0.44 at $r = 8.5$. Figure 12-14 shows a loss in bmep of 4% when spark is retarded 10° from optimum. For the change in compression ratio, $R_i = 0.44/0.405 = 1.085$. From Fig 9-26, fmep is estimated at 28 psi. Therefore, from eq 12-5,

$$\text{bmep}_2 = 100(0.96)\left\{\frac{1.085 - \frac{28}{128}}{1 - \frac{28}{128}}\right\} = 105$$

$\text{imep}_1 = 100 + 28 = 128$, $\text{imep}_2 = 105 + 28 = 133$, $\text{isfc}_1 = 0.50(100/128) = 0.39$. Since fuel flow is unchanged, $\text{isfc}_2 = 0.39(128/133) = 0.375$ and from eq 12-7, $\text{bsfc}_2 = 0.375(133/105) = 0.475$

Example 12-10. Use of Characteristic Performance Curves. An automobile engine having the characteristics shown in Fig 12-16 has 8 cylinders, 4-in bore, and $3\frac{1}{2}$-in stroke. It drives a passenger automobile which requires 35 hp at 60 mph from the engine on a level highway. The rear axle ratio is 3.0, which in high gear (1:1) gives 2200 revolutions per mile.

(*a*) Compute miles per gal of gasoline at 60 mph level road.

(*b*) Compute the gear-box ratio for best mileage and the miles per gal for this gear ratio.

Solution: (*a*) Piston area = 8(12.55) = 100 in^2. Piston speed at 60 mph = $2200(3.5)\frac{2}{12} = 1280$ ft/min. bmep = 35(33,000)4/100(1280) = 36 psi.

Figure 12-16 shows bsfc at this point to be 0.63; therefore, with 6 lbm fuel per gallon,

$$\text{miles per gal} = \frac{60(6)}{35(0.63)} = 16.3$$

(*b*) Power required by a car is the same at any gear ratio. Following a line of $P/A_p = 0.35$ on Fig 12-16 shows minimum bsfc = 0.51 at bmep = 90, $s = 500$. The new mileage is computed

$$\text{mpg} = \frac{60(6)}{35(0.51)} = 20$$

and the gear box ratio, engine to drive shaft is

$$1.0\left(\frac{500}{1280}\right) = 0.39$$

Example 12-11. Use of Performance Maps. A certain electric power station needs 5000 hp from new Diesel engines of the type whose characteristics are shown in Fig 12-17. The maximum continuous rating of these engines is at 1800 ft/min and bmep = 100. The engines cost $60 per rated hp and the carrying charges, including maintenance and housing, are 20% of the engine cost. Fuel costs $0.10 per gal. Will it pay to operate the engines at their best-economy point rather than at the rating point? Operation will be continuous, 24 hr per day at 5000 hp.

Solution: From Fig 12-17, the bsfc at rating (s = 1800, bmep = 100) is 0.42. The best economy is bsfc = 0.37 at s = 1200, bmep = 85. The total rated power required to operate at the best economy point is

$$5000\,\frac{(100)1800}{(85)1200} = 8830 \text{ hp}$$

The extra carrying cost per year will be

$$(8830 - 5000)(60)0.20 = \$46{,}000$$

The cost of fuel saved in one year will be, at 7.6 lbm per gallon,

$$5000(24)365(0.42 - 0.37)0.10/7.6 = \$28{,}800$$

The investment in extra engine power is not justified.

Example 12-12. Optimum Scavenging Ratio. Determine the scavenging ratio for best output and for best fuel economy for a two-stroke Diesel engine with the following specifications:

$F_R' = 0.6$, $r = 17$, $p_3/p_1 = 70$, $s = 2000$ ft/min, $C = 0.025$, gear driven compressor with 0.80 efficiency, light Diesel oil. No aftercooler, atmospheric conditions 14.7 psia, 100°F. Scavenging efficiency vs scavenging ratio from eq 7-14.

Solution: From Fig 4-6, fuel-air cycle efficiency = 0.54(0.49/0.47) = 0.56, actual indicated efficiency = 0.56(0.85) = 0.475. From Table 3-1, $F_c = 0.0666$,

$$Q_c = 18{,}250, \qquad F'Q_c\eta' = 0.6(0.0666)18{,}250(0.475) = 346$$

$$\text{isfc} = \frac{2545}{0.475(18{,}250)} = 0.294$$

$$\rho_s = 2.7(14.7)/T_i = 39.7/T_i$$

$$\text{imep} = \frac{778}{144}\left(\frac{39.7}{T_i}\right) e_s(346)\frac{17}{16} = 78{,}800\,\frac{e_s}{T_i}$$

From eq 10-26,

$$\frac{\text{cmep}}{\text{imep}} = \frac{1}{346}\left(\frac{0.24\,T_iY_c}{0.80\Gamma}\right) = 0.000866\,\frac{T_iY_c}{\Gamma}$$

From Fig 9-28 and eq 9-16,

$$\text{fmep} = 20 + 0.08(\text{imep} - 100)$$

From eq 7-19,

$$R_s = 2(0.025)\left(\frac{16}{17}\right)\left(\frac{a_i}{33.3}\right)\left(\frac{p_i}{14.7}\right)\phi_1 = 0.000096a_ip_i\phi_1$$

where ϕ_1 is the compressible-flow function (Fig A-2) for p_e/p_i.

From the above equations, the following tabulation can be made:

p_2/p_1	Y_c	T_i	a_i	ϕ_1	R_s	e_s	imep	Γ	$\frac{\text{cmep}}{\text{imep}}$	cmep	fmep	bmep	bsfc
1	2	3	4	5	6	7	8	9	10	11	12	13	14
1.25	0.0656	606	1202	0.472	1.0	0.64	83	0.640	0.054	4.5	20	59	0.415
1.35	0.089	622	1220	0.517	1.2	0.70	89	0.583	0.082	7.3	20	71	0.369
1.50	0.125	648	1250	0.550	1.46	0.77	94	0.527	0.133	12.3	20	62	0.445
2.0	0.218	713	1310	0.577	2.13	0.88	97	0.413	0.326	31.6	20	45	0.634

1 independent variable
2 Fig 10-2
3 $560(1 + Y_c/0.80)$
4 $49\sqrt{T_i}$
5 Fig A-2
6 previous equation
7 eq 7-14
8 previous equation
9 e_s/R_s
10 previous equation
11 imep(cmep/imep)
12 Fig 9-27
13 imep-cmep-fmep
14 (imep/bmep)isfc

The optimum scavenging ratio for both output and fuel economy is 1.2.

Supercharged Engines and Their Performance —thirteen

DEFINITIONS

A four-stroke engine is defined as *supercharged* when, through the use of a compressor, its inlet pressure is higher than that of the surrounding atmosphere. A two-stroke engine is called *supercharged* when it is equipped with an exhaust-driven turbine.

Figure 13-1 shows several possible arrangements of engine, compressor, and turbine. The following designations are used:

A. Engine with compressor but no turbine. Unsupercharged two-stroke engines and many supercharged aircraft and Diesel engines are this type.

B. Engine with free exhaust-driven compressor. Engines so equipped are said to be *turbo-supercharged.*

C. Compressor, engine, and turbine all geared together. The Wright "Turbo-Compound" airplane engine is a commercial example. (See ref 13.21.) The Napier Nomad (ref 13.22) was an experimental engine of this type.

D. Gas-generator type. In this case an engine drives only the compressor. Air from the compressor flows through the engine, and the exhaust gases drive a power turbine. The experimental "Orion" power

plant (ref 13.23) and most *free-piston* power units (refs 13.30—) are this type.

A common variant of arrangement B consists of two stages of compression, the first stage being turbine driven and the second geared to the engine. This arrangement is common in two-stroke engines, where it

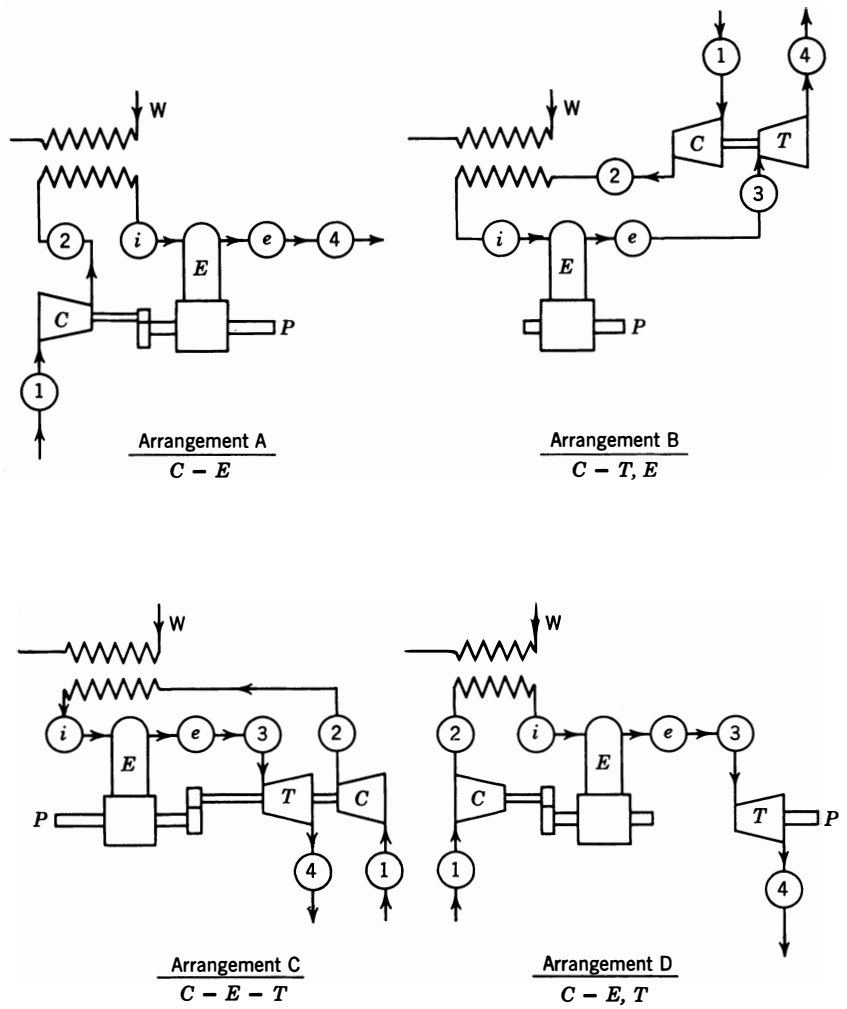

Fig 13-1. Compressor-engine-turbine arrangements: *C* indicates compressor; *E* indicates engine; *P* indicates power take-off; *T* indicates turbine; *W* indicates coolant entering aftercooler.

is difficult to design a type B arrangement which will properly scavenge the engine at all speeds and loads. (See refs 13.08, 13.26.)

Wherever a compressor is used it is possible to insert a cooler on the upstream side of the compressor or between compressor stages. (See Chapter 10.)

In arrangements containing an exhaust turbine the use of an *afterburner*, which consists of a combustion chamber between engine and turbine, has also been suggested as a means of increasing the overload output of the plant, as for take-off purposes. However, no such arrangement is yet in commercial use.

Notation. The following system of notation is used in subsequent figures and discussion in order to identify the stations at which pressures, temperatures, and other fluid characteristics are measured or defined.

Station 1. Entrance to the compressor. In most cases the conditions at this point will be close to those of the surrounding atmosphere
Station 2. Compressor outlet and entrance to aftercooler (if used)
Station i. Engine inlet system
Station e. Engine exhaust system
Station 3. Turbine nozzle box
Station 4. Turbine exhaust. In most cases the turbine exhausts to atmospheric pressure
Station W. Coolant entering aftercooler or intercooler

Unless otherwise noted, steady-state stagnation values are assumed at the above measuring points.

Reasons for Supercharging

Supercharging may be used for any one, or any combination, of the following purposes: to increase in the maximum output of a given engine, to maintain sea-level power at higher altitudes, to reduce the size of an engine required for a given duty, and to improve fuel economy for engines used mostly at or near full load.

SUPERCHARGING OF SPARK-IGNITION ENGINES

In the case of spark-ignition engines, the use of supercharging is complicated by the problem of detonation or "knocking." This phenomenon is discussed in detail in Chapters 2 and 4 of Volume 2, where it is shown that with most available fuels the maximum allowable mep is limited by the occurrence of detonation.

Figure 13-2 shows knock-limited performance as a function of compression ratio, inlet-air density, and fuel octane number for a spark-ignition engine at one particular set of operating conditions, including best power spark timing and fuel-air ratio, and constant inlet-air temperature. It is

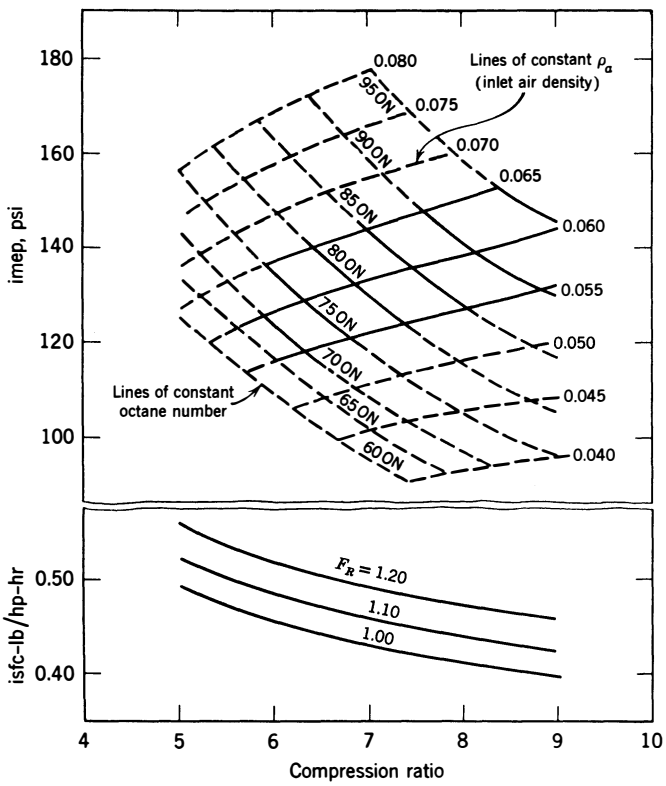

Fig 13-2. Detonation-limited imep and octane requirement vs. compression ratio and inlet density. ON = fuel octane number; imep values are for 1500 rpm; $F_R = 1.2$; $T_i = 70°F$. (Barber, ref. 12.41)

evident that with a given fuel the compression ratio must be reduced as the imep is increased by raising the inlet density. For example, with a 90-octane fuel the engine gives 148 imep at inlet density 0.065 at compression ratio 7.6. To raise the imep to 170 psi requires reducing the compression ratio to 6.5, with an inlet density of 0.078. The increase in indicated specific fuel consumption is 7%, for a 15% gain in specific output. In an actual case, the inlet temperature rises as the inlet pressure is increased; this would require an even lower compression ratio. It is evident that the supercharging of spark-ignition engines requires a compromise between power output and efficiency.

SUPERCHARGING OF AIRCRAFT ENGINES

Superchargers were first developed for airplane engines, for the purpose of offsetting the drop in air density as altitude increases (see pp. 433–436). Credit for the invention of the turbosupercharger (type B, Fig 13-1), around 1915, is given to Rateau. [For a history of aircraft superchargers see Taylor, *Aircraft Propulsion* (Smithsonian Institution Press, 1971).]

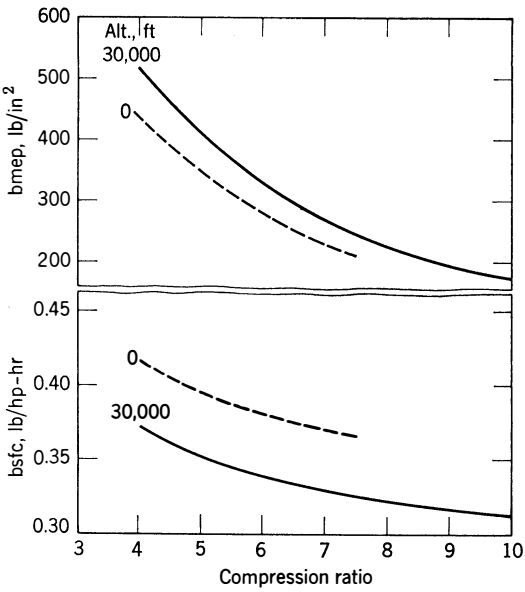

Fig 13-3. Effect of compression ratio and altitude on net mean effective pressure and net specific fuel consumption of a compound aircraft engine (type C, Fig 13-1): knock-limited operation with AN-F-28 fuel; $F_R=1.2$; $p_e=p_i$. (Humble and Martin, ref 13-25)

The General Electric Company took up the development of that type and was a principal supplier of aircraft turbochargers until reciprocating engines were superseded by jet engines for large military and commercial aircraft.

Early large aircraft engines usually used type A, with centrifugal superchargers built into the engine structure and geared to the crankshaft. These could sustain sea-level power to 10,000–15,000 feet. Where still higher altitude capability was required, a turbocharger was added, usually with an intercooler, to serve as a first stage of compression (ref. 13.16). One of the last of the large radial engines used arrangement C, called "turbo-compound," with three exhaust-driven power turbines geared to the crankshaft plus a gear-driven centrifugal supercharger (ref. 13.21). Figure 13-3 shows the effect of compression ratio on the knock-limited performance of this very highly developed supercharged engine. A compression ratio of 7.2 was finally chosen for production. This was the last of the large reciprocating airplane engines.

A high-altitude supercharger system makes it possible to supercharge an aircraft engine to extra high power for takeoff. Since this phase lasts only a very short time, fuel economy is unimportant. Measures to allow extra-high output without detonation include a very rich fuel-air ratio and water or water-alcohol injection. Aircraft gasoline has much higher resistance to detonation that motor-vehicle gasoline (see Volume 2, pp. 145–147).

Contemporary reciprocating spark-ignition airplane engines are built in sizes ranging up to about 500 hp. When supercharged, they use turbo rather than gear-driven superchargers (see Volume 2, table 10-15, p. 421).

SUPERCHARGING OF AUTOMOBILE ENGINES

Since the engines of passenger automobiles and other light vehicles operate at light loads most of the time, efficiency under supercharged conditions can be sacrificed for efficient performance in the light-load range.

As shown in Chapter 2 of Volume 2, for an engine using a given fuel, as the inlet pressure is increased detonation can be delayed by retarding the spark, by increasing the fuel-air ratio, and (as a last resort) by reducing the compression ratio. In the case of automobile engines, present practice in applying supercharging is to retard the spark and enrich the mixture to allow the highest supercharger pressure feasible with minimum reduction in the compression ratio.

The use of superchargers for road vehicles was rare before the development and introduction in the late 1970s of electronic (computerized) control systems with the necessary sensors and actuators to control not only spark timing and fuel-air ratio but also many other variables that affect engine performance and the onset of detonation. A most important sensor in a supercharged engine is one that signals detonation by responding to its characteristic vibration frequency (see Volume 2, Chapter 2). The control system can then adjust ignition timing, supercharger pressure, fuel-air ratio, and many other variables to the most favorable values for maximum engine torque without detonation. With equipment of this type, remarkable gains in vehicle performance have been achieved by supercharging without serious reduction in road fuel economy. Few manufacturers have yet employed supercharging for reducing the size and/or the speed of the engine rather than increasing road performance. The use of those alternatives should offer significant gains in road fuel economy.

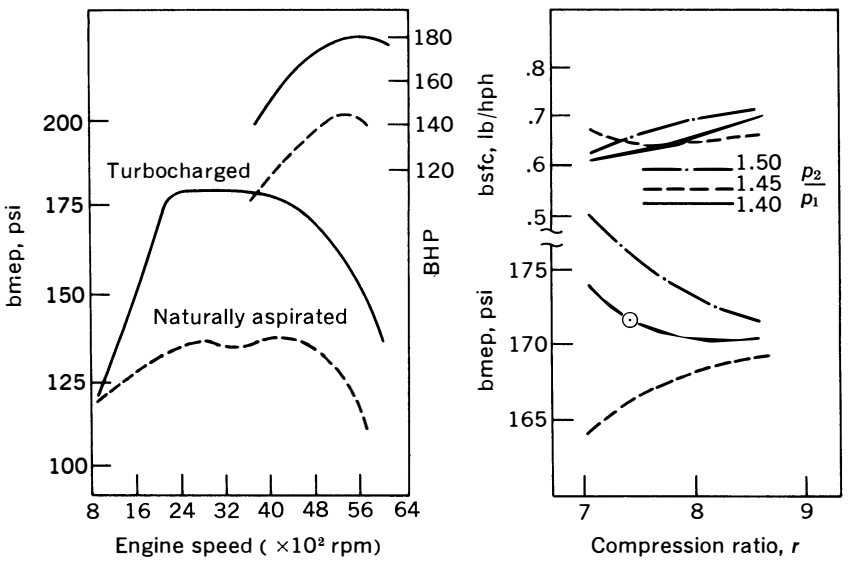

Fig. 13-4. Full-throttle performance of 1982 spark-ignition automobile engine, supercharged and unsupercharged. Engine is vertical 4-cylinder, 3.39-in. bore, 3.1-in. stroke, 168 in.^{3} (2.75 liters), with compression ratios of 7.4 (supercharged) and 8.8 (unsupercharged). (a) Performance; (b) bmep and bsfc vs. r at three supercharger pressure ratios, where circled point is chosen design point. From Matsumura et al., "The Turbocharged 2.8 liter Engine for the Datsun 280ZX," SAE Paper 820442, Report SP-514, February 1982, reprinted with permission from the Society of Automotive Engineers, Inc., the copyright holder.

Figure 13-4 shows full-throttle performance of a typical 1982 spark-ignition automobile engine, supercharged and unsupercharged. These data are at the detonation limit as controlled by signals from a knock detector. This engine is equipped with fuel injection at the inlet ports and with a very complete electronic system that controls not only spark timing but also many other engine variables so as to give best performance with minimum fuel consumption and lowest practicable exhaust emissions (see also Volume 2, Chapters 6 and 7).

Table 13-1 gives comparisons between supercharged and unsupercharged automobile engines. When installed in the same car, the supercharged versions give 5%–15% lower road mileage.

SUPERCHARGING OF DIESEL ENGINES

In Diesel engines, supercharging introduces no fuel or combustion difficulties. Actually, the higher compression temperature and pressure resulting from supercharging tend to reduce the ignition-delay period, and thus to improve the combustion characteristics with a given fuel or to allow the use of fuel of poorer ignition quality. (See discussions of Diesel combustion in ref. 1.10 and in Volume 2.) Thus, the limits on specific output of supercharged Diesel engines are set chiefly by considerations of reliability and durability.

As the specific output increases, due to supercharging, cylinder pressures and heat flow must increase accordingly, and therefore both mechanical and thermal stresses increase unless suitable design changes can be made to control them. Whether or not such stress increases lead to unsatisfactory reliability and durability depends on the quality of the design, the type of service, and the specific output expected. References 13.4 ff. give some record of actual experience in this regard.

Another consideration that makes supercharging of Diesel engines attractive is that, for a given power output, it is possible to use lower fuel-air ratios as the engine's inlet density is increased. When starting with an engine designed for unsupercharged operation, it is often found that an increase in power and an improvement in reliability and durability can be obtained by supercharging. This comes about when the increase in air flow achieved by supercharging is accompanied by a somewhat smaller increase in fuel flow, which leads to lower combustion, expansion, and exhaust temperatures and to reduced smoke and deposits.

Table 13-1 Supercharged (S) and Unsupercharged (U) Spark-Ignition Engines

		Cylinder Arrangement, Number	Bore, Stroke (in.)	Displ. ($in.^3$)	r	bhp	rpm	bmep (psi)	s (ft/min)	Spec. Output	bhp ratio, S/U
Audi	S	I-5	3.13	131	7.0	130	5400	146	3060	3.79	1.30
5000T (1983)	U		3.40		8.2	100	5100	119	2890	3.10	
Chrysler	S	I-4	3.44	135	8.2	142	5600	149	3378	3.81	1.45
2.2L (1984)	U		3.62		9.0	98	5200	111	3137	2.63	
Datsun	S	V-6	3.43	181	7.4	180	5600	141	3052	3.25	1.24
280ZX (1983)	U		3.27		8.3	145	5200	122	2834	2.62	
Ford	S	I-4	3.78	140	8.0	142	5000	161	2600	3.16	1.58
Mustang (1983)	U		3.12		9.0	90	4600	111	2392	2.00	
Honda	S	I-4	2.6	75.2	7.5	100	5500	192	3245	4.67	1.49
City turbo (1984)	U		3.54		10.0	67	5500	127	3245	3.11	
Lotus	S	I-4	3.74	133	7.5	210	6250	200	3125	3.16	1.31
Esprit (1983)	U		3.00		8.5	160	6500	197	3250	2.01	
Mitsubishi	S	I-2	2.76	33	9.0	39	5500	169	2567	3.31	1.26
Minica (1984)	U		2.80		9.0	31	5500	134	2567	2.63	
Volvo (1984)	S	I-4	3.78	141	8.7	157	5400	163	2783	3.51	1.41
B21FT, B23F	U		3.15		9.5	111	5400	115	2783	2.48	
Saab 2L	S	I-4	3.54	121	8.5	135	4800	184	2456	3.42	1.23
(1984)	U		3.07		9.3	110	5250	137	2686	2.79	
Avco Lycoming	S	O-6	$5\frac{1}{8}$	542	7.3	350	2575	200	1878	2.84	1.35
T10-450-J,	U		$4\frac{3}{8}$		8.5	260	2700	141	1969	2.10	
10-450-D (1984)											

1983 data from *Automotive Industries* (Chilton), April 1983; 1984 data from manufacturers' publications. All are automobile engines except the Avco aircraft engines.

The emphasis on fuel conservation in the 1970s stimulated the use of supercharging to improve the fuel economy of those Diesel engines that run at or near full load for long periods of time. This category includes marine, stationary, and heavy-road-vehicle engines. By improving structural design, many engines in these services are supercharged to high mean effective pressure, often accompanied by reduced piston speed, with resulting improved mechanical efficiency. This trend has been especially notable for the giant marine engines used in long-distance ocean service (tankers and cargo ships). Some of these have brake thermal efficiencies at cruise rating of close to 50% (see Volume 2, Figs. 11-18, 11-20, 11-21).

Supercharging of Automobile Diesel Engines

In most cases, Diesel passenger cars are offered as an alternative to similar vehicles with spark-ignition engines. Since the output of an unsupercharged Diesel engine is lower than that of its spark-ignition counterpart of the same cylinder dimensions and the weight is usually somewhat greater, either poorer vehicle performance must be accepted, or a larger engine must be used, or the Diesel must be supercharged. The latter solution is now frequent.

Most passenger-car Diesels use divided combustion chambers (generally designated "indirect injection," or IDI), because such chambers tend to give lower emission levels than open ("direct injection," or DI) chambers. IDI chambers also have advantages in cold-weather starting. Figure 13-5 gives performance data for a typical 1982 Diesel automobile engine, supercharged and naturally aspirated. Figure 13-6 is a cross-section of its turbosupercharger. (Figures 13-5 and 13-6 are from Brandstetter and Dziggel, "The 4- and 5-Cylinder Diesel Engines for Volkswagen and Audi," Paper no. 820441, SAE Report SP-514, February 1982, and are reprinted with the permission of the copyright holder, the Society of Automotive Engineers. The engine is a 4-cylinder vertical in-line with a bore and stroke of 3×3.4 in., a displacement of 98 in.^{3}, and an r value of 23.)

Where limits on exhaust emissions are in force, as in the United States, a changeover to Diesel power must be accompanied by emission-control devices, as explained in Volume 2, Chapter 7. When electronic systems are used for this purpose they are designed to include controls for fuel flow and injection timing that adjust to the best fuel economy consistent with atmospheric and engine conditions and minimum undesirable emissions. Such systems are still under active development.

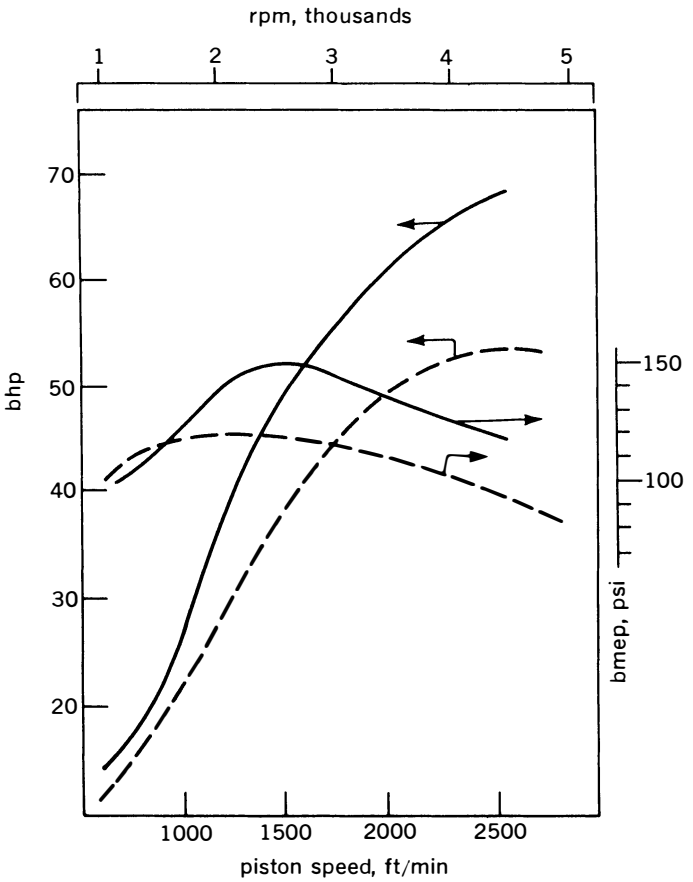

Fig 13-5. Full-throttle performance of a typical automobile Diesel engine, supercharged (solid lines) and unsupercharged (broken lines).

SUPERCHARGING FOR HEAVY VEHICLES

Most heavy road vehicles (trucks and buses) use Diesel engines, many of them supercharged and many of these with aftercooling. Open combustion chambers (DI) are generally used. Data for engines of this type are included in Table 13-2 here and in Table 10-8 of Volume 2.

Although four-cycle engines predominate, there are a considerable number of two-cycle engines in this category (see Volume 2, Fig 11-13). When these engines are supercharged, the scavenging pump is usually retained, with the turbosupercharger feeding into the pump inlet.

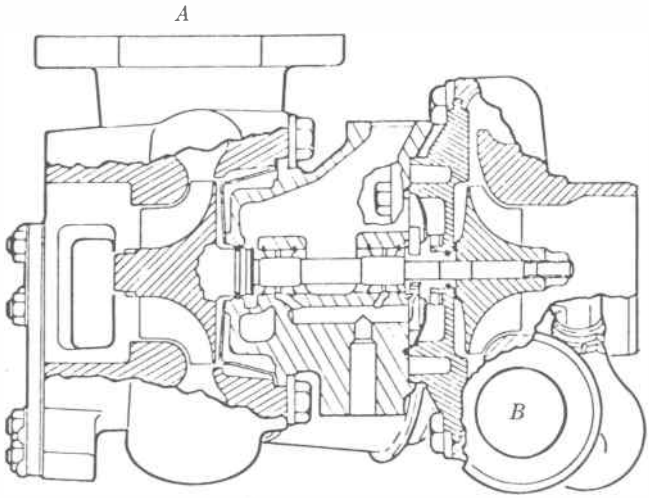

Fig 13-6. Cross-sectional view of turbosupercharger for engine of fig 13-5. (A) Exhaust inlet; (B) compressor outlet.

Diesel-Engine Compression Ratio. In Diesel engines changes in compression ratio have a limited effect on efficiency. (See Fig 4-6.) In order to avoid excessive peak pressures, there is a tendency to use the lowest compression ratio consistent with easy starting. Engines confined within heated rooms, such as large marine and stationary power plants, have a great advantage here, as is also the case when superchargers are separately driven and the temperature rise thus provided is available for starting.

AFTERCOOLING

Figure 13-7 shows compressor outlet temperature vs. pressure ratio assuming 75% compressor efficiency and 75% aftercooler effectiveness (see pp. 392 and 400). The desirability of aftercooling is evident. Whether it is used depends on space, weight, cost, and availability of a suitable cooling medium. For moving vehicles, the coolant must be the atmosphere and space, weight, and cost are always limited. The result in practice is that aftercooling is more often used in the larger and more expensive passenger cars and is used more widely in heavy vehicles.

Aftercooling in vehicles may be accomplished with a water-cooled exchanger connected to the engine cooling system, with a suitably en-

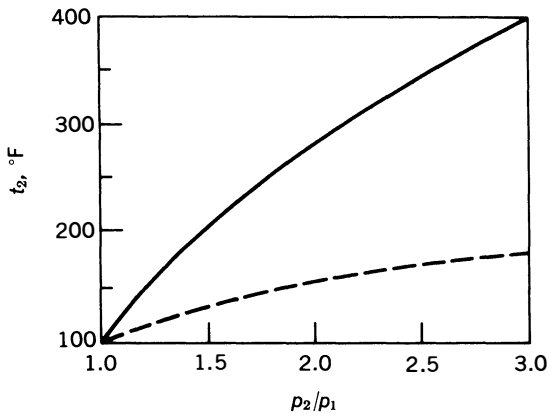

Fig 13-7. Temperature rise due to supercharging. p_2/p_1 = compressor pressure ratio; t_2 = compressor outlet temperature; compressor inlet temperature = 100°F. Solid line: without aftercooling. Broken line: aftercooler with 100°F coolant, effectiveness 0.75 (see p. 392).

larged radiator. Alternatively, a separate water-cooled system with its own radiator is possible. A third alternative is an air-to-air exchanger between the compressor and the engine inlet manifold (see Volume 2, Fig 11-9). These alternatives are discussed further in SAE Report SP-524, 1983, paper 821051 by Emmerling and Kiser.

FURTHER READING

More complete tabular data on supercharged engines will be found in Chapters 10 and 11 of Volume 2.

The reports of the Society of Automotive Engineers (see p. 522) are recommended for further reading on supercharged engines for road vehicles. Important recent reports include nos. SP-514 (1982), SP-524 (1983), P122 (1983), PT-23 (1983), and MEP153 (1982).

PERFORMANCE COMPUTATIONS

The performance of supercharged engines can be predicted with reasonable accuracy by means of the relations developed up to this point in this book.

For the sake of convenience, the basic performance equations developed in other chapters are assembled in Appendix 8. The quantities which

Table 13-2 Typical Supercharged Diesel Engines, 1983

	Service	Cylinder Arrangement, Number	Bore, Stroke (in.)	Displ. ($in.^3$)	r	bhp	rpm	bmep (psi)	s (ft/min)	bsfc (lb/hph)	Spec. Output
Mercedes	A	I-5	3.58	183	21.5	123	4350	122	2639	27 mpg†	2.45
300TD			3.64								
Peugeot	A	I-4	3.70	141	21.0	80	4150	108	2255	28 mpg†	1.85
2.3L			3.26								
Volvo	A	I-6	3.01	145	23.0	103	4800	117	2720	30 mpg†	2.42
780 GLE			3.40								
Volkswagen	A	I-4	3.01	97	23.0	70	4500	127	2550	0.530	2.45
and Audi			3.40								
Caterpillar	T	I-6	4.75	638		350	1800	241	1800	0.340	3.29
3406-B			6.00								
Cummins	T	I-6	4.92	611	16.3	270	1900	184	1694	0.329	2.36
L-10 270 (1984)			5.35								
GM Detroit	T	V-8	4.25	568	17.0	370$_s$	2100	123	1750	—	3.25
8V-71TA		2C	5.00								
GM Electro-	L	V-16	9$\frac{1}{16}$	10,322	16.0	3800	950	154	1583	0.336	3.68
Electromotive		2C	10								
16-F3A											
Sulzer	L	V-16	9.84	14,357	12.2	4506	1000	249	1967	—	3.70
16AT25			11.80								
Hanshin	M	I-6	17.3	48,940	12.5	4000	220	294	1270	0.297	2.82
6EL44			34.7								
Sulzer	M	I-12	31.5	883,741		48,360	87	223	1370	0.280	5.17
RTA84		2C	94.5								

Service: A, automobiles; T, trucks and buses; L, rail locomotives; M, large marine. 2C, two-cycle.

†For automobile engines the fuel consumption is usually given in terms of miles per gallon in a given vehicle, as measured by official U.S. EPA tests. The figures given apply to cars of approximately equal weight. Data are relative only.

The last two engines in the table are examples of marine engines highly supercharged for fuel economy. The Sulzer, being a two-cycle engine, has the equivalent of 446 $lb/in.^2$ bmep in a four-cycle engine. The bsfc shows the remarkable brake thermal efficiency of 49%. The constant-volume fuel-air-cycle efficiency at an estimated $F_r = 0.6$ ($r = 12$) (from Fig 4-5, p. 82) is 0.53.

must be evaluated in order to use these equations are as follows (excluding coefficients depending on units of measure alone):

Efficiencies
- Indicated, η' (based on fuel retained)
- Compressor, η_c
- Turbine, η_{ts} or η_{kb}

Parameters of effectiveness
- Volumetric efficiency, e_v
- Scavenging ratio, R_s
- Trapping efficiency, Γ
- Cooler effectiveness, C_c

Important design ratios
- Compression ratio, r
- Turbine-nozzle area/piston area, A_n/A_p
- Engine flow coefficient, C

Properties of fuel and air
- Heat of combustion, Q_c
- Specific heat of inlet air, C_{p1}
- Specific heat of exhaust gases, C_{pe}
- Atmospheric water-vapor content, h

Operating variables
- Fuel-air ratio, F' (based on fuel retained)
- Mean piston speed, s
- Compressor-inlet pressure, p_1
- Compressor-inlet temperature, T_1
- Compressor pressure ratio, p_2/p_1
- Aftercooler coolant temperature, T_w
- Aftercooler pressure loss p_i/p_2

Evaluation of Variables in Performance Equations

For new designs, or for existing designs under unknown conditions, it is necessary to assign realistic values to the dimensionless parameters previously listed, in order to use the performance equations. The following methods are based on the discussion and analysis in the preceding chapters of this book.

Indicated Efficiency. $\eta' = (0.80 - 0.90)\eta$ of equivalent fuel-air cycle. (See Chapter 5.)

Compressor Efficiency. Estimate this quantity from Figs 10-6–10-9.

Turbine Efficiency. (See Chapter 10.) Suggested design values:

$$\eta_{ts} = 0.85, \qquad \eta_{kb} = 0.70$$

Volumetric Efficiency. Chapter 6 discusses the question of the volumetric efficiency of four-stroke engines and its relation to design and operating conditions. The Illustrative Examples in Chapter 6 show in detail how volumetric efficiency may be estimated.

Scavenging Ratio. This ratio is determined by compressor characteristics and their relation to engine characteristics. (See Chapter 7.) Except for crankcase-scavenged engines, the compressor design is usually chosen to give a scavenging ratio between 1.00 and 1.4 at the rating point. (See Chapter 7 for crankcase-scavenged characteristics.)

Engine Flow Coefficient. This parameter depends on port sizes and port design in relation to piston area. (See Chapter 7.) Figures 7-10–7-12 show values achieved in practice.

Trapping Efficiency. Chapters 6 and 7 discuss this factor in detail. Figures 6-22 and 7-7–7-9 may be used in making estimates of this parameter. (See also Illustrative Examples in Chapters 6 and 7.)

Use of Intercooler or Aftercooler. In general, charge cooling is desirable, but it is not justified unless a supply of coolant at a temperature well below compressor-outlet temperature is available. Effectiveness values from 0.6–0.8 are achievable in practice, depending on how much space and weight are allowable for the unit. Reference 13.10 shows the effect of charge cooling on a type A aircraft engine.

Compression Ratio. The choice of compression ratio for supercharged engines is discussed in this chapter.

Nozzle Area for Steady-Flow Turbines. For this type the desired exhaust pressure must first be established. In type B installations the exhaust pressure is chosen so that the turbine power balances the compressor power under the desired operating condition. Example 10-4 illustrates this computation. The ratio p_4/p_3 is then determined, and the turbine nozzle area can be computed from the steady-flow orifice equations of Appendix 3.

In two-cycle engines, if p_4/p_3 is high enough to require a p_c/p_i ratio greater than that necessary for the desired scavenging ratio, a gear-driven scavenging pump must be used in series with the turbine-driven compressor. Four-stroke engines will operate with p_e/p_i ratios slightly greater than 1.0 without serious effects on performance.

For type C installations (all units geared together) refs 13.13–13.16 show that the optimum exhaust pressure for maximum output is equal to or slightly less than the inlet pressure, whereas that for maximum economy tends toward higher ratios of exhaust to inlet pressure.

Only steady-flow turbines have been used with type D installations. The turbine nozzle area is chosen to achieve the design-point pressure ratio across the turbine. (See Illustrative Examples at the end of this chapter.)

Nozzle-Area for Blowdown Turbines. Figure 10-14 has shown that for a given mass flow the smaller the nozzle area the greater the turbine output. For free-turbine (type B) installations the nozzle area is chosen to give turbine power equal to compressor power. Again, in two-stroke engines it may not be possible to secure enough turbine power to give

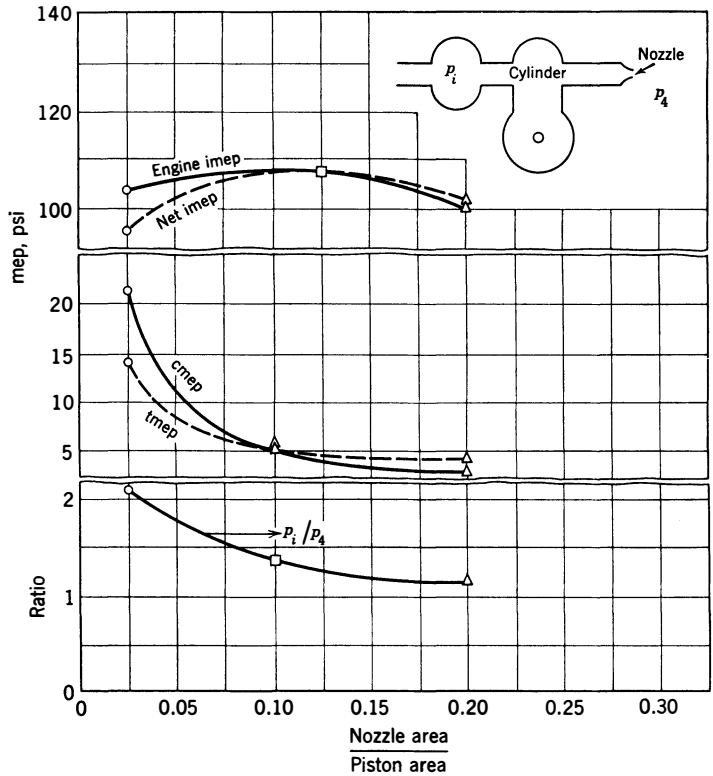

Fig 13-8. Effect of nozzle-area on the performance of compressor, engine, and blowdown turbine: net imep = imep − cmep + tmep; p_2/p_i = compressor pressure ratio; GM-71 Diesel cyl; s = 1330 ft/min; $\dot{M}_a$ = 0.09 lb/sec; F_R = 0.4; T_i = 75–82°F; p_4 = 14.5 psia. Tests made with GM-71 single cylinder. Exhaust pipe 2 ft long. Well-rounded nozzles, coefficient ⌣1.0. Thrust at nozzle was measured on circular plate 1 in from nozzle outlet. tmep is turbine output in terms of engine mep, calculated from thrust at 70% kinetic efficiency. cmep is compressor (scavenging-pump) power in terms of engine mep, 75% adiabatic efficiency. (Crowley et al., ref 10.69)

the desired scavenging ratio, in which case a gear-driven scavenging pump must be added in series with the turbine-driven unit.

Figure 13-8 shows results of tests in which the nozzle area for a blowdown turbine was varied while mass air flow was held constant by appropriate adjustment of the engine inlet pressure. A two-stroke Diesel engine was used. These curves show that turbine mep and the required compressor mep both increase as nozzle area decreases. If the three units are geared together, maximum output occurs at A_n/A_p near 0.10. This is also the smallest nozzle area with which the turbine will drive the compressor with sufficient power to maintain the air flow constant and with the assumed compressor and turbine efficiencies. The engine used had a low flow coefficient (curve *e* of Fig 7-12). With a larger flow coefficient, or higher component efficiencies, a more favorable ratio of turbine to compressor mep would be obtained.

The optimum ratio of nozzle area to piston area will undoubtedly vary somewhat with component characteristics and operating regime. Area ratios used in practice are shown in Table 13-3.

Table 13-3

Turbine-Nozzle Areas Used in Practice

Engine Type	Service	Cycle	Turbine Type	Effective A_n/A_p *
Spark ignition	aircraft	4	blowdown	0.06±
Diesel	railroad	4	blowdown	0.05–0.07
Diesel	large marine	4	blowdown	0.04–0.05
Diesel	large marine	2	steady flow	0.001–0.0015
Spark ignition	gas	4	blowdown	0.049

* Effective nozzle area is actual area × flow coefficient. For blowdown turbines nozzle area of one group is divided by area of one piston. For steady-flow turbines total nozzle area/total piston area is given. Figures are taken from recent design data.

Properties of Fuel and Fuel-Air Mixtures. These are discussed in Chapter 3 and presented in summary form in Table 3-1.*

* For purposes of calculating engine performance the following assumptions give results of sufficient accuracy:

	k	C_p	Sound Velocity a
Air	1.40	0.24	$49\sqrt{T}$
Exhaust gas	1.34	0.27	$48\sqrt{T}$

Units are in lbm, ft, sec, Btu, °R.

Fuel-Air Ratio. The effects of fuel-air ratio and the appropriate fuel-air ratios to use under various conditions are discussed briefly in Chapter 12. More complete treatment of this subject may be found in ref 1.10 and in Vol 2 of this series.

Mean Piston Speed. Due to the influence of piston speed on friction m.e.p. (Chap. 9) and on volumetric or scavenging efficiency (Chaps. 6 and 7), the full-load power of any engine will reach a peak volume as speed increases, provided stress limitations allow operation at this point. For both spark-ignition and Diesel engines, performance maps (Figs. 12-16, 17, 18) nearly always show best fuel economy in the range 1000–1400 ft/min. Engines designed to operate at constant speed tend to be rated in that range. Road-vehicle engines are usually rated at or near their peak power.

Current practice in ratings is illustrated in tables 13-1 and 13-2 and in the tables of Vol. 2, Chap. 10. Speeds much above 3000 ft/min. are used only for specially designed sports or racing engines.

Compressor Inlet Pressure, Temperature, and Vapor Content. These are usually at or near those of the surrounding atmosphere. In new designs allowance should be made for the highest temperature, highest humidity, and lowest barometric pressure under which the designed output is expected, and also for pressure loss in air cleaners and ducts.

Compressor Pressure Ratio. For spark-ignition engines the higher this ratio the lower the compression ratio, as explained earlier in this chapter. Figures 13-2–13-4 will be helpful in deciding on the compression ratio to be used.

In Diesel engines no fuel limitations are involved, and the output is limited almost entirely by considerations of reliability and durability, as affected by maximum cylinder pressures and heat flow per unit wall area. In general, higher pressure ratios may be used as more aftercooling can be employed and compression ratios can be lowered. Few commercial Diesel engines are designed for pressure ratios greater than 2.5. Free-piston units are generally designed for pressure ratios of 4 to 6.

In new designs a plot of performance characteristic against p_2/p_1 is essential before deciding on the pressure ratio at which to rate the engine. The construction of such plots is discussed in the following section.

Aftercooler Characteristics. To decide on aftercooler characteristics or whether or not a cooler is to be used requires data on the highest coolant temperature which is likely to prevail under service conditions. Pressure losses through aftercoolers can generally be held below 4% of the inlet absolute pressure.

Examples of Performance Computations

The utility of performance computations based on the equations in Appendix 8 and on the foregoing discussion is illustrated here by a few examples. Methods of calculation are shown in detail in the Illustrative Examples at the end of this chapter.

Example 1. Determine the best fuel-air ratio to use in a type C, supercharged, two-stroke Diesel engine, assuming that stress considera-

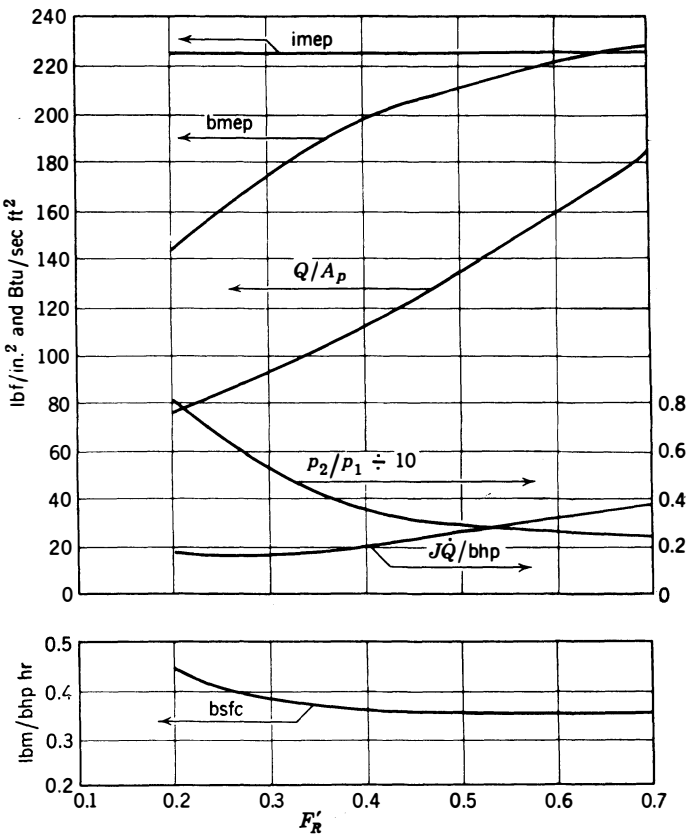

Fig 13-9. Effect of combustion fuel-air ratio on performance of C-E-T system: two-stroke engine, type C, Fig 13-1; $R_s = 1.4$; $e_s = 0.75$; $p_e/p_i = 0.80$; $C_c = 0.50$; $T_w = T_i = 560°R$; $\eta_c = 0.75$; $\eta_{ts} = 0.80$; $\eta_{kb} = 0.70$; $A_n/A_p = 0.12$; bore = 12 in; imep = 224 psi.

tions limit the imep to 224 psi. The imep will be held constant by lowering the supercharger pressure ratio as the combustion fuel-air ratio is increased.

Figure 13-9 shows plots of bmep, bsfc, and heat-flow parameters vs fuel-air ratio for this example. Heat-flow parameters were computed from Fig 8-11. Other assumptions used are given below the figure.

From the plot it is evident from the point of view of brake specific output and fuel economy that the highest practicable fuel-air ratio should be used. Smoke and deposits usually limit F_R' to 0.6 or less.

If stresses caused by heat flow are limiting, the plot shows that the lowest ratio of heat flow to brake power occurs at $F_R' = 0.3$. For a given brake output, however, the engine would have to have 20% more piston area at this fuel-air ratio than at $F_R' = 0.5$, and the brake specific fuel consumption would be 5% greater.

Example 2. Determine relative characteristics of arrangements, B, C, D (Fig 13-1) for high-output Diesel engines.

The following arrangements will be considered:

1. Four-stroke engine, with free turbo-compressor, arrangement B
2. Four-stroke engine with turbine and compressor geared to shaft, arrangement C
3. Four-stroke engine driving compressor and furnishing hot gas to a steady-flow power turbine, arrangement D
4. Same as 2, except that a two-stroke engine is used
5. Same as 3, except that a two-stroke engine is used. (This is the usual free-piston arrangement)

Systems 1, 2, and 4 are assumed to use combined blowdown and steady-flow turbines in order to secure the maximum feasible turbine output. Other assumptions are given in Table 13-4.

All of the engines have been assumed to have the same combustion fuel-air ratio and the same indicated efficiency. Another important assumption is that the piston speed of the four-stroke engines is 2000 ft/min and of the two-stroke engines, 1800 ft/min. This relation is based on the difficulties involved in properly scavenging two-stroke engines at high piston speed (see Chapter 7) and on current practice which indicates generally lower piston speeds for two-stroke engines in commercial practice. (See Table 13-2.) If the two-stroke engines were to be operated at 2000 ft/min piston speed, their specific output would be approximately 10% higher and their fuel economy slightly reduced, as compared to the results obtained at 1800 ft/min. These are *design-point* computa-

Table 13-4

Assumptions Used for Fig 13-10

Arr. No	Cycle	Type Fig 13-1	s ft/ min	$\frac{p_e}{p_i}$	Highest T_e °R	η_{kb}	C_c	$C_n A_n / A_p$	at $p_2/p_1 = 6$ Γ	e_v	R_s	For all arrangements p_2/p_1	r	η'	$\frac{p_{max}}{p_1}$	p_{max} psia	isfc
1	4	B	2000	var	1648	0.70	0.5	0.12	0.81	1.36	—	1	15	0.455	65	955	0.302
2	4	C	2000	1.0	1818	0.70	0.5	0.12	1.0	1.02	—	2	14	0.445	60	1760	0.309
3	4	D	2000	1.0	1540	0	0	—	0.45	1.16	—	3	13	0.435	55	2430	0.316
4	2	C	1800	0.9	1378	0.70	0.5	0.20	0.54	—	1.4	4	12	0.425	50	2940	0.323
4A *	2	C	1800	0.8	1378	0.70	0.5	0.20	0.54	—	1.4	5	11	0.415	45	3300	0.331
5	2	D	1800	0.9	1530	0	0	—	0.44	—	1.9	6	10	0.405	40	3530	0.340
5A *	2	D	1800	0.8	1530	0	0	—	0.44	—	1.9						

For all arrangements $F_R = 0.60$, $\eta_c = 0.75$, $h = 0$, $T_1 = 560°\text{R}$, $\eta_{ts} = 0.80$, $F_c = 0.0667$, $Q_c = 18{,}500$. For No. 3, enough compressor air is bypassed to the turbine so that cmep/bmep = 1.0. For 5 and 5*A*, R_s is adjusted so that cmep/bmep = 1.0. For two-stroke engines e_s vs R_s = the perfect-mixing curve, $\text{fmep}_0 = 18$ psi. For four-stroke engines, $e_{vb} = 0.85$ with no overlap, $\text{fmep}_0 = 30$ psi.

* 4*A* and 5*A* are the same as 4 and 5, except that p_e/p_i is 0.8 instead of 0.9.

p_{max} is maximum cylinder pressure.

tions; that is, the optimum design of compressor, engine, and turbine is used at each value of the pressure ratio. For a fixed design these curves would apply only at one particular pressure ratio and would give inferior performance as the pressure ratio was varied on either side of the design point.

The compressor pressure ratio, p_2/p_1, was taken as the independent variable. Imep, bmep, specific output, and specific fuel consumption are plotted against p_2/p_1 in Fig 13-10. Computations were made by means of the relations given in Appendix 8.

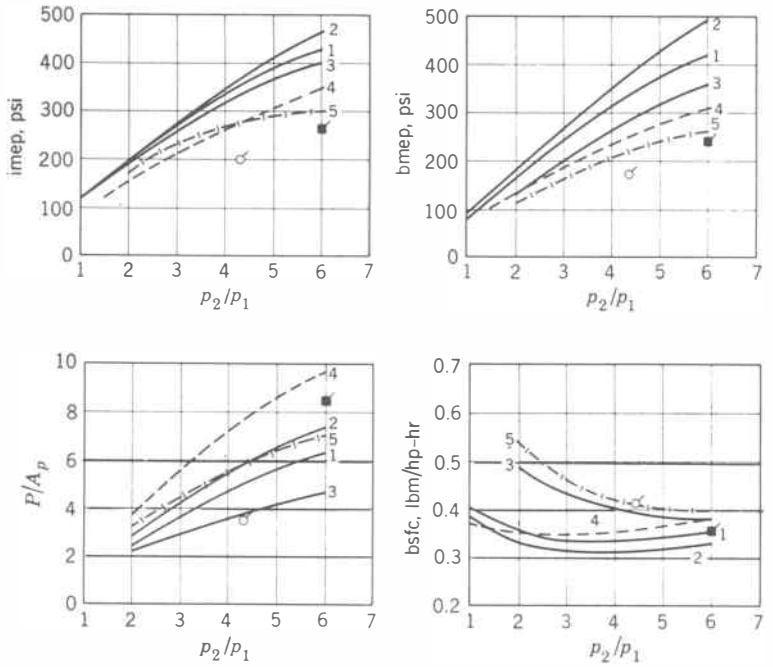

Fig 13-10. Performance of Diesel compressor-engine-turbine combinations (see Fig 13-1):

1 Four-cycle engine, free turbosupercharger, type B, p_e/p_i variable
2 Four-cycle engine, turbine and compressor geared to shaft, type C, $p_e/p_i = 1.0$
3 Four-cycle engine drives compressor, generating gas for a power turbine, type D, $p_e/p_i = 1.0$. Air not needed by engine is bypassed to turbine
4 Two-cycle engine, turbine and compressor geared to shaft, type C, $p_e/p_i = 0.9$
5 Two-cycle, free-piston gas generator with power turbine, type D, $p_e/p_i = 0.9$. Scavenging ratio varied to keep engine power equal to compressor power. In all cases $F_R' = 0.6$. See Table 13-4 for other details

HIGHLY SUPERCHARGED DIESEL ENGINES

For purposes of the discussion, let highly supercharged Diesel engines be those operated with a compressor-pressure ratio greater than 2.

Figure 13-10 makes it possible to examine the relative characteristics of five different types of highly supercharged engines. In the discussion which follows it is assumed that arrangement No 5 is a two-stroke engine of the free-piston design which is later discussed in some detail.

Relative Type Characteristics. Let it be assumed that for adequate reliability and durability the four-stroke engines, arrangements 1, 2, and 3 of Fig 13-10, and the free-piston engine, No 5, are limited to an imep of 250 psi and that the two-stroke crankshaft engine, No 4, is limited to 200 psi. These limitations, based on experience to date (1958), would appear reasonable.

Table 13-5, taken from Fig 13-10, compares the five types on this

Table 13-5

Comparative Performance of Engines of Fig 13-10 with imep and Piston Speed Limited to Assumed Maximum Service Values

Engine No	Cycle	Type	Maximum imep	Maximum s	p_2/p_1	bmep	P/A_p	bsfc
1	4	B	250	2000	2.65	217	3.3	0.34
2	4	C	250	2000	2.65	240	3.6	0.32
3	4	D	250	2000	2.90	195	2.9	0.44
4	2	C	200	1800	2.75	175	4.8	0.35
5	2	D	250	1800	3.50	185	5.0	0.44

See Table 13-4 for further details.

basis. From this table it is seen that under the assumed limitations the four-stroke B and C engines, Nos 1 and 2, are the most economical, whereas the highest specific outputs are attainable from two-stroke engines Nos 4 and 5. The type D engines, Nos 3 and 5, are poorest in fuel economy.

Highly supercharged Diesel engines must incorporate refinements in design for taking care of the high thermal and mechanical stresses that are unavoidable when very high specific outputs are developed. Table 13-5 shows that arrangement C, an engine with turbine and compressor geared to the shaft (No 2 in the table), gives performance appreciably

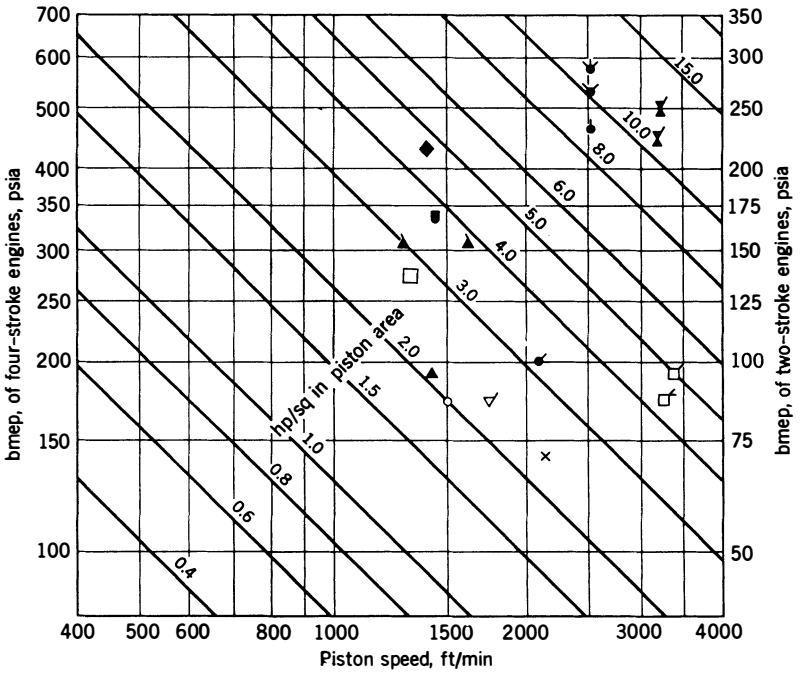

Symbol	Make	Cycle	Scav.	Service	Status	Regime	Type	Ref.
●	Napier Nomad	2	L	a	e	TO	C	13.22
●	Napier Nomad	2	L	a	e	TOW	C	13.22
●	Napier Nomad	2	L	a	e	TOWA	C	13.22
⧗	Junkers Jumo 207	2	OP	a	e	TO	B	13.44
▲	GM	2	PV	l	s	M	AB	13.29
▲	GM	2	PV	m	s	M	AB	13.09
●	FM	2	OP	l	s	M	AB	13.29
▽	ALCO	4		l	s	M	B	13.29
▮	Gotawerken	2	OP	m	s	M	A	13.291
○	Maybach	4		l	s	M	B	13.29
□	Cummins	4		r	e	M	A	13.091
□	Hanshin	4		m	s	M	B	mf
◆	Sulzer	2	PV	m	s	M	B	mf

Fig 13-11. Ratings of highly supercharged Diesel engines. Symbols: L=loop-scavenged; OP=opposed-piston; PV=poppet exhaust valves; a=aircraft; l=locomotive; m=marine; r=racing; t=tank (military); e=experimental; s=in service; TO=take-off; TOW=take-off with water injection; TOWA=take-off with water injection and afterburner; M=maximum rating. Type letters refer to Fig 13-1. mf=manufacturer's specifications.

better than a similar engine with free turbo compressor, No. 1, at the same stress level. However, since the use of a free turbo compressor eliminates gearing between engine and turbo-compressor unit, it is the most popular in both four-stroke and two-stroke practice. In two-stroke engines for road vehicles, which have to run over a wide range of speeds and loads, the engine-driven scavenging pump is retained, with the turbosupercharger feeding into it.

Figure 13-11 shows piston speed, bmep, and specific output for a number of highly supercharged Diesel engines. The Napier "Nomad" was an experimental two-cycle sleeve-valve airplane engine that used the type C system. It never saw service (ref. 13.22). The Junkers "Jumo" was an opposed-piston, two-cycle, six-in-line airplane engine. When supercharged, it used a type B arrangement. It was used in German civilian and military aircraft up to the end of World War II.

FREE-PISTON POWER PLANTS

Figure 13-12 shows an arrangement for a free-piston Diesel power plant that attracted much attention in the 1950s. Without the power turbine, small units of this type were used as air compressors in German submarines. With the power-turbine element the system is basically type D (fig 13-1). A calculated performance of such a unit is shown in fig 13-10 (curves 5). Attached directly to the Diesel pistons are the compressor pistons with the necessary *bounce chambers*. The compressor acts as scavenging pump for the cylinders, and the exhaust gases are led through suitable ducts to the power turbine.

It has been generally assumed that the free-piston Diesel cylinder could be operated at much higher imep than has proved feasible with a conventional Diesel engine. Development work has not yet convincingly supported this assumption.

Under the limitations assumed in Table 13-5, the highest specific output is possible with the two-stroke type D engine, that is, the free-piston type. However, it should be remembered that in this engine there must be a turbine and reduction gear in addition to the gas-generating unit. Thus the whole power plant will be larger and heavier than indicated by the specific output figures. Free-piston units have been rated at piston speeds considerably less than the 1800 ft/min assumed in Table 13-5 and therefore give lower specific outputs than those shown in that table.

The free-piston power plant has the following theoretical advantages over conventional Diesel engines of equal piston area:

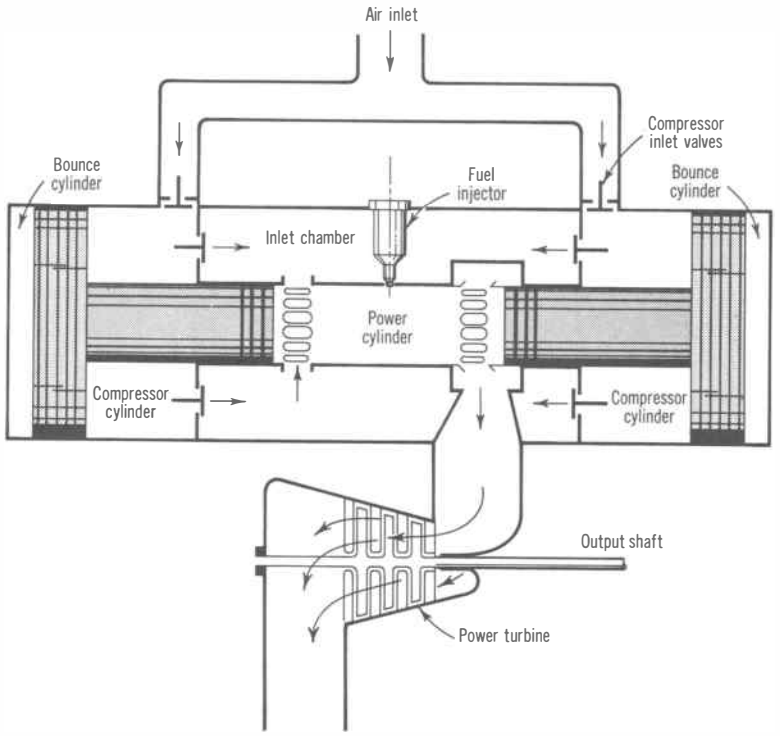

Fig 13-12. Diagrammatic section of a free-piston power unit.

1. Replacement of the crankshaft and connecting rods of a conventional engine by a gas turbine may save some weight and will simplify problems of lubrication and of vibration control (the opposed-piston units are perfectly balanced).

2. A number of gas-generator units can be connected in parallel to a single power turbine. This feature makes it easy to take advantage of the weight- and space-saving features of small cylinders as opposed to large ones. (See Chapter 11.)

3. The free-piston Diesel engine apparently has greater tolerance of low-ignition-quality fuel than a comparable conventional engine because the compression stroke will usually continue until ignition occurs. Thus the compression ratio adjusts to the fuel's ignition requirements.

4. If such a power plant is used for road or rail vehicles, the turbine will act as a torque convertor with a ratio of stall torque to rated torque of about 2.0. Thus a somewhat less elaborate transmission can be employed than in a conventional engine. Also, if the torque-conversion

feature is used, no cooling system is required to take care of the convertor losses, since these are discharged in the exhaust from the turbine.

On the other hand, several serious disadvantages appear to be characteristic of such systems. These include the following:

1. Relatively poor fuel economy at rated output, as indicated by Fig 13-10 and Table 13-5 (No 5).
2. Still poorer relative fuel economy at part load and particularly at very light loads. However, there are some applications, such as marine service, in which light-load operation is so brief that this defect would not be considered serious.

The basic reason for the poor part-load efficiency of this power plant is that the speed of reciprocation of the gas-generator units is confined within much narrower limits than that of the conventional reciprocating engine. The free-piston unit must run at a frequency controlled by the mass of the piston assembly and the gas pressure used to return the pistons, and the stroke must always be long enough to uncover the ports. Up to the present time it has been found necessary, in order to run the turbine at light loads, to waste some of the air from the compressor. As long as this method of operation prevails, the efficiency at light loads obviously will be low.

3. The geared power turbine running on hot gas is an expensive and highly stressed piece of equipment.

A number of power plants of this type were developed for marine and stationary service after World War II. General Motors even built one for an automobile. The results in each case have been unsatisfactory, and the type may now be considered obsolete. See Volume 2, p. 583, and references 13.30–13.392 in this volume.

EFFECTS OF p_e/p_i RATIO

Figure 13-13 shows the effects on specific output and fuel economy of changing p_e/p_i from 0.9 to 0.8 and compressor efficiency from 0.75 to 0.85. These curves show that type D units are somewhat more sensitive to such changes than are type C units. Achieving a pressure ratio of 0.9 across a two-stroke engine at high piston speeds and high scavenging ratios would require engine flow coefficients considerably higher than those now current. (See Fig 7-12.) Compressor efficiencies of 0.85 are difficult to achieve in the types appropriate for use with reciprocating engines. (See Chapter 10.)

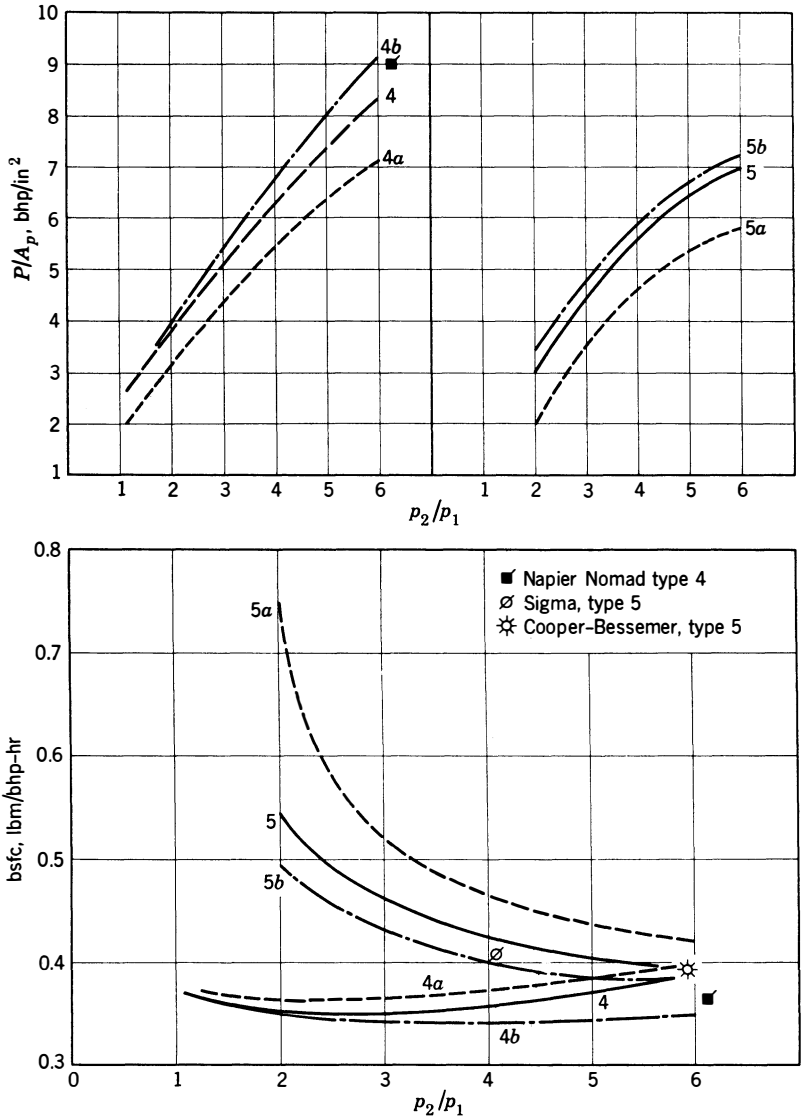

Fig 13-13. Effect of exhaust-to-inlet pressure ratio and compressor efficiency on performance of two-stroke C-E-T combinations:

Curve	Arrangement	p_e/p_i	η_c
4	C	0.9	0.75
4*a*	C	0.8	0.75
4*b*	C	0.9	0.85
5	D	0.9	0.75
5*a*	D	0.8	0.75
5*b*	D	0.9	0.85

The foregoing examples show how the material presented in this book can be brought together and used to solve practical design problems. Details of the methods of computation used, together with other examples of performance calculations, may be found in the Illustrative Examples which follow.

ILLUSTRATIVE EXAMPLES

(Measuring stations are defined by Fig 13-1)

Example 13-1. Turbo-Compound Spark-Ignition Engine. Calculate the power output and fuel economy of the Wright Turbo-compound air-cooled airplane engine at take-off, 2900 rpm, $p_i = 29.4$ psi, $F_R = 1.49$. Specifications are arrangement C, Fig 13-1, no aftercooler, 18 cylinders, 6.125-in bore x 6.312-in stroke, $r = 6.70$. Blowdown exhaust turbines. Fuel injected into cylinders during compression.

Assumptions: Turbine nozzle, $CA_n/A_p = 0.06$, atmospheric conditions 14.7 psi, 520°R, $h = 0.009$, compressor efficiency, 0.80, turbine kinetic efficiency, 0.75, $Z = 0.5$, valve overlap 90°, inlet closes 60° late.

Solution: Preliminary computations: $F = 1.49(0.0670) = 0.10$, piston speed = $2900(6.321)\frac{2}{12} = 3050$ ft/min = 51 ft/sec, piston area = $18(29.5) = 530$ in^2, p_2/p_1 for compressor = $29.4/14.7 = 2.0$.

Inlet temperature is computed from eq 10-9 and from Fig 10-2. At pressure ratio 2.0, $Y_c = 0.22$, $T_2 = 520(1 + (0.22)/0.80) = 520 + 143 = 663$, and, since there is no cooler, $T_i = T_2 = 663$°R.

From eq 6-6,

$$\rho_a = \frac{29.4(2.7)}{663}\left(\frac{1}{1 + 1.6(0.009)}\right) = 0.118 \text{ lbm/ft}^3$$

Volumetric efficiency is computed in accordance with Chapter 6 as follows: From Fig 6-13, e_v at $Z = 0.5$ is 0.83, with base conditions given on that figure. Correction for fuel-air ratio (Fig 6-18) = 1.0. Correction for inlet temperature (Fig 6-19) = $\sqrt{\frac{663}{580}} = 1.07$. Correction for T_c applies to water-cooled engines only—assume no correction here. Correction for valve overlap (Fig 6-22) at p_e/p_i is 0.51, $e_v/e_{vb} = 1.19$, $\Gamma = 0.93$. Correction for inlet timing—none.

$$e_v = 0.83(1.07)(1.19) = 1.07$$

$$e_v' = e_v\Gamma = 1.07(0.93) = 1.00$$

Indicated Efficiency: $F_R' = 1.49/0.93 = 1.6$. Fuel-air cycle efficiency at this ratio is 0.24 from Fig 4-5.

$$F' = 1.6(0.0670) = 0.107, \qquad F = 1.49(0.0670) = 0.10$$

$$F'Q_c\eta_i = (0.107)19{,}020(0.24)(0.85) = 413$$

$$\text{imep} = \frac{778}{144}(0.118)(1.0)413 = 264 \text{ psi}$$

Compressor mep: From eq 10-26,

$$\frac{\text{cmep}}{\text{imep}} = \frac{1}{413}\left(\frac{0.24(520)0.22}{0.80(0.93)}\right) = 0.089$$

$$\text{cmep} = 264(0.089) = 23.5 \text{ psi}$$

Turbine mep: Preparing to use Fig 10-14, $(T_e - T_i)$, from Fig 10-11, at $F_R = 1.49$ is estimated at 1200°F and therefore $T_e = T_3 = 663 + 1200 = 1863$°R.

$$a = 48\sqrt{1863} = 2080 \text{ ft/sec}$$

$$\dot{M} = (1 + F)(1 + h)\rho_a e_v A_p s/4 = 1.10(1.009)0.118(1.07)A_p 51/4 = 1.79A_p$$

$$\frac{p_e C_n A_n g_0}{\dot{M}a} = \frac{(144)14.7(0.06)(32.2)}{1.79(2080)} = 1.11$$

u/a_3 from the four-stroke spark-ignition curve of Fig 10-14 is 1.18 and $u = 1.18(2080) = 2460$ ft/sec.

From eq 10-37,

$$\frac{\text{tmep}}{\text{imep}} = \frac{1.10(1.009)}{413}\frac{(2460)^2 0.75}{50{,}000(0.93)} = 0.264$$

$$\text{tmep} = 264(0.264) = 70 \text{ psi}$$

Friction mep: From Fig 9-27, the motoring friction mep for an aircraft engine at 3060 ft/min is 33 psi. From eq 9-16, and Fig 9-31,

$$\text{fmep} = 33 + 1.2(14.7 - 29.4) + 0.03(264 - 100) = 30 \text{ psi}$$

Performance:

$$\text{bmep} = 264 - 30 - 23.5 + 70 = 280 \text{ psi}$$

$$\text{bhp} = 280(530)51/550(4) = 3440$$

$$\text{isfc} = 2545/0.85(0.24)19{,}020 = 0.66$$

$$\text{bsfc} = 0.66(264)/280 = 0.622$$

This engine is rated by the manufacturer at 3400 hp for take off.

Example 13-2. Supercharged Four-Stroke Diesel Engine, Steady-Flow Turbine. Compute power and fuel economy of a four-stroke Diesel engine with the following specifications: 8 cylinders, 8 x 10 in, $r = 15$, 1020 rpm $F_R' = 0.6$, inlet pressure, 30 psia, exhaust pressure, 24 psia, single-stage steady-flow turbine and centrifugal compressor both geared to the crankshaft. Valve overlap is 140° and inlet valve closes 60° late. $Z = 0.4$. Max. cylinder pressure is limited to 1800 psia. Atmospheric conditions are 14.7 psi pressure, 100°F, $h = 0.005$. Aftercooler has 0.70 effectiveness with coolant temperature 80°F, 3% pressure loss. Fuel is medium Diesel oil.

Solution: Preliminary calculations: $F' = 0.6(0.0664) = 0.04$, piston area $= 8(50.2) = 403$ in^2. Piston speed $= 1020(10)\frac{2}{12} = 1700$ ft/min, 28.3 ft/sec.

$$p_2 = 30/0.97 = 31 \text{ psia}$$

$$p_2/p_1 = 31/14.7 = 2.1, \qquad p_e/p_i = \tfrac{24}{30} = 0.8$$

Inlet Conditions:

$$Y_c = 0.235 \text{ from Fig 10-2}$$

$$T_2 = 560(1 + 0.235/0.81) = 560 + 162 = 722°\text{R}$$

$$T_i = 722 - 0.70(722 - 540) = 722 - 127 = 595°\text{R}$$

$$\rho_a = 2.7(30)/(1 + 1.6(0.005))595 = 0.135 \text{ lbm/ft}^3$$

Volumetric Efficiency: From Fig 6-13, base value is 0.83. Correction for fuel-air ratio from Fig 6-18 = 1.057, inlet temp correction $\sqrt{\frac{595}{580}} = 1.025$, valve overlap correction, Fig 6-22, $(p_r/p_i = 0.80)1.3$, $\Gamma = 0.82$. Therefore,

$$e_r = 0.83(1.057)1.025(1.3) = 1.17$$

$$e_r\Gamma = 1.17(0.82) = 0.96$$

imep: At $p_{\max}/p_1 = \frac{1800}{30} = 60$, $r = 15$, fuel-air cycle efficiency (Fig 4-6) is 0.51 and $\eta' = 0.85(0.51) = 0.432$.

$$F'Q_c\eta' = 0.04(18{,}000)(0.432) = 310$$

$$\text{imep} = \tfrac{778}{144}(0.135)0.96(310) = 218$$

$$\frac{\text{cmep}}{\text{imep}} = \frac{1}{310}\left[\frac{0.24(162)}{0.82}\right] = 0.153$$

$$\text{cmep} = 218(0.153) = 33 \text{ psi}$$

tmep: From Fig 10-11, at over-all fuel-air ratio, $F_R = 0.6(0.82) = 0.49$. T_e is computed as $595 + 840 = 1435°\text{R}$.

tmep: Fig 10-12 shows that at $p_3/p_4 = 24/14.7 = 1.63$ best turbine efficiency $= 0.81$, $F = 0.49(0.0667) = 0.0328$. Y_t at $p_4/p_3 = 1/1.63 = 0.613$, from Fig 10-2, is 0.12. Then,

$$\frac{\text{tmep}}{\text{imep}} = \frac{1.0328}{310}\left[\frac{0.27(1435)(0.12)0.81}{0.82}\right] = 0.153$$

$$\text{tmep} = 0.153(218) = 33$$

Fmep: From Fig 9-27, motoring mep is estimated at 27 psi. Correcting this value by means of eq 9-16 and Fig 9-31,

$$\text{fmep} = 27 + 0.3(24 - 30) + 0.04(2.18 - 100) = 30 \text{ psi}$$

$$\text{bmep} = 218 - 33 - 30 + 33 = 188$$

$$\text{bhp} = \frac{188(403)1700}{(33{,}000)4} = 970$$

$$\text{isfc} = 2545/0.432(18{,}000) = 0.33$$

$$\text{bsfc} = 0.33(218)/188 = 0.382$$

Note that compressor and turbine have equal power and that gearing to the crankshaft would be unnecessary at this operating point.

Example 13-3. Supercharged Two-Stroke Diesel. Estimate the power and fuel economy of a two-stroke engine of the same number of cylinders and cylinder dimensions as the four-stroke engine of example 13-2. Assume that, for the same reliability, piston speed must be reduced 20%, imep 20%, and maximum cylinder pressure to 1500 psia. The engine uses cylinders similar to configuration II of Fig 7-7. Other specifications are scavenging ratio 1.2, single stage centrifugal scavenging pump and steady-flow exhaust turbine, both geared to shaft and each having 0.80 efficiency. All other operating conditions are the same as in example 13-2.

Preliminary Computations: For $R_s = 1.2$, Fig 7-7 shows that $e_s = 0.58$ and $\Gamma = 0.48$. From the specification, imep $= 218(0.80) = 174$.

From eq 7-10,

$$\tfrac{7}{144}\tfrac{7}{8}\rho_s\eta_i(0.58)(0.04)(18{,}000)\tfrac{1}{14}\tfrac{5}{4} = 174$$

or $\rho_s\eta_i = 0.072$.

Exhaust Pressure: Estimating η_i at 0.42 (3% less than four-stroke engine) gives $\rho_s = 0.169$, and, estimating T_i at 600°R, $2.7(p_e)/600 = 0.169$ and $p_e = 37.5$ psia. Figure 7-11 shows that the flow coefficient of this cylinder type is 0.023 at 1700(0.80) = 1360 ft/min = 22.6 ft/sec. $R_s s/C(r - 1/r) = 1.2(22.6)/0.023(\tfrac{14}{15}) = 1263$ and, from Fig 7-13, $p_i/p_e = 1.19$. The estimates must now be verified.

Indicated Efficiency: $p_{max}/p_1 = 1500/37.5 = 40$. Figure 4-6 shows that fuel-air cycle efficiency is about 0.50. Therefore, indicated efficiency may be 0.50(0.85) = 0.425 for a four-stroke engine, or 0.425(0.97) = 0.413 for the two-stroke engine. The assumption of 0.42 is close enough and will be used.

Inlet Conditions:

$$p_i = 37.5(1.19) = 44.6 \text{ psia}$$

$$p_2/p_1 = 44.6/(0.97)14.7 = 3.12$$

$$Y_c = 0.383 \quad \text{and} \quad T_2 = 560(1 + 0.383/0.80) = 830°\text{R}$$

$$T_i = 830 - 0.70(830 - 540) = 615°\text{R}$$

T_i was underestimated Taking a new estimate of T_i at 630°R,

$$p_e = 37.3(630)/600 = 39.2$$

$$p_i = 39.2(1.19) = 46.7, \qquad p_2 = 46.7/0.97 = 48.2$$

$$p_2/p_1 = 48.2/14.7 = 3.28, \qquad Y_c = 0.403$$

$$T_2 = 560(1 + 0.403/80) = 842°\text{R}$$

$$T_i = 842 - 0.70(842 - 540) = 626°\text{R}$$

This is close to the estimate. Therefore, p_i will be taken as 46.7 psi and T_i as 626°R.

$$\rho_s = 2.7(39.2)/626 = 0.169$$

$$F'Q_c\eta' = 0.04(18{,}000)0.42 = 302$$

$$\text{imep} = \tfrac{7}{144}\tfrac{7}{8}(0.169)0.58(302)\tfrac{1}{14}\tfrac{5}{4} = 171$$

which verifies the requirement as closely as necessary.

cmep: From eq 10-26,

$$\frac{\text{cmep}}{\text{imep}} = \frac{1}{302}\left(\frac{0.24(560)0.403}{0.80(0.48)}\right) = 0.468$$

$$\text{cmep} = 0.468(171) = 80$$

tmep: $F_R = 0.6(0.48) = 0.288$, $F = 0.288(0.0667) = 0.0192$.

From Fig 10-11, $T_e = 626 + 510 = 1136°\text{R}$, $p_4/p_3 = 14.7/39.2 = 0.375$, and Y_t, from Fig 10-2, is 0.21. From eq 10-36,

$$\frac{\text{tmep}}{\text{imep}} = \frac{1.0192}{302}\left(\frac{0.27(1136)0.21(0.80)}{0.48}\right) = 0.352$$

$$\text{tmep} = 0.352(171) = 60$$

fmep: From Fig 9-27, motoring mep at 1700(0.80) = 1360 ft/min is 15 psi. Correction by eq 9-16 and Fig 9-28,

$$\text{fmep} = 15 + 0.068(171 - 100) = 20 \text{ psi}$$

$$\text{bmep} = 171 - 80 - 20 + 60 = 131$$

$$\text{bhp} = 131(403)1360/2(33{,}000) = 1100$$

$$\text{isfc} = 2545/18{,}000(0.42) = 0.337$$

$$\text{bsfc} = 0.337(171)/131 = 0.440$$

Example 13-4. More-Complete-Expansion Engine. Some four-stroke engines are designed to use an expansion ratio larger than the compression ratio, the latter being limited either by detonation or by maximum cylinder pressure. In order to accomplish this result, the expansion ratio is set by selecting the appropriate combustion-chamber volume and the compression ratio is reduced below this value by very early closing of the inlet valve. Compare this arrangement with a normal one under the following assumptions. Four-stroke Diesel engine, $F_R' = 0.6$, piston speed 1800 ft/min, inlet air standard dry (60°F, 14.7 psi) $r = 15$, cooler effectiveness, 0.8, cooler coolant temperature, 60°F, 3% pressure loss in coolers. Pressure at beginning of inlet stroke limited to 1.5 atm,

Normal Engine	Special Engine
$p_2/p_1 = 1.5$	$p_2/p_1 = 2.0$
Valve overlap = 90°	Inlet-valve closing timed so that pressure at beginning of compression is 1.5 atm
Coolant temp, 160°F	
$Z = 0.4$, $\gamma = 1.0$	
$F' = 0.04$, $F_R' = 0.6$	Other conditions same as for normal engine
Medium Diesel fuel	
Turbosupercharger drives compressor at $p_e/p_i = 0.80$	

Solution:

	Normal	Special
Y_c, Fig 10-2	0.13	0.30
$T_1 Y_c/\eta_c$	85	195
T_2	605	715
$T_i(e_c = 0.8)$	553	575
ρ_a	0.108	0.172
p_i	21.6	28.6
p_e	17.6	22.8

The air in the special engine is delivered to the cylinder at an inlet temperature of 575°R, and the inlet valve is closed so as to expand this air from 2 to 1.5 atm at the end of the inlet stroke. The relative mass of air taken in by the two engines can be estimated on the basis of the theoretical temperature at beginning of expansion without heat transfer or mixing with residuals; that is, T_1 theoretical for normal engine = T_i = 553°R, T_1 theoretical for special engine = 575 × $(1.5/2.0)^{0.285}$ = 497°R, relative mass = $\frac{553}{497}$ = 1.11 in favor of the special engine.

Volumetric Efficiency of Normal Engine: At Z = 0.4, the base value from Fig 6-13 is 0.83. Inlet-temp correction $\sqrt{\frac{553}{580}}$ = 0.975, fuel-air ratio correction (Fig 6-18) = 1.057, coolant-temp correction, negligible, valve overlap correction (Fig 6-22) = 1.12, Γ = 0.97,

$$e_v = 0.83(0.975)(1.057)1.12 = 0.957$$

$$e_v\Gamma = 0.957(0.97) = 0.93$$

Volumetric Efficiency for the Special Engine: The inlet valve of the special engine is so timed that its retained air capacity is equal to that of the normal engine increased in proportion to the density at the beginning of compression, that is, by the factor 1.11. In other words, pressures during compression are equal, but temperatures are lower in the special engine by the factor 1/1.11.

isfc: Assuming 85% of fuel-air cycle efficiency at p_3/p_i = 70, the indicated efficiency of both engines is 0.54(0.85) = 0.46 and isfc = 2545/18,000(0.46) = 0.308.

imep: $F'Q_c\eta'$ = 0.04(18,000)0.46 = 332 for both engines.

For normal engine from eq 6-9,

$$\text{imep} = \tfrac{778}{144}(0.108)0.93(332) = 180$$

For the special engine, since the efficiency and fuel-air ratio are the same,

$$\text{imep} = 180(1.11) = 198$$

fmep: From Fig 9-26, fmep_0 = 28 and, from eq 9-16 and Fig 9-28, with p_e/p_i = 0.80,

$$\text{fmep (normal engine)} = 28 + 0.3(17.6 - 22) + 0.04(180 - 100) = 30$$

$$\text{fmep (special engine)} = 28 + 0.3(23.5 - 29.4) + 0.04(198 - 100) = 30$$

$$\frac{\text{bhp (special engine)}}{\text{bhp (normal engine)}} = \frac{198 - 30}{180 - 30} = 1.12$$

$$\text{bsfc (normal engine)} = 0.308(180)/(180 - 30) = 0.370$$

$$\text{bsfc (special engine)} = 0.308(198)/(198 - 30) = 0.364$$

Under the assumptions, the special engine shows a small improvement in both output and fuel economy. It should be noted that this advantage is based on the assumption that both engines are running at their practical limit of imep and piston speed and that the higher allowable imep of the special engine is due to its lower cyclic temperatures. Otherwise, the inlet pressure of the normal engine could be increased to give equal performance.

Example 13-5. Optimum Scavenging Ratio, Supercharged. If the engine of example 12-12 is supercharged to an exhaust pressure of 2 atm and equipped with a steady-flow exhaust turbine of 0.80 efficiency geared to the crankshaft, what is the optimum scavenging ratio? An aftercooler of effectiveness 0.75, coolant temperature 90°F is added.

Solution: For the cooler, from eq 10-40,

$$T_i = T_2 - 0.75(T_2 - 550)$$

and for the turbine, $p_4/p_3 = 0.5$ and, from Fig 10-2, $Y_t = 0.17$; from eq 10-36,

$$\frac{\text{tmep}}{\text{imep}} = \frac{1 + F}{346}\left(\frac{0.27T_e(0.17)0.80}{\Gamma}\right) = 0.000106\,\frac{(1 + F)T_e}{\Gamma}$$

Equations from example 12-12 will be modified as follows:

$$R_s = (0.000096/2)a_i\rho_i\phi_1 = 0.000048a_i\rho_i\phi_1$$

$$\text{imep} = 78{,}800(2)e_s/T_i = 157{,}600e_s/T_i$$

cmep/imep remains the same as in example 12-12.

The following tabulation can be made:

p_2/p_1	p_2	p_i	p_i/p_e	Y_c	T_2	T_i	a_i	ϕ_1	R_s	e_s	Γ
1	2	3	4	5	6	7	8	9	10	11	12
2.58	37.9	36.7	1.25	0.310	778	607	1205	0.472	1.00	0.64	0.64
2.78	41.0	39.7	1.35	0.338	748	612	1211	0.517	1.20	0.70	0.58
3.10	45.6	44.0	1.50	0.370	820	618	1215	0.550	1.41	0.75	0.53
4.13	60.7	58.8	2.00	0.477	895	630	1230	0.577	2.00	0.86	0.43

p_2/p_1	imep	$\frac{\text{cmep}}{\text{imep}}$	cmep	F_R	$T_3 - T_i$	T_3	$\frac{\text{tmep}}{\text{imep}}$	tmep	fmep	bmep	bsfc
1	13	14	15	16	17	18	19	20	21	22	23
2.58	166	0.255	42.4	0.39	690	1297	0.212	35.2	26	134	0.364
2.78	180	0.303	54.5	0.35	610	1222	0.217	39.7	27	137	0.386
3.10	191	0.377	70.0	0.32	560	1178	0.232	43.0	28	136	0.415
4.13	215	0.605	130.0	0.26	470	1000	0.240	52.6	30	138	0.458

1	Independent variable	9	Fig A-2	17	Fig 10-11
2	$14.7(p_2/p_1)$	10	Previous equation	18	$T_i + T_3 - T_i$
3	$0.97p_2$	11	$e_s = 1 - e^{-R_s}$	19	From previous equation
4	$p_i/29.4$	12	e_s/R_s	20	imep × col 19
5	Fig 10-2	13	Previous equation	21	From Fig 9-28 and eq 9-16
6	$560(1 + Y_c/0.80)$	14	Equation of example 12-12	22	imep − cmep − fmep + tmep
7	$T_2 - 0.75(T_2 - 550)$	15	imep (cmep/imep)	23	0.294 (imep/bmep)
8	$49\sqrt{T_i}$	16	0.6Γ		

The tabulation shows a scavenging ratio of 1.0, or even less, to be optimum for fuel economy. Since power is nearly independent of scavenging ratio, 1.0 is optimum for power also. A larger flow coefficient would greatly improve the performance of this engine and would probably raise the optimum scavenging ratio.

Example 13-6. Free-Piston Engine. Estimate the maximum output and fuel economy at maximum output of a free-piston, exhaust-turbine arrangement of the type shown in Fig 13-12 under the following conditions: bore 6-in, stroke (each of two cylinders), 8 in, mean piston speed, 1200 ft/min, comp ratio at max output, 12, inlet pressure, 4 atm, atmospheric temperature, 100°F, turbine inlet pressure, 3.2 atm, fuel-air ratio adjusted so that Diesel cylinder output meets compressor requirements, turbine efficiency (steady flow), 0.80, compressor efficiency, 0.80, scavenging ratio, 1.4, fuel is medium Diesel oil, $F_c = 0.0664$, $Q_c = 18{,}000$ Btu/lb, max pressure is 50 times inlet pressure.

Solution: For this type of power plant, the indicated output of the engine minus friction must equal the power required by the compressor. In other words, eq 10-26 must be written

$$\frac{\text{cmep}}{\text{imep}} = \frac{1}{F'Q_c\eta'}\left[\frac{C_pT_1Y_c}{\eta_c\Gamma}\right] = 1 + \frac{\text{fmep}}{\text{imep}}$$

For this problem $T_1 = 560$°R, Y_c, from Fig 10-2, = 0.485. For the opposed-piston type of cylinder at $R_s = 1.4$, Fig 7-9 shows $e_s = 0.74$, $\Gamma = 0.74/1.4 = 0.53$. At 1200 ft/min piston speed, Fig 9-27 shows a motoring friction for two-stroke engines of 15 psi. If we assume that the rings and pistons of the compressor would have the same friction as the crankshaft system of a Diesel engine, this figure could be used as a first approximation for the free-piston estimate, and fmep is taken at 15 psi, provided imep is near 100 psi.

Equation 10-26 can now be written

$$\frac{1}{F'\eta'(18{,}000)}\left[\frac{0.24(560)0.485}{0.80(0.53)}\right] = 1 - \frac{15}{\text{imep}}$$

or

$$F'\eta' = \frac{1}{117(1 - 15/\text{imep})}$$

Furthermore, $T_i = 560 + 560(0.485)/0.80 = 900$°R, $\rho_s = 2.7(3.2)14.7/900 = 0.141$ lbm/ft^3, and, therefore, from eq 7-9,

$$\text{imep} = \tfrac{7}{1}\tfrac{7}{4}\tfrac{8}{4}(0.141)1.4(0.53)(\tfrac{1}{1}\tfrac{2}{1})F'\eta'(18{,}000) = 11{,}100F'\eta'$$

A combination of the foregoing two equations gives

$$F'\eta'\left(1 - \frac{15}{11{,}100F'\eta'}\right) = \frac{1}{117}$$

$$F'\eta' = 0.0099$$

To find the separate values of F' and η', tabulate from Fig 4-6 as follows:

F'	F'/F_c	η fuel-air from Fig 4-6	$\eta' = 0.85\eta$	$F'\eta'$
0.03	0.452	0.54	0.460	0.0138
0.02	0.302	0.57	0.484	0.0097
0.025	0.377	0.56	0.447	0.0112
0.023	0.357	0.562	0.450	0.0103
0.022	0.332	0.565	0.452	0.0099

The correct values are evidently $F' = 0.022$ and $\eta' = 0.452$. The imep is then 11,100(0.0099) = 110, which is near enough 100 psi so that the original estimate of 15 psi fmep is correct. $F = 0.022(0.53) = 0.0117$.

Turbine Performance: From Fig 10-11 at $F_R = 0.022(0.53)/0.0664 = 0.175$, $T_e = T_i + 320 = 560(1 + 0.485/0.80) + 320 = 1220°\text{R}$, $p_6/p_5 = 14.7/14.7(4)(0.80) = 0.313$, and, from Fig 10-2, $Y_t = 0.251$.

From eq 10-36,

$$\frac{\text{tmep}}{\text{imep}} = \frac{1.0117}{18{,}000(0.0099)}\left(\frac{0.27(1220)0.251(0.80)}{0.53}\right) = 0.712$$

$$\text{tmep} = 0.712(110) = 78.5$$

Power output is entirely from the turbine. The piston area of the gasifier is 2(28.3) = 56.6 in^2 and therefore

$$\text{bhp} = \frac{56.6(78.5)1200}{(2)33{,}000} = 81$$

$$\text{isfc} = 2545/0.452(18{,}000) = 0.312$$

$$\text{bsfc} = 0.312(110)/78.5 = 0.437$$

It should be noted that the examples of Chapter 13 involve every preceding chapter in this volume, with the exception of Chapter 2. It is hoped that the foregoing examples will serve as a final illustration of the practical application of the material in this volume.

appendix one—— Symbols and Their Dimensions

Symbol	Name	Dimension
A	area	L^2
a	velocity of sound	Lt^{-2}
amep	accessory-drive mep	FL^{-2}
B	a coefficient	any
B	barometric pressure	FL^{-2}
Btu	British thermal unit	Q
b	bore	L
bpsa	best-power spark advance	1 *
bmep	brake mean effective pressure	FL^{-2}
bsfc	brake specific fuel consumption	$MF^{-1}L^{-1}$
C	a flow coefficient,	1
	a dimensionless coefficient, or	1
	clearance (of a bearing)	L
C_c	cooler effectiveness	1
C_i	inlet-valve flow coefficient	1
C_e	exhaust-valve flow coefficient	1
C_p	specific heat at constant pressure	$QM^{-1}\Theta^{-1}$
C_v	specific heat at constant volume	$QM^{-1}\Theta^{-1}$
cm	centimeter	L
cmep	mean effective pressure to drive compressor	FL^{-2}
D	diameter	L
d	diameter	L

* The number 1 indicates no dimension.

d	differential operator	—
d	depth of wear	L
E	internal energy (excluding potential, electric, etc.) per unit mass	QM^{-1}
E^*	Same for (1 + F) lbm	QM^{-1}
$E°$	Same for 1 lb mole	QM^{-1}
E_{lg}	internal energy of liquid referred to gaseous state	QM^{-1}
e_v	measured or actual volumetric efficiency	1
e_v'	volumetric efficiency based on air retained	1
e_{vi}	volumetric efficiency with the ideal induction process	1
e_{vh}	volumetric efficiency without heat transfer	1
e_{vy}	volumetric efficiency when $p_y y/p_i = 1.0$	1
e_{vo}	volumetric efficiency at reference conditions, or *base* volumetric efficiency	1
e_s	scavenging efficiency	1
F	force (fundamental unit)	F
F	fuel-air ratio	1
F'	combustion fuel-air ratio	1
F_c	stoichiometric fuel-air ratio	1
F_R	$= F/F_c$	1
°F	degrees Fahrenheit	Θ
f	residual-gas fraction, coefficient of friction	1
fmep	imep-bmep, friction mean effective pressure	FL^{-2}
ft	foot or feet	L
G	mass flow/unit area, or "mass velocity"	$ML^{-2}t^{-1}$
g	acceleration of gravity	Lt^{-2}
g_0	force-mass-acceleration coefficient or Newton's law coefficient	$MLt^{-2}F^{-1}$
H	enthalpy/unit mass	QM^{-1}
H_{lg}	enthalpy of liquid referred to gaseous state	QM^{-1}
H_0	stagnation enthalpy/unit mass	QM^{-1}
H^*	enthalpy of (1 + F) lbm	QM^{-1}
$H°$	enthalpy/lb mole	QM^{-1}
h	mass ratio water vapor to air	1
h	heat-transfer coefficient	$Q\Theta^{-1}L^{-2}t^{-1}$
h	hardness	FL^{-2}
hp	horsepower	FLt^{-1}
hp-hr	horsepower hour	FL
I	mass moment of inertia	ML^2
imep	indicated mean effective pressure	FL^{-2}
isfc	indicated specific fuel consumption	$MF^{-1}L^{-1}$
in	inches	L
J	Joule's law coefficient	FLQ^{-1}
K	coefficient with dimensions	any
k	specific heat ratio C_p/C_v	1
k_g	thermal-conductivity coefficient of gas	$QL^{-1}\Theta^{-1}t^{-1}$
k_c	coefficient of heat conductivity of coolant	$QL^{-1}\Theta^{-1}t^{-1}$
k_w	coefficient of heat conductivity of a solid wall	$QL^{-1}\Theta^{-1}t^{-1}$
k_s	stiffness coefficient	FL^{-1}
L	length (fundamental unit)	L

l	length	L
lbm	pound mass	M
lbf	pound force	F
M	mass (fundamental unit)	M
$\dot{M}$	mass flow per unit time	Mt^{-1}
$\dot{M}^*$	critical mass flow per unit time	Mt^{-1}
M	Mach number	1
m	molecular weight	1
mep	mean effective pressure	FL^{-2}
min	minute	t
mmep	mechanical-friction mean effective pressure	FL^{-2}
N	revolutions per unit time	t^{-1}
n	a number	1
n	an exponent	1
0	zero	1
P	power	FLt^{-1}
P	load due to pressure	F
P	Prandtl number	1
p	pressure, absolute	FL^{-2}
pmep	pumping mean effective pressure	FL^{-2}
p_0	stagnation pressure, absolute	FL^{-2}
psia	pounds per square inch absolute	FL^{-2}
psi	pounds per square inch	FL^{-2}
Q	quantity of heat (fundamental unit)	Q
$\dot{Q}$	heat flow per unit time	Qt^{-1}
Q_c	heat of combustion per unit mass	QM^{-1}
q	internal energy of residual gas per unit mass	QM^{-1}
R	a design ratio (R_1, $R_2 \cdots R_n$)	1
R	universal gas constant	$FL\Theta^{-1}M^{-1}$
°R	degrees Rankine (°F + 460)	Θ
R_i	ratio imep to reference imep	1
R_s	scavenging efficiency	1
R	Reynolds number	1
r	compression ratio	1
r_p	pressure ratio (absolute)	1
rpm	revolutions per minute	t^{-1}
S	stroke	L
S	entropy per unit mass	$Q\Theta^{-1}M^{-1}$
s	mean piston speed	Lt^{-1}
sec	second	t
sfc	specific fuel cons.	$MF^{-1}L^{-1}$
T	temperature (fundamental unit)	Θ
T_0	stagnation temperature	Θ
t	time (fundamental unit)	t
t	thickness	L
tmep	turbine mean effective pressure	FL^{-2}
U	internal energy, total from all sources	Q
u	velocity (usually of a fluid stream)	Lt^{-1}
V	volume	L^3

V^*	volume of (1 + F) lbm	ML^{3-1}
V°	volume of 1 lb mole	ML^{3-1}
V_c	maximum cylinder volume	L^3
V_d	displacement volume	L^3
v	volume of a unit mass	L^3M^{-1}
W	weight, load	F
w	work	FL
w_s	shaft work	FL
x	an unknown quantity	any
x	a length	L
Y_c	adiabatic compression factor, $(p_2/p_1)^{(k-1)/k} - 1$	1
Y_t	adiabatic expansion factor, $1 - (p_2/p_1)^{(k-1)/k}$	1
y	ratio of stroke at inlet-valve closing to total stroke	1
y	a length	L
Z	inlet-valve Mach index	1
Z'	inlet Mach index with $C = 1$	—
α	ratio of inlet work to ideal inlet work	1
α	an angle or a ratio	1
β	an angle or a ratio	1
Γ	trapping efficiency	1
γ	ratio exhaust-valve-to-inlet valve flow capacity = C_eA_e/C_iA_i	1
Δ	increment sign (ΔT, Δp, etc.)	—
δ	partial differential sign	—
ϵ	base of Naperian logarithms	1
ζ	a dimensionless coefficient used with compressors	1
η	efficiency	1
η'	efficiency based on fuel retained for combustion	—
η_0	efficiency of the fuel-air cycle	1
η_i	indicated efficiency	1
η_c	compressor efficiency	1
η_{ts}	turbine efficiency, steady-flow	1
η_{kb}	blowdown-turbine kinetic efficiency	1
η_m	mechanical efficiency	1
Θ	temperature (fundamental unit)	Θ
θ	crank angle	1
Λ	reduced port area divided by piston area	1
μ	viscosity	$FL^{-2}t$
π	circumference/diameter	1
ρ	density	ML^{-3}
ρ_a	density of air at inlet valve	ML^{-3}
ρ_i	inlet density	ML^{-3}
ρ_0	stagnation density	ML^{-3}
ρ_s	scavenging density	ML^{-3}
σ	unit stress	FL^{-2}
τ	torque	FL
ϕ	a function of what follows	—
ϕ_1	compressible-flow function (Fig A-2)	1
ϕ_2	compressible-flow function (Fig A-3)	1

ψ	a function of what follows	—
Ω	angular velocity	t^{-1}
ω	angular frequency	t^{-1}

SUBSCRIPTS AND SUPERSCRIPTS

Subscript	Meaning
a	air or atmosphere
b	brake, base value
c	coolant or combustion or conductivity or compressor or chemically correct
d	displacement (volume)
e	exhaust
f	fuel
g	gas
i	inlet, indicated, ideal
l	liquid
m	mixture of fuel and air
n	natural (frequency)
n	turbine nozzle
0	reference state or stagnation state
p	refers to horsepower constant, or piston, or pressure
R	relative or ratio
r	residual gas
s	stiffness, sensible, surface, scavenging
v	volumetric, or constant-volume, or water vapor
w	wall (material) or water
x	at point of inlet-valve opening
y	at point of inlet-valve closing
$'$	indicates special condition
$^\circ$	leading, degrees of temperature
$^\circ$	following, per lb mole or degrees of angle
^{n}	exponent for Reynolds number
^{m}	exponent for Prandtl number
1, 2, etc A, B, etc	subscripts referring to specified locations or conditions or to points in the cycle
*	applies to (1 + F) lbm or indicates critical flow

Properties of a Perfect Gas —— appendix two

A perfect gas is defined as a gas having constant specific heat and conforming to the equation of state:

$$pV = \frac{M}{m} RT \tag{A-1}$$

where p = unit pressure of gas
V = total volume of gas
M = mass of gas
m = molecular weight of gas (m for air = 29)
T = absolute temperature of gas
R = universal gas constant which in English units is 1545 ft lbf per °R for m pounds of gas

Since a perfect gas is assumed to have a constant specific heat, the specific heat ratio $k = C_p/C_v$ is constant. Combining this relation with A-1 gives

$$C_p - C_v = R/mJ \tag{A-2}$$

From the definitions of internal energy and enthalpy per unit mass

$$E = C_v(T - T_b) \tag{A-3}$$

$$H = E + pV/J = E + \frac{RT}{mJ} \tag{A-4}$$

where T_b is the *base* temperature, that is, the temperature at which E is taken as zero.

For a reversible adiabatic process in a perfect gas from state (1) to state (2)

$$p_2/p_1 = (V_1/V_2)^k \tag{A-5}$$

$$T_2/T_1 = (p_2/p_1)^{(k-1)/k} = (V_1/V_2)^{k-1} \tag{A-6}$$

Stagnation Temperature of a Perfect Gas. From the definition of stagnation enthalpy (eq 1-19) for a perfect gas we define the stagnation temperature of a perfect gas as

$$T_0 = \frac{H_0}{C_p} = T + u^2/2Jg_0C_p \tag{A-7}$$

In real gases not near the condensation point of any of their components a stationary thermometer placed in the moving stream measures more nearly stagnation temperature than static, or *true*, temperature. Some thermometers measure stagnation temperature very well. (See ref A-2.2.)

Stagnation pressure, or *total* pressure, as it is more often called, is the pressure resulting when a moving fluid is brought to rest reversibly and adiabatically. Thus, from eq A-6, the total pressure of a perfect gas is given by the relation

$$p_0 = p\left(\frac{T_0}{T}\right)^{k/(k-1)} \tag{A-8}$$

In real gases a *Pitot* tube, that is, a small tube with its opening facing directly upstream, measures total pressure quite closely, provided the velocity of the gas is less than sonic velocity. (See ref A-2.3.)

Density of a Perfect Gas. Since density is defined as M/V, eq A-1 can be written

$$\rho = pm/RT \tag{A-9}$$

The *stagnation* density is computed by using p_0 and T_0 in the above expression. Stagnation density does not represent a real density, but it is a useful quantity in the study of the flow of gases discussed in Appendix 3.

Velocity of Sound in a Perfect Gas. The velocity of sound, a, in a perfect gas is expressed by the relations

$$a^2 = \frac{g_0kp}{\rho} = (k-1)g_0JC_pT = \frac{g_0kRT}{m} \tag{A-10}$$

where a is the velocity of sound waves, that is, pressure waves of an amplitude which is small compared to the absolute pressure of the gas. When $k = 1.4$ and $m = 29$ (air)

$$a = 49\sqrt{T} \tag{A-11}$$

in units of ft/sec and °R.

appendix three— Flow of Fluids*

Ideal Flow in Passages of Varying Area. Many engineering problems involve the flow of fluids through passages of varying area. To deal with such cases a useful approximation is the assumption that the stream of fluid has uniform velocity, temperature, and pressure across any section at right angles to the flow. Another useful assumption is that the flow is reversible and adiabatic, that is, without appreciable friction or flow of heat between the fluid and the passage walls. Flow under these circumstances is called *ideal flow*.

Figure A-1 shows a passage of varying area. Section 1 is upstream of the smallest cross section, section 2 is the smallest cross section, and section 3 is downstream of the smallest cross section. Under the above assumptions it is evident that

$$\dot{M} = A\rho u \tag{A-12}$$

where $\dot{M}$ = mass flow per unit time
A = local cross-sectional area
ρ = local density
u = local velocity

From expression 1-21, if there is no shaft work or heat transfer,

$$H_{02} - H_{01} = 0 \tag{A-13}$$

* For more complete treatment of this subject see refs A-3.0–3.85.

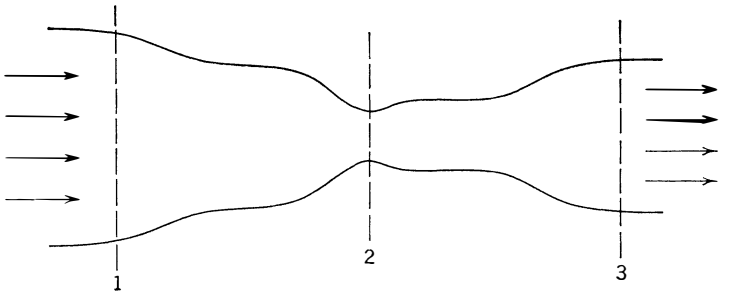

Fig A-1. Generalized flow passage.

Ideal Flow of a Perfect Gas. By combining eqs A-12 and A-13 and using the characteristics of perfect gases given in Appendix 2 it can be shown that for a perfect gas

$$\dot{M} = A_2 p_{01} \left(\sqrt{\frac{g_0 m k}{R T_{01}}} \right) \phi_1 \tag{A-14}$$

$$= A_2 a_{01} \rho_{01} \phi_1 \tag{A-15}$$

The above equation may also be written as a modified hydraulic equation:

$$\dot{M} = A_2 \sqrt{2 g_0 \rho_{01} \, \Delta p} \; \phi_2 \tag{A-16}$$

In the above equations $\dot{M}$ is the mass flow of gas per unit time and

$$\phi_1 = \sqrt{\frac{2}{k-1} (r_p^{2/k} - r_p^{(k+1)/k})} \tag{A-17}$$

$$\phi_2 = \phi_1 \sqrt{k/2(1 - r_p)} \tag{A-18}$$

a_{01} is the velocity of sound corresponding to T_{01}

$$\Delta p = p_{01} - p_2$$

$$r_p = p_2/p_{01} = 1 - \Delta p/p_{01}$$

Values of ϕ_1 and ϕ_2 when $k = 1.4$ are plotted in Figs A-2 and A-3.

Critical Flow. For given values of p_{01} and T_{01} the maximum mass flow occurs when the velocity of sound is reached at the smallest cross section. This condition is called *choking flow*, or *critical flow*, and is

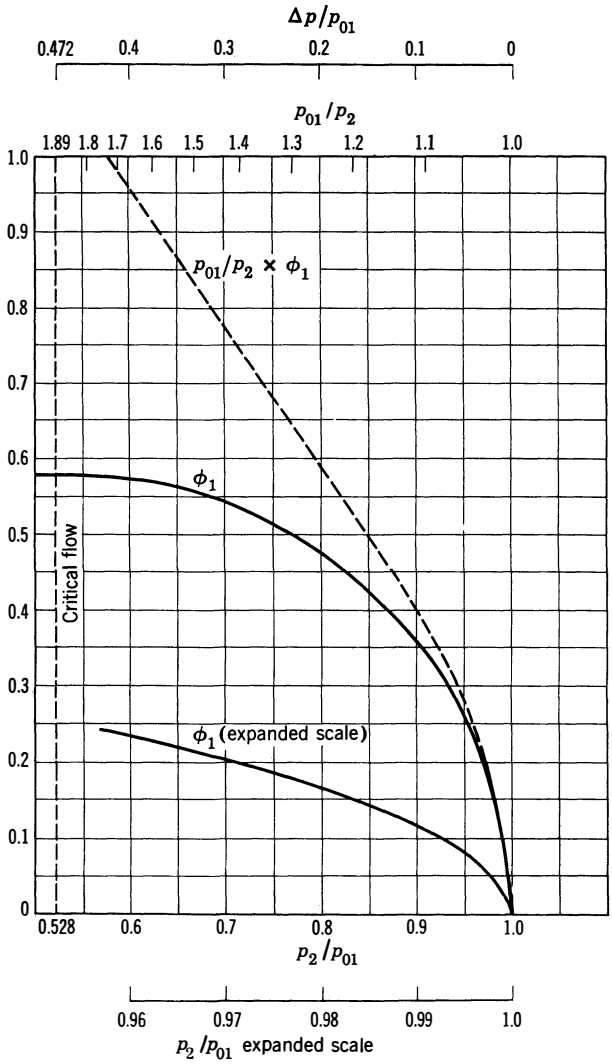

Fig A-2. Compressible-flow functions, $k = 1.4$:

$$\phi_1 = \sqrt{\frac{2}{k-1}\left[\left(\frac{p_2}{p_{01}}\right)^{\frac{2}{k}} - \left(\frac{p_2}{p_{01}}\right)^{\frac{k+1}{k}}\right]}$$

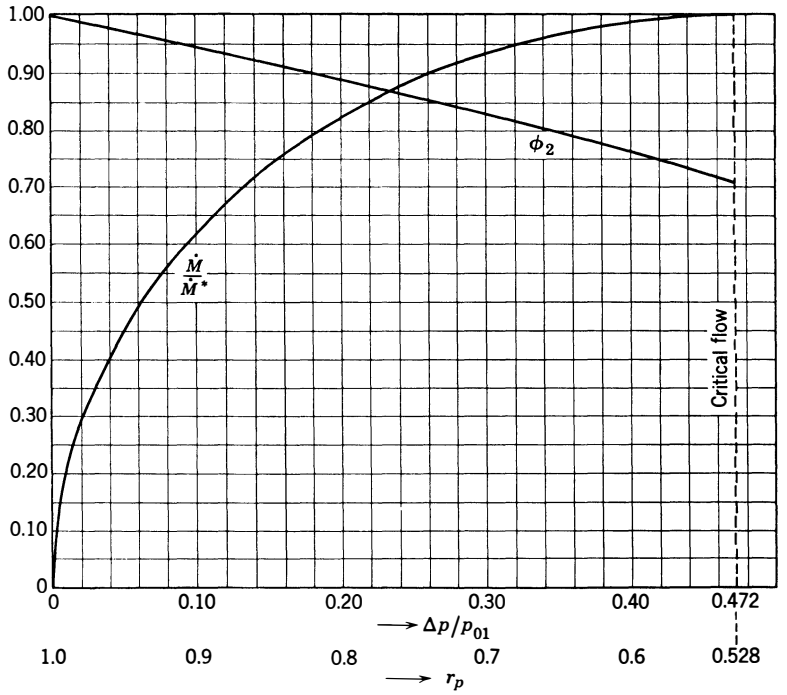

Fig A-3. Flow function and relative mass flow of a perfect gas, $k = 1.4$:

$$\phi_2 = \phi_1 \text{ (Fig A-2)} \times \sqrt{\frac{k}{2(1 - r_p)}}$$

$$\dot{M}/\dot{M}^* = \phi_2/0.705$$

designated by an asterisk. At this point

$$(p_2/p_{01})^* = \left(\frac{2}{k+1}\right)^{k/(k-1)} \qquad \text{(A-19)}\dagger$$

for $k = 1.4$, $(p_2/p_{01})^* = 0.528$.

Also,

$$\phi_1{}^* = \sqrt{\left(\frac{2}{k+1}\right)^{(k+1)/(k-1)}} \qquad \text{(A-20)}$$

$$= 0.578 \quad \text{when} \quad k = 1.4$$

† An excellent approximation to eq A-19 for the useful values of k is $(p_2/p_{01})^* = 1/(1.05 + 0.6k)$.

and

$$\phi_2{}^* = 0.705 \quad \text{when} \quad k = 1.4 \tag{A-21}$$

Thus

$$M^* = A_2 a_{01} \rho_{01} \sqrt{\left(\frac{2}{k+1}\right)^{(k+1)/(k-1)}} \tag{A-22}$$

for air

$$M^* = 0.53 A_2 p_{01} / \sqrt{T_{01}}$$

where $k = 1.4$, $\dot{M}^*$ is in lbm/sec, and T_{01} is in °R. When p_{01} is in psi, A_2 is in square inches. When p_{01} is in lb/ft^2, A_2 is in square feet.

Flow in Terms of Critical Flow. A convenient approach to many problems in fluid flow is through the ratio $\dot{M}/\dot{M}^*$, that is, the ratio of actual flow to choking flow. By combining eqs A-14–A-16 with expression A-22, when $k = 1.4$,

$$\frac{\dot{M}}{\dot{M}^*} = \frac{\phi_1}{0.578} \tag{A-23}$$

$\dot{M}/\dot{M}^*$ for $k = 1.4$ is plotted in Fig A-3.

Ideal Liquids. An ideal liquid has no viscosity and its density is constant. The ideal flow of such a liquid through the passage of Fig A-1 can be written

$$M_l = A_2 \rho u_2 = A_2 \sqrt{2 g_0 \rho \, \Delta p} \tag{A-24}$$

where $\Delta p = p_{01} - p_2$. Equation A-24 is the familiar Bernoulli equation.

Flow of Actual Fluids. It is obvious that an actual case of fluid flow never duplicates exactly the assumptions which we have used for the ideal case. In practice, this discrepancy is usually taken care of by introducing a *flow coefficient*, C, which is defined as

$$C = \frac{\text{actual mass flow}}{\text{ideal mass flow through reference area}}$$

so that

$$\dot{M}_{\text{actual}} = C \dot{M}_{\text{ideal}} \tag{A-25}$$

If the reference area is taken as the area A_2, C is generally less than unity, although it may approach unity under favorable circumstances. The departure of C from unity is due to uneven velocity distribution across the flow section, to viscosity, and to the fact that the measured pressures may not be the pressures defined for ideal flow.

Experience shows that C is a function of the *shape* of the passage, including the position and shape of the pressure measuring orifices, the

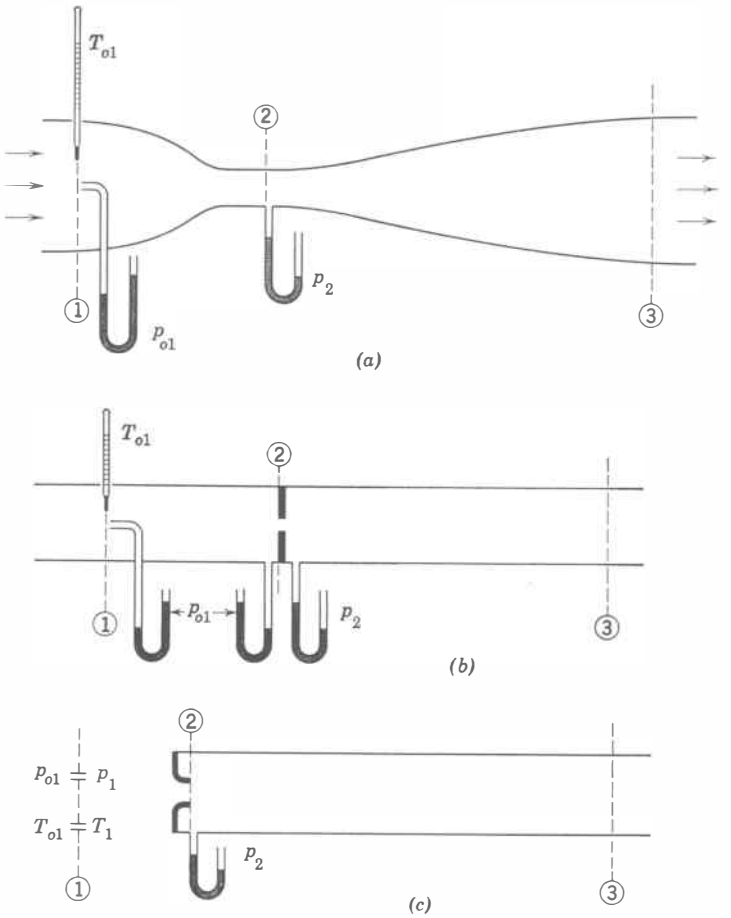

Fig A-4. Fluid flowmeters: (*a*) venturi meter; (*b*) orifice meter in a passage; (*c*) orifice meter from atmosphere.

characteristics of the fluid, and the velocity at the smallest cross section. For *similar* passages, that is, passages of the same shape but of different size, it has been shown that C is a function of the following nondimensional coefficients:

R, the Reynolds number,* $\rho u L/\mu g_0$

M, the Mach number,* u/a

* A more complete discussion of the significance of these numbers is given in Chapter 6.

where, at the smallest cross section, or *throat*,

ρ = fluid density
u = average fluid velocity
μ = fluid viscosity
a = velocity of sound in the fluid
L = characteristic dimension of the flow passage.

For Mach numbers in the throat less than about 0.7 the effect of **M** on C is small, and for passages of the same shape the coefficient can be taken to depend on the Reynolds number only. A more convenient form of the Reynolds number is obtained by substituting $\dot{M}/\rho A$ for u when A is the throat area. If $\dot{M}/A$, the mass flow per unit throat area, is designated by G, the Reynolds number can be written

$$\mathbf{R} = GL/\mu g_0 \tag{A-26}$$

which is a convenient form because it avoids the necessity for measuring ρ and u in the throat.

Figure A-4 shows several common forms of flow measuring passages. Data on the values of C for various fluids in such passages are given in refs A-3.2–3.81.

An essential precaution to be taken in using all such meters is that the flow be steady, that is, free from pulsations of appreciable magnitude. (See refs A-3.82–A-3.84.)

Analysis of Light-Spring Indicator Diagrams —appendix four

Derivation of Eq 6-13. From the general energy equation for the inlet process between x, inlet opening, and y, inlet closing, assuming no effective valve overlap, referring to Fig 6-6:

$$(M_i + M_r)E_y - M_iE_i - M_rE_r = Q - \frac{w}{J} \qquad \text{(A-27)}$$

where M_i = mass of fresh mixture
M_r = mass of residual gases
E = internal energy per unit mass
Q = net heat received
w = net work produced

The net work of the process is

$$w = -p_iV_d\,e_v + \int_x^y p\,dv \qquad \text{(A-28)}$$

Also,

$$M_i = \rho_iV_d\,e_v \qquad \text{where } \rho_i \text{ is fresh-mixture density}$$

$$M_r = V_x\,\rho_x$$

$$(M_i + M_r) = V_y\,\rho_y$$

For perfect gases

$$E = C_v T$$

$$\rho = \frac{pm}{RT}$$

where C_v = specific heat at constant volume

T = absolute temperature

m = molecular weight

R = universal gas constant

Let C_v and m be the same for fresh mixture and residuals and let

$$Q = M_i C_p \, \Delta T = (V_d \, \rho_i e_v) C_p \, \Delta T \tag{A-29}$$

By making the above substitutions,

$$(V_y p_y) \frac{C_v m}{R} - (V_d p_i e_v) \frac{C_v m}{R} - (V_x p_x) \frac{C_v m}{R}$$

$$= V_d \, \rho_i e_v C_p \, \Delta T + \frac{e_v p_i V_d}{J} - \frac{1}{J} \int_x^y p \, dv \tag{A-30}$$

Simplifying

$$V_y p_y - V_x p_x = V_d p_i e_v + \frac{R}{JmC_v} \left[V_d \, \rho_i e_v C_p \, \Delta T J + e_v p_i V_d - \int_x^y p \, dv \right] \tag{A-31}$$

For perfect gases

$$R/JmC_v = (k - 1)$$

$$C_p/C_v = k$$

By remembering that $\rho_i = p_i m/RT_i$, $(V_d + V_x)/V_x = r$, making the above substitutions, and rearranging,

$$e_v = \frac{1}{1 + (\Delta T/T_i)} \left\{ \frac{(k - 1)\alpha}{k} + \frac{(p_y y/p_i) r - (p_x/p_i)}{k(r - 1)} \right\} \tag{A-32}$$

where

$$\alpha = \int_x^y \frac{p \, dv}{p_i V_d} \tag{A-33}$$

Equation A-32 is given in the text as eq 6-13.

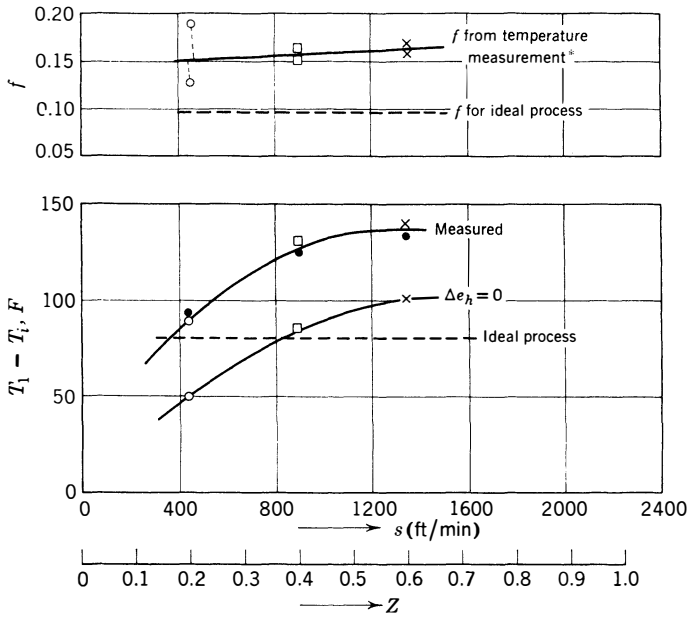

	Run	Speed	p_e	p_i	p_e/p_i
○	(1)	600 rpm	14.7 psia	14.6 psia	1.01
□	(7)	1200 rpm	14.7 psia	14.3 psia	1.03
×	(10)	1800 rpm	14.7 psia	14.1 psia	1.04
●					

T_c = 200°F T_i = 160°F r = 6
F = 0.078 (iso-octane)
k = 1.345
*Gas temperature used in calculation of f is from measurements of sound velocity

Fig A-5. Residual-gas fraction and $(T_1 - T_i)$ from indicator diagrams and gas-temperature measurements.

For the idealized cycle of Fig 6-3, $\Delta T = 0$, $\alpha = 1$, $p_y y/p_i = 1.0$, $p_x/p_i = p_e/p_i$, and

$$e_{vi} = \frac{k-1}{k} + \frac{r - p_e/p_i}{k(r-1)} \tag{A-34}$$

Temperature at End of Induction. From the perfect gas law, assuming specific heats and molecular weights of fresh mixture and residuals are the same,

$$\frac{T_y}{T_i} = \left(\frac{M_i}{M_y}\right)\left(\frac{p_y}{p_i}\right)\left(\frac{V_y}{V_i}\right) \tag{A-35}$$

Since

$$\frac{M_i}{M_y} = 1 - f$$

and

$$e_v = \frac{V_i y}{V_y(r - 1/r)}$$

eq A-35 can be written

$$T_y = T_i \left(\frac{p_y}{p_i}\right)\left(\frac{r}{r-1}\right)\frac{y(1-f)}{e_v} \tag{A-36}$$

All quantities on the right-hand side except f, the residual gas fraction, can be measured. On the other hand, if T_y can be measured, f can be computed. Values of T_y measured by the sound-velocity method are given in Fig A-5 with corresponding values of f computed from the foregoing relation.

T_y increases as piston speed increases because e_v decreases and f increases more than enough to offset any decrease in p_y.

Heat Transfer by Forced Convection between a Tube and a Fluid —— appendix five

Referring to Fig 6-10,

$$\dot{Q} = \dot{M}C_p\,\Delta T = h\pi DL(T_s - T_x) \qquad \text{(A-37)}$$

		Dimensions
where $\dot{Q}$ =	heat flow per unit time from wall to fluid between sections 1 and 2	Qt^{-1}
$\dot{M}$ =	mass flow of fluid per unit time	Mt^{-1}
ΔT =	$T_2 - T_1$	Θ
T_1 =	fluid mean temperature at section 1	Θ
T_2 =	fluid mean temperature at section 2	Θ
T_s =	inner surface temperature of tube	Θ
T_x =	mean temperature of fluid between sections 1 and 2	Θ
h =	coefficient of heat transfer	$Qt^{-1}L^{-2}\Theta^{-1}$
C_p =	gas specific heat	$QM^{-1}\Theta^{-1}$

For turbulent flow

$$h \cong \frac{Kk_c}{D}\,\mathbf{R}^{0.8}\mathbf{P}^{0.4} \qquad \text{(A-38)}$$

where K = dimensionless constant
$\mathbf{R}$ = tube Reynolds number
$\mathbf{P}$ = gas Prandtl number, $C_p\mu g_0/k_c$

The Reynolds number can be written

$$\mathbf{R} = \frac{u\rho D}{\mu g_0} = \frac{GD}{\mu g_0} \tag{A-39}$$

		Dimensions
where u	= mean fluid velocity	Lt^{-1}
ρ	= mean fluid density	ML^{-3}
μ	= mean fluid viscosity	$FL^{-2}t$
k_c	= fluid heat conductivity	$QL^{-1}t^{-1}\Theta^{-1}$
$u\rho$	$= 4\dot{M}/\pi D^2 = G$	$ML^{-2}t^{-1}$

Substituting eqs A-38 and A-39 in eq A-35 gives

$$\Delta T = \frac{Kk_c}{\dot{M}C_p}\left(\frac{u\rho D}{\mu g_0}\right)^{0.8} \pi L(T_s - T_x)\mathbf{P}^{0.4} \tag{A-40}$$

For a gas at moderate temperature the quantities k_c, C_p, μ, and the Prandtl number can be considered constant. In this case eq A-40 can be written

$$\Delta T = C(GD)^{-0.2}\frac{L}{D}\left\{T_s - T_x\right\} \tag{A-41}$$

where C is a constant $= 4Kk_c/C_p(\mu g_0)^{0.8}\mathbf{P}^{0.4}$.

Flow through Two Orifices in Series —— appendix six

In Fig A-6 the top diagram shows two orifices in series. Let the following assumptions be made: perfect gas, velocity ahead of second orifice low. Then

$$\dot{M} = C_1 A_1 \rho_1 a_1 \phi_1 \left(\frac{p_2}{p_1}\right) = C_2 A_2 \rho_2 a_2 \phi_1 \left(\frac{p_3}{p_2}\right) \qquad \text{(A-42)}$$

where C = orifice coefficient
A = area of orifice
ρ = density
a = sonic velocity = $\sqrt{kg_0RT/m}$
ϕ_1 = the function given in Fig A-2
R = universal gas constant
k = ratio of specific heats
T = absolute temperature
m = molecular weight
g_0 = Newton's law coefficient.

For air $a = 49\sqrt{T}$ ft/sec when T is in °R.

If adiabatic flow is assumed, $T_2 = T_1$, $a_1 = a_2$, and $\rho_2/\rho_1 = p_2/p_1$. (Note that the subscript $_1$ denotes the stagnation condition upstream of the first orifice.)

Then

$$\phi_1\left(\frac{p_2}{p_1}\right) = \left(\frac{p_2}{p_1}\right)\phi_1\left(\frac{p_3}{p_2}\right)\frac{C_2A_2}{C_1A_1} \tag{A-43}$$

Let M_1 be the flow through A_1 when A_2 is so large that $p_2 \cong p_3$. Then

$$\frac{M}{M_1} = \frac{\phi_1(p_2/p_1)}{\phi_1(p_3/p_1)} \tag{A-44}$$

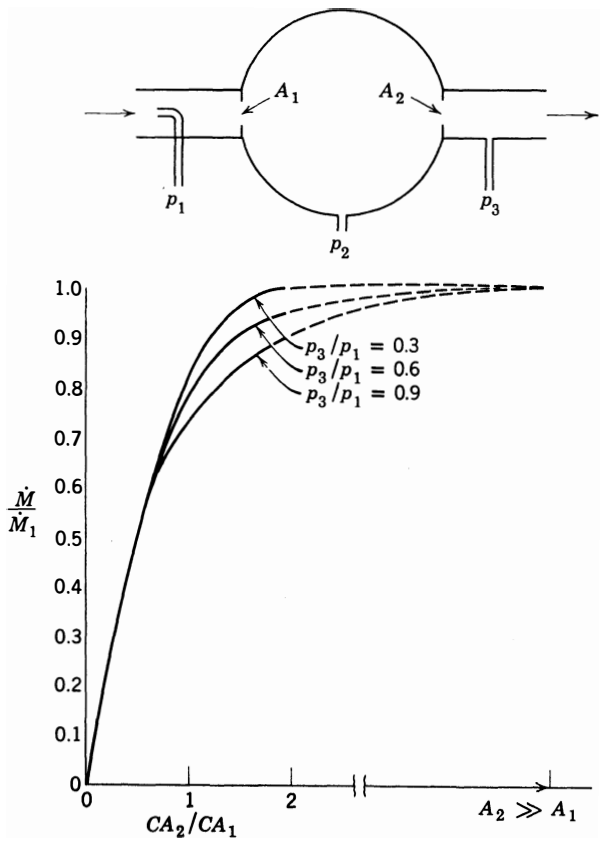

Fig A-6. Compressible flow through two orifices in series: CA_1 = coefficient × area of upstream orifice; CA_2 = coefficient × area of downstream orifice; $\dot{M}$ = mass flow through the system; $\dot{M}_1$ = mass flow when A_2 is very much larger than A_1; velocity ahead of A_2 assumed very small.

Stresses Due to Motion and Gravity in Similar Engines —appendix seven

Similar Engines. These are taken as engines in which all corresponding length ratios are the same and in which the same materials are used in corresponding parts. Such engines can be completely described by the following notation:

Typical dimension	L
Design (length) ratios	$R_1, R_2, R_3 \cdots R_n$
A bill of materials	

Basic properties of the materials can be specified by the value for a given material. For example, all moduli of elasticity are proportional to a characteristic modulus, E; all densities of material are proportional to a characteristic density ρ; the same can be said for heat conductivities, etc.

Inertia and Gravitational Stresses. Insofar as stresses due to inertia and gravity are concerned, only the following properties are important:

Name	Symbol	Dimension
Characteristic length	L	L
Design ratios	$(R_1 \cdots R_n)$	1
Characteristic density	ρ	ML^{-3}
Characteristic modulus of elasticity	E	FL^{-2}
Angular velocity	Ω	t^{-1}
Crank angle	θ	1
Viscosity of lubricant	μ	$FL^{-2}t$
Acceleration of gravity	g	Lt^{-2}
Newton's law constant	g_0	$MLt^{-2}F^{-1}$

Introducing the typical stress σ, which has the dimensions FL^{-2}, we can write the dimensionless equation

$$\phi_1\left(\frac{\rho L^2\Omega^2}{\sigma g_0}, \frac{\rho L^2\Omega^2}{Eg_0}, \frac{g\rho L}{\sigma g_0}, \frac{\mu(L\Omega)}{EL}, \theta, R_1 \cdots R_n\right) = 0$$

where ϕ_1 indicates a function of what follows. The third term in parentheses describes a parameter controlling stresses due to gravity. It is evident that these stresses vary with the typical length, L. However, in engines the gravitational stresses are negligible. Omitting this term and solving for the typical stress,

$$\sigma = \frac{\rho(L\Omega)^2}{g_0}\,\phi_2\left(\frac{\rho(L\Omega)^2}{Eg_0}, \frac{\mu(L\Omega)}{EL}, \theta, R_1 \cdots R_n\right)$$

where ϕ_2 is a function different from ϕ_1. The term after the equality sign indicates that stresses computed on a rigid-body base ($E = \infty$) are proportional to ρ times the square of the linear velocity. The first term in the parenthesis can also be written as Ω/ω_n where ω_n is the undamped natural vibration frequency of any typical engine component. As we have seen in Chap 9, the viscosity μ should be proportional to L, in which case the second term in parenthesis depends on $(L\Omega)/E$ only. Together, the first two terms in parenthesis control the friction and vibration stresses. For similar machines (ρ, E, $R_1 \cdots R_n$, all the same) it is thus evident that stresses due to inertia forces will be the same at the same values of $(L\Omega)$ and θ.

Basic Engine-Performance Equations —appendix eight

The following is a compendium of the basic relations used in Chapters 12 and 13. Definitions of the symbols are given in Appendix 1 and also where each equation first appears.

$$\text{bmep} = \text{imep} - \text{fmep} \tag{9-1}$$

where fmep = mmep + pmep + amep + cmep − tmep.

$$\text{imep}_4 = J\rho_a e_v \Gamma F' Q_c \eta' \tag{6-9}$$

$$\text{imep}_2 = JR_s \Gamma \rho_s F' Q_c \eta' \left(\frac{r}{r-1}\right) \tag{7-10}$$

$J = 5.4$ when imep is in psi, ρ_s is in lbm/ft^3, and Q_c is in Btu/lbm.

$$\rho_a = \frac{29p_i}{RT_i} \Big/ \left(1 + F_i \frac{29}{m_f} + 1.6h\right) \tag{6-6}$$

$$\rho_s = \frac{29p_e}{RT_i} \Big/ \left(1 + F_i \frac{29}{m_f} + 1.6h\right) \tag{7-3}$$

$29/R = 2.7$ when pressure is in psia, temperature in °R, density in lbm/ft^3.

The following relations are dimensionless when consistent units are used:

$$\frac{\text{cmep}}{\text{imep}} = \frac{1 + F_i}{Q_c F' \eta_i'} \left\{ \frac{C_{p1} T_1 Y_c}{\eta_c \Gamma} \right\} \tag{10-26}$$

$$\frac{\text{tmep}_s}{\text{imep}} = \frac{1 + F}{Q_c F' \eta_i'} \left\{ \frac{C_{pe} T_e Y_t \eta_t}{\Gamma} \right\} \tag{10-36}$$

$$\frac{\text{tmep}_b}{\text{imep}} = \frac{1 + F}{Q_c F' \eta_i'} \left\{ \frac{u^2 \eta_{kb}}{2 g_0 J \Gamma} \right\} \tag{10-37}$$

Fuel Economy Relations

$$\text{isfc} = 1/JQ_c\eta_i \tag{1-6}$$

$1/J = 2545$ when isfc is in lbm/hp-hr and Q_c is in Btu/lbm (1-12)

$$\text{isac} = \text{isfc}/F \tag{1-7}$$

$$\text{bsfc} = \text{isfc}\left(\frac{\text{imep}}{\text{bmep}}\right)$$

Mean Effective Pressure

Calculated from speed, power, or torque:

$$\begin{aligned} \text{mep} &= K_1 P/V_d N \\ &= K_2 P/A_p s \\ &= K_3 \tau/V_d \end{aligned}$$

In English measure, for four-cycle engines:

$$K_1 = 792{,}000 \qquad K_2 = 132{,}000 \qquad K_3 = 151$$

P = horsepower (33,000 ft-lbf per min), V_d = piston displacement (in^3), N = revolutions per minute, A_p = piston area (in^2), s = mean piston speed (feet per min), τ = torque (ft-lbf).

In metric measure, for four-cycle engines:

$$K_1 = 1224 \times 10^3 \qquad K_2 = 24{,}471 \qquad K_3 = 1.2563$$

P = power (kilowatts), V_d = piston displacement (liters), N = revolutions per minute, A_p = piston area (cm^2), s = mean piston speed (meters per minute), τ = torque (kg-meters).

For two-cycle engines, divide all values of K by 2.

Bibliography

Abbreviations

Unless otherwise noted, sources are in the United States.

The number following the source name is the volume or serial number.

AER	*Aeronautical Engineering Review,* pub IAS
AIMME	American Institute of Mining and Metallurgical Engineers
AM	*Applied Mechanics,* pub ASME
API	American Petroleum Institute
ASME	American Society of Mechanical Engineers
ASTM	American Society for Testing Materials
CIMCI	Congrès International des Moteurs à Combustion Interne
CIT	California Institute of Technology, Pasadena, Calif.
DEMA	Diesel Engine Manufacturers Association, Chicago, Ill.
EES	Engineering Experiment Station
IAS	Institute of Aeronautical Sciences
ICE	Internal-Combustion Engine(s)
IME	Institution of Mechanical Engineers, London
IEC	*Industrial Engineering Chemistry, Philadelphia, Pa.*
JSME	Japanese Society of Mechanical Engineers, Tokyo
Jour AS	*Journal of the Institute of Aeronautical Sciences*
Jour Appl Phys	*Journal of Applied Physics*
Jour Appl Mech	*Journal of Applied Mechanics,* pub ASME
Mech Eng	*Mechanical Engineering,* pub ASME
MIT	Massachusetts Institute of Technology, Cambridge, Mass.
MTZ	*Motortechnische Zeitschrift*
NACA	National Advisory Committee for Aeronautics *ARR* Advance research reports

NACA	*MR* Memorandum reports
	TR Technical reports
	TN Technical notes
	TM Technical memoranda
	WR Wartime reports
p	page
pub	published by
SAE	Society of Automotive Engineers
SAL	Sloan Laboratories for Aircraft and Automotive Engines, MIT
SME	Society of Mechanical Engineers
VDI	*Zeitschrift des Vereines deutscher Ingenieure,* Berlin
WADC	Wright Air Development Center, Dayton, Ohio
ZVDI	*Zeitschrift des Vereines deutscher Ingenieure,* Berlin

Chapter 1 Introduction, Symbols, Units, Definitions

Historical

1.01 Encyclopedia Britannica 14th ed articles entitled "Aero Engines" "Diesel Engines" "Internal Combustion Engines" "Oil Engines"
1.02 Clerk *The Gas Engine* Wiley NY 1886
1.03 Vowles and Vowles *The Quest for Power* Chapman and Hall (London) 1931
1.04 Taylor "History of the Aeronautical Engine" *Aviation* Aug 1926
1.05 Diesel and Strossner *Kampf um eine Maschine* (in German) E Schmidt Verlag Berlin 1952 (History of Dr. Diesel and his engines)
1.06 Beck et al. "The First Fifty Years of the Diesel Engine in America" *ASME NY spec pub* 1949
1.061 Historical number of *Diesel Progress* Los Angeles May 1948

Internal-Combustion Engines—Elementary and Descriptive

1.07 Heldt *High-Speed Combustion Engines* Chilton Co Phila 1956
1.08 Ober and Taylor *The Airplane and Its Engine* McGraw-Hill 1949

Internal-Combustion Engines—Analytical

1.10 Taylor and Taylor *The Internal Combustion Engine* Int Textbook Co Scranton Pa ed 1949 revised 1960
1.11 Rogowski *Elements of Internal Combustion Engines* McGraw-Hill NY 1953
1.12 Ricardo *Engines of High Output* Van Nostrand NY 1927
1.13 Ricardo and Clyde *The High Speed Internal Combustion Engine* Blackie and Son London 1941
1.14 Pye *The Internal Combustion Engine* Vol 1 Oxford University Press 1937 Vol II *The Aero Engine* Oxford University Press 1934
1.15 List *Thermodynamik der Verbrennungskraftmaschine* 3 vol Springer-Verlag Vienna 1950
1.16 Heywood *Internal-Combustion Engine Fundamentals* McGraw-Hill New York 1985

ENGINE BALANCE

1.2 Root *Dynamics of Engine and Shaft* Wiley NY 1932

THERMODYNAMICS

1.3 Keenan and Shapiro "History and Exposition of the Laws of Thermodynamics" *Mech Eng* Nov 1947
1.4 Keenan *Thermodynamics* Wiley NY 1941

EXHAUST-TEMPERATURE MEASUREMENT

1.5 Boyd et al. "A Study of Exhaust-Gas Temperature Measurement" Thesis MIT library June 1947

Chapter 2 Air Cycles

2.1 Van Duen and Bartas "Comparison of Actual Engine Cycle with Theoretical Fuel-air Cycle" Thesis MIT library June 1950
2.2 Phillips "Comparison of the Relative Efficiencies of the Actual Cycle, Fuel-air Cycle, and Air Cycle" Thesis MIT library June 1941
2.3 Spero and Sommer "Comparison of Actual to Theoretical Cycles" Thesis MIT library June 1944
2.4 Taylor and Taylor *The Internal-Combustion Engine* Int Textbook Co NY 1949 revised 1960

Chapter 3 Thermodynamics of Working Fluids

THEORY

3.10 Loeb *Kinetic Theory of Gases* McGraw-Hill NY 1927
3.11 Knudsen *Kinetic Theory of Gases* Methuen (London) 1934
3.12 Sears *An Introduction to Thermodynamics, The Kinetic Theory of Gases, and Statistical Mechanics* Addison-Wesley Cambridge Mass 1950

PROPERTIES OF AIR AND OTHER GASES

3.20 Hottel et al. *Thermodynamic Charts for Combustion Processes* parts I and II Wiley 1949 (see also bibliography included)
3.21 Keenan and Kaye *Gas Tables* Wiley NY 1948
3.22 Goff et al. "Zero-Pressure Thermodynamic Properties of Some Monatomic Gases" *Trans ASME* 72 Aug 1950
3.23 Goff and Gratch "Zero-Pressure Thermodynamic Properties of Carbon Monoxide and Nitrogen" *Trans ASME* 72 Aug 1950
3.24 Akin "The Thermodynamic Properties of Helium" *Trans ASME* 72 Aug 1950
3.25 Andersen "Some New Values of the Second Enthalpy Coefficient for Dry Air" *Trans ASME* 72 Aug 1950

3.26 Johnston and White "Pressure-Volume-Temperature Relationships of Gaseous Normal Hydrogen from its Boiling Point to Room Temperature and from 0–200 Atmospheres" *Trans ASME* 72 Aug 1950

PROPERTIES OF FUELS

3.30 Holcomb and Brown "Thermodynamic Properties of Light Hydrocarbons" (includes pure hydrocarbon compounds and natural gases) *Ind Eng Chem* 34 May 1942 plus revised chart p 384 1943

3.31 Schiebel and Othmer "Hydrocarbon Gases, Specific Heats and Power Requirements for Compression" *Ind Eng Chem* 36 June 1944

3.32 Brown "A Series of Enthalpy-entropy Charts for Natural Gases" *AIMME Tech Pub* 1747 1944

3.33 Maxwell *Data Book on Hydrocarbons* Van Nostrand 1950

3.34 ASTM *Handbook of Petroleum Products.* See also ASTM Standards, issued periodically

PROPERTIES OF FUEL-AIR MIXTURES

3.40 Pflaum *I.S Diagramme für Verbrennungsgase und ihre Anwendung auf die Verbrennungsmaschine VDI* Verlag (Berlin) 1932

3.41 Gilliland "P-V-T-Relations of Gaseous Mixtures" *Ind Eng Chem* 28 Feb 1936

3.42 Tanaka et al. "Entropy Diagrams for Combustion Gases of Gas Oil" *Tokyo Imp Univ Aero Res Inst Rep* 144 Sept 1936

3.43 Hershey, Eberhardt, and Hottel "Thermodynamic Properties of the Working Fluid in Internal Combustion Engines" *Jour SAE* 39 Oct 1936

3.431 Tsien and Hottel "Note on Effect of Hydrogen-Carbon Ratio etc" *Jour AS* 5 Mar 1938

3.44 Wiebe et al. "Mollier Diagrams for Theoretical Alcohol-Air and Octane-Water-Air Mixtures" *Ind Eng Chem* 34 May 1942 plus corrected charts 36 July 1944 p 673

3.45 Oleson and Wiebe "Thermodynamics of Producer Gas Combustion" (includes charts for burned and unburned mixtures) *Ind Eng Chem* 37 July 1945

3.46 Gilchrist "Chart for Investigation of Thermodynamic Cycles in IC Engines and Turbines" *IME* (London) 159 1948

3.47 Walker and Rogers "The Development of Variable Specific Heat Charts and Graphs and Their Application to ICE Problems" *Proc IME* (London) 159 1948

3.48 Turner and Bogart "Constant-Pressure Combustion Charts Including Effects of Diluent Additions" (diluents include water, alcohol, ammonia, dissociation not included) *NACA TR* 937 1949

3.49 Hottel et al. "Thermodynamic Charts for Combustion Processes" *NACA TN* 1883 1949 (see also reference 3.20)

3.50 Hoge "Compilation of Thermal Properties of Wind-Tunnel and Jet-Engine Gases at the National Bureau of Standards" *Trans ASME* 72 Aug 1950

3.51 McCann et al. "Thermodynamic Charts for Internal-Combustion Engine Fluids" (same base as ref 3.20) *NACA TN* 1883 July 1949

3.52 Huff and Gordon "Tables of Thermodynamic Functions for Analysis of Aircraft-Propulsion Systems" *NACA TN* 2161 Aug 1950
3.53 Kaye "Thermodynamic Properties of Gas Mixtures Encountered in Gas-Turbine and Jet-Propulsion Processes" *Jour Appl Mech* 15 1948 p 349
3.54 Logan and Treanor "Polytropic Exponents for Air at High Temperatures" *Jour AS* 24 1957

Chapter 4 Fuel-Air Cycles

4.1 Goodenough and Baker "A Thermodynamic Analysis of Internal Combustion Engine Cycles *U of Ill EES Bull* 160 1927
4.2 Tsien and Hottel "Note on Effect of Hydrogen-Carbon Ratio of Fuel on Validity of Mollier Diagrams for Internal Combustion Engines" *Jour IAS* 5 March 1938
4.3 Hottel and Eberhardt "Flame Temperatures in Engines" *Chem Reviews* 21 1937
4.4 Van Deun and Bartas "Comparison of Actual Engine Cycle with Theoretical Fuel-Air Cycle" Thesis MIT library June 1950
4.5 Center and Chisholm "Indicated Thermal Efficiency at Low Engine Speeds" Thesis MIT library June 1951
4.6 Takata and Edwards "Idling and Light Load Operation of a Gasoline Engine" two reports on file in Sloan Laboratories MIT Jan and Feb 1942
4.7 Farrell "A Study of Highly Throttled Engine Conditions" Thesis MIT library June 1941
4.8 Collmus and Freiberger "Gasoline Consumption of a Highly Throttled Multi-Cylindered Engine" Thesis MIT library June 1945
4.81 D'Alleva and Lovell "Relation of Exhaust Gas Composition to Air-Fuel Ratio" *Jour SAE* 38 March 1936
4.82 Houtsma et al. "Relation of Scavenging Ratio and Scavenging Efficiency in the Two-Stroke Compression Ignition Engine Thesis MIT library June 1950
4.90 Streid "Gas Turbine Fundamentals" *Mech Eng* June 1947
4.901 Vincent *Theory and Design of Gas Turbines and Jet Engines* Chap IV McGraw-Hill NY 1950
4.902 Mallinson et al. "Part Load Performance of Various Gas-Turbine Engine Schemes" *Proc Inst Mech Eng* (London) 159 1948
4.91 Livengood et al. "Ultrasonic Temperature Measurement in Internal Combustion Engine Chamber" *Jour Acoustical Soc Am* Sept 1954
4.92 Livengood et al. "Measurement of Gas Temperature in an Engine by the Velocity of Sound Method" *Trans SAE* 66 1958

Chapter 5 The Actual Cycle

Pressure Indicators

5.01 Dickinson and Newell "A High-Speed Engine Pressure Indicator of the Balanced Diaphragm Type" NACA TR 107 1921

5.02 "The Dobbie-McInnes Farnboro Electric Indicator" bull Dobbie-McInnes 57 Bothwell St Glasgow Scotland
5.03 Taylor and Draper "A New High-Speed Engine Indicator" *Mech Eng* March 1933 (modern version manufactured by American Instrument Co Silver Spring Md)
5.031 Ranck "MIT Indicator Gives Fast Check on Engine Performance" *Oil and Gas Journal* May 11 1959
5.04 Livengood "Improvement of Accuracy of Balanced-Pressure Indicators and Development of an Indicator Calibrating Machine" *NACA TN* 1896 June 1949
5.05 Rogowski "P-V Conversion Machine" *DEMA Bull* 14 Jan 9 1956
5.06 Draper and Li "A New High Performance Engine Indicator of the Strain Gage Type" *Jour AS* 16 Oct 1949
5.07 Kistler "SLM Pressure Indicator" *DEMA Bull* 14 Jan 9 1956 (capacity type electric indicator)
5.08 Robinson et al. "New Research Tool Aids Combustion Analysis" *SAE preprint* 256 Jan 1958 and abstract in *Jour SAE* Jan 1958 (combination of SLM indicator with spark plug)
5.09 McCullough "Engine Cylinder-Pressure Measurements" *Trans SAE* 61 1953 p 557 (discussion of various indicator types and their uses)
5.091 Li "High-Frequency Pressure Indicators for Aerodynamic Problems" *NACA TN* 3042 Nov 1953
5.092 Vinycomb "Electronic Engine Indicators with Special Reference to Some Recent American Designs" *Proc IME* London 164 1951 p 195
5.093 Robison et al. "Investigating Combustion in Unmodified Engines" *Trans SAE* 66 1958 p 549

Temperature—Measuring Methods

5.10 Hershey and Paton "Flame Temperatures in an Internal Combustion Engine Measured by Spectral Line Reversal" *U of Ill EES Bull* 262 1933
5.11 Rassweiler and Withrow "Flame Temperatures Vary with Knock and Combustion-Chamber Position" *Jour SAE* 36 April 1935
5.12 Brevoort "Combustion-Engine Temperatures by the Sodium-Line Reversal Method" *NACA TN* 559 1936
5.13 Chen et al. "Compression and End-Gas Temperature from Iodine Absorption Spectra" *Trans SAE* 62 1954 p 503
5.15 Livengood et al. "Ultrasonic Temperature Measurement in Internal-Combustion Engine Chamber" *Jour Acoustical Soc Am* 26 Sept 1954
5.16 Livengood et al. "Measurement of Gas Temperatures by the Velocity of Sound Method" *Trans SAE* 66 1958 p 683 (see also ref 1.5)

Comparison of Actual and Fuel-Air Cycles

(See also ref 5.16)

5.20 Spero and Sommer "Comparison of Actual to Theoretical Engine Cycles" Thesis MIT library May 1944
5.21 Van Deun and Bartas "Comparison of Actual Engine Cycle with Theoretical Fuel-Air Cycle" Thesis MIT library May 1950

NONSIMULTANEOUS BURNING

(See also ref 1.10)

5.22 Hopkinson "Explosions in Gaseous Mixtures and the Specific Heat of the Products" *Engineering* (London) 81 1906

MEASUREMENTS OF TEMPERATURE AND PRESSURE IN DIESEL ENGINES

5.30 Uyehara et al. "Diesel Combustion Temperatures—Influence of Operating Variables" *Trans ASME* 69 July 1947 p 465

5.301 Uyehara and Myers "Diesel Combustion Temperatures—Influence of Fuels" *Trans SAE* 3 Jan 1949 p 178

5.31 Millar et al. "Practical Application of Engine Flame Temperature Measurements" *Trans SAE* 62 1954 p 515

5.32 Crowley et al. "Utilization of Exhaust Energy of a Two-Stroke Diesel Engine" Thesis MIT library May 1957

Chapter 6 Air Capacity of Four-Stroke Engines

AIR-MEASURING TECHNIQUES

6.01 *Fluid Meters: Their Theory and Application* 4th ed ASME NY 1940

INDICATOR DIAGRAM ANALYSIS

6.10 Grisdale and French "Study of Pumping Losses with the MIT High-Speed Indicator" Thesis MIT library May 1948

6.11 Mehta "Influence of Inlet Conditions on the Constant-Volume Fuel-Air Cycle" Thesis MIT library Nov 1945

6.12 Draper and Taylor "A New High-Speed Engine Indicator" *Mech Eng* 55 Mar 1933

EFFECTS OF OPERATING VARIABLES

6.20 Livengood et al. "The Volumetric Efficiency of Four-Stroke Engines" *Trans SAE* 6 Oct 1952 p 617

6.21 Malcolm and Pereira "The Effect of Inlet Temperature on Volumetric Efficiency at Various Fuel-Air Ratios" Thesis MIT library May 1944

6.22 Markell and Taylor "A Study of the Volumetric Efficiency of a High-Speed Engine" *AER* 2 Nov 1943

6.23 Markell and Li "A Study of Air Capacity of an Automobile Engine" Thesis MIT library May 1942

6.24 Foster "The Quiescent Chamber Type Compression-Ignition Engine" *NACA TR* 568 1936

6.25 Roensch and Hughes "Evaluation of Motor Fuels · · ·" *Trans SAE* 5 Jan 1951

6.26 Johnson "Supercharged Diesel Performance vs. Intake and Exhaust Conditions" *Trans SAE* 61 1953 p 34

6.27 Gibson et al. "Combustion Chamber Deposition and Power Loss" *Trans SAE* 6 Oct 1952 p 567

6.28 Schmidt "The Induction and Discharge Process and Limitations of Poppet Valve Operation in a Four-Stroke Aero Engine" Luftfahrt-Forschung 16 1939 p 251 RTP translation 2495 Durand Publishing Co in care of CIT Pasadena 4 Calif.

ATMOSPHERIC EFFECTS

6.29 See refs 12.10–12.189

EFFECTS OF FUEL EVAPORATION, FUEL INJECTION, ETC.

6.30 Taylor et al. "Fuel Injection with Spark Ignition in an Otto-Cycle Engine" *Trans SAE* 25 1931-2 p 346

6.31 Rogowski and Taylor "Comparative Performance of Alcohol-Gasoline Blends" *Jour AS* Aug 1941

HEAT TRANSFER TO INLET GASES

6.32 Forbes and Taylor "Rise in Temperature of the Charge in its Passage through the Inlet Valve and Port of the Air-Cooled Aircraft Engine Cylinder" *NACA TN* 839 Jan 1942

6.321 Wu "A Thermodynamic Analysis of the Inlet Process of a Four-Stroke Internal Combustion Engine" Thesis MIT library Feb 1947

6.322 Taylor and Toong "Heat Transfer in Internal-Combustion Engines" *ASME paper* 57-HT-17 Penn State Coll Aug 1957 (see also abstract in *Mech Eng* Oct 1957 p 961)

6.323 Hirao "The Thermal Effect upon the Charging Efficiency of a 4-Cycle Engine" (in Japanese with English summary) SMI Tokyo 19 1953

VALVE FLOW CAPACITY, MACH INDEX, ETC.

6.40 Wood et al. "Air Flow Through Intake Valves" *Jour SAE* June 1942

6.41 Livengood and Stanitz "The Effect of Inlet-Valve Design, Size, and Lift on the Air Capacity and Output of a Four-Stroke Engine" *NACA TN* 915 1943

6.42 Tsu "Theory of the Inlet and Exhaust Processes of the ICE" *NACA TN* 1446 1949

6.43 Eppes et al. "The Effect of Changing the Ratio of Exhaust-Valve Flow Capacity to Inlet-Valve Flow Capacity on Volumetric Efficiency and Output of a Single-Cylinder Engine" *NACA TN* 1365 Oct 1947

6.44 Livengood and Eppes "Effect of Changing Manifold Pressure, Exhaust Pressure, and Valve Timing on the Air Capacity and Output of a Four-stroke Engine Operated with Inlet Valves of Various Diameters and Lifts" *NACA TN* 1366 Dec 1947

6.45 Livengood and Eppes "Effect of Changing the Stroke on Air Capacity, Power Output, and Detonation of a Single-Cylinder Engine" *NACA ARR* 4E24 Feb 1945

6.46 Stanitz et al. "Steady and Intermittent-flow Coefficients of Poppet Intake Valves" *NACA TN* 1035 Mar 1946

VALVE TIMING

6.50 Taylor "Valve Timing of Engines Having Intake Pressure Higher than Exhaust Pressure" *NACA TN* 405 1932

6.501 Schey and Bierman "The Effect of Valve Timing on the Performance of a Supercharged Engine at Altitude and an Unsupercharged Engine at Sea Level" *NACA TR* 390 1931

6.51 Boman et al. "Effect of Exhaust Pressure on a Radial Engine with Valve Overlap of 40°" *NACA TN* 1220 Mar 1947

6.52 Humble et al. "Effect of Exhaust Pressure on Performance with Valve Overlap of 62°" *NACA TN* 1232 Mar 1947

6.53 See ref 6.74

6.54 Stem and Deibel "The Effect of Valve Overlap on the Performance of a Four-stroke Engine" Thesis MIT library Jan 1955

6.55 Creagh et al. "An Investigation of Valve-Overlap Scavenging over a Wide Range of Inlet and Exhaust Pressures" *NACA TN* 1475 Nov 1947

6.56 See ref 13.17

6.57 See ref 13.19

INLET DYNAMICS

6.60 Reynolds et al. "The Charging Process in a High-Speed, Four-Stroke Engine" *NACA TN* 675 Feb 1939

6.61 Morse et al. "Acoustic Vibrations and Internal-Combustion Engine Performance" *Jour Appl Phys* 9 1938

6.62 Loh "A Study of the Dynamics of the Induction and Exhaust Systems of a Four-Stroke Engine by Hydraulic Analogy" Thesis MIT library Sept 1946

6.621 Orlin et al. "Application of the Analogy Between Water Flow with a Free Surface and Two-Dimensional Compressible Gas Flow" *NACA TN* 1185 Feb 1947

6.63 Taylor et al. "Dynamics of the Inlet System of a Four-Stroke Single-Cylinder Engine" *Trans ASME* 77 Oct 1955 p 1133

6.64 Glass and Kestin "Piston Velocities and Piston Work" *Aircraft Eng* (London) June 1950

EXHAUST-SYSTEM EFFECTS

6.70 Stanitz "Analysis of the Exhaust Process" *Trans ASME* 73 April 1951 p 327

6.71 Taylor "Effect of Engine Exhaust Pressure on the Performance of Engine-Compressor-Turbine Units" *Trans SAE* 54 Feb 1946 p 64

6.72 Hussmann and Pullman "Formation and Effects of Pressure Waves in Multi-Cylinder Exhaust Manifolds" U.S. Navy ONR N6onr 269 Penn State College Dec 1953

6.73 Hamabe "A Consideration on the Size of the Exhaust Valve and Suction Valve of a High Speed ICE" *Trans SME* Tokyo 4 No. 17

6.74 Desman and Doyle "Effect of Exhaust Pressure on Performance of a 12-cyl Engine" *NACA TN* 1367 1947

Chapter 7 Two-Stroke Engines

General

7.01 Rogowski and Taylor "Scavenging the Two-Stroke Engine" *Trans SAE* 1953
7.02 List "Der Ladungswechsel der Verbrennungskraftmaschine" part 2 der Zweitakt Springer-Verlag Vienna 1950
7.03 "Technology Pertaining to Two-Stroke Cycle Spark-Ignition Engines" SAE Report PT-26 1982

Scavenging Efficiency and Its Measurement

7.10 Irish et al. "Measurement of Scavenging Efficiency of the Two-Stroke Engine—A Comparison and Analysis of Methods" Thesis MIT library 1949
7.11 Spanogle and Buckley "The NACA Combustion Chamber Gas-sampling Valve and some preliminary Test Results" *NACA TN* 454 1933
7.12 Schweitzer and DeLuca "The Tracer Gas Method of Determining the Charging Efficiency of Two-Stroke-Cycle Diesel Engines" *NACA TN* 838 1942
7.13 Curtis "Improvements in Scavenging and Supercharging" *Diesel Power* Sept 1933
7.14 "Scavenging of Two-Cycle Engines" *Sulzer Tech Review* 4 1933
7.15 Boyer et al. "A Photographic Study of Events in a 14 in Two-Cycle Gas-Engine Cylinder" *Trans ASME* 76 1954 p 97 (Schlieren photos of air motion with Miller high-speed camera)
7.16 D'Alleva and Lovell "Relation of Exhaust Gas Composition to Air-Fuel Ratio" *Trans SAE* 38 Mar 1936
7.161 Gerrish and Meem "Relation of Constituents in Normal Exhaust Gas to Fuel-Air Ratio" *NACA TR* 757 1943
7.162 Elliot and Davis "The Composition of Diesel Exhaust Gas" *SAE preprint* 387 Nov 1949
7.17 Ku and Trimble "Scavenging Characteristics of a Two-Stroke Cycle Engine as Determined by Skip-Cycle Operation" *Jour Research* U.S. Bu Standards 57 Dec 1956
7.18 Spannhake "Procedures Used in Development of Barnes and Reinecke Air Force Diesel Engine" *Trans SAE* 61 1953 p 574
7.19 Rogowski and Bouchard "Scavenging a Piston-Ported Two-Stroke Cylinder" *NACA TN* 674 1938
7.20 Rogowski et al. "The Effect of Piston-Head Shape, Cylinder-Head Shape and Exhaust Restriction on the Performance of a Piston-Ported Two-Stroke Cylinder" *NACA TN* 756 1940
7.21 Houtsma et al. "Correlation of Scavenging Ratio and Scavenging Efficiency in the Two-Stroke Compression Ignition Engine" Thesis MIT library 1950
7.22 Hagen and Koppernaes "Influence of Exhaust-Port Design and Timing on Performance of Two-Stroke Engines" Thesis MIT library Aug 1956
7.23 Taylor et al. "Loop Scavenging vs. Through Scavenging of Two-Cycle Engines" *Trans SAE* 66 1958 p 444

7.24 Taylor "An Analysis of the Charging Process in the Two-Stroke Engine" *SAE preprint* June 1940

PERFORMANCE OF TWO-STROKE ENGINES

7.30 Shoemaker "Automotive Two-Cycle Diesel Engines" *Trans SAE* 43 Dec 1938 p 485

7.31 "Trials of a 5500 BHP Sulzer Marine Engine" *Sulzer Tech Review* 2 1935

7.32 Reid and Earl "Examination and Tests of a Six-Cylinder Opposed Piston, Compression Ignition Aero Engine of 16.6 Litres Displacement" *RAE Report EA* 216 May 1944 (British) (description and performance tests of captured Junkers Jumo 207 engine including air flow measurements)

7.321 Chatterton "The Napier Deltic Diesel Engine" *Trans SAE* 64 1956 (multicylinder op engine data on valve timing performance, etc)

7.33 "The Trunk-Piston Two-Stroke MAN Engine Type GZ" *Diesel Engine News* 25 April 1952 pub Maschinenfabrik Augsburg-Nurnberg A.G. Werk Augsburg Germany

7.34 Rogowski and Taylor "Part-Throttle Operation of a Piston-Ported Two-Stroke Cylinder" *NACA TN* 919 Nov 1943

7.35 See refs 13.22 and 13.44

7.36 Dickson and Wellington "Loop Scavenging Used in New 3000-rpm Diesel" *Jour SAE* June 1953 p 48 (GM-51 series)

7.37 List "High-Speed, High-Output, Loop-Scavenged Two-Cycle Diesel Engines" *Trans SAE* 65 1957 p 780

7.38 Grant "Outboard Engine Fuel Economy" *Jour SAE* Nov 1957 p 62

7.390 Wynne "Performance of a Crankcase-Scavenged Two-Stroke Engine" Thesis MIT library Jan 1953 (flow coefficients of automatic valves—vol eff of crankcase)

7.391 Zeman "The Recent Development of Two-Stroke Engines" ZVDI 87 Part 1 RTP translation 2470 Part II translation 2382 Durand Publishing Co in care of CIT Pasadena 4 Calif.

7.3911 "Outboard Motors and Their Operation" *Lubrication* 39 Jan 1953 (The Texas Co)

7.392 Kettering "History and Development of the 567 Series General Motors Locomotive Engine" published by Electro-Motive Division, GMC Jan 1952

7.3921 Rising "Air Capacity of a Two-Stroke Crankcase-Scavenged Engine" Thesis MIT library May 1959

PORT FLOW COEFFICIENTS

7.4 Toong and Tsai "An Investigation of Air Flow in Two-Stroke Engine" Thesis MIT library 1948 (see also refs 7.21–7.24)

EXHAUST BLOWDOWN EFFECTS

7.50 Wallace and Nassif "Air Flow in a Naturally Aspirated Two-Stroke Engine" *Proc IME* (London) 168 1954

7.51 Weaving "Discharge of Exhaust Gases in Two-Stroke Engines" *IME Internal Combustion Engine Group Proc* 1949 (Study of "blowdown process" from a vessel of fixed volume in both sonic and subsonic regions. Experiments with port and sleeve arrangement, and with poppet valve. Brief reference to Kadenacy effect. Extensive discussion)

7.52 Belilove "Improving Two-Stroke Cycle Engine Performance by Exhaust-Pipe Turning" *Diesel Power and Diesel Trans* July 1943

7.53 Cockshutt and Schwind "A Study of Exhaust Pipe Effects in the MIT Two-Stroke Engine" Thesis MIT library Sept 1951

7.54 Hussmann and Pullman "Formation and Effects of Pressure Waves in Multi-cylinder Exhaust Manifolds" Penn State College Dec 1953 US Navy report (Report on several years' work at Penn State College with air model and various exhaust manifolds. Theoretical computations compared with test measurements)

Effects of Inlet and Exhaust Conditions

7.60 Mitchell and Vozella "Effect of Inlet Temperature on Power of a Two-Stroke Engine" Thesis MIT library June 1945

7.61 See ref 12.183

Supercharging Two-Stroke Engines

See refs 13.00–13.26

Free-Piston Two-Stroke Engines

7.8 See refs 13.30–13.391

Chapter 8 Heat Losses

Heat Transfer, General

8.01 McAdams *Heat Transmission* McGraw-Hill NY 1954

8.02 Eckert and Drake *Introduction to the Transfer of Heat and Mass* McGraw-Hill NY 1950

8.03 Croft *Thermodynamics, Fluid Flow and Heat Transmission* McGraw-Hill NY 1938

8.04 Kay *Fluid Mechanics and Heat Transfer* Cambridge University Press (England) 1957

Heat Transfer in Tubes

8.10 Pinkel "A Summary of NACA Research on Heat Transfer and Friction for Air Flowing Through Tube With Large Temperature Difference" *Trans ASME* Feb 1954

8.11 Martinelli et al. "Heat Transfer to a Fluid Flowing Periodically at Low Frequencies in a Vertical Tube" *Trans ASME* Oct 1943

8.12 Warren and Loudermilk "Heat Transfer Coefficients for Air and Water Flowing Through Straight, Round Tubes" NACA RME50E23 Aug 1950
8.13 Toong "A New Examination of the Concepts of Adiabatic Wall Temperature and Heat-Transfer Coefficient" *Proc Nat Cong Appl Mech* 1954

Heat Transfer in Engines

8.20 Nusselt "Der Wärmeübergang in der Gasmaschine" *ZVDI* (Berlin) 1914
8.21 David "The Calculation of Radiation Emitted in Gaseous Explosions from Pressure Time Curve" *Phil Mag* (London) 39 Jan 1920 p 66
8.211 David "An Analysis of Radiation Emitted in Gaseous Explosions" *Phil Mag* (London) 39 Jan 1920 p 84
8.22 Eichelberg "Temperaturverlauf und Wärmespannungen in Verbrennungsmotoren" *ZVDI* (Berlin) 263 1923
8.23 Nusselt "Der Wärmeübergang in der Verbrennungskraftmaschine" *ZVDI* (Berlin) 264 1923
8.24 Nusselt "Der Wärmeübergang in der Dieselmaschine" *ZVDI* (Berlin) April 3 1926
8.25 Eichelberg "Some New Investigations in Old Internal-Combustion Engine Problems" *Engineering* (London) Oct 27–Dec 22 1939
8.26 Baker and Laserson "An Investigation into the Importance of Chemiluminescent Radiation in Internal Combustion Engines" *Proc London Conference on Heat Transmission* Sept 1951 (ASME pub)
8.27 Englisch *Verschleiss, Betriebzahlen und Wirtschaftlichkeit von Verbrennungskraftmaschinen* Springer Verlag (Vienna) 1943
8.28 Alcock et al. "Distribution of Heat Flow in High-duty Internal-Combustion Engines" Int Congress ICE Zurich 1957 (measures heat flux along bore and through cylinder head)

Heat Transfer in Engines—NACA Work

8.30 Pinkel "Heat-Transfer Processes in Air-Cooled Engine Cylinders" *NACA TR* 612 1938
8.31 Pinkel and Ellerbrook "Correlation of Cooling Data from an Aircooled Cylinder and Several Multi-Cylinder Engines" *NACA TR* 683 1940
8.32 Brimley and Brevoort "Correlation of Engine Cooling Data" NACA MR-L5A17 Jan 1945
8.33 Kinghorn et al. "A Method for Correlating Cooling Data of Liquid Cooled Engines and Its Application to the Allison V-3420 Engine" NACA L-782 MR-L5D03 May 1945
8.34 Pinkel et al. "Heat Transfer Processes in Liquid-Cooled Engine Cylinders" NACA E-131 ARR E5J31 Nov 1945
8.35 Zipkin and Sanders "Correlation of Exhaust-Valve Temperatures with Engine Operating Conditions" *NACA TR* 813 1945
8.36 Povolny et al. "Cylinder-Head Temperatures and Coolant Heat Rejection of a Multi-Cylinder Liquid-Cooled Engine of 1650-Cubic-Inch Displacement" *NACA TN* 2069 Apr 1950

8.37 Lundin et al. "Correlation of Cylinder-Head Temperatures and Coolant Heat Rejections of a Multi-cylinder Liquid-Cooled Engine of 1710-Cubic-Inch Displacement" *NACA Report* 931 1949
8.38 Manganiello and Stalder "Heat-Transfer Tests of Several Engine Coolants" *NACA ARR* E-101 Feb 1945
8.381 Sanders et al. "Operating Temperatures of Sodium-Cooled Exhaust Valve . . ." *NACA TN* 754 1943

Heat Transfer in Engines—MIT Work

8.40 Goldberg and Goldstein "An Analysis of Direct Heat Losses in an Internal-Combustion Engine" Thesis MIT library 1933
8.41 Meyers and Goelzer "A Study of Heat Transfer in Engine Cylinders" Thesis MIT library 1948
8.42 Smith et al. "A Study of the Effect of Engine Size on Heat Rejection" Thesis MIT library 1950
8.43 Cansever and Batter "A Study of Heat Transfer in Geometrically Similar Engines" Thesis MIT library 1953
8.44 Taylor "Heat Transmission in Internal Combustion Engines" *Proc Conference on Heat Transmission* London Sept 1951 (ASME pub)
8.45 Ku "Factors Affecting Heat Transfer in the Internal-Combustion Engine" *NACA TN* 787 Dec 1940
8.46 Lundholm and Steingrimsson "A Study of Heat Rejection in Diesel Engines" Thesis MIT library 1954
8.47 Toong et al. "Heat Transfer in Internal-Combustion Engines" Report to Shell Co MIT library (Sloan Automotive Branch) 1954
8.48 Hoey and Kaneb "A Study of Heat Transfer to Engine Oil" Thesis MIT library 1943
8.49 Simon et al. "An Investigation of Heat Rejection to the Engine Oil in an Internal Combustion Engine" Thesis MIT library 1944
8.491 Meng and Wu "The Direct Heat Loss in Internal-Combustion Engines" Thesis MIT library 1943

Stresses Due to Thermal Expansion

8.50 Goodier "Thermal Stresses" *Jour Appl Mech* ASME Mar 1937
8.51 Kent "Thermal Stresses in Spheres and Cylinders Produced by Temperatures Varying with Time" *Trans ASME* 54 1932

Heat Loss and Detonation

8.6 Bierman and Covington "Relation of Preignition and Knock to Allowable Engine Temperatures" *NACA ARR* 3G14 E-134 July 1943

Heat Losses and Design

8.70 Sulzer "Recent Measurements on Diesel Engines and Their Effect on Design" *Sulzer Tech Rev* 2 1939
8.71 Hoertz and Rogers "Recent Trends in Engine Valve Design and Maintenance" *Trans SAE* 4 July 1950

8.72 Flynn and Underwood "Adequate Piston Cooling" *Trans SAE* 53 Feb 1945
8.73 Sanders and Schramm "Analysis of Variation of Piston Temperature with Piston Dimensions and Undercrown Cooling" *NACA Report* 895 1948

RADIATOR DESIGN

8.80 Brevoort "Radiator Design" *NACA WR* L-233 July 1941
8.81 Gothert "The Drag of Airplane Radiators with Special Reference to Air Heating (Comparison of Theory and Experiment)" *NACA TM* 896 1938
8.82 Barth "Theoretical and Experimental Investigations of the Drag of Installed Aircraft Radiators" *NACA TM* 932 1938
8.83 Winter "Contribution to the Theory of the Heated Duct Radiator" *NACA TM* 893
8.84 Linke "Experimental Investigations on Freely Exposed Ducted Radiators" (From Jahrbuch 1938 der Deutschen Luftfahrtforschung) *NACA TM* 970 March 1941
8.85 Nielsen "High-Altitude Cooling, III—Radiators" *NACA WR* L-773 Sept 1944

MEASUREMENT OF SURFACE TEMPERATURE

8.9 Geidt "The Determination of Transient Temperatures and Heat Transfer at a Gas-Metal Surface applied to a 40 mm Gun Barrel" *Jet Propulsion* April 1955

Chapter 9 Friction, Lubrication, and Wear

There is an enormous literature on the theory and practice of lubrication, friction, and wear. This bibliography attempts to select those items most pertinent to the subject of engine friction.

GENERAL

9.01 Hersey *Theory of Lubrication* Wiley NY 1938
9.02 Norton *Lubrication* McGraw-Hill NY 1942
9.03 Shaw and Macks *Analysis and Lubrication of Bearings* McGraw-Hill NY 1949 (contains extensive bibliography)
9.04 Wilcock and Booster *Bearing Design and Application* McGraw-Hill NY 1957
9.05 Strang and Lewis "On the Mechanical Component of Solid Friction" *Jour Appl Phys* 20 Dec 1949 p 1164
9.06 Burwell and Strang "The Incremental Coefficient of Friction—A Non-Hydrodynamic Component of Boundary Lubrication" *Jour Appl Phys* 20 Jan 1949 p 79

OIL VISCOSITY

9.10 Reynolds "On the Theory of Lubrication" *Tran Roy Phil Soc* 177 1886 *Papers on Mech and Phys Subjects* Vol 2 Macmillan NY 1901
9.11 Herschel "Viscosity and Friction" *Trans SAE* 17 1922
9.12 Texas Co "Viscosity" *Lubrication* pub Texas Co May and June 1950

9.13 Fleming et al. "The Performance of High VI Motor Oils" *Trans SAE* 4 July 1950 p 410 (effects of viscosity on engine starting and oil consumption)

Journal-Bearing Friction

9.20 McKee and McKee "Journal-Bearing Friction in the Region of Thin-Film Lubrication" *Jour SAE* Sept 1932

9.21 McKee and McKee "Friction of Journal Bearings as Influenced by Clearance and Length" *Trans ASME* 51 1929

9.22 McKee and White "Oil Holes and Grooves in Plain Journal Bearings" *Trans ASME* 72 Oct 1950 p 1025

9.23 Barnard et al. "The Mechanism of Lubrication III, The Effect of Oiliness" *Jour IEC* Apr 1924

9.24 Underwood "Automotive Bearings" *ASTM Symposium on Lubricants* 1937

9.241 Stone and Underwood "Load Carrying Capacity of Journal Bearings" *Trans SAE* 1 Jan 1947

9.25 Bloch "Fundamental Mechanical Aspects of Thin-Film Lubrication" *Delft Publication III* (Shell Laboratories Holland) Feb 27 1950

9.26 Burwell "The Calculated Performance of Dynamically Loaded Sleeve Bearings" *Jour Appl Mech* Dec 1949 p 358 (see also part II [corrections] *Jour Appl Mech* 16-4 Dec 1949 p 358)

9.27 Simons "The Hydrodynamic Lubrication of Cyclically Loaded Bearings" *ASME paper* 49-A-41 Jan 1950

9.271 Buske and Rolli "Measurement of oil-film pressures in journal bearings under constant and variable loads" *NACA TM* 1200 Nov 1949

9.272 Shaw and Nussdorfer "An Analysis of the Full-Floating Journal Bearing" *NACA RM* E7A28a Jan 1947

9.273 Dayton et al. "Discrepancies between Theory and Practice of Cyclically Loaded Bearings" *NACA TN* 2545 Nov 1951

Oil Flow in Bearings

9.28 Boyd and Robinson "Oil Flow and Temperature Relations in Lightly Loaded Journal Bearings" *Trans ASME* Vol 70 No 3 p 257 April 1948

9.281 McKee "Oil Flow in Plain Journal Bearings" *Trans ASME* July 1952 p 841

9.282 Wilcock and Rosenblatt "Oil Flow, Key Factor in Sleeve-Bearing Performance" *Trans ASME* July 1952 p 849

Sliding Bearings

9.30 Michell "The Lubrication of Plane Surfaces" *Zeitschrift Math Phys* (Leipzig) 50 1904

9.31 Martin "Theory of the Michell Thrust Bearing" *Engineering* (London) Feb 20 1920

9.32 Charnes and Saibel "On the Solution of the Reynolds Equation for Slider-Bearing Lubrication I" *Trans ASME* July 1952 p 867

9.33 Fogg "Film Lubrication of Parallel Thrust Surfaces" *Proc Inst ME* (London) 155 1946

Oscillating Bearings

9.34 Underwood and Roach "Slipper Type Bearings for Two-Cycle Diesel Connecting Rods" *SAE preprint* 715 Jan 1952

Antifriction Bearings

9.35 Ferretti "Experiments with Needle Bearings" *NACA TM* 707 May 1933

9.351 Getzlaff "Experiments on Ball and Roller Bearings Under Conditions of High Speed and Small Oil Supply" *NACA TM* 945 July 1940

9.352 Barwell and Webber "The Influence of Combined Thrust and Radial Loads on Performance of High-Speed Ball Bearings" *Proc 7th Cong* AM 4 1948 p 257

Friction of Pistons and Rings

9.40 Hersey "Bibliography on Piston-Ring Lubrication" *NACA TN* 956 Oct 1944

9.41 Wisdom and Brooks "Observations of the Oil Film between Piston Ring and Cylinder of a Running Engine" *Australian Res Council for Aero* 37 1947

9.42 Shaw and Nussdorfer "Visual Studies of Cylinder Lubrication" I *NACA ARR* E5H08 Sept 1945

9.421 Ibid Part II

9.43 Forbes and Taylor "A Method for Studying Piston-Ring Friction" *NACA WR* W-37 1943

9.44 Tischbein "The Friction of Pistons and Rings" *NACA TM* 1069 Mar 1945

9.45 Stanton "The Friction of Pistons and Rings" *Aero Res Comm* (British) R and M 931 1924

9.451 Hawkes and Hardy "Friction of Piston Rings" *Trans. NE Coast Inst. Eng. & Shipbuilders* 1935

9.46 Robertson and Ford "An Investigation of Piston Ring Groove Pressures" *Diesel Power* Oct 1934

9.47 U of Minnesota "Gas Pressure Behind Piston Rings" *Aut Ind* July 25 1936 p 118

9.48 Leary and Jovellanos "A Study of Piston and Piston-Ring Friction" *NACA ARR*-4J06 Nov 1944

9.481 Livengood and Wallour "A Study of Piston-Ring Friction" *NACA TN* 1249 1947

9.482 Gibson and Packer "Effect of Ring Tension, Face Width and Number of Rings on Piston-Ring Friction" Thesis MIT library May 1951

9.483 Courtney et al. "Lubrication Between Piston Rings and Cylinder Walls" *Engineering* (London) 161 1946

9.484 Ebihara "Researches on the Piston Ring" *NACA TM* 1057 Feb 1944

9.49 "Investigations into the Behavior of Lubricating Oil in the Working Cylinders of Diesel Engines" *Sulzer Tech Rev* 3 1943

Bearing Loads

9.50 Taylor "Bearing Loads in Radial Engines" *Trans SAE* 25-26 1930–1931 p 546

9.501 Manson and Morgan "Distribution of Bearing Reactions on a Rotating Shaft Supported on Multiple Journal Bearings" *NACA TN* 1280 May 1947
9.502 Shaw and Macks "In-Line Engine Bearing Loads" "Radial-Engine Bearing Loads" *NACA ARR* E5H04 E5H10a and E5H10b Oct 1945 and *TN* 1206 Feb 1947 (see also ref 9.03)

MEASUREMENT OF ENGINE FRICTION

9.51 McLeod "The Measurement of Engine Friction" *SAE preprint* Jan 1937
9.52 Light and Karlson "A Comparison of Motoring Friction and Firing Friction in an Internal-Combustion Engine" Thesis MIT library May 1950
9.53 Taylor and Rogowski "Loop Scavenging vs. Through Scavenging of Two-Cycle Engines" *Trans SAE* 66 1958 (see last figure)
9.54 Gish et al. "Determination of True Engine Friction" (comparison of indicated and motoring friction) *Trans SAE* 66 1958 p 649

ENGINE FRICTION, GENERAL

9.55 Moss "Motoring Losses in Internal Combustion Engines" *Aero Res Comm* (British) R and M 1128 July 1927
9.56 Sparrow and Thorne "The Friction of Aviation Engines" *NACA TR* 262 1927
9.561 Taylor "The Effect of Gas Pressure on Piston Friction" *Trans SAE* 38 May 1936
9.562 Moore and Collins "Friction of Compression-Ignition Engines" *NACA TN* 577 Aug 1936
9.563 Richter "Internal Power, Frictional Power, and Mechanical Efficiencies of Internal Combustion Engines" *Maschinenbau und Wärmewirtschaft* Oct-Dec 1947 Reviewed in *Engineers' Digest* 5 Aug 1948
9.564 Geogi "Some Effects of Motor Oils and Additives on Engine Fuel Consumption" *Trans SAE* 62 1954 p 385 (viscosity index effects—no oiliness effects measurable)
9.57 Roensch "Thermal Efficiency and Mechanical Losses of Automotive Engines" *Trans SAE* March 1949
9.58 "Friction Analysis of the Liberty 12 Engine" *U.S. Air Service Report* Ser No 1675 July 19 1921
9.581 See ref 6.45
9.582 Aroner and O'Reilly "An Investigation of Friction in M.I.T. Four-Stroke Geometrically Similar Engines" Thesis MIT library May 1951
9.583 Harvey "Reducing Friction Losses Through Engine Design" *GM Engineering Staff Product Series 4 Report* 4-24-6 July 15 1948
9.584 Meyer et al. "Engine Cranking at Arctic Temperatures" *Trans SAE* 63 1955 p 515

PUMPING LOSSES IN FOUR-STROKE ENGINES

9.60 Hale and Olmstead "Some Factors Affecting Friction in an Internal-Combustion Engine" Thesis MIT library May 1937
9.61 Grisdale and French "Study of Pumping Losses with the MIT High Speed Indicator" Thesis MIT library May 1948

9.62 Taylor "Valve Timing of Engines Having Inlet Pressure Higher Than Exhaust Pressure" *NACA TN* 405 1932

ENGINE-FRICTION

(Aircraft Engines)

9.701 See ref 12.12
9.702 See ref 12.13
9.703 Manufacturers' tests unpublished
9.704 Manufacturers' tests unpublished

(Automobile Engines)

9.710 Zeder "New Horizons in Engine Development" *Trans SAE* 6 Oct 1952
9.711 MacPherson "The New Ford Six-Cylinder Engine" *Trans SAE* 6 July 1952
9.712 Stevenson "The New Ford V-8 Engine" *Trans SAE* 62 1954 p 595
9.713 Hardig et al. "The Studebaker V-8 Engine" *Trans SAE* 5 Oct 1951 p 447
9.714 Furphy "Part Load Performance of a Typical Automobile Engine" Thesis MIT library May 1948
9.715 Matthews "New Buick V-8 Engine" *Trans SAE* 61 1953 p 478

(Two-Stroke Engines)

9.720 See ref 7.30
9.721 See ref 7.34

(Four-Stroke Diesel Engines)

9.730 Unpublished tests by Texas Co
9.731 MAN Four-Cycle Marine Diesel Engine—Manufacturer's tests
9.732 Eaton and Meyer "Effect of Supercharging on Performance of a Commercial Diesel Engine" Thesis MIT library May 1944

MINIATURE ENGINES

9.74 Smith et al. "Study of Miniature Engine—Generator Sets" *WADC Tech Report* 53-180 Part V ASTIA Document AD 130940 Oct 1956

WEAR

There is an enormous body of literature on basic wear research, wear of bearings, and general engine wear. Particular attention is invited to publications in the field of engine wear in the Transactions of the Society of Automotive Engineers since about 1940. See also

9.80 Oberle "Hardness, Elastic Modulus, Wear of Metal" *Trans SAE* 6 1952
9.801 "Cylinder Wear, A Compilation (Bibliography) of Pertinent Articles" pub Texas Co NY 1947
9.81 *Proc Special Conference on Friction and Surface Finish* pub MIT June 1940
9.82 Poppinga *Verschleiss und Schmierung insbesondere von Kolbenringen und Zylindern* J W Edwards Chicago 1946
9.83 Burwell et al. "Mechanical Wear" *Jour ASTM* Jan 1950 (report on MIT wear conference June 1948)
9.84 *Proc 1958 Symposium on Engine Wear* pub Southwest Research Institute San Antonio Texas

Chapter 10 Compressors, Exhaust Turbines, Heat Exchangers

General

10.01 von der Nuell "Superchargers and Their Comparative Performance" *Trans SAE* 6 Oct 1952 Competent discussion of many aspects of compressor-engine-turbine problems. Includes performance curves of centrifugal, vane, and Roots type compressors. Discusses questions of matching with engines etc

10.02 Reiners and Schwab "Turbosupercharging of High Speed Diesel Engines" *SAE Paper* No 634 Aug 1952. Discussion of centrifugal vs positive displacement blowers

10.03 "Sulzer Turbo-Compressors" *Sulzer Tech Rev* No 2 1950 Discusses the application of centrifugal and axial compressors to large Diesel engines

10.04 Bullock et al. "Method of Matching Performance of Compressor Systems with that of Aircraft Power Sections" *NACA TR* 815 1945

Piston Compressors

10.10 Costagliola "Dynamics of a Reed Type Valve" Thesis MIT library 1947 Tests of a piston compressor and source of data for Fig 10-6

10.11 "Discharge Regulation in Piston-Type Compressors" *Sulzer Tech Rev* 2 1949 Shows compressor indicator cards and discusses control problems

10.12 Wynne "Performance of a Crankcase-Scavenged Two-Stroke Engine" Thesis MIT Jan 1953 Measures volumetric efficiency of a crankcase-type compressor

10.13 Ku "Note on Flow Characteristics of the Reciprocating Compressor" *Nat Bur Standards Rep* 3468 July 1954 Discussion of the design of a multistage piston compressor including effects of over-all pressure ratio, clearance ratio, piston area ratio, and leakage

Roots-Type Compressors

(See also ref 10.01)

10.20 Hiersch "Proposed Exrcssions for Roots Supercharger Design and Efficiency" *Trans ASME* Nov 1943

10.21 Pigott "Various Types of Compressors for Supercharging" *Trans SAE* 53 1945 (Study of leakage, windage and bearing losses in Roots compressor. Experimental data on an NACA Roots compressor)

10.22 Schey and Wilson "An Investigation of the Use of Discharge Valves and an Intake Control for Improving the Performance of NACA Roots-type Supercharger" *NACA TR* 303 1928

10.23 Ware and Wilson "Comparative Performance of Roots-Type Aircraft Engine Superchargers as Affected by Change in Impeller Speed and Displacement" *NACA TR* 284 1928 (Exhaustive tests—source of data for Fig 10-7)

10.24 Ryde "The Positive-Displacement Supercharger" *Trans SAE* 50 July 1942 (Discussion of applications. Some performance data)

Lysholm and Vane Compressors

(See also ref 10.21)

10.30 Wilson and Crocker "Fundamentals of the Elliott-Lysholm Compressor" *Mech Eng* 68 June 1946 Includes drawings and performance curves

10.31 Lysholm "A New Rotary Compressor" *Proc Inst Mech Eng* (London) 150 July 1943 History of development with drawings and performance curves

10.32 Schey and Ellerbrock "Comparative Performance of a Powerplus Vane Type Supercharger and an NACA Roots Type Supercharger" *NACA TN* 426 1932 Shows performance curves for vane type (See also ref 10.01)

Centrifugal Compressors

(See also ref 10.01)

10.40 Campbell and Talbert "Some Advantages and Limitations of Centrifugal and Axial Aircraft Compressors" *Jour SAE* 53 Oct 1945 Useful design information Source of Fig 10-9

10.41 Sheets "The Flow Through Centrifugal Compressors and Pumps" *Trans ASME* 72 Oct 1950 Analytic solution and experimental investigation on velocity and pressure distribution, surge, and blade stalling

10.42 Bullock and Finger "Surging in Centrifugal and Axial Flow Compressors" *Trans SAE* 6 April 1952 Theoretical and experimental treatment of surge

10.43 Sheets "The Flow Through Centrifugal Compressors and Pumps" *Trans ASME* 72 October 1950 Analytic solution and experimental investigation on velocity pressure distribution, surge, and stalling

10.44 Ku and Wang "A Study of the Centrifugal Supercharger" *NACA TN* 1950 Oct (Thermodynamics, hydrodynamics, dynamics, and stress analysis of the centrifugal compressor)

Mechanical Compressor Drives

(See also ref 10.01 and 10.03)

10.50 Kinkaid "Two-Speed Supercharger Drives" *Trans SAE* 50 Mar 1942 Details of gear drives used in aircraft engines

10.51 Fox "Seals for Preventing Oil Leakage in High-Speed Superchargers" *Prod Eng* 17 Feb 1946

10.52 "Construction and Operation of new McCulloch Supercharger" *Aut Ind* Oct 15 1953 Describes a mechanical drive using steel balls

10.53 Fangman and Hoffman "Supercharger Shaft Dynamics" *SAE preprint* 7A Jan 1958 (problems of torsional vibration)

10.54 Puffer "Aircraft Turbosupercharger Bearings—Their History, Design and Application Technique" *Trans ASME* 73 1951

Exhaust-Gas Energy and Temperature

10.60 Pinkel and Turner "Thermodynamic Charts for Computation of the Performance of Exhaust-Gas Turbines" NACA ARR 4B25 E-23 Oct 1945

10.61 Pinkel "Utilization of Exhaust Gas of Aircraft Engines" *Trans SAE* 54 1946 Excellent review of practical and theoretical aspects. Source of curve *a*, Fig 10-14.

10.62 Schweitzer and Tsu "Energy in the Engine Exhaust" *ASME paper* No 48-A-56 Dec 1948 Curves of recoverable energy as a function of release temperature, release pressure, and atmospheric pressure

10.63 Stanitz "Analysis of the Exhaust Process in Four-Stroke Reciprocating Engines" *ASME paper* 50-OGP-4 June 1950 Computations of cylinder blowdown as a function of valve characteristics

10.64 Brown-Boveri "The Utilization of Exhaust-Gas Energy in the Supercharging of the Four-Stroke Diesel Engine" *Brown-Boveri Review* 11 Nov 1950 Theory and experiment on blowdown energy, pressure waves etc

10.65 Schweitzer et al. "The Blowdown Energy in Piston Engines and Its Utilization in Turbines" Department of Engineering Research Penn State College July 1953 Study using a special type of blowdown valve

10.66 Johnson "Supercharged Diesel Performance vs. Intake and Exhaust Conditions" *Trans SAE* 61 1953 Includes extensive exhaust-temperature measurements

10.67 Sonderegger "The Blowdown Energy in Piston Engines and its Utilization in Turbines" Penn State College Report on Dept Eng Res US Navy contract NONR-656 (02)

10.68 Witter and Lobkovitch "Development of a Design Parameter for Utilization of Exhaust Gas from Two-Stroke Diesel Engine" Thesis MIT library June 1958

10.69 Crowley et al. "Utilization of Exhaust-Gas Energy of a Two-Stroke Diesel Engine" Thesis MIT library May 1957

10.691 Hussman et al. "Exhaust Blowdown Energy" USN Office of Naval Research Contract Nonr-656(02) Task No. NR 097-195 (comprehensive report of research at Penn State U. Includes calculations of blowdown energy together with tests on models and with four-stroke and two-stroke engines)

Blowdown Turbines

10.70 Turner and Desmond "Performance of a Blowdown Turbine Driven by Exhaust Gas of Nine-Cylinder Radial Engine" *NACA TR* 786 1944 Source of data for Fig 10–14 Gives curves of kinetic efficiency

10.71 Buchi "Exhaust Turbo-supercharging of Internal-Combustion Engines" Monograph No. 1 *Jour Franklin Inst* July 1953 Discussion of aplication of blowdown turbine to engines, including design of exhaust pipes, no. of cylinders etc

10.72 Wiegand and Eichberg "Development of the Turbo-Compound Engine" *Trans SAE* 62 1954 Performance data on blowdown turbine as well as its effect on engine performance (See also *Auto Ind* March 1 1954)

10.73 Wieberdink and Hootsen "Supercharging by Means of Turbo-blowers Applied to Two-Stroke Diesel Engines of Large Output" *Proc CIMCI* La Haye 1955 Shows diagrams of exhaust pressure and exhaust temperature vs crank-angle for a blowdown turbine

10.74 Van Asperen "Development and Service Results of a High Powered Turbo-Charged Two-Cycle Marine Diesel Engine" *Proc CIMCI* La Haye 1955 Complete description of engine and supercharger system, including curves of cylinder pressure and nozzle pressure for a blowdown turbine. Source of graph I, Fig 10–13

10.75 De Klerk "Exhaust-Gas Turbo-supercharged Four-stroke Rail Traction Engines" *Proc CIMCI* La Haye 1955 Details and performance curves. Source of graph II, Fig 10–13

10.76 Nagao and Shimamoto "On the Transmission of Blow-Down Energy in the Exhaust System of a Diesel Engine" *Bull JSME* 5 1959 p 170 (significant experiments with an air model accompanied by theoretical analysis)

Axial Turbines

10.80 Ainley "The Performance of Axial-Flow Turbines" *Proc IME* 1948 159 p 230

10.81 Talbert and Smith "Aerothermodynamic Design of Turbines for Aircraft Power Plants" *Jour IAS* 15 1948 p 556

10.82 Ohlsson "Partial Admission, Low Aspect Ratios, and Supersonic Speeds in Small Turbines" Sc.D. Thesis ME Dept MIT Jan 1956

Radial Turbines

10.83 Balje "A Contribution to the Problem of Designing Radial Turbomachines" *Trans ASME* May 1952

10.84 Jamison "The Radial Turbine" *Gas Turbine Principles and Practices* Ed Roxbee-Cox George Newnes Ltd London 1955

10.85 von der Nuell "Single-Stage Radial Turbines for Gaseous Substances with High Rotative and Low Specific Speed" *Trans ASME* May 1952

10.86 Wosika "Radial Flow Compressors and Turbines for the Simple Small Gas Turbine" *Trans ASME* Nov 1952

10.87 "Constructional Details of New Miehle-Dexter Turbo-Supercharger" *Auto Ind* June 1 1955 (description of a radial-flow turbine combined with radial-flow compressor on one wheel)

Heat Exchangers

10.90 McAdams *Heat Transmission* McGraw-Hill 1942

10.91 Kays and London *Compact Heat Exchangers* National Press Palo Alto Calif 1955

10.92 Fairall "A New Method of Heat-Exchanger Design . . ." *Trans ASME* 80 Apr 1958 Optimization for various types of flow and various design requirements Includes bibliography (See also ref 12.177)

Chapter 11 Influence of Cylinder Size on Engine Performance

General Theory of Dimensions

11.01 Bridgeman *Dimensional Analysis* Yale U Press 1932

11.02 "Law of Similitude in Flow Problems" *Sulzer Tech Rev* No 1 1947

11.03 Hunsaker "Dimensional Analysis and Similitude in Mechanics" *ASME Appl Mech von Karman Anniversary Vol* 1941

11.04 Murphy *Similitude in Engineering* Ronald Press NY 1950

11.05 Buckingham "Dimensional Analysis" *Phil Mag* 48 1924

11.06 Rayleigh "The Principle of Similitude" *Nature* (London) 95 1915

11.07 Sedov "Similarity and Dimensional Methods in Mechanics" trans from Russian by Holt, Academic Press Inc NY 1959

EFFECTS OF CYLINDER SIZE

11.10 Coppens "The Characteristic Curves of Liquid Fuel Engines" *Jour IAE* London Dec 1932

11.11 Lutz "Ähnlichkeitsbetrachtungen bei Brennkraftmaschinen" *Ingenieur Archiv* Bd IV 1933 (Eng trans *NACA TM* 978 May 1941)

11.12 Taylor "Design Limitations of Aircraft Engines" *SAE preprint* June 1934 Pub in *Aero Digest* Jan 1935 Abstracted in *Auto Ind* June 23 1934

11.13 Riekert and Held "Leistung und Warmeabfuhr bei geometrisch ahnlichen Zylindern" *Jahrbuch deutscher Luftfahrtforschung* 1938 (Eng trans *NACA TM* 977 May 1941)

11.14 Everett and Keller "Mechanical Similitude Applied to Internal-Combustion Engines Tests" *PGCOA Report* ET 30 Jan 1939

11.15 Kamm "Ergebnisse von Versuchen mit geometrischahnlich gebauten Zylindern verschiedener Grosse und Folgerungen für die Flugmotorenentwicklung" *Schriften der deutschen Akademie der Luftfahrtforschung* Heft 12 March 1939

11.16 Schron *Die Dynamik der Verbrennungskraftmaschine* Springer Verlag Wien 1942

11.17 Jackson "Future Possibilities of Diesel Road Locomotives" *Mech Eng* May 1943

11.18 Riekert "Piston Area as the Basis of Similarity Consideration" The Engineers' Digest May 1944

11.19 Taylor and Taylor *The Internal-Combustion Engine* Int Textbook Co Scranton Pa 1948

11.20 Mikel and McSwiney "A Study of the Laws of Similitude Using a 2½" GS Engine" Thesis MIT library June 1949

11.21 Lobdell and Clark "A Study of Similitude Using the Four-Inch GS Engine" Thesis MIT library June 1949

11.22 Breed and Cowdery "A Study of Similitude Using the Six-Inch GS Engine" Thesis MIT library June 1949

11.23 Gaboury et al. "A Study of Friction and Detonation in Geometrically Similar Engines" Thesis MIT library June 1950

11.24 Taylor "Effect of Size on the Design and Performance of Internal-Combustion Engines" *Trans ASME* July 1950

11.26 Taylor "Correlation and Presentation of Diesel Engine Performance Data" *Trans SAE* April 1951

11.29 Jendrassik "Practice and Trend in Development of Diesel Engines with Particular Reference to Traction" *Proc Inst Locomotive Eng* (London) 1951

11.30 Taylor "Heat Transmission in Internal-Combustion Engines" *ASME paper* Sept 1951

11.31 Destival "L'Effet d'echelle dans les moteurs et les turbines" *Jour SIA* (Paris) Feb 1952

11.32 Smith et al. "A Study of the Effect of Engine Size on Heat Rejection" Thesis MIT library June 1952

11.33 Batter and Cansever "A Study of Heat Transfer in Geometrically Similar Engines" Thesis MIT library Jan 1954
11.34 Taylor "The Relation of Cylinder Size to the Design and Performance of Diesel-Engine Installations for Railway and Marine Service" *Proc CIMCI La Haye* 1955
11.35 Ohio State U "Study of Miniature Engine Generator Sets" *WADC TR* 53-180 1953–1956
11.36 Taylor "Size Effects in Friction and Wear" *Proc Conf on Friction and Wear* Southwest Research Inst San Antonio Texas May 1956
11.37 Taylor and Toong "Heat Transfer in Internal Combustion Engines" *Mech Eng* Oct 1957 p 961
11.38 Taylor "Dimensional Considerations in Friction and Wear" *Mech Wear* Ed by J T Burwell Jan 1950 p 1–7 Am Soc for Metals
11.39 Talbot and Gall "A Study of Octane Requirement as a Function of Cylinder Size" Theses MIT library June 1958
11.40 Lutz "Dynamic Similitude in Internal Combustion Engines" *NACA TM* 978 May 1941
11.41 Talbot "A Study of Octane Requirement as a Function of Size in Geometrically Similar Engines" MIT Thesis 1958
11.42 Gall "A Study of the Detonation Characteristics of Geometrically Similar Engines" MIT Thesis 1958
11.43 Taylor and Gall "The Effect of Cylinder Size on Octane Requirement" progress report to Shell Oil Co Sept 1957–1958 MIT library
11.44 Hamzeh and Nunes "Highest Useful Compression Ratio for Geometrically Similar Engines" Thesis MIT library 1959

MULTIENGINE INSTALLATIONS

11.50 Jackson "Future Possibilities of Diesel Road Locomotives" *Mech Eng* May 1943
11.51 Nordberg Mfg Co "A Multi-Engined Cargo Vessel" Bull 176 1950
11.52 Sulzer "The Propulsion Machinery of M S Willem Ruys" *Sulzer Tech Rev* 4 1951
11.53 Steiger "Direct and Geared Propulsion of Diesel-Engined Ships" *Sulzer Tech Rev* 1 1951

EXAMPLES OF SIMILAR ENGINES IN PRACTICE

11.6 Hulsing and Erwin "GM Diesel's Additional Engines, New Vees and In-Lines" *SAE preprint 1R* Jan 12 1959 (see especially Fig 32)

Chapter 12 The Performance of Unsupercharged Engines

ATMOSPHERE, EFFECT ON ENGINE PERFORMANCE

12.10 Dickinson et al. "Effect of Compression Ratio, Temperature, and Humidity on Power" *NACA TR* 45 1919
12.11 Gage "A Study of Airplane Engine Tests" *NACA TR* 46 1920

12.12 Sparrow and White "Performance of a Liberty-12 Airplane Engine" *NACA TR* 102 1920
12.13 Sparrow and White "Performance of a 300-Horsepower Hispano-Suiza Engine" *NACA TR* 103 1920
12.14 Gage "Some Factors of Airplane Engine Performance" *NACA TR* 108 1921
12.15 Sparrow "Performance of a Mayback 300-Horsepower Airplane Engine" *NACA TR* 134 1921
12.16 Sparrow "Performance of a B.M.W. 185-Horsepower Airplane Engine" *NACA TR* 135 1922
12.17 Stevens "Variation of Engine Power with Height" *Aero Res Comm* (London) R and M 960 1924
12.171 Garner and Jennings "The Variation of Engine Power with Height" *Aero Res Comm* (London) R and M 961 1924
12.172 Sparrow "Aviation Engine Performance" *Jour Franklin Inst* 200 Dec 1925 p 711
12.173 Maitland and Nutt "Flight Tests on the Variation of the Range of an Aircraft with Speed and Height" *Aero Res Comm* (London) R and M 1317 1929
12.174 Pierce "Altitude and the Aircraft Engine" *Trans SAE* 47 Oct 1940 p 421
12.175 Sarracino "New Method of Calculating the Power at Altitude of Aircraft Engines Equipped with Superchargers on the Basis of Tests Made under Sea-Level Conditions" *NACA TM* 981 July 1941
12.176 Ragazzi "The Power of Aircraft Engines at Altitude" *NACA TM* 895 May 1939
12.177 Droegmueller et al. "Relation of Intake Charge Cooling to Engine Performance" *Trans SAE* 52 Dec 1944 p 614
12.178 Gagg and Farrar "Altitude Performance of Aircraft Engines Equipped with Gear-Driven Superchargers" *Trans SAE* 29 June 1934 p 217
12.179 Maganiello et al. "Compound Engine Systems for Aircraft" *Trans SAE* 4 Jan 1950 p 79
12.180 Moore and Collins "Compression-Ignition Engine Performance at Altitude" *NACA TN* 619 Nov 1937
12.181 Johnson "Supercharged Diesel Performance vs. Intake and Exhaust Conditions" *Trans SAE* 61 1953 p 34
12.182 Barth Lyon and Wallis "Altitude Performance of Electro Motive 567 Engine" *SAE preprint* 533 Oil and Gas Power Conf Nov 2–3 1950
12.183 Guernsey "Altitude Effects on 2-stroke Cycle Automotive Diesel Engines" *Trans SAE* 5 Oct 1951 p 488
12.184 Taylor "Correcting Diesel Engine Performance to Standard Atmospheric Conditions" *Trans SAE* 32 July 1937 p 312
12.185 Gardiner "Atmospheric Humidity and Engine Performance" *Trans SAE* 24 Feb 1929 p 267
12.186 Jones *Report No 20 project XA-202* Wright Aero Corp Nov 1 1946
12.187 Brooks "Horsepower Correction for Atmospheric Humidity" *Trans SAE* 24 1929 p 273
12.188 Potter et al. "Weather or Knock" *Trans SAE* 62 1954 p 346
12.189 Welsh "The Effect of Humidity on Reciprocating Engine Performance" Wright Aero Corp Serial Rep 1232 Jan 19 1948

Power Losses, Accessories, etc.

12.2 Burke et al. "Where Does All the Power Go?" *Trans SAE* 65 1957 p 713 (See also Chap 9 refs)

Spark-Ignition Engine Performance. Fuel-Air Ratio Effects

12.30 Fawkes et al. "The Mixture Requirements of an Internal Combustion Engine at Various Speeds and Loads" Thesis MIT library 1941

12.31 Berry and Kegerris "The Carburetion of Gasoline" *Purdue U EES Bull* 5 1920

12.32 Berry and Kegerris "Car Carburetion Requirements" *Purdue U EES Bull* 17 1924

12.33 Sparrow "Relation of Fuel-Air Ratio to Engine Performance" *NACA TR* 189 1924

Detonation Limits

12.34 Texas Co "Passenger Car Trends Affecting Fuels and Lubricants" *Lubrication* (Texas Co Pub) 44 Feb 1958

12.35 Bartholomew et al. "Economic Value of Higher Octane Gasoline" Ethyl Corp Report TA-105 Mar 1958

12.36 Bigley et al. "Effects of Engine Variables on Octane Number Requirements of Passenger Cars" *Jour API* 1952

12.37 Roensch and Hughes "Evaluation of Motor Fuels for High-Compression Engines" *Trans SAE* 5 Jan 1951

12.38 Edgar et al. "Antiknock Requirements of Commercial Vehicles" *Trans SAE* 4 Jan 1950

12.39 Davis "Factors Affecting the Utilization of Antiknock Quality in Automobile Engines" *Trans IME* (London) Auto Div III 1951–1952

12.40 Eatwell et al. "The Significance of Laboratory Octane Numbers in Relation to Road Anti-knock Performance" *Trans IME* (London) Auto Div III 1951–1952

12.41 Barber "Knock-Limited Performance of Several Automobile Engines" *Trans SAE* 2 July 1948 p 401

12.42 Chandler and Enoch "Once More About Mechanical Octanes" *SAE preprint* 684 Jan 9–13 1956

12.43 Heron and Felt "Cylinder Performance, Compression Ratio and Mechanical Octane Number Effects" *Trans SAE* 4 Oct 1950 p 455

12.44 Roensch "Thermal Efficiency and Mechanical Losses of Automotive Engines" *SAE preprint* 316 March 8–10 1949

12.45 Caris et al. "Mechanical Octanes for Higher Efficiency" *Trans SAE* 64 1956 p 76

12.46 Campbell et al. "Increasing the Thermal Efficiencies of Internal-Combustion Engines" *Trans SAE* 3 April 1949

12.47 Bigley et al. "Effects of Engine Variables on Octane Number Requirements of Passenger Cars" *Proc API* Refining Section Vol 32 M part 3 1952 p 174

12.48 Bartholomew et al. "Economic Value of Higher-Octane Gasoline" *Ethyl Corp Report* TA-10T March 1958

12.49 Caris et al. "A New Look at High-Compression Engines" *Trans SAE* 67 1959 (Tests at compression ratios 9–25. Thermal, mechanical, and volumetric efficiencies vs r)

Diesel-Engine Performance

(See also refs 1.1 and 1.2)

12.50 Taylor and Huckle "Effect of Turbulence on the Performance of a Sleeve-Valve Compression-Ignition Engine" *Diesel Power* Sept 1933

12.51 Whitney "High Speed Compression-Ignition Performance—Three Types of Combustion Chamber" *Trans SAE* 37 Sept 1935 p 328

12.52 Foster "The Quiescent-Chamber Type Compression-Ignition Engine" *NACA TR* 568 1936

12.53 Moore and Collins "Pre-Chamber Compression—Ignition Engine Performance" *NACA TR* 577 1937

12.54 Ricardo "The High-Speed Compression-Ignition Engine" *Aircraft Eng* (London) May 1929

12.55 Ricardo "Diesel Engines" *Jour Royal Soc Arts* (London) Jan and Feb 1932

12.56 Pye "The Origin and Development of Heavy-Oil Aero Engines" *Jour Royal Aero Soc* (London) Vol 35 p 265 April 1931

12.57 Dicksee "Some Problems Connected with High-Speed Compression-Ignition Engine Development" *Proc Inst Auto Eng* (London) March 1932

12.58 Whitney and Foster "The Diesel as a High-Output Engine for Aircraft" *Trans SAE* 33 1938 p 161

12.59 Ricardo and Pitchford "Design Developments in European Automotive Diesel Engines" *Trans SAE* 32 1937

12.60 Dicksee *The High-Speed Compression-Ignition Engine* Blackie and Son (London) 1940

12.61 "Diesel-Engine Characteristics vs Year" *Diesel Progress* Los Angeles May 1946 p 216

12.62 McCulla "Ratings of Diesels Depend on—Smoke, Piston Temperature, Exhaust Temperature" *SAE preprint* 64A Oct 1958

Road Vehicle Economy—Effects of Gear Ratio

12.70 Caris and Richardson "Engine-Transmission Relationships for Higher Efficiency" *Trans SAE* 61 p 81

12.71 Mitchell "Drive Line for High-Speed Truck Engines" *Trans SAE* 62 1954 p 397

12.72 Shaefer "Transmission Developments for Trucks and Busses" *SAE preprint* 341 Aug 1954

Diesel vs Gasoline Engines in Service

12.73 Shoemaker and Gadebusch "Effect of Diesel Fuel Economy on High-Speed Transportation" *Trans SAE* 54 April 1946

12.74 Bryan "Diesel Power Economics Applied to Farm Tractor Operation" *Trans SAE* 1 Jan 1947
12.75 Willett "Gasoline vs Diesel Engines for Trucks" *SAE preprint* 275 Jan 10–14 1949
12.76 Hatch "Diesel vs Gasoline Engines for City Buses" *SAE preprint* 273 Jan 10–14 1949
12.77 Bachman "Diesel Engines in Trucks" *Trans SAE* 32 1937 p 173

Chapter 13 Supercharged Engines and Their Performance

(See also Chapter 10 and its refs and refs 1.01, 12.175, 12.177–8, 12.43)

Supercharging, Theory and Practice

13.00 Vincent *Supercharging the Internal-Combustion Engine* McGraw-Hill 1948 (elementary theory and extensive descriptive material as of date of publication)
13.01 *Brown-Boveri Review* "Problems of Turbocharger Design and Manufacture" No. 11 Nov 1950 p 420 (general article on design, manufacture and engine-performance effects of turbosuperchargers)
13.02 Ricardo "The Supercharging of Internal Combustion Engines" *Proc IME* 1950 162 p 421 (general comments on supercharging S.I. and C.I. engines)
13.03 *Motortechnische Zeitschrift* articles on Supercharging, Franckh'sche Verlagshandlung ABT Technik Feb 1952 (turbosupercharging of Diesel engines, in German. Also data on rotary compressors etc)
13.04 Buchi "Exhaust Turbosupercharging of Internal Combustion Engines" *Jour Franklin Inst Monograph* 1 July 1953 (authentic discussion by originator of the blowdown turbine)
13.05 Arvano "Performances of Supercharged Four-Cycle Diesel Engines" Report 2 Inst of Technology Nikon University Tokyo Nov 1954 (in English. Extensive test data and discussion)
13.06 Smith "A High Supercharge Two-Stroke Diesel Engine" *SAE preprint* 401 Oct 1954 (complete test data on GM 1-71 two-stroke engine with various compression ratios)
13.07 Birmann "New Developments in Turbosupercharging" *SAE preprint* 250 Jan 1954 (blowdown and steady-flow turbo applications)
13.08 *Proc Congrès International des Moteurs à Combustion Interne* The Hague 1955 (contains a number of useful articles on the supercharging of four-stroke locomotive engines and large two-stroke marine engines)
13.09 Louzecky "Design and Development of a Two-Cycle Turbocharged Diesel Engine" *ASME paper* No 56-A-100 Nov 1956 (blowdown type turbosupercharger applied to GM Marine Diesel. Performance included)
13.091 Reiners and Wollenweber "Turbosupercharging High-Output Diesel Engines" *SAE preprint* 673 Jan 1956 (application to a four-stroke engine. Comparison with Roots gear-driven installation)
13.092 Weider "Some Problems Incurred in Supercharging Gasoline Engines" *Trans SAE* 1 Oct 1947 p 680 (Roots vs centrifugal, octane no. limitations)
13.093 Taylor and Ku "Spark Control of Supercharged Aircraft Engines" *Jour IAS* 3 July 1936 p 326

13.10 Wood and Brimley "A Study of the Effect of Aftercooling on the Power and Weight of a 2000-Horsepower Air-Cooled Engine Installation" *NACA MR* L-705 Sept 1944

13.11 Sanders and Mendelson "Calculations of the Performance of a Compression-Ignition Engine-Compressor-Turbine Combination" *NACA ARR* E5K06 Dec 1945

13.12 Hannum and Zimmerman "Calculations of Economy of 18-Cylinder Radial Aircraft Engine with Exhaust-Gas Turbine Geared to the Crankshaft" *NACA ARR* E5K28 *TN* E-32 Dec 1945

13.13 Turner and Noyes "Performance of a Composite Engine" *NACA TN* 1447 Oct 1947

13.14 Desmon and Doyle "Effect of Exhaust Pressure on Performance of a 12-Cylinder Liquid-cooled Engine" *NACA TN* 1367 July 1947

13.15 Taylor "Effect of Engine Exhaust Pressure on Performance of Compressor-Engine-Turbine Units" *Trans SAE* 54 Feb 1946 p 64

13.16 Gerdan and Wetzler "The Allison V-1710 Exhaust Turbine Compounded Reciprocating Aircraft Engine" *Trans SAE* 2 April 1948 p 191

13.17 Boman and Kaufman "Effect of Reducing Valve Overlap on Engine and Compound-Power-Plant Performance" *NACA TN* 1612 June 1948

13.18 Manganiello et al. "Compound Engine Systems for Aircraft" *Trans SAE* 4 1950 p 79

13.19 Eian "Effect of Valve Overlap and Compression Ratio on Measured Performance with Exhaust Pressure of Aircraft Cylinder and on Computed Performance of Compound Power Plant" *NACA TN* 2025 Feb 1950

13.20 Morley *Performance of a Piston Type Aero Engine* Pitman 1951

13.21 Wiegand and Eichberg "Development of the Turbo-Compound Engine" *Trans SAE* 62 1954 p 265

13.22 Sammons and Chatterton "Napier Nomad Aircraft Diesel Engine" *Trans SAE* 63 1955 p 107

13.23 Hooker "A Gas-Generator Turbocompound Engine" *Trans SAE* 65 1957 p 293

13.24 Bulletin of Hanshin Diesel Works, 1983, Kobe, 650, Japan

13.25 Humble and Martin "The Four-stroke Spark-ignition Compound Engine" *IAS preprint* 145 March 19 1948

13.26 Hines and Reed "Turbocharging Development for Loop-Scavenged Two-Cycle Gas Engines" *Proc 29th Oil and Gas Power Conf ASME* May 1957 (cut and try methods of fitting turbosuperchargers to large spark-ignition two-cycle gas engines)

13.27 Haas "The Continental 750-HP Aircooled Diesel Engine" *Trans SAE* 65 1957 p 641

13.28 *Automotive Industries* Annual statistical issue (March 15 each year) Chilton Co Phila

13.29 "Diesel Engine Catalog" pub annually *Diesel Progress* Los Angeles 46 Calif

13.291 "A Highly-supercharged Opposed-piston Engine" *The Motor Ship* (London) July 1953 (Götaverken marine engine)

13.292 May and Reddy "Supercharging the Series 71 Engine" *Trans SAE* 66 1958 p 100

13.293 Nagao et al. "Basic Design of Turbosupercharged Two-Cycle Diesel" and "Evaluation of Capacity of Auxiliary Blower . . ." *Bull JSME* 2 1959 p 156 and p 163 (computations based on well-chosen assumptions)

Engines, Compound, Free-Piston

13.30 Eichelberg "The Free-Piston Gas Generator" Translated from Schweiz Bauzeitung 1948 Nos 48 and 49 Jean Frey AG Zurich 1948

13.31 Farmer "Free-Piston Compressor Engines" *Proc IME* (London) 156 1947 p 253

13.32 London "Free-Piston and Turbine Compound Engine Cycle Analysis" *ASME paper* No 53-A-212 Nov–Dec 1953 and *Trans ASME* Feb 1955

13.33 London "The Free-Piston and Turbine Compound Engine—Status of the Development" *Trans SAE* 62 1954 p 426

13.34 Payne and McMullen "Performance of Free-Piston Gas Generator" *Trans ASME* 76 1954 p 1

13.35 Soo and Morain "Some Design Aspects of Free-Piston Gas-Generator-Turbine Plant" Part I *ASME paper* 55-A-146 Part II *ASME paper* 55-A-155 1955

13.36 Scanlan and Jennings "Bibliography—Free-Piston Engines and Compressors" *Mech Eng* April 1957 p 339

13.37 Moiroux "A Few Aspects of the Free-Piston Gasifier" lecture presented at MIT June 1957 (copies on file in Sloan Laboratories)

13.38 Flynn "Observations on 25,000 Hours of Free-Piston Engine Operation" *Trans SAE* 65 1957 p 508

13.39 Underwood "The GMR 4-4 Hyprex Engine" *Trans SAE* 65 1957 p 377

13.391 "History and Description of the Free-Piston Engine" *Diesel Times* (pub Cleveland Diesel Div GM) March–April 1957

13.392 Barthalon and Horgen "French Experience with Free Piston Engines" *ASME paper* 56A209 Nov 1956 and *Mech Eng* May 1957 p 428 (summary of development and present status by largest producer of free-piston engines)

Reliability and Durability of Supercharged Engines

13.40 *Proc Congrès International des Moteurs a Combustion Interne* 1955 The Hague papers No C-1 C-2

13.41 Hill "Railroad Experience with a Turbosupercharged Two-Cycle Diesel Engine" *SAE preprint* 800 Aug 6–8 1956

13.42 Kettering "History and Development of the 567 Series General Motors Locomotive Engine" *ASME paper* Nov 29 1951 (technical problems in an unsupercharged engine, later supercharged)

13.43 McCulla "How a Diesel Engine Rates Itself" *SAE preprint* 64A June 1958 (discussion of limitations on supercharged output—peak pressures, temperatures, etc)

13.44 Gerecke "Entwicklung und Betriebsverhalten des Feuerringes als Dichtelement hochbeanspruchter Kolben" (Development and Tests of "Fire" Rings as Critical Element in High-Output Pistons) *MTZ* 6 June 1953 p 182 second installment 11 Nov 1953 p 333 (development work and tests on the Junkers Jumo 207 diesel aircraft engine)

13.441 May and Reddy "Turbosupercharging the Series 71 Engine" *Trans SAE* 66 1957 (shows exhaust valves to be critical, four valves ran cooler than two, see excerpt in *Auto Ind* July 1957 p 39)

13.45 McCulla "Rating of Diesel Engines Depends on Such Critical Parameters as Smoke, Piston Temperature, Exhaust Temperature" *SAE preprint* 64A, Oct 1958 abstract in *Jour SAE* Oct 1958
(See also refs 13.16, 13.21, 13.23)

COMPARISON OF POWER-PLANT TYPES

13.50 Caris "Are Piston Engines Here to Stay?" *SAE preprint* Oct 8 1956

13.51 Boegehold "The Cycle Race" *Aut Ind* July 15 1956

13.52 Shoemaker and Gadebusch "Effect of Diesel Fuel Economy on High-Speed Transportation" *Trans SAE* 54 April 1946 p 153

Appendix 2 Properties of a Perfect Gas

A-2.0 Ladenburg et al. "Physical Measurements in Gas Dynamics and Combustion" Princeton U Press 1954

A-2.1 Baker et al. *Temperature Measurement in Engineering* Wiley 1953

A-2.2 Moffatt "Multiple-Shielded High-Temperature Probes—Comparison of Experimental and Calculated Errors" *SAE preprint* T13 Jan 1952

A-2.3 Herschel and Buckingham "Investigation of Pitot Tubes" *NACA TN* 2 1915

Appendix 3 Flow of Fluids

A-3.0 Shapiro and Hawthorne "The Mechanics and Thermodynamics of Steady One-Dimensional Gas Flow" *Jour Appl Mech Trans ASME* 69 1947

A-3.1 Hunsaker and Rightmire *Engineering Applications of Fluid Mechanics* McGraw-Hill 1947

A-3.2 ASME "Fluid Meters: Their Theory and Application" 5th Ed *ASME* NY 1959

A-3.3 Folsom "Determination of ASME Nozzle Coefficients for Variable Nozzle External Dimensions" *Trans ASME* July 1950

A-3.4 Smith "Calculation of Flow of Air and Diatomic Gases" *Jour IAS* 13 June 1946

A-3.5 Peterson "Orifice Discharge Coefficients in the Viscous-Flow Range" *Trans ASME* Oct 1947

A-3.6 Grace and Lapple "Discharge Coefficients of Small-Diameter Orifices and Flow Nozzles" *Trans ASME* 73 July 1951

A-3.7 Cunningham "Orifice Meters With Supercritical Compressible Flow" *Trans ASME* 73 July 1951

A-3.8 Linden and Othmer "Air Flow Through Small Orifices in the Viscous Region" *Trans ASME* 71 Oct 1949

A-3.81 Gellales "Coefficients of Discharge of Fuel-Injection Nozzles for Compression-Ignition Engines" *NACA TR* 373 1931

A-3.82 Deschere "Basic Difficulties in Pulsating-Flow Metering" *Trans ASME* 74 Aug 1952

A-3.83 Hall "Orifice and Flow Coefficients in Pulsating Flow" *Trans ASME* 74 Aug 1952

A-3.84 Baird and Bechtold "The Dynamics of Pulsative Flow Through Sharp-Edged Restrictions" *Trans ASME* 74 Nov 1952

A-3.85 Oppenheim "Pulsating-Flow Measurements" (a literature survey) *ASME paper* 53-A-157 Dec 1953

Additional References, Chapters 3–5

14.1 Edson and Taylor "The Limits of Engine Performance" *SAE preprint* 633E, 1963 also, SAE Special Pub. Vol 7, 1964 (basis of Fig 4-5*a–dd*)

14.2 Edson "The Influence of Compression Ratio and Dissociation on . . . Thermal Efficiency" *Trans SAE* 70 1962 p 665 (fuel-air cycles up to compression ratio 300)

14.3 Newhall and Starkman "Thermodynamic Properties of Octane and Air for Engine Performance Calculations" *SAE preprint* 633G Jan 1963 also *SAE* Special Pub. Vol 7, 1964 (these charts cover wider range than charts C-1 through C-4 in the back cover)

14.4 Kerley and Thurston "The Indicated Performance of Otto Cycle Engines" *Trans SAE* 70 1962 p 5 (engine tests with compression ratios 7-14 and relative fuel-air ratios 0.52-1.5. Indicator diagrams included. Gasoline and methanol fuels)

14.5 Van der Werf "The Idealized Limited-Pressure Compression-Ignition Cycle," *ASME paper No* 63-OGP-5 March 1964

14.6 Vickland et al. "A Consideration of the High Temperature Thermodynamics of Internal Combustion Engines" *Trans SAE* 70 1962 p 785 (equilibrium compositions for octane at 0.8, 1.0, 1.2 equivalence ratios)

Air Pollution by Internal-Combustion Engines and Its Control

Springer and Patterson, *Engine Emissions; Pollutant Formation and Measurement*, New York, Plenum Press, 1973.

Vehicle Emissions, Part I, 1955–62, Part II, 1963–66, Part III in process, 1976. Each part is a collection of important papers by various authors published by Society of Automotive Engineers, Warrendale, Pa. 15096.

Tabaczynski, Heywood, and Keck. *Time Resolved Measurements of Hydrocarbon Mass Flowrate in the Exhaust of a Spark-Ignition Engine*, paper no. 720112, SAE, Warrendale, Pa. 15096, 1972.

Heywood and Keck, *Formation of Hydrocarbons and Oxides of Nitrogen in Automobile Engines*, Environmental Science and Technology, Vol. 7, 1973.

Heywood and Tabaczniski, Current Developments in Spark-Ignition Engines," SAE paper 760606, August 1976—Included in SAE Report No. SP-409, 1976.

See also publications listed on page 522, and Chapters 6 and 7 of Volume 2.

Index

Aftercooler, 392, 400, 467
  choice of, for supercharged engines, 471
  example of, 400
  use of, 466, 468
Air, compression of, dry, example, 62
    with water vapor, example, 62, 63
    with water vapor and fuel, 64
Air, flow of, *see* Fluids, flow of
Air, properties of, heat capacity, 43
    internal energy, 43
      see also Chart C-1 in pocket. on back cover
    specific heat, 43
    thermodynamic properties, 42–44
      see also Chart C-1
    see also Atmosphere
Air capacity, *see* Capacity, air
Air consumption, engine, 9, 10, 19, 20, 21
Air pollution, vi, vii, 465
  references for, 555, 556
Altitude, effect on engine performance, 433–436
    example of, 451, 452
    knock-limited compression ratio, as affected by, 460
    on brake mep, 436
    on power, 435, 436
    on power of aircraft engines, 460, 461.
    on specific fuel consumption, 435
Altitude, standard, table of, 434
  density vs, 434
  pressure vs, 434
  temperature vs, 435
  viscosity vs, 434
Analysis, dimensional, in compressor problems, 368, 369
    in friction problems, journal bearings, 316–318
      pumping friction, 342, 343
    in stress problems, 518, 519
    in turbine problems, 387, 388
    in volumetric efficiency problems, 167–171
Atmosphere, composition of, 41, 42
  moisture content of, 41

Atmosphere, effect on engine performance, 427–436
Diesel engines, 428, 429, 433
examples of, 452
humidity, 430–433
example of, 450, 451
pressure, 427–436
temperature, 427–430
example of, 450
see also Altitude, standard, table of; Humidity; Pressure, atmospheric; Temperature, atmospheric
Auxiliary friction, 355

Base, thermodynamic, definition of, 24
Bearing loads, 324, 325
Bearings, antifriction, 326, 327
journal, 317–322
coefficients of friction of, 318–322
deflection of, 317
effect of grooves and oil holes, 321
Petroff's equation, 318, 319
Sommerfeld variable, 318–321
stability of, 319, 320
oscillating, 322
sliding, 322, 323
coefficient of friction of, 323
illustration of, 323
theory of, 322, 323
Bore, cylinder, effect on brake mep, 404
effect on cost, 413
effect on efficiency, 408
effect on octane requirement, 402, 414
effect on piston speed, 404
effect on specific output, 405
effect on weight, 407, 414, 417
vs year for passenger-car engines, 423
see also Size, cylinder
Brake mean effective pressure, *see* Mean effective pressure, brake
Burning, *see* Combustion

Cam contour, 202
Capacity, of engines, 11
vs efficiency, 11, 12
Capacity, air, definitions for, 148, 149
effects of design on, 187–204
Capacity air, effects of design on, bore size, 178–180
compression ratio, 195–196
exhaust-valve capacity, 193
inlet-valve size and design, 171–177
stroke-bore ratio, 194–195
temperature effects, 188
valve timing, 188–193
illustrative examples of, 205–210
measurement of, 150
method of estimating, 204, 205
of four-stroke engines, 147–205
relation to power, 9, 10, 21, 147–148
see also Efficiency, volumetric
Charge, definition of, 149
Charts, thermodynamic, discussion of, 59–61
transfer between, 60, 62
use of, 49–61
see Charts C-1 through C-4 in pocket inside back cover
Coefficient, flow, for a passage, 18
for two orifices in series, 516–517
of commercial and experimental types, 232
of loop-scavenged cylinders, 230–232
of poppet-valve cylinder, 231, 232
of two-stroke engines, 228–234
definition of, 228
scavenging ratio, pressure ratio, and piston-speed effects, 229–233, 234
see also Fluids, flow of
Combustion, energy of, 54, 55
of residual gases, 55
heat of, 53, 54
determination of, 53, 54
progressive, 109–112
computation of cycle with, 110, 111
diagram of, 110
effect on temperatures and pressures, 111, 112
thermodynamic computations of, examples, 64–66
thermodynamics of, 52, 53
Compression, adiabatic, 363, 364
Y-factor, 364
Compression ratio, choice of, for supercharged engines, 470

Compression ratio, definition of, 27, 216
effect on bmep with various maximum cylinder pressures, 460
effect on performance, 443–445
of Diesel engines, 445
of spark-ignition engines, 443–445
effect on thermal efficiency, of actual cycles, 130, 134
of air cycles, 27–33
of engines, 134, 443–445
of fuel-air cycles, 82–89
effect on volumetric efficiency, 156, 157, 195
knock-limited, 444, 445
vs imep, 459
of Diesel engines, 445, 467
of two-stroke engines, 216, 445
typical, in practice, 461
vs year, 424
Compressor conditions, choice of, for supercharged engines, 473
Compressor-engine relations, 380, 381
compressor-to-engine mep, 381
Compressors, 362–381
axial, 365, 367, 378
centrifugal, 365, 367, 370, 378–380, 395
example of, 395
performance curves of, 379
performance of, 378–380
characteristics of, 368, 369–379
crankcase type, 375, 376
drives for, 392–394
electric, 393
exhaust-turbine, 393, 394
mechanical, 393
general equations for, 368, 369
ideal, 362, 363
Lysholm, 366, 378
oscillating, 366
performance curves, 369–372, 379
piston type, 366, 370, 373–376, 395
design of, 375, 376
efficiency of, 371, 375
example of, 395, 396
Mach index of, 374
performance curves of, 370, 371
valves for, 371–375
valve stresses in, 375
Compressors, piston type, volumetric efficiency of, 372, 373
Roots type, 366, 376–378, 395
example of, 395
ideal and actual, 377, 378
performance curves for, 372
performance of, 372, 376–378
pressure diagram for, 377
types of, 365–367
vane type, 366, 376
Conductivity, thermal, of air, 290
of water, 269
Consumption, air, *see* Air consumption; Capacity, air
Consumption, fuel, specific, brake, atmospheric effects on, 426, 438, 439
definition of, 10, 11
effects of fuel-air ratio, 438, 439, 474
equations for, 426, 521
for aircraft engines, 463–465
for automotive engines, 446
for Diesel engines, 448, 449
formulas for, 426
of supercharged engines, 463–465, 474–493
of unsupercharged engines, 425–449
indicated, definition of, 10, 11
equations for, 426, 521
vs compression ratio, 459
total, 418
Cooling, effect of high-conductivity materials, 282, 283
of cylinder-heads, pistons and valves, 281, 282
of large cylinders, 280, 281
see also Heat losses; Heat transfer
Cycles, actual, effect of operating variables on, 107–142
in Diesel engines, 135–143
in spark-ignition engines, 127–133
illustrative examples of, 143–146
Cycles, air, 23–39
comparison with fuel-air cycles, 70, 73, 93–96
comparison with real cycles, 35, 36
constant pressure, 30

Cycles, air, constant volume, 24–29
comparison with fuel-air cycle, 70, 95
characteristics of, 28, 29
diagrams of, 25
example of, 37, 38
definitions of, 23, 24
equivalent, 24
gas-turbine, 33, 34
p-V diagram for, 34
Lenoir, 38, 39
limited-pressure, 30–34
compared with fuel-air cycle, 73
characteristics of, 32, 33
diagram of, 31
mixed, 30
Cycles, fuel-air, 67–106
assumptions for, 68, 69
comparison with air cycles, 70, 73, 93–96
comparison with real cycles, 134, 142, 143
characteristics of, 82–89
constant volume, 69–72
characteristics of, 71, 82–87
construction of, 69–71
diagram of, 70
examples of, 97–100
definitions of, 67, 68
equivalent, 89–93
determination of mass, 91
determination of residuals, 91, 93
determination of volume, 90
method of construction, 88–92
exhaust-gas characteristics of, 97
gas-turbine, 74–76
construction of, 74–76
diagram of, 75
examples of, 103–106
illustrative examples of, 97–105
limited pressure, characteristics of, 88, 89
construction of, 72–74
diagram of, 73
example of, 101, 102
with ideal inlet and exhaust process, characteristics of, 82–89
discussion of, 76–81
Cycles, fuel-air, volumetric efficiency of, 78, 79, 86, 87
more-complete-expansion, 488
Cyclic process, definition of, 23
Cylinders, stroke-bore ratio, 194, 195, 236, 237
two-stroke, choice of type, 247–252
design of, 236–252
exhaust-port to inlet-port area, 239–240
port-area to piston area, 237–238
port height, 239
stroke-bore ratio, 236–237
loop-scavenged type, 212–214, 225–227, 230–232, 238–251
limitations of, 241
with automatic inlet valves, 242
with mechanical exhaust valve, 212, 244
maximum port areas vs cylinder type, 248
opposed-piston type, 212, 227, 232, 238, 246, 251
poppet-valve type, 212, 214, 226, 227, 231, 232, 238, 243, 245, 246, 249, 251, 252
porting of, commercial, 238, 246
reverse-loop-scavenged type, 212, 251
type, effect on scavenging efficiency, 249–250
type-designation, 212
very small, 409
see also Bore, cylinder; Engine, two-stroke; Size, cylinder

Definitions, general, 7, 8
of engine types, 8
relating to engine performance, 8, 9
Density, inlet, 149–152, 217
effect of atmospheric conditions on, 427
formulas for, 520
Detonation, in supercharged engines, 459–462. *see also* Vol. 2, Chap. 2

Detonation limits, 459
Development of engines, vs time, 422, 423, 424, 449
423, 424
example of, 449
Durability, engine, 418

Efficiency, brake thermal, definition of, 9
(References to this quantity occur frequently, especially in Chapters 9–13)
compressor, 469
engine, *see* Efficiency, thermal
indicated, definition of, 9
(References to this quantity appear frequently, especially in Chapters 1–5)
mechanical, 9, 313, 314
scavenging, 218–227, 245, 249
definition of, 218
design effects on, 225–227, 236–254
effect of cylinder type, 249, 250
effect of exhaust-port to inlet-port ratio, 225, 226
effects of operating conditions, 225–227
piston speed, 225, 226
scavenging ratio, 225–227
measurement of, 221–224
by model tests, 224
gas-sampling method, 222, 223
indicated mep method, 221, 222
tracer-gas method, 224
of commercial engines, 227
scavenging ratio, relation to, 219, 225–227, 245
test results, 225–230
with ideal scavenging process, 219
with perfect mixing, 219, 220
Efficiency, thermal, basic definition of, 9
of air cycles, 28, 29, 33
of engines, as affected by cylinder bore, 408, 409
as affected by heat loss, 303
brake, 9
definition of, 8, 9
indicated, 9
of Diesel engines, 142, 143
Efficiency, thermal, of fuel-air cycles, 71–89
constant volume, 71, 82–87
gas turbine, 75
limited pressure, 73, 88, 89
see also Efficiency, brake thermal; Efficiency, indicated
Efficiency trapping, definition of, 190, 218
in four-stroke engines, 190
effect of valve overlap, 191
in two-stroke engines, 218, 219
definition of, 218
with perfect mixing, 219
of supercharged engines, 470
Efficiency, turbine, 383–389, 469
blowdown type, 388, 389
steady-flow type, 385
Efficiency volumetric, 149–210
based on dry air, 150, 153
definition of, 149
design effects, 156–200
compression ratio, 195
exhaust-valve capacity, 193, 194
inlet-pipe size, 200
inlet pressure and compression ratio, no overlap, 156
inlet-valve closing, 191, 192
stroke-bore ratio, 194, 195
valve overlap, 188–191
effect of operating conditions on, 181–191
coolant temperature, 187
fuel-air ratio, 181–183
fuel evaporation, 183, 184
fuel injection, 185
inlet temperature, 181, 182, 186
latent heat of fuel, 185
pressure ratio, inlet to exhaust, 181, 189, 191
evaluation of, for supercharged engines, 469
from the indicator diagram, 158–164
pressure effects, 166
work effect, 167
general equation for, 170
heat-transfer effects, 163–166
influence on design, 187–203
Mach-index effects, 171–175
measurement of, 150–154

Efficiency, volumetric, of commercial engines, 203, 204
of fuel-air cycles with ideal inlet and exhaust process, 78, 79, 86, 87, 158
of MIT similar engines, 179
operating conditions, effect of, 171–187
over-all, 150
plot showing various effects, from indicator diagrams, 163
relation to mean effective pressure, 154
residual-gas temperature effect, 157
Reynolds index effects, 177–179
size effects, 179–181
surface-temperature effects, 165, 166

Emissions, exhaust, *see* Air pollution

Energy, general equation of, 12, 13
application of, 18, 19
internal, 12, 13
of air, 43, chart C-1
of combustion, 54, 55
of fuel, 45–47
of fuel-air mixtures, 48, 52, 53, 55 Charts C-1 through C-4
of perfect gas, 24

Engine, turbo-compound, example of, 484, 485
performance of, 464, 465

Engines, automotive, compression ratio of, 424
definition of, 419
development of, vs time, 423
effect of number of cylinders on, example, 414, 415
Diesel, compression ratio of, 467
definition of, 8
efficiency of, 142, 143
highly supercharged, 478–484
graph showing performance data, 480
large, 410, 411
performance of, supercharged, 463–493
unsupercharged, 425–429, 433–441, 448, 449, 452

Engines, Diesel, ratings of, supercharged, 469
supercharging of, 463–493
free-piston, 481–483
performance, example of, 491–493
heat, 2
classification of, 2
hot air, 2
industrial, 419
internal-combustion, advantages of, 1, 2, 3
basic types of, 8
classification of, 1, 2
jet, 2
marine, 2, 419
model airplane, 410, 411
more-complete-expansion, 488
multiple, 412–417
examples of, 415–417
similar, definition of, 175, 176
detonation limits of, 402
MIT similar engines, 178
single-cylinder, equipped with surge tanks, 17
small, 409, 411
stationary, 2, 419
steam, 2
supercharged, 456–493
arrangements of, 457
definitions for, 456–458
examples of, 478, 479, 485–493
oversupercharged engine, example of, 488, 489
performance of, 456–493
equations for, 520, 521
two-stroke, 211–260
cylinder types, 212, 263, 264
definitions for, 211–213
effect of inlet and exhaust-system design on, 252–254
flow coefficient of, 261, 262
illustrative examples for, 260, 265
indicator diagrams for, 140, 213, 214, 244
optimum scavenging ratio, supercharged, 490, 491
unsupercharged, 454, 455
supercharging of, 259, 260
see also Cylinders, two-stroke; Efficiency, scavenging

Engine types, definition of, carbureted, 8
carburetor, 8
compression ignition, 8
Diesel, 8
external combustion, 1
injection, 8
internal combustion, 1
spark-ignition, 8
Enthalpy, of air, 43, Chart C-1
definition of, 15
of combustion, 53, 54
of fuel, 45–47
of fuel-air mixtures, 49, 52, 53, Charts C-1 through C-4
of a perfect gas, 24
stagnation, 15
Entropy, of fuel-air mixtures, 51, Charts C-1 through C-4
vs internal energy for air cycle, 25
Equilibrium, chemical, constant of, 56
discussion of, 56–59
example of, 56, 57
Evaporation, fuel, effect on volumetric efficiency, 183
enthalpy of, 45, 46, 63
Examples, illustrative, 19–21, 37–39, 62–66, 97–106, 143–146, 205–210, 260–265, 308–311, 356–361, 394–400, 414–417, 449–455, 484–493
Exchanger, heat, 271, 272, 311, 392
diagram of, 271
equations for, 272
example of, 311
see also Aftercooler; Radiator, coolant
Exhaust gas, composition of, 223
energy of, 381, 382
sampling valve for, 222
specific heat of, 383, 394, 472
temperature of, 105, 106, 384
Exhaust pipe, *see* Exhaust systems
Exhaust pressure, effect on mean gas temperature, 286
to inlet pressure, ratio of, effect on compressor mep, 235
effect on engine performance, 384, 483, 484
effect on fuel-air cycles with ideal induction process, 86, 87
Exhaust pressure, to inlet pressure, ratio of, effect on pumping mep, 342–344, 352, 354
effect on scavenging ratio in two-stroke engines, 229–234
effect on volumetric efficiency, 156–164, 170, 181
Exhaust process, energy of, 381–383
ideal, four-stroke, 76–80
fuel-air cycles with, 81–89
pumping loss of, 340–343
two-stroke, 80, 81
see also Exhaust gases; Exhaust pressure
Exhaust smoke, 419
Exhaust stroke, *see* Exhaust process
Exhaust systems, design of, for four-stroke engines, 201, 202
for two-stroke engines, 252–254
effect of pipe length on volumetric efficiency, 201, 202
Exhaust temperature, 383, 384
of fuel-air cycle, 105, 106
vs fuel-air ratio, 384
Exhaust turbines, *see* Turbine, exhaust

Finning for air-cooled cylinders, 306
Flow coefficient, for orifices and passages, *see* Fluids, flow of
for two-stroke engines, 228–234, 470
example of, 262
Flowmeters, 508
Flow of gases and liquids, *see* Fluids, flow of
Fluid, working, thermodynamics of, 40–66
approximate, treatment of, 61, 62
see also Fuel-air mixture
Fluids, flow of, 503, 509
coefficient of, 507, 508
compressible, functions for, 505, 506
critical, 504, 505
ideal, 503, 504
in passage of varying area, 503, 504
measurement of, 508, 509
of actual fluids, 507, 508
of ideal liquids, 507
through engines, *see* Capacity, air; Engines, two-stroke; Scavenging ratio; Volumetric efficiency

Fluids, flow of, through fixed passages, 17, 18
through two orifices in series, 233, 234, 516, 517
Free-piston engines, *see* Engines, free-piston
Friction, auxiliary, 355
dry, 314
engine, 312–361
estimates of, 353–355
correction for motoring test, 353, 354
examples of, 356–361
motoring tests for, 347–353
accuracy of, 348–350
comparison with indicated results, 349
effect of compression ratio, 352
effect of time, 348
results on commercial engines, 350, 351
throttling effect, 352, 353, 361
of four-stroke engines, vs piston speed, 350
of two-stroke engines, vs piston speed, 351
fluid, 314–317
theory of, 316
journal bearing and sliders, 317–323
mean effective pressure, 313, 327
definition of, 313
auxiliary, 313
compressor, 313
mechanical, 313, 327
pumping, 79, 313, 343
turbine, 313, 391, 521
of exhaust stroke, 341
of four-stroke engines, 350, 360
of inlet stroke, 342, 343
of two-stroke engines, 351, 361
mechanical, 313–338
distribution of, 330, 331
effect of design on, 335–337
cylinder size, 338
stroke-bore ratio, 337, 338, 359
effect of operating variables on, 331–333, 359
cylinder pressure, 331, 332, 359
Friction, mechanical, effect of operating variables on, oil viscosity, jacket temperature, and speed, 336
measurement of, 328
of four-stroke and two-stroke engines, 329
of pistons and rings, 332–336
special test engine for, 334
vs crank angle, 335
viscosity effects on, 332, 333, 336
of two-stroke engines, 329, 351
partial film, definition of, 314
discussion of, 317
pumping, 339–352, 361
effect of design on, 344–347
exhaust system, 347
exhaust-valve opening, 346
inlet-pipe length, 345
throttling, 345, 352, 361
effect of operating conditions on, fuel-air ratio, 347
inlet and exhaust pressure, 339–344
effect of size on, 344
indicator diagrams of, 339, 344, 345, 348
of ideal cycles, 339
of real cycles, 339–345, 348
rolling, 314, 317
Fuel, effect on volumetric efficiency, 185
mass flow of, 9
properties of, 44, 47
composition, 46, 47
enthalpy, 45
heat of combustion, 9, 46, 47
internal energy, 45
measurement of, 53, 54
sensible properties, 44
specific gravity, 46, 47
table of, 46, 47
see also Fuel-air medium; Consumption, fuel
Fuel-air cycles, *see* Cycles, fuel-air
Fuel-air mixture, composition of, 40, 41, 46, 47, 58
examples for, 62–66
properties of, 46–61, 183 and Charts C-1 through C-4
discussion of, 48–52

Fuel-air ratio, chemically correct, 46, 47
combustion, 217–224
definition of, 217
effect on Diesel-engine performance, 474
relation to performance, 218, 474
use in measuring scavenging efficiency, 222–224
vs exhaust-gas composition, 223
definition of, 9
effect on detonation, 439, 440
effect on engine performance, 437–439
detonation, 439, 440, 460
Diesel engines, 439, 474
economy, 438, 439
example of, 452
indicated mep, 437
spark-ignition engines, 436, 460
supercharged engines, 460, 474
effect on exhaust-gas composition, 223
effect on fuel-air cycles, 82, 84, 86, 89
effect on fuel economy, 438, 439
effect on mean gas temperature, 285
effect on molecular weight, 50
effect on properties of octane-air mixtures, 183
for best economy, 438, 439
for best power, 438
measurement of, by exhaust analysis, 223, 224
in inlet manifold, 153
relative, 51
trapped, 216, 218, 224
see also Fuel-air ratio, combustion
values of product $F\eta$, 437
values used in practice, 440
Fuel consumption, *see* Consumption, fuel
Fuel economy, *see* Consumption, fuel, specific; Efficiency, thermal

Gas, *see* Fluids, flow of; Fuel-air mixture
Gas, flow of, *see* Fluids, flow of
Gas, perfect, definition of, 23
law of, 7, 23
properties of, 500–502
residual, characteristics of, 50
definition of, 149
effect on volumetric efficiency, 157, 158
Gas residual, fraction of, actual and computed, 512
effect on fuel-air cycle, 100, 101
in constant-volume cycles, 82, 83
in limited-pressure cycles, 88, 89
measurement of, 125
real vs ideal values, 125
in fuel-air mixtures, 48–61
internal energy of, 55
molecular weight of, 50
properties of, *see* Chart C-1 for $f = 1.0$
molecular weight of, 50
Gas constant, universal, 7, 23
dimensions of, 7
value of, 7, 23
Gas temperature, *see* Temperature, gas

Heat, definition of, 6, 7
flowing into system, 9
of combustion, 9
measurement of, 53, 54
of fuels, table, 46, 47
relation to work, 6, 7
specific, of air, 23, 394, 472
of exhaust gas, 383, 394, 472
of fuel-air media, 47, 58
of fuels, 46
of gases, 58
to water jackets, *see* Heat losses
see also Heat flow; Heat losses; Heat transfer
Heat addition, choice of value for air cycle, 29
Heat conductivity, effect of path length, 287
of air, 290
of water, 269
related to heat transfer, 269, 514, 515
Heat exchanger, *see* Exchanger, heat
Heat flow, effect of fuel-air ratio on, in supercharged Diesel engine, 474
in Diesel engines, example of, 310, 311
local, example, 308
measurement of, 287
parameters for, 275, 277, 278
effect of changes in, 283

Heat flow, effect of fuel-air ratio on, quantitative use of heat-flowequations, 283–287
to water jackets, 288–302
examples of, 309–311
see also Heat losses; Heat transfer
Heat losses, 266–312
control of, 303
distribution of, in cylinder, 302
effect of cylinder design, 303
effect of cylinder size, 279, 280
effect of operating variables on, 291–302
brake mep, 301
coolant temperature, 299
detonation, 296, 297
engine deposits, 300
exhaust pressure, 293, 294
fuel-air ratio, 294, 295
inlet pressure, 292, 293
inlet temperature, 298, 299
piston speed, 292, 293, 301
spark advance, 295, 296
effect on efficiency, 303
general consideration of, 266
illustrative examples of, 308–311
indicated vs jacket, 126
in Diesel engines, 141, 292
in gas turbines, 307
map of, 301
per unit area, 277
per unit piston area, 290
ratio to heat of combustion, 291
ratio to power, 291
relation to efficiency, 303
sources of, 267
Heat of friction, 274
Heat transfer, 267–299
by conduction, 267
by convection, 268–271
between tube and fluid, 514, 515
equation for forced convection, 269
forced convection, 268–271
by radiation, 267, 268
in engines, 273, 274
coefficient of, 269
in engines, 289, 299
over-all, 287–290
effect of geometry, 274
Heat transfer, effect on volumetric efficiency, 163–166
in engines, 273–280
basic equations for, 274
implications of equations, 277–283
validity of equations, 276, 277
in MIT similar engines, 276
in tubes, 268–270
model for heated tube, 165, 514, 515
processes of, 267–271
see also Heat flow; Heat losses
Horsepower, United States and British standard, 10
see also Power
Humidity, allowance for in thermodynamic charts, 51
example of, 64
effect on performance, 430–434
effect on detonation, 432, 433
effect on Diesel engines, 433
effect on efficiency, 431
effect on thermodynamic properties of air, 42

Indicated efficiency, *see* Efficiency, indicated
Indicated mep, *see* Mean effective pressure, indicated
Indicated power, *see* Power, indicated
Indicator diagram, effect of operating conditions on, 128–133
compression ratio, 130
exhaust pressure, 132
fuel-air ratio, 133
inlet pressure, 131
spark advance, 128
speed, 129
light-spring, 159, 161, 162, 339, 344, 345, 348
analysis of, 510–513
effect on volumetric efficiency, 158–164
for similar engines, 180
of piston friction, 335
of Roots compressor, 377
pressure-crank-angle, 117
pressure-volume, 90, 108, 118, 123, 124, 128–133, 139, 140
analysis of, 108

Indicator diagram, pressure-volume, for air cycles, 25, 28, 31, 34
for Diesel engines, 139, 140
for fuel-air cycles, 123, 124, 139, 140
for gas turbines, 34, 75
for spark-ignition engines, 123, 124, 128–133
for two-stroke engines, 118, 213, 214
Indicators, engine, electric types, 119
MIT balanced-pressure type, 114–119
diagram of, 116
diagrams by, 117, 118
Induction process, actual, diagrams of, 159, 161, 162, 339
equations for, 159–161, 510–513
temperature at end of, 512, 513
volumetric efficiency of, 157, 163–210
ideal, 76–80, 155–158, 512
characteristics of fuel-air cycles with, 81–89
description of, 76, 77, 149, 155
diagrams for, 77, 155
equations for, 77–79, 157, 512
work of, 79, 80, 159
two-stroke, 80, 81
Injection, fuel, effect on volumetric efficiency, 185
water-alcohol, 440
Inlet pipe, effects of length and diameter on volumetric efficiency, 196–200
see also Inlet system
Inlet pressure, *see* Pressure ratio; Exhaust to inlet
Inlet process, *see* Induction process
Inlet system, design of, 196–200, 252, 253
for four-stroke engines, 196–200
for two-stroke engines, 252, 253
effect on inlet density, 201
effect on volumetric efficiency, 196–201
losses in, 201
multicylinder, 201
pressure loss in, 201
temperature rise in, 201
Intercooler, 470
see After cooler

Joules law coefficient, 9

Leakage in the actual cycle, 109
Load, definition of, 419
Loop scavenging, *see* Scavenging, loop
Losses, actual vs fuel-air cycle, analysis of, 122–127
discussion of, 112–114
exhaust loss, 114
heat loss, 112, 113, 126, 303
see also Heat losses
in Diesel engines, 135–142
time loss, 112, 113, 136, 137

Mach index, applied to inlet valve, 171–176
of commercial engines, 176
of flow passages, 507
of turbines and compressors, 368–372, 379
Maintenance, engine, 418
Mean effective pressure, auxiliary, 313
formulas for, 426, 520, 521
knock-limited, 444, 438, 439
maximum, 420
of unsupercharged engines, 420–436
rated, in practice, 404
vs compression ratio, 444
vs compression ratio and maximum cylinder pressure, 460
vs fuel-air ratio, 438, 439
vs piston speed, for aircraft engines, 463–465
for automotive engines, 446
for Diesel engines, 448
for various engines, 421
vs year, 422–424
compressor, 313, 381
formula for, 521
of reciprocating compressor, 375
of scavenging pumps, 235
definition of, 27
friction, *see* Friction, mean effective pressure
indicated, discussion of, 426–429
formulas for, 426, 428, 437, 520
knock-limited, vs bore, 402
vs compression ratio, 459, 460, 462
vs maximum cylinder pressure, 131

Mean effective pressure, indicated, of Diesel engines, at constant fuel-pump setting, 428, 429
vs compressor pressure ratio, 477
vs piston speed, 448, 449
of spark-ignition aircraft engines, 422
net, 79, 80
turbine, 313, 391, 521
formulas for, 391, 521
Mean effective pressure of air cycles, 25–28, 31, 34
examples of, 37–39
Mean effective pressure of fuel-air cycles, 69, 70, 82–89
examples of, 97–104
Mean effective pressure of mechanical friction, 313, 327
Mean effective pressure of pumping, 79, 313
Medium, fuel air, *see* Fuel-air mixture
Mixing, fuel and air, 52
example of, 63, 64
incomplete, 109
Mixture, fresh, definition of, 149
Mixture, fuel-air, *see* Fuel-air mixture
Models, use of for scavenging-efficiency measurement, 224
Molecular weight, change with combustion, 57, 58
of fuel-air mixtures, 46, 47, 50
formulas for, 49
of fuels, 46, 47
Motoring test, for friction, 347–353
see also Friction, engine

Newton's law, statement of, 6
constant of, 6
Nusselt number, of engines, 276, 288, 289
definition of, 270
plotted vs Reynolds number for air and water in tubes, 270
for engines, 276, 289

Octane number, 402, 424, 459
of automotive gasoline vs year, 424
Octane requirement, as affected by cylinder bore, 402
Octane requirement, vs compression ratio and fuel-air ratio, 459
Octene, properties of with air, *see* charts C-1 through C-4 in pocket on back cover
sensible enthalpy of, 45
Output, estimate based on energy balance, 20
see also Power
Output, specific, definition of, 420
of aircraft engine, 463
of Diesel engines, 405, 448
highly-supercharged, 479
vs compressor pressure ratio, 477, 483
of passenger-car engine, 446
of various engines, 421, 447
rated, in practice, 405, 421
Overlap, valve, *see* Valve timing

Performance, engine, basic equations for, 520, 521
basic measure of, 419, 420
characteristic curves of, 445–449
for aircraft engines, 463–465
for automotive engine, 446
for Diesel engines, 448, 449
use of, examples, 453, 454
definitions for, 419
Performance of supercharged engines, 456–493
definitions for, 456–458
Diesel engines, 466–484, 486–493
computations for, 468–474
evaluation of variables for, 469–473
examples of, 474, 478, 483–493
free-piston type, 480–484
table of assumptions for, 476
vs compressor pressure ratio, 477, 483
vs fuel-air ratio, 474
with steady-flow supercharger, example, 486, 487
equations for, 520, 521
spark-ignition engines, 462–466
aircraft, 462–466
automotive, 459–462

Performance of two-stroke engines, vs compressor-pressure ratio, 477, 483
vs flow coefficient, 258
vs fuel-air ratio, 474
vs scavenging ratio, 258
Performance of unsupercharged engines, 418–455
Diesel engines at constant fuel-pump setting, 428, 429
vs atmospheric conditions, 427–433
altitude, 433–436
humidity, 430–433
pressure, 427–430
temperature, 427–430
vs compression ratio, 443–445
vs fuel-air ratio, 437–441
vs spark timing, 441–443
vs time, 423, 425
Petroff's equation, 318, 319, 357
Pipe, exhaust, *see* Exhaust systems
Pipe, inlet, *see* Inlet pipe, Inlet system
Piston, free, *see* Engines, free piston
Piston and ring friction, 332–336
measurements of, 333–335
special test engine for, 334
see also Friction
Piston area, relation to power, 402, 405, 420, 421, 446–448, 477, 478, 483
see also Output, specific
Piston speed, references to this highly important parameter occur throughout this book. The more important ones are noted below.
choice of, 472, 473
definition of, 419
of two engines of extremely different size, 411
rated, in practice, 404, 467
relation to brake mean effective-pressure, 421, 446–449, 463, 479
relation to detonation, 402
relation to friction, 327–332, 336–341, 350–361
relation to indicated mean effective pressure, 448, 449
relation to power, 421, 446, 447, 463, 479
relation to power to scavenge, 235–236
Piston speed, relation to scavenging ratio and scavenging efficiency, 225–228, 240, 245, 249
relation to stresses, 518, 519
relation to two-stroke engine flow coefficient, 228–233
relation to volumetric efficiency, 150–154, 171–179, 189–204
vs bore, 404
vs year, 423, 424
Port area, reduced, 244, 246
Ports, cylinder, *see* Cylinders, two-stroke, design of; Port timing
Port timing, of commercial engines, 238, 243, 246
symmetrical vs unsymmetrical, 243, 245, 249
Power, accessory, 312
compressor, 312
engine, absolute maximum, 419
brake, definition of, 9
cost of, 413
indicated, 9
installed in the United States, 4
maximum rated, 419, 420
normal rated, 419
rated, 419
relation of, to air capacity, fuel-air ratio, heat of combustion and efficiency, 9–11
vs bore, 405
vs compressor pressure ratio, 477, 483
vs efficiency, 9–12
vs piston area, 406, 411
vs piston displacement, 406, 411
vs piston speed, 421, 446, 447, 463, 479
pumping, 312
rated, *see* Power, engine, rated
turbine, 312
Power plant, classification of, 2
free-piston, 480–484
types of, 1–5
Power production in the United States, 5
Power to cool, 305
Power to scavenge two-stroke engines, 235–236

Prandtl number, 270,
of air, 290
of gases, 269
of water, 269
related to volumetric efficiency, 169
Pressure, measurement of, 114–119
indicators for, 114–119
see also Indicators, engine
atmospheric, effect on performance, 427–436
three cases of, 430
barometric, effect on engine performance, 427, 428, 430
effect on inlet density, 427
exhaust, *see* Exhaust pressure, pressure ratio, exhaust to inlet
inlet, *see* Pressure ratio; exhaust to inlet
mean effective, *see* Mean effective pressure
stagnation, 501
Pressure ratio, compressor, choice of, 473
effect on engine performance, 477–483
exhaust-to-inlet
effect on performance of C-E-T combinations, 483
effect on volumetric efficiency, 161–164, 181, 189, 191
relation to scavenging ratio, 228–235
gas turbine, 33–35, 74–77, 102
Pressure-volume diagrams, *see* Indicator diagrams
Process, cyclic, 9, 12
exhaust, *see* Exhaust process
induction, *see* Induction process
inlet, *see* Induction process
steady-flow, 14, 15
thermodynamic, 12–15
example of, 37, 38
Pump, scavenging, centrifugal type, 255, 257
crankcase type, 255, 256
displacement type, 254–256
piston type, 255
Roots type, 255
types of, 255
Pumping friction, *see* Friction, pumping
Pumping mean effective pressure, *see* Friction, pumping; Friction, mean effective pressure
Pumping work with ideal inlet process, 79

Quantity of heat, 6, 7
see also Heat

Radiator, coolant, design of, 304–305
equations for, 304–306
Rating, of engines, 419–425
commercial ratings, 420–425
definitions, 419
example of, 449, 450
plots of, 405, 421
ratio to piston area, 406
Ratio, compression, *see* Compression ratio
Ratio, fuel-air, *see* Fuel-air ratio
Ratio, pressure, *see* Pressure ratio
Ratio, scavenging, *see* Scavenging ratio
Reliability, engine, 418
Residual gases, *see* Gas, residual
Reynolds number, in fluid flow, 168, 509
in heat transfer, 165, 269–293, 515, 516
coolant side, 275
gas side, 275, 276, 280, 288, 289, 293
local, 275
definition of, 177
relation to volumetric efficiency, 168, 177
Rpm, *see* Speed, engine

Scavenging, definitions for, 216
description of, 213–215
efficiency, *see* Efficiency, scavenging
ideal process, 215, 216
with perfect mixing, 219, 220
light-spring diagrams of, 213, 244
loop, comparison with other methods, 227, 249, 250
definition of, 211, 212
porting for, 225, 240, 241–244
exhaust-to-inlet port ratio, 225, 241
power required for, 235, 236
symbols for, 216, 217

Scavenging pumps, *see* Pumps, scavenging
Scavenging ratio, choice of, 257, 469
definition of, 217
effect of operating conditions on, 234, 235
formulas for, 217, 218
measurement of, 220, 221
optimum, 258, 259
examples of, 454, 455, 490, 491
relation to scavenging efficiency, 219–228, 245
with long exhaust pipes, 254
Short circuiting, in two-stroke engines, 220
Similar engines, 175–179
definition of, 175
MIT similar engines, 179
Similitude, definition of, 175, 176
in commercial engines, 403
effect on scavenging ratio, 228, 229
effect on volumetric efficiency, 170–175
see also Size, cylinder; Size, engine
Size, cylinder, discussion of, 401–413
effect on costs, 413
effect on design for heat flow, 281, 282
effect on efficiency, 408
examples of, 414, 415
effect on stresses, 518, 519
effect on surface temperatures, 279, 280
effect on volumetric efficiency, 179–181
effect on wear, 355, 356
effects of, in practice, 403–409
examples of, 410, 411, 414–417
implications of size effects, 412
influence on engine performance, 401–417
in two-stroke cylinders, 247
examples of, 401–407
knock-limited imep vs bore, 402
limits on, due to heat flow, 279–283
example of, 308, 309
octane requirement vs bore, 402
example of, 414, 415
Size, engine, comparison of very large and very small engines, 410, 411
effect on stresses, 518, 519
effect on wear, 355, 356
extreme example of, 411
see also Size, cylinder
Slider, plain, 322
Smoke, *see* Exhaust smoke
Smoke limit, definition of, 419
Sommerfeld variable, 318–321
see also Bearings, journal
Sound, velocity of, in air, 234, 394
in a perfect gas, 501, 502
in compressor performance, 368–379
in exhaust gases, 383, 394, 472
effect on turbine performance, 385–389
in fuel-air mixtures, 46, 47, 183, 472
in inlet gas, 168, 170–175
Spark advance, *see* Spark timing
Spark timing, effect on performance, 441–443
charts for, 442, 443
effect on indicator diagram, 128
example of, 452, 453
for best power, 127
Specific fuel consumption, *see* Consumption, fuel, specific
Specific gravity of fuels, 46, 47
Specific heat, *see* Heat, specific
Specific output, *see* Output, specific
Speed, engine, definition of, 419
range of, 418
rated, 419
vs year for passenger-car engines, 423
piston, *see* Piston speed
Steady-flow process, application to engines, 16, 17
definition of, 14
equations for, 15
Stresses, due to gas pressure, 401, 519
example of, 416
due to gravity, 519
due to inertia, 401, 518, 519
example of, 416
equation for, 519
thermal, 278–283

Stroke, vs year for passenger-car engines, 423
Stroke-bore ratio, effects on volumetric efficiency, 194, 195
of two-stroke cylinders, 236, 237
Subscripts, list of, 499
Supercharged engines, 456–493
arrangements of, 457
Diesel, 465, 467
spark-ignition, 462, 463
see also Performance, engine
Superchargers, *see* Compressors
Supercharging, 456–493
of aircraft engines, 460, 461
of auto engines, 461, 462, 464, 465
of Diesel engines, 463–467, 478–483
of free-piston engines, 480–482
of spark-ignition engines, 459–462
of turbo-compound engine, 460, 461
examples of 484–493
of two-stroke engines, 259, 260
reasons for, 458
Symbols, discussion of, 5
list of, 495–499

Tanks, surge, applied to engine, 17
Temperature, atmospheric, effect on bmep, 429
effect on detonation, 429, 430
effect on performance, 427–436
vs altitude, 434
compression, at beginning of, actual vs ideal, 512, 513
for fuel-air cycles, 85
from sound-velocity measurements, 125, 512
at compressor outlet, 365
coolant, choice of, 304, 305
effect on volumetric efficiency, 187
exhaust, of fuel-air cycles, 97
example of, 105, 106
of engines, 383, 384
gas, mean, 283–286
measurement of, 119–122
sodium-line reversal, 119, 121
spectroscopic methods, 119
Temperature, gas, measurement of, sound-velocity method, 119–122
inlet, effect on volumetric efficiency, 181, 182, 186, 187
measurement of, 17, 153
mean gas, 275–286
evaluation of, 283, 284
exhaust-pressure effect, 286
for inlet process, 169
inlet-temperature effect, 285, 286
values of vs fuel-air ratio, 285, 286
rise through inlet system, effect of design on, 188
relation to volumetric efficiency, 160–165
stagnation, of a perfect gas, 501
surface, in engines, 275, 276, 280, 281, 282
effect of cylinder size, 279, 280
effect of design changes, 282, 283
in similar engines, 281
local, 278, 279
example of, 308
measurement of, 287
of exhaust valve, 279, 280
of piston crown, 279
of port bridges, 279
of spark-plug points, 279
in heat exchangers, 272
Thermodynamics, of air cycles, 22–39
of fuel-air cycles, 67–106
of working fluids, 40–66
Thermodynamic properties, of air, Chart C-1
of fuel-air mixtures, Charts C-1 through C-4 (in pocket inside back cover)
Timing, port, *see* Port timing
Timing, spark, *see* Spark timing
Timing, valve, *see* Valve timing
Torque, engine, definition of, 419
Transient operation, 418
Trapping efficiency, *see* Efficiency, trapping
Trends, engine, vs time, 423–425
Turbine, exhaust, 383–392
blowdown type, 385–390
examples of, 398, 399
combination with engine, 391, 394

Turbine, exhaust, mixed flow type, 389, 390
example of, 398, 399
nozzle area of blowdown turbines, 470–472
in practice, 472
steady-flow turbines, 470
steady-flow type, 383–385
example of, 396
gas, advantages of, 3
classification of, 2
cycles for, 33, 34, 74–76
examples of, 102–105
definition of, 8
Turbo-supercharger, performance of, 391
examples of, 396–399
Two-stroke cylinders, *see* Cylinders, two-stroke
Two-stroke engines, *see* Engines, two-stroke

Units of measure, 5–7
fundamental, 5, 6
force, 5, 6
length, 5, 6
mass, 5, 6
quantity of heat, 6
temperature, 6
time, 5, 6

Valve, exhaust, for four-stroke engines, effect of capacity on volumetric efficiency, 193, 194
effect of closing time, 346
exhaust, for two-stroke engines, 212
effect on flow, 233
size of, 239–242
timing of, 214, 242–247
inlet, for four-stroke engines, effect on volumetric efficiency, 171–175, 193
capacity of valve, 171–175
closing time, 193
flow coefficient of, 171–175
Z-factor, 171–175
for two-stroke engines, *see* Ports and Port timing
sampling, for exhaust blowdown, 222
Valve overlap, *see* Valve timing
Valve timing, effect of exhaust opening, 346, 347
effect of inlet closing on volumetric efficiency, 191, 192
effect of valve overlap on volumetric efficiency, 188–191
effect on volumetric efficiency with various inlet pipes, 196, 197
relation to inlet pipe dimensions and volumetric efficiency, 196, 197
Velocity, sonic, *see* Sound, velocity of
Viscosity, conversion of, 315, 316
definition of, 314–317
of air, 290
of lubricant, effect on friction in engines, 332
in journal bearings, 316–322
with pistons, 332, 333
with sliders, 322–323
of water, 260
required for similar engines, 338
vs bore, 338
Volume, cylinder, displacement, 79, 149, 160
total, 217, 218
total vs displacement, 218
engine, specific, 420
of air, Chart C-1
of fuel-air mixtures, 46, 47, and Charts C-1 through C-4
of fuel vapor, 46, 47
Volumetric efficiency, *see* Efficiency, volumetric

Water, heat transfer with, 270
properties of, 269
Water vapor, *see* Humidity
Wear, of engines, 355, 356
damage, as related to bore, 403
general, 355
size effects, 355, 356, 403
Weights, of engines, relation to bore, 402, 407
relation to displacement, 407
vs cylinder size, 407
Work, in relation to energy and heat, 9–15
of air cycles, 26–34
of fuel-air cycles, 69–76

Work, of inlet stroke, 167
pumping work, 79

Z-factor, 173–177
definition of, 173
Z-factor, effect on volumetric efficiency, 174, 175
in practice, 176
maximum value of, 175
see also Mach index, inlet

1984 References for Vol. 1

Since the Bibliography beginning on page 523 was printed, the literature on the subject of internal-combustion engines has grown beyond the possibility of detailed listing. Publications in English for following continuing developments include:

Publications of the Society of Automotive Engineers (SAE) Warrendale, PA, 15096, as follows:

Automotive Engineering, a monthly magazine including reviews of current practice and condensations of important papers.

SAE Reports, classified by subject matter and containing selected *SAE Papers* on various subjects. Lists of each year's reports are available annually on request.

Individual *SAE Papers*, available in limited quantities on application or at SAE meetings.

Automotive Engineer, monthly, Box 24, Bury St. Edmunds, Suffolk, IP326BW, England. Published bi-monthly by Inst. of Mechanical Engineers, Automotive Division.

Bulletin of Marine Engineering Society in Japan, quarterly. The Marine Engineering Society of Japan, 1-2-2 Uchisaiwai-Cho, Chiyoda-Peu, Tokyo, 100 Japan.

Chilton Automotive Industries, monthly. Chilton Way, Radnor, PA, 19089. Statistical issue, April each year.

Diesel and Gas Turbine World Wide Catalog, 13555 Bishop Court, Brookfield, Wisconsin, 53005-0943. Annual.

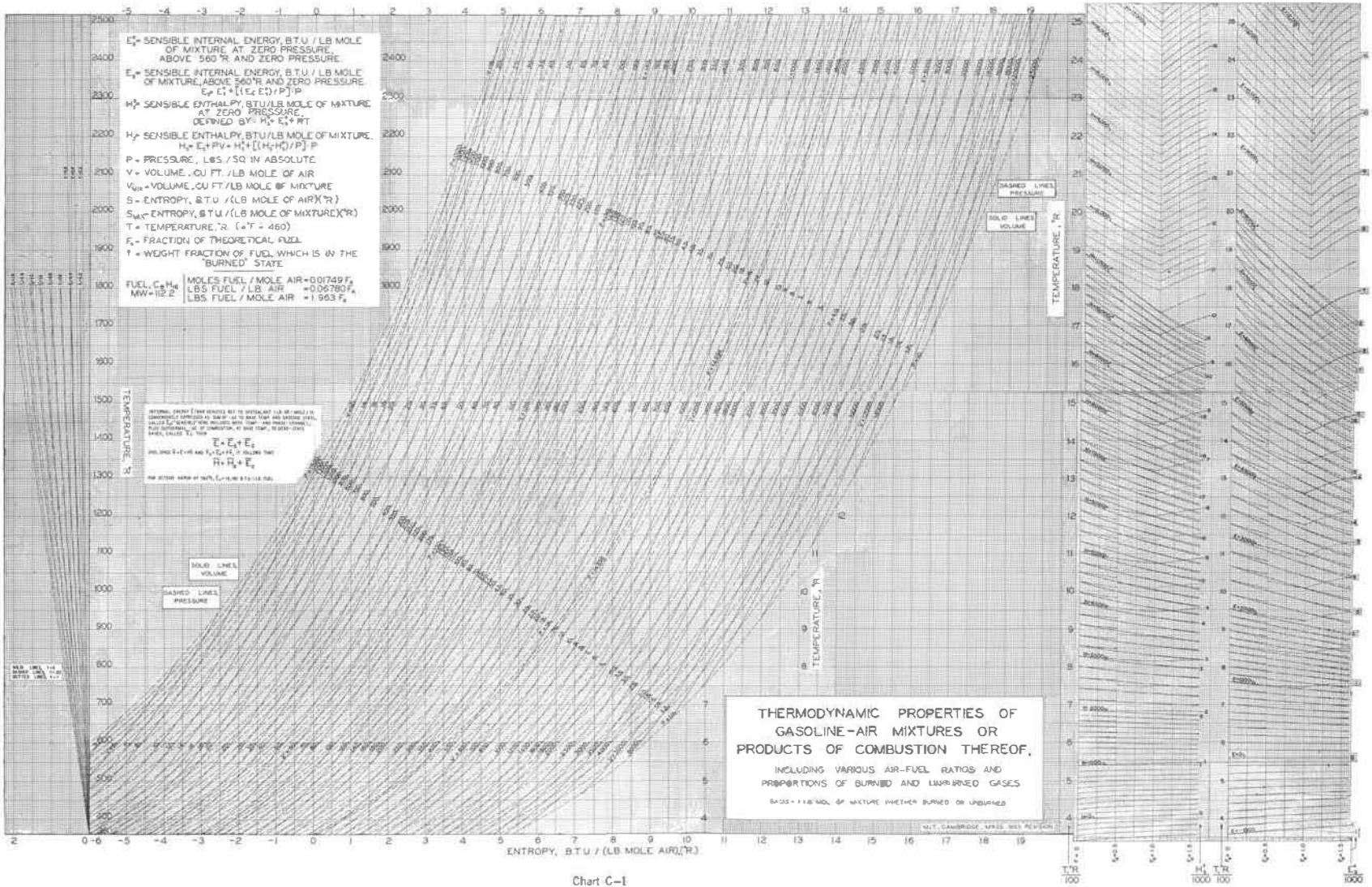
E_s° = SENSIBLE INTERNAL ENERGY, B.T.U. / LB MOLE OF MIXTURE AT ZERO PRESSURE, ABOVE 560 °R AND ZERO PRESSURE.
E_s = SENSIBLE INTERNAL ENERGY, B.T.U. / LB MOLE OF MIXTURE, ABOVE 560 °R AND ZERO PRESSURE. $E_s = E_s^\circ + [(E_s - E_s^\circ)/P] \cdot P$
H_s° = SENSIBLE ENTHALPY, BTU/LB MOLE OF MIXTURE AT ZERO PRESSURE, DEFINED BY $H_s^\circ = E_s^\circ + RT$
H_s = SENSIBLE ENTHALPY, BTU/LB MOLE OF MIXTURE. $H_s = E_s + PV = H_s^\circ + [(H_s - H_s^\circ)/P] \cdot P$
P = PRESSURE, LBS. / SQ IN ABSOLUTE
V = VOLUME, CU FT. / LB MOLE OF AIR
V_{MIX} = VOLUME, CU FT. / LB MOLE OF MIXTURE
S = ENTROPY, B.T.U. / (LB MOLE OF AIR)(°R)
S_{MIX} = ENTROPY, B.T.U. / (LB MOLE OF MIXTURE)(°R)
T = TEMPERATURE, °R (= °F + 460)
F_c = FRACTION OF THEORETICAL FUEL
f = WEIGHT FRACTION OF FUEL WHICH IS IN THE "BURNED" STATE
FUEL, C_8H_{16} MW = 112.2
MOLES FUEL / MOLE AIR = 0.01749 F_c
LBS FUEL / LB AIR = 0.06780 F_c
LBS. FUEL / MOLE AIR = 1.963 F_c
$E + E_s + E_c$
$H + H_s + E_c$
SOLID LINES VOLUME
DASHED LINES PRESSURE
DASHED LINES PRESSURE
SOLID LINES VOLUME
TEMPERATURE, °R
TEMPERATURE, °R
TEMPERATURE, °R
ENTROPY, B.T.U. / (LB MOLE AIR)(°R)
THERMODYNAMIC PROPERTIES OF GASOLINE-AIR MIXTURES OR PRODUCTS OF COMBUSTION THEREOF.
INCLUDING VARIOUS AIR-FUEL RATIOS AND PROPORTIONS OF BURNED AND UNBURNED GASES
BASIS - 1 LB MOL OF MIXTURE WHETHER BURNED OR UNBURNED
M.I.T. CAMBRIDGE, MASS. 1951 REVISION
T °R / 100
H_s° / 1000
T °R / 100
E_s / 1000

Chart C-1

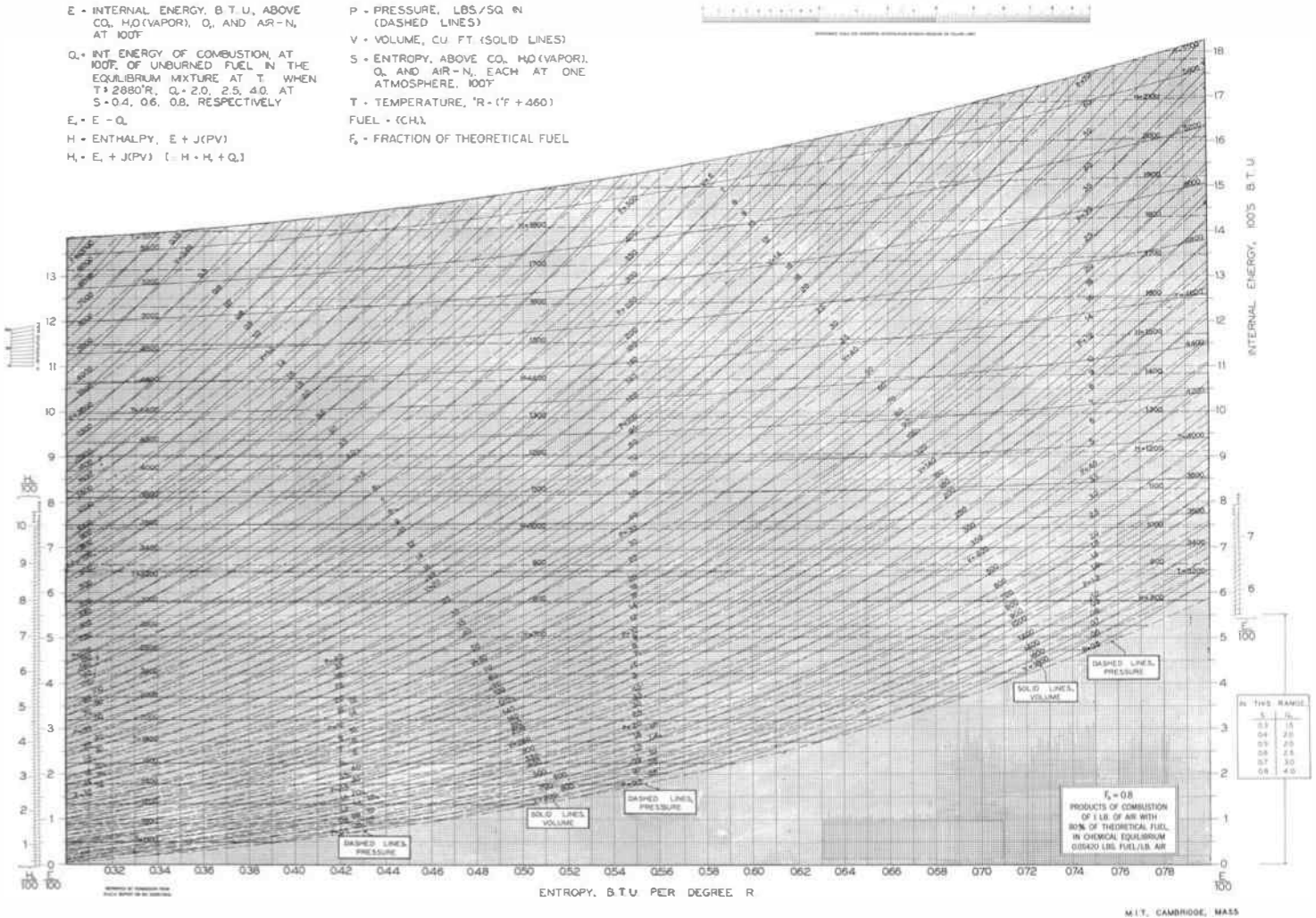
E - INTERNAL ENERGY, B.T.U. ABOVE CO2, H2O (VAPOR), O2, AND AR-N2 AT 100°F
Q - INT. ENERGY OF COMBUSTION, AT 100°F, OF UNBURNED FUEL IN THE EQUILIBRIUM MIXTURE AT T WHEN T = 2880°R, Q = 2.0, 2.5, 4.0, AT S = 0.4, 0.6, 0.8, RESPECTIVELY
E1 = E - Q
H = ENTHALPY, E + J(PV)
H1 = E1 + J(PV) (H = H1 + Q)
P - PRESSURE, LBS./SQ. IN. (DASHED LINES)
V - VOLUME, CU. FT. (SOLID LINES)
S - ENTROPY, ABOVE CO2, H2O (VAPOR), O2 AND AIR-N2, EACH AT ONE ATMOSPHERE, 100°F
T - TEMPERATURE, °R = (°F + 460)
FUEL = (CH2)x
Fo - FRACTION OF THEORETICAL FUEL
INTERNAL ENERGY, 1000'S B.T.U.
ENTROPY, B.T.U. PER DEGREE R
DASHED LINES, PRESSURE
SOLID LINES, VOLUME
DASHED LINES, PRESSURE
SOLID LINES, VOLUME
DASHED LINES, PRESSURE
Fo = 0.8
PRODUCTS OF COMBUSTION OF 1 LB. OF AIR WITH 80% OF THEORETICAL FUEL IN CHEMICAL EQUILIBRIUM
0.05420 LBS. FUEL/LB. AIR
IN THIS RANGE
M.I.T., CAMBRIDGE, MASS.

Chart C1-2

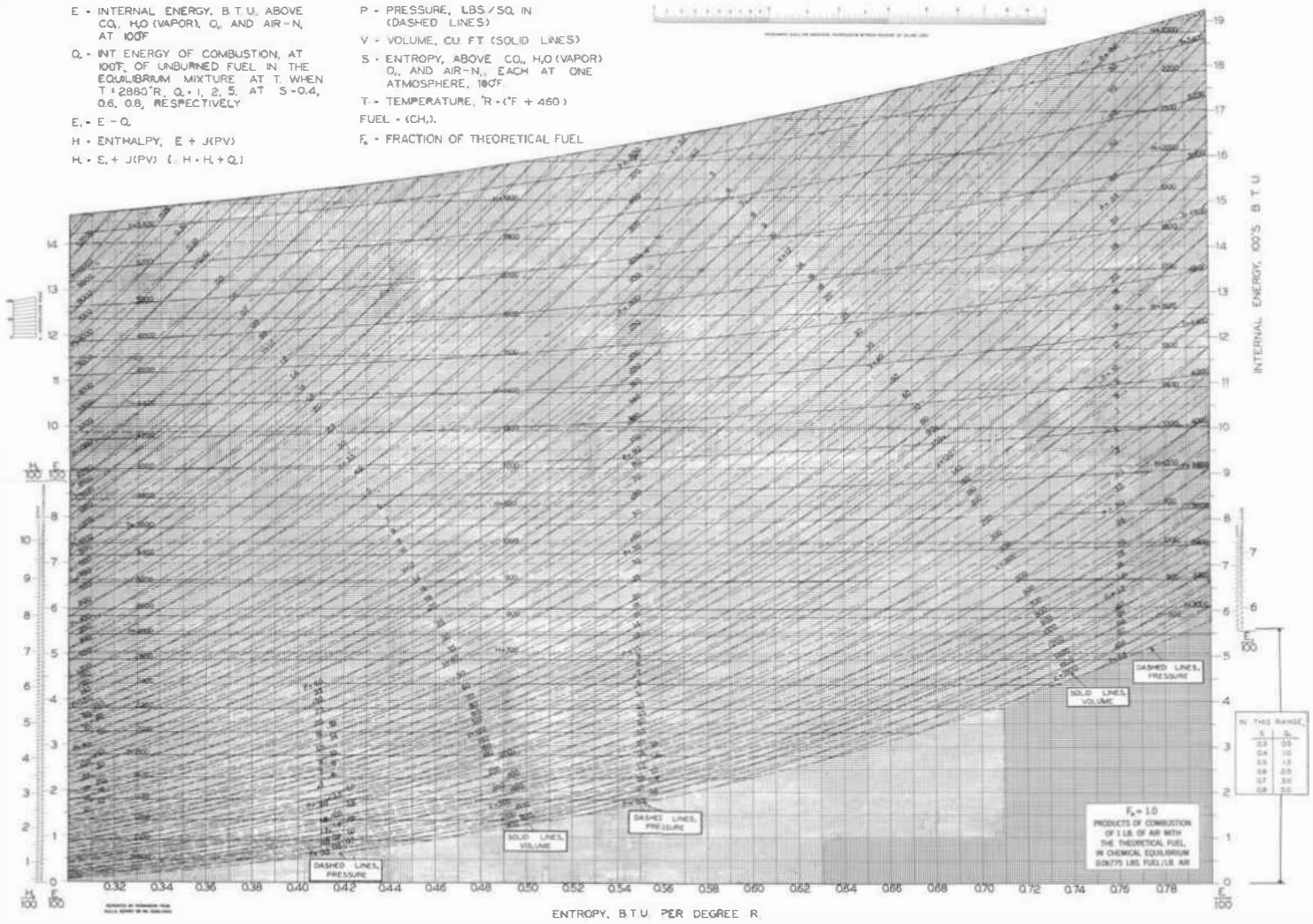
E - INTERNAL ENERGY, B.T.U. ABOVE CO2, H2O (VAPOR), O2, AND AIR - N2 AT 100°F
Qp - INT. ENERGY OF COMBUSTION, AT 100°F, OF UNBURNED FUEL IN THE EQUILIBRIUM MIXTURE AT T, WHEN T = 2880°R, Qp = 1, 2, 5, AT S = 0.4, 0.6, 0.8, RESPECTIVELY
E1 = E - Qp
H = ENTHALPY, E + J(PV)
H1 = E1 + J(PV) (H = H1 + Qp)
P - PRESSURE, LBS / SQ. IN (DASHED LINES)
V - VOLUME, CU. FT. (SOLID LINES)
S - ENTROPY, ABOVE CO2, H2O (VAPOR) O2, AND AIR - N2, EACH AT ONE ATMOSPHERE, 100°F
T - TEMPERATURE, °R = (°F + 460)
FUEL = (CH2).
Fa = FRACTION OF THEORETICAL FUEL
INTERNAL ENERGY, 100'S B.T.U.
DASHED LINES, PRESSURE
SOLID LINES, VOLUME
DASHED LINES, PRESSURE
SOLID LINES, VOLUME
DASHED LINES, PRESSURE
Fa = 1.0
PRODUCTS OF COMBUSTION OF 1 LB. OF AIR WITH THE THEORETICAL FUEL IN CHEMICAL EQUILIBRIUM
0.0775 LBS. FUEL/LB. AIR
IN THIS RANGE,
ENTROPY, B.T.U. PER DEGREE R.
M.I.T., CAMBRIDGE, MASS.

Chart C-3

E - INTERNAL ENERGY, B.T.U., ABOVE CO_2, H_2O (VAPOR), O_2, AND AIR - N_2 AT 100°F

Q_p - INT. ENERGY OF COMBUSTION, AT 100°F, OF UNBURNED FUEL IN THE EQUILIBRIUM MIXTURE AT T. WHEN T = 2880°R, Q_p = 336.

E_1 = E - Q_p

H - ENTHALPY, E + J(PV)

H_1 = E_1 + J(PV) [= H - H_f + Q_p]

P - PRESSURE, LBS / SQ. IN. (DASHED LINES)

V - VOLUME, CU. FT. (SOLID LINES)

S - ENTROPY, ABOVE CO_2, H_2O (VAPOR), O_2, AND AIR - N_2, EACH AT ONE ATMOSPHERE, 100°F

T - TEMPERATURE, °R - (°F + 460)

FUEL - $(CH_2)_x$

F_r - FRACTION OF THEORETICAL FUEL

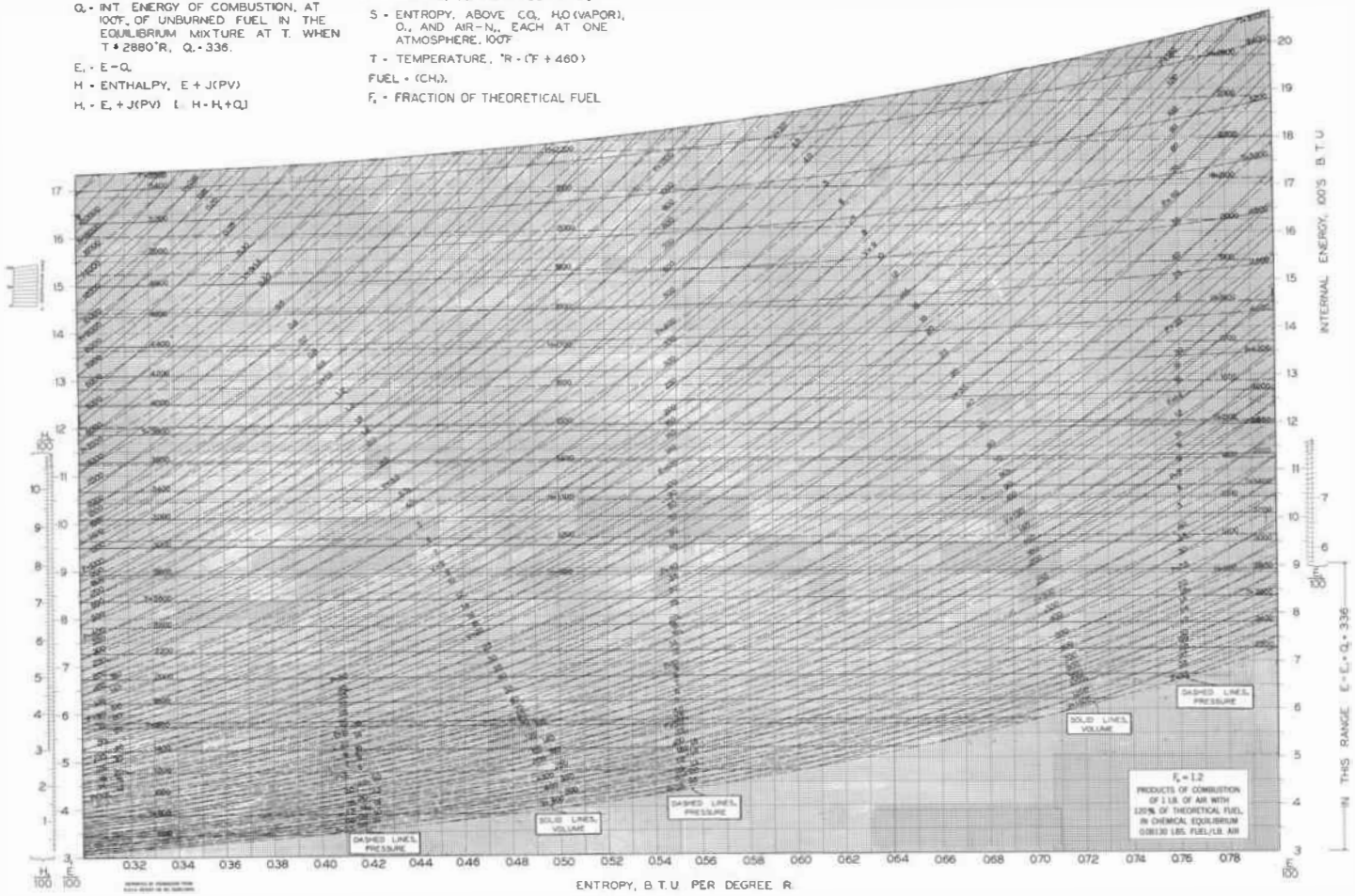

M.I.T. CAMBRIDGE, MASS.

Chart C-4